Rhodium and Iridium Pincer Complexes Supported by Bis(phosphino)silyl Ligation: Applications in Bond Cleavage Chemistry

by

Erin Morgan

Submitted in partial fulfilment of the requirements
for the degree of Doctor of Philosophy

at

Dalhousie University
Halifax, Nova Scotia
May 2013

DALHOUSIE UNIVERSITY

DEPARTMENT OF CHEMISTRY

The undersigned hereby certify that they have read and recommend to the Faculty of Graduate Studies for acceptance a thesis entitled "Rhodium and Iridium Pincer Complexes Supported by Bis(phosphino)silyl Ligation: Applications in Bond Cleavage Chemistry" by Erin Morgan in partial fulfilment of the requirements for the degree of Doctor of Philosophy.

Dated: May 22, 2013

External Examiner: _____

Research Supervisor: _____

Examining Committee: _____

_____

_____

Departmental Representative: _____

DALHOUSIE UNIVERSITY

DATE: May 22, 2013

AUTHOR: Erin Morgan

TITLE: Rhodium and Iridium Pincer Complexes Supported by Bis(phosphino)silyl Ligation: Applications in Bond Cleavage Chemistry

DEPARTMENT OR SCHOOL: Department of Chemistry

DEGREE: PhD CONVOCATION: October YEAR: 2013

_____

Signature of Author

Table of Contents

List of Tables

List of Figures

List of Schemes

Abstract

Group 9 transition metal pincer complexes have shown tremendous utility in a variety of E-H (E = main group element) bond activation reactions. In an effort to access new types of highly reactive pincer-like transition metal complexes this research focuses on the development of new late metal complexes supported by tridentate bis(phosphino)silyl ligands of the type $[\kappa^3\text{-}(2\text{-}R_2PC_6H_4)_2SiMe]^-$ ([R-PSiP]; R = Cy, ^{i}Pr). The incorporation of a strongly electron donating and highly trans-labilizing silyl group at the central anionic position may promote the formation of new coordinatively unsaturated compounds capable of enhanced reactivity. In this regard, the synthesis of coordinatively unsaturated Rh and Ir complexes supported by R-PSiP ligation and their ability to activate E-H bonds will be detailed.

The synthesis of Cy-PSiP ligated Rh and Ir species and the ability to access the products of N–H bond oxidative addition with these species was investigated. Both [Cy-PSiP]Rh and [Cy-PSiP]Ir complexes were shown to form isolable complexes of the type [Cy-PSiP]M(H)(NHR) (M = Rh, R = aryl; M = Ir, R = H, aryl). However, attempts to generate such amido hydride complexes by N-H activation of the corresponding amine led to divergent reactivity, where adducts of the type [Cy-PSiP]Rh(NH_2R) were obtained for Rh, while N-H bond oxidative addition was observed for Ir to form the targeted amido hydride complexes, including a rare example of ammonia N-H bond oxidative addition to form a monomeric, terminal parent amido complex that was crystallographically characterized. Due to the scarcity of transition metal complexes that are capable of N-H bond oxidative addition, a thorough investigation of the N-H bond activation mediated by [Cy-PSiP]Rh and Ir with various N-H containing substrates, including alkyl amines, hydrazine derivatives, and benzamides was initiated. Extension of this reactivity to the related diisopropylphosphino derivative [^{i}Pr-PSiP]Ir^I was also probed, as the resulting complexes were envisioned to be less susceptible to potential cyclometalation processes.

Indeed, oxidative addition of primary alkyl amines, hydrazines, and benzamides was observed for [R-PSiP]Ir. These results comprise an unprecedented example of a metal complex that is capable of facile N-H bond activation in such a wide range of substrates, including challenging substrates such as ammonia and alkyl amines. A rare example of Rh-mediated N-H oxidative addition was also observed for the reaction of [Cy-PSiP]Rh^I with benzophenone hydrazone.

The potential for these [R-PSiP]Ir(H)(NHR) complexes to insert unsaturated substrates was investigated, as the development of new pathways for the formation of C-N bonds via transition metal catalyzed N-H bond oxidative addition to a metal center followed by insertion of an alkene or alkyne into the M-N or M-H bond may provide a new pathway for accessing intermolecular amination reactions. Insertion chemistry attempts with various alkenes, alkynes, allenes, C=O and C≡N containing compounds is described.

Lastly, the synthesis of Ir^{III} complexes of the type $\{[R\text{-}PSiP]IrR'\}^+X^-$ (R = Cy, ^{i}Pr; R' = H, Me; X = OTf, BF_4, $B(C_6F_5)_4$) and their interactions with the C-H bonds of arenes and aldehydes, as well as, the Si-H bonds of hydrosilanes is detailed. The Si-H bond activation chemistry observed was typically influenced by the counter anion X. Thus, the more coordinating anions OTF and BF_4 were shown to coordinate to and stabilize the highly electrophilic Si in transiently generated Ir silylene species.

List of Abbreviations and Symbols Used

η = hapticity (contiguous donor atoms)
κ = hapticity (non-contiguous donor atoms)
Anal. Calcd. = Analysis Calculated
Å = angstrom
COD = 1,5-cyclooctadiene
COE = cyclooctene
COSY = Homonuclear Shift *CO*rrelation *S*pectroscop*Y*
Cp* = pentamethylcylcopentadienyl
Cy = cyclohexyl
[Cy-PSiP] =

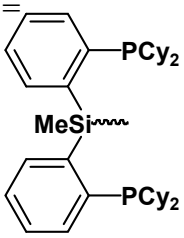

d = doublet
δ = chemical shift
DEPT = *D*istortionless *E*nhancement by *P*olarization *T*ransfer
E = main group element
equiv = equivalents
Et = ethyl
h = hour
HMBC = *H*eteronuclear *M*ultiple *B*ond *C*orrelation
HSQC = *H*eteronuclear *S*ingle *Q*uantum *C*orrelation
Hz = hertz
IR = infrared
^{i}Pr = isopropyl
[^{i}Pr-PCP] =

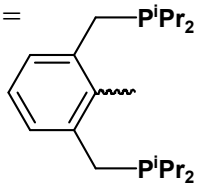

**$^{n}J_{XX`}$** = n bond coupling constant between atom X and atom X`
L = two-electron donor ligand
m = multiplet
M = generic transition metal *or* mol/L
Me = methyl
Mes = 2,4,6-trimethylphenyl
min = minutes
NMR = Nuclear Magnetic Resonance
[NSiN] =

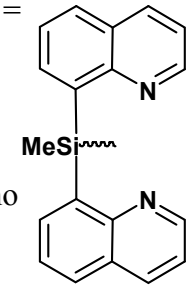

o = ortho
ORTEP = Oak Ridge Thermal Ellipsoid Plot
p = para
ppm = parts per million
Ph = phenyl
[POCOP] =

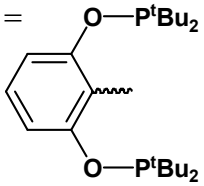

q = quartet
R = alkyl or aryl group
s = singlet
t = triplet
^{t}Bu = *tert*-butyl
[^{t}Bu-PCP] =

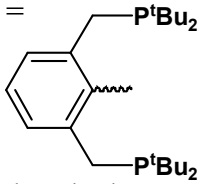

TBA = *tert*-butyl ethane
TBE = *tert*-butyl ethylene
THF = tetrahydrofuran
TMS = trimethylsilyl
TOF = turn over frequency
TON = turn over number

Acknowledgements

There are many individuals I am grateful to for their assistance during my time in graduate school. My first debt of gratitude must go to my supervisor, Dr. Laura Turculet for both her time and ideas in helping me complete this research. Her knowledge, inspiration, support, and mentorship have helped to shape both the direction of my work and the type of scientist I would like to become.

The members of the Turculet group, past and present, have immensely contributed to both personal and professional development. I couldn't have imagined a better group of people to go through this experience with. I particularly want to thank Morgan MacInnis for not letting me take things too seriously, Sam Mitton for acting as my life coach, and Adam Ruddy for both enlightening me with daily doses of internet happenings and DJing our days in the lab. The countless discussions and support helped me make it through. I must also extend thanks to some current and former members of the Stradiotto research group, especially Kevin Hesp, Pam Alsabeh, and Sarah Crawford for invaluable discussions and general helpfulness.

I want to thank the members of my supervisory committee, Dr. Mark Stradiotto, Dr. Kevin Grundy, and Dr. Norm Schepp for their support over the course of my degree. I would also like to acknowledge Drs. Robert McDonald and Mike Ferguson at the University of Alberta for their excellent work in collecting and solving X-ray crystal data, as well as Dr. Mike Lumsden of the NMR^3, for his assistance and expertise in the collection of NMR data. As well, I wish to acknowledge the numerous administrative staff in the Dalhousie Chemistry Department for their assistance, specifically Giselle Andrews for her dedication to graduate student's success.

I would like to extend special thanks to my friends, who have made up an invaluable support system. Firstly, Dea Chute and Jamie Kneen have motivated me to become as strong and inspiring as them. Vanessa Marx and Kelly Resmer who helped me enjoy the first few years of life in Halifax. Furthermore, I'd like to thank Erica Zirpolo and Lauren Florko who have taught me the importance of balance and the significance of surrounding yourself with those who make you laugh.

Lastly, this thesis would not have been possible without the love and support of my family. I would not have contemplated this road if not for my parents, Leslie and George, who from day one nurtured my natural curiosity, instilled within me a drive to succeed, and provided the foundation of love and encouragement to help me realize my goals. My sister Hayley, who has become one of my best friends through this journey, has shown me the significance of taking advantage of your abilities and compassion to make a difference in the world. I would also like to thank my grandmother Reta who has taught me the importance of both standing up for what you believe in and rewarding yourself with a glass (or half glass) of wine, as well as my grandfather Michael who's unwavering pride in 'his girls' inspires me to be a better person. To my family, thank you.

Chapter 1: Introduction

1.1 Overview

One of the most important applications of modern organometallic chemistry is the utilization of transition metal complexes to catalyze chemical reactions in an efficient and selective manner.[1] The conversion of abundant and easily accessible substrates (such as alkanes, alkenes, CO, CO_2, H_2, H_2O, N_2, and NH_3) into functionalized products in an efficient catalytic cycle is crucial to the production of both commodity chemicals on an industrial scale, as well as fine chemicals and pharmaceuticals. The tremendous impact of homogeneous transition metal catalysis was recognized in the awarding of the 2001, 2005, and 2010 Nobel Prizes in Chemistry for developments in asymmetric catalysis[2], olefin metathesis,[3] and palladium-catalyzed cross-coupling,[4] respectively. Although such advances have wide-ranging applications, they are ultimately rooted in the fundamental study of transition metal reactivity. As such, the starting point for the discovery of new and/or improved metal-mediated syntheses is the design of metal complexes that exhibit novel reactivity. Key to this endeavour is the construction of new types of ancillary ligands that are able to stabilize a reactive metal center in a unique coordination environment while simultaneously conferring desirable reactivity properties.

In this context, the research described in this thesis involves the use of novel bis(phosphino)silyl 'pincer'-type ancillary ligands. Specifically, the development of complexes containing such silyl pincer ligands coordinated to Group 9 transition metals (Rh and Ir) and the corresponding reactivity of these new complexes with E-H (E = main group element) bonds will be addressed. To place the work described in this document in context, an overview of previous noteworthy advances from the field of transition metal pincer chemistry will be presented. This overview will emphasize breakthroughs that highlight the utility of Group 9 metal pincer complexes in achieving challenging C-H, N-H, and Si-H bond cleavage reactions and in the subsequent selective functionalization of such fragments.

1.2 Pincer Ligand Design and Influence Over Metal Reactivity

The choice of ancillary ligand(s) can influence the structure and reactivity of a transition metal complex via a combination of steric and electronic effects. In this regard, pincer ligands offer an attractive means of controlling these factors due to their relatively modular design. Pincer ligands are a class of tridentate ancillary ligands that feature an LXL-type (L = neutral donor, X = anionic donor) donor framework and that typically coordinate to the metal center in a meridional fashion (Figure 1-1).[5] Upon coordination to a metal center, such tridentate ligands afford enhanced stability to the resulting complex. This stability can be attributed to the chelating nature of the pincer ligand, which typically leads to the formation of two five-membered metallacycles upon complexation. The enhanced stability imparted by pincer ligands can lead to novel reactivity for the ensuing complexes, especially in comparison with related monodentate, non-chelating ancillary ligand systems.

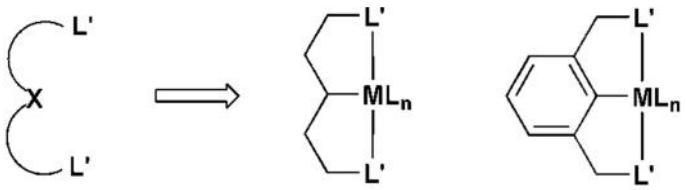

Figure 1-1. Traditional LXL pincer ligand design

Variations that involve changing the neutral donor groups (L), the nature of the central anionic donor (X), as well as the composition of the pincer ligand backbone can have a dramatic effect on the chemistry of the ensuing pincer metal complexes. A wide variety of neutral L donors have been employed in the LXL pincer design. Traditionally, the most commonly utilized neutral donors are phosphine[5d] and amine[6] groups, but examples that feature neutral O,[7] S,[8] Se,[9] as well as C-,[10] Si-[11] and Ge-based[11a] donors have also been reported. The substitution at these donor atoms also impacts the steric and electronic profile of the metal center through the use of steric bulk and/or electron

donating/withdrawing substituents. By comparison, substantially less variability at the central X donor position has been reported, and with few exceptions,[12-15] the central anionic donor has typically been limited to carbon (alkyl or aryl)[5] or nitrogen (amido)[16] donors. Finally, the backbone of the pincer framework can be comprised of either aliphatic or aromatic moieties, the choice of which can alter the rigidity of the ligand scaffold as well as the donor properties of the L and X donors, leading to notable differences in reactivity.[17]

Although it is apparent that ligand variability in such pincer architectures is immense, by far the most prominent examples of pincer complexes in the literature feature bis(phosphino) L donors and a central carbon-based X donor. It is therefore appropriate to begin a discussion of pincer ligand development with the prominent PCP-supported complexes.

1.3 Development of PCP Pincer Chemistry

Pioneering work in the field of pincer chemistry was initiated by Shaw and coworkers[18] nearly 40 years ago. These initial studies focused on the formation of late metal PCP pincer complexes by the chelate assisted metalation of an aromatic or aliphatic C-H bond (Figure 1-2).[18] Throughout these investigations it was noted that PCP pincer complexes were much more stable than traditional complexes containing analogous monodentate phosphine ligands. Since the initial groundbreaking work of Shaw and coworkers, the field of transition metal pincer chemistry has greatly expanded into its own sub-discipline of organometallic chemistry.

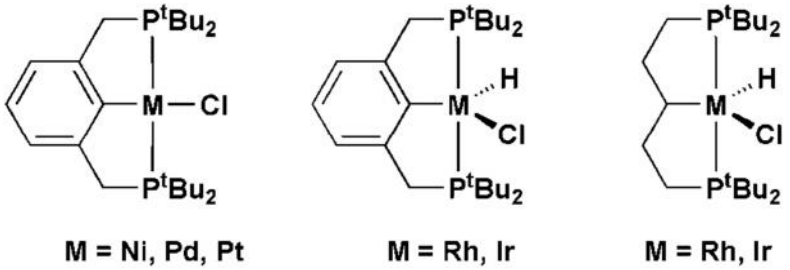

Figure 1-2. PCP pincer complexes synthesized by Shaw and co-workers

Chelate-assisted cyclometalation remains the most common approach for the synthesis of new late metal PCP pincer complexes.[5a] This synthetic route involves M-C bond formation via initial coordination of the phosphine donors of the ligand precursor to the metal, such that the cleavage of an sp^2- or sp^3-hybridized C-H bond becomes a more facile intramolecular process. Although this synthetic route has been successfully utilized to generate PCP pincer complexes, it is nonetheless often plagued by long reaction times and high temperatures. The C-H bond cleavage step is often facilitated by increasing the electron donating ability of the phosphine donors in order to promote oxidative addition. Thus, alkyl substituted phosphine donors help to promote the oxidative addition step.[5b]

Although numerous examples of platinum group metal PCP pincer complexes have been prepared and studied since the initial discoveries of Shaw and co-workers, this thesis will focus specifically on advances involving the chemistry of Group 9 (Rh and Ir) metal PCP complexes, and the utility of these species for the intermolecular cleavage and functionalization of C-H, N-H, and Si-H bonds. The groups of Goldman, Jensen, Brookhart, and Hartwig have accomplished major breakthroughs in these areas, and their contributions will be highlighted in the following sections.

1.4 (PCP)Ir Catalyzed C-H Bond Activation Chemistry

1.4.1 Development of Alkane Dehydrogenation Chemistry

The selective functionalization of unactivated alkanes is viewed as one of the greatest challenges in modern organometallic chemistry.[19,20] A key step in the conversion of alkanes into functionalized products involves C-H bond activation (or cleavage) at a reactive metal center. Although there are different classes of reactions that can achieve C-H bond activation, significant research efforts have focused on the direct oxidative addition of a C-H bond to a low-valent metal center to form a hydridoalkyl metal species (Figure 1-3).

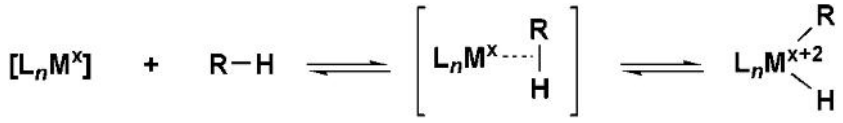

Figure 1-3. Oxidative addition of a C-H bond to a metal center

Pioneering work by both the Bergman and Graham groups in the early 1980s demonstrated that transition metal mediated intermolecular alkane C-H bond oxidative addition was indeed possible in a stoichiometric fashion and that the products of C-H activation were isolable.[21] To achieve C-H bond cleavage, both groups used photolysis to generate an electronically unsaturated Ir^{I} species capable of oxidatively adding alkane C-H bonds (Scheme 1-1).

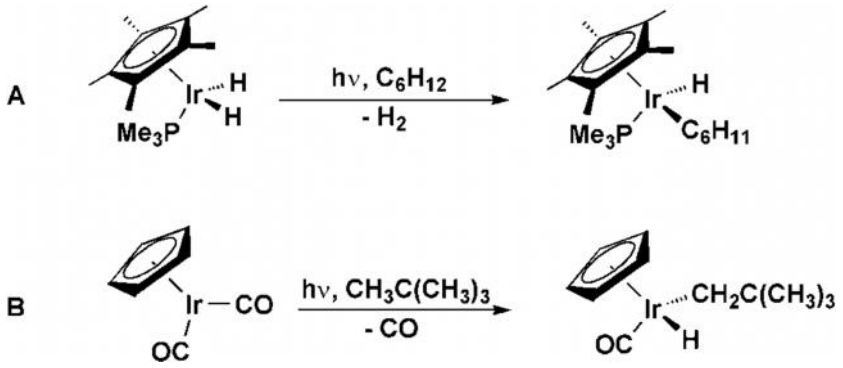

Scheme 1-1. Early examples of C-H bond activation

Although C-H bond activation at a metal center has proven possible in a stoichiometric fashion, significant challenges remain with respect to practical alkane functionalization.[19] One reaction being investigated toward these ends is metal-mediated alkane dehydrogenation to a terminal alkene. As this reaction is thermodynamically uphill, an alternative being pursued is metal-mediated transfer dehydrogenation, where a hydrogen acceptor is used to shift the equilibrium of the reaction (Figure 1-4).

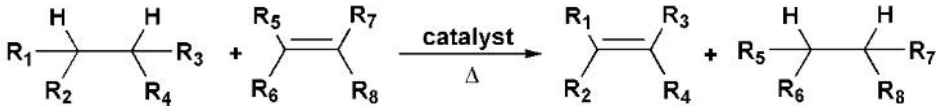

Figure 1-4. Net transfer dehydrogenation reaction

The highly desirable process of *n*-alkane dehydrogenation to a terminal alkene through metal-mediated transfer dehydrogenation was probed using various transition metal complexes.[22] The first efficient system for the thermal transfer dehydrogenation of alkanes was developed by Goldman and coworkers using the Rh catalyst $Rh(PMe_3)_2Cl(CO)$ with a sacrificial alkene hydrogen acceptor.[23] Although this system showed promise for alkane dehydrogenation, a large excess of the sacrificial alkene was required and the turnover numbers were limited due to competitive (non-transfer) hydrogenation of the alkene product. It was clear that a more efficient catalytic system was needed to achieve effective homogeneous alkane dehydrogenation.

1.4.2 Catalytic Dehydrogenation of Cyclic Alkanes by a (PCP)Ir Pincer Complex

A breakthrough in the catalytic dehydrogenation of alkanes was established by Jensen and Goldman who independently reported on a (PCP)Ir pincer system capable of highly efficient cycloalkane dehydrogenation (Figure 1-5).[24]

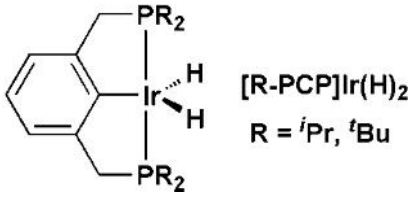

Figure 1-5. [R-PCP]Ir(H)$_2$ pincer complex used for catalytic alkane dehydrogenation

One of the primary challenges associated with alkane dehydrogenation is that heating to relatively high temperatures is required to overcome the uphill thermodynamics of the reaction at room temperature. Under such conditions, many of the organometallic complexes that had previously been investigated as catalysts for this reaction undergo decomposition. For instance, Crabtree and coworkers had previously shown that $[IrH_2(Me_2CO)_2(P(p\text{-}FC_6H_4)_3)_2][SbF_6]$ was able to effect the dehydrogenation of alkanes at 150 ºC in the presence of the hydrogen acceptor *tert*-butylethylene (TBE), but the system failed to catalytically turn over because the catalyst decomposed at the elevated temperatures required for the release of the alkene from intermediate complexes.[25] Complexes of the type [R-PCP]Ir(H)$_2$ (R-PCP = 2,6-$(R_2PCH_2)_2C_6H_3$) utilized by Jensen and Goldman proved advantageous as they exhibited greatly enhanced thermal stability relative to previous systems without pincer ligands, even at temperatures up to 200 ºC.[26] The enhanced stability imparted by the pincer ligand allowed for the use of elevated temperatures to complete the catalytic cycle for dehydrogenation of alkanes.

Initial reports of (PCP)Ir-catalyzed alkane dehydrogenation from the Jensen group involved combining an excess of cyclooctane (COA) with the sacrificial alkene TBE and 0.01 mol % of [^{t}Bu-PCP]Ir(H)$_2$ under an Ar atmosphere.[24a] At 200 ºC the dehydrogenation of COA occurred with a turnover frequency (TOF) of ca. 12 turnovers min^{-1} to produce the desired cyclooctene (COE) product. It was also found that catalyst decomposition did not occur at elevated temperatures, which was a great improvement on previous catalysts used for alkane dehydrogenation. In a follow-up study, [^{t}Bu-PCP]Ir(H)$_2$ was also shown to catalyze the transfer dehydrogenation of cycloalkanes such

as cyclohexane and methylcyclohexane to arenes with rates comparable to those found for the dehydrogenation of cyclooctane.[24b]

Under similar conditions, the ability of [^{t}Bu-PCP]Rh(H)$_2$ to effect alkane dehydrogenation was much less and rates of 1.8 turnovers h^{-1} were observed at 200 ºC, with significant catalyst decomposition observed after 24 h at this temperature.[24a] This was surprising since prior to the reported [^{t}Bu-PCP]IrH$_2$ catalyst, only Rh catalysts had been catalytically active in the transfer dehydrogenation of alkanes.[23] It has been postulated, on the basis of computational studies, that the [R-PCP]Rh-mediated C-H bond activation of alkanes may be unfavorable by comparison with the Ir system, leading to the observed low activity of the Rh catalysts.[26]

Focusing on the [^{t}Bu-PCP]Ir(H)$_2$ system, it was found that catalytic activity was suppressed both by the presence of N_2 as well as high concentrations of alkene, including both the sacrificial alkene (TBE) and the dehydrogenated product (COE).[24a] To achieve higher TONs, TBE was periodically added to the reaction mixture in small increments and under such conditions TOFs of 12 turnovers min^{-1} were maintained until prominent product inhibition was observed after a total of 1000 turnovers. In order to avoid catalyst inhibition by N_2, the reaction mixtures were thoroughly degassed prior to heating.

The proposed overall mechanism of transfer dehydrogenation of alkanes by [^{t}Bu-PCP]Ir(H)$_2$ (Scheme 1-2) involves initial dehydrogenation of the dihydride by the sacrificial alkene (TBE), which is achieved by coordination of TBE to Ir followed by irreversible insertion of the alkene into the Ir-H bond.[27] This is followed by reductive elimination of *tert*-butylethane (TBA), which has been observed by NMR spectroscopy. A new Ir product assigned as the highly unsaturated, 14-electron [^{t}Bu-PCP]Ir^I species is generated by this reductive elimination step. This intermediate could not be isolated, however it was characterized in situ by both ^{31}P and ^{1}H NMR spectroscopy.[27] Although the 14-electron [^{t}Bu-PCP]Ir^I species was proposed based on solution NMR studies, the possibility of agostic interactions or solvent coordination to the highly unsaturated Ir center cannot be discounted.

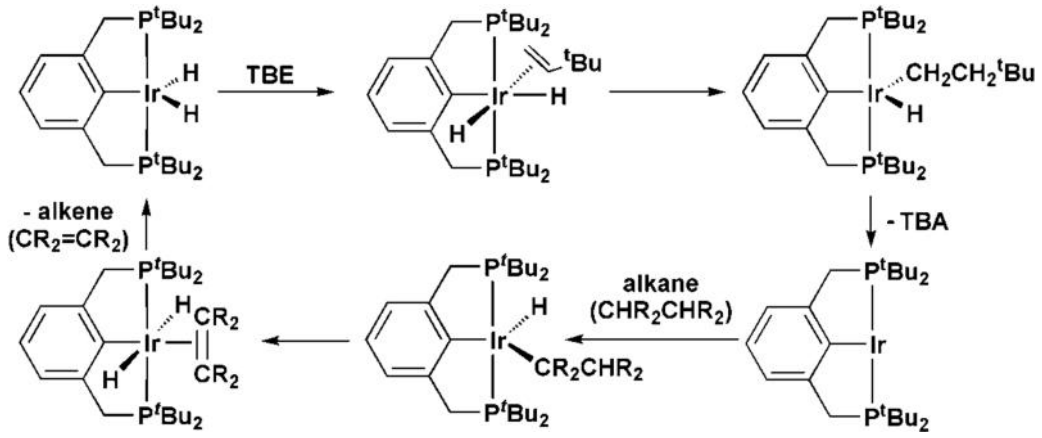

Scheme 1-2. Proposed mechanism for [R-PCP]Ir-mediated alkane dehydrogenation with TBE as the hydrogen acceptor

The alkane dehydrogenation portion of the catalytic cycle is proposed to occur via C-H bond activation of the alkane substrate by the [^{t}Bu-PCP]Ir^{I} intermediate, which is likely to occur via C-H bond oxidative addition to form a hydrido alkyl Ir^{III} species (Scheme 1-2).[28] Subsequent β-hydride elimination generates a dihydrido alkene complex. Upon loss of the coordinated alkene, [^{t}Bu-PCP]Ir(H)$_2$ is regenerated and can reenter the catalytic cycle.

1.4.3 Catalytic Alkane Dehydrogenation of Linear Alkanes by a (PCP)Ir Complex

The catalytic ability of the [R-PCP]Ir(H)$_2$ pincer system was further extended by changing the substituents on the phosphorus donor of the pincer ligand from ^{t}Bu to ^{i}Pr groups. The pincer complex [^{i}Pr-PCP]Ir(H)$_2$ was able to mediate transfer dehydrogenation of linear *n*-alkanes for the formation of terminal alkenes (Scheme 1-3A).[29] This reaction has immense potential, as terminal alkenes are the precursors for many industrially relevant chemical products. Furthermore, this system represents the first reported catalyst to achieve functionalization of the terminal position of a linear alkane under thermal conditions.

Since internal alkenes are thermodynamically favored over terminal alkenes, the ability to produce the desired terminal alkene products was a remarkable breakthrough. Substitution of the ^{t}Bu groups on the [R-PCP] ligand phosphine donors with ^{i}Pr groups led to the formation of a more active dehydrogenation catalyst, such that the major kinetic product became the terminal alkene. In addition, it was postulated that the terminal alkene product could be prevented from isomerizing to an internal alkene by competition with another alkene, such as the hydrogen acceptor itself. Isomerization is traditionally thought to occur through coordination of the terminal alkene to the metal center, followed by a 2,1-insertion into a metal hydride bond (Scheme 1-3B). A β-hydride elimination follows, producing the internal alkene. However, more recent experimental and theoretical studies indicate that the [^{t}Bu-PCP]Ir system mediates the isomerization of terminal alkenes via a formal 1,3-hydride shift through a π-allyl complex formed by dissociation of the Ir-olefin π-bond followed by sp^3-C–H bond activation (Scheme 1-3C).[30]

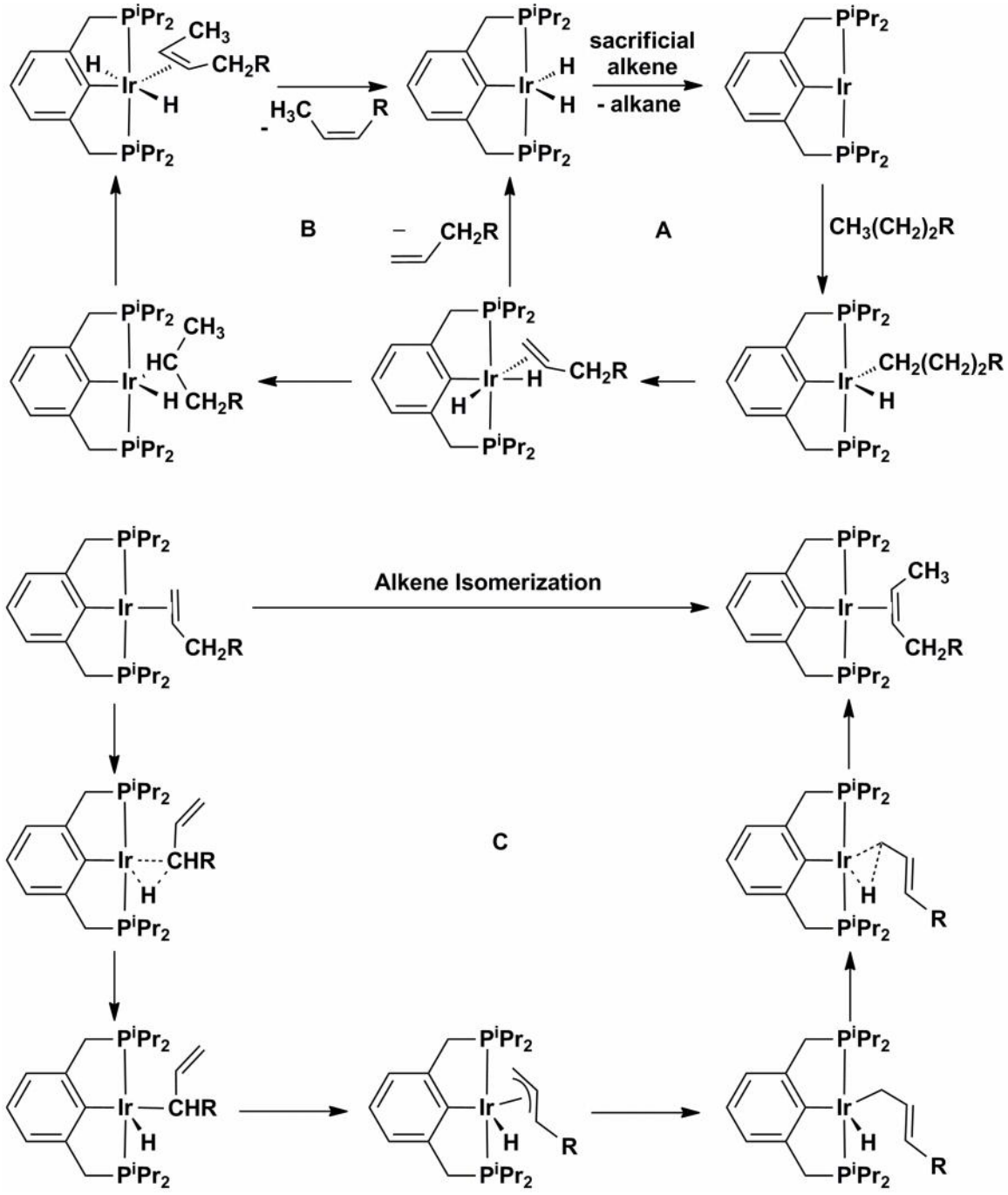

Scheme 1-3. Proposed mechanism for **(A)** [^{i}Pr-PCP]Ir-mediated linear alkane dehydrogenation, **(B)** traditional isomerization of α-olefins to internal olefins and **(C)** π-Allyl pathway for isomerization of α-olefins

To improve on the isomer distribution of the alkene products, the catalytic system was modified such that the sacrificial alkene acting as the hydrogen acceptor was switched from TBE to either norbornene or 1-decene. This modification was found to affect the observed distribution of alkene isomers and it was proposed that the isomer distribution was determined by the competition between the sacrificial alkene and product terminal alkene for insertion into the Ir-H bond of [^{i}Pr-PCP]Ir(H)$_2$. Thus, in the reaction of *n*-octane with [^{i}Pr-PCP]Ir(H)$_2$, when 1-decene was used as the hydrogen acceptor, after 111 turnovers in 90 minutes, an 80% yield of 1-octene was found.[29] Extended reaction times caused the distribution of alkene products to gradually shift to the thermodynamically preferred internal alkenes.

1.4.4 Acceptorless Catalytic Alkane Dehydrogenation by a (PCP)Ir Complex

For the catalytic dehydrogenation of alkanes to be feasible on an industrial scale, a system that does not require a sacrificial hydrogen acceptor is desired. Once again an Ir PCP-type pincer complex was found to be an efficient catalyst for acceptorless alkane dehydrogenation. Initial studies by Jensen, Goldman and co-workers used the [^{t}Bu-PCP]Ir(H)$_2$ precatalyst to attempt acceptorless alkane dehydrogenation.[31] Due to the high thermal stability of the pincer complex, the precatalyst was refluxed in a high boiling alkane solvent, such as cyclodecane. Heating the reaction mixture to 201 ºC led to cyclodecene formation concurrent with H_2 liberation, which was removed from the reaction mixture by a purge of Ar. After 24 hours, 360 turnovers were observed. Although elevated temperatures were used, the pincer system showed high thermal stability enabling the acceptorless dehydrogenation of alkanes.

A much more efficient acceptorless catalytic alkane dehydrogenation system was developed by Goldman and coworkers using the less sterically demanding ^{i}Pr derivative [^{i}Pr-PCP]Ir(H)$_2$.[32] Remarkably, the dehydrogenation of cyclooctane (in refluxing cyclooctane) occurred at a rate of > 94 turnovers h^{-1} (compared to the 11 turnovers h^{-1}

observed with the ^{t}Bu derivative) and the dehydrogenation of cyclodecane (in refluxing cyclooctane) occurred at a rate of 460 turnovers h^{-1}. In addition, the [^{i}Pr-PCP]Ir(H)$_2$ precatalyst was also able to catalyze the acceptorless dehydrogenation of linear alkanes, though the efficiency was much more limited than that of cycloalkanes.

Despite the remarkable thermal stability of these Ir pincer complexes, decomposition can still occur after prolonged reaction times at the increased temperatures required to overcome the high enthalpic barrier associated with acceptorless alkane dehydrogenation. As a result, Goldman and coworkers modified the [^{i}Pr-PCP]Ir(H)$_2$ catalyst by changing the ^{i}Pr substituents on phosphorus to adamantyl groups with hopes of yielding a more thermally robust catalyst without sacrificing catalytic activity.[33] It was anticipated that the cage structure of the adamantyl groups might be more resistant to cyclometallation and P–C bond cleavage, which are potential decomposition pathways. Indeed, [Ad-PCP]Ir(H)$_2$ was found to be more thermally robust at higher temperatures (250 ºC) and had greater total turnover numbers for the dehydrogenation of both cycloalkanes and linear alkanes, despite slightly lower initial turnover frequencies than the [^{t}Bu-PCP]Ir and [^{i}Pr-PCP]Ir systems.

Experimental and computational studies support a mechanism for acceptorless alkane dehydrogenation that involves H_2 reductive elimination as the rate determining step to generate a (PCP)Ir^{I} intermediate that subsequently undergoes C-H bond activation of the substrate alkane (Scheme 1-4).[34]

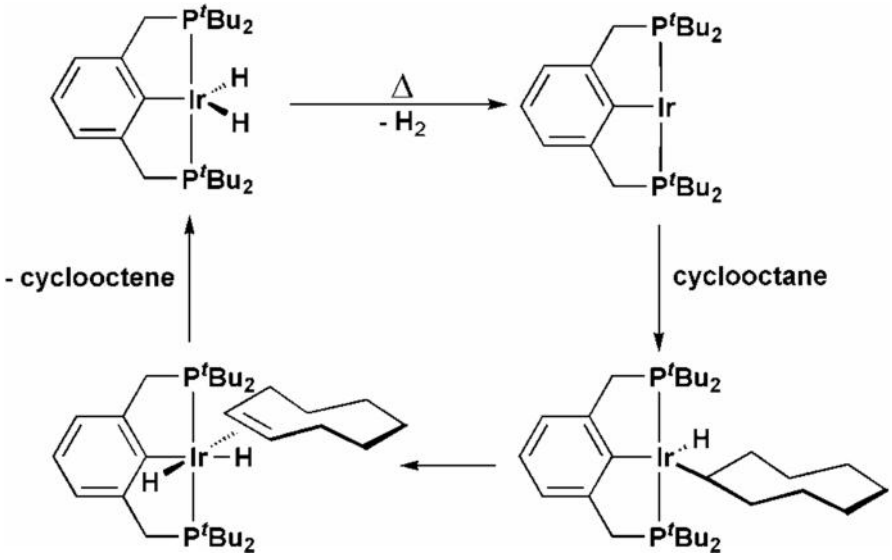

Scheme 1-4. Proposed mechanism for catalytic alkane dehydrogenation without a hydrogen acceptor

1.4.5 Highly Active Bis(phosphinite) Ir Complexes for the Catalytic Transfer Dehydrogenation of Alkanes

Until 2004, the Goldman/Jensen [R-PCP]Ir(H)$_2$ precatalyst (described in the previous sections) was the benchmark for alkane transfer dehydrogenation both in the presence and absence of a hydrogen acceptor.[24, 26-34] Subsequent work conducted by the Brookhart group on the synthesis of new Ir bis(phosphinite) PCP complexes of the form [C$_6$H$_3$-2,6-(OP(^{t}Bu)$_2$)$_2$]Ir(H)Cl ([POCOP]Ir(H)Cl; Figure 1-6) expanded the utility of PCP-type pincer complexes as alkane dehydrogenation catalysts.[35]

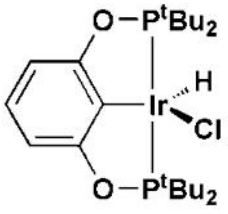

[POCOP]Ir(H)(Cl)

Figure 1-6. [POCOP]Ir(H)Cl pincer complex developed by Brookhart and co-workers for catalytic alkane dehydrogenation

The rationale behind the synthesis of such bis(phosphinite) complexes was that there may be an advantage to using a more electron withdrawing pincer ligand to generate a somewhat electron deficient Ir center, which could bind alkenes less strongly thereby leading to increased turnover in alkane dehydrogenation. Indeed, it was found that these bis(phosphinite) pincer species exhibited unprecedented TOFs in alkane dehydrogenation and were less susceptible to TBE and product inhibition than the previously described [R-PCP]Ir analogues.

In situ reactions were conducted to generate the coordinatively unsaturated [POCOP]Ir^{I} intermediate analogous to the highly reactive [PCP]Ir^{I} species observed by Goldman, Jensen and coworkers. Treatment of [POCOP]Ir(H)Cl with NaO^{t}Bu proved to be an efficient means of generating [POCOP]Ir^{I} upon loss of HO^{t}Bu and NaCl.[35] Combining this unsaturated species with the alkane substrate and TBE as a hydrogen acceptor led to efficient dehydrogenation, with TONs ranging from 1480-2070 (depending on the alkane used) and TOFs of up to 2.4 s^{-1} at 200 ºC. When the Goldman and Jensen [PCP]$Ir(H)_2$ precatalyst was utilized under the same reaction conditions, TONs of about 230 were obtained, exemplifying the enhanced activity of the bis(phosphinite) Ir catalysts.[35]

To further investigate the nature of the catalytically active species, [POCOP]Ir(H)Cl was reacted with NaO^{t}Bu in neat COA in the absence of TBE. Two new products were observed in this reaction and these were identified as [POCOP]$Ir(H)_2$ and [POCOP]Ir(COE) by ^{31}P and ^{1}H NMR spectroscopy.[35] The formation of these products was rationalized by initial dehydrochlorination of [POCOP]Ir(H)Cl to generate the 14-electron fragment [POCOP]Ir^{I}, which undergoes oxidative addition of a C-H bond of COA followed by β-hydride elimination to generate [POCOP]$Ir(H)_2$ and one equiv of COE. The liberated COE could then be trapped by another [POCOP]Ir^{I} fragment to yield [POCOP]Ir(COE) (Scheme 1-5).

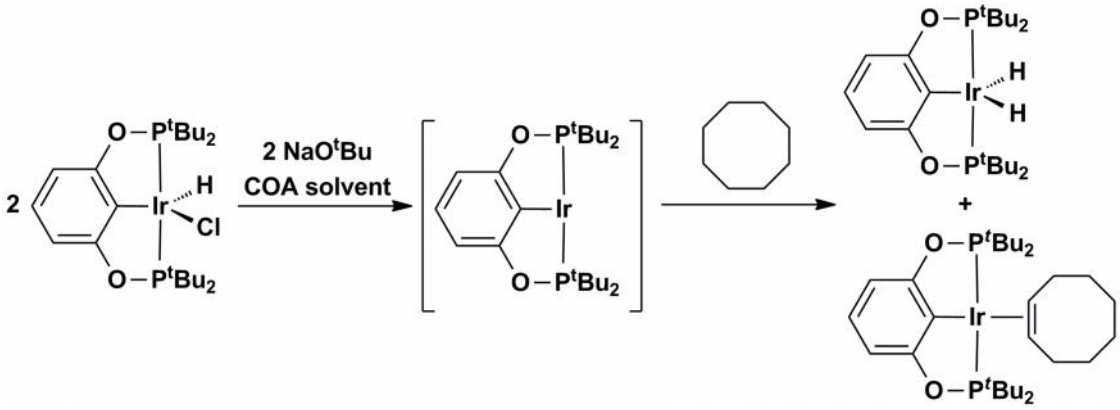

Scheme 1-5. Generation of $[POCOP]Ir(H)_2$ and [POCOP]Ir(COE) by dehydrochlorination of [POCOP]Ir(H)Cl in neat COA

A comparison of the bisphosphinite [POCOP]Ir system to the Goldman/Jensen [PCP]Ir catalyst showed several important differences.[35b] While the Goldman/Jensen electron rich $[PCP]Ir^{I}$ intermediate was capable of oxidatively adding an sp^2-CH bond in TBE through oxidative addition leading to strong catalyst inhibition, Brookhart's $[POCOP]Ir^{I}$ intermediate simply coordinates the olefin through the π-bond (Figure 1-7). Although it was originally postulated that these differences in reactivity were due to the less electron rich nature of the metal center in the [POCOP]Ir system (due to the presence of the electronegative oxygen atoms in the ligand backbone), it was later found that sterics, not electronics, affect the reactivity to a greater extent.[36] According to recent DFT calculations, the [PCP]Ir metal center is much more sterically hindered than that in [POCOP]Ir. These results were supported experimentally by comparing the crystallographically characterized complexes [^{t}Bu-POCOP]Ir(CO) and [^{t}Bu-PCP]Ir(CO), which feature P–Ir–P bond angles of 157.55(3) and 164.510(8), respectively, where the smaller angle in the (POCOP)Ir complex indicated a more open geometry about the metal center.[37] Thus due to the differences in sterics between the two catalytically active species, the rate determining step for alkane dehydrogenation by $[POCOP]Ir^{I}$ is olefin coordination, rather than reductive elimination of TBA, as was observed for the more hindered [PCP]Ir system.[35,36]

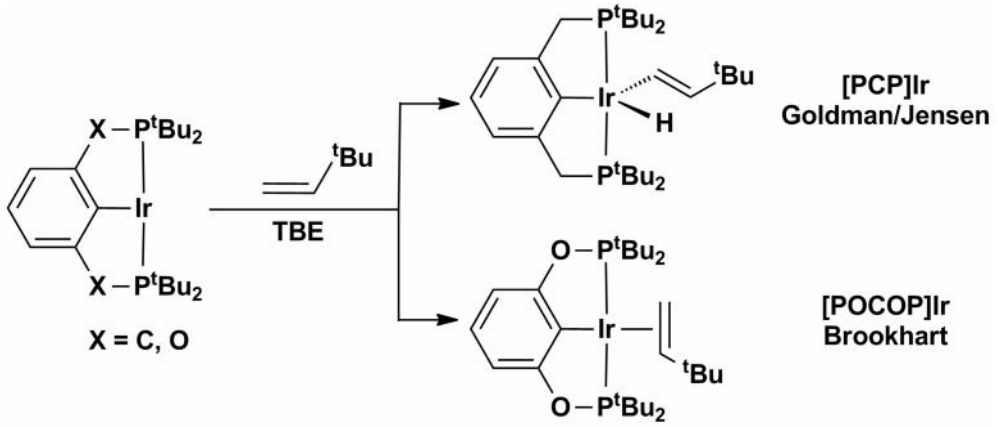

Figure 1-7. Comparison of the interaction of 14-electron $[PCP]Ir^{I}$ and $[POCOP]Ir^{I}$ fragments with olefins

1.5 (PCP)Ir-Catalyzed N-H Bond Oxidative Addition Chemistry

1.5.1 Generation of (PCP)Ir(NH_2)(H) from Activation of the N-H Bonds of Ammonia

The noteworthy reactivity of PCP pincer complexes has not been limited to C-H bond activation and functionalization. Another significant feature of these pincer systems is the ability to mediate other E-H bond oxidative addition reactions, most notably the cleavage of N-H bonds.

Due to the tremendous utility of platinum-group metal complexes in E-H bond cleavage chemistry and catalysis, there is significant interest in developing such late transition complexes that can insert into the N-H bonds of ammonia and other simple amines and anilines through oxidative addition, with the goal of developing mild and selective catalytic amination reactions. However, there have been relatively few well-documented examples of N-H bond oxidative addition of amines to date, and only a handful of examples that involve ammonia activation.[38] This scarcity may be attributed to the inherent ability of NH_3 to form stable Werner-type coordination complexes that do not react further to achieve N-H bond cleavage. As a result, prior to the work described in this thesis, only one example of an isolable, monomeric late metal $L_nM(H)(NH_2)$ species obtained from N-H bond oxidative addition of ammonia had been reported. This

ground breaking initial work was reported by Zhao, Goldman, and Hartwig, who used a (PCP)Ir pincer complex to achieve ammonia activation.[38a]

Initial investigations into N-H bond cleavage by PCP-type pincer complexes began with a study of the reactivity of [^{t}Bu-PCP]Ir(H)$_2$ with aniline as well as ammonia.[39] The reaction of [^{t}Bu-PCP]Ir(H)$_2$ with a hydrogen acceptor such as TBE or norbornene was used to generate the highly reactive, coordinatively and electronically unsaturated [^{t}Bu-PCP]Ir^I intermediate, which was reacted in situ with an amine (Scheme 1-6). When aniline was used as the amine, N-H bond oxidative addition occurred to form the desired anilido hydride complex [^{t}Bu-PCP]Ir(H)(NHPh).[39] However, divergent reactivity was observed with ammonia, which rather than undergo oxidative addition formed the Ir^I ammonia adduct [^{t}Bu-PCP]Ir(NH$_3$) (Scheme 1-6). In order to further probe this reactivity, the parent amido hydride Ir^{III} complex [^{t}Bu-PCP]Ir(NH$_2$)(H) was synthesized via addition of NH$_3$ to [^{t}Bu-PCP]Ir(H)(Cl), followed by reaction with KN(SiMe$_3$)$_2$ at low temperatures to dehydrochlorinate the intermediate complex [^{t}Bu-PCP)Ir(H)(Cl)(NH$_3$).[39] This reaction sequence produced the desired amido hydride complex [^{t}Bu-PCP]Ir(NH$_2$)(H), which upon warming to room temperature, reductively eliminated NH$_3$ to form [^{t}Bu-PCP]Ir(NH$_3$). This was the first indication that oxidative addition of NH$_3$ was viable, but the resulting amido hydride Ir complex was likely less thermodynamically stable than the Ir^I ammonia adduct.

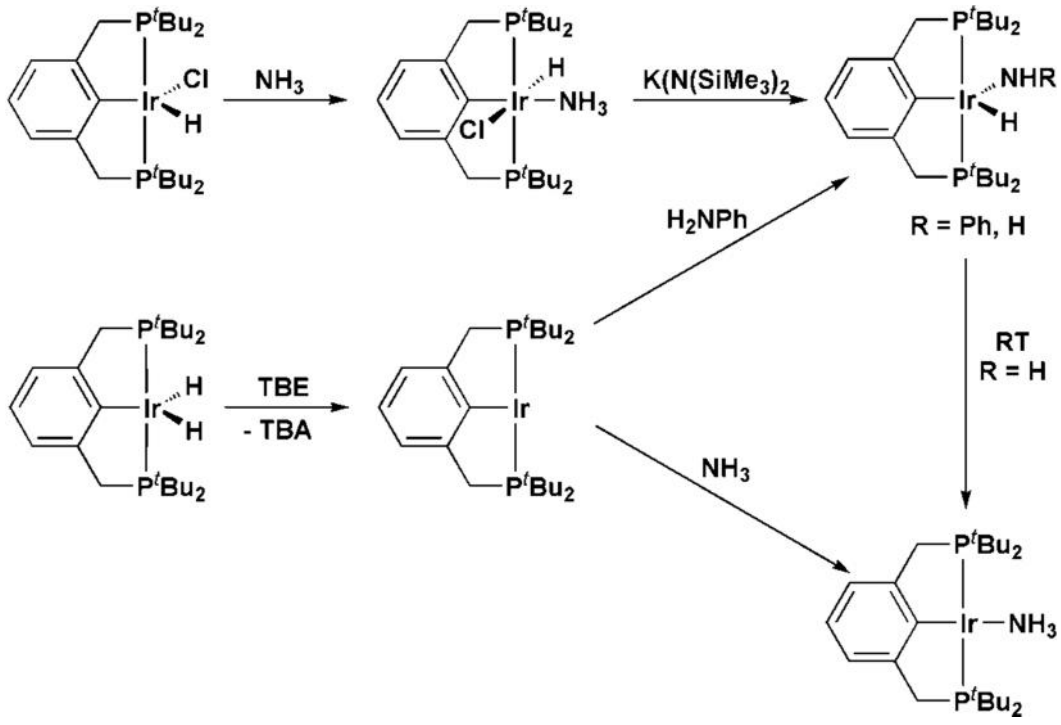

Scheme 1-6. Generation of [^{t}Bu-PCP]Ir(H)(NHR) species through N-H activation

The thermodynamic instability of [^{t}Bu-PCP]Ir(H)(NH$_2$) limited the utility of this complex for further study into the details of N-H bond oxidative addition and the potential functionalization of ammonia. Goldman, Hartwig and coworkers sought to form a more stable monomeric amido hydride complex through modification of the pincer ligand. It was proposed that increasing the electron donating ability of the pincer ligand might render the Ir^{III} oxidation state more favourable, thereby allowing for the isolation of the N-H bond oxidative addition product. Towards this end, the introduction of an aliphatic pincer ligand backbone enabled the formation of an isolable Ir^{III} amido hydride complex (Scheme 1-7).[38a]

Treatment of the polyhydride complex [(^{t}Bu$_2$P(CH$_2$)$_2$)$_2$CH]Ir(H)$_4$ with excess propene or 1-pentene dehydrogenated the pincer complex and generated the corresponding Ir^I alkene complex (Scheme 1-7). The alkene complex, in turn, reacted with an excess (four equiv) of ammonia at room temperature to generate the Ir^{III} amido hydride species [(^{t}Bu$_2$P(CH$_2$)$_2$)$_2$CH]Ir(H)(NH$_2$) upon liberation of the alkene (Scheme 1-

17).[46a] Unlike the previously studied [^{t}Bu-PCP]Ir system, [(^{t}Bu$_2$P(CH$_2$)$_2$)$_2$CH]Ir(H)(NH$_2$) was isolated and crystallographically characterized.[38a]

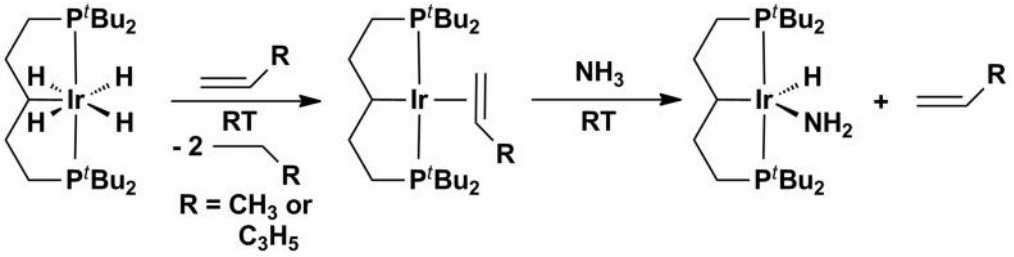

Scheme 1-7. Formation of a monomeric Ir^{III} amido hydride complex via ammonia N-H bond activation

To investigate the thermodynamics of the ammonia N-H bond oxidative addition reaction, Hartwig and co-workers sought to determine the stability of the amido hydride complex relative to the corresponding Ir^I alkene complex [(^{t}Bu$_2$P(CH$_2$)$_2$)$_2$CH]Ir(1-pentene).[38a] Upon combining ammonia, 1-pentene, and [(^{t}Bu$_2$P(CH$_2$)$_2$)$_2$CH]Ir(1-pentene) (0.03 M in diethyl ether-d_{10}) in a 15:30:1 ratio, the resulting equilibrium distribution was a 3.9:1 ratio of the amido hydride Ir^{III} complex to the Ir^I pentene complex and a 1:2.3 ratio of dissolved ammonia to pentene. Addition of the same ratio of ammonia and pentene to a 0.03 M solution of the amido hydride complex led to the same ratio of the amido hydride Ir^{III} complex to the Ir^I pentene complex. These experiments yielded an equilibrium constant of 9 for the conversion of the alkene complex to the amido hydride species. By comparison, the reaction of the alkene complex with H$_2$N(3,5-Me$_2$C$_6$H$_3$) revealed that the formation of the hydrido arylamide oxidative addition product was thermodynamically less favorable than the analogous reaction with ammonia, with an equilibrium constant of 0.09. This result is somewhat surprising given the N-H bond strength and greater acidity of the aromatic amine.

Mechanistic studies of ammonia N-H bond cleavage by [(^{t}Bu$_2$P(CH$_2$)$_2$)$_2$CH]Ir(1-pentene) were also conducted.[38a] Isotopic labelling studies using ND$_3$ were consistent

with a mechanism involving oxidative addition of ammonia to a [(^{t}Bu$_2$P(CH$_2$)$_2$)$_2$CH]Ir^I intermediate, as deuterium incorporation was only observed at the Ir-*H* and Ir-N*H*$_2$ positions; these observations preclude a possible mechanism involving N-H addition across the Ir-C bond of a cyclometalated Ir^{III} intermediate. Kinetic studies were also conducted to further distinguish between an associative pathway for N-H bond cleavage, in which ammonia coordinates to [(^{t}Bu$_2$P(CH$_2$)$_2$)$_2$CH]Ir(1-pentene), versus a dissociative pathway, in which the alkene first dissociates from the Ir center to generate a three-coordinate [(^{t}Bu$_2$P(CH$_2$)$_2$)$_2$CH]Ir species that subsequently reacts with ammonia. The rate of the reaction was found to be dependent on the concentration of alkene, which is consistent with the dissociative mechanism.

1.5.2 N-H Bond Activation of Hydrazines via (PCP)Ir Complexes

The study of N-H bond oxidative addition of ammonia can be plagued by reductive elimination chemistry, preventing thorough investigation into the nature of the bond cleavage chemistry (*vide supra*). As an alternative, organic substrates designated as ammonia equivalents can be utilized to better understand N-H bond cleavage chemistry. Hartwig and coworkers have recently reported on the synthesis of hydrazido hydride complexes formed by the N-H bond oxidative addition of hydrazine derivatives to both aromatic (PCP)Ir^I and aliphatic (PCP)Ir^I complexes.[40] Initial studies revealed that the addition of 1.1 equiv. of benzophenone hydrazone (NH_2NCPh_2) to both [^{t}Bu-PCP]Ir(H)Ph or [(^{t}Bu$_2$P(CH$_2$)$_2$)$_2$CH]Ir(1-pentene) lead to the formation of stable hydrazido hydride products of the type [^{t}Bu-PCP]Ir(H)($NHNPh_2$) and [(^{t}Bu$_2$P(CH$_2$)$_2$)$_2$CH]Ir(H)($NHNPh_2$) after 5 min at room temperature. These products were proposed to form via N-H bond activation of NH_2NCPh_2 by [^{t}Bu-PCP]Ir^I or [(^{t}Bu$_2$P(CH$_2$)$_2$)$_2$CH]Ir^I after loss of benzene or 1-pentene, respectively (Scheme 1-8). The resulting hydrazido hydride products were not susceptible to reductive elimination, even in the presence of excess (10 equiv) benzene or 1-pentene.[40]

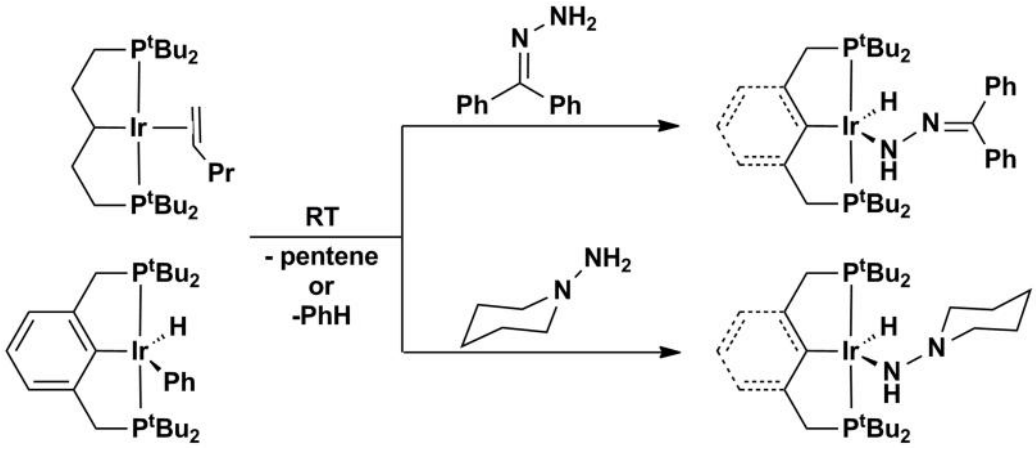

Scheme 1-8. Synthesis of (PCP)Ir hydrazido hydride complexes via N-H bond activation

N-H bond oxidative addition of 1-aminopiperidine ($NH_2NC_5H_{10}$) was also mediated by [^{t}Bu-PCP]Ir^I and [(^{t}Bu$_2$P(CH$_2$)$_2$)$_2$CH]Ir^I to form either [^{t}Bu-PCP]Ir(H)($NHNC_5H_{10}$) or [(^{t}Bu$_2$P(CH$_2$)$_2$)$_2$CH]Ir(H)(NC_5H_{10}), respectively (Scheme 1-8). Although the latter complex was stable at room temperature for days, a second N-H bond activation was observed for [^{t}Bu-PCP]Ir(H)($NHNC_5H_{10}$) upon mild heating to give a rare example of an Ir aminonitrene complex, [^{t}Bu-PCP]Ir($N{=}NC_5H_{10}$) and H_2 (Scheme 1-9). The nature of the aminonitrene Ir–N bond was examined with DFT calculations and the results showed that the primary Ir–N interaction involves donation from the lone pair on N to the metal center, with little backbonding from the metal.

The reactivity of $MePhNNH_2$ and Me_2NNH_2 was also explored. The reaction of [^{t}Bu-PCP]Ir^I with either $MePhNNH_2$ or Me_2NNH_2 provided two products, [^{t}Bu-PCP]Ir(N=NRR') (R = Ph, R' = Me; or R = R' = Me) and [^{t}Bu-PCP]Ir(H)$_2$(C≡NR) (R = Ph, Me). The aminonitrene product resulted from double N–H bond activation of the hydrazine derivative, while the isocyanide product likely formed by an initial C–H bond oxidative addition of an N-*Me* group followed by N–N bond cleavage via β-NH_2 elimination, and subsequent C–H bond activation of the resulting imine before deinsertion of the isocyanide group (Scheme 1-9).

The hydrazine N-H bond cleavage chemistry detailed by Hartwig and co-workers is a rare example of N-H bond oxidative addition and represents an important step towards understanding such reactions involving electron rich late metal centers. This work lays the foundation for the development of catalytic chemistry that parallels existing E-H addition reactions such as hydrogenation, hydroboration, and hydrosilylation.

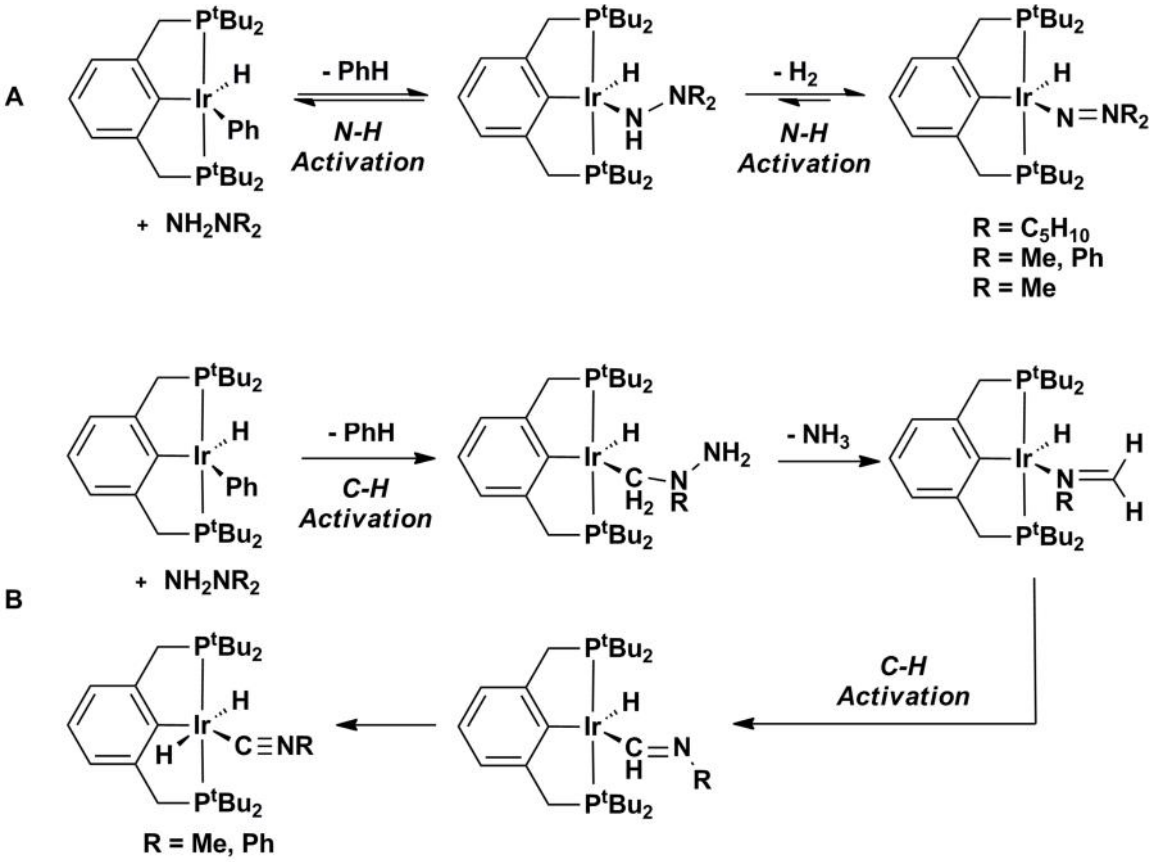

Scheme 1-9. Generation of (**A**) aminonitrene and (**B**) isocyanide (PCP)Ir complexes

1.5.3 Investigations into N-H Bond Activation by Bis(phosphinite) Ir Pincer Complexes

Having examined the reactivity of electron-deficient bis(phosphinite) [POCOP]Ir pincer complexes with C-H bonds (*vide supra*), Brookhart and co-workers also sought to extend their reactivity studies to the activation of the N-H bonds.[41] Previous work had shown that the reaction of [POCOP]Ir(H)Cl with NaO^{t}Bu leads to the

generation of a highly reactive [POCOP]Ir^{I} intermediate, which exhibited aggressive reactivity with alkane C-H bonds.[35] This same intermediate was also found to react with the N-H bonds of anilines and benzamides. Treatment of [POCOP]Ir^{I} with a variety of anilines in benzene solution at room temperature produced three products in equilibrium – [POCOP]Ir(H)(Ph), [POCOP]Ir(H)(NHAr) and the Lewis base adduct [POCOP]Ir(NH_2Ar) (Scheme 1-10; Ar = *p*-X-C_6H_3; X = OMe, Me, H, Cl, or CF_3).[41] This product mixture indicates that C-H bond activation of the benzene solvent is competitive with N-H bond activation. Thus, [POCOP]Ir(H)(Ph) was formed by the reaction of [POCOP]Ir^{I} with benzene, while [POCOP]Ir(H)(NHAr) and [POCOP]Ir(NH_2Ar) result from the interaction of [POCOP]Ir^{I} with aniline (Scheme 1-10). Equilibrium constants connecting these three species were measured and were found to be dependent on the nature of the *para*-substituent on the aniline. As expected, as the basicity of the aniline increased with more electron donating *para*-substituents, the Lewis base complex [POCOP]Ir(NH_2Ar) was found to dominate the product distribution. However, as the para-substituent was replaced with more electron withdrawing groups, the basicity of the aniline decreased and the aniline oxidative addition product [POCOP]Ir(H)(NHAr) was observed as the major product. Brookhart and co-workers propose that the latter effect is due to decreased repulsion between filled metal d_π–orbitals and N p-orbitals. The rates of reductive elimination from [POCOP]Ir(H)(NHAr) were measured by heating the Ir^{III} complexes in the presence of ethylene as a trapping ligand, to form the Ir^{I} ethylene adduct [POCOP]Ir(C_2H_4). The reductive elimination barriers fall in the range of 21-22 kcal/mol and increased with the electron-withdrawing ability of the anilines employed. By comparison, the barrier of C-H bond reductive elimination from [POCOP]Ir(H)(Ar) (Ar = 3,5-$Me_2C_6H_3$) was determined to be 14.1 kcal/mol.

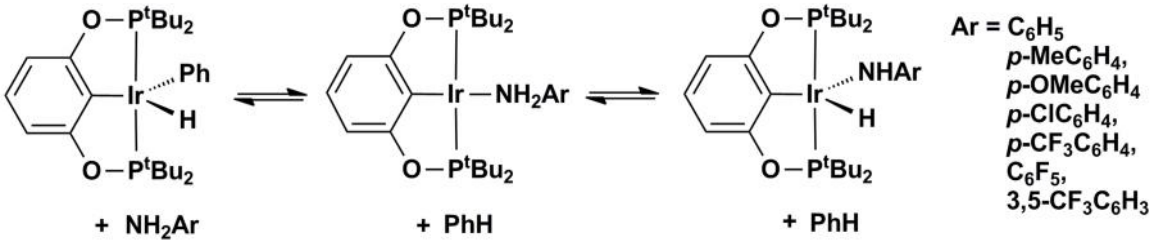

Scheme 1-10. Equilibria between products resulting from the reaction of [POCOP]Ir^{I} with anilines in benzene solution

Related N-H bond activation studies with benzamides yielded quantitatively the Ir^{III} oxidative addition products [POCOP]Ir(H)(NHC(O)Ar).[41] X-ray analysis of the isolated amido hydride products indicated significant interaction between the carbonyl O and the Ir center. The barrier to reductive elimination from the benzamide complexes was determined to be substantially higher than for the related anilido complexes, and the increased binding energy of the benzamide group to Ir was ascribed to the presence of stabilizing Ir-O interactions as well as to a decrease in the repulsive d_{π}-p interaction due the strong electron withdrawing ability of the benzamide group.

The work of Brookhart and co-workers represents one of the few detailed mechanistic studies of N-H bond activation at a late metal center. It is anticipated that further mechanistic understanding of such reactivity, along with the further development of new complexes that can undergo N-H bond cleavage reactions will enable the development of catalytic cycles that incorporate N-H bond activation steps to achieve useful organic transformations. In particular, the functionalization of ammonia is a highly desirable target.

1.5.4. N–H Bond Activation via Metal Ligand Cooperation

The N–H bond activation chemistry described thus far has involved formal oxidative addition in order to achieve cleavage of the N–H bond. However, another possible route that has recently emerged in the literature for the activation of difficult to cleave E–H bonds (E = main group element; H, B, C, N, O, etc.) involves metal ligand

cooperativity where no change in formal oxidation state of the metal occurs. This bond cleavage mechanism features aromatization–dearomatization of the pincer ligand backbone mediated by proton transfer from the substrate to the dearomatized ligand, leading to net E–H bond cleavage in concert with aromatization of the pincer ligand (Scheme 1-11).

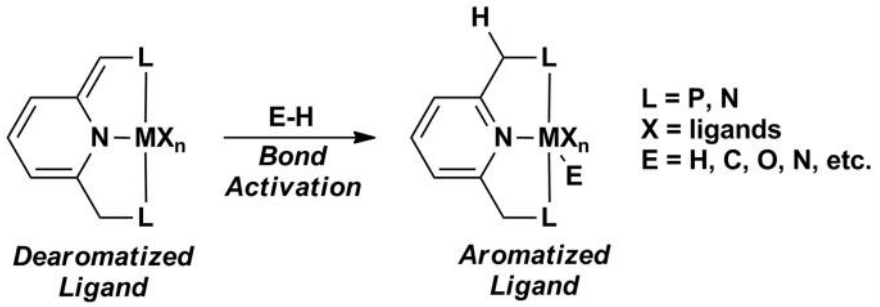

Scheme 1-11. General mode of bond activation through metal ligand cooperativity

Milstein and co-workers have developed a novel class of pyridine based ^{R}PNP and ^{R}PNN (^{R}PNP = 2,6-$(CH_2\text{-}PR_2)_2C_5H_3N$; ^{R}PNN = 2-$(CH_2\text{-}PR_2)$-6-$(CH_2\text{-}NEt_2)C_5H_3N$; R = ^{t}Bu, ^{i}Pr) pincer complexes that have shown tremendous utility in bond activation and catalysis through metal ligand cooperation by aromatization–dearomatization[42] (Scheme 1-11). The reaction of [^{tBu}PNP*]Ru(H)(CO) (* designates dearomatized version of the ligand) with electron poor anilines, such as 4-nitroaniline and 2-chloro-4-nitroaniline, at room temperature lead to N–H bond activation where the proton was transferred to the unsaturated ligand arm and aromatization of the central pyridine ring occurred (Scheme 1-12). Reaction of [^{tBu}PNP*]Ru(H)(CO) with halo anilines resulted in equilibria of the starting complex with the N–H activation product, suggesting reversibility of the N–H bond cleavage process at room temperature (Scheme 1-12).[43a]

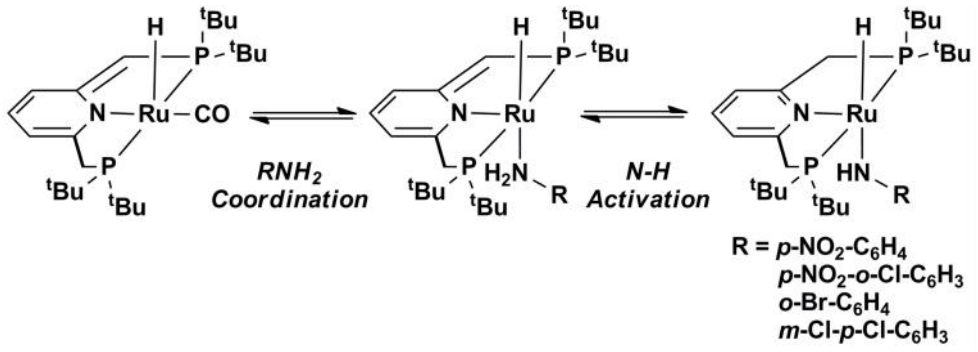

Scheme 1-12. Aniline N-H bond activation via metal-ligand cooperativity

More electron rich amines such as H_2NPh, NH_3 and H_2N^iPr appeared to either form the corresponding amine complexes [^{tBu}PNP*]Ru(H)(NH_2R), or did not react at all at room temperature. Although these electron rich amines did not appear to undergo N–H bond cleavage, mechanistic studies showed that N-H bond activation of such substrates is kinetically accessible. Treatment of a benzene-d_6 solution of [^{tBu}PNP*]Ru(H)(CO) with ND_3 led to the selectively deuterated product [^{tBu}PNP*]Ru(H)(ND_3), where one of the two methylene CH_2 arm signals has also been deuterated, as indicated by its disappearance in the ^{1}H NMR spectrum of the complex. No exchange was noted between the methylene C-*H* and C-*D*, indicating that the activation process likely occurred in an intramolecular manner on one face of the ligand. This was the first report of reversible N–H bond activation of ammonia via metal-ligand cooperativity.[43a]

Furthermore, heating of [^{tBu}PNP*]Ru(H)(CO) with 5 equivalents of H_2N^iPr in a sealed J. Young tube for one week at 80 ºC generated a 1:1 mixture of a *trans*-dihydride complex [^{tBu}PNP*]Ru($H)_2$(CO) and [^{tBu}PNP*]Ru(H)(CO). It was proposed that the dihydride product likely formed after an initial N–H activation of H_2N^iPr, followed by H_2 elimination to produce [^{tBu}PNP*]Ru(NH^iPr)(CO). Subsequent β-hydride elimination, followed by H_2 addition could provide the *trans*-dihydride product observed (Scheme 1-13). DFT calculations supported this proposal, as barriers between the H_2N^iPr adduct and the corresponding Ru amido complex were between 10 – 20 kcal/mol and therefore accessible at room temperature.[43a]

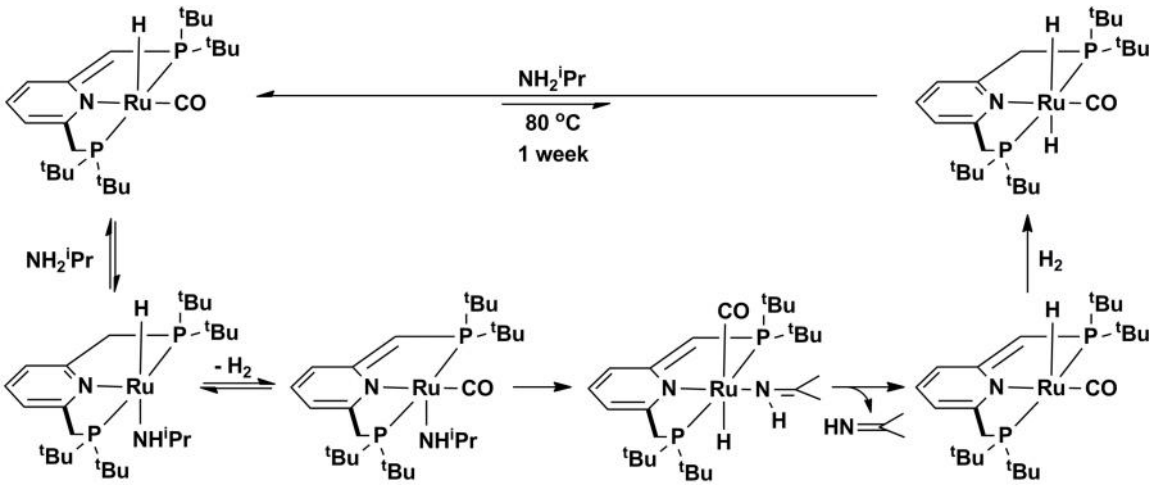

Scheme 1-13. Potential pathway for N-H bond activation of $NH_2{}^iPr$ by [^{tBu}PNP*]Ru

Activation of the N–H bonds of anilines by dearomatized ^{tBu}PNN and ^{iPr}PNP Rh complexes was also recently reported.[43b] The reaction of [^{tBu}PNN*]Rh(L') (L' = N_2, C_2H_4) and [^{iPr}PNP*]Rh(L') (L' = C_2H_4, COE) with various anilines at 60 ºC yielded stable Rh anilido products of the type [^{R}PNL]Rh(NHAr) (^{R}PNL = ^{tBu}PNN, ^{iPr}PNP; Ar = C_6H_5, *o*-Br-C_6H_4, *m*-Cl-*p*-Cl-C_6H_3, *p*-NO_2-C_6H_4) via a similar pathway to that documented for [^{tBu}PNP*]Ru (Scheme 1-12). Upon reaction of the anilido complexes with CO or PEt_3, the N–H bond reformed, to eliminate free aniline and the respective dearomatized complex [^{R}PNL*]Rh(L') (L' = CO, PEt_3), which highlights the reversible nature of the N–H bond cleavage process in this system.

In agreement with the trends in reactivity observed in the [^{tBu}PNP*]Ru system, N–H activation was faster with electron poor anilines (i.e. *p*-nitroaniline) compared to the more electron rich anilines.[43] This same trend was also observed by Brookhart and coworkers (*vide supra*) in the oxidative addition of the N–H bond of various anilines with [POCOP]Ir.[41]

Although the mechanism for N-H bond cleavage involving ^{R}PNP- and ^{R}PNN-ligated Ru and Rh complexes differs from the oxidative addition route for bond cleavage involving (PCP)Ir and (POCOP)Ir, this work highlights the challenges associated with N-H bond cleavage of a variety of amines. Notably, this work showed a rare indirect

example of N-H bond cleavage involving an alkyl amine. No other examples late metal mediated N-H bond cleavage in alkyl amines have been reported in the literature thus far. Therefore, the pursuit of new transition metal complexes that are capable of N-H bond cleavage in alkyl amines remains an active area of investigation.

1.6. Cationic Bis(phosphinite) Ir^{III} Pincer Complexes in Stoichiometric and Catalytic Bond Functionalization

Iridium bis(phosphinite) pincer complexes have shown effectiveness in alkane dehydrogenation chemistry and N–H bond activation (*vide supra*). Treatment of [POCOP]Ir(H)Cl with NaO^{t}Bu proved to be an efficient means of generating [POCOP]Ir^I, the active species in this type of bond cleavage chemistry. Alternatively, Brookhart and co-workers have demonstrated that the cationic Ir^{III} bis(phosphinite) pincer complex $\{[POCOP]Ir(H)(CH_2Cl_2)\}^+[BArF]^-$ (BArF = 3,5-$(CF_3)C_6H_3$) can be accessed by abstraction of the chloride ligand from [POCOP]Ir(H)Cl with NaBArF in CH_2Cl_2 (Scheme 1-14A). The resulting in situ generated solvated cationic monohydride complex has displayed intriguing bond activation activity, including the catalytic reduction of dichloromethane to methane using Et_3SiH as the reducing agent.[44a] Unfortunately catalytic studies of the in situ generated $[POCOP]Ir(H)^+$ complex produced inconsistent results and as such, alternative cationic bis(phosphinite) iridium complexes were targeted.

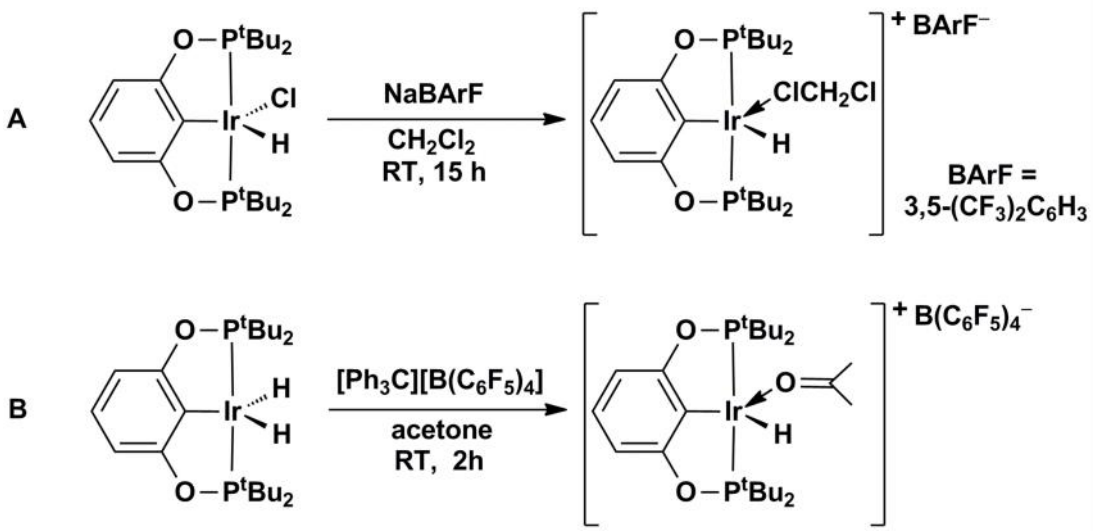

Scheme 1-14. Synthesis of cationic bis(phosphinite) iridium complexes (**A**) $\{[POCOP]Ir(H)(CH_2Cl_2)\}^+[BArF]^-$ and (**B**) $[[POCOP]Ir(H)(acetone)]^+[B(C_6F_5)_4]^-$

Towards these ends, the solvated complex $\{[POCOP]Ir(H)(acetone)\}^+[B(C_6F_5)_4]^-$ was synthesized by treatment of $[POCOP]Ir(H)_2$ with $(Ph_3C)[B(C_6F_5)_4]$ in acetone (Scheme 1-14B). Remarkably, this complex was shown to be a highly active catalyst for the reduction of alkyl chlorides, bromides, iodides, and some fluorides to alkanes utilizing Et_3SiH as the reductant.[44] The reduction of primary and secondary alkyl halides catalyzed by $[POCOP]Ir(H)(acetone)^+$ was typically executed in chlorobenzene or in neat alkyl halides at either 23 or 60 ºC. For instance, using 0.5 mol % catalyst loading and 3 equiv. Et_3SiH, 1-bromopentane was reduced to pentane after 1.5 hours at 60 ºC in greater than 99 % conversion. $[POCOP]Ir(H)(acetone)^+$ also proved to be a highly efficient catalyst for the reduction of benzyl halides. Specifically, with 0.075 mol % of $[POCOP]Ir(H)(acetone)^+$, rapid and complete reduction of benzyl bromide to toluene was observed to occur in 2.5 h.

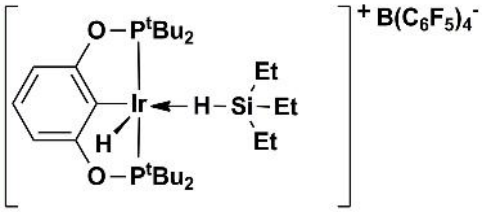

Figure 1-8. Structure of the η^1-silane complex [POCOP]Ir(H)(η^1-$HSiEt_3$)$^+$

A potential catalytic cycle involving an η^1-silane complex of the type [POCOP]Ir(H)(η^1-$HSiEt_3$)$^+$ (Figure 1-8) as an intermediate was proposed (Scheme 1-15). This electrophilic Ir silane complex, which was isolated and characterized structurally and spectroscopically, was found to possess an unprecedented binding mode of the silane to the Ir^{III} center with Et_3SiH bound in an η^1 fashion, rather than the typical η^2-SiH coordination mode where the silane is bound side on.[45] This [POCOP]Ir(H)(η^1-$HSiEt_3$)$^+$ complex was proposed to transfer Et_3Si^+ to the alkyl halide to form a silyl-substituted halonium ion, Et_3SiXR^+ (X = Cl, Br, I, F), which subsequently reacts with an equivalent of the neutral complex [POCOP]$Ir(H)_2$ to produce the reduced alkane and $XSiEt_3$ and to regenerate [POCOP]$Ir(H)^+$ (Scheme 1-15).

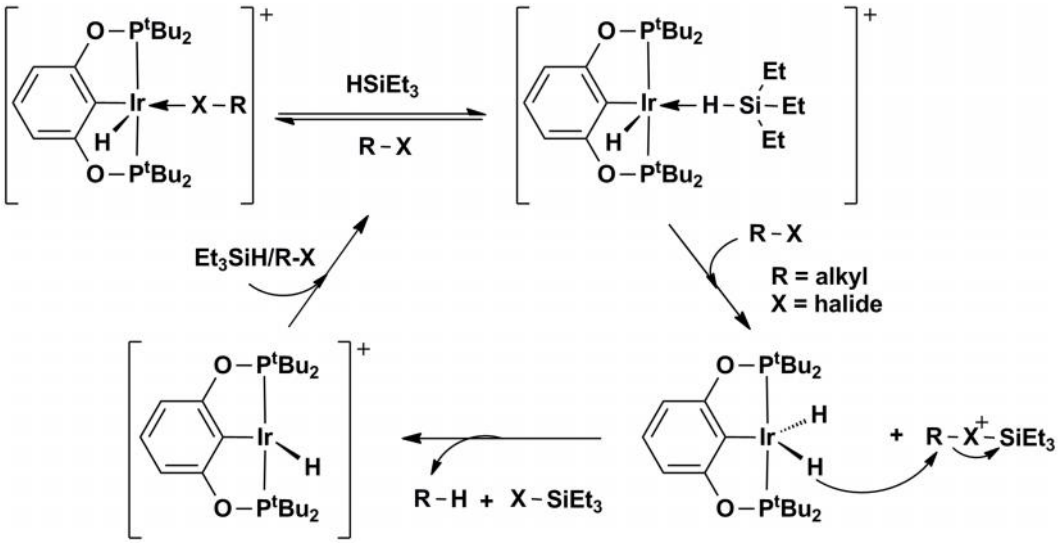

Scheme 1-15. Proposed catalytic cycle for (POCOP)Ir catalyzed reduction of alkyl halides by Et_3SiH

In an extension of this reduction chemistry, cationic Ir^{III} bis(phosphinite) complexes were also shown to catalytically cleave and reduce a variety of alkyl ethers in the presence of Et_3SiH.[46] Thus, treatment of a room temperature solution of [POCOP]Ir(H)(acetone)$^+$ (1 mol%) and Et_3SiH in dichlorobenzene with an alkyl ether produced alkyl triethylsilyl ethers and alkanes (Scheme 1-16). In some cases the newly generated triethylsilyl ether underwent a second C-O cleavage reaction to form hexaethyldisiloxane (Et_3SiOEt_3) and an additional equivalent of alkane (Scheme 1-16). This reductive cleavage chemistry was applied to a wide variety of unactivated alkyl ethers including primary, secondary, and tertiary alkyl ethers as well as aryl alkyl ethers and even poly(ethylene)glycol.

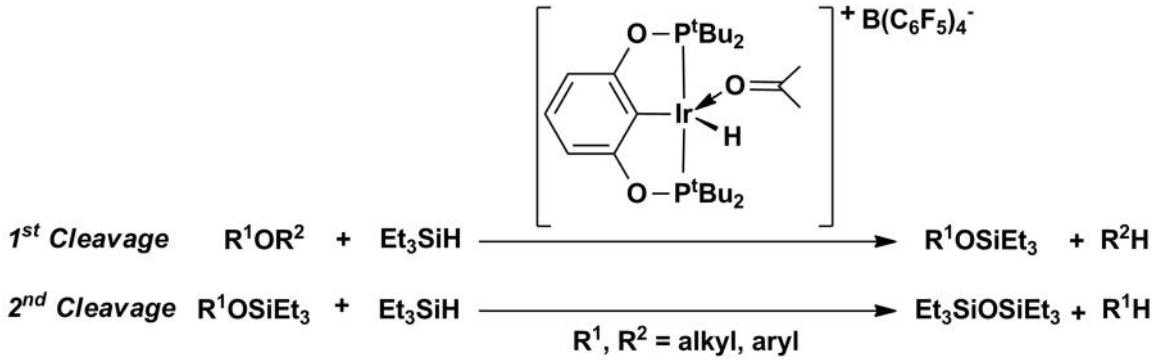

Scheme 1-16. Cleavage of aryl and alkyl ethers catalyzed by $[[POCOP]Ir(H)(acetone)]^{+}[B(C_6F_5)_4]^{-}$

The proposed catalytic cycle for ether cleavage and reduction by $[POCOP]Ir(H)(acetone)^{+}$ involves similar components as the cycle described for alkyl halide reduction (Scheme 1-15). Upon generation of $[POCOP]Ir(H)(\eta^1\text{-}HSiEt_3)^{+}$, Et_3Si^{+} is transferred to the ether (R^1OR^2 where R^1, R^2 = alkyl, aryl) to produce the corresponding oxonium ion $(R^1R^2OSiEt_3)^{+}$ and $[POCOP]Ir(H)_2$. The neutral dihydride complex then reduces $(R^1R^2OSiEt_3)^{+}$ to the corresponding alkane (R^1H or R^2H) and silyl ether (R^1OSiEt_3 or R^2OSiEt_3) products, forming the monohydride complex $[POCOP]Ir(H)^{+}$. The catalytic cycle is completed by the reaction of Et_3SiH with $[POCOP]Ir(H)^{+}$ to reform $[POCOP]Ir(H)(\eta^1\text{-}HSiEt_3)^{+}$ (Scheme 1-17).

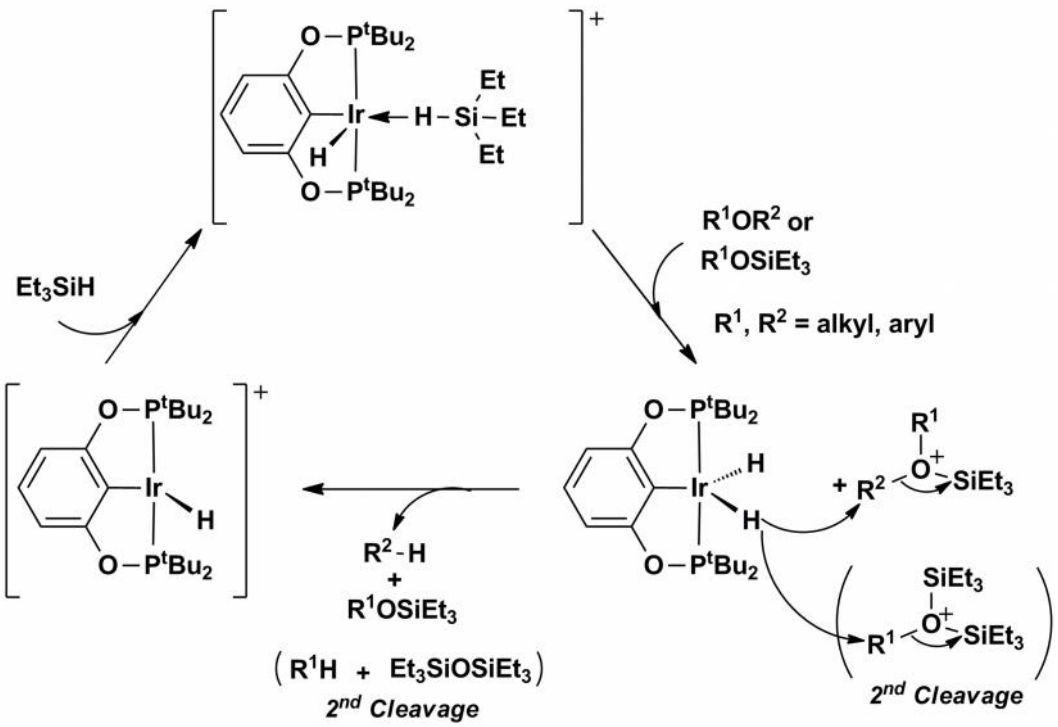

Scheme 1-17. Proposed catalytic cycle for (POCOP)Ir catalyzed ether cleavage

In the course of exploring the catalytic reduction of alkyl halides and ethers by [POCOP]Ir(H)(acetone)$^+$, the acetone hydrosilylation product $Et_3SiOCH(CH_3)_2$ was also observed. It was therefore postulated that the reduction chemistry facilitated by such cationic Ir^{III} bis(phosphinite) species could be extended to the hydrosilylation of other carbonyl compounds.[47] Indeed, the catalytic hydrosilylation of ketones, aldehydes, esters and amides by [POCOP]Ir(H)(acetone)$^+$ in the presence of excess Et_3SiH has been reported. The reaction of most ketones is complete in under 0.5 h at room temperature with TONs on the order of ca. 200. The hydrosilylation of benzaldehyde with 1.2 equiv Et_3SiH provided the corresponding silyl benzyl ether quantitatively in 0.3 h without the secondary cleavage of the silyl ether, which is known to occur in other systems.[46a] The hydrosilylation of esters and amides occurs at slower rates relative to ketones and aldehydes and results in over-reduction to afford cleavage of C-O bonds.[47a] The catalytic hydrosilylation of epoxides was also conducted with 0.5 mol % [POCOP]Ir(H)(acetone)$^+$ in the presence of 1.5 equiv. Et_3SiH at room temperature.[47b] It was determined that the

resulting silyl-protected alcohols originated from rapid isomerization of the epoxide to a ketone that underwent subsequent hydrosilylation.

Mechanistic studies revealed that the hydrosilylation of carbonyl compounds occurs through Et_3Si^+ transfer to the carbonyl fragment by [POCOP]Ir(H)(η^1-$HSiEt_3$)$^+$ to form an oxocarbenium ion $(Et_3SiOCR^1R^2)^+$ that is subsequently reduced by [POCOP]$Ir(H)_2$ (Scheme 1-18).[47] Low temperature NMR studies showed that the adduct [POCOP]Ir(H)$(O{=}CR^1R^2)^+$ and the η^1-silane complex are in equilibrium before hydrosilylation occurs, and the ketone complex is the likely resting state of the catalyst.

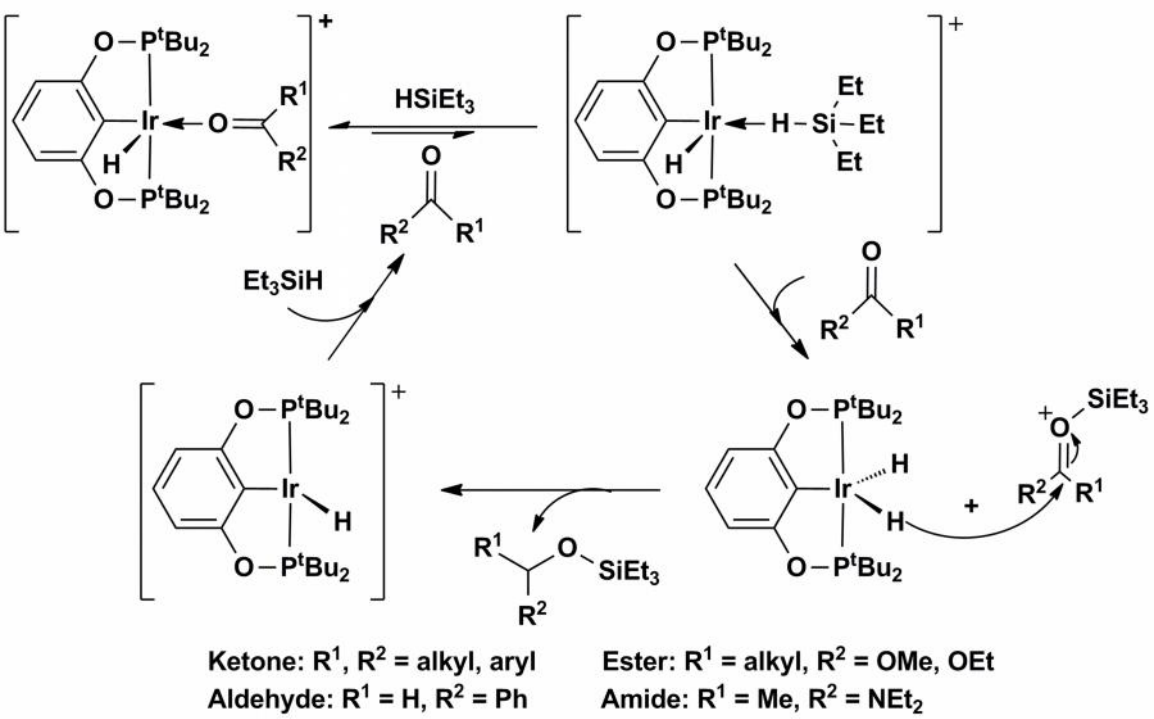

Scheme 1-18. Proposed catalytic cycle for (POCOP)Ir catalyzed hydrosilylation of carbonyl containing compounds

The reduction of carbonyl containing compounds by the η^1-silane complex [POCOP]Ir(H)(η^1-silane)$^+$ has also been recently extended to the catalytic hydrosilylation of carbon dioxide to methane with trialkylsilane as the reducing agent.[48] The reaction 0.3 mol% [POCOP]Ir(H)(acetone)$^+$ with 1 atm of CO_2 and 300 equivalents of various tertiary silanes at 23 ºC formed mixtures of bis(silyl)acetals, methyl silylethers, bis(silyl)ethers,

and methane. Less bulky silanes such as Me_2EtSiH and Me_2PhSiH led to both higher catalytic activity and increased selectivity for methane formation, with no detection of bis(silyl)acetal and methyl silyl ether intermediates. When Me_2PhSiH was used as the silane with a 0.0077 mol % loading of Ir, greater than 8200 TONs were achieved (where a TON indicates consumption of 1 equiv of silane). In addition, long catalyst lifetimes were observed as introduction of CO_2 after the reaction seemed to have stopped reinitiated catalysis with comparable rates and TONs to the first catalytic run.

A catalytic cycle was proposed for the reduction of CO_2 involving the initial reaction of [POCOP]Ir(H)(acetone)$^+$ with R_3SiH to generate [POCOP]Ir(H)(η^1-silane)$^+$ (Scheme 1-19). The silane complex reacts with CO_2 to yield a formoxysilane and [POCOP]Ir(H)$^+$, which can go on to regenerate [POCOP]Ir(H)(η^1-silane)$^+$. The formoxysilane is subsequently reduced in a reaction with [POCOP]Ir(H)(η^1-silane)$^+$ to form the bis(silyl)acetal $CH_2(OSiR_3)_2$. Successive subsequent hydrosilylations of $CH_2(OSiR_3)_2$ mediated by [POCOP]Ir(H)(η^1-silane)$^+$ lead to the formation of methane as well as two equivalents of the bis(silyl)ether $(R_3Si)_2O$.

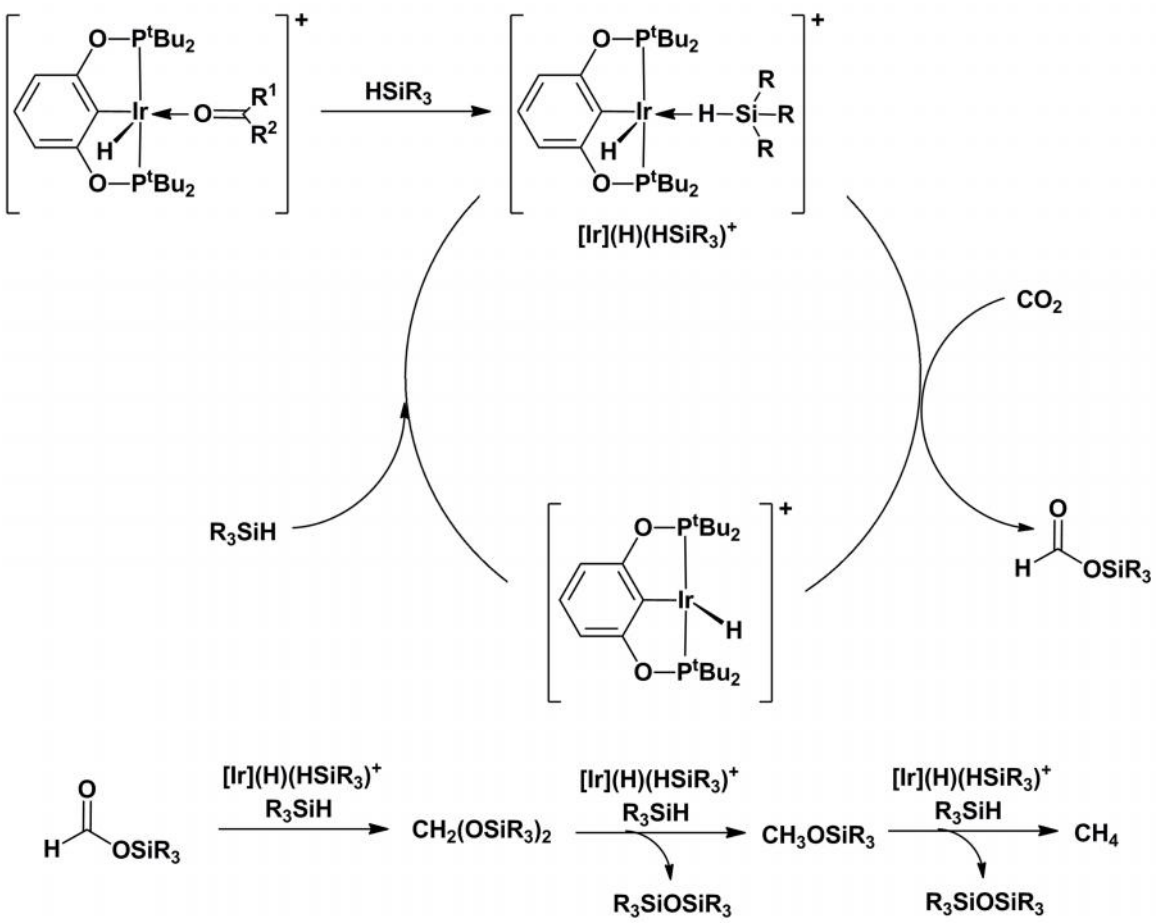

Scheme 1-19. Proposed catalytic cycle for CO_2 reduction to CH_4 by [POCOP]Ir(H)$^+$ and R_3SiH

Lastly, cationic iridium^{III} bis(phosphinite) complexes have also found application as pre-catalysts for the reduction of tertiary amides to amines with diethylsilane as the reductant.[49] In recent years, the reduction of tertiary amides via metal catalyzed hydrogenation has been investigated due to the need for more selective methods of synthesis for tertiary amines, though mechanistic details about this transformation have been lacking. Initial studies found that the combination of [POCOP]Ir(H)(acetone)$^+$ (0.5 mol %) with Et_2SiH_2 (3 equiv) at 60 ºC enabled the catalytic reduction of aromatic, aliphatic, heteroaromatic and heterocyclic amides to tertiary amines.[49] Unlike the systems described above for the reduction of carbonyl compounds, CO_2, alkyl halides and ethers, mechanistic studies revealed that the catalytically relevant species in the reduction

of tertiary amides was not the silane complex [POCOP]Ir(H)(η^1-silane)$^+$. Rather, the neutral iridium^V silyl trihydride complex [POCOP]Ir(H)$_3$(SiEt$_2$H) was determined to be the active species for the reduction of tertiary amides (Figure 1-9, Scheme 1-20).[49]

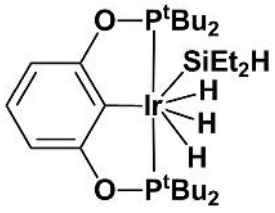

[POCOP]Ir(H)$_3$(SiEt$_2$H)

Figure 1-9. Strucutre of neutral Ir^V silyl trihydride for catalytic reduction of tertiary amides to amines

The catalyst resting state for amide hydrosilylation were first probed by carrying out the reaction of [POCOP]Ir(H)(acetone)$^+$ with excess Et$_2$SiH$_2$ in the presence of NEt$_3$ as a model for the basic amide and amine product. An equilibrium mixture of neutral Ir^{III} complex [POCOP]Ir(H)(SiEt$_2$H) and Ir^V species [POCOP]Ir(H)$_3$(SiEt$_2$H) was found to be the resting state during catalysis. This observation suggested that the in situ generated silane complex [POCOP]Ir(H)(H$_2$SiEt$_2$)$^+$ (resulting from the reaction of [POCOP]Ir(H)(acetone)$^+$ with excess Et$_2$SiH$_2$) was deprotonated by NEt$_3$ to form [POCOP]Ir(H)(SiEt$_2$H) and Et$_3$NH$^+$. The reaction of [POCOP]Ir(H)(SiEt$_2$H) with H$_2$ (from the hydrolysis of Et$_2$SiH$_2$ and adventitious water) provides the Ir^V complex [POCOP]Ir(H)$_3$(SiEt$_2$H).[49] These neutral silyl hydride complexes could be rationally prepared by treatment of [POCOP]Ir(H)(Cl) with NaO^{t}Bu in the presence of excess Et$_2$SiH$_2$ at 60 ºC for 4 h.

In order to assess the feasibility of these neutral Ir^{III} and Ir^V silyl hydride complexes for the catalytic reduction of tertiary amides, 1 mol% of a mixture of [POCOP]Ir(H)(SiEt$_2$H) and [POCOP]Ir(H)$_3$(SiEt$_2$H) (0.9:0.1 ratio) was treated with *N,N*-dimethylbenzamide and Et$_2$SiH$_2$. After 1 h, the amide was converted to the hemiaminal ether and only minimal amine product was observed, even after prolonged reaction times.

Since the reduction of *N,N*-dimethylbenzamide with [POCOP]Ir(H)(acetone)$^+$ and excess Et_2SiH_2 formed only *N,N*-dimethylbenzamine, these differing results suggested that the conjugate acid R_3NH^+ was catalyzing the conversion of the hemiaminal to the corresponding amine. Consequently, treatment of the hemiaminal ether with 1 mol% of $[Et_3NH][B(C_6F_5)_4]$ enabled quantitative amine formation. Further investigation revealed that the rate of conversion of the hemiaminal ether was dependent on the ammonium salt and silane concentration, which indicated that the silane was the hydride donor for the initial reduction chemistry. As such, since the iridium(V) complex [POCOP]Ir(H)$_3$(SiEt$_2$H) has a much more active 'Et_2SiH^+' donor, it was determined to be the active catalyst for the conversion of amide to hemiaminal ether.[49]

Based on the above results, a catalytic cycle was proposed for the reduction of tertiary amides to amines with Et_2SiH_2 (Scheme 1-20). Treatment of [POCOP]Ir(H)(acetone)$^+$ with excess Et_2SiH_2 provides a mixture of [POCOP]Ir(H)(SiEt$_2$H) and [POCOP]Ir(H)$_3$(SiEt$_2$H), the later complex being the catalytically active species. [POCOP]Ir(H)$_3$(SiEt$_2$H) transfers Et_2SiH^+ to the amide substrate to form an oxocarbenium ion intermediate and [POCOP]Ir(H)$_3^-$, which can react together to yield a hemiaminal and [POCOP]Ir(H)$_2$. The neutral Ir dihydride complex can reenter the catalytic cycle by reacting with Et_2SiH_2 to regenerate the active catalyst, [POCOP]Ir(H)$_3$(SiEt$_2$H). In order to obtain the final amine product, the hemiaminal reacts with a weak acid (such as Et_3NH^+) to generate an iminium ion that is then further reduced to the amine by Et_2SiH_2 (Scheme 1-20). Since it was found that adventitious H_2 encourages the formation of the catalytically active [POCOP]Ir(H)$_3$(SiEt$_2$H), the most active catalytic system was achieved under an atmosphere of H_2.

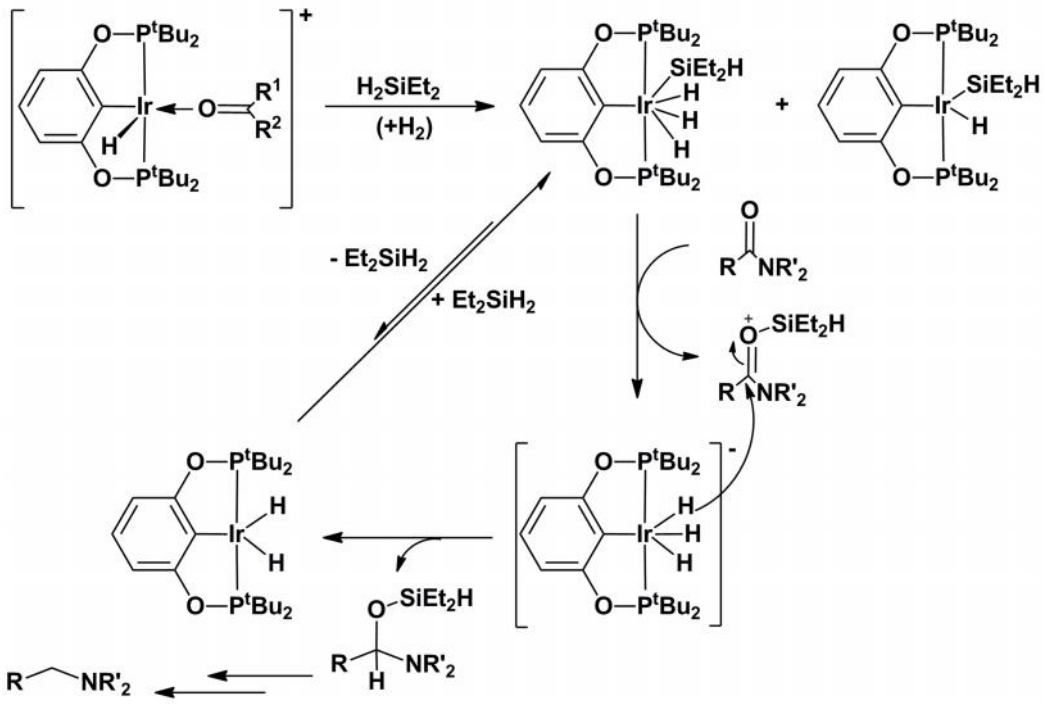

Scheme 1-20. Proposed catalytic cycle for reduction of tertiary amines by $[POCOP]Ir(H)_3(SiEt_2H)$

1.7 Alternative Pincer Designs – Silyl Pincer Complexes

The pincer complexes that have been discussed thus far exclusively feature a PCP or PNP-type donor framework. The study of transition metal pincer chemistry has in fact focused almost exclusively on such PCP/PNP ligated complexes. However, as was noted previously, LXL pincer-type ligands have a modular design that allows for variability at both the neutral (L) and anionic (X) donor positions. Despite this feature, relatively little attention has been given to varying the nature of the central anionic donor. As such, the chemistry of pincer complexes with ligands bearing other types of central donor groups is an emerging area, with examples of pincer ligation featuring X = P,[12] B,[13] Sn,[14] Ge,[14] and Si[15] having been recently reported. It is anticipated that such novel pincer systems will

display interesting new reactivity due to changes in the electronic characteristics of the central donor group.

Of these alternative pincer designs, silyl-based LSiL pincers are the most established and well-studied. Due to the decreased electronegativity of Si (relative to C), the substitution of Si for C in a pincer complex is predicted to enable the synthesis of increasingly electron rich metal complexes that may more readily undergo oxidative addition reactions. Silyl groups are also highly *trans*-labilizing, which can encourage coordinative unsaturation in the resulting metal complexes – a necessary requirement for further reactivity.[50] Such features may lead to significant structural and reactivity differences between PCP- and PSiP-supported metal complexes. Indeed, PSiP ligation has been utilized to prepare unprecedented four-coordinate, trigonal pyramidal Ru complexes, and computational studies have confirmed the key role of the strongly σ-donating silyl group in enforcing the unusual coordination geometry. [15f]

Silyl PSiP ligands were first reported by Stobart and co-workers in the 1980s, who prepared a series of platinum group metal complexes supported by various mono- and bis(phosphino)silyl ligands featuring either aliphatic or benzylic backbones (Figure 1-10C).[51] These early studies primarily addressed the fundamental coordination chemistry of such (phosphino)silyl ligands, specifically focusing on the trans-labilizing effect of silicon and the stabilization of the M-Si linkage by the chelate effect (Figure 1-10A). There was little investigation into the organometallic reactivity of these compounds and their utility in E-H bond cleavage reactions of the type that have been highlighted for PCP pincer complexes was not evaluated.

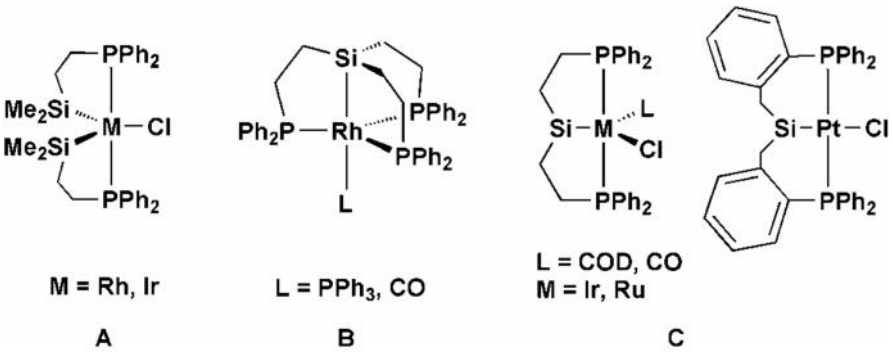

Figure 1-10. Previously reported bi-, tri- and tetradentate phosphinosilyl complexes

More recently, Tilley and co-workers developed an NSiN pincer-type ancillary ligand based on the bis(8-quinolyl)silyl framework (Figure 1-11).[52] The coordination chemistry of NSiN with Rh, Ir and Pt was investigated. Although Pt and Rh complexes supported by NSiN ligation proved relatively unreactive,[52b,d] the Ir analogues were shown to activate the Si-H bond of tertiary alkyl and aryl hydrosilanes.[52c] Ir complexes supported by NSiN ligation were also shown to catalyze arylsilane redistribution of a variety of primary and secondary aryl silanes, as well as dehydrogenative arene silylation of various arenes with a primary silane.[52c] However, these [NSiN]Ir catalysts were not very active and lead to poor product yields.[52c]

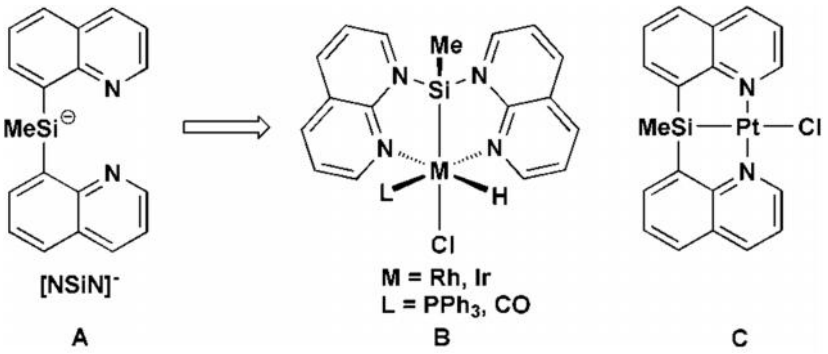

Figure 1-11. Rh, Ir and Pt complexes featuring the tridentate bis(8-quinolyl)silyl (NSiN) ligand

Although the Tilley NSiN ligand system was shown to lead to isolable late transition metal silyl pincer complexes, a major drawback of the quinolyl-based ligand

framework is the lack of modularity. Due to the nature of the quinolyl donors, substitution at nitrogen is not readily modified, which limits the ability to fine tune the steric and electronic properties of this tridentate ligand. Furthermore, N-based peripheral donors are anticipated to afford late metal complexes that are not very electron-rich, and thus may not readily undergo oxidative addition reactions with substrates such as hydrocarbons.

In an effort to further develop the reactivity and bond activation chemistry of pincer complexes featuring a central silyl donor, work in the Turculet group has targeted a new class of bis(phosphino)silyl pincer ligands of the type [κ^3-(2-$R_2PC_6H_4)_2SiMe$]$^-$ ([R-PSiP], R = alkyl or aryl; Figure 1-12).[15] By comparison with the Stobart phosphinosilyl ligand architectures, the reduced conformational flexibility and lack of β-hydrogens associated with the *ortho*-phenylene backbone of [R-PSiP] is anticipated to provide enhanced stability and selectivity in metal-mediated substrate transformations. Furthermore, in comparison with the quinolyl-based NSiN system studied by Tilley and co-workers, [R-PSiP] ligation offers the opportunity to readily tune the steric and electronic properties of the phosphino donors; the phosphino groups are also more compatible than quinolyl groups with the preparation of electron-rich platinum group metal derivatives. Thus far, [R-PSiP] metal complexes have been shown to participate in a wide variety of E-H bond activation reactions,[15a,b,d,e] and have also been shown to be catalytically active in reactions such as transfer hydrogenation of ketones,[15a] hydrosilylation of CO_2 to form methane,[15g,i-n]

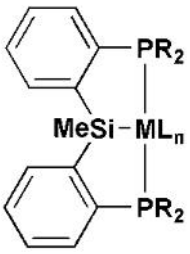

M = late transition metal

Figure 1-12. Bis(phosphino)silyl pincer complexes being pursued in the Turculet group

The work described in the following chapters builds on previous work from the Turculet group dealing with the synthesis and reactivity of new [R-PSiP]Rh and [R-PSiP]Ir pincer complexes.[15a,b] The studies presented herein will address the synthesis of new coordinatively and electronically unsaturated Rh and Ir complexes supported by [R-PSiP] ligation and the reactivity of such complexes with C-H and a variety of N-H bonds. Mechanistic investigations of this E-H bond activation chemistry that implicate a highly reactive, 14-electron [PSiP]Ir^{I} intermediate will also be discussed. Moreover, results of attempted functionalization of N–H bond through insertion of unsaturated substrates into the Ir–N bond of synthesized amido hydride complexes will be addressed. Finally extension of the [R-PSiP]Ir^{I} bond cleavage chemistry to cationic [R-PSiP]Ir^{III} complexes and their reactivity will also be presented.

Chapter 2: Synthesis and Reactivity of New Bis(phosphino)silyl Rh and Ir Amido Hydride Pincer Complexes - A Rare Example of N-H Bond Oxidative Addition of Ammonia

2.1 Introduction

As highlighted in Chapter 1, Group 9 metal pincer complexes have demonstrated an aptitude for cleaving C-H and N-H bonds in organic substrates such as hydrocarbons and amines, respectively. Although some promising breakthroughs towards efficient catalytic processes that involve such bond cleavage steps have been achieved, there are still many avenues left to pursue. In order to advance this field, a significant portion of current research efforts are focused on investigating alternative pincer ligand architectures and their influence on reactivity at the metal center. Towards this end, research in the Turculet group has focused on a pincer ligand design featuring a central silyl donor.[15a-g] The incorporation of strongly electron donating and *trans*-labilizing silyl groups into such multidentate ligand architectures may promote the formation of electron-rich and coordinatively unsaturated complexes that can readily undergo oxidative addition of a variety of σ-bonds.

Although metal-silicon chemistry has been well studied across the transition series,[53] the incorporation of a silyl donor into a pincer ancillary ligand framework has not been widely explored. As highlighted in the introduction of this thesis, while a few previous examples of silyl pincer complexes have appeared in the literature, very little exploration of the reactivity of such complexes has been reported.[15,51,52] Investigations in the Turculet group have focused on new tridentate bis(phosphino)silyl ligands of the type [κ^3-(2-$R_2PC_6H_4)_2SiMe]^-$ ([R-PSiP], R = aryl or alkyl; Figure 2-1). Unlike previously reported tridentate phosphinosilyl ligands,[51] the [R-PSiP] ligand architecture features a relatively rigid *o*-phenylene backbone lacking β-hydrogens, which is anticipated to lead to stable organometallic pincer metal complexes. Furthermore, the ligand design is modular, in that the substitution at phosphorus is readily modified in order to alter the steric and electronic profile of the phosphine donors.

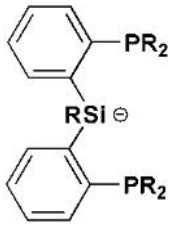

Figure 2-1. Bis(phosphino)silyl ligand design pursued in the Turculet group

Initial investigations have shown that [R-PSiP]-supported pincer complexes can exhibit aggressive reactivity.[15a-g] Specifically, coordinatively unsaturated Ir complexes supported by the new bis(phosphino)silyl ligand [Cy-PSiP] were reported to undergo facile intermolecular arene sp^2-C-H bond cleavage reactions. This represents the first example of room temperature arene C-H bond activation by a silyl pincer complex.[15b]

This chapter will detail the continued study of Group 9 metal [R-PSiP] pincer complexes, with the goals of improving the understanding of [R-PSiP]Ir-mediated C-H bond cleavage chemistry, as well as extending this reactivity to the activation of N-H bonds.

2.2 Results and Discussion

The synthesis of the [Cy-PSiP]H ligand precursor, which has been reported previously,[15b] is readily achieved in three synthetic steps (Scheme 2-1). The initial Pd coupling reaction between Cy_2PH and 2-iodobromobenzene in the presence of Cs_2CO_3 yielded 2-dicyclohexylphosphino bromobenzene in 85 % yield. Lithiation of the aryl phosphine with ^{n}BuLi, followed by *in situ* treatment with 0.5 equiv of $MeSiHCl_2$, afforded [Cy-PSiP]H in 69% isolated yield (Scheme 2-1).

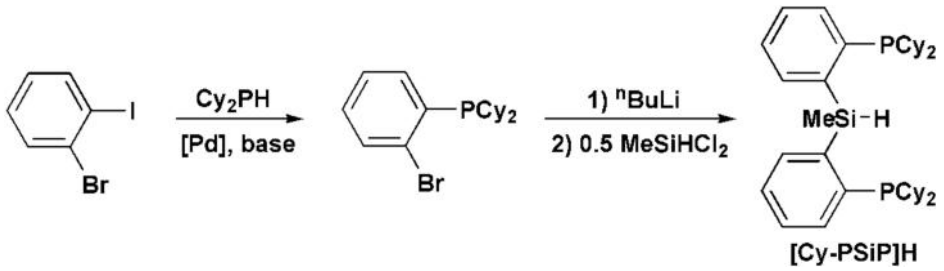

Scheme 2-1. Synthesis of the [Cy-PSiP]H ligand precursor

Oxidative addition of the Si-H bond in [Cy-PSiP]H to a low valent metal center has been shown to lead to metalation of the ligand and the formation of the desired silyl pincer complexes.[15b] Specifically focusing on the chemistry of Rh and Ir complexes supported by [Cy-PSiP] ligation, previous work has demonstrated that five-coordinate complexes of the type [Cy-PSiP]M(H)Cl are readily prepared by the reaction of [Cy-PSiP]H with 0.5 equiv of $[(COE)_2MCl]_2$ (**2-1**, M = Ir; **2-2**, M = Rh; COE = cyclooctene).[15b] Attempted alkylation of either **2-1** or **2-2** with alkyl lithium reagents such as MeLi led to the formation of short-lived [Cy-PSiP]M(H)(alkyl) intermediates that were shown to rapidly eliminate the corresponding alkane and, in the case of M = Ir, mediate intermolecular aryl C-H bond cleavage processes, including arene exchange, at room temperature (Scheme 2-2).[15b] These results constitute the first reported example of intermolecular C-H bond cleavage mediated by a silyl pincer complex.

In an effort to expand on these initial results, one goal of the current work is to attempt to shed additional light on the mechanism of C-H bond cleavage by [Cy-PSiP]-supported Ir complexes. A possible mechanism for this sp^2-C–H bond activation chemistry involves C-H bond oxidative addition to a highly reactive, 14-electron [Cy-PSiP]Ir^I intermediate species that is generated *in situ* via alkane or arene reductive elimination from [Cy-PSiP]Ir(H)(alkyl) or [Cy-PSiP]Ir(H)(aryl), respectively. Such a mechanism has been postulated previously for related C-H bond cleavage chemistry involving [PCP]Ir pincer complexes.[26,28,34,54]

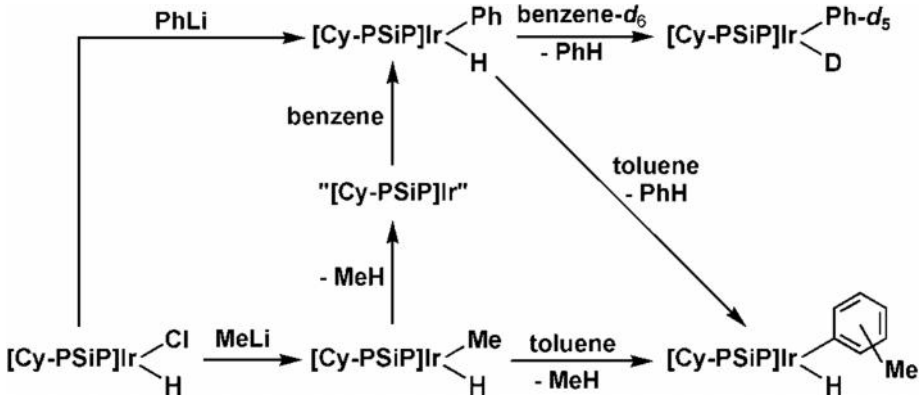

Scheme 2-2. C-H bond activation chemistry mediated by [Cy-PSiP]Ir^{I}

In this context, the trapping, isolation and study of reactive [Cy-PSiP]M^{I} intermediates represents one avenue of investigation, as the viability of [Cy-PSiP]M^{I} species (M = Rh, Ir) has not previously been demonstrated. Furthermore, an additional goal of the current work is to study the capability of the [Cy-PSiP]M system to carry out additional aggressive E-H bond cleavage reactions. In this regard, N-H bonds were considered suitable candidates for further investigation due to the comparable homolytic bond strengths of C-H and N-H bonds.[55]

2.2.1 Synthesis and Characterization of [Cy-PSiP]ML Complexes

Initial attempts to probe the reactivity of **2-1** and **2-2** aimed to prepare M^{III} complexes of the type [Cy-PSiP]M(H)(alkyl) (M = Rh, Ir) by the treatment of either **2-1** or **2-2** with alkyl lithium reagents such as MeLi. In the case of Ir, as mentioned above, the resulting [Cy-PSiP]Ir(H)(alkyl) species was shown to eliminate the corresponding alkane (methane, if MeLi was used) and undergo intermolecular C-H bond cleavage of the arene solvent at room temperature to generate complexes of the type [Cy-PSiP]Ir(H)(aryl) (Scheme 2-2).[15b] Complexes of the type [Cy-PSiP]Ir(H)(aryl) underwent arene exchange reactions and were susceptible to arene loss when exposed to vacuum, which precluded their isolation. Experiments utilizing benzene-d_6 as the reaction solvent led to the formation of [Cy-PSiP]Ir(D)(Ph-d_5), where ^{2}H incorporation was observed exclusively at the hydride and Ph positions (^{2}H NMR). In the case of Rh,

loss of methane was detected upon the reaction of **2-2** with MeLi in benzene solution, but intermolecular C-H bond activation of the benzene solvent was not observed. Instead, an unidentified Rh-containing product exhibiting a broadened $^{31}P\{^{1}H\}$ NMR signal centered at 62.9 ppm ($^{1}J_{RhP}$ = 162 Hz) and broadened ^{1}H NMR signals resulted.[15b]

To better understand the reactivity of **2-1** and **2-2** with alkyl lithium reagents, alkylation reactions were pursued in the non-aromatic solvent cyclohexane-d_{12}.[15b] When one equiv of MeLi (1.6 M in Et_2O) was added to **2-1** in cyclohexane-d_{12}, ^{1}H NMR analysis revealed complete consumption of **2-1** and the formation of methane. Broad aromatic and cyclohexyl resonances, as well as a broad Ir-H signal centered around -11.3 ppm were also observed. The $^{31}P\{^{1}H\}$ NMR spectrum of the reaction mixture exhibited a complex multiplet centered at 56.2 ppm. Both ^{1}H and ^{31}P spectral features did not vary appreciably between –90-90 ºC. Although the presence of an Ir-H resonance may indicate the formation a cyclometalated species where Ir has inserted into one of the P*Cy* C-H groups, this product could not be unambiguously identified due to the broad nature of the NMR resonances. The addition of an excess (100 equiv) of benzene to this reaction mixture led to the formation of [Cy-PSiP]Ir(H)Ph.

When one equiv of MeLi was reacted with **2-2** in cyclohexane-d_{12} solution, the same unidentified Rh-containing product previously observed in attempted alkylation reactions in arene solvents was once again observed upon loss of methane.[15] The broadened $^{31}P\{^{1}H\}$ and ^{1}H NMR resonances were not resolved between –90-100 ºC and no evidence of a Rh-H was observed.

Several mechanistic possibilities for the C-H bond cleavage chemistry observed can be proposed, including: (a) alkane reductive elimination from [Cy-PSiP]M(H)(alkyl) followed by C-H bond oxidative addition of the arene solvent to a 14-electron [Cy-PSiP]Ir^{I} intermediate (or a related agostic complex); and (b) alkane reductive elimination from [Cy-PSiP]M(H)(alkyl) followed by intramolecular cyclometalation to afford a metalated [Cy-PSiP]Ir^{III} hydride complex that undergoes subsequent σ-bond metathesis with an arene C-H bond. The results obtained thus far are more consistent with a

mechanism of type (a), as mechanism (b) would result in ^{2}H incorporation into the ligand P*Cy* groups, which was not observed by ^{2}H NMR spectroscopy. Although a possible cyclometalated species was detected for M = Ir, this species can also serve as a source of 14-electron [Cy-PSiP]Ir^I upon C-H bond reductive elimination. The broadened features of the NMR spectra observed for the intermediates generated in cyclohexane-d_{12} solution could potentially arise from fluxional processes involving rapid, reversible intramolecular metalation of a P*Cy* C-H bond by the [Cy-PSiP]M^I fragment. Although the related Rh complex does not undergo intramolecular C-H bond activation, it is possible that [Cy-PSiP]Rh^I species are generated just the same. Related 14-electron Rh and Ir species have previously been proposed in both [PCP]M^I and [PNP]M^I systems.[26,34,35,54,56]

Attempts to isolate the [Cy-PSiP]M^I reactive intermediates have proven unsuccessful thus far. Such coordinatively and electronically unsaturated species are highly reactive and rarely isolable.[57] In light of this, efforts were made to trap these species with an L-type neutral donor ligand in order to prove the viability of [Cy-PSiP]M^I intermediates (Scheme 2-3). In this regard, a cyclohexane solution of **2-1** was reacted with Me_3SiCH_2Li to generate [Cy-PSiP]Ir^I. The reaction mixture was subsequently degassed and 1 atm of ethylene gas was added to the reaction mixture to trap the intermediate. Following heating at 65 ºC for 16 h a new product identified as [Cy-PSiP]Ir(C_2H_4) (**2-3,** Scheme 2-3) was observed (^{1}H and ^{31}P NMR) and subsequently isolated as an orange solid in 89% yield. The ^{31}P NMR spectrum of **2-3** features a single resonance at 65.4 ppm corresponding to the symmetry equivalent phosphine donors of the [Cy-PSiP] ligand. The ^{1}H and ^{13}C NMR spectra of **2-3** display a single set of [Cy-PSiP] ligand backbone aromatic resonances, consistent with a C_s-symmetric complex. Also, signals for the coordinated ethylene ligand were observed at 2.68 and 37.1 ppm in the ^{1}H NMR and ^{13}C NMR spectra of **2-3**, respectively.

A similar route was pursued to prepare and isolate [Cy-PSiP]Ir(PMe_3) (**2-4**, Scheme 2-3). A benzene solution of **2-1** was treated with Me_3SiCH_2Li to generate the [Cy-PSiP]Ir(H)Ph species which quickly eliminated benzene upon subsequent treatment

with PMe_3. The solution turned dark red over 20 minutes at room temperature and the new product, identified as **2-4** by ^1H and ^{31}P NMR spectroscopy, was isolated as a dark red solid in 77% yield. Complex **2-4** exhibited C_s symmetry in solution, as evidenced by the presence of a single $^{31}P\{^1H\}$ NMR resonance at 70.6 ppm (d, $^2J_{PP}$ = 7 Hz) corresponding to the [Cy-PSiP] ligand phosphorus donors. The $^{31}P\{^1H\}$ NMR spectrum of **2-4** also features a resonance at -21.2 ppm (t, $^2J_{PP}$ = 7 Hz), which corresponds to the Ir-bound PMe_3 ligand. In addition, the ^1H and ^{13}C NMR spectra of **2-4** (benzene-d_6) featured a single set of [Cy-PSiP] ligand backbone aromatic resonances, as well as resonances consistent with the coordinated PMe_3 ligand (^1H, 1.53 ppm, d, 9 H, $^2J_{HP}$ = 6 Hz; $^{13}C\{^1H\}$, 25.2, d, $^1J_{CP}$ = 20 Hz).

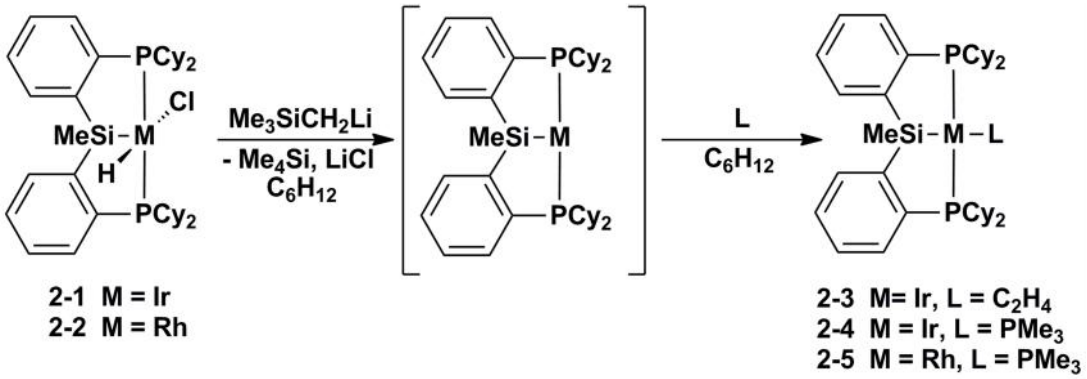

Scheme 2-3. Trapping of [Cy-PSiP]M^I species with neutral L-type donor ligands

Similar trapping experiments were also completed to assess the viability of [Cy-PSiP]Rh^I intermediates (Scheme 2-3). Indeed, addition of PMe_3 to *in situ* generated [Cy-PSiP]Rh^I led to complete conversion to the new complex [Cy-PSiP]Rh(PMe_3) (**2-5**), as evidenced by the appearance of two new $^{31}P\{^1H\}$ NMR resonances at 70.8 (dd, 2 P, $^1J_{PRh}$ = 166 Hz, $^2J_{PP}$ = 22 Hz, Cy-*P*Si*P*) and -33.1 ppm (dt, 1 P, $^1J_{PRh}$ = 128 Hz, $^2J_{PP}$ = 22 Hz, *P*Me_3). Complex **2-5** was isolated as a red solid in 56% yield. The ^1H and ^{13}C NMR features of **2-5** (benzene-d_6) are consistent with the formation of a C_s-symmetric species, as indicated by the presence of a single set of [Cy-PSiP] ligand backbone resonances. In addition, resonances consistent with the coordinated PMe_3 ligand are also observed (^1H,

1.38 ppm, d, 9 H, $^{2}J_{HP}$ = 3 Hz; $^{13}C\{^{1}H\}$, 23.5 ppm, d, $^{1}J_{CP}$ = 12 Hz). The X-ray crystal structure of complex **2-5** (Figure 2-2, Table 2-1) confirmed the formation of a four-coordinate complex. Surprisingly the geometry at the metal center is significantly distorted from square planarity, as indicated by the P3-Rh-Si bond angle of 147.61(2)º. This unusual structure is unexpected given that examples of related square planar complexes of the type [Cy-PSiP]MR (M = Ni, Pd, Pt) are known, including structurally characterized examples where R is a relatively bulky ligand such as diphenylsilyl.[15c] No such deviation from square planar geometry was observed in these Group 10 complexes. Although this distortion can be ascribed to crystalline packing effects, it is also possible that this structural feature arises due to electronic factors related to the strongly *trans*-labilizing properties of Si. Comparably, Grushin and coworkers have reported studies on the intramolecular exchange of phosphine substituents in polyphosphine complexes of the type $(PPh_3)_3RhX$ (X = H, Me, Ph, CF_3) which also exhibit distorted square planar geometries, with P-Rh-P angles of less than 150º.[58] When X has a high trans labilizing influence, this distortion was attributed to both steric and electronic factors to promote movement of the phosphine trans to X towards an axial position and subsequent reduction of the P-Rh-P angle as the remaining phosphines move toward the vacant site.[58]

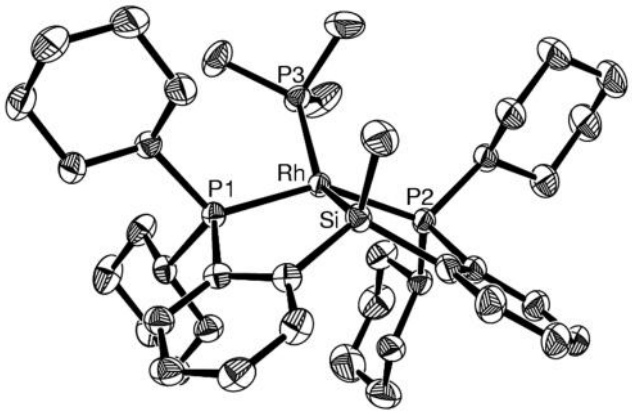

Figure 2-2. The crystallographically determined structure of **2-5**, shown with 50% displacement ellipsoids. All H atoms have been omitted for clarity.

Table 2-1. Selected interatomic distances (Å) and angles (º) for **2-5**

Bond Lengths (Å)			
Rh-P1	2.2668(4)	Rh-P3	2.3597(5)
Rh-P2	2.2703(4)	Rh-Si	2.2872(5)
Bond Angles (º)			
P1-Rh-P2	146.00(2)	P2-Rh-P3	103.86(2)
P1-Rh-P3	105.62(2)	P3-Rh-Si	147.61(2)

The successful isolation of complexes of the type [Cy-PSiP]ML confirms for the first time that Rh^I and Ir^I species supported by the [Cy-PSiP] ligation are viable. Furthermore, the trapping of intermediates generated by alkane elimination from [Cy-PSiP]M(H)(alkyl) supports the hypothesis that [Cy-PSiP]M^I species are generated *in situ* in these reaction mixtures. The large distortion from square planarity observed in the solid state structure of **2-5** suggests that these [Cy-PSiP]M^I species may be highly strained, which may play a role in their reactivity towards E–H bonds.

2.2.2 Synthesis and Characterization of [Cy-PSiP]M(H)(NHR) Complexes

Significant research interest exists in developing new atom-efficient and selective catalytic amination reactions, as amine functional groups are present in many pharmaceutical and industrially relevant compounds. Although there are numerous possible mechanisms by which metal-catalyzed amination may proceed, there is interest in developing late transition metal complexes that can insert into the N-H bonds of amines, and especially ammonia, through oxidative addition reactions, as such reactivity parallels other highly successful catalytic reactions that incorporate E-H bond oxidative addition steps, including hydrogenation, hydrosilation and hydroboration. Unfortunately, the oxidative addition of N-H bonds is challenging due to the presence of a lone pair of electrons on nitrogen, which can simply coordinate to a transition metal to form a stable σ-complex rather than undergo N-H bond cleavage. As such, there are relatively few

well-documented examples of such N-H bond cleavage chemistry,[38-40,41] and catalytic amination reactions that utilize N-H bond oxidative addition steps remain an elusive goal.

As described in the introduction of this document, there is some precedent in the literature for PCP-type Ir pincer complexes being able to activate N-H bonds.[38a,39,40,41] Given the rarity of such reactivity, the development of alternate transition metal complexes that are capable of mediating N-H bond oxidative addition is highly desirable, as such studies may afford insights into the development of new catalytic amination reactions. In this regard, [Cy-PSiP] ligated Rh and Ir species are attractive candidates for the study of N-H bond activation reactions.

In this context, the direct synthesis of amido hydride complexes of the type [Cy-PSiP]M(H)(NHR) (M = Rh, Ir) was initially targeted in this study, as these are the type of complexes expected to result from N-H bond oxidative addition of amines to [Cy-PSiP]M^{I}. To establish the viability of such N-H bond activation products they were rationally prepared by reacting either **2-1** or **2-2** with one equiv of the corresponding lithium amide reagent in THF solution at room temperature (Scheme 2-4). Two sets of anilido hydride complexes of Rh and Ir were synthesized using this route – [Cy-PSiP]M(H)(NHPh) (M = Ir, **2-6**; M = Rh, **2-8**) and [Cy-PSiP]M(H)(NH-2,6-$Me_2C_6H_3$) (M = Ir, **2-7**; M = Rh, **2-9**).

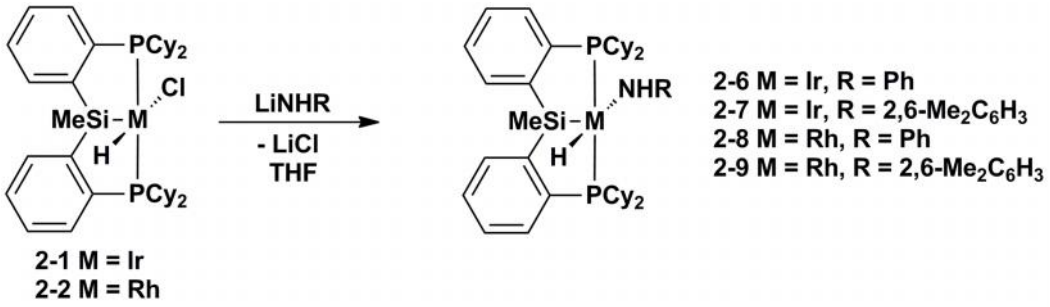

Scheme 2-4. Synthesis of [Cy-PSiP]M(H)(NHR) complexes (R = Ph, 2,6-$Me_2C_6H_3$) via a salt metathesis route

In all cases, the formation of the anilido hydride complexes appeared to be quantitative by ^{31}P-NMR spectroscopy and these complexes were all isolated as orange or red solids in yields ranging from 80-89%. Spectroscopic data of the isolated complexes, including solution ^{1}H, ^{13}C, and ^{31}P NMR spectra indicate the formation of C_s-symmetric species. Thus, the ^{31}P NMR spectra in all cases feature a single resonance corresponding to symmetry equivalent [CyPSiP] ligand phosphine donors (Table 2-2). Furthermore, the ^{1}H NMR spectra (benzene-d_6) of all amido hydride complexes feature a characteristic downfield-shifted hydride resonance, consistent with the formulations given in Scheme 2-4. In addition, ^{29}Si and ^{15}N spectroscopic data support the structures depicted in Scheme 2-4 (Table 2-2).

Table 2-2. Selected NMR spectroscopic data (ppm) for complexes **2-1**, **2-2** and **2-6** – **2-9**

Complex	^{31}P{^{1}H} NMR	^{1}H NMR hydride[a]	^{1}H NMR N***H***[a,b]	^{15}N NMR[b]	^{29}Si NMR[c]
[Cy-PSiP]Ir(H)Cl (**2-1**)	61.1	-23.79 (t)	-	-	7.7
[Cy-PSiP]Ir(H)(NHPh) (**2-6**)	55.1	-21.16 (t)	6.90	-260.8	13.3
[Cy-PSiP]Ir (H)(NH(2,6-$Me_2C_6H_3$)) (**2-7**)	52.8	-21.94 (t)	5.98	-265.0	12.1
[Cy-PSiP]Rh(H)Cl (**2-2**)	59.8 (d)	-18.80 (dt)	-	-	42.5
[Cy-PSiP]Rh(H)(NHPh) (**2-8**)	59.6 (d)	-16.86 (dt)	4.57	-275.9	44.0
[Cy-PSiP]Rh(H)(NH(2,6-$Me_2C_6H_3$)) (**2-9**)	57.3 (d)	-17.27 (dt)	3.28	-293.0	43.9

[a] benzene-d_6; [b] ^{1}H-^{15}N HMQC; [c] ^{1}H-^{29}Si HMBC

The solid state structures of [Cy-PSiP]Rh(H)(NHPh) (**2-8**), [Cy-PSiP]Ir(H)(NHPh) (**2-6·OEt$_2$**), and [Cy-PSiP]Ir(H)(NH(2,6-$Me_2C_6H_3$)) (**2-7**) were determined using single crystal X-ray diffraction techniques (Figure 2-3; Table 2-3). In all three cases the five-coordinate structures exhibit distorted square-based pyramidal coordination geometry at the metal center, with Si occupying the apical coordination site. Interestingly, the structures feature relatively acute Si–M–H1 angles (**2-8**, 67.8º; **2-6·OEt$_2$**, 67.5º; **2-7**, 68.8º)[58] similar to those previously observed for **2-1** and **2-2** in the solid state (M = Ir, 68.7(18)º; M = Rh, 65.8(12)º).[15b] As such, the geometry at the metal center can also be described as "Y-shaped", in which the anilido ligand is positioned opposite to the acute angle of the "Y". Such Y-shaped coordination geometry has

previously been observed for five-coordinate d^6 complexes and is attributed to electronic effects.[59] The structures also feature relatively short Si···H1 distances of 2.22 (**2-6·OEt$_2$**), 2.25 (**2-7**), and 2.19 (**2-8**) Å, respectively, that are comparable to those observed for **2-1** and **2-2** (M = Rh, 2.14(3) Å; M = Ir, 2.24(5) Å).[15b] Although these Si···H1 distances fall within the range indicative of an Si-H interaction (typically 1.7 – 2.4 Å;[60] sum of van der Waals radii = 3.4 Å) no evidence for such an interaction was observed in solution for **2-1** and **2-2** ($^2J_{SiH}$ < 10 Hz).[61] It is noteworthy that these anilido hydride complexes adopt a structure that differs substantially from that of [^{t}Bu-PCP]Ir(H)(NHPh), which adopts a square pyramidal geometry with the hydride and anilido ligands positioned *cis* to each other and the hydride in the apical position.[39] The Ir–N interatomic distances in **2-6·OEt$_2$** (2.056(2) Å) and **2-7** (2.077(3) Å) are similar to that observed for [^{t}Bu-PCP]Ir(H)(NHPh) (Ir–N = 2.082(2) Å).[39] By comparison, complex **2-8** features a Rh–N distance of 2.123(5) Å, which is slightly longer than that observed for the Ir complexes.

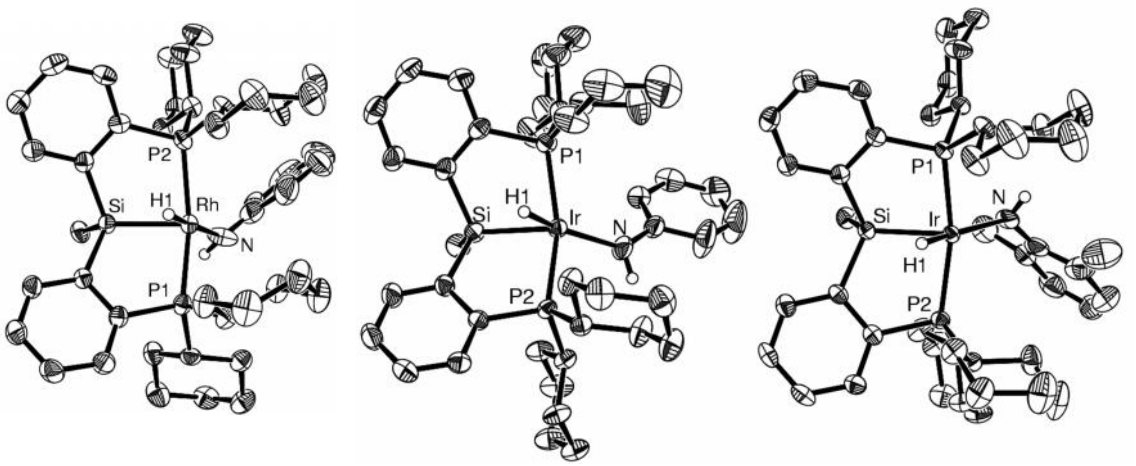

2-8 **2-6·OEt$_2$** **2-7**

Figure 2-3. The crystallographically determined structures of **2-8, 2-6·OEt$_2$**, and **2-7** shown with 50% displacement ellipsoids. With the exception of H1 and N-*H* all H atoms, as well as the Et_2O and solvate, have been omitted for clarity.

Table 2-3. Selected interatomic distances (Å) and angles (º) for **2-8**, **2-6·OEt$_2$**, and **2-7**.

Bond Lengths (Å)				
2-8	Rh-P1	2.287(15)	Rh-H1	1.55
	Rh-P2	2.3155(15)	Rh-N	2.123(5)
	Rh-Si	2.2430(14)		
2-6·OEt$_2$	Ir-P1	2.3112(7)	Ir-H1	1.55
	Ir-P2	2.2939(7)	Ir-N	2.056(2)
	Ir-Si			
2-7	Ir-P1	2.2872(8)	Ir-H1	1.55
	Ir-P2	2.3016(8)	Ir-N	2.077(3)
	Ir-Si	2.2791(8)		
Bond Angles (º)				
2-8	P1-Rh-P2	156.35(5)	Si-Rh-H1	67.8
	Si-Rh-N	118.28(15)	N-Rh-H1	173.9
2-6·OEt$_2$	P1-Ir-P2	158.06(3)	Si-Ir-H1	67.5
	Si-Ir-N	137.35(8)	N-Ir-H1	154.4
2-7	P1-Ir-P2	162.01(3)	Si-Ir-H1	68.8
	Si-Ir-N	129.72(11)	N-Ir-H1	160.7

A notable feature of the [Cy-PSiP]-supported anilido hydride complexes **2-6** – **2-8** is the fact that they do not readily undergo N-H bond reductive elimination, even in arene solvents. Previously, Hartwig and co-workers demonstrated that in benzene solution [^{t}Bu-PCP]Ir(H)(NHPh) exists in equilibrium with the benzene C-H bond activation product [^{t}Bu-PCP]Ir(H)Ph.[39] Related bisphosphinite [POCOP]Ir(H)(NHR) anilido hydride complexes reported by Brookhart and co-workers also exist in equilibrium with the benzene C-H bond activation product [POCOP]Ir(H)Ph.[41] Compared to these previously reported complexes the [Cy-PSiP]M anilido hydride complexes reported herein exhibit no spectroscopic evidence of an equilibrium between N-H and C-H bond activation products. This suggests that complexes of the type [Cy-PSiP]M(H)(NHR) (M = Rh, Ir) may undergo substantially different reactivity from previously reported PCP analogues.

2.2.3 Synthesis and Characterization of the Parent Amido Hydride Complex [Cy-PSiP]Ir(H)(NH_2)

A long sought after goal of catalytic amination chemistry is the development of reactions for the direct amination of substrates with ammonia, which is an abundant source of nitrogen.[62] The development of ammonia N-H bond oxidative addition chemistry is therefore highly desirable, as this may lead to the discovery of new reaction pathways. However, examples of organometallic species capable of ammonia N-H bond oxidative addition are exceedingly rare; only one example of a stable, isolable $L_nM(H)(NH_2)$ species produced from the oxidative addition of ammonia has been documented and this transformation was mediated by a [^{t}Bu-PCP]Ir pincer complex.[38a] As such, there is significant interest in the discovery and study of alternative organometallic species that can undergo ammonia N-H bond cleavage chemistry, as this may lead to the development of new catalytic reactions for ammonia functionalization.

In this regard, the direct synthesis of parent amido hydride complexes of the type [Cy-PSiP]M(H)(NH_2) (M = Rh, Ir) were targeted in our study, as these are the type of complexes expected to result from N-H bond oxidative addition of ammonia to [Cy-PSiP]M^I. Late transition metal parent amido complexes are quite rare, and can be challenging to synthesize.[38,63] As salt metathesis of the metal chloride complexes **2-1** and **2-2** with lithium anilides proved successful for the synthesis of anilido hydride Rh and Ir complexes, a similar route was attempted for the synthesis of the related parent amido complexes. Thus, treatment of **2-1** with five equiv of $LiNH_2$ in THF solution led to the clean formation of [Cy-PSiP]Ir(NH_2)(H) (**2-10**, Scheme 2-5) upon heating at 65 ºC for 12 h. Excess $LiNH_2$ was used due to the poor solubility of $LiNH_2$ in THF. Complex **2-10** was isolated as a yellow solid in 92% yield. Attempts to synthesize an Rh analogue of the type [Cy-PSiP]Rh(NH_2)(H) were not successful. The reaction of **2-2** with five equiv of $LiNH_2$ in THF solution typically led to a reaction mixture containing numerous unidentified products (^{31}P NMR). No pure materials could be isolated from such reaction mixtures.

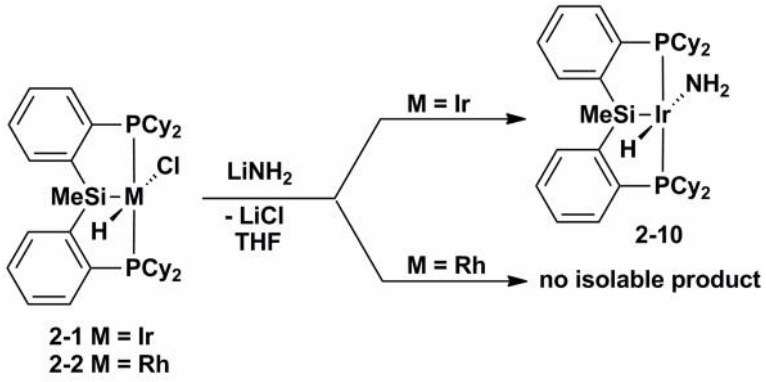

Scheme 2-5. Synthesis of the parent amido hydride complex [Cy-PSiP]Ir(H)(NH_2) (**2-10**) via a salt metathesis route utilizing $LiNH_2$

Complex **2-10** exhibits C_s symmetry in solution, as indicated by the presence of a single ^{31}P NMR resonance at 55.5 ppm corresponding to the symmetry equivalent phosphine donors of the [Cy-PSiP] ligand. The ^{1}H-NMR spectrum of **2-10** (benzene-d_6) features a hydride resonance at -20.13 ppm (t, $^{2}J_{HP}$ = 15 Hz) as well as a broad triplet at 5.03 ppm ($^{3}J_{HP}$ = 6 Hz) which corresponds to the IrNH_2 protons. The latter resonance correlates to a ^{15}N NMR resonance observed at -309.8 ppm in a ^{1}H–^{15}N HMQC experiment (referenced to $MeNO_2$).

The solid state structure of [Cy-PSiP]Ir(H)NH_2 (**2-10**) was determined using single crystal X-ray diffraction techniques (Figure 2-4, Table 2-4). In direct analogy with the iridium anilido hydride solid state structures for **2-6·OEt₂** and **2-7**, the geometry about the five coordinate iridium center is described as distorted square-based pyramidal with silicon in the apical position. The structure of **2-10** features a relatively acute Si–M–H1 angle of 66.2(17)°, comparable to those previously observed for the five coordinate iridium hydride structures in the solid state (67.5 – 68.8°). The Ir–N interatomic distance in **2-10** (1.980(4) Å) is shorter than those observed for the aryl amido hydride complexes **2-6·OEt₂** (2.056(2) Å) and **2-7** (2.077(3) Å) and comparable to that observed for the related complex [$CH(CH_2CH_2P^tBu_2)_2$]Ir(H)(NH_2) (1.999(4) Å).[38a]

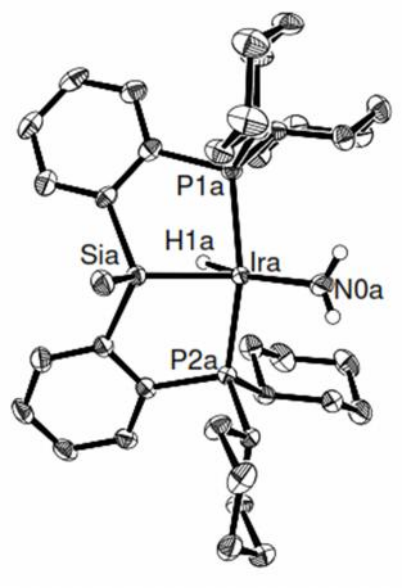

Figure 2-4. The crystallographically determined structures of **2-10** shown with 50% displacement ellipsoids. Only one of the two crystallographically-independent molecules of **2-10** is shown. With the exception of H1 and N-*H* atoms, all H atoms have been omitted for clarity.

Table 2-4. Selected interatomic distances (Å) and angles (º) for **2-10**.

Bond Lengths (Å)			
Ir-P1	2.2760(9)	Ir-H1	1.40(4)
Ir-P2	2.2823(9)	Ir-N	1.980(4)
Ir-Si	2.2808(10)		
Bond Angles (º)			
P1-Ir-P2	162.87(4)	Si-Ir-H1	66.2(17)
Si-Ir-N	138.93(13)	N-Ir-H1	154.7(17)

Note: Distances and angles of only one of the two crystallographically-independent molecules of **2-10** are given

Interestingly, **2-10** does not readily undergo N-H bond reductive elimination, even in arene solvents. No evidence for N-H bond reductive elimination was observed at room temperature or at 65 °C (72 h) when **2-10** was dissolved in arene solvents; only under forcing conditions (100 °C, 48 h, benzene-d_6) was NH_3 reductive elimination observed to cleanly generate [Cy-PSiP]Ir(D)(Ph-d_5).

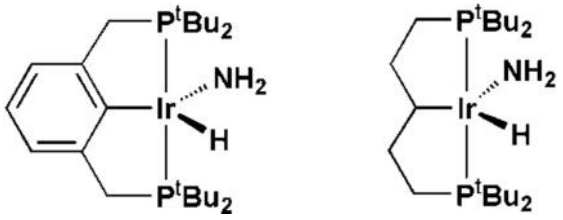

Figure 2-5. Previously reported amido hydride Ir complexes supported by PCP-type pincer ligands

Comparison of **2-10** to other late transition metal parent amido hydride complexes is limited to a $(DMPE)_2Ru(H)(NH_2)$ synthesized by salt metathesis,[63b] and two PCP-type pincer complexes (Figure 2-5), both of which appear to be significantly more susceptible to N-H bond reductive elimination than **2-10**. Hartwig and co-workers reported the generation of [^{t}Bu-PCP]Ir(H)(NH_2) by dehydrohalogenation of [^{t}Bu-PCP]Ir(H)(Cl)(NH_3) with $KN(SiMe_3)_2$; this complex was found to undergo N–H bond reductive elimination above -10 ºC in THF solution to form [^{t}Bu-PCP]Ir(NH_3).[39] In a subsequent study, Hartwig and co-workers also synthesized [$CH(CH_2CH_2P^tBu_2)_2$]Ir(H)(NH_2) via ammonia N–H bond oxidative addition.[38a] While the latter complex is stable in alkane and ethereal solvents at room temperature, in benzene-d_6 solution [$CH(CH_2CH_2P^tBu_2)_2$]Ir(H)(NH_2) undergoes deuterium incorporation into the backbone methine position of the pincer ligand, possibly via a mechanism involving N-H reductive elimination.[64] Furthermore, a mixture of [$CH(CH_2CH_2P^tBu_2)_2$]Ir(H)(NH_2) and [$CH(CH_2CH_2P^tBu_2)_2$]Ir(1-pentene) was formed upon treatment of the latter with excess 1-pentene (Et_2O-d_{10} or benzene-d_6), indicating facile and reversible reductive elimination of ammonia.[38a] In contrast, when **2-10** was treated with an atmosphere of ethylene at room temperature in benzene-d_6 solution no reaction occurred. Furthermore, treatment of **2-10** with one equiv of PMe_3 led to the quantitative formation of [Cy-PSiP]Ir(H)(NH_2)(PMe_3) (**2-10·PMe$_3$**; ^{1}H and ^{31}P NMR). Surprisingly, attempts to isolate this complex led to loss of PMe_3 (rather than N–H reductive elimination) to reform **2-10** upon exposure to vacuum (Scheme 2-6). These observations suggest that [Cy-PSiP] ligation is capable of significantly stabilizing amido hydride complexes from N–H bond reductive elimination.

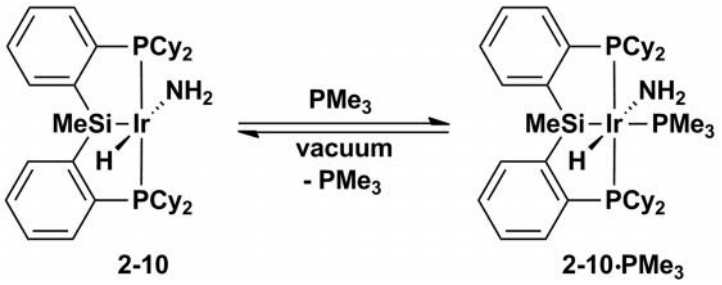

Scheme 2-6. Synthesis of [Cy-PSiP]Ir(H)(NH_2)(PMe_3) (**2-10·PMe$_3$**)

2.2.4 Generation of [Cy-PSiP]Ir(H)(NHR) through N-H Bond Activation

As previously described in Chapter 1, electron rich late metal centers are viable candidates for amine N-H bond activation by oxidative addition. Having shown that amido hydride complexes of the type [Cy-PSiP]M(H)(NHR) (M = Rh, Ir) are readily synthesized and are isolable, it seemed feasible that such complexes may be generated by N-H bond oxidative addition of the corresponding amine to *in situ* generated "[Cy-PSiP]M" (Scheme 2-7).

Toward these ends, [Cy-PSiP]Ir(H)Cl (**2-1**) was first treated with one equiv of Me_3SiCH_2Li in cyclohexane-d_{12} solution. An immediate color change from yellow to orange was observed and monitoring of the reaction mixture by ^{31}P and ^{1}H NMR spectroscopy indicated that **2-1** was completely consumed and an equivalent of Me_4Si was generated. The $^{31}P\{^{1}H\}$ NMR spectrum of the reaction mixture featured a very broad resonance at 56.2 ppm, consistent with formation of the product of C-H reductive elimination (*vide supra*). The reaction mixture was then treated with one equiv of H_2NPh. Subsequent heating at 65 ºC for 16 h led to quantitative formation of [Cy-PSiP]Ir(H)(NHPh) (**2-6**) (^{1}H and ^{31}P NMR). Using this N-H bond activation pathway, this reaction was also conducted on a preparative scale and **2-6** was cleanly isolated as an orange solid in 96% yield by this route.

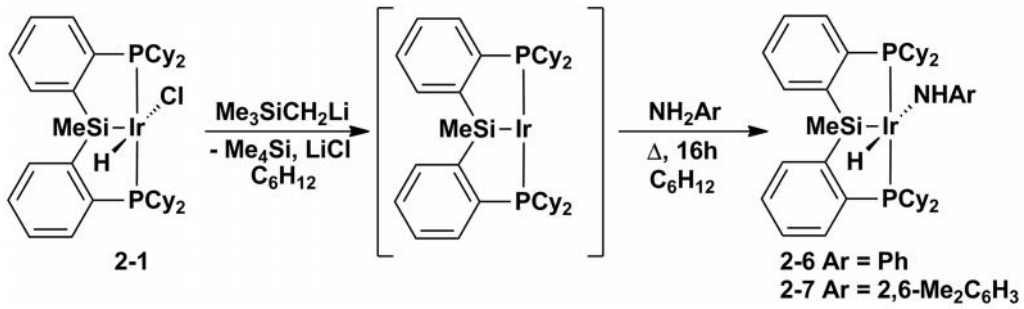

Scheme 2-7. Synthesis of [Cy-PSiP]Ir(H)(NHAr) through N-H bond activation of H_2NAr

A similar N-H bond activation route was also utilized for the preparation of the more sterically hindered anilido hydride complex **2-7**. Complex **2-7** was obtained by following a procedure similar to that used to synthesize **2-6**, with quantitative conversion obtained (^{31}P and ^{1}H NMR) after 72 h of heating at 65 ºC using 20 equiv of $H_2N(2,6\text{-}Me_2C_6H_3)$ in cyclohexane-d_{12} solution.

Given that **2-6** was readily accessed via N-H bond activation of aniline in cyclohexane solution, the analogous reaction in benzene solution was also pursued in order to determine if C–H bond activation of the solvent would be competitive with aniline N–H bond activation. Consequently, when **2-1** was reacted with Me_3SiCH_2Li in benzene-d_6 at room temperature, ^{1}H and ^{31}P NMR spectroscopy indicated the formation of Me_4Si and [Cy-PSiP]Ir(D)(Ph-d_5), which had previously been observed.[15b] When this reaction mixture was treated *in situ* with one equiv of H_2NPh, 35% conversion to **2-6** was observed (^{1}H and ^{31}P NMR) after 72 h of heating at 65 ºC, and quantitative conversion was not attained even after 168 h of heating at this temperature. By comparison, when 20 equiv of H_2NPh were utilized in this reaction, quantitative conversion to **2-6** (^{1}H and ^{31}P NMR) was obtained after 70 h of heating at 65 ºC. The observed reactivity in benzene solution suggests that although C-H bond activation competes with N-H bond activation under these conditions, the thermodynamics of N–H bond activation are more favourable than arene C–H bond activation. This observation is in agreement with previous examples involving PCP-type Ir pincer systems, in which the N-H bond cleavage product

was also thermodynamically preferred.[39,41] However, as described earlier in this document, the [Cy-PSiP] pincer complexes described herein are substantially more resistant to reductive elimination in the presence of benzene than the previously reported PCP systems. The resistance of [Cy-PSiP]Ir(H)(NH_2R) species to N-H bond reductive elimination is noteworthy and may play an important role in further developing the chemistry of such complexes.

2.2.5 Generation of [Cy-PSiP]Ir(H)(NH_2) through N-H Bond Activation

Having shown that [Cy-PSiP]Ir species are able to mediate N-H bond cleavage of anilines, including sterically hindered anilines, ammonia N-H bond activation was pursued as a route to prepare the parent amido hydride complex [Cy-PSiP]Ir(H)(NH_2) (**2-10**). Prior to this work, only one example of an isolable, monomeric late transition metal $L_nM(H)(NH_2)$ species obtained from oxidative addition of N-H bonds in ammonia had been reported, as highlighted in Chapter 1.[38a]

Treatment of **2-1** with one equiv of Me_3SiCH_2Li in cyclohexane-d_{12} solution led to the formation of Me_4Si and complete consumption of **2-1** (^{1}H and ^{31}P NMR), as has been previously documented. The reaction mixture was subsequently degassed via three freeze-pump-thaw cycles and an excess of anhydrous gaseous ammonia (ca. 1 atm) was introduced (Scheme 2-8). Although no initial reaction was observed at room temperature, heating at 65 ºC for 14 h led to 72% conversion to **2-10**, as evidenced by solution NMR data. The ^{31}P NMR spectrum of the reaction mixture exhibited a single resonance at 55.5 ppm, consistent with the formation of **2-10**. The ^{1}H NMR spectrum of the product also matched that of the previously prepared **2-10**, featuring a hydride resonance at -20.13 ppm (t, $^2J_{HP}$ = 15 Hz), and a broad triplet at 5.03 ppm ($^3J_{HP}$ = 6 Hz) which corresponded to the Ir-NH_2 protons. In a preparative scale experiment, **2-10** was obtained as a yellow solid in 69% yield by this ammonia N–H bond activation pathway.

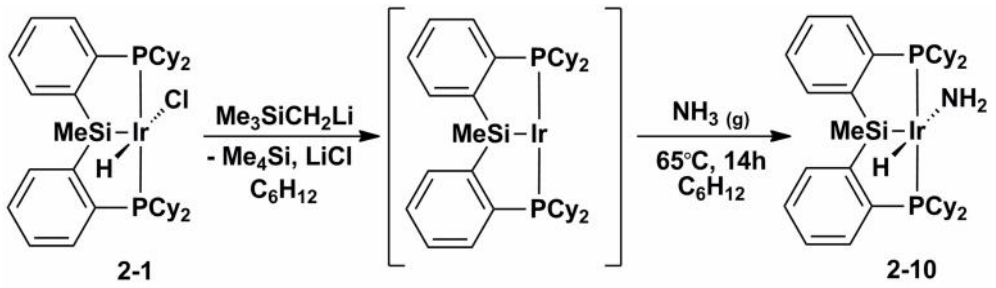

Scheme 2-8. Synthesis of [Cy-PSiP]Ir(H)(NH_2) (**2-10**) via N-H bond activation of ammonia

The N-H bond activation of ammonia was also pursued in benzene solution in order to determine if C-H bond activation of the solvent would compete with N-H bond activation of ammonia. Thus, treatment of **2-1** with Me_3SiCH_2Li in benzene-d_6 at room temperature led to the formation of Me_4Si and [Cy-PSiP]Ir(D)(Ph-d_5) (^{1}H and ^{31}P NMR), as previously documented. This reaction mixture was subsequently degassed via three freeze-pump-thaw cycles and treated with ca. 1 atm of anhydrous gaseous ammonia. After heating for 144 h at 65 ºC, 45% conversion to **2-10** was observed (^{31}P and ^{1}H-NMR). Further heating led to multiple unidentified products and no further conversion to **2-10**. These results indicate that ammonia N-H bond activation is indeed competitive with sp^2-C-H bond activation and demonstrate a rare example of ammonia N-H bond cleavage in the presence of a large excess of relatively reactive sp^2-hybridized benzene C-H bonds. The relative stability of isolated **2-10** in benzene solution (*vide supra*) is noteworthy, and may play an important role in developing the reactivity of such N-H bond activation products.

2.2.6 Generation of Rh^I species of the type [Cy-PSiP]Rh(NH_2R)

In an effort to extend the N-H bond cleavage chemistry observed for [Cy-PSiP]Ir to Rh, analogous reactions utilizing [Cy-PSiP]Rh species were carried out utilizing both anilines as well as ammonia. However, attempts to form amido hydride N–H bond

activation products led instead to the apparent generation of Rh^I amine adducts (Scheme 2-9).

Treatment of [Cy-PSiP]Rh(H)Cl (**2-2**) with one equiv of Me_3SiCH_2Li in cyclohexane-d_{12} solution resulted in an immediate colour change from yellow to red-orange. The ^1H and ^{31}P NMR spectra of the reaction mixture indicated the full consumption of **2-2** along with the formation of one equiv of Me_4Si. Furthermore, a broad resonance was observed at 62.9 ppm ($^1J_{RhP}$ = 162 Hz) in the ^{31}P NMR spectrum of the reaction mixture, consistent with formation of a Rh^I product resulting from C-H reductive elimination from [Cy-PSiP]Rh(H)(CH_2SiMe_3) (*vide supra*). The reaction mixture was subsequently treated with 20 equiv of H_2NPh. This led to the quantitative generation (^1H and ^{31}P NMR) of a new Rh complex tentatively assigned as [Cy-PSiP]Rh(NH_2Ph) (**2-11**). The $^{31}P\{^1H\}$ NMR spectrum of **2-11** features a resonance at 54.7 ppm (d, $^1J_{RhP}$ = 182 Hz) corresponding to the symmetry equivalent phosphine donors of the [Cy-PSiP] ligand. The ^{13}C and ^1H-NMR spectra of **2-11** contain a single set of resonances for the aromatic ligand backbone, consistent with a C_s symmetric complex. The ^1H NMR spectrum of **2-11** does not feature a hydride resonance, which is consistent with the absence of N-H bond oxidative addition to Rh. Subsequent heating of **2-11** at 65 ºC for 72 h led to only ca. 25% conversion to the anilido hydride complex **2-8**. Unfortunately, the isolation of **2-11** was prevented by decomposition of the complex upon exposure to vacuum to remove excess aniline.

Similarly, when ca. 1 atm of anhydrous gaseous ammonia was added to a degassed solution of in situ generated [Cy-PSiP]Rh^I, a new product tentatively assigned as the ammonia adduct [Cy-PSiP]Rh(NH_3) (**2-12)** was observed to form quantitatively (^1H and ^{31}P NMR, Scheme 2-9). The $^{31}P\{^1H\}$ NMR spectrum of the reaction mixture containing **2-12** features a single resonance at 54.4 ppm (d, $^1J_{RhP}$ = 180 Hz), which corresponds to the symmetry equivalent phosphine donors of the [Cy-PSiP] ligand. The ^{13}C and ^1H-NMR spectra of **2-12** feature a single set of peaks for the aromatic ligand backbone, consistent with the formation of a C_s-symmetric complex. Furthermore, the

^{1}H NMR spectrum of **2-12** does not contain a Rh-hydride resonance, consistent with the formation of an ammonia adduct, as opposed to an amido hydride Rh complex. As in the case of **2-11**, the isolation of **2-12** was prevented by decomposition upon exposure to vacuum. Subsequent heating of **2-12** at 65 °C for 48 h did not lead to further reaction.

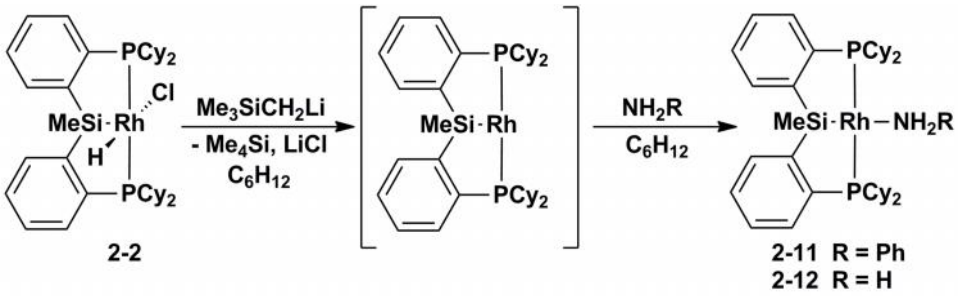

Scheme 2-9. Generation of Rh^I amine adducts [Cy-PSiP]Rh(NH_2R) (R = Ph, H)

Given that complexes of the type [Cy-PSiP]Rh(H)(NHR) have proven isolable from salt metathesis reactions involving lithium amide reagents and [Cy-PSiP]Rh(H)Cl, the observation that amine adducts are formed upon reacting *in situ* generated [Cy-PSiP]Rh^I with aniline and ammonia suggests that the barrier to N-H bond oxidative addition is prohibitively high in the case of Rh.

2.3 Preliminary Investigations into the Mechanism of Ir-Mediated N–H Bond Activation

There are various possible mechanisms for the formation of amido hydride complexes from the reaction of anilines and ammonia with a [Cy-PSiP]Ir species. For example, a possible mechanistic pathway leading to N-H bond cleavage may involve a 14-electron [Cy-PSiP]Ir^I intermediate (or an agostic analogue) generated by the reductive elimination of alkane from [Cy-PSiP]Ir(H)(alkyl); this [Cy-PSiP]Ir^I can, in turn, oxidatively add the N-H bond of aniline or ammonia. Alternatively, intramolecular C-H bond activation of a P*Cy* substituent by [Cy-PSiP]Ir^I may occur, leading to the formation

of a cyclometalated Ir^{III} intermediate that can, in turn, react with an N-H bond to generate the observed amido hydride product.

In an effort to begin to understand the mechanism of [Cy-PSiP]Ir-mediated N-H bond cleavage, preliminary ^2H labelling experiments utilizing ammonia-d_3 were carried out. Treatment of **2-1** with NpLi in cyclohexane-d_{12} solution led to the rapid reductive elimination of NpH, as has been previously documented. Subsequent reaction of the degassed mixture with ca. 1 atm of ammonia-d_3 led to the quantitative formation of [Cy-PSiP]Ir(D)(ND_2) (**2-10-*d*$_3$**) after 20 h of heating at 65 ºC (^1H and ^{31}P NMR). ^2H NMR analysis of the reaction mixture in benzene solution indicated that deuterium incorporation had occurred exclusively at the hydride (-20.13 ppm) and amide positions (5.03 ppm). Moreover, no deuterium incorporation into the ligand P*Cy*$_2$ fragments was observed. These results are consistent with a reaction pathway involving a [Cy-PSiP]Ir^I 14 e^- intermediate, or a reactive equivalent such as an agostic species (Scheme 2-10). Coordination of ammonia to such a [Cy-PSiP]Ir^I intermediate was not directly observed, however there is indirect evidence for the formation of such an intermediate from related [Cy-PSiP]Rh chemistry (*vide supra*). The intermediate [Cy-PSiP]Ir(NH_3) could then undergo N-H bond oxidative addition to generate **2-10** (Scheme 2-10). The proposal of a 14 e^- [Cy-PSiP]Ir^I reactive intermediate agrees with previous results involving sp^2-C–H bond activation by [Cy-PSiP]Ir (*vide supra*). Related 14 e^- (PCP)M^I species (M = Rh or Ir) have also been proposed as reactive intermediates in E-H bond activation reactions.[26,28,34,35,38a,41,54,56]

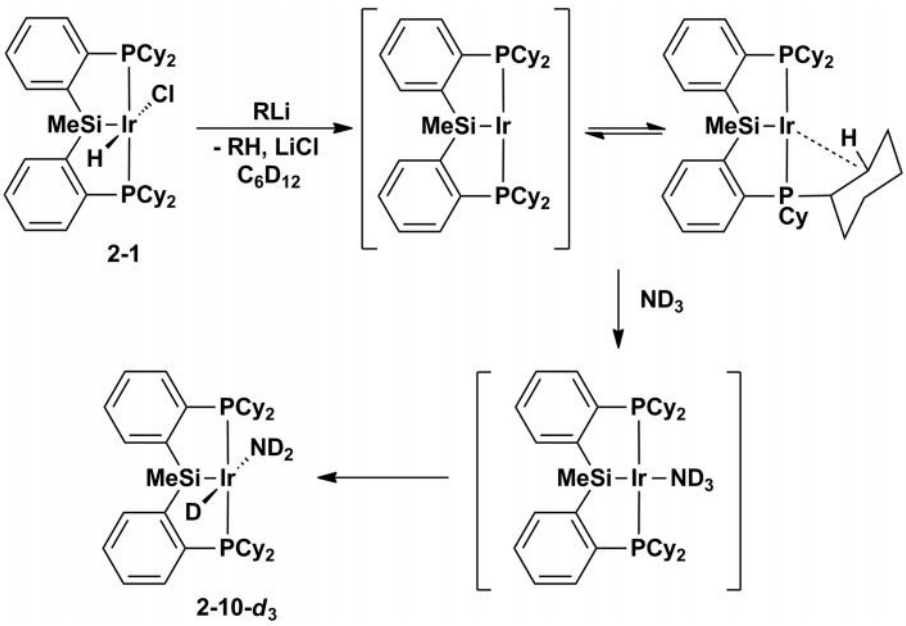

Scheme 2-10. Proposed mechanism for the formation of [Cy-PSiP]Ir(D)(ND_2) (**2-10-d_3**) through oxidative addition of ND_3 via a [Cy-PSiP]Ir^I intermediate

The reaction of **2-10** with an atmosphere of ammonia-d_3 was also carried out in order to assess whether [Cy-PSiP]Ir(H)(NH_2) underwent exchange with free ammonia. After 14 h at room temperature in cyclohexane-d_{12} solution, ^2H incorporation was observed exclusively at the Ir-NH_2 position (^1H and ^2H NMR). These results suggest that this exchange process likely does not occur by a simple reductive elimination of NH_3 followed by oxidative addition of ND_3. A possible mechanism might involve coordination of ND_3 to **2-10**, followed by deprotonation of the coordinated ND_3 by the NH_2 ligand (Scheme 2-11). Subsequent loss of NH_2D from the Ir coordination sphere would generate the observed product.

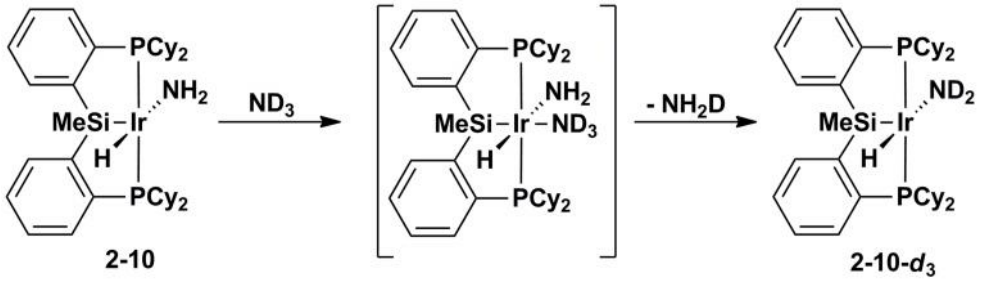

Scheme 2-11. Possible mechanism for reaction of [Cy-PSiP]Ir(H)(NH_2) with ND_3

2.4 Conclusions

The work discussed in this chapter highlights the continuing study of new bis(phosphino)silyl Rh and Ir pincer complexes, including their ability to activate E-H bonds. Specifically, previous work showed that the [Cy-PSiP] pincer framework was capable of supporting Ir complexes that underwent remarkably facile sp^2-C-H bond activation through a [Cy-PSiP]Ir^I reactive intermediate. This work showcased the utility of this reactive intermediate in effecting the N-H bond activation of anilines as well as a rare example of ammonia N-H bond activation under relatively mild conditions to form complexes of the type [Cy-PSiP]Ir(H)(NHR). These complexes were shown to be more resistant to N-H bond reductive elimination in the presence of alkenes and arenes, relative to their (PCP)Ir counterparts, emphasizing the unique reactivity properties imparted by a silyl pincer ligand. The example of ammonia N-H bond activation presented is exceedingly rare, and may provide inroads to new atom-economical chemical transformations that incorporate N-H bond oxidative addition steps in the functionalization of this abundant feedstock.

2.5 Experimental Section

2.5.1 General Considerations

All experiments were conducted under nitrogen in an MBraun glovebox or using standard Schlenk techniques. Dry, oxygen-free solvents were used unless otherwise indicated. All non-deuterated solvents were deoxygenated and dried by sparging with nitrogen and subsequent passage through a double-column solvent purification system purchased from MBraun Inc. Tetrahydrofuran and diethyl ether were purified over two activated alumina columns, while benzene, toluene, and pentane were purified over one activated alumina column and one column packed with activated Q-5. All purified solvents were stored over 4 Å molecular sieves. Benzene-d_6 and cyclohexane-d_{12} were degassed via three freeze-pump-thaw cycles and stored over 4 Å molecular sieves. The compounds [Cy-PSiP]Rh(H)Cl,[15b] [Cy-PSiP]Ir(H)Cl,[15b] Me_3SiCH_2Li,[65] $PhCH_2K$,[66] and

NpLi[67] were prepared according to literature procedures. Anhydrous ammonia and ethylene were purchased from Air Liquide Canada and used as received. All other reagents, including ammonia-d_3 were purchased from Aldrich and used without further purification. Unless otherwise stated, ^{1}H, ^{13}C, ^{31}P NMR, ^{15}N, and ^{29}Si characterization data were collected at 300K on a Bruker AV-500 spectrometer operating at 500.1, 125.8, 202.5, 50.7 and 99.4 MHz (respectively) with chemical shifts reported in parts per million downfield of $SiMe_4$ (for ^{1}H, ^{13}C, and ^{29}Si), $MeNO_2$ (for ^{15}N), or 85% H_3PO_4 in D_2O (for ^{31}P). ^{1}H and ^{13}C NMR chemical shift assignments are based on data obtained from ^{13}C-DEPTQ, ^{1}H-^{1}H COSY, ^{1}H-^{13}C HSQC, and ^{1}H-^{13}C HMBC NMR experiments. ^{29}Si NMR assignments are based on ^{1}H-^{29}Si HMQC and ^{1}H-^{29}Si HMBC experiments. ^{15}N NMR assignments are based on ^{1}H-^{15}N HMQC experiments. In some cases, fewer than expected unique ^{13}C NMR resonances were observed, despite prolonged acquisition times. Elemental analyses were performed by Canadian Microanalytical Service Ltd. of Delta, British Columbia, Canada and by Columbia Analytical Services of Tucson, Arizona. Infrared spectra were recorded as Nujol mulls between NaCl plates using a Bruker VECTOR 22 FT-IR spectrometer at a resolution of 4 cm^{-1}. X-ray data collection, solution, and refinement were carried out by Drs. Robert MacDonald and Michael J. Ferguson at the University of Alberta X-ray Crystallography Laboratory, Edmonton, Alberta.

2.5.2 Synthetic Details and Characterization Data

[Cy-PSiP]Ir(C_2H_4) (2-3). A solution of **2-1** (0.100 g, 0.122 mmol) in ca. 10 mL of cyclohexane was treated with Me_3SiCH_2Li (0.012 g, 0.122 mmol). The resulting orange solution was transferred to a resealable thick-walled glass vessel equipped with a Teflon stopcock and was degassed by three freeze-pump-thaw cycles. The vessel was then charged with ca. 1 atm ethylene gas, and the resulting reaction mixture was heated at 65 °C for 16 h. The volatile components were subsequently removed under vacuum, the residue was extracted with ca. 10 mL of cyclohexane, and the extract was filtered through

Celite. The filtrate was dried in vacuo, and the remaining residue was triturated with pentane (3 × 5 mL) to afford **2-3** as an orange powder (0.088 g, 89%). ^{1}H NMR (500 MHz, benzene-d_6): δ 8.24 (d, 2 H, J = 7 Hz, H_{arom}), 7.52 (m, 2 H, H_{arom}), 7.32 (t, 2 H, J = 7 Hz, H_{arom}), 7.18 (t, 2 H, J = 7 Hz, H_{arom}), 2.68 (s, 4 H, C_2H_4), 2.59 (m, 4 H, P*Cy*), 2.05 – 1.98 (overlapping resonances, 6 H, P*Cy*), 1.73 – 1.04 (overlapping resonances, 30 H, P*Cy*), 0.88 – 0.79 (overlapping resonances, 7 H, P*Cy* + Si*Me*; Si*Me* at 0.86 ppm). ^{13}C{^{1}H} NMR (125.8 MHz, benzene-d_6): δ 160.1 (m, C_{arom}), 145.4 (m, C_{arom}), 132.8 (apparent t, J = 12 Hz, CH_{arom}), 130.0 (CH_{arom}), 129.6 (CH_{arom}), 127.3 (CH_{arom}), 41.0 (apparent t, J = 14 Hz, CH_{Cy}), 37.1 (C_2H_4), 36.4 (apparent t, J = 16 Hz, CH_{Cy}), 30.9 (CH_{2Cy}), 30.4 (CH_{2Cy}), 29.8 (CH_{2Cy}), 29.6 (CH_{2Cy}), 28.6 – 27.2 (overlapping resonances, CH_{2Cy}), 6.4 (Si*Me*). ^{31}P{^{1}H} NMR (202.5 MHz, benzene-d_6): δ 65.4. ^{29}Si NMR (99.4 MHz, benzene-d_6): δ 60.1. Anal. Calcd for $C_{39}H_{59}P_2IrSi$: C, 57.82; H, 7.34. Found: C, 57.58; H, 7.28.

[Cy-PSiP]Ir(PMe$_3$) (2-4). Method 1: A solution of **2-1** (0.050 g, 0.061 mmol) in ca. 10 mL of benzene was treated with Me_3SiCH_2Li (0.006 g, 0.061 mmol). The reaction mixture was subsequently treated with PMe_3 (6.3 μL, 0.005 g, 0.061 mmol), and allowed to stand at room temperature for 20 minutes, over the course of which the solution turned dark red in color. The reaction mixture was filtered through Celite and the filtrate solution was evaporated to dryness. The remaining residue was triturated with pentane (3 × 5 mL) to afford **2-4** as a dark red solid (0.040 g, 77%). **Method 2:** A solution of Me_3SiCH_2Li (0.0011 g, 0.012 mmol) in ca. 0.4 mL of cyclohexane-d_{12} was added to a solution of **2-1** (0.010 g, 0.012 mmol) in ca. 0.4 mL of cyclohexane-d_{12}. An immediate color change from yellow to orange was observed. The reaction mixture was analyzed by ^{1}H and ^{31}P NMR spectroscopy to confirm the complete consumption of [Cy-PSiP]Ir(H)Cl and the formation of 1 equiv. of Me_4Si. The reaction mixture was subsequently treated with PMe_3 (1.3 μL, 0.001 g, 0.012 mmol), and allowed to stand at room temperature for 20 minutes, over the course of which the solution turned dark red in color. ^{1}H and ^{31}P NMR analysis of the reaction mixture indicated the quantitative

formation of **2-4**. ^{1}H NMR (500 MHz, benzene-d_6): δ 8.41 (d, 2 H, J = 7 Hz, H_{arom}), 7.60 (m, 2 H, H_{arom}), 7.36 (t, 2 H, J = 7 Hz, H_{arom}), 7.23 (t, 2 H, J = 7 Hz, H_{arom}), 2.68 (m, 2 H, P*Cy*), 2.22 (br d, 2 H, J = 13 Hz, P*Cy*), 2.11 – 1.12 (overlapping resonances, 49 H, P*Cy* + P*Me*$_3$; P*Me*$_3$ at 1.53 ppm, d, $^{2}J_{HP}$ = 6 Hz), 0.95 (s, 3 H, Si*Me*). ^{13}C{^{1}H} NMR (125.8 MHz, benzene-d_6): δ 160.8 (m, C_{arom}), 147.8 (m, C_{arom}), 133.1 (apparent t, J = 11 Hz, CH$_{arom}$), 130.2 (CH$_{arom}$), 129.5 (CH$_{arom}$), 126.9 (CH$_{arom}$), 42.2 (apparent t, J = 10 Hz, CH$_{Cy}$), 37.7 (apparent t, J = 15 Hz, CH$_{Cy}$), 31.9 (CH$_{2Cy}$), 31.0 (CH$_{2Cy}$), 30.1 – 27.0 (overlapping resonances, CH$_{2Cy}$), 25.2 (d, $^{1}J_{CP}$ = 20 Hz, P*Me*$_3$), 8.7 (Si*Me*). ^{31}P{^{1}H} NMR (202.5 MHz, benzene-d_6): δ 70.6 (d, $^{2}J_{PP}$ = 7 Hz, Cy-*P*Si*P*), -21.2 (t, $^{2}J_{PP}$ = 7 Hz, *P*Me$_3$). ^{29}Si NMR (99.4 MHz, benzene-d_6): δ 68.0. Anal. Calcd for $C_{40}H_{64}P_3IrSi$: C, 55.98; H, 7.52. Found: C, 55.57; H, 7.27.

[Cy-PSiP]Rh(PMe$_3$) (2-5). Method 1: A solution of **2-2** (0.060 g, 0.082 mmol) in ca. 7 mL of THF was treated with PMe$_3$ (8.5 μL, 0.006 g, 0.082 mmol), and the resulting reaction mixture was allowed to stir at room temperature for ca. 30 min. A solution of PhCH$_2$K (0.011 g, 0.082 mmol) in ca. 3 mL of THF was then added to the reaction mixture at room temperature. A color change to dark red was observed. The volatile components of the reaction mixture were removed under vacuum and the remaining residue was extracted with ca. 10 mL of benzene. The benzene extract was filtered through Celite and evaporated to dryness. The residue was washed with 3 × 5 mL of pentane and dried in vacuo to afford **2-5** as a red solid (0.035 g, 56%). **Method 2:** A solution of Me$_3$SiCH$_2$Li (0.0013 g, 0.014 mmol) in ca. 0.4 mL of cyclohexane-d_{12} was added to a solution of **2-2** (0.010 g, 0.014 mmol) in ca. 0.4 mL of cyclohexane-d_{12}. An immediate color change from yellow to red-orange was observed. The reaction mixture was analyzed by ^{1}H and ^{31}P NMR spectroscopy to confirm the complete consumption of [Cy-PSiP]Rh(H)Cl and the formation of 1 equiv. of Me$_4$Si. Neat PMe$_3$ (1.4 μL, 0.0011 g, 0.014 mmol) was added to the reaction mixture, resulting in an immediate color change to dark red. At this point ^{1}H and ^{31}P NMR analysis of the reaction mixture indicated the quantitative formation of **2-5**. ^{1}H NMR (500 MHz, benzene-d_6): δ 8.34 (d, 2 H, J = 7 Hz,

H_{arom}), 7.58 (d, 2 H, J = 7 Hz, H_{arom}), 7.36 (t, 2 H, J = 7 Hz, H_{arom}), 7.24 (t, 2 H, J = 7 Hz, H_{arom}), 2.45 (m, 2 H, P*Cy*), 2.17 – 1.09 (overlapping resonances, 49 H, P*Cy* + P*Me*$_3$; P*Me*$_3$ at 1.38 ppm, d, $^2J_{HP}$ = 3 Hz), 0.91 (s, 3 H, Si*Me*), 0.86 (m, 2 H, P*Cy*). $^{13}C\{^1H\}$ NMR (125.8 MHz, benzene-d_6): δ 160.8 (m, C_{arom}), 147.2 (m, C_{arom}), 133.0 (apparent t, J = 12 Hz, CH_{arom}), 130.3 (CH_{arom}), 129.3 (CH_{arom}), 126.9 (CH_{arom}), 41.1 (apparent t, J = 7 Hz, CH_{Cy}), 37.6 (apparent t, J = 11 Hz, CH_{Cy}), 32.4 (CH_{2Cy}), 31.3 (CH_{2Cy}), 30.9 (CH_{2Cy}), 29.6 (CH_{2Cy}), 28.7 (CH_{2Cy}), 27.8 – 27.5 (overlapping resonances, CH_{2Cy}), 27.1 (CH_{2Cy}), 23.5 (d, $^1J_{CP}$ = 12 Hz, P*Me*$_3$), 9.6 (Si*Me*). $^{31}P\{^1H\}$ NMR (202.5 MHz, benzene-d_6): δ 70.8 (dd, 2 P, $^1J_{PRh}$ = 166 Hz, $^2J_{PP}$ = 22 Hz, Cy-*P*Si*P*), -33.1 (dt, 1 P, $^1J_{PRh}$ = 128 Hz, $^2J_{PP}$ = 22 Hz, *P*Me$_3$). ^{29}Si NMR (99.4 MHz, benzene-d_6): δ 69.7. Anal. Calcd for $C_{40}H_{64}P_3RhSi$: C, 62.49; H, 8.39. Found: C, 62.24; H, 8.18. X-Ray quality crystals of **2-5** were grown from a concentrated benzene solution at room temperature.

[Cy-PSiP]Ir(H)(NHPh) (2-6). Method 1: A solution of LiNHPh (0.010 g, 0.098 mmol) in ca. 5 mL of THF was added dropwise via pipette to a solution of **2-1** (0.080 g, 0.098 mmol) in ca. 5 mL of THF at room temperature. An immediate color change from yellow to red was observed. The reaction mixture was evaporated to dryness, and the remaining residue was extracted with ca. 10 mL of benzene. The benzene extract was filtered through Celite and the filtrate was dried under vacuum. The remaining solid residue was triturated with pentane (3 × 5 mL) to afford **2-6** as a red solid (0.069 g, 80%). **Method 2** - *NMR-scale***:** A solution of Me_3SiCH_2Li (0.0011 g, 0.012 mmol) in ca. 0.4 mL of cyclohexane-d_{12} was added to a solution of [Cy-PSiP]Ir(H)Cl (0.010 g, 0.012 mmol) in ca. 0.4 mL of cyclohexane-d_{12}. An immediate color change from yellow to orange was observed. The reaction mixture was analyzed by ^{1}H and ^{31}P NMR spectroscopy to confirm the complete consumption of [Cy-PSiP]Ir(H)Cl and the formation of 1 equiv. of Me_4Si. Aniline (1.1 μL, 0.0011 g, 0.012 mmol) was added to the reaction mixture, and the solution was heated at 65 °C for 16 h, at which point ^{1}H and ^{31}P NMR analysis of the reaction mixture indicated the quantitative formation of **2-6**. **Method 2** – *preparative-scale***:** A solution of Me_3SiCH_2Li (0.0046 g, 0.049 mmol) in ca.

2 mL of cyclohexane was added to a solution of [Cy-PSiP]Ir(H)Cl (0.040 g, 0.049 mmol) in ca. 5 mL of cyclohexane. An immediate color change from yellow to orange was observed. An aliquot of the reaction mixture was analyzed by ^{1}H and ^{31}P NMR spectroscopy to confirm the complete consumption of [Cy-PSiP]Ir(H)Cl and the formation of 1 equiv. of Me_4Si. Aniline (4.5 μL, 0.0046 g, 0.049 mmol) was added to the reaction mixture, and the solution was heated at 65 °C for 16 h, at which point ^{1}H and ^{31}P NMR analysis of the reaction mixture indicated the quantitative formation of **2-6**. The reaction mixture was evaporated to dryness, and the remaining residue was extracted with ca. 10 mL of benzene. The benzene extract was filtered through Celite and the filtrate was dried under vacuum. The remaining solid residue was triturated with pentane (3 × 5 mL) to afford **2-6** as a red solid (0.041 g, 96%). **Method 3:** A solution of Me_3SiCH_2Li (0.0011 g, 0.012 mmol) in ca. 0.4 mL of benzene-d_6 was added to a solution of [Cy-PSiP]Ir(H)Cl (0.010 g, 0.012 mmol) in ca. 0.4 mL of benzene-d_6. An immediate color change from yellow to orange was observed. The reaction mixture was analyzed by ^{1}H and ^{31}P NMR spectroscopy to confirm the complete consumption of [Cy-PSiP]Ir(H)Cl and the formation of 1 equiv. of Me_4Si. Aniline (22.0 μL, 0.022 g, 0.240 mmol) was added to the reaction mixture, and the solution was heated at 65 °C for 70 h, at which point ^{1}H and ^{31}P NMR analysis of the reaction mixture indicated the quantitative formation of **2-6**. ^{1}H NMR (500 MHz, benzene-d_6): δ 8.10 (d, 2 H, J = 7 Hz, H_{arom}), 7.44 (m, 2 H, H_{arom}), 7.26 – 7.17 (overlapping resonances, 6 H, H_{arom}), 7.11 (t, 2 H, J = 7 Hz, H_{arom}), 6.90 (br t, 1 H, $^{3}J_{HP}$ = 4 Hz, N*H*), 6.84 (t, 1 H, J = 7 Hz, H_{arom}), 2.61 (m, 2 H, P*Cy*), 2.47 (br t, 2 H, J = 12 Hz, P*Cy*), 2.32 (br d, 2 H, J = 13 Hz, P*Cy*), 2.07 – 1.10 (overlapping resonances, 34 H, P*Cy*), 0.89 (s, 3 H, Si*Me*), 0.77 (m, 4 H, P*Cy*), -21.16 (t, 1 H, $^{2}J_{HP}$ = 17 Hz, Ir*H*). ^{1}H NMR (500 MHz, cyclohexane-d_{12}): δ 7.99 (d, 2 H, J = 7 Hz, H_{arom}), 7.47 (m, 2 H, H_{arom}), 7.21 (t, 2 H, J = 7 Hz, H_{arom}), 7.12 (t, 2 H, J = 7 Hz, H_{arom}), 6.91 (t, 2 H, J = 7 Hz, H_{arom}), 6.75 (d, 2 H, J = 7 Hz, H_{arom}), 6.55 – 6.52 (overlapping resonances, 2 H, H_{arom} + N*H*), 2.64 (m, 2 H, P*Cy*), 2.33 (br t, 2 H, J = 12 Hz, P*Cy*), 2.09 (br d, 2 H, J = 12 Hz, P*Cy*), 2.04 – 0.88 (overlapping resonances, 36 H, P*Cy*), 0.59 (m, 2

H, P*Cy*), 0.41 (s, 3 H, Si*Me*), -21.22 (t, 1 H, $^{2}J_{HP}$ = 17 Hz, Ir*H*). $^{13}C\{^{1}H\}$ NMR (125.8 MHz, benzene-d_6): δ 165.0 (C_{arom}), 159.3 (m, C_{arom}), 144.4 (m, C_{arom}), 132.4 (apparent t, J = 9 Hz, CH_{arom}), 130.9 (CH_{arom}), 129.5 (CH_{arom}), 129.1 (CH_{arom}), 127.3 (CH_{arom}), 121.7 (CH_{arom}), 117.9 (CH_{arom}), 35.5 (apparent t, J = 16 Hz, CH_{Cy}), 33.5 (apparent t, J = 11 Hz, CH_{Cy}), 31.0 (CH_{2Cy}), 30.8 (CH_{2Cy}), 30.6 (CH_{2Cy}), 28.5 (CH_{2Cy}), 28.2 (CH_{2Cy}), 27.8 – 27.6 (overlapping resonances, CH_{2Cy}), 27.1 (CH_{2Cy}), 6.2 (Si*Me*). $^{31}P\{^{1}H\}$ NMR (202.5 MHz, benzene-d_6): δ 55.1. $^{31}P\{^{1}H\}$ NMR (202.5 MHz, cyclohexane-d_{12}): δ 55.3. ^{29}Si NMR (99.4 MHz, benzene-d_6): δ 13.3. ^{15}N NMR (50.7 MHz, benzene-d_6): δ -260.8. IR (Nujol, cm^{-1}): 3371 (br, w, N-H), 2134 (m, Ir-H). Anal. Calcd for $C_{43}H_{62}IrNP_2Si$: C, 59.01; H, 7.14; N, 1.60. Found: C, 59.38; H, 7.22; N, 1.48. X-Ray quality crystals of **2-6·OEt$_2$** were grown from a concentrated Et_2O solution at -30 °C.

[Cy-PSiP]Ir(H)[NH(2,6-Me$_2$C$_6$H$_3$)] (2-7). Method 1: A solution of LiNH(2,6-$Me_2C_6H_3$) (0.019 g, 0.150 mmol) in ca. 5 mL of THF was added dropwise via pipette to a solution of [Cy-PSiP]Ir(H)Cl (0.123 g, 0.150 mmol) in ca. 5 mL of THF at room temperature. An immediate color change from yellow to orange was observed. The reaction mixture was evaporated to dryness, and the remaining residue was extracted with ca. 10 mL of benzene. The benzene extract was filtered through Celite and the filtrate was dried under vacuum. The remaining solid residue was triturated with pentane (3 × 5 mL) to afford **2-7** as an orange solid (0.118 g, 87%). **Method 2:** A solution of Me_3SiCH_2Li (0.0011 g, 0.012 mmol) in ca. 0.4 mL of cyclohexane-d_{12} was added to a solution of [Cy-PSiP]Ir(H)Cl (0.010 g, 0.012 mmol) in ca. 0.4 mL of cyclohexane-d_{12}. An immediate color change from yellow to orange was observed. The reaction mixture was analyzed by ^{1}H and ^{31}P NMR spectroscopy to confirm the complete consumption of [Cy-PSiP]Ir(H)Cl and the formation of 1 equiv. of Me_4Si. Neat $H_2N(2,6\text{-}Me_2C_6H_3)$ (29.5 μL, 0.029 g, 0.240 mmol) was added to the reaction mixture, and the solution was heated at 65 °C for 72 h, at which point ^{1}H and ^{31}P NMR analysis of the reaction mixture indicated the quantitative formation of **2.7**. ^{1}H NMR (500 MHz, benzene-d_6): δ 8.13 (d, 2 H, J = 7 Hz, H_{arom}), 7.45 (m, 2 H, H_{arom}), 7.24 – 7.18 (overlapping resonances, 4 H,

H_{arom}), 7.12 (t, 2 H, J = 7 Hz, H_{arom}), 6.89 (t, 1 H, J = 7 Hz, H_{arom}), 5.98 (br t, 1 H, $^3J_{HP}$ = 5 Hz, N*H*), 2.67 (s, 3 H, 2,6-$Me_2C_6H_3$), 2.59 (s, 3 H, 2,6-$Me_2C_6H_3$), 2.50 (br t, 2 H, J = 12 Hz, P*Cy*), 2.30 (br d, 2 H, J = 13 Hz, P*Cy*), 1.96 – 1.12 (overlapping resonances, 38 H, P*Cy*), 0.94 (s, 3 H, Si*Me*), 0.69 (m, 2 H, P*Cy*), -21.94 (t, 1 H, $^2J_{HP}$ = 16 Hz, Ir*H*). $^{13}C\{^1H\}$ NMR (125.8 MHz, benzene-d_6): δ 162.9 (C_{arom}), 159.7 (apparent t, J = 21 Hz, C_{arom}), 144.9 (apparent t, J = 28 Hz, C_{arom}), 132.8 (apparent t, J = 21 Hz, C_{arom}), 132.4 (apparent t, J = 9 Hz, CH_{arom}), 131.2 (C_{arom}), 130.4 (CH_{arom}), 129.2 (CH_{arom}), 127.2 (CH_{arom}), 120.0 (CH_{arom}), 35.3 (apparent t, J = 16 Hz, CH_{Cy}), 34.0 (apparent t, J = 11 Hz, CH_{Cy}), 30.6 (CH_{2Cy}), 30.3 (CH_{2Cy}), 29.5 (CH_{2Cy}), 28.2 (CH_{2Cy}), 28.1 (CH_{2Cy}), 27.7 (CH_{2Cy}), 27.5 – 27.3 (overlapping resonances, CH_{2Cy}), 26.9 (CH_{2Cy}), 21.0 (2,6-$Me_2C_6H_3$), 20.9 (2,6-$Me_2C_6H_3$), 5.0 (Si*Me*). $^{31}P\{^1H\}$ NMR (202.5 MHz, benzene-d_6): δ 52.8. ^{29}Si NMR (99.4 MHz, benzene-d_6): δ 12.1. ^{15}N NMR (50.7 MHz, benzene-d_6): δ -265.0. IR (Nujol, cm^{-1}): 3377 (br, w, N-H), 2116 (m, Ir-H). Anal. Calcd for $C_{45}H_{66}IrNP_2Si$: C, 59.84; H, 7.36; N, 1.55. Found: C, 59.44; H, 7.49; N, 1.43. X-Ray quality crystals of **2-7** were grown from a concentrated pentane/THF solution at -30 °C.

[Cy-PSiP]Rh(H)(NHPh) (2-8). A solution of LiNHPh (0.011 g, 0.110 mmol) in ca. 5 mL of THF was added dropwise via pipette to a solution of [Cy-PSiP]Rh(H)Cl (0.080 g, 0.110 mmol) in ca. 5 mL of THF at room temperature. An immediate color change from light yellow to red was observed. The reaction mixture was evaporated to dryness, and the remaining residue was extracted with ca. 10 mL of benzene. The benzene extract was filtered through Celite and the filtrate was dried under vacuum. The remaining solid residue was triturated with pentane (3 × 5 mL) to afford **2-8** as a red-orange solid (0.077 g, 89%). ^1H NMR (500 MHz, benzene-d_6): δ 7.97 (d, 2 H, J = 7 Hz, H_{arom}), 7.40 (m, 2 H, H_{arom}), 7.25 – 7.21 (overlapping resonances, 4 H, H_{arom}), 7.14 (t, 2 H, J = 7 Hz, H_{arom}), 6.94 (d, 2 H, J = 7 Hz, NPh_{ortho}), 6.69 (t, 1 H, J = 7 Hz, NPh_{para}), 4.57 (s, 1 H, N*H*), 2.48 (m, 2 H, P*Cy*), 2.37 (m, 2 H, P*Cy*), 2.23 (m, 4 H, P*Cy*), 1.95 – 1.11 (overlapping resonances, 34 H, P*Cy*), 0.90 (m, 2 H, P*Cy*), 0.87 (s, 3 H, Si*Me*), -16.86 (apparent q, 1 H, $^2J_{HP} \sim {}^1J_{HRh}$ = 16 Hz, Rh*H*). $^{13}C\{^1H\}$ NMR (125.8 MHz, benzene-d_6): δ

164.0 (C_{arom}), 157.5 (m, C_{arom}), 142.0 (m, C_{arom}), 131.6 (apparent t, J = 10 Hz, CH_{arom}), 130.0 (CH_{arom}), 128.9 (CH_{arom}), 128.4 (CH_{arom}), 127.5 (CH_{arom}), 118.2 (NPh_{ortho}), 112.8 (NPh_{para}), 35.3 (apparent t, J = 12 Hz, CH_{Cy}), 33.7 (apparent t, J = 9 Hz, CH_{Cy}), 30.8 (CH_{2Cy}), 30.2 (CH_{2Cy}), 29.7 (CH_{2Cy}), 27.6 (CH_{2Cy}), 27.2 – 26.9 (overlapping resonances, CH_{2Cy}), 26.2 (CH_{2Cy}), 8.9 (Si*Me*). $^{31}P\{^{1}H\}$ NMR (202.5 MHz, benzene-d_6): δ 59.6 (d, $^{1}J_{PRh}$ = 122 Hz). ^{29}Si NMR (99.4 MHz, benzene-d_6): δ 44.0. ^{15}N NMR (50.7 MHz, benzene-d_6): δ -275.9. IR (Nujol, cm^{-1}): 3340 (br, w, N-H), 2019 (m, Rh-H). Anal. Calcd for $C_{43}H_{62}RhNP_2Si$: C, 65.72; H, 7.95; N, 1.78. Found: C, 65.41; H, 7.82; N, 1.62. X-Ray quality crystals of **2-8** were grown from a concentrated Et_2O/THF solution at -30 °C.

[Cy-PSiP]Rh(H)[NH(2,6-$Me_2C_6H_3$)] (2-9). A solution of LiNH(2,6-$Me_2C_6H_3$) (0.014 g, 0.110 mmol) in ca. 5 mL of THF was added dropwise via pipette to a solution of [Cy-PSiP]Rh(H)Cl (0.080 g, 0.110 mmol) in ca. 5 mL of THF at room temperature. An immediate color change from light yellow to red-orange was observed. The reaction mixture was evaporated to dryness, and the remaining residue was extracted with ca. 10 mL of benzene. The benzene extract was filtered through Celite and the filtrate was dried under vacuum. The remaining solid residue was triturated with pentane (3 × 5 mL) to afford **2-9** as an orange solid (0.077 g, 84%). ^{1}H NMR (500 MHz, benzene-d_6): δ 7.98 (d, 2 H, J = 7 Hz, H_{arom}), 7.42 (m, 2 H, H_{arom}), 7.23 (t, 2 H, J = 7 Hz, H_{arom}), 7.17 (br s, 2 H, H_{arom}), 7.13 (t, 2 H, J = 7 Hz, H_{arom}), 6.36 (t, 1 H, J = 7 Hz, H_{arom}), 3.28 (s, 1 H, N*H*), 2.63 (br s, 3 H, 2,6-$Me_2C_6H_3$), 2.42 (br s, 3 H, 2,6-$Me_2C_6H_3$), 2.33 – 2.09 (overlapping resonances, 8 H, P*Cy*), 1.84 – 1.10 (overlapping resonances, 34 H, P*Cy*), 0.97 (m, 2 H, P*Cy*), 0.92 (s, 3 H, Si*Me*), -17.27 (apparent q, 1 H, $^{2}J_{HP} \sim {}^{1}J_{HRh}$ = 17 Hz, Rh*H*). $^{13}C\{^{1}H\}$ NMR (125.8 MHz, benzene-d_6): δ 163.8 (C_{arom}), 157.8 (m, C_{arom}), 143.1 (m, C_{arom}), 132.4 (apparent t, J = 9 Hz, CH_{arom}), 130.4 (CH_{arom}), 129.6 (CH_{arom}), 127.9 (CH_{arom}), 112.5 (CH_{arom}), 36.6 (apparent t, J = 12 Hz, CH_{Cy}), 35.5 (apparent t, J = 8 Hz, CH_{Cy}), 30.9 (CH_{2Cy}), 30.5 (CH_{2Cy}), 30.1 (CH_{2Cy}), 28.3 (CH_{2Cy}), 27.9 – 27.5 (overlapping resonances, CH_{2Cy}), 26.9 (CH_{2Cy}), 20.8 (br, 2,6-$Me_2C_6H_3$), 19.9 (br, 2,6-$Me_2C_6H_3$), 8.9 (Si*Me*).

$^{31}P\{^{1}H\}$ NMR (202.5 MHz, benzene-d_6): δ 57.3 (d, $^{1}J_{PRh}$ = 129 Hz). ^{29}Si NMR (99.4 MHz, benzene-d_6): δ 43.9. ^{15}N NMR (50.7 MHz, benzene-d_6): δ -293.0. IR (Nujol, cm^{-1}): 3359 (br, w, N-H), 1999 (m, Rh-H). Anal. Calcd for $C_{45}H_{66}RhNP_2Si$: C, 66.40; H, 8.17; N, 1.72. Found: C, 66.05; H, 7.81; N, 1.68.

[Cy-PSiP]Ir(H)(NH_2) (2-10). Method 1: A slurry of $LiNH_2$ (0.006 g, 0.261 mmol) in ca. 5 mL of THF was added dropwise via pipette to a solution of [Cy-PSiP]Ir(H)Cl (0.040 g, 0.049 mmol) in ca. 5 mL of THF at room temperature. The yellow reaction mixture was transferred to a resealable thick-walled glass vessel containing a magnetic stir bar and equipped with a Teflon stopcock and was heated at 65 °C for 12 h, over the course of which a color change to orange was observed. The reaction mixture was cooled to room temperature and evaporated to dryness, and the remaining residue was extracted with ca. 10 mL of benzene. The benzene extract was filtered through Celite and the filtrate was dried under vacuum. The remaining solid residue was triturated with pentane (3 × 5 mL) to afford **2-10** as a yellow solid (0.036 g, 92%). **Method 2** – *NMR scale***:** A solution of Me_3SiCH_2Li (0.0017 g, 0.018 mmol) in ca. 0.4 mL of cyclohexane-d_{12} was added to a solution of [Cy-PSiP]Ir(H)Cl (0.015 g, 0.018 mmol) in ca. 0.4 mL of cyclohexane-d_{12}. An immediate color change from yellow to orange was observed. The reaction mixture was analyzed by ^{1}H and ^{31}P NMR spectroscopy to confirm the complete consumption of [Cy-PSiP]Ir(H)Cl and the formation of 1 equiv. of Me_4Si. The reaction mixture was then filtered through Celite to remove LiCl, and was transferred to a J-Young NMR tube. The solution was degassed via three freeze-pump-thaw cycles, and an atmosphere of anhydrous ammonia was introduced. The reaction mixture was heated at 65 °C for 14 h. Analysis of the reaction mixture by ^{1}H and ^{31}P NMR spectroscopy confirmed the formation of **2-10** (72%) as well as unidentified side-products at δ ^{31}P 97.0 (5%), 94.1 (5%) and 37.9 - 36.6 (18%). **Method 2** – *preparative scale***:** A solution of Me_3SiCH_2Li (0.0069 g, 0.073 mmol) in ca. 2 mL of cyclohexane-d_{12} was added to a solution of [Cy-PSiP]Ir(H)Cl (0.060 g, 0.073 mmol) in ca. 5 mL of cyclohexane-d_{12}. An immediate color change from yellow to

orange was observed. An aliquot of the reaction mixture was analyzed by ^{1}H and ^{31}P NMR spectroscopy to confirm the complete consumption of [Cy-PSiP]Ir(H)Cl and the formation of 1 equiv. of Me_4Si. The reaction mixture was then filtered through Celite to remove LiCl, and was transferred to a resealable thick-walled glass vessel equipped with a Teflon stopcock. The solution was degassed via three freeze-pump-thaw cycles, and an atmosphere of anhydrous ammonia was introduced. The reaction mixture was heated at 65 °C for 14 h. The reaction mixture was cooled to room temperature and evaporated to dryness, and the remaining residue was washed with ca. 2 mL of cold (-30 °C) pentane, then dried in vacuo to afford **2-10** as a yellow solid (0.040 g, 69%). **Method 3:** A solution of Me_3SiCH_2Li (0.0023 g, 0.024 mmol) in ca. 0.4 mL of benzene-d_6 was added to a solution of [Cy-PSiP]Ir(H)Cl (0.020 g, 0.024 mmol) in ca. 0.4 mL of benzene-d_6. An immediate color change from yellow to orange was observed. The reaction mixture was analyzed by ^{1}H and ^{31}P NMR spectroscopy to confirm the complete consumption of [Cy-PSiP]Ir(H)Cl and the formation of 1 equiv. of Me_4Si. The reaction mixture was then filtered through Celite to remove LiCl, and was transferred to a J-Young NMR tube. The solution was degassed via three freeze-pump-thaw cycles, and an atmosphere of anhydrous ammonia was introduced. The reaction mixture was heated at 65 °C for 144 h. Analysis of the reaction mixture by ^{1}H and ^{31}P NMR spectroscopy confirmed the formation of **2-10** (45%) as well as [Cy-PSiP]Ir(D)(Ph-d_5) (δ ^{31}P 56.8, 20%) and unidentified side-products at δ ^{31}P 95.6 (10%), 94.1 (10%) and 37.3 (15%). ^{1}H NMR (500 MHz, benzene-d_6): δ 8.16 (d, 2 H, J = 7 Hz, H_{arom}), 7.49 (m, 2 H, H_{arom}), 7.24 (t, 2 H, J = 7 Hz, H_{arom}), 7.12 (t, 2 H, J = 7 Hz, H_{arom}), 5.03 (br t, 2 H, $^{3}J_{HP}$ = 6 Hz, NH_2), 2.61 (br d, 2 H, J = 12 Hz, P*Cy*), 2.47 (br t, 2 H, J = 11 Hz, PC*H*), 2.20 (br t, 2 H, J = 12 Hz, PC*H*), 2.11 (m, 2 H, P*Cy*), 1.94 (m, 4 H, P*Cy*), 1.84 (br d, 2 H, J = 12 Hz, P*Cy*), 1.67 – 1.05 (overlapping resonances, 26 H, P*Cy*), 0.97 (m, 2 H, P*Cy*), 0.94 (s, 3 H, Si*Me*), 0.82 (m, 2 H, P*Cy*), -20.13 (t, 1 H, $^{2}J_{HP}$ = 15 Hz, Ir*H*). ^{1}H NMR (500 MHz, cyclohexane-d_{12}): δ 7.98 (d, 2 H, J = 7 Hz, H_{arom}), 7.47 (m, 2 H, H_{arom}), 7.19 (t, 2 H, J = 7 Hz, H_{arom}), 7.10 (t, 2 H, J = 7 Hz, H_{arom}), 4.58 (br s, 2 H, NH_2) 2.45 (br m, 2 H, P*Cy*), 2.35 (br d, 2 H, J =

11 Hz, P*Cy*), 2.18 – 1.02 (overlapping resonances, 38 H, P*Cy*), 0.82 (m, 2 H, P*Cy*), 0.44 (s, 3 H, Si*Me*), -20.34 (t, 1 H, $^{2}J_{HP}$ = 15 Hz, Ir*H*). $^{13}C\{^{1}H\}$ NMR (125.8 MHz, benzene-d_6): δ 161.0 (m, C_{arom}), 144.4 (m, C_{arom}), 132.0 (apparent t, J = 9 Hz, CH_{arom}), 130.4 (CH_{arom}), 128.8 (CH_{arom}), 126.6 (CH_{arom}), 34.2 – 33.9 (overlapping resonances, CH_{Cy}), 30.3 (CH_{2Cy}), 30.2 (CH_{2Cy}), 29.2 (CH_{2Cy}), 28.0 (CH_{2Cy}), 27.7 – 26.9 (overlapping resonances, CH_{2Cy}), 26.5 (CH_{2Cy}), 6.0 (Si*Me*). $^{31}P\{^{1}H\}$ NMR (202.5 MHz, benzene-d_6): δ 55.5. $^{31}P\{^{1}H\}$ NMR (202.5 MHz, cyclohexane-d_{12}): δ 55.7. ^{29}Si NMR (99.4 MHz, benzene-d_6): δ 14.6. ^{15}N NMR (50.7 MHz, benzene-d_6): δ -309.8. IR (Nujol, cm^{-1}): 3418 (w, N-H), 3340 (w, N-H), 2129 (m, M-H). Anal. Calcd for $C_{37}H_{58}IrNP_2Si$: C, 55.61; H, 7.32; N, 1.75. Found: C, 55.30; H, 7.18; N, 1.38. X-Ray quality crystals of **2-10** were grown from a concentrated benzene solution at room temperature.

Generation of [Cy-PSiP]Ir(H)(NH_2)(PMe_3) (2-10·PMe_3). A room temperature solution of **2-10** (0.015 g, 0.019 mmol) in ca. 0.8 mL of benzene-d_6 was treated with PMe_3 (2.0 μL, 0.0015 g, 0.019 mmol). The reaction mixture was transferred to an NMR tube and analyzed by use of NMR techniques, which confirmed the quantitative consumption of **2-10** and the clean formation of putative **2-10·PMe_3**. Attempts to isolate **2-10·PMe_3** by removing the volatile components in vacuo resulted in reformation of **2-10**, as indicated by ^{1}H and ^{31}P NMR spectroscopy of the residue. ^{1}H NMR (500 MHz, benzene-d_6): δ 8.27 (d, 2 H, J = 7 Hz, H_{arom}), 7.38 (m, 2 H, H_{arom}), 7.22 (t, 2 H, H_{arom}), 7.09 (t, 2 H, H_{arom}), 3.13 (m, 2 H, P*Cy*), 2.88 (br m, 2 H, P*Cy*), 2.13 – 1.06 (overlapping resonances, 43 H, P*Cy* + PMe_3; PMe_3 at 1.61 ppm, d, $^{2}J_{HP}$ = 6 Hz), 1.01 (s, 3 H, Si*Me*), 0.71 (m, 4 H, P*Cy*), 0.46 (m, 2 H, P*Cy*), -1.38 (br s, 2 H, NH_2), -13.77 (dt, 1 H, $^{2}J_{HPcis}$ = 22 Hz, $^{2}J_{HPtrans}$ = 127 Hz, Ir*H*) $^{13}C\{^{1}H\}$ NMR (125.8 MHz, benzene-d_6): δ 160.5 (m, C_{arom}), 146.4 (m, C_{arom}), 133.2 (apparent t, J = 9 Hz, CH_{arom}), 129.2 (CH_{arom}), 128.2 (CH_{arom}), 126.7 (CH_{arom}), 37.1 (apparent t, J = 10 Hz, CH_{Cy}), 35.6 (apparent t, J = 14 Hz, CH_{Cy}), 29.9 (CH_{2Cy}), 29.4 (CH_{2Cy}), 28.9 (CH_{2Cy}), 28.4 – 26.3 (overlapping resonances, CH_{2Cy}), 19.4 (br d, $^{1}J_{CP}$ = 27 Hz, PMe_3), 5.8 (Si*Me*). $^{31}P\{^{1}H\}$ NMR (202.5 MHz,

benzene-d_6): δ 28.9 (br s, 2 P, *P*Si*P*), -55.7 (br s, 1 P, *P*Me_3). ^{29}Si NMR (99.4 MHz, benzene-d_6): δ 22.9.

Generation of [Cy-PSiP]Rh(NH_2Ph) (2-11). A solution of Me_3SiCH_2Li (0.0020 g, 0.021 mmol) in ca. 0.4 mL of cyclohexane-d_{12} was added to a solution of [Cy-PSiP]Rh(H)Cl (0.015 g, 0.021 mmol) in ca. 0.4 mL of cyclohexane-d_{12}. An immediate color change from yellow to red-orange was observed. The reaction mixture was analyzed by ^{1}H and ^{31}P NMR spectroscopy to confirm the complete consumption of [Cy-PSiP]Rh(H)Cl and the formation of 1 equiv. of Me_4Si. Aniline (38.3 μL, 0.039 g, 0.420 mmol) was added to the reaction mixture, and the solution was subsequently analyzed by use of NMR techniques, which confirmed the clean formation of putative **2-11**. The coordinated aniline in **2-11** was readily displaced in vacuo, precluding the isolation of this compound. Moreover, the presence of excess aniline in the in situ generated solution of **2-11** precluded the comprehensive assignment of ^{1}H and ^{13}C NMR resonances for this complex. ^{1}H NMR (500 MHz, cyclohexane-d_{12}): δ 7.99 (d, 2 H, J = 7 Hz, H_{arom}), 7.38 (br m, 2 H, H_{arom}), 7.21 (m, 2 H, H_{arom}), 7.12 (m, 2 H, H_{arom}), 2.26 – 0.79 (overlapping resonances, 44 H, P*Cy*), 0.40 (s, 3 H, Si*Me*). ^{13}C{^{1}H} NMR (125.8 MHz, cyclohexane-d_{12}): δ 132.0 (CH_{arom}), 128.2 (CH_{arom}), 126.5 (CH_{arom}), 40.2 (CH_{Cy}), 38.6 (CH_{Cy}), 31.8 (CH_{2Cy}), 31.3 (CH_{2Cy}), 30.5 (CH_{2Cy}), 29.7 (CH_{2Cy}), 28.0 – 26.6 (overlapping resonances, CH_{2Cy}), 8.9 (Si*Me*). ^{31}P{^{1}H} NMR (202.5 MHz, cyclohexane-d_{12}): δ 54.7 (d, $^1J_{PRh}$ = 182 Hz). ^{29}Si NMR (99.4 MHz, cyclohexane-d_{12}): δ 59.3.

Generation of [Cy-PSiP]Rh(NH_3) (2-12). A solution of Me_3SiCH_2Li (0.0020 g, 0.021 mmol) in ca. 0.4 mL of cyclohexane-d_{12} was added to a solution of [Cy-PSiP]Rh(H)Cl (0.015 g, 0.021 mmol) in ca. 0.4 mL of cyclohexane-d_{12}. An immediate color change from yellow to red-orange was observed. The reaction mixture was analyzed by ^{1}H and ^{31}P NMR spectroscopy to confirm the complete consumption of [Cy-PSiP]Rh(H)Cl and the formation of 1 equiv. of Me_4Si. The reaction mixture was then filtered through Celite to remove LiCl, and was transferred to a J-Young NMR tube. The solution was degassed via three freeze-pump-thaw cycles, and an atmosphere of

anhydrous ammonia was introduced, resulting in a color change to light orange. The reaction mixture was subsequently analyzed by use of NMR techniques, which confirmed the clean formation of putative **2-12**. The coordinated amine in **2-12** was readily displaced in vacuo, precluding the isolation of this compound. Moreover, the presence of excess ammonia in the in situ generated solution of **2-12** prevented the unequivocal assignment of the RhN*H*$_3$ ^{1}H NMR resonance for this complex. ^{1}H NMR (500 MHz, cyclohexane-d_{12}): δ 7.98 (d, 2 H, J = 7 Hz, H_{arom}), 7.37 (m, 2 H, H_{arom}), 7.18 (t, 2 H, J = 7 Hz, H_{arom}), 7.10 (t, 2 H, J = 7 Hz, H_{arom}), 2.22 (br m, 2 H, P*Cy*), 2.14 (br m, 4 H, P*Cy*), 2.03 (t, 2 H, J = 12 Hz, P*Cy*), 1.80 – 1.09 (overlapping resonances, 36 H, P*Cy*), 0.26 (s, 3 H, Si*Me*). ^{13}C{^{1}H} NMR (125.8 MHz, cyclohexane-d_{12}): δ 162.0 (m, C_{arom}), 146.6 (m, C_{arom}), 132.4 (apparent t, J = 12 Hz, CH$_{arom}$), 129.2 (CH$_{arom}$), 128.4 (CH$_{arom}$), 126.9 (CH$_{arom}$), 41.7 (apparent t, J = 7 Hz, CH$_{Cy}$), 41.0 (apparent t, J = 8 Hz, CH$_{Cy}$), 32.7 (CH$_{2Cy}$), 30.9 (CH$_{2Cy}$), 28.5 – 28.2 (overlapping resonances, CH$_{2Cy}$), 27.7 (CH$_{2Cy}$), 27.4 (CH$_{2Cy}$), 8.9 (Si*Me*). ^{31}P{^{1}H} NMR (202.5 MHz, cyclohexane-d_{12}): δ 54.4 (d, $^1J_{PRh}$ = 180 Hz). ^{29}Si NMR (99.4 MHz, cyclohexane-d_{12}): δ 60.8.

2.5.3 Crystallographic Solution and Refinement Details

Crystallographic data for each of **2-5**, **2-6·OEt$_2$**, **2-7**, and **2-8** were obtained at 193(±2) K, while data for **2-10** were obtained at 173(±2) K on a Bruker D8/APEX II CCD diffractometer using a graphite-monochromated Mo Kα (λ = 0.71073 Å) radiation, employing a sample that was mounted in inert oil and transferred to a cold gas stream on the diffractometer. Programs for diffractometer operation, data collection, and data reduction (including SAINT) were supplied by Bruker. Gaussian integration (face-indexed) was employed as the absorption correction method for **2-5**, **2-6·OEt$_2$**, **2-7**, and **2-8**, while multi-scan (*TWINABS*) was used for **2-10**. For **2-5**, **2-6·OEt$_2$**, **2-7**, and **2-8** the structures were solved by use of the Patterson search/structure expansion, while the for **2-10** the structure was solved by use of direct methods. All structures were refined by use of full-matrix least-squares procedures (on F^2) with R_1 based on $F_o^2 \geq 2\sigma(F_o^2)$ and wR_2

based on $F_o^2 \geq -3\sigma(F_o^2)$. Unless otherwise specified, anisotropic displacement parameters were employed throughout for the non-hydrogen atoms. During the structure solution process for **2-6·OEt$_2$** an equiv. of Et_2O was located in the asymmetric unit. Disorder involving this solvent molecule and the N-*Ph* group was identified during refinement. The non-hydrogen atoms of the disordered Et_2O solvate were refined over two positions, where O1S and C1S - C4S were refined with an occupancy factor of 0.65, while O2S and C5S - C8S were refined with an occupancy factor of 0.35. Distances involving analogous pairs of atoms within the solvent diethyl ether molecule were constrained to be equal (within 0.03 Å) during refinement: d(O1S–C1S) = d(O2S–C5S); d(O1S–C3S) = d(O2S–C7S); d(C1S–C2S) = d(C5S–C6S); d(C3S–C4S) = d(C7S–C8S); d(O1S···C2S) = d(O2S···C6S); d(O1S···C4S) = d(O2S···C8S); d(C1S···C3S) = d(C5S···C7S). The carbon atoms of the N-*Ph* group in **2-6·OEt$_2$** were refined over two positions, where C2A – C7A were refined with an occupancy factor of 0.65, while C2B – C7B were refined with an occupancy factor of 0.35. The N–C2A and N–C2B distances within the HNPh ligand were constrained to be equal (within 0.01 Å) during refinement. During the structure solution process for **2-10**, two crystallographically independent molecules of [Cy-PSiP]Ir(H)(NH_2) (A and B) were located in the asymmetric unit; for convenience, only molecule A is discussed in the text. Furthermore, in the case of **2-10** the crystal used for data collection was found to display non-merohedral twinning. Both components of the twin were indexed with the program *CELL_NOW* (Bruker AXS Inc., Madison, WI, 2004). The second twin component can be related to the first component by 180º rotation about the [1 0 0] axis in real space and about the [1 1/4 0] axis in reciprocal space. Integrated intensities for the reflections from the two components were written into a *SHELXL-97* HKLF 5 reflection file with the data integration program *SAINT* (version 8.27B), using all reflection data (exactly overlapped, partially overlapped and non-overlapped). The refined value of the twin fraction (*SHELXL-97* BASF parameter) was 0.1061(10). The Ir-*H* in **2-10** was located in the difference map and refined isotropically. The Rh-*H* in **2-8** and the Ir-*H* in **2-7** were each located in the

difference map and refined with the restraint that in each case the M-*H* distance was fixed at 1.55 Å, thereby allowing for the determination of the hydride isotropic thermal parameter. In the final refinement cycles, this distance restraint was removed; the previously determined hydride thermal parameter was retained and the hydride position was refined by use of a riding model in which the hydride positional changes matched those of the attached metal center. For **2-6·OEt$_2$** the Ir-*H* was not located in the difference map. Instead, an initial Ir-*H* position similar to that found in **2.7** was selected, and in the subsequent refinement cycles the Ir-H distance was fixed (1.55 Å) and the other parameters (X-Ir-H angles, Ir-*H* thermal parameter) were allowed to vary. The Ir-*H* position in **2-6·OEt$_2$** following refinement in this manner was similar to that found in **2.7**. The N-*H* in **2-8**, **2-6·OEt$_2$** and **2-7** were each located in the difference map and refined with the restraint that in each case the N-*H* distance was fixed at 0.88 Å. The N-*H* atoms in **2-10** (H1NAand H1NB) were each located in the difference map and refined isotropically. Otherwise, all hydrogen atoms were added at calculated positions and refined by use of a riding model employing isotropic displacement parameters based on the isotropic displacement parameter of the attached atom. Additional crystallographic information is provided in Appendix A.

Chapter 3: A Thorough Investigation of N–H Bond Activation Mediated by [R-PSiP]M

3.1 Introduction

As discussed previously in this document, the design and synthesis of new classes of late transition metal complexes that are capable of mediating N-H bond oxidative addition of a variety of amines under relatively mild conditions to form stable products is an important goal, as it could provide insight into the development of new pathways for amine and ammonia functionalization. Given the rarity of systems capable of such reactivity, the discovery of transition metal complexes that can mediate N-H bond oxidative addition is highly desirable.

In addition to the previously highlighted examples of N-H bond activation of anilines and ammonia, there is some precedent in the literature for PCP-type Ir pincer complexes that are able to activate alternative types of N-H bonds. Hartwig reported N-H bond cleavage of hydrazines by [^{t}Bu-PCP]Ir^I species.[40] In contrast to the reactivity observed for aniline and ammonia N-H bond cleavage products in this system,[38a,39] hydrazido hydride complexes resulting from the oxidative addition of hydrazines were not susceptible to N-H bond reductive elimination, although in some cases other reactivity involving further N-H and/or C-H bond activation processes was observed. In addition, as part of a detailed mechanistic study of the reactivity of [POCOP]Ir^I with a variety of anilines in benzene solution, Brookhart and coworkers also investigated the reactivity of the [POCOP]Ir^I species with benzamides. The oxidative addition products formed were much more stable than the anilido hydride complexes resulting from N-H oxidative addition of anilines, likely due to the interaction of the carbonyl oxygen with the Ir metal center (Scheme 1-10).[41] Beyond these studies, no examples of isolable amido hydride complexes resulting from N-H bond oxidative addition of simple unactivated amines, such as alkyl amines, can be found in the literature. Furthermore, to date no system that can effect N-H bond oxidative addition in a wide range of amines, including alkyl amines, anilines, ammonia, benzamides and hydrazines has been reported.

As detailed in Chapter 2, the attempted alkylation of the bis(phosphino)silyl Ir complex [Cy-PSiP]Ir(H)Cl (Cy-PSiP = κ^3-(2-$Cy_2PC_6H_4)_2SiMe^-$) transiently generated highly reactive Ir^I species of the type [Cy-PSiP]Ir^I that were shown to undergo N-H bond oxidative addition of anilines and ammonia under relatively mild conditions. The resulting [Cy-PSiP]Ir(H)(NHR) (R = H, aryl) products proved remarkably resistant to N-H bond reductive elimination, even in the presence of arene solvents, which is in direct contrast to the reactivity observed in (PCP)Ir systems that can undergo similar bond activation processes (*vide supra*).

Since N-H oxidative addition processes are exceedingly rare and have not been studied in detail, especially across a series of different types of N-H containing molecules, a thorough investigation of N-H bond activation mediated by [Cy-PSiP]Rh^I and Ir^I species with various N-H containing substrates, including alkyl amines, hydrazine derivatives, and benzamides was initiated. Extension of this reactivity to the related diisopropylphosphino derivative [^{i}Pr-PSiP]Ir^I was also investigated, as such diisopropylphosphino silyl pincer complexes were envisioned to be less susceptible to potential cyclometalation side reactions than their dicyclohexylphosphino counterparts. In addition, ^{i}Pr-PSiP ligation may offer more diagnostic ^{1}H and ^{13}C NMR features, which may make it easier to spectroscopically analyze reaction products.

3.2 Results and Discussion

3.2.1 Generation of [^{i}Pr-PSiP]Ir^I

The tertiary silane ligand precursor [^{i}Pr-PSiP]H (**3-1**) was prepared utilizing similar steps to those previously developed by our group for the synthesis of the related tertiary silanes [Ph-PSiP]H and [Cy-PSiP]H (Scheme 3-1).[15a,b] An initial Pd-coupling step was utilized to prepare the known compound 2-$^i Pr_2PC_6H_4Br$ from $^i Pr_2PH$ and 2-bromoiodobenzene.[68,69] 2-$^i Pr_2PC_6H_4Br$ underwent lithium halogen exchange with ^{n}BuLi at -40 °C in Et_2O solution to form the known compound 2-$^i Pr_2PC_6H_4Li{\cdot}(OEt_2)_{0.7}$,[70] which was obtained in 63% yield following recrystallization from Et_2O at -35°C. The reaction

of 2-$^{i}Pr_2PC_6H_4Li{\cdot}(OEt_2)_{0.7}$ with half an equivalent of Cl_2SiMeH at -78 °C in hexanes led to the formation of the tertiary silane ligand precursor [^{i}Pr-PSiP]H (**3-1**), which was isolated in 87% yield as a yellow oil.[71] The ^{31}P NMR spectrum of **3-1** features a singlet at 0.4 ppm corresponding to the [^{i}Pr-PSiP]H phosphino groups. The ^{1}H and ^{13}C NMR spectra of **3-1** (benzene-d_6) feature a single set of aromatic ligand backbone resonances. In addition, the ^{1}H NMR spectrum of **3-1**contains a diagnostic resonance at 6.27 ppm that corresponds to the Si-*H* of the tertiary silane product.

Treatment of **3-1** with 0.5 equiv of $[Ir(COE)_2Cl]_2$ (COE = cyclooctene) led to the formation of [^{i}Pr-PSiP]Ir(H)Cl (**3-2**, Scheme 3-1, 81% isolated yield). Complex **3-2** exhibits NMR features similar to those of the related Cy-PSiP derivative, [Cy-PSiP]Ir(H)Cl (**2-1**), including a single sharp ^{31}P NMR resonance at 69.7 ppm and an Ir hydride resonance observed in the ^{1}H NMR spectrum (benzene-d_6) at -23.90 ppm (*cf.* 61.1 and -23.79 ppm for **2-1**, respectively).

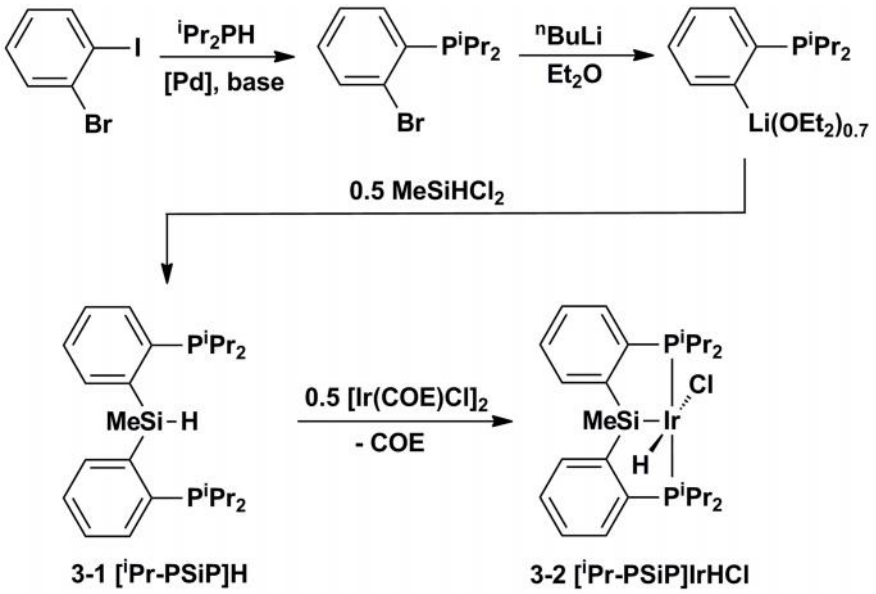

Scheme 3-1. Synthesis of [^{i}Pr-PSiP]H (**3-1**) and [^{i}Pr-PSiP]IrHCl (**3-2**)

An X-ray crystal structure of **3-2** (Figure 3-1) confirmed the formation of a five-coordinate complex in which the phosphine donors are approximately trans-oriented (P1-

Ir-P2 = 163.31(3)º), similar to previously reported **2-1** and the related Rh analogue [Cy-PSiP]Rh(H)Cl (**2-2**).[15b] The coordination geometry at Ir is approximately square-based pyramidal, with Si occupying the apical coordination site, and can also be described as "Y-shaped".[59]

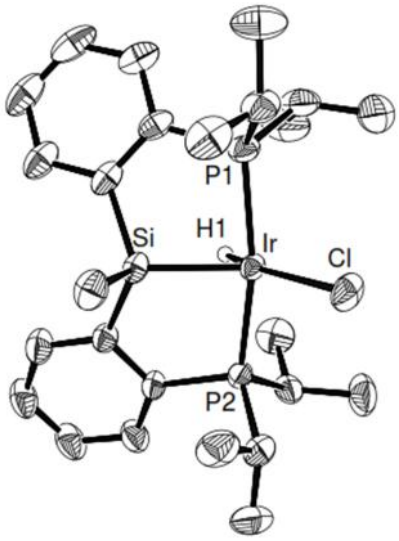

Figure 3-1. The crystallographically determined structure of **3-2** shown with 50% displacement ellipsoids. With the exception of H1, all H atoms have been omitted for clarity.

Table 3-1. Selected interatomic distances (Å) and angles (º) for **3-2**.

Bond Lengths (Å)			
Ir-P1	2.2936(9)	Ir-H1	1.40(3)
Ir-P2	2.2913(8)	Ir-Cl	2.4017(8)
Ir-Si	2.2646(9)		
Bond Angles (º)			
P1-Ir-P2	163.31(3)	Si-Ir-H1	72.4(13)
Si-Ir-Cl	131.61(3)	Cl-Ir-H1	155.7(13)

It was previously reported that the attempted alkylation of **2-1** with a lithium alkyl reagent in benzene solution led to the evolution of the corresponding alkane and the formation of the benzene activation product [Cy-PSiP]Ir(H)Ph (Scheme 2-2).[15b] In an effort to demonstrate that **3-2** was capable of similar C-H bond cleavage chemistry, treatment of a room temperature benzene solution of **3-2** with Me_3SiCH_2Li led to the

rapid generation of Me_4Si and the quantitative (by ^{31}P NMR) formation of the corresponding benzene activation product [^{i}Pr-PSiP]Ir(H)Ph (**3-3,** Scheme 3-2), which was isolated in 93% yield. Complex **3-3** was also independently synthesized (91% isolated yield) by the reaction of **3-2** with PhLi. Interestingly, unlike the analogous complex [Cy-PSiP]Ir(H)Ph that eliminated benzene and decomposed upon exposure to vacuum, complex **3-3** proved to be isolable, possibly due to slightly decreased steric pressure in the Ir coordination sphere for the isopropyl(phosphino) derivative.

The *in situ* observation of a putative 14-electron Ir^{I} intermediate in the C-H bond activation of benzene was targeted by carrying out the alkylation of **3-2** in cyclohexane-d_{12} solution (Scheme 3-2). At room temperature, this reaction gave rise quantitatively to a new [^{i}Pr-PSiP]Ir-containing species (**3-4**) that exhibits broad NMR features, including a ^{31}P NMR signal at 66.8 ppm, and a ^{1}H NMR resonance centered at -11.5 ppm that is consistent with the formation of an Ir hydride species. Neither the ^{1}H nor ^{31}P NMR spectral features observed for **3-4** varied significantly between -90 - 90 °C (methylcyclohexane-d_{14}). These observations are comparable with the results obtained in the alkylation of **2-1** in cyclohexane-d_{12} solution (*cf.* broad $^{31}P\{^{1}H\}$ NMR signal at 56.2 ppm, and broad ^{1}H NMR resonance centered at -11.3 ppm),[15b] and suggest the formation of a cyclometalated variant of [^{i}Pr-PSiP]Ir. As is the case for the [Cy-PSiP]Ir system, attempts to isolate complex **3-4** were unsuccessful. However, *in situ* generated **3-4** appears to serve as a source of [^{i}Pr-PSiP]Ir^{I}. To trap **3-4**, a cyclohexane solution of **3-2** was treated with an equivalent of Me_3SiCH_2Li to generate **3-4**; the reaction mixture was subsequently degassed and 1 atm of ethylene gas was introduced. An immediate colour change to bright orange was observed and quantitative (by ^{31}P NMR) formation of the ethylene complex [^{i}Pr-PSiP]Ir$(C_2H_4)_2$ (**3-5**, Scheme 3-2) was observed. A single ^{31}P NMR resonance at 72.0 ppm and ^{29}Si shift of 58.1 ppm were observed for the C_s symmetric product (*cf.* 65.4 and 60.1 ppm, respectively for **2-1**). The coordination of two molecules of ethylene to the Ir center in **3-5** was confirmed ^{1}H NMR spectroscopy, and once again highlights the decreased steric crowding in ^{i}Pr-PSiP-ligated Ir relative to the

Cy-PSiP analogue, which can only accommodate one ethylene ligand. Furthermore, treatment of a reaction mixture containing *in situ* generated **3-4** with an excess (ca. 2 mL, 250 equivalents) of benzene led to the quantitative formation of the C-H activation product **3-3** (Scheme 3-1), indicating that **3-4** is the active species initiating the bond cleavage chemistry.

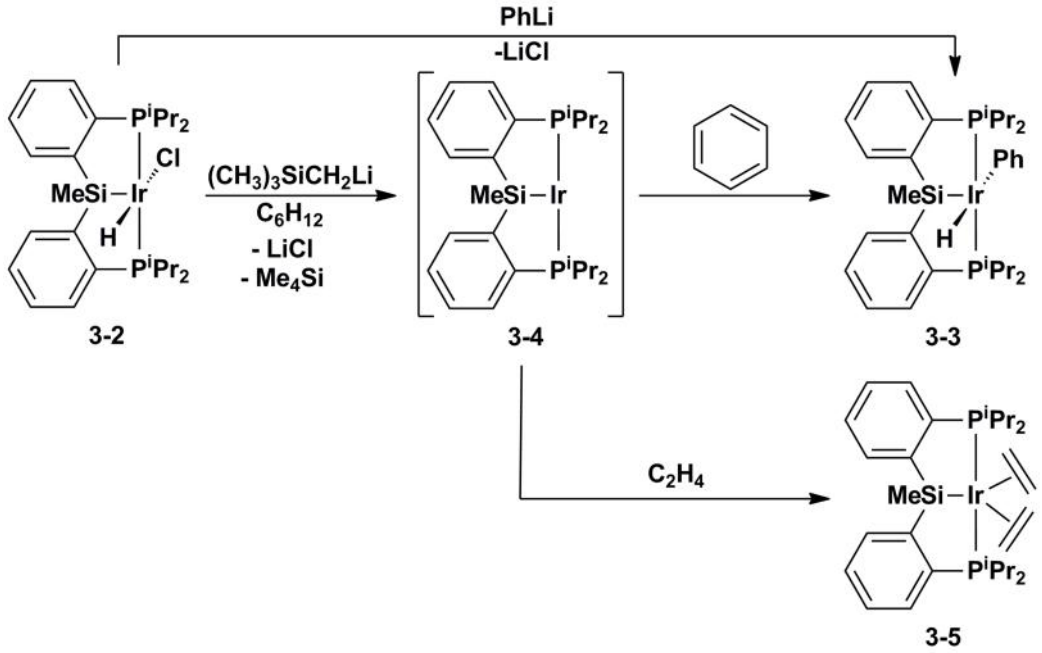

Scheme 3-2. Synthesis of (a) [^{i}Pr-PSiP]Ir(H)Ph (**3-3**) via C-H activation by [^{i}Pr-PSiP]Ir^I (**3-4**) and (b) [^{i}Pr-PSiP]Ir(C_2H_4)$_2$ (**3-5**)

3.2.2 N-H Bond Activation of Aniline and Ammonia by [^{i}Pr-PSiP]Ir^I

Having shown that an ^{i}Pr-PSiP analogue (**3-4**) of [Cy-PSiP]Ir^I can be accessed in situ, and that this highly reactive species can mediate benzene C-H bond activation to yield **3-3**, the ability of **3-4** to mediate N-H bond cleavage in aniline and ammonia in a manner comparable to [Cy-PSiP]Ir was investigated. The direct synthesis of the N-H bond cleavage products of the type [^{i}Pr-PSiP]Ir(H)(NHR) (R = H, Ph) were first targeted to assess the viability of [^{i}Pr-PSiP]Ir to support amido hydride products. Thus, treatment of **3-2** with one equiv of LiNHPh in THF at room temperature led to clean formation of

[^{i}Pr-PSiP]Ir(H)(NHPh) (**3-6**, Scheme 3-3). Complex **3-6** was isolated as a red solid in 97% isolated yield. The corresponding synthesis of [^{i}Pr-PSiP]Ir(H)(NH_2) (**3-7**) was achieved by treating **3-2** with 5 equiv $LiNH_2$ in THF solution and heating at 65 °C for 16 h to produce **3-7** as an orange solid in 90% isolated yield (Scheme 3-3). The ^{31}P NMR spectrum of **3-6** features a resonance at 61.6 ppm, while that of **3-7** features a resonance at 63.1 ppm, consistent with symmetry equivalent phosphine donors. The ^{1}H NMR (benzene-d_6) spectrum of **3-6** exhibits a hydride resonance at -20.18 ppm (t, $^{2}J_{HP}$ = 15 Hz), and that of **3-7** contains a similar resonance at -20.12 ppm (t, $^{2}J_{HP}$ = 15 Hz), both of which are consistent with the hydride NMR shifts of the corresponding [Cy-PSiP]Ir analogues (cf. -21.16 ppm for **2-6** and -20.13 ppm for **2-10**). The ^{1}H NMR spectra of **3-6** and **3-7** also feature a characteristic N-H resonance at 6.84 and 5.06 ppm, respectively. These resonances correspond to ^{15}N NMR resonances of -259.9 and -307.4 ppm in ^{1}H-^{15}N HMQC experiments. Complexes **3-6** and **3-7** are stable both in the solid state and in solution, including benzene solution, with no evidence for reductive elimination of aniline or ammonia even under vacuum (0.01 mm Hg). This is comparable to the previously reported Cy-PSiP analogues that proved similarly resistant to N-H reductive elimination. By comparison, complexes of the type [PCP]Ir(H)(NHR')[46a,47] (PCP = 2,6-($CH_2P^{t}Bu_2)_2C_6H_3$; R' = H, aryl) and [POCOP]Ir(H)(NHR")[50] (POCOP = 2,6-($OP^{t}Bu_2)_2C_6H_3$; R" = aryl) undergo much more facile N-H bond reductive elimination, and for example exist in equilibrium with the corresponding phenyl hydride species in benzene solution.

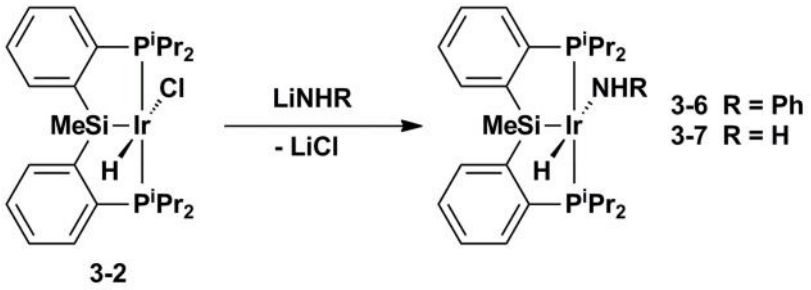

Scheme 3-3. Synthesis of [^{i}Pr-PSiP]Ir(H)NHR complexes (**3-6,** R = Ph; **3-7**, R = H) via a salt metathesis route

In an effort to access complexes **3-6** and **3-7** via N-H bond oxidative addition to [^{i}Pr-PSiP]Ir^I, **3-2** was treated with one equiv of Me_3CCH_2Li in cyclohexane-d_{12} solution, which led to the evolution of Me_4C, accompanied by the complete consumption of **3-2** and the quantitative (^{1}H and ^{31}P NMR) formation of **3-4**. Treatment of this reaction mixture with one equiv of $PhNH_2$ led to the formation of **3-6** after 14 hours at 80 °C. Alternatively, treatment of the aforementioned reaction mixture with an excess of anhydrous ammonia (ca. 1 atm) led to the quantitative (^{31}P and ^{1}H NMR) formation of **3.7** after heating at 65 °C for 14 h (Scheme 3-4).

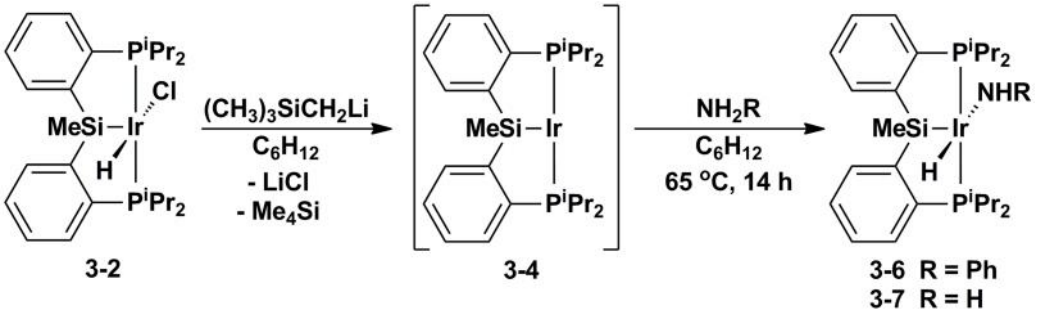

Scheme 3-4. Synthesis of [^{i}Pr-PSiP]Ir(H)NHR (**3-6,** R = Ph; **3-7**, R = H) through N-H bond activation

3.2.3 N-H Bond Activation of Alkyl Amines by [R-PSiP]Ir^I (R = Cy, ^{i}Pr)

The N-H bonds of alkyl amines are more difficult to oxidatively add than those of anilines due to the increased basicity of the lone pair on nitrogen, which favours the formation of amine adducts rather than metal insertion into the N-H bond. As such, there

have been no reported examples of N-H bond oxidative addition of alkyl amines at a platinum group metal center in the literature. As discussed in Chapter 1, a recent example of N-H bond activation of isopropylamine was reported, but the mode of activation involved metal/ligand cooperativity, not oxidative addition. Furthermore the N-H activation product could not be isolated.[43] Therefore, this challenging reaction was targeted to demonstrate that the electron-rich Ir center of the [PSiP]Ir^{I} fragment could mediate the oxidative addition of such highly Lewis basic amines.

The direct synthesis of the alkyl amido hydride complexes that would be the products of N-H bond oxidative addition to [R-PSiP]Ir^{I} (R = ^{i}Pr, Cy) was attempted initially by a salt metathesis route utilizing amido lithium reagents. Thus, treatment of either **2-1** or **3-2** with one equiv of Li(NHR') (R' = Ad, ^{t}Bu, Cy) led to the room temperature, immediate formation of the corresponding isolable amido hydride complexes (Scheme 3-5; **3-8**, R = Cy, R' = Ad; **3-9**, R = Cy, R' = ^{t}Bu; **3-10**, R = R' = Cy; **3-11**, R = ^{i}Pr, R' = Ad; **3-12**, R = ^{i}Pr, R' = ^{t}Bu) in 76–89% yields . Spectroscopic data for the isolated complexes, including solution ^{1}H, ^{13}C, and ^{31}P NMR (benzene-d_6) spectra indicate the formation of C_s-symmetric species. Additionally, the ^{1}H NMR spectra of complexes **3-8** – **3-12** each feature a downfield-shifted hydride resonance, as well as a characteristic N-H resonance (confirmed by the use of ^{1}H-^{15}N HMQC spectroscopy), consistent with the formation of the targeted amido hydride Ir complexes. In addition, ^{29}Si and ^{15}N spectroscopic data support the structures represented in Scheme 3-4 (Table 3-2). Notably, **3-10** exhibits diffent NMR features than the other alkyl amido hydride products and it is possible that the product may not simply be an oxidative addition product. However, there were no characteristic ^{1}H or ^{13}C NMR resonances to indicate evidence of β-hydride elimination. Attempts to synthesize [^{i}Pr-PSiP]Ir(H)(NHCy) via a salt metathesis route led to complex reaction mixtures where no clean products were isolated. The reduced steric bulk of ^{i}Pr compared to Cy substituents on the ligand phosphine donors may allow further reactivity to occur at the Ir center in the [^{i}Pr-PSiP]Ir(H)(NHCy) complex, leading to the formation of multiple products.

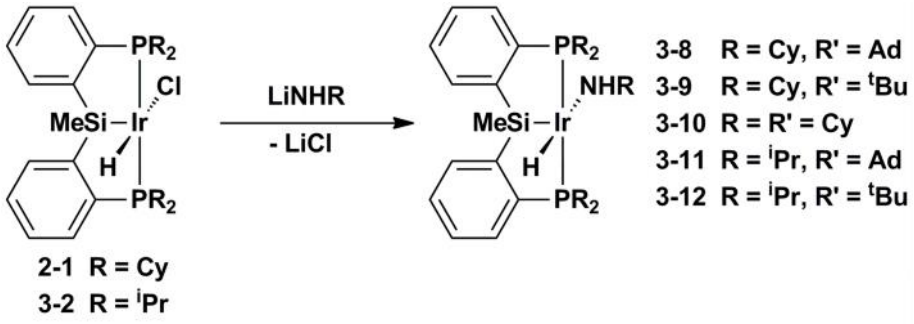

Scheme 3-5. Synthesis of [R-PSiP]Ir(H)(NHR') complexes (R = Cy, ^{i}Pr; R' = Ad, ^{t}Bu, Cy) via a salt metathesis route

Table 3-2. Selected NMR spectroscopic data (ppm) for complexes **3-8** – **3-12.**

Complex	$^{31}P\{^{1}H\}$ NMR	^{1}H NMR hydride[a]	^{1}H NMR N*H*[a,b]	^{15}N NMR[b]	^{29}Si NMR[c]
[Cy-PSiP]Ir(H)(NHAd) (**3-8**)	52.1	-20.73 (t)	6.59	-216.8	16.2
[Cy-PSiP]Ir(H)(NH^{t}Bu) (**3-9**)	52.0	-20.78 (t)	6.67	-219.2	16.0
[Cy-PSiP]Ir (H)(NHCy) (**3-10**)	54.8	-18.37 (t)	–[d]	–[d]	23.2
[^{i}Pr-PSiP]Ir(H)(NHAd) (**3-11**)	58.9	-20.83 (t)	6.70	-213.4	16.8
[^{i}Pr-PSiP]Ir(H)(NH^{t}Bu) (**3-12**)	51.9	-20.91 (t)	6.80	-215.7	16.7

[a] benzene-d_6; [b] ^{1}H-^{15}N HMQC; [c] ^{1}H-^{29}Si HMBC; [d] Not observed by ^{1}H-^{15}N HMQC

Complexes **3-8** – **3-12** are stable both in the solid state and in solution (including benzene solution) and do not appear to undergo N-H bond reductive elimination. This is consistent with the stability observed for [R-PSiP]Ir(H)(NHR') (R = Cy, ^{i}Pr; R' = aryl, H) species, which are also resistant to N-H reductive elimination.

The solid state structures of [Cy-PSiP]Ir(H)(NHAd) (**3-8**) and [^{i}Pr-PSiP]Ir(H)(NHAd) (**3-11**) were determined using single crystal X-ray diffraction and in both cases confirm the connectivity proposed for these complexes (Figure 3-2, Table 3-3). As in the case of complex **3-2**, as well as the related anilido hydride species [Cy-PSiP]Ir(H)(NH(aryl)) (aryl = Ph, **2-6**; 2,6-$Me_2C_6H_3$, **2-7**) that have been crystallographically characterized, the R-PSiP ligand coordinates to the Ir center such that the phosphino donors are trans-disposed (P1-Ir-P2 = 154.61(2)º for **3-8** and 155.84(6)º for **3-11**), and the coordination geometry can be described as distorted square based pyramidal with Si in the apical site. The Ir–N bond distance of 2.018(2) Å observed for

3-8 is slightly shorter than those previously reported for (Cy-PSiP)Ir(H)(NHPh) (**2-6·Et$_2$O**, 2.056(2) Å) and (Cy-PSiP)Ir(H)(NH(2,6-Me$_2$C$_6$H$_3$)) (**2-7**, 2.077(3) Å).

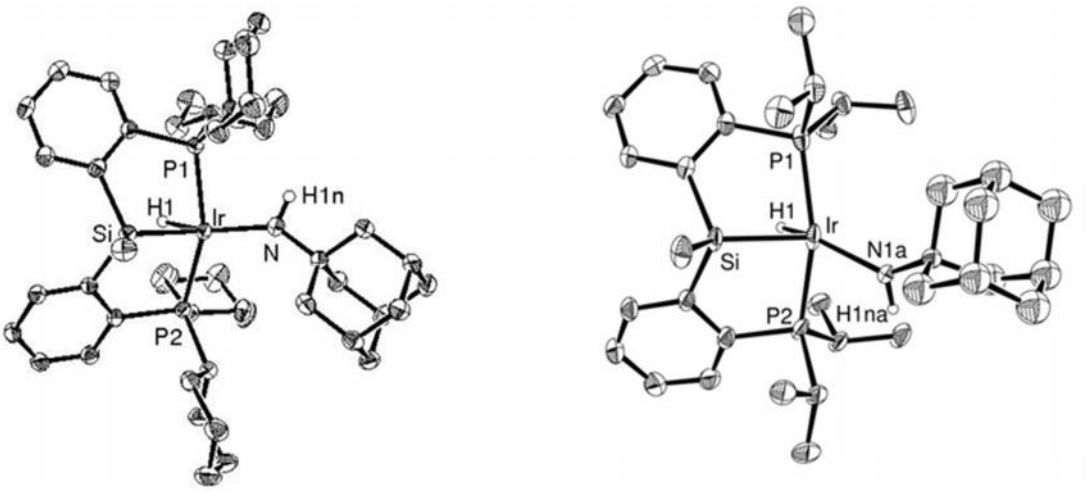

3-8 **3-11**

Figure 3-2. The crystallographically determined structures of **3-8** and **3-11** shown with 50% displacement ellipsoids. With the exception of H1 and the N-*H* atoms, all H atoms have been omitted for clarity.

Table 3-3. Selected interatomic distances (Å) and angles (º) for **3-8**, and **3-11**.

Bond Lengths (Å)				
3-8	Ir-P1	2.2832(7)	Ir-H1	1.55
	Ir-P2	2.3105(7)	Ir-N	2.018(2)
	Ir-Si	2.2941(8)		
3-11	Ir-P1	2.2991(18)	Ir-H1	1.54(6)
	Ir-P2	2.298(2)	Ir-N	2.088(8)
	Ir-Si	2.2887(14)		
Bond Angles (º)				
3-8	P1-Ir-P2	154.61(2)	Si-Ir-H1	72.6
	Si-Ir-N	131.03(7)	N-Ir-H1	153.7
3-11	P1-Ir-P2	155.84(6)	Si-Ir-H1	70(2)
	Si-Ir-N	135.4(2)	N-Ir-H1	147(2)

Having demonstrated that Ir alkylamido hydride complexes supported by R-PSiP ligation are synthetically accessible, the synthesis of such species by N-H bond oxidative

addition of alkyl amines was pursued in an analogous manner to the arylamido hydride and parent amido hydride complexes described in Chapter 2. Towards this end, the hydrido chloride species **2-1** or **3-2** were initially treated with one equiv of Me_3SiCH_2Li in cyclohexane-d_{12} solution, which led to the immediate evolution of Me_4Si and the quantitative (by ^1H and ^{31}P NMR) consumption of the corresponding hydrido chloride complex in order to provide in situ access to [R-PSiP]Ir^I species (*vide supra*). Having confirmed spectroscopically that the starting hydrido chloride complex was consumed in its entirety, an excess (ca. 20 equiv) of the appropriate alkyl amine was added to the reaction mixture. Heating of the resulting reaction mixtures at 65 ºC for 14 h led to the quantitative formation of the [Cy-PSiP]Ir amido hydride species **3-8**, **3-9** and **3-10** resulting from N-H bond activation of H_2NAd, H_2N^tBu and H_2NCy (Scheme 3-6). In the case of [^{i}Pr-PSiP]Ir, after heating the reaction mixtures at 65 ºC for 14 h, NMR analysis indicated 50% conversion to **3-11** and greater than 90% conversion to **3-12**. These represent the first reported examples of N-H bond oxidative addition of alkyl amines.

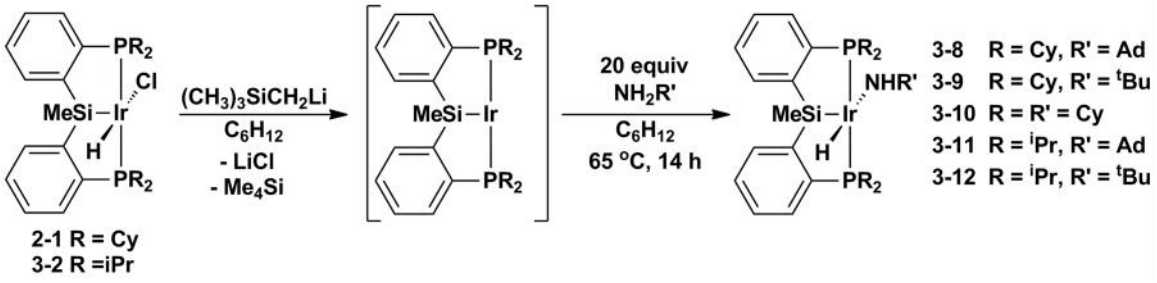

Scheme 3-6. Synthesis of [R-PSiP]Ir(H)(NHR') complexes by N-H bond activation of alkyl amines

The extension of this chemistry to alkyl amines containing potentially reactive β-hydrogen substituents was also investigated. The direct synthesis of amido hydride complexes featuring *n*-propylamido and *n*-octylamido ligands by the reaction of **2-1** or **3-2** with the corresponding lithium amide reagent were attempted. Treatment of a benzene-d_6 solution of **2-1** or **3-2** with ^{n}PrNHLi led to the immediate formation of new products

with ^{31}P NMR resonances at 48.7 (**3-13**) and 57.9 (**3-14**), respectively. ^{1}H and ^{13}C NMR spectroscopy indicated the formation of C_s-symmetric species with a single set of aromatic resonances for the pincer ligand backbone. In addition, two broad hydride signals (at δ -11.00 (s) and -14.10 (d) for **3-13**, as well as δ -11.46 (s) and -14.35 (d) for **3-14**) in a 1:2 ratio were observed in both reactions by ^{1}H NMR spectroscopy. Analogous reactivity was observed for the reaction of **2-1** and **3-2** with ^{n}OctNHLi in benzene-d_6 to yield **3-13** and **3-14**, respectively, as indicated by ^{31}P and ^{1}H NMR spectroscopy. Attempts to isolate **3-13** and **3-14** were not successful as exposure to vacuum led to decomposition. As such, the products of these reactions could not be unambiguously identified. The observation of multiple hydride resonances for **3-13** and **3-14** by ^{1}H NMR spectroscopy indicates that likely β-hydride elimination, as well as additional N-H and/or C-H bond cleavage processes are occurring during the course of these reactions. Generation of [R-PSiP]Ir^{I} species by treatment of **2-1** or **3-2** with one equivalent of Me_3SiCH_2Li in cyclohexane (*vide supra*), followed by subsequent treatment with 20 equivalents of either $^{n}PrNH_2$ or $^{n}OctNH_2$ resulted in partial conversion to **3-13** or **3-14**, respectively, upon heating for 14 h at 70 ^{o}C. Prolonged heating did not drive these reactions to completion.

The N-H bond activation reactivity of benzylamine was also investigated (Scheme 3-7). Treatment of a cyclohexane solution containing in situ generated [Cy-PSiP]Ir^{I} (*vide supra*) with one equivalent of H_2NCH_2Ph afforded a white precipitate after heating for 12 hours at 65 °C. Spectroscopic analysis (benzene-d_6) of the precipitate is consistent with the formation of the desired N-H bond activation product [Cy-PSiP]Ir(H)($NHCH_2Ph$) (**3-15**) in 41% isolated yield. Interestingly, the solution NMR data for **3-15** indicates that this complex adopts a C_1-symmetric structure in which the Cy-PSiP ligand is bound in a facial manner, such that one phosphino donor is bound *trans* to a hydride ligand, while the other phosphino group is coordinated trans to the benzylamido ligand (Scheme 3-7). Thus, the ^{31}P NMR spectrum of **3-15** features two doublets at 44.9 and 14.7 ppm, respectively, with a coupling constant of 12 Hz. Furthermore, the ^{1}H NMR spectrum of

3-15 contains a hydride resonance that appears as a doublet of doublets at -9.04 ppm ($^2J_{HPtrans}$ = 135 Hz; $^2J_{HPcis}$ = 22 Hz). The diastereotopic benzylic protons corresponding to the $NHCH_2Ph$ ligand give rise to resonances at 4.27 (dd, J_{HH} = 13 Hz, J_{HNH} = 5 Hz) and 3.72 in the ^1H NMR spectrum of **3-15**. Interestingly, the former resonance correlates to the Cy-PSiP ligand Si in a ^1H-^{29}Si HMBC experiment, which suggests the possibility of an agostic interaction with the Ir metal center (Figure 3-3).

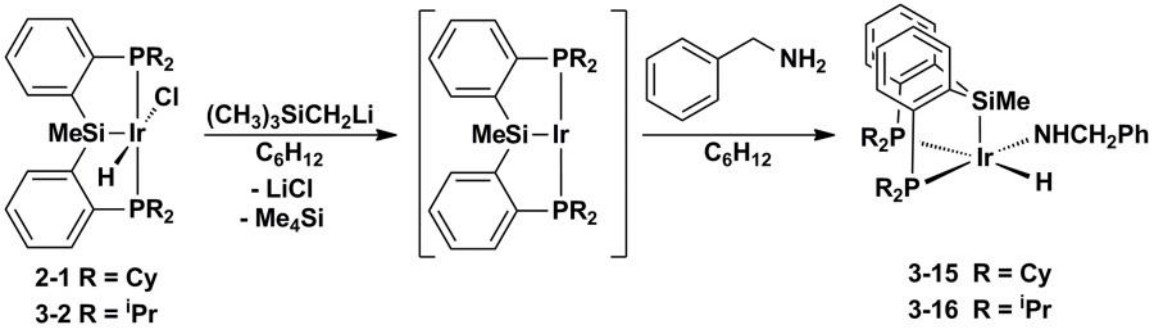

Scheme 3-7. Synthesis of [R-PSiP]Ir(H)$NHCH_2Ph$ through N-H bond activation of NH_2CH_2Ph

In a related experiment, treatment of a cyclohexane solution containing in situ generated [^{i}Pr-PSiP]Ir^I (*vide supra*) with one equivalent of H_2NCH_2Ph afforded a new product identified as the corresponding amido hydride complex [^{i}Pr-PSiP]Ir(H)($NHCH_2Ph$) (**3-16**, 96% isolated yield, Scheme 3-7) on the basis of spectroscopic evidence. The solution NMR data (^{31}P, ^1H) for **3-16** are in agreement with the formation of a C_1-symmetric product analogous to **3-15** (Figure 3-3), where the ^{i}Pr-PSiP ligand is bound in a facial manner and there is a potential agostic interaction between the Ir metal center and one of the benzylic protons at 4.17 ppm (dd, 1 H, J_{HH} = 13 Hz, J_{HNH} = 5 Hz), as a correlation between this proton and Si (^1H-^{29}Si HMBC) was observed. The $^1J_{CH}$ of this resonance was found to be 139 Hz (^1H coupled ^1H-^{13}C HSQC). Although this value is not within the range of typical agostic $^1J_{CH}$ values (75-110 Hz), the analysis is complicated by potential dynamic processes leading to an averaging of the agostic C-H interaction and non-agostic C-H.[72]

Remarkably, the N-H bond oxidative addition of benzylamine by [^{i}Pr-PSiP]Ir^{I} occurs at room temperature, whereas heating for 12 hours at 65 °C is required for the synthesis of the Cy-PSiP analogue, **3-15**. The ease with which [^{i}Pr-PSiP]Ir^{I} is able to activate the N-H bond of benzylamine demonstrates the impact that phosphine substituents have on the resulting chemistry at Ir, and may reflect decreased steric bulk in the coordination sphere of [^{i}Pr-PSiP]Ir.

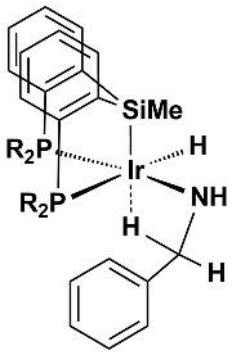

Figure 3-3. The proposed structure for [R-PSiP]Ir(H)NHCH$_2$Ph complexes

The N-H bond activation of secondary alkyl amines by [R-PSiP]Ir^{I} (R = Cy, ^{i}Pr) was also investigated. Exposure of a cyclohexane solution containing in situ generated [Cy-PSiP]Ir^{I} to either 1 or 5 equivalents of ^{i}Pr$_2$NH or Me$_2$NH led to the formation of complex reaction mixtures that contained numerous unidentified products, as well as **3-13** (^{31}P-NMR). Similar treatment of a cyclohexane solution containing in situ generated [^{i}Pr-PSiP]Ir^{I} with Me$_2$NH also led to the formation of a complex reaction mixture that contained **3-14** (^{31}P-NMR). By comparison, the analogous reaction involving treatment of [^{i}Pr-PSiP]Ir^{I} with ^{i}Pr$_2$NH in cyclohexane-d_{12} solution cleanly generated **3-14** (^{1}H, ^{31}P NMR). This reactivity suggests that numerous reaction pathways are accessible in these examples, including N-H activation and possible β-H elimination. By comparison, the heterocycles piperidine (C$_5$H$_{10}$NH, 2 equiv) and morpholine (O(CH$_2$CH$_2$)$_2$NH, 2 equiv) did not undergo any reactivity under similar conditions.

The reaction of in situ generated [R-PSiP]Ir^{I} (R = Cy, ^{i}Pr) with five equivalents of the secondary amine HNMePh (65 ºC, 16 h, cyclohexane) led to the quantitative (^{31}P

NMR) formation of new products (**3-17** for R = Cy and **3-18** for R = ^{i}Pr) that each feature a single ^{31}P NMR resonance (53.9 ppm for **3-17** and 63.7 ppm for **3-18**). Complexes **3-17** and **3-18** are formulated as adducts of the type [R-PSiP]Ir(H)$_2$(NH(CH$_3$)Ph) based on solution NMR data (benzene-d_6), including the appearance of two hydride resonances in the ^{1}H NMR spectrum (for **3-17**: -9.86 (td, 1 H, $^{2}J_{PH}$ = 15 Hz, $^{2}J_{HH}$ = 3 Hz) and -14.10 ppm (td, 1 H, $^{2}J_{PH}$ = 20 Hz, $^{2}J_{HH}$ = 3 Hz; for **3-18**: -10.26 (td, 1H, $^{2}J_{PH}$ = 15 Hz, $^{2}J_{HH}$ = 4 Hz and -14.10 ppm (td, 1 H, $^{2}J_{PH}$ = 20 Hz, $^{2}J_{HH}$ = 4 Hz)). Furthermore, a ^{1}H NMR resonance at 2.30 ppm (d, J = 5 Hz) for **3-17** could be attributed to an N-methyl group based on ^{1}H-^{13}C HMQC and ^{13}C DEPT NMR experiments. A possible route for the formation of complexes **3-17** and **3-18** involves initial N-H activation of N-methylaniline to form the unobserved amido hydride species [R-PSiP]Ir(H)(NMePh), followed by subsequent β-hydride elimination to yield an imine (Scheme 3-8). In the presence of excess aniline, an equivalent of HNMePh can coordinate to the metal center to produce the target complex.

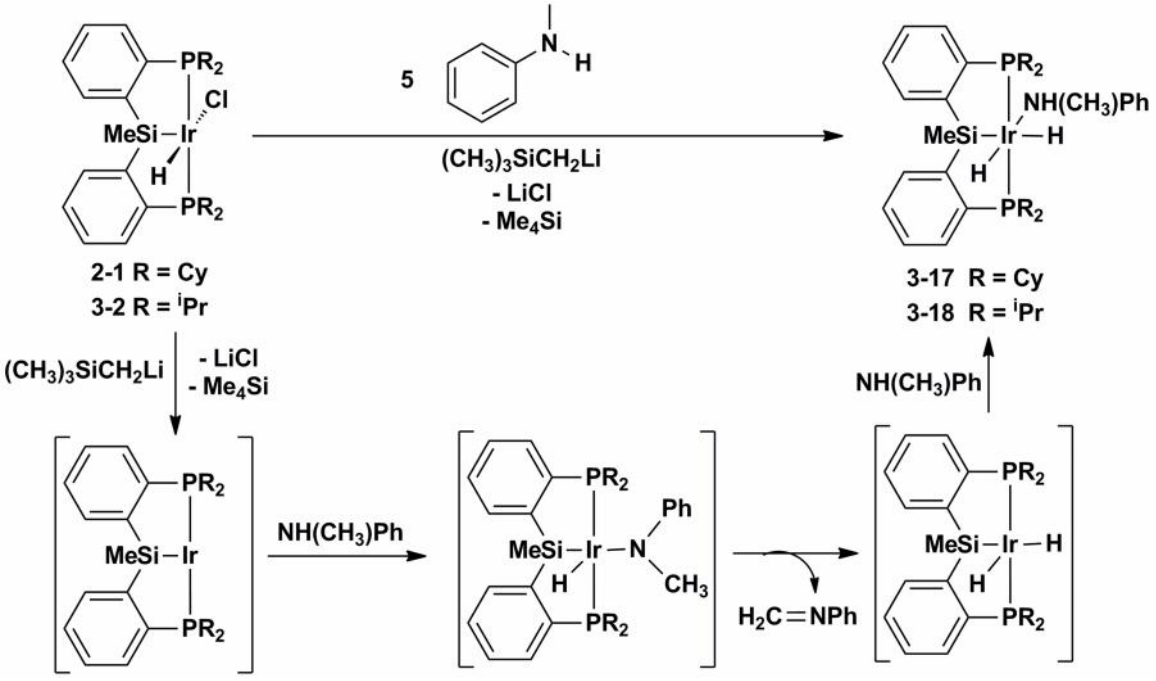

Scheme 3-8. Proposed synthesis of [R-PSiP]Ir(H)$_2$(NH(CH$_3$)Ph) (**3-17**, R = Cy; **3-18**, R = ^{i}Pr)

3.2.4 N-H Bond Activation of Hydrazines by [R-PSiP]Ir^{I}

In an effort to expand the scope of N-H bond oxidative addition by [R-PSiP]Ir^{I} (R = Cy, ^{i}Pr), the reactivity of hydrazine derivatives was investigated in this context. Hydrazine derivatives are often utilized as ammonia surrogates in cases where reactivity with ammonia is not feasible, and are thus of synthetic utility in the synthesis of amines. However, only one previous example of N-H bond oxidative addition of hydrazines to a single metal center to form isolable hydrido hydrazido complexes has been previously reported.[40] As detailed in Chapter 1, Hartwig and co-workers have demonstrated that (PCP)Ir^{I} species (PCP = $CH(CH_2CH_2P^tBu_2)_2$ or 2,6-$(CH_2P^tBu_2)_2C_6H_3$) undergo facile N-H bond activation of hydrazines, and in some cases subsequent α-H migration resulted in the formation of aminonitrene species.

The direct synthesis of the hydrazido hydride complexes that would result from N-H bond oxidative addition of hydrazine to [R-PSiP]Ir^{I} (R = ^{i}Pr, Cy) was targeted initially in order to determine if such species are isolable. Thus, the lithium salts of 1-aminopiperidine ($C_5H_{10}NNH_2$) and 4-methyl-1-aminopiperazine ($MeN(CH_2CH_2)_2NNH_2$) were reacted with hydrido chloride complexes **2-1** or **3-2**, respectively, in THF at room temperature, to furnish the desired hydrido hydrazido species (R-PSiP)Ir(H)(NHNR') (Scheme 3-9; **3-19**, R = Cy, R' = C_5H_{10}; **3-20**, R = Cy, R' = $(CH_2CH_2)_2NMe$; **3-21**, R = ^{i}Pr, R' = C_5H_{10}; **3-22**, R = ^{i}Pr, R' = $(CH_2CH_2)_2NMe$) quantitatively by ^{31}P NMR spectroscopy. These complexes were isolated as orange solids in 73 – 96% yields. The ^{31}P NMR spectra of complexes **3-19** – **3-22** indicate nonequivalent phosphino groups, as evidenced by the observation of an AB spin system centered at 55.6, 55.8, 62.6, and 62.7 ppm, respectively. This phenomenon is likely due to hindered rotation about the Ir–N bond, as was previously observed for related (PCP)Ir hydrazido hydride complexes reported by Hartwig and co-workers.[40] Furthermore, the ^{1}H NMR spectra of complexes **3-19** – **3-22** featured a characteristic hydride resonance (-20.33 – -20.64 ppm), as well as an N-H resonance (6.45 – 6.58 ppm) that was assigned on the basis of ^{1}H-^{15}N HMQC data, both characteristic of the targeted hydrazido hydride species (Table 3-4).

Complexes **3-19** – **3-22** were stable at room temperature both in solution and in the solid state, and did not undergo reductive elimination or α-H migration, even upon heating up to 70 ºC (benzene-d_6) over the course of 3 days.

Table 3-4. Selected NMR spectroscopic data (ppm) for complexes **3-19** – **3-22**

Complex	$^{31}P\{^1H\}$ NMR	^1H NMR hydride[a]	^1H NMR N*H*[a,b]	^{15}N NMR[b]	^{29}Si NMR[c]
[Cy-PSiP]Ir(H)NHNC$_5$H$_{10}$ (**3-19**)	55.6	-20.64 (t)	6.51	- 185.0	15.1
[Cy-PSiP]Ir(H)NHN(CH$_2$CH$_2$)$_2$NMe (**3-20**)	55.8	-20.62 (t)	6.45	-190.2	14.9
[^{i}Pr-PSiP]Ir(H)NHNC$_5$H$_{10}$ (**3-21**)	62.6	-20.33 (t)	6.58	-182.7	15.4
[^{i}Pr-PSiP]Ir(H)NHN(CH$_2$CH$_2$)$_2$NMe (**3-22**)	62.7	-20.40 (t)	6.50	-189.2	15.2

[a] benzene-d_6; [b] ^{1}H-^{15}N HMQC; [c] ^{1}H-^{29}Si HMBC

The solid state structure of **3-22** was determined using single crystal X-ray diffraction techniques and is consistent with the formulation of **3-22** as a five-coordinate hydrazido hydride complex (Figure 3-4, Table 3-5). As in the case of complexes **3-8** and **3-11**, the PSiP ligand coordinates to the Ir center such that the phosphino donors are trans-disposed (P1-Ir-P2 = 160.69(3)º), and the coordination geometry can be described as distorted square based pyramidal with Si in the apical site. The short Ir-N bond distance of 1.985(3) Å (cf. 2.018(2) Å for **3-8**, 2.056(2) Å for (Cy-PSiP)Ir(H)NHPh (**2-6·OEt$_2$**), and 2.077(3) Å for (Cy-PSiP)Ir(H)NH(2,6-Me$_2$C$_6$H$_3$) (**2-7**)) is comparable to those reported previously for the related (PCP)Ir complexes [(^{t}Bu$_2$PCH$_2$CH$_2$)$_2$CH]Ir(H)(NH(NC$_5$H$_{10}$)) (Ir-N = 1.9875(18) Å), [(^{t}Bu$_2$PCH$_2$CH$_2$)$_2$CH]Ir(H)NHNCPh$_2$ (Ir-N = 2.018(7) Å), and [2,6-(CH$_2$PtBu$_2$)$_2$C$_6$H$_3$]Ir(H)NHNCPh$_2$ (Ir-N = 2.022(3) Å)[40] and indicates potential Ir-N double bond character. This potential π-donation from the nitrogen lone pair to Ir would lead to hindered rotation about the Ir-N bond and could provide an explanation for the nonequivalent phosphino groups observed in solution (*vide supra*).

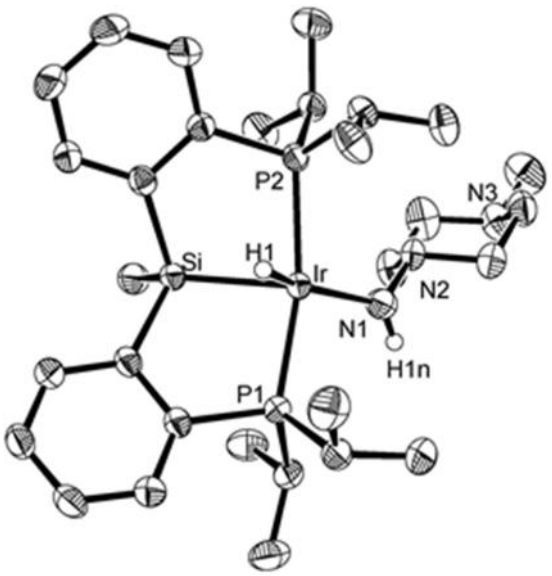

Figure 3-4. The crystallographically determined structure of **3-22**, shown with 50% displacement ellipsoids. With the exception of H1 and N-*H*, all H atoms have been omitted for clarity

Table 3-5. Selected interatomic distances (Å) and angles (º) for **3-22**.

Bond Lengths (Å)			
Ir-P1	2.2715(7)	Ir-H1	1.52(3)
Ir-P2	2.2908(7)	Ir-N	1.985(3)
Ir-Si	2.2833(7)	N-N	1.395(3)
Bond Angles (º)			
P1-Ir-P2	160.69(3)	Si-Ir-H1	68.5(12)
Si-Ir-N	137.92(8)	N-Ir-H1	153.6(12)

Having demonstrated that PSiP-supported Ir hydrazido hydride complexes are indeed isolable, the synthesis of such complexes by N-H bond activation of hydrazine derivatives was attempted. Treatment of a cyclohexane solution containing in situ generated [R-PSiP]Ir^{I} (R = Cy, ^{i}Pr) (*vide supra*) with 1.1 equiv of 1-aminopiperazine or 4-methyl-1-aminopiperidine resulted in the quantitative (^{31}P NMR) formation of the corresponding N-H bond cleavage products **3-19** – **3-22** upon heating of the reaction mixtures at 65 °C for 14 h. The hydrazido hydride complexes **3-19** – **3-22** prepared via this N-H bond activation process were isolated in yields comparable (78 – 91%) to those

obtained in the direct synthesis of these species from complexes **2-1** or **3-2**, respectively (Scheme 3-9). Related reactions utilizing either [Cy-PSiP]Ir^{I} or [^{i}Pr-PSiP]Ir^{I} and benzophenone hydrazone resulted in complex reaction mixtures (^{31}P NMR) from which no isolable products were obtained. This reactivity is not surprising given the potential for competing C(sp^{2})–H activation of the aryl groups of benzophenone hydrazone that could be facilitated by [R-PSiP]Ir^{I} species.

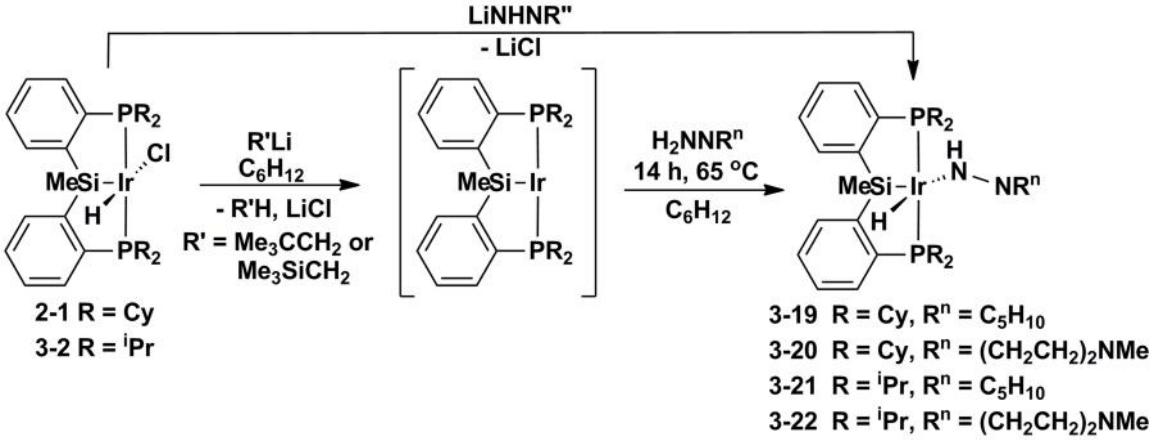

Scheme 3-9. Synthesis of [R-PSiP]Ir(H)NHNR^{n} via salt metathesis and N-H bond activation routes

3.2.5 N-H Activation of Benzamides by [R-PSiP]Ir^{I}

The N-H bond oxidative addition of benzamides by [R-PSiP]Ir^{I} (R = Cy, ^{i}Pr) was also investigated in the course of this study. Treatment of a cyclohexane solution containing in situ generated [R-PSiP]Ir^{I} (R = Cy, ^{i}Pr) with 1.1 equiv of $H_2N(CO)Ph$ or $H_2N(CO)(C_6F_5)$ led to the quantitative formation (^{31}P NMR) of the corresponding Ir^{III} oxidative addition products [R-PSiP]Ir(H)(NHC(O)R') (Scheme 3-10; **3-23**, R = Cy, R' = Ph; **3-24**, R = Cy, R' = C_6F_5; **3-25**, R = ^{i}Pr, R' = Ph; **3-26**, R = ^{i}Pr, R' = C_6F_5) upon heating of the reaction mixtures for 2 hours at 65 ºC. Complexes **3-23** – **3-26** were isolated as pale yellow solids in 70 - 99% yields, and are stable both in solution and in the solid state.

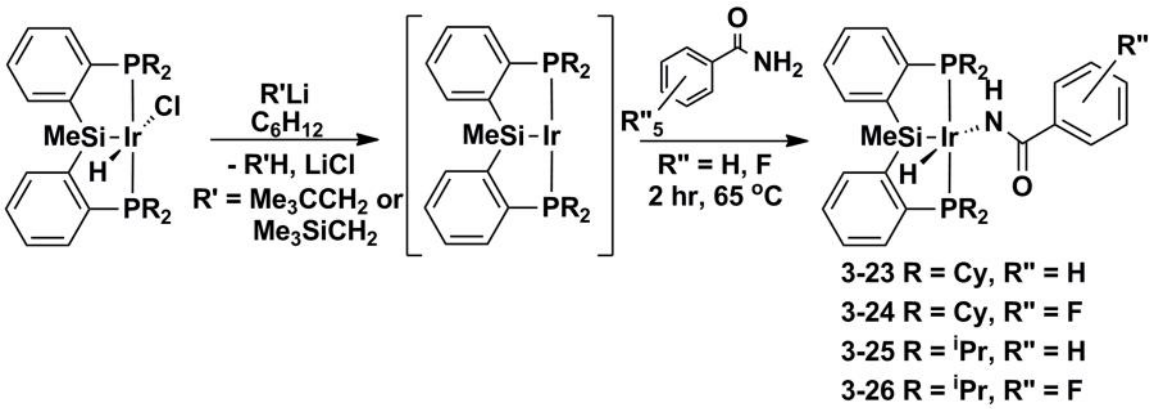

Scheme 3-10. Synthesis of [R-PSiP]Ir(H)NH(CO)Ar through N-H bond activation of benzamides

The ^{31}P NMR spectra of **3-23** – **3-26** feature a single resonance in the range of 50.9 - 60.1 ppm, consistent with the formation of C_s-symmetric complexes in solution. The ^{1}H NMR spectra (benzene-d_6) of **3-23** – **3-26** feature a hydride resonance (-20.89 – -21.28 ppm), as well as a characteristic N-H resonance in the range of 5.24 - 5.73 ppm that was assigned on the basis of ^{1}H-^{15}N HMQC data. The IR spectra of complexes **3-23** – **3-26** do not feature an amide carbonyl stretch, likely due to coordination of the carbonyl group to the Ir center to form κ^2-amide species.[41,73] Indeed, the X-ray crystal structure of **3-24** (Figure 3-5, Table 3-6) features a short Ir–O distance of 2.4285(14) Å, which falls in the range of Ir-O bond distances reported for other Ir^{III} κ^2-amide complexes (2.290 - 2.550 Å).[41,73] The amide nitrogen is coordinated trans to the hydride ligand (N-Ir-H = 167.8(9)º), as has been the case for all structurally characterized products of N-H bond oxidative addition to [R-PSiP]Ir^{I}, while the carbonyl oxygen is positioned trans to silicon (Si-Ir-O = 169.84(4)º). The Ir–N bond distance of 2.1615(19) Å is longer than those reported for the aryl and alkyl amido hydride complexes [Cy-PSiP]Ir(H)NHPh (**2.6**, 2.056 (2) Å) and [Cy-PSiP]Ir(H)NHAd (**3-8**, 2.018 (2) Å), but is comparable to the related κ^2-amide complex [POCOP]Ir(H)(NHC(O)Ph), which features an Ir-N distance of 2.171(3) Å.[41]

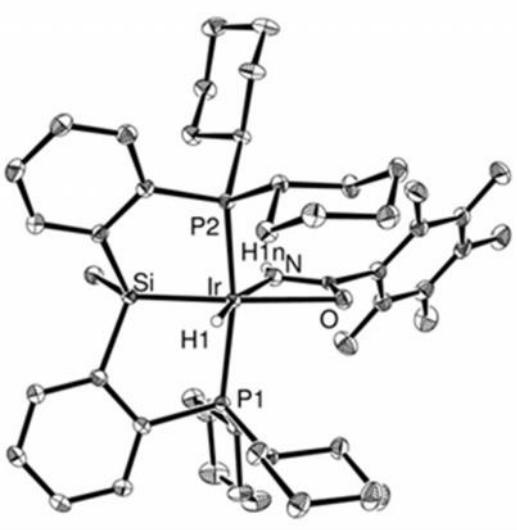

Figure 3-5. The crystallographically determined structure **3-24** shown with 50% displacement ellipsoids. With the exception of H1 and N-*H*, all H atoms have been omitted for clarity.

Table 3-6. Selected interatomic distances (Å) and angles (º) for **3-24**.

Bond Lengths (Å)			
Ir-P1	2.2942(5)	Ir-H1	1.51(2)
Ir-P2	2.2926(5)	Ir-N	2.1615(19)
Ir-Si	2.2636(5)	Ir-O	2.4285(14)
Bond Angles (º)			
P1-Ir-P2	162.273(18)	Si-Ir-H1	79.3(9)
Si-Ir-N	112.81(5)	N-Ir-H1	167.8(9)
Si-Ir-O	169.84(4)	O-Ir-N	57.03(6)

Only one prior example of N-H bond oxidative addition of benzamides has been reported by Brookhart and co-workers.[41] Thus the reactivity exhibited by the [R-PSiP]Ir fragment represents another rare example of N-H bond oxidative addition. The relatively facile N-H bond activation observed for benzamides (2 h at 65 ºC) compared to aryl and alkyl amines (14 h at 65 ºC), reflects the fact that amide N-H bonds are likely more activated toward bond cleavage than amine N-H bonds due to the presence of electron withdrawing substituents.

3.2.6 Reactivity of [Cy-PSiP]Rh^{I} with N–H Bonds

In addition to the N-H bond oxidative chemistry observed with [R-PSiP]Ir (R = Cy, ^{i}Pr) complexes, there was interest in investigating the reactivity of related Rh complexes with N-H bonds. In Chapter 2 attempts to synthesize rhodium amido hydride complexes of the type [Cy-PSiP]Rh(H)NHR from the reaction of [Cy-PSiP]Rh(H)Cl (**2-2**) with LiNHR were discussed. Efforts towards the synthesis of the product of ammonia N-H bond cleavage by the reaction of **2-2** with $LiNH_2$ led to complex reaction mixtures with no isolable products (Scheme 2-5). Conversely, the anilido hydride complex [Cy-PSiP]Rh(H)(NHPh) formed readily upon treatment of **2-2** with LiNHPh, and proved to be isolable and resistant to N-H bond reductive elimination (Scheme 2-4). Attempts to form the amido and anilido hydride products by N-H bond activation of ammonia or aniline, respectively, utilizing in situ generated [Cy-PSiP]Rh^{I} were not successful. Instead, the quantitative formation of Rh^{I} amine adducts of the type [Cy-PSiP]Rh(NH_2R) (Scheme 2-9, R = H, Ph) was observed. Attempts to isolate these adducts were unsuccessful as the coordinated amine was removed upon exposure to vacuum.

In an effort to expand on these initial studies, further exploration of N-H bond activation of other types of amine-containing substrates utilizing [R-PSiP]Rh (R = Cy, ^{i}Pr) was conducted in parallel with studies on [R-PSiP]Ir mediated N-H bond cleavage. Preparation of a Rh precursor complex of the type [^{i}Pr-PSiP]Rh(H)Cl (**3-27**) was attempted by treatment of **3-1** with a series of Rh starting materials, including $[Rh(COD)Cl]_2$, $[Rh(COE)Cl]_2$, and $RhCl(PPh_3)_3$. Unfortunately, we were unable to cleanly isolate the targeted Rh complex **3-27** by any of these routes. As such, the study of N-H bond activation is restricted to the chemistry of the [Cy-PSiP]Rh fragment.

As in the case of the related Ir species, initial investigations focused on the reactivity of alkyl amine substrates. We were unable to directly synthesize complexes of the type [Cy-PSiP])Rh(H)(NHR) (R = Ad, ^{t}Bu, Cy) by the reaction of **2-2** with the corresponding LiNHR species in THF, as such reactions immediately led to intractable reaction mixtures from which no pure material could be isolated. Conversely, treatment

of a benzene-d_6 solution of **2-2** with $TMSCH_2Li$ resulted in an immediate colour change from yellow to dark red. Complete consumption of **2-2** and formation of Me_4Si was observed (^1H and ^{31}P NMR). Subsequently five equiv of NH_2R (R = Ad, ^{t}Bu, Cy) were added to the reaction mixture which led to the rapid and quantitative (^{31}P NMR) formation of new Rh complexes, which were tentatively assigned as the corresponding amine adducts [Cy-PSiP]Rh(NH_2R) (Scheme 3-11; **3-28**, R = Ad; **3-29**, R = ^{t}Bu; **3-30**, R = Cy). As was previously observed for the related complexes [Cy-PSiP]Rh(NHR) (R = H, Ph), these alkyl amine adducts could only be observed in situ, as the amine was easily removed upon exposure of the complexes to vacuum, which prevented their isolation. The ^{31}P NMR spectra of in situ generated **3-28** – **3-30** feature a single resonance in the range of 52.1 - 54.8 ppm. The ^1H NMR spectra of these complexes lack the characteristic upfield shifted hydride resonance that would be expected if the targeted amido hydride species had been generated. The ^{13}C and ^1H-NMR spectra of **3-28** – **3-30** feature a single set of peaks for the aromatic ligand backbone, indicating symmetry in the C_s-symmetric complexes. No further reactivity was observed upon heating of complexes **3-28** – **3-30** in benzene-d_6 solution (up to 100 ºC).

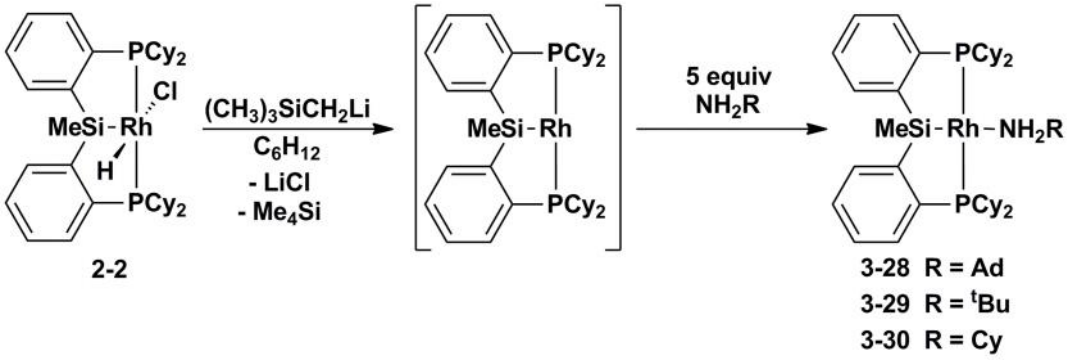

Scheme 3-11. Generation of Rh^I alkyl amine adducts [Cy-PSiP]Rh(NH_2R) (R = Ad, ^{t}Bu, Cy)

Interestingly, the reaction of **2-2** with one equiv of LiNHR' (R' = ^{n}Pr, ^{n}Oct) in THF solution cleanly generated amine adducts of the type (Cy-PSiP)Rh(NH_2R') (Scheme 3-12; **3-31**, R' = ^{n}Pr; **3-32**, R' = ^{n}Oct). As in the case of **3-28** – **3-30**, these complexes

could only be observed in situ, as the amine was easily removed upon exposure of the complexes to vacuum, which prevented their isolation. Thus treatment of **2-2** with the appropriate lithium salt in benzene-d_6 yielded **3-31** and **3-32** allowed characterization of these amine adducts which exhibited a single set of ligand aromatic resonances (^{1}H and ^{13}C) and no upfield hydride resonance was observed. Formation of **3-31** and **3-32** in these reactions is consistent with facile N-H bond reductive elimination from complexes of the type [Cy-PSiP]Rh(H)(NHR'). Thus it appears that unlike the anilido hydride complex [Cy-PSiP]Rh(H)(NHPh) (**2-8**) that proved resistant to N-H bond reductive elimination, related alkyl amido hydride complexes readily undergo alkyl amine reductive elimination. Complexes **3-31** and **3-32** were also synthesized via treatment of in situ generated [Cy-PSiP]Rh^I with 5 equiv of the appropriate amine.

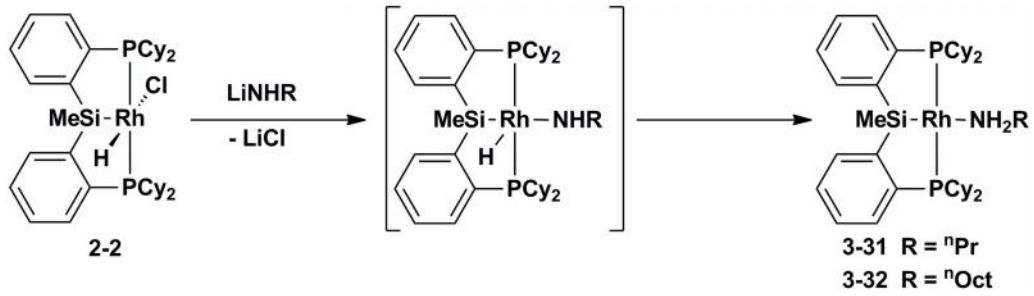

Scheme 3-12. Generation of Rh^I amine adducts [Cy-PSiP]Rh(NH_2R) (R = ^{n}Pr, ^{n}Oct)

Although the Rh^I amine adducts **3-28** – **3-32** were not isolable, an isolable amine adduct [Cy-PSiP]Rh(NH_2CH_2Ph) (**3-33**) that survived exposure to vacuum by the treatment of in situ generated [Cy-PSiP]Rh^I (*vide supra*) with one equiv of benzylamine (Scheme 3-13). Complex **3-33** was isolated as an orange solid in 93% yield. The ^{31}P NMR spectrum of **3-33** contains a resonance at 54.3 ppm (d, $^1J_{RhP}$ = 180 Hz), consistent with the ^{31}P chemical shift range observed for **3-28** – **3-32**, while the ^{1}H NMR spectrum (benzene-d_6) features a single set of PSiP ligand and benzylamine aromatic resonances as well as a resonance at 3.89 ppm (br singlet) that integrates as two protons and corresponds to the NH_2 group of the coordinated benzylamine (confirmed by a ^{1}H-^{15}N

HMQC experiment). Heating of **3-33** (70 ºC for 1 days in benzene-d_6 solution) did not result in subsequent N-H bond activation.

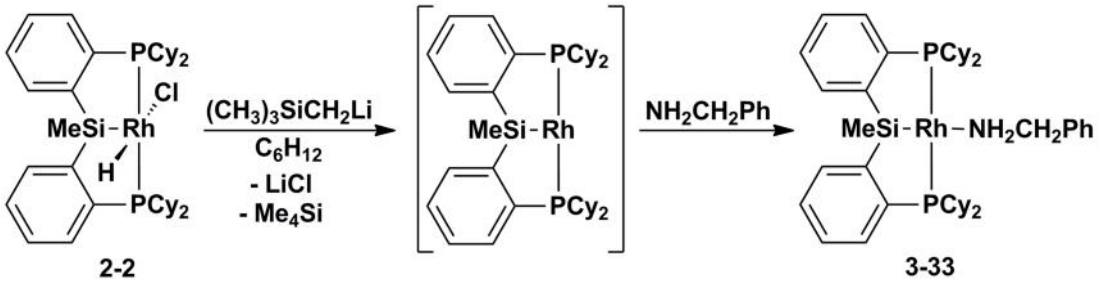

Scheme 3-13. Synthesis of Rh^I amine adduct [Cy-PSiP]Rh(NH_2CH_2Ph) (**3-33**)

The reactivity of (Cy-PSiP)Rh species with hydrazine derivatives was also investigated. Direct synthesis of isolable hydrido hydrazido complexes of the type [Cy-PSiP]Rh(H)(NHNR) (Scheme 3-14; **3-34**, R = C_5H_{10}; **3-35**, R = $(CH_2CH_2)_2NMe$) was achieved by the reaction of **2-2** with the lithium salts of 1-aminopiperadine ($C_5H_{10}NNH_2$) and 4-methyl-1-aminopiperazine ($MeN(CH_2CH_2)_2NNH_2$), respectively. These products of N-H bond activation of hydrazine derivatives were isolated as orange solids in 69 – 90 % yield. Both **3-34** and **3-35** are stable both in the solid state and in solution, and as in the case of the Ir analogues **3-19** – **3-22**, no subsequent reductive elimination or α-H migration was observed. The ^{31}P NMR spectra of complexes **3-34** and **3-35** exhibit broad singlets at 63.6 and 63.7 ppm, respectively. This phenomenon is likely due to hindered rotation about the Rh–N bond, as was previously observed for related Ir hydrazido hydride complexes **3-19** – **3-22** (*vide supra*). Furthermore, the ^1H NMR spectra of complexes **3-34** and **3-35** featured a characteristic hydride resonance (-16.74 and -16.78 ppm, respectively), as well as an N-H resonance (4.75 and 4.69 ppm, respectively) that was assigned on the basis of ^1H-^{15}N HMQC data, both characteristic of the targeted hydrazido hydride species.

Attempts to generate complexes **3-34** and **3-35** by N-H bond activation of the corresponding hydrazines using in situ generated [Cy-PSiP]Rh^I led to the quantitative

(^{31}P NMR) formation of Rh^{I} hydrazine adducts of the type [Cy-PSiP]Rh(NH_2NR) (Scheme 3-14; **3-36**, R = C_5H_{10}; **3-37**, R = $(CH_2CH_2)_2NMe$). As was previously observed for amine and aniline adducts of (Cy-PSiP)Rh, complexes **3-36** and **3-37** could only be observed in situ and decomposed upon attempted isolation. The formation of these Rh^{I} adducts in the presence of one equiv of the corresponding hydrazine derivative was monitored by ^{31}P and ^{1}H NMR spectroscopy (benzene-d_6 solution), which were consistent with the clean generation of new (Cy-PSiP)Rh species that do not exhibit a Rh-H resonance and feature a ^{1}H NMR resonance at 3.56 and 3.45 ppm, respectively, corresponding to the NH_2 group of the coordinated hydrazine. No further reactivity was observed upon heating of **3-36** or **3-37** up to 70 ºC for 2 days in benzene-d_6 solution.

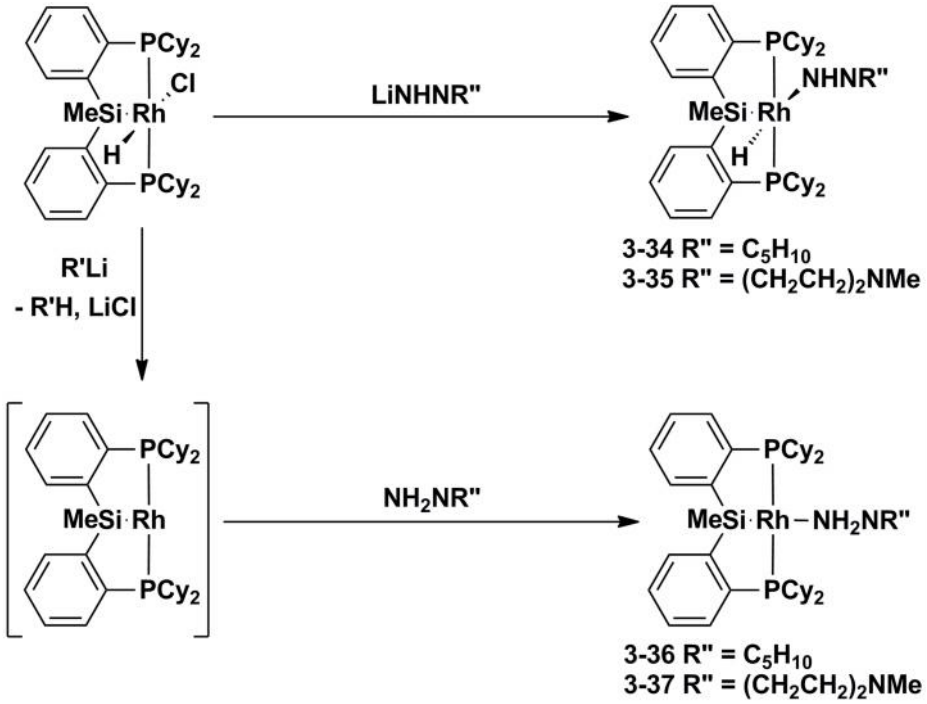

Scheme 3-14. Synthesis of [Cy-PSiP]Rh(H)NHNR" complexes via salt metathesis and generation of Rh^{I} hydrazine adducts [Cy-PSiP]Rh(NH_2NR")

Although we were unable to isolate bulk samples of complexes **3-36** and **3-37**, a minute amount of crystalline material was obtained from a reaction mixture containing **3-**

37, which enabled the solid state characterization of this complex by use of single crystal X-ray diffraction techniques (Figure 3-6, Table 3-7). The Rh center in **3-37** exhibits the expected square planar coordination geometry (Si-Rh-N1 = 168.05(8)º, P1-Rh-P2 = 152.25(3)º), with the hydrazine ligand coordinated trans to Si. The Rh-N1 distance of 2.295(3) Å is significantly longer than the Rh-N distance of 2.123(5) Å observed for the anilido hydride complex [Cy-PSiP]Rh(H)(NHPh) and the Ir-N distance of 1.985(3) Å observed for the Ir hydrazido hydride complex [^{i}Pr-PSiP]Ir(H)(NHN(CH_2CH_2)$_2$NMe) (**3-22**).

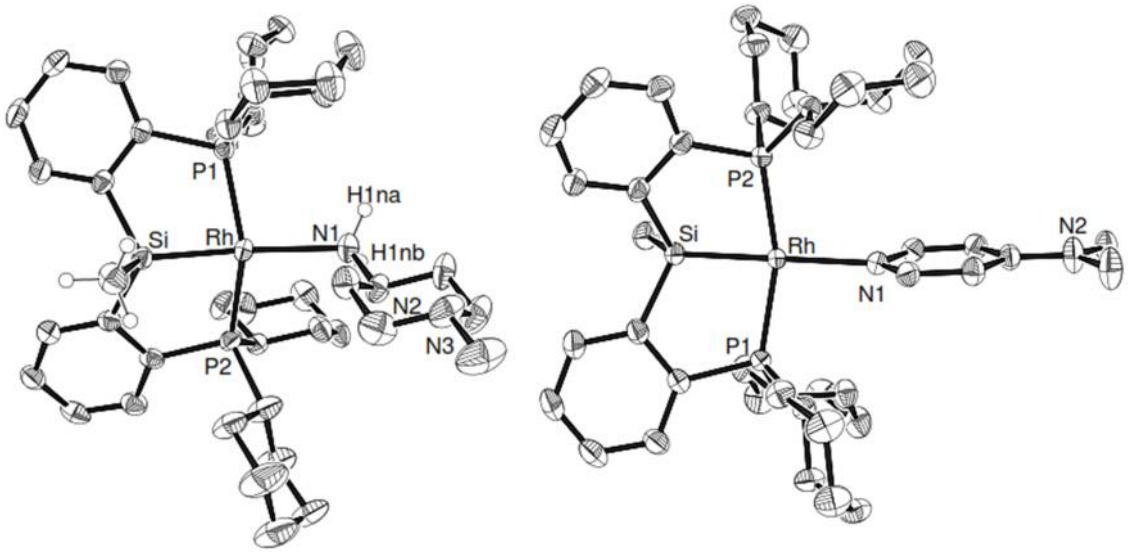

3-37 **3-38**

Figure 3-6. The crystallographically determined structures of **3-37** and **3-38·Et_2O** shown with 50% displacement ellipsoids. With the exception of H1 and N-*H*, all H atoms, as well as the Et_2O solvate, have been omitted for clarity.

Table 3-7. Selected interatomic distances (Å) and angles (º) for **3-37**, and **3-38·Et$_2$O**

Bond Lengths (Å)				
3-37	Rh-P1	2.2674(8)	Rh-N1	2.295(3)
	Rh-P2	2.2616(9)	N1-N2	1.443(4)
	Rh-Si	2.2482(8)		
3-38·Et$_2$O	Rh-P1	2.2628(4)	Rh-N1	2.2027(14)
	Rh-P2	2.2678(4)		
	Rh-Si	2.2634(5)		
Bond Angles (º)				
3-37	P1-Rh-P2	152.25(3)	Si-Rh-N	168.05(8)
3-38·Et$_2$O	P1-Rh-P2	161.216(16)	Si-Rh-N	179.77(4)

As a comparison, an easily isolable Rh^I adduct was synthesized and the resulting X-ray crystal structure was studied. In this regard, *in situ* generation of [Cy-PSiP]Rh^I from **2-2** and $TMSCH_2Li$ in benzene solution followed by addition of 4-dimethylaminopyridine (DMAP) yielded a new product with a ^{31}P NMR resonance centered at 53.0 ppm, after stirring at room temperature for 0.5 h. The [Cy-PSiP]Rh(DMAP) pyridine adduct (**3-38**) was easily isolated in 95 % yield (Scheme 3-15). Spectroscopic data supported the formation of a C_s-symmetric complex with one set of ligand aryl resonances (^1H and ^{13}C NMR) as well as a broad singlet for the two Me groups of the coordinated DMAP ligand. The resulting X-ray crystal structure of **3-38** was obtained and confirmed the proposed geometry. The structure of **3-38** exhibited a Rh-N distance of 2.2027(14) Å, which is close to that observed for **3-37** (Figure 3-6).

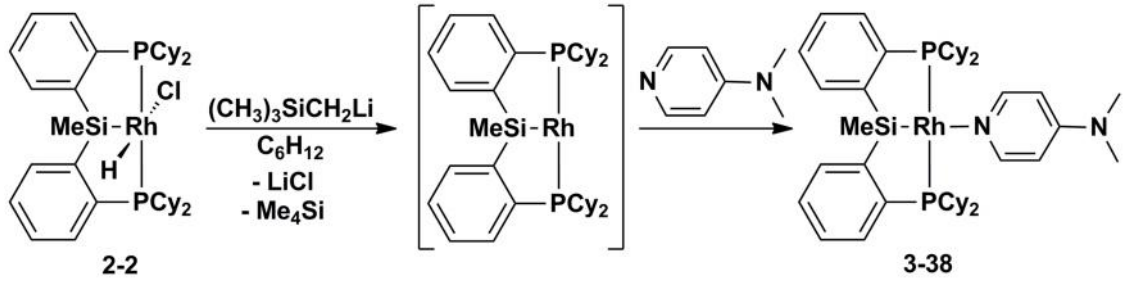

Scheme 3-15. Synthesis of Rh^I pyridine adduct [Cy-PSiP]Rh(DMAP) (**3-38**)

Remarkably, the reaction of *in situ* generated [Cy-PSiP]Rh^{I} with benzophenone hydrazone led to the first example of N-H bond activation mediated by a bis(phosphino)silyl rhodium complex (Scheme 3-16). Upon addition of one equiv of benzophenone hydrazone to a benzene-d_6 solution of *in situ* generated [Cy-PSiP]Rh^{I} at room temperature the formation of two new Rh-containing species was observed by ^{31}P NMR spectroscopy. The major product (**3-39**) gives rise to a ^{31}P NMR resonance at 55.9 ppm (d, $^{1}J_{RhP}$ = 184 Hz), while the minor product (**3-40**) gives rise to a resonance at 63.1 ppm (d, $^{1}J_{RhP}$ = 122 Hz; 9:1 ratio of **3-39**:**3-40**). After standing at room temperature for three days, the ratio of **3-39**:**3-40** was circa 1:1. Subsequent heating of the reaction mixture for 14 h at 65 ºC led to quantitative conversion to **3-40**, which was isolated in 86% yield in a preparative scale reaction. The ^{1}H NMR spectrum of isolated **3-40** is consistent with a hydrido hydrazido complex of the type [Cy-PSiP]Rh(H)(NH-N=CPh_2) and features a Rh-H resonance at -17.3 ppm, as well as a resonance at 8.35 ppm that integrates as one proton and corresponds to the N-H proton of the Rh bound NH-N=CPh_2 ligand. ^{1}H NMR analysis of the reaction mixture containing **3-39** and **3-40** indicates that complex **3-40** does not give rise to a Rh-H resonance, and thus we tentatively assign this intermediate in the formation of **3-39** as the Rh^{I} adduct [Cy-PSiP]Rh(NH_2-N=CPh_2) (Scheme 3-16). Rhodium complexes that can mediate N-H bond oxidative addition are relatively rare.[16b]

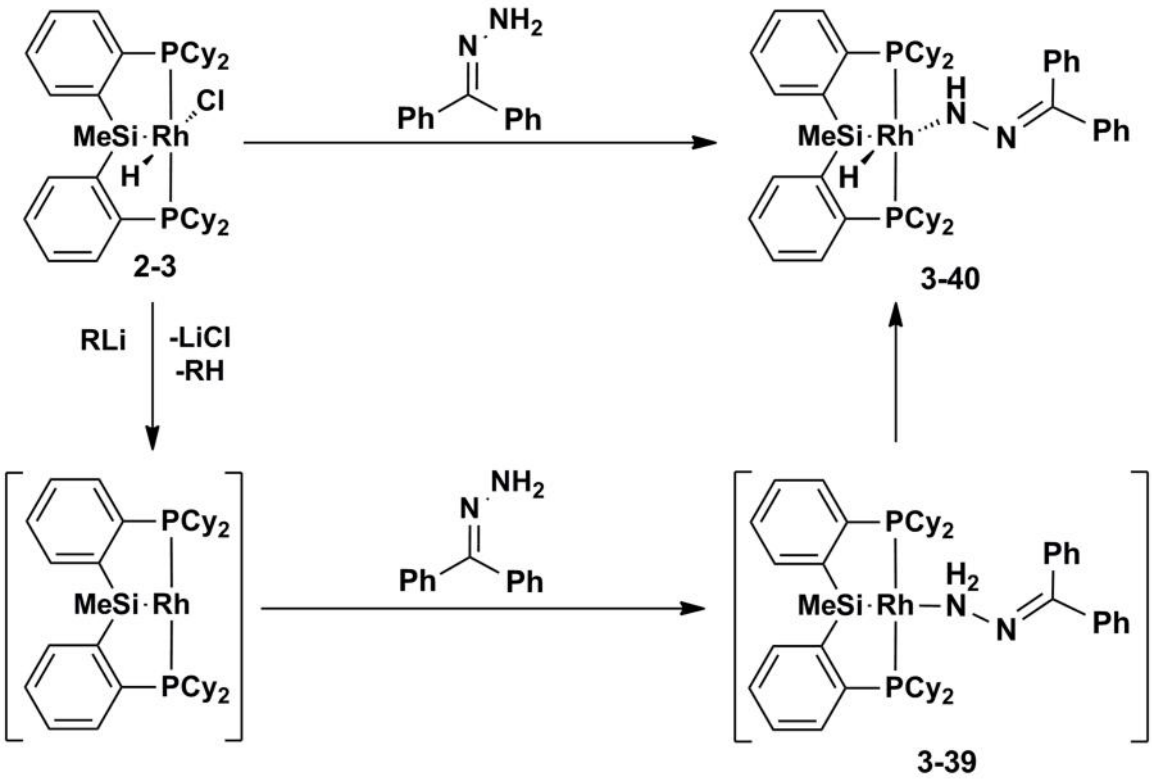

Scheme 3-16. Synthesis of [Cy-PSiP]Rh(H)NH-N=CPh_2 (**3-40**) via N-H bond activation

To further probe the scope of this Rh-mediated N-H bond oxidative addition, [Cy-PSiP]Rh^I was reacted with 4,4'-dichlorobenzophenone hydrazone and 4,4'-dimethoxybenzophenone hydrazone (Scheme 3-17). Treatment of in situ generated [Cy-PSiP]Rh^I with 1 equiv of 4,4'-dichlorobenzophenone hydrazone led to the formation of a new product (**3-41**) that has been assigned as the Rh^I adduct [Cy-PSiP]Rh(NH_2-N=C(*p*-$ClC_6H_4)_2$) on the basis of ^1H and ^{31}P NMR spectroscopy. Complex **3-41** was isolated in 83% yield and exhibited a single ^{31}P resonance at 47.3 ppm (d, $^1J_{RhP}$ = 113 Hz) corresponding to the symmetry equivalent phosphine donors of the [Cy-PSiP] ligand. The ^1H NMR spectrum of **3-41** does not feature a hydride resonance, which is consistent with a lack of N-H bond oxidative addition to Rh. Prolonged heating (70 ºC for 72 h) of a benzene-d_6 solution of complex **3-41** did not encourage any further reactivity. Conversely, treatment of *in situ* generated [Cy-PSiP]Rh^I with 1 equiv of 4,4'-

dimethoxybenzophenone hydrazone led to the formation of a complex reaction mixture from which no clean (Cy-PSiP)Rh-containing product could be isolated.

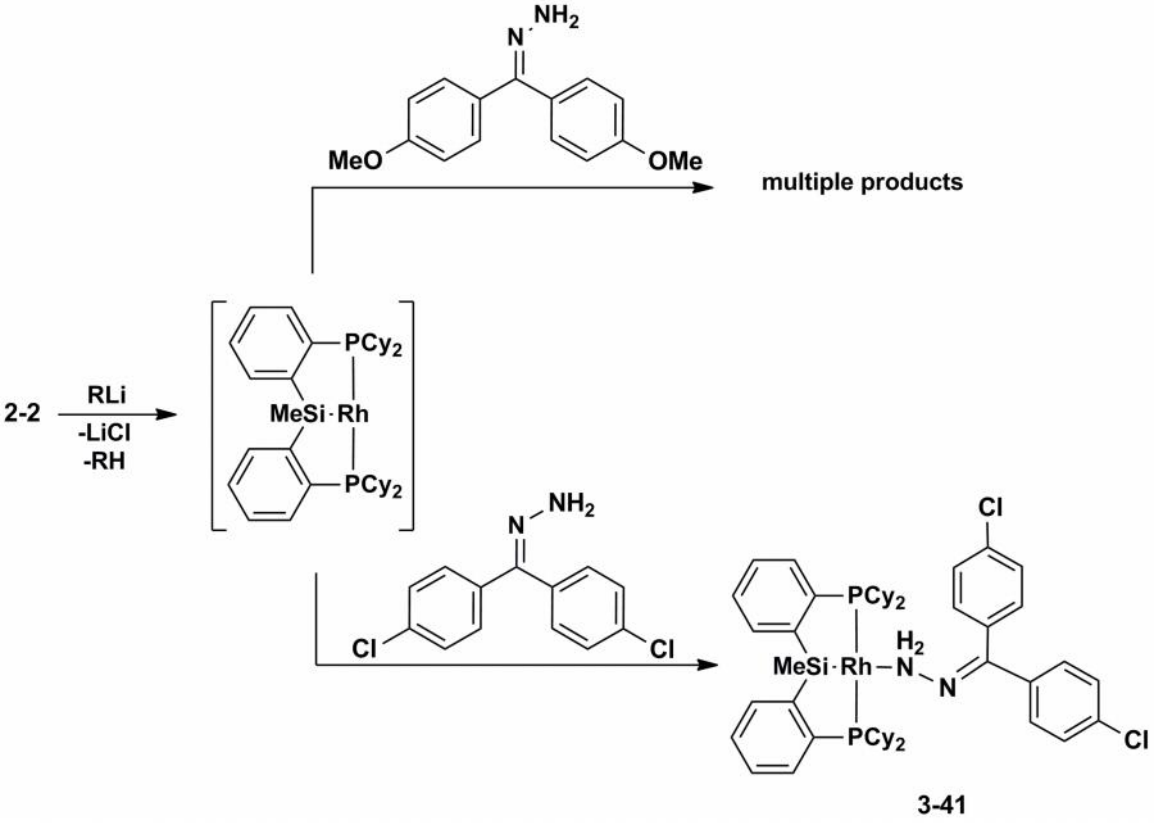

Scheme 3-17. Reactivity of [Cy-PSiP]Rh^{I} with benzophenone hydrazone derivatives

The observed reactivity of [Cy-PSiP]Rh^{I} with the N-H bond of benzophenone hydrazone stands in contrast to what has previously been observed for the reaction of [Cy-PSiP]Rh^{I} with aryl amines, alkyl amines, and ammonia, where amine adducts are formed preferentially. This difference in reactivity may be explained by the subtle relationship between more basic amines (alkyl amines, ammonia) being able to coordinate strongly to transition metal centers, while less basic amines (benzophenone hydrazone), although not able to coordinate as strongly to the metal center, are more likely to undergo N-H bond cleavage chemistry due to the weaker N-H bond. As a result, the weaker N-H bond in benzophenone hydrazone may be easier to cleave by the less

electron rich Rh center, compared to the [R-PSiP]Ir systems which are capable of cleaving a variety of N-H bonds.

3.3 Conclusions

In summary, the ability of Rh and Ir bis(phosphino)silyl pincer complexes to mediate N-H bond activation has been thoroughly investigated, including a comprehensive study of the interaction of [Cy-PSiP]Rh^{I} and [R-PSiP]Ir^{I} (R = Cy, ^{i}Pr) with the N-H bonds of anilines, alkyl amines, hydrazines, benzamides, and ammonia. Alkyl amines are inherently more difficult to activate due to the propensity for the more basic lone pair on nitrogen to coordinate to a metal center rather than undergo oxidative addition. Remarkably, the highly reactive [R-PSiP]Ir^{I} (R = Cy, ^{i}Pr) intermediates were shown to mediate the oxidative addition of highly Lewis basic amines, such as adamantylamine, *tert*-butylamine, cyclohexyl amine and benzyl amine. This represents the first known example of facile N-H bond oxidative addition of alkyl amines to form isolable amido hydride complexes. The reactivity of primary and secondary alkyl amines that contained β-hydrogens was complicated by possible β-hydride elimination. In addition, the N-H bond oxidative addition of hydrazine derivatives was also investigated. The N-H bonds of 1-aminopiperidine and 4-methyl-1-aminopiperazine were activated, showing the variability in N-H bonds that are cleaved by the [R-PSiP]Ir^{I} system. Finally, the facile N-H bond activation of benzamides by [R-PSiP]Ir^{I} was also documented.

In contrast to the N-H bond cleavage reactivity observed for [Cy-PSiP]Ir^{I}, the Rh analogue [Cy-PSiP]Rh^{I} reacted with primary and secondary alkyl amines, as well as with hydrazine derivatives to form simple amine adducts, in direct relation to the reactivity previously observed for this fragment with ammonia and anilines. Although for the most part such amine adducts were stable only in the presence of excess amine and were not isolable, the benzyl amine adduct [Cy-PSiP]Rh(NH_2CH_2Ph) proved to be isolable. Interestingly, the first example of [Cy-PSiP]Rh^{I} mediated N-H bond activation was observed with the hydrazine derivative benzophenone hydrazone to yield [Cy-

PSiP]Rh(H)($NHNCPh_2$). This represents a rare example of N-H bond activation mediated by Rh.

The remarkable ability of bis(phosphino)silyl ligated Ir complexes to mediate the N-H bond activation of a wide variety of amine substrates represents the first documented example of such comprehensive N-H bond oxidative addition chemistry. This reactivity will enable the careful investigation of the chemical transformations of such late metal amido complexes, with the ultimate goal of developing of new pathways for the formation of C-N bonds.

3.5 Experimental Section

3.5.1 General Considerations

All experiments were conducted under nitrogen in an MBraun glovebox or using standard Schlenk techniques. Dry, oxygen-free solvents were used unless otherwise indicated. All non-deuterated solvents were deoxygenated and dried by sparging with nitrogen and subsequent passage through a double-column solvent purification system purchased from MBraun Inc. Tetrahydrofuran and diethyl ether were purified over two activated alumina columns, while benzene, toluene, and pentane were purified over one activated alumina column and one column packed with activated Q-5. All purified solvents were stored over 4 Å molecular sieves. Benzene-d_6 and cyclohexane-d_{12} were degassed via three freeze-pump-thaw cycles and stored over 4 Å molecular sieves. The compounds [Cy-PSiP]Rh(H)Cl,[15b] [Cy-PSiP]Ir(H)Cl,[15b] Me_3SiCH_2Li,[66] and NpLi[67] were prepared according to literature procedures. Anhydrous ammonia and ethylene were purchased from Air Liquide Canada and used as received. All other reagents were purchased from Aldrich and used without further purification. Unless otherwise stated, ^1H, ^{13}C, ^{31}P NMR, ^{15}N, and ^{29}Si characterization data were collected at 300K on a Bruker AV-500 spectrometer operating at 500.1, 125.8, 202.5, 50.7 and 99.4 MHz (respectively) with chemical shifts reported in parts per million downfield of $SiMe_4$ (for ^1H, ^{13}C, and ^{29}Si), $MeNO_2$ (for ^{15}N), or 85% H_3PO_4 in D_2O (for ^{31}P). ^1H and ^{13}C NMR chemical shift

assignments are based on data obtained from ^{13}C-DEPTQ, ^{1}H-^{1}H COSY, ^{1}H-^{13}C HSQC, and ^{1}H-^{13}C HMBC NMR experiments. ^{29}Si NMR assignments are based on ^{1}H-^{29}Si HMQC and ^{1}H-^{29}Si HMBC experiments. ^{15}N NMR assignments are based on ^{1}H-^{15}N HMQC experiments. In some cases, fewer than expected unique ^{13}C NMR resonances were observed, despite prolonged acquisition times. Elemental analyses were performed by Canadian Microanalytical Service Ltd. of Delta, British Columbia, Canada and by Columbia Analytical Services of Tucson, Arizona. Infrared spectra were recorded as Nujol mulls between NaCl plates using a Bruker TENSOR 27 FT-IR spectrometer at a resolution of 4 cm^{-1}. X-ray data collection, solution, and refinement were carried out by Drs. Robert MacDonald and Michael J. Ferguson at the University of Alberta X-ray Crystallography Laboratory, Edmonton, Alberta.

3.5.2 Synthetic Details and Characterization Data

[^{i}Pr-PSiP]H (3-1). A solution of 2-^{i}Pr$_2$PC$_6$H$_4$Li·(Et$_2$O)$_{0.7}$ (0.40 g, 1.58 mmol) in ca. 2 mL of hexanes was cooled to -78 °C and subsequently treated with 0.5 equiv of Cl$_2$SiMeH (0.091 g, 0.79 mmol). The resulting clear peach solution was allowed to warm to room temperature over the course of 18 h, and the volatile components of the reaction mixture were then removed in vacuo. The remaining residue was dissolved in ca. 5 mL of benzene and filtered through Celite. The filtrate solution was dried in vacuo to afford **3-1** (0.29 g, 87%) as a pale yellow oil. ^{1}H NMR (500.1 MHz, benzene-d_6): δ 7.71 (d, 2 H, J = 7 Hz, H_{arom}), 7.36 (d, 2 H, J = 7 Hz, H_{arom}), 7.19 – 7.12 (overlapping resonances, 4 H, H_{arom}), 6.27 (m, 1 H, Si*H*), 1.97 – 1.88 (overlapping resonances, 4 H, P^{i}*Pr*), 1.12 – 1.06 (overlapping, 12 H, P^{i}*Pr*), 0.92 (d, 3 H, Si*Me*, $^{3}J_{HH}$ = 4 Hz), 0.90 – 0.84 (m, 12 H, P^{i}*Pr*). ^{13}C{^{1}H} NMR (125.8 MHz, benzene-d_6): δ 147.3 (d, J = 45 Hz, C_{arom}), 144.9 (d, J = 17 Hz, C_{arom}), 138.0 (d, J_{CP} = 15 Hz, *C*H$_{arom}$), 132.5 (*C*H$_{arom}$), 129.4 (*C*H$_{arom}$), 128.8 (*C*H$_{arom}$), 26.2 (d, J_{CP} = 15 Hz, *C*H$_{iPr}$), 25.8 (d, J_{CP} = 14 Hz, *C*H$_{iPr}$), 21.2 – 20.7 (overlapping resonances, *C*H$_{3iPr}$), -1.1 (Si*Me*). ^{31}P{^{1}H} NMR (202.5 MHz, benzene-d_6):

δ 0.4 (s). ^{29}Si NMR (99.4 MHz, benzene-d_6): δ75.4. IR (Thin Film, cm^{-1}): 2177 (m, Si-H).

[^{i}Pr-PSiP]Ir(H)Cl (3-2). A solution of **3-1** (0.63 g, 1.49 mmol) in ca. 13 mL of THF was added to $[Ir(COE)_2Cl]_2$ (0.66 g, 0.75 mmol). The mixture was heated at 80 °C for 3 days, prior to removing the volatile components in vacuo. The resulting brown oil was extracted with ca. 10 mL benzene, and the extract was filtered through a plug of Celite and silica. The yellow filtrate solution was retained and concentrated to dryness. The remaining residue was subsequently triturated with hexanes (4 × 2 mL) to afford **3-2** (0.79 g, 81%) as a yellow solid. ^{1}H NMR (500.1 MHz, benzene-d_6): δ 7.95 (d, 2 H, J = 7 Hz, H_{arom}), 7.26 (m, 2 H, H_{arom}), 7.17 (m, 2 H, H_{arom}), 7.06 (m, 2 H, J = 7 Hz, H_{arom}), 3.04 (m, 2 H, P^{i}*Pr*), 2.62 (m, 2 H, P^{i}*Pr*), 1.49 – 1.21 (overlapping resonances, 12 H, P^{i}*Pr*), 1.08 – 1.02 (overlapping resonances, 6 H, P^{i}*Pr*), 0.88 – 0.80 (overlapping resonances, 6 H, P^{i}*Pr*), 0.74 (s, 3 H, Si*Me*), -23.90 (t, 1 H, Ir-*H*, $^2J_{HP}$ = 12 Hz). ^{13}C{^{1}H} NMR (125.8 MHz, benzene-d_6): δ 158.5 (C_{arom}), 142.8 (C_{arom}), 132.2 (apparent t, C_{arom}, J = 9 Hz), 131.2 (C_{arom}), 129.9 (C_{arom}), 127.9 (C_{arom}), 26.3 (apparent t, CH$_{iPr}$, J_{CP} = 15 Hz), 25.3 (apparent t, CH$_{iPr}$, J_{CP} = 12 Hz). ^{31}P{^{1}H} NMR (101.3 MHz, benzene-d_6): δ 68.9 (s). ^{29}Si NMR (99.4 MHz, benzene-d_6): δ8.4. IR (Thin Film, cm^{-1}): 2215 (m, Ir-H). Anal. Calcd for $C_{25}H_{40}ClIrP_2Si$: C, 45.61; H, 6.12. Found: C, 45.39; H, 6.16. X-Ray quality crystals of **3-2** were grown from slow evaporation of a concentrated benzene solution at room temperature.

[^{i}Pr-PSiP]Ir(H)Ph (3-3). Method 1 – A solution of PhLi (1.8 mol/L in $^{n}Bu_2O$, 50.7 μL, 0.092 mmol) was added to a room temperature cyclohexane solution of **3-2** (0.060 g, 0.09 mmol). The reaction mixture was concentrated to dryness, and the remaining residue was taken up in ca. 3 mL of benzene, filtered through Celite and dried under vacuum. The remaining solid residue was triturated with pentane (4 × 2 mL) to afford **3-3** as a pale yellow solid (0.058 g, 91%). **Method 2** – *NMR scale*: A solution of Me_3SiCH_2Li (0.007 g, 0.075 mmol) in ca. 0.5 mL benzene-d_6 was added to a solution of **3-2** (0.047 g, 0.075 mmol) in ca. 0.5 mL benzene-d_6. The reaction mixture was analyzed

after 2 hours at which point ^{1}H and ^{31}P NMR analysis of the reaction mixture indicated complete consumption of **3-2** and formation of 1 equiv. of Me_4Si, and quantitative formation of **3-3**. ^{1}H NMR (500.1 MHz, benzene-d_6): δ 7.95 (m, 2 H, H_{arom}), 7.45 (m, 2 H, H_{arom}), 7.21 – 7.17 (overlapping resonances, 4 H, H_{arom}), 7.17 – 7.10 (overlapping resonances, 3 H, H_{arom}), 6.99 (m, 2 H, H_{arom}), (2.85 (m, 2 H, P^{i}*Pr*), 2.39 (m, 2 H, P^{i}*Pr*), 1.31 (m, 6 H, P^{i}*Pr*), 1.01 (m, 12 H, P^{i}*Pr*), 0.80 (m, 6 H, P^{i}*Pr*), 0.52 (s, 3 H, Si*Me*), -11.95 (t, 1 H, $^{2}J_{HP}$ = 16 Hz, Ir-*H)*. ^{13}C{^{1}H} NMR (125.8 MHz, benzene-d_6): δ 178.2 (C_{arom}, IrPh), 157.4 (C_{arom}), 143.8 (C_{arom}), 132.3 (CH_{arom}), 130.5 (CH_{arom}), 129.8 (CH_{arom}), 129.5 (CH_{arom}), 127.9 (CH_{arom}), 113.6 (CH_{arom}), 30.0 ($CH_{iPr,}$), 29.3 (CH_{ipr}), 21.0 (CH_{3iPr}), 20.1 (CH_{3iPr}), 19.3 (CH_{3iPr}), 17.9 (CH_{3iPr}), 4.7 (Si*Me*). ^{31}P{^{1}H} NMR (202.5 MHz, benzene-d_6): δ 65.3. ^{29}Si NMR (99.4 MHz, benzene-d_6): δ 7.00.

[^{i}Pr-PSiP]Ir(C_2H_4)$_2$ (3-5). A solution of **3-2** (0.100 g, 0.15 mmol) in ca. 10 mL cyclohexane was treated with Me_3SiCH_2Li (0.014 g, 0.15 mmol). The resulting orange solution was transferred to a resealable thick-walled glass vessel equipped with a Teflon stopcock and was subsequently degassed via three freeze-pump-thaw cycles. The vessel was then charged with ca. 1 atm ethylene gas, resulting in an immediate colour change to bright orange. The reaction mixture was filtered through Celite and the filtrate dried in vacuo before the remaining residue was triturated with pentane (3 x 5 mL) to afford **3-5** as an orange powder (0.084 g, 86%). ^{1}H NMR (500.1 MHz, benzene-d_6): δ 8.17 (d, 2 H, *J* = 7 Hz, H_{arom}), 7.36 (d, 2 H, *J* = 7 Hz, H_{arom}), 7.28 (t, 2 H, *J* = 7 Hz, H_{arom}), 7.12 (m, 2 H, H_{arom}), 2.67 (m, 2 H, CH_{iPr}), 2.58 – 2.54 (overlapping resonances, 6 H, C_2H_4 + CH_{iPr}), 1.39 (s, 4 H, C_2H_4), 1.04 (m, 6 H, CH_{3iPr}), 0.97 – 0.85 (overlapping resonances, 12 H, CH_{3iPr}), 0.80 (s, 3 H, Si*Me*), 0.72 (m, 6 H, CH_{3iPr}). ^{13}C{^{1}H} NMR (125.8 MHz, benzene-d_6): 159.7 (apparent t, *J* = 29 Hz, C_{arom}), 145.2 (apparent t, *J* = 24 Hz, C_{arom}), 132.7 (apparent t, *J* = 11 Hz, CH_{arom}), 130.1 (CH_{arom}), 129.5 (CH_{arom}), 127.3 (CH_{arom}), 36.3 (CH_{2C2H4}), 31.0 (apparent t, *J* = 15 Hz, CH_{iPr}), 27.8 (CH_{2C2H4}), 26.8 (apparent t, *J* = 15 Hz, CH_{iPr}), 20.5 (CH_{3iPr}), 20.2 (CH_{3iPr}), 19.6 (CH_{3iPr}), 18.9 (CH_{3iPr}), 5.8 (Si*Me*). ^{31}P{^{1}H} NMR (202.5 MHz, benzene-d_6): δ 72.0 (s). ^{29}Si NMR (99.4 MHz, benzene-d_6): δ 58.1.

[^{i}Pr-PSiPIr(H)NHPh (3-6). Method 1 – A solution of LiNHPh (0.008 g, 0.087 mmol) in ca. 5 mL THF was added to a solution of **3-2** (0.054 g, 0.087 mmol) and allowed to stir at room temperature for 5 minutes. The reaction mixture was evaporated to dryness, and the remaining residue was extracted with ca. 5 mL benzene which was further filtered through Celite and dried under vacuum. The remaining solid residue was triturated with pentane (4 × 2 mL) to afford **3-6** as a pale yellow solid (0.057 g, 97%). **Method 2** – *NMR scale*: A solution of NpLi (0.001 g, 0.015 mmol) in ca. 0.3 mL of cyclohexane-d_{12} was added to a solution of **3-2** (0.010 g, 0.015 mmol) in ca. 0.3 mL of cyclohexane-d_{12}. The reaction mixture was analyzed by ^{1}H and ^{31}P{^{1}H} NMR spectroscopy to ensure complete consumption of **3-2** and formation of 1 equiv of Me_4C. Aniline (1.4 μL, 0.0014 g, 0.015 mmol) was added to the reaction mixture, and the solution was heated at 80°C for 14 h, at which point ^{1}H and ^{31}P NMR analysis of the reaction mixture indicated the quantitative formation of **3-6**. ^{1}H NMR (500 MHz, benzene-d_6): δ 8.06 (d, 2 H, J = 7 Hz, H_{arom}), 7.27 (m, 2 H, H_{arom}), 7.23 (t, 2 H, J = 7 Hz, H_{arom}), 7.18 (t, 2 H, J = 7 Hz, H_{arom}), 7.11 (d, 2 H, J = 7 Hz, H_{arom}), 7.05, (d, 2 H, J = 7 Hz, H_{arom}), 6.87 – 6.84 (overlapping resonances, 2 H, H_{arom} + N*H*; NH at 6.84 ppm based on ^{15}N-^{1}H HSQC), 2.55 (m, 2 H, P^{i}*Pr*), 2.36 (m, 2 H, P^{i}*Pr*), 1.18 (m, 6 H, P^{i}*Pr*), 0.99 – 0.92 (overlapping resonances, 12 H, P^{i}*Pr*), 0.88 – 0.83 (overlapping resonances, 9 H, P^{i}*Pr* + Si*Me*; SiMe at 0.87), -21.59 (t, 1 H, $^{2}J_{HP}$ = 17 Hz, Ir*H*). ^{13}C{^{1}H} NMR (125.8 MHz, benzene-d_6): δ 165.1 (C_{arom}), 159.3 (apparent t, J = 20 Hz, C_{arom}), 144.0 (apparent t, J = 29 Hz, C_{arom}), 132.2 (apparent t, J = 8 Hz, CH$_{arom}$), 130.5 (CH$_{arom}$), 129.4 (CH$_{arom}$), 128.7 (CH$_{arom}$), 127.1 (CH$_{arom}$), 121.9 (CH$_{arom}$), 118.1 (CH$_{arom}$), 25.8 (apparent t, J = 15 Hz, CH$_{iPr}$), 24.5 (apparent t, J = 10 Hz, CH$_{iPr}$), 21.0 (CH$_{3iPr}$), 20.4 (CH$_{3iPr}$), 19.2 (CH$_{3iPr}$), 17.3 (CH$_{3iPr}$), 5.5 (Si*Me*). ^{31}P{^{1}H} NMR (202.5 MHz, benzene-d_6): δ 61.6. ^{29}Si NMR (99.4 MHz, benzene-d_6): δ 13.7. ^{15}N NMR (50.7 MHz, benzene-d_6): δ –259.9 IR (Nujol, cm-1): 3375 (w, N-H), 2130 (m, Ir-H).

[^{i}Pr-PSiP]Ir(H)(NH$_2$) (3-7). **Method 1**: A slurry of $LiNH_2$ (0.014 g, 0.61 mmol) in ca. 4 mL of THF was added dropwise via pipette to a solution of **3-2** (0.080 g, 0.13

mmol) in ca. 4 mL of THF at room temperature. The yellow reaction mixture was transferred to a resealable thick walled glass vessel containing a magnetic stir bar and equipped with a Teflon stopcock and was heated at 65 °C for 12 h, over the course of which a color change to orange was observed. The reaction mixture was cooled to room temperature and evaporated to dryness, and the remaining residue was extracted with ca. 8 mL of benzene. The benzene extract was filtered through Celite and the filtrate was dried under vacuum. The remaining solid residue was triturated with pentane (3 × 5 mL) to afford **3-7** as a yellow solid (0.075 g, 90%). **Method 2** – *NMR scale*: A solution of Me_3SiCH_2Li (0.0021 g, 0.023 mmol) in ca. 0.4 mL of cyclohexane-d_{12} was added to a solution of **3-2** (0.015 g, 0.023 mmol) in ca. 0.4 mL of cyclohexane-d_{12}. An immediate color change from yellow to orange was observed. The reaction mixture was analyzed by ^{1}H and ^{31}P NMR spectroscopy to confirm the complete consumption of **3-2** and the formation of 1 equiv. of Me_4Si. The reaction mixture was then filtered through Celite to remove LiCl, and was transferred to a J-Young NMR tube. The solution was degassed via three freeze-pump-thaw cycles, and an atmosphere of anhydrous ammonia was introduced. The reaction mixture was heated at 65 °C for 14 h. Analysis of the reaction mixture by ^{1}H and ^{31}P NMR spectroscopy confirmed the formation of **3-7**. ^{1}H NMR (500 MHz, benzene-d_6): δ 8.11 (d, 2 H, J = 7 Hz, H_{arom}), 7.37 (m, 2 H, H_{arom}), 7.22 (t, 2 H, J = 7 Hz, H_{arom}), 7.09 (t, 2 H, J = 7 Hz, H_{arom}), 5.06 (br s, 2 H, NH_2), 2.45 (m, 2 H, P^i*Pr*), 2.20 (m, 2 H, P^i*Pr*), 1.24 (m, 6 H, P^i*Pr*), 1.16 (m, 6 H, P^i*Pr*), 1.05 (m, 6 H, P^i*Pr*), 0.88 – 0.84 (overlapping resonances, 9 H, P^i*Pr* + Si*Me*; SiMe at 0.87), -20.18 (t, 1 H, $^2J_{HP}$ = 15 Hz, Ir*H*). ^{13}C{^{1}H} NMR (125.8 MHz, benzene-d_6): δ 161.8 (m, C_{arom}), 145.5 (m, C_{arom}), 132.6 (apparent t, J = 9 Hz, CH$_{arom}$), 130.8 (CH$_{arom}$), 129.5 (CH$_{arom}$), 127.2 (CH$_{arom}$), 25.2 (apparent t, J = 15 Hz, CH$_{iPr}$), 24.8 (apparent t, J = 13 Hz, CH$_{iPr}$), 21.1 (CH$_{3iPr}$), 17.9 (CH$_{3iPr}$), 6.3 (Si*Me*). ^{31}P{^{1}H} NMR (202.5 MHz, benzene-d_6): δ 62.8. ^{29}Si NMR (99.4 MHz, benzene-d_6): δ 15.5. ^{15}N NMR (50.7 MHz, benzene-d_6): δ -307.4. IR (thin film, cm-1): 3377 (w, N-H), 3335 (w, N-H), 2133 (m, M-H). Anal. Calcd for $C_{25}H_{42}IrNP_2Si$: C, 47.00; H, 6.63; N, 2.19. Found: C, 46.83; H, 6.75; N, 2.45.

[Cy-PSiP]Ir(H)NHAd (3-8). Method 1: A solution of LiNH(Ad) (0.019g, 0.122 mmol) in ca. 5 mL of THF was added dropwise via pipette to a solution of **2-1** (0.100 g, 0.122 mmol) in ca. 5 mL of THF at room temperature. An immediate color change from yellow to light yellow was observed. The reaction mixture was evaporated to dryness, and the remaining residue was extracted with ca. 10 mL of benzene. The benzene extract was filtered through Celite and the filtrate was dried under vacuum. The remaining solid residue was triturated with pentane (3 × 5 mL) to afford **3-8** as an yellow solid (0.146 g, 89%). **Method 2:** A solution of Me_3CCH_2Li (0.0011 g, 0.012 mmol) in ca. 0.4 mL of cyclohexane-d_{12} was added to a solution of **2-1** (0.010 g, 0.012 mmol) in ca. 0.4 mL of cyclohexane-d_{12}. An immediate color change from yellow to orange was observed. The reaction mixture was analyzed by ^1H and ^{31}P NMR spectroscopy to confirm the complete consumption of [Cy-PSiP]Ir(H)Cl and the formation of 1 equiv. of CMe_4. An excess of H_2NAd (0.037 g, 0.244 mmol) was added to the reaction mixture, and the solution was heated at 65 °C for 14 h, at which point ^1H and ^{31}P NMR analysis of the reaction mixture indicated the quantitative formation of **3-8**. ^1H NMR (500 MHz, benzene-d_6): δ 8.18 (d, 2 H, J = 7 Hz, H_{arom}), 7.48 (m, 2 H, H_{arom}), 7.24 (t, 2 H, J = 7 Hz, H_{arom}), 7.12 (t, 2 H, J = 7 Hz, H_{arom}), 6.59 (apparent t, 1 H, J = 8 Hz, N*H*), 2.56 (m, 6 H, P*Cy*), 2.22 (m, 2 H, P*Cy*), 1.97 (m, 6 H, P*Cy*), 1.92 (s, 6 H, H_{Ad}), 1.89 – 1.22 (overlapping resonances, 25 H, P*Cy* + H_{Ad}), 1.01 (s, 3 H, Si*Me*), 0.95 (apparent d, 1 H, J = 7 Hz, H_{Ad}), 0.89 – 0.77 (overlapping resonances, 10 H, P*Cy* + H_{Ad}), 0.71 (m, 3 H, P*Cy*) -20.73 (t, 1 H, $^2J_{HP}$ = 19 Hz, Ir*H*). $^{13}C\{^1H\}$ NMR (125.8 MHz, benzene-d_6): δ 159.9 (C_{arom}), 132.4 (apparent t, J = 8 Hz, CH_{arom}), 130.0 (CH_{arom}), 129.1 (CH_{arom}), 126.7 (CH_{arom}), 50.4 (CH_{2Ad}), 37.7 (CH_{2Ad}), 34.2 (overlapping resonances, CH_{Cy}), 31.8 (CH_{Ad}), 30.6 – 27.0 (overlapping resonances, CH_{2Cy} + CH_{Ad}), 6.1 (Si*Me*). $^{31}P\{^1H\}$ NMR (202.5 MHz, benzene-d_6): δ 52.1 (br s). ^{29}Si NMR (99.4 MHz, benzene-d_6): δ 16.2. ^{15}N NMR (50.7 MHz, benzene-d_6): δ -216.8. IR (Thin Film, cm^{-1}): 3353 (br, w, N-H), 2130 (m, Ir-H). X-Ray quality crystals of **3-8** were grown from a concentrated Et_2O/THF solution at -30 °C.

[Cy-PSiP]Ir(H)NH^{t}Bu (3-9). Method 1: A solution of LiNH(^{t}Bu) (0.014g, 0.183 mmol) in ca. 5 mL of THF was added dropwise via pipette to a solution of **2-1** (0.150 g, 0.183 mmol) in ca. 5 mL of THF at room temperature. An immediate color change from yellow to dark yellow/orange was observed. The reaction mixture was evaporated to dryness, and the remaining residue was extracted with ca. 10 mL of benzene. The benzene extract was filtered through Celite and the filtrate was dried under vacuum. The remaining solid residue was triturated with pentane (3 × 5 mL) to afford **3-9** as an orange solid (0.132 g, 86%). **Method 2:** A solution of Me_3CCH_2Li (0.0011 g, 0.012 mmol) in ca. 0.4 mL of cyclohexane-d_{12} was added to a solution of **2-1** (0.010 g, 0.012 mmol) in ca. 0.4 mL of cyclohexane-d_{12}. An immediate color change from yellow to orange was observed. The reaction mixture was analyzed by ^{1}H and ^{31}P NMR spectroscopy to confirm the complete consumption of **2-1** and the formation of 1 equiv. of CMe_4. An excess of H_2N^tBu (25.8 μL, 0.0089 g, 0.244 mmol) was added to the reaction mixture, and the solution was heated at 65 °C for 14 h, at which point ^{1}H and ^{31}P NMR analysis of the reaction mixture indicated the quantitative formation of **3-9**. ^{1}H NMR (500 MHz, benzene-d_6): δ 8.18 (d, 2 H, J = 7 Hz, H_{arom}), 7.48 (m, 2 H, H_{arom}), 7.23 (t, 2 H, J = 7 Hz, H_{arom}), 7.12 (t, 2 H, J = 7 Hz, H_{arom}), 6.67 (apparent t, 1 H, J = 7 Hz, N*H*), 2.54 – 2.48 (overlapping resonances, 6 H, P*Cy*), 1.99 (m, 6 H, P*Cy*), 1.85 (m, 3 H, P*Cy*), 1.76 – 1.54 (overlapping resonances, 13 H, P*Cy*), 1.54 (s, 9 H, NH^t*Bu*), 1.34 – 1.19 (overlapping resonances, 12 H, P*Cy*), 1.00 (s, 3 H, Si*Me*), 0.81 (m, 2 H, P*Cy*), 0.71 (m, 2 H, P*Cy*) -20.78 (t, 1 H, $^2J_{HP}$ = 19 Hz, Ir*H*). ^{13}C{^{1}H} NMR (125.8 MHz, benzene-d_6): δ 160.0 (C_{arom}), 145.5 (C_{arom}), 132.4 (apparent t, J = 9 Hz, CH_{arom}), 130.1 (CH_{arom}), 129.1 (CH_{arom}), 126.7 (CH_{arom}), 36.5 (CH_{3tBu}), 34.5 – 34.1 (overlapping resonances, CH_{Cy}), 30.9 – 30.4 (overlapping resonances, CH_{2Cy}), 28.5 – 27.7 (overlapping resonances, CH_{2Cy}), 27.0 (CH_{2Cy}), 5.8 (Si*Me*). ^{31}P{^{1}H} NMR (202.5 MHz, benzene-d_6): δ 52.0 (br s). ^{29}Si NMR (99.4 MHz, benzene-d_6): δ 16.0. ^{15}N NMR (50.7 MHz, benzene-d_6): δ - 219.2. IR (Nujol, cm^{-1}): 3331 (br, w, N-H), 2206 (m, Ir-H). Anal. Calcd for $C_{41}H_{66}IrNP_2Si$: C, 57.58; H, 7.78; N, 1.64. Found: C, 57.25; H, 7.61; N, 1.37.

[Cy-PSiP]Ir(H)NHCy (3-10). Method 1: A solution of LiNHCy (0.010g, 0.098 mmol) in ca. 4 mL of THF was added dropwise via pipette to a solution of **2-1** (0.080 g, 0.098 mmol) in ca. 4 mL of THF at room temperature. A gradual color change from yellow to dark orange was observed over 24 hours at room temperature. The reaction mixture was evaporated to dryness, and the remaining residue was extracted with ca. 8 mL of benzene. The benzene extract was filtered through Celite and the filtrate was dried under vacuum. The remaining solid residue was triturated with pentane (3 × 5 mL) to afford **3-10** as an orange solid (0.077 g, 89%). **Method 2:** A solution of Me_3SiCH_2Li (0.0014 g, 0.015 mmol) in ca. 0.4 mL of cyclohexane-d_{12} was added to a solution of **2-1** (0.012 g, 0.015 mmol) in ca. 0.4 mL of cyclohexane-d_{12}. An immediate color change from yellow to orange was observed. The reaction mixture was analyzed by ^{1}H and ^{31}P NMR spectroscopy to confirm the complete consumption of **2-1** and the formation of 1 equiv. of $SiMe_4$. H_2NCy (1.7 μL, 0.0015 g, 0.244 mmol) was added to the reaction mixture, and the solution was heated at 65 °C for 14 h, at which point ^{1}H and ^{31}P NMR analysis of the reaction mixture indicated the quantitative formation of **3-10**. ^{1}H NMR (500 MHz, benzene-d_6): δ 8.17 (d, 2 H, J = 7 Hz, H_{arom}), 7.48 (m, 2 H, H_{arom}), 7.26 (t, 2 H, J = 7 Hz, H_{arom}), 7.12 (m, 2 H, H_{arom}), 2.63 (m, 2 H, P*Cy*), 2.53 (m, 4 H, P*Cy*), 2.34 (m, 4 H, P*Cy*), 2.11 – 1.14 (overlapping resonances, 30 H, P*Cy* + NH*Cy*), 0.99 (s, 3 H, Si*Me*), 0.88 – 0.83 (overlapping resonances, 16 H, P*Cy* + NH*Cy*), -18.37 (t, 1 H, $^{2}J_{HP}$ = 16 Hz, Ir*H*). $^{13}C\{^{1}H\}$ NMR (125.8 MHz, benzene-d_6): δ 161.9 (apparent t, J = 23 Hz, C_{arom}), 144.9 (C_{arom}), 132.8 (apparent t, J = 8 Hz, CH_{arom}), 130.6 (CH_{arom}), 129.3 (CH_{arom}), 127.0 (CH_{arom}), 38.3 (CH_2), 38.0 (CH_2), 36.1 (apparent t, J = 13 Hz, CH_{Cy}), 34.2 (apparent t, J = 15 Hz, CH_{Cy}), 30.6 (CH_{2Cy}), 30.3 (CH_{2Cy}), 30.0 (CH_{2Cy}), 29.0 – 26.9 (overlapping resonances, CH_{2Cy}), 7.4 (Si*Me*). $^{31}P\{^{1}H\}$ NMR (202.5 MHz, benzene-d_6): δ 54.8. ^{29}Si NMR (99.4 MHz, benzene-d_6): δ 23.2. ^{15}N NMR (50.7 MHz, benzene-d_6): δ -307.4. IR (Thin Film, cm^{-1}): 3358 (br, w, N-H), 2112 (m, Ir-H). Anal. Calcd for

[^{i}Pr-PSiP]Ir(H)NHAd (3-11). Method 1: A solution of LiNH(Ad) (0.019 g, 0.12 mmol) in ca. 4 mL of THF was added dropwise via pipette to a solution of **3-2**

(0.080 g, 0.12 mmol) in ca. 4 mL of THF at room temperature. An immediate color change from yellow to light orange was observed. The reaction mixture was evaporated to dryness, and the remaining residue was extracted with ca. 8 mL of benzene. The benzene extract was filtered through Celite and the filtrate was dried under vacuum. The remaining solid residue was triturated with pentane (3 × 5 mL) to afford **3-11** as an yellow solid (0.070 g, 76%). **Method 2:** A solution of Me_3CCH_2Li (0.0018 g, 0.023 mmol) in ca. 0.4 mL of cyclohexane-d_{12} was added to a solution of **3-2** (0.015 g, 0.023 mmol) in ca. 0.4 mL of cyclohexane-d_{12}. An immediate color change from yellow to orange was observed. The reaction mixture was analyzed by ^{1}H and ^{31}P NMR spectroscopy to confirm the complete consumption of **3-2** and the formation of 1 equiv. of CMe_4. An excess of H_2NAd (0.069 g, 0.46 mmol) was added to the reaction mixture, and the solution was heated at 65 °C for 14 h, at which point ^{1}H and ^{31}P NMR analysis of the reaction mixture indicated 50% conversion to **3-11**. ^{1}H NMR (500 MHz, benzene-d_6): δ 8.15 (d, 2 H, J = 8 Hz, H_{arom}), 7.33 (m, 2 H, H_{arom}), 7.20 (t, 2 H, J = 7 Hz, H_{arom}), 7.08 (t, 2 H, J = 7 Hz, H_{arom}), 6.70 (apparent t, 1 H, J = 7 Hz, N*H*), 2.69 (br m, 2 H, P^i*Pr*), 2.57 (br m, 2 H, P^i*Pr*), 2.19 (br s, 2 H, H_{Ad}), 1.93 – 1.90 (overlapping resonances, 6 H, H_{Ad}), 1.75 (m, 3 H, H_{Ad}), 1.53 – 1.47 (m, 4 H, H_{Ad}), 1.29 (m, 6 H, P^i*Pr*), 1.11 – 1.07 (m, 12 H, P^i*Pr*), 0.99 (s, 3 H, Si*Me*), 0.87 (m, 6 H, P^i*Pr*), -20.83 (t, 1 H, $^2J_{HP}$ = 19 Hz, Ir*H*). ^{13}C{^{1}H} NMR (125.8 MHz, benzene-d_6): δ 159.9 (C_{arom}), 132.3 (apparent t, J = 9 Hz, CH_{arom}), 130.0 (CH_{arom}), 129.3 (CH_{arom}), 126.6 (CH_{arom}), 57.8 (C_{Ad}), 50.3 (CH_{2Ad}), 47.0 (CH_{2Ad}), 37.7 (CH_{2Ad}), 37.0 (CH_{2Ad}), 31.8 (CH_{Ad}), 30.7 (CH_{Ad}), 25.0 (br m, CH_{iPr}), 21.2 (CH_{3iPr}), 20.7 (CH_{3iPr}), 19.8 (CH_{3iPr}), 17.3 (CH_{3iPr}), 5.8 (Si*Me*). ^{31}P{^{1}H} NMR (202.5 MHz, benzene-d_6): δ 58.9 (br s). ^{29}Si NMR (99.4 MHz, benzene-d_6): δ 16.8. ^{15}N NMR (50.7 MHz, benzene-d_6): δ -213.4. IR (Nujol, cm^{-1}): 3234 (br, w, N-H), 2126 (m, Ir-H). X-Ray quality crystals of **3-11** were grown from a concentrated pentane solution at -30 ºC.

[^{i}Pr-PSiP]Ir(H)NH^{t}Bu (3-12). Method 1: A solution of LiNH(^{t}Bu) (0.010g, 0.122 mmol) in ca. 4 mL of THF was added dropwise via pipette to a solution of **3-2**

(0.080 g, 0.122 mmol) in ca. 4 mL of THF at room temperature. An immediate color change from yellow to dark yellow/orange was observed. The reaction mixture was evaporated to dryness, and the remaining residue was extracted with ca. 8 mL of benzene. The benzene extract was filtered through Celite and the filtrate was dried under vacuum. The remaining solid residue was triturated with pentane (3 × 5 mL) to afford **3-12** as an orange solid (0.072 g, 87%). **Method 2:** A solution of Me_3CCH_2Li (0.0018 g, 0.023 mmol) in ca. 0.4 mL of cyclohexane-d_{12} was added to a solution of **3-2** (0.015 g, 0.023 mmol) in ca. 0.4 mL of cyclohexane-d_{12}. An immediate color change from yellow to orange was observed. The reaction mixture was analyzed by ^{1}H and ^{31}P NMR spectroscopy to confirm the complete consumption of **3-2** and the formation of 1 equiv. of CMe_4. An excess of H_2N^tBu (48.3 μL, 0.033 g, 0.456 mmol) was added to the reaction mixture, and the solution was heated at 65 °C for 14 h, at which point ^{1}H and ^{31}P NMR analysis of the reaction mixture indicated greater than 90% conversion to **3-12**. ^{1}H NMR (500 MHz, benzene-d_6): δ 8.14 (d, 2 H, J = 7 Hz, H_{arom}), 7.32 (m, 2 H, H_{arom}), 7.19 (t, 2 H, J = 7 H_{arom}), 7.07 (t, 2 H, J = 7 Hz, H_{arom}), 6.80 (apparent t, 1 H, J = 7 Hz, N*H*), 2.63 – 2.55 (overlapping resonances, 4 H, P^i*Pr*), 1.52 (s, 9 H, CH_{3tBu}), 1.26 (m, 6 H, P^i*Pr*), 1.06 (m, 12 H, P^i*Pr*), 0.98 (s, 3 H, Si*Me*), 0.86 (m, 6 H, P*Cy*), -20.91 (t, 1 H, $^{2}J_{HP}$ = 19 Hz, Ir*H*). $^{13}C\{^{1}H\}$ NMR (125.8 MHz, benzene-d_6): δ 160.0 (C_{arom}), 150.9 (C_{arom}), 132.5 (apparent t, J = 9 Hz, CH_{arom}), 130.2 (CH_{arom}), 129.5 (CH_{arom}), 126.8 (CH_{arom}), 36.6 (CH_{3tBu}), 25.1 (CH_{3tBu}), 24.0 (CH_{tBu}), 21.3 (CH_{3iPr}), 20.9 (CH_{3iPr}), 19.8 (CH_{3iPr}), 17.5 (CH_{3iPr}), 5.8 (Si*Me*). $^{31}P\{^{1}H\}$ NMR (202.5 MHz, benzene-d_6): δ 51.9 (br s). ^{29}Si NMR (99.4 MHz, benzene-d_6): δ 16.7. ^{15}N NMR (50.7 MHz, benzene-d_6): δ -215.7. IR (Nujol, cm^{-1}): 3234 (br, w, N-H), 2388 (m, Ir-H).

[Cy-PSiP]Ir(H)NHCH$_2$Ph (3-15). A solution of PhLi (50.9 μL, 1.8 M in $(C_4H_9)_2O$, 0.092 mmol) was added to a room temperature solution of **2-1** (0.075 g, 0.092 mmol) in ca. 8 mL of cyclohexane. An immediate color change from yellow to orange was observed. Neat H_2NCH_2Ph (10.0 μL, 0.010 g, 0.0916 mmol) was added to the reaction mixture, and the solution was heated at 65 °C for 12 h to yield a white solid in a

bright orange solution. The solution was removed by pipet and the resulting solid was triturated with pentane (3 × 5 mL) to afford **3-15** as an white solid (0.034g, 41 %). ^{1}H NMR (500 MHz, benzene-d_6): δ 8.18 (d, 1 H, J = 7 Hz, H_{arom}), 7.86 (d, 1 H, J = 7 Hz H_{arom}), 7.62 (m, 1 H, H_{arom}) 7.32 – 7.26 (overlapping resonances, 3 H, H_{arom}), 7.19 – 7.17 (m, 1 H, H_{arom}), 7.10 (m, 2 H, H_{arom}), 7.03 – 6.94 (overlapping resonances, 3 H, H_{arom}), 6.73 (t, 1 H, J = 7 Hz, H_{arom}), 4.27 (apparent dd, 1 H, $^{2}J_{HH}$ = 13 Hz, $^{3}J_{HNH}$ = 5 Hz, CH_2) 3.72 (td, 1 H, J_1 = 25 Hz, J_2 = 4 Hz, CH_2), 3.42 (m, 1 H, P*Cy*), 2.87 (m, 1H, P*Cy*), 2.70, (m, 2 H, P*Cy*), 2.48 (m, 1 H, P*Cy*), 2.26 (m, 1 H, P*Cy*), 1.95 (m, 2 H, P*Cy*), 1.85 – 1.20 (overlapping resonances, 25 H, P*Cy*), 1.12 (s, 3 H, Si*Me*), 1.08 – 0.97 (overlapping resonances, 8 H, P*Cy*), 0.67 (m, 1H, P*Cy*), 0.53 (m, 1 H, P*Cy*), 0.02 (m, 1H, P*Cy*), -0.54 (m, 1H, P*Cy*), -9.04 (dd, 1 H, $^{2}J_{HPtrans}$ = 135 Hz, $^{2}J_{HPcis}$ = 22 Hz, Ir*H*). ^{13}C{^{1}H} NMR (125.8 MHz, THF-d_8): δ 161.1 (C_{arom}), 158.6 (C_{arom}), 150.1 (C_{arom}), 147.3 (C_{arom}), 142.1 (CH$_{arom}$), 133.6 (apparent d, J = 19 Hz, CH$_{arom}$), 132.8 (apparent d, J = 19 Hz, CH$_{arom}$), 130.3 (CH$_{arom}$), 129.2 (CH$_{arom}$), 129.0 (apparent d, J = 16 Hz, CH$_{arom}$), 127.9-127.8 (CH$_{arom}$), 127.3 (CH$_{arom}$), 125.2 (CH$_{arom}$), 120.7 (apparent d, J = 21 Hz CH$_{arom}$), 59.1 (CH$_2$), 31.8 (CH$_{2Cy}$), 31.7 (CH$_{2Cy}$), 30.9 (CH$_{2Cy}$), 30.1 (CH$_{2Cy}$), 29.9 (CH$_{2Cy}$), 29.5 (CH$_{2Cy}$), 29.4 (CH$_{2Cy}$), 29.3 (CH$_{2Cy}$), 29.2 (CH$_{2Cy}$), 29.1 (CH$_{2Cy}$), 28.9 (CH$_{2Cy}$), 28.8 (CH$_{2Cy}$), 28.6 (CH$_{2Cy}$), 28.5 (CH$_{2Cy}$), 28.0 (CH$_{2Cy}$), 27.8 (CH$_{2Cy}$), 27.7 (CH$_{2Cy}$), 27.4 (CH$_{2Cy}$), 27.3 (CH$_{2Cy}$), 27.2 (CH$_{2Cy}$), 0.6 (Si*Me*). ^{31}P{^{1}H} NMR (202.5 MHz, benzene-d_6): δ 44.9 (d, $^{2}J_{PPcis}$ = 12 Hz), 14.7 (d, $^{2}J_{PPcis}$ = 12 Hz). ^{29}Si NMR (99.4 MHz, benzene-d_6): δ 23.1. IR (Nujol, cm^{-1}): 3322 (br, w, N-H), 2008 (m, Ir-H). Anal. Calcd for $C_{45}H_{64}IrNP_2Si$: C, 59.43; H, 7.25; N, 1.58. Found: C, 59.75; H, 7.06; N, 1.30.

[^{i}Pr-PSiP]Ir(H)NHCH$_2$Ph (3-16). A solution of Me_3SiCH_2Li (0.007 g, 0.08 mmol) in ca. 3 mL of cyclohexane was added to a solution of **3-2** (0.052 g, 0.08 mmol) in ca. 3 mL of cyclohexane. An immediate color change from yellow to orange was observed. Neat H_2NCH_2Ph (8.6 μL, 0.0085 g, 0.08 mmol) was added to the reaction mixture, and the solution was stirred at room temperature for 20 minutes. The reaction mixture was filtered through Celite and the filtrate was dried under vacuum. The

remaining solid residue was triturated with pentane (3 × 5 mL) to afford **3-16** as an orange solid (0.056 g, 96 %). ^{1}H NMR (500 MHz, benzene-d_6): δ 8.20 (d, 1 H, J = 7 Hz, H_{arom}), 7.88 (d, 1 H, J = 7 Hz H_{arom}), 7.55 (m, 1 H, H_{arom}) 7.35 – 7.31 (overlapping resonances, 2 H, H_{arom}), 7.19 – 7.05 (overlapping resonances, 6 H, H_{arom}), 6.93 (t, 1 H, J = 7 Hz, H_{arom}), 6.74 (t, 1 H, J = 7 Hz, H_{arom}), 4.17 (dd, 1 H, $^{2}J_{HH}$ = 13 Hz, $^{3}J_{HNH}$ = 5 Hz, CH_2) 3.61 (td, 1 H, J_1 = 18 Hz, J_2 = 5 Hz, CH_2), 2.88 (m, 1 H, P^{i}Pr), 2.26 (m, 1H, NH), 2.33, (septet, 1 H, J = 7 Hz, P^{i}Pr), 2.06 (m, 1 H, P^{i}Pr), 1.90 (m, 1 H, P^{i}Pr), 1.42 (m, 3 H, P$^{i}Pr_2$), 1.20 (dd, 3 H, $^{3}J_{HP}$ = 17 Hz, $^{3}J_{HH}$ = 8 Hz, P^{i}Pr), 1.11 (s, 3 H, SiMe), 0.96 (dd, 3 H, $^{3}J_{HP}$ = 15 Hz, $^{3}J_{HH}$ = 7 Hz, P^{i}Pr), 0.85 (dd, 3 H, $^{3}J_{HP}$ = 15 Hz, $^{3}J_{HH}$ = 7 Hz, P^{i}Pr), 0.74 – 0.67 (overlapping resonances, 6 H, P^{i}Pr), 0.35 (m, 3 H, P^{i}Pr), -0.18 (dd, 3 H, $^{3}J_{HP}$ = 14 Hz, $^{3}J_{HH}$ = 7 Hz, P^{i}Pr), -9.09 (dd, 1 H, $^{2}J_{HPtrans}$ = 135 Hz, $^{2}J_{HPcis}$ = 22 Hz, IrH). ^{13}C{^{1}H} NMR (125.8 MHz, benzene-d_6): δ 160.6 (C_{arom}), 158.4 (C_{arom}), 150.1 (C_{arom}), 149.0 (C$_{arom}$), 142.7 (CH$_{arom}$), 142.3 (C_{arom}), 133.5 (CH$_{arom}$), 132.7 (CH$_{arom}$), 130.0 (CH$_{arom}$), 129.4 (CH$_{arom}$), 129.2 (CH$_{arom}$), 127.6 (CH$_{arom}$), 127.3 (CH$_{arom}$), 126.0 (CH$_{arom}$), 121.4 (CH$_{arom}$), 121.1 (CH$_{arom}$), 58.9 (CH$_2$), 30.6 (CH$_{iPr}$), 29.8 (CH$_{iPr}$), 28.6 (CH$_{iPr}$), 27.9 (CH$_{iPr}$), 27.5 (CH$_{3iPr}$), 27.1 (CH$_{3iPr}$), 20.8 (CH$_{3iPr}$), 20.1 (d, J = 14 Hz, CH$_{3iPr}$), 19.8 – 19.6 (overlapping resonances, CH$_{3Cy}$), 19.3 – 19.1 (overlapping resonances, CH$_{3Cy}$), 1.0 (SiMe). ^{31}P{^{1}H} NMR (202.5 MHz, benzene-d_6): δ 48.9 (d, $^{2}J_{PPcis}$ = 12 Hz), 21.2 (d, $^{2}J_{PPcis}$ = 12 Hz). ^{29}Si NMR (99.4 MHz, benzene-d_6): δ 22.9. ^{15}N NMR (50.7 MHz, benzene-d_6): δ -397.9. IR (Nujol, cm^{-1}): 3383 (br, w, N-H), 2034 (m, Ir-H).

[Cy-PSiP]Ir(H)$_2$N(CH$_3$)Ph (3-17) A solution of Me$_3$CCH$_2$Li (0.012 g, 0.12 mmol) in ca. 4 mL of cyclohexane was added to a solution of **2-1** (0.100 g, 0.12 mmol) in ca. 4 mL of cyclohexane. An immediate color change from yellow to orange was observed. Neat HN(CH$_3$)Ph (66.2 μL, 0.065 g, 0.61 mmol) was added to the reaction mixture, and the solution was heated at 65 °C for 14 h. A gradual color change from orange to dark orange was observed. The reaction mixture was evaporated to dryness, and the remaining residue was extracted with ca. 8 mL of benzene. The benzene extract was filtered through Celite and the filtrate was dried under vacuum. The remaining solid

residue was triturated with pentane (3 × 5 mL) to afford **3-17** as an orange solid (0.104 g, 96%). ^{1}H NMR (500 MHz, benzene-d_6): δ 8.33 (d, 2 H, J = 7 Hz, H_{arom}), 7.48 (m, 2 H, H_{arom}), 7.29 (t, 2 H, J = 7 Hz, H_{arom}), 7.19 – 7.10 (overlapping resonances, 3 H, H_{arom}), 6.85 (apparent t, 2 H, J = 7 Hz, H_{arom}), 6.74 (apparent t, 1 H, J = 7 Hz, H_{arom}), 6.39 (d, 1 H, J = 7 Hz, H_{arom}), 3.92 (br s, 1 H, N*H*), 2.56 (m, 4 H, P*Cy*), 2.30 (d, 3 H, $^{3}J_{HNH}$ = 5 Hz, NCH_3), 2.23 (m, 4 H, P*Cy*), 1.96 – 1.85 (overlapping resonances, 10 H, P*Cy*), 1.70 – 0.75 (overlapping resonances, 28 H, P*Cy* + Si*Me*; SiMe at 1.17 ppm), -9.86 (dt, 1 H, $^{2}J_{HP}$ = 15 Hz, $^{2}J_{HH}$ = 3 Hz, Ir*H*), -14.10 (dt, 1H, $^{2}J_{HP}$ = 20 Hz, $^{2}J_{HH}$ = 3 Hz, Ir*H*). ^{13}C{^{1}H} NMR (125.8 MHz, benzene-d_6): δ 162.3 (apparent t, J = 20 Hz, C_{arom}), 146.5 (apparent t, J = 28 Hz, C_{arom}), 133.6 (apparent t, J = 10 Hz, CH$_{arom}$), 132.1 (C_{arom}), 129.9 (CH$_{arom}$), 129.6 (apparent d, J = 18 Hz, CH$_{arom}$), 127.1 (CH$_{arom}$), 126.9 (CH$_{arom}$), 125.8 (CH$_{arom}$), 112.9 (CH$_{arom}$), 40.0 (apparent t, J = 13 Hz, CH$_{Cy}$), 33.4 (apparent t, J = 18 Hz, CH$_{Cy}$), 30.7 (CH$_{3NCH3}$), 30.4 (CH$_{2Cy}$), 29.2 (CH$_{2Cy}$), 28.8 (CH$_{2Cy}$), 28.2 – 27.0 (overlapping resonances CH$_2$), 7.2 (Si*Me*). ^{31}P{^{1}H} NMR (202.5 MHz, benzene-d_6): δ 53.9. ^{29}Si NMR (99.4 MHz, benzene-d_6): δ 35.8. IR (Thin Film, cm^{-1}): 2095 (m, Ir-H), 2008 (m, Ir-H).

[^{i}Pr-PSiP]Ir(H)$_2$N(CH$_3$)Ph (3-18) A solution of Me_3CCH_2Li (0.010 g, 0.11 mmol) in ca. 0.4 mL of cyclohexane was added to a solution of **3-2** (0.070 g, 0.11 mmol) in ca. 0.4 mL of cyclohexane. An immediate color change from yellow to orange was observed. Neat HN(CH$_3$)Ph (57.5 μL, 0.056 g, 0.53 mmol) was added to the reaction mixture, and the solution was heated at 65 °C for 14 h. A gradual color change from orange to dark orange was observed. The reaction mixture was evaporated to dryness, and the remaining residue was extracted with ca. 1 mL of benzene. The benzene extract was filtered through Celite and the filtrate was dried under vacuum. The remaining solid residue was triturated with pentane (3 × 2 mL) to afford **3-18** as an orange solid (0.073 g, 92%). ^{1}H NMR (500 MHz, benzene-d_6): δ 8.29 (d, 2 H, J = 7 Hz, H_{arom}), 7.35 (m, 2 H, H_{arom}), 7.26 (t, 2 H, J = 7 Hz, H_{arom}), 7.12 (t, 2 H, J = 7 Hz, H_{arom}), 7.02 (d, 2 H, J = 7 Hz, H_{arom}), 6.81 (t, 2 H, J = Hz, H_{arom}), 6.74 (m, 1 H, H_{arom}), 3.49 (br s, 1H, N*H*), 2.32 –

2.25 (overlapping resonances, 4 H, P^{i}*Pr*), 2.03 (br m, 3 H, NC*H*$_3$), 1.43 (m, 6 H, P^{i}*Pr*), 1.17 (m, 6 H, P^{i}*Pr*), 1.10 (s, 3 H, Si*Me*), 0.98 (m, 6 H, P^{i}*Pr*), 0.79 (m, 6 H, P^{i}*Pr*), -10.26 (td, 1 H, $^{2}J_{HP}$ = 15 Hz, $^{2}J_{HH}$ = 3 Hz, Ir*H*), -14.41 (td, 1H, $^{2}J_{HP}$ = 20 Hz, $^{2}J_{HH}$ = 3 Hz, Ir*H*). ^{13}C{^{1}H} NMR (125.8 MHz, benzene-d_6): δ 161.9 (apparent t, J = 20 Hz, C_{arom}), 153.2 (C_{arom}), 146.9 (apparent t, J = 29 Hz, C_{arom}), 133.5 (apparent t, J = 9 Hz, CH$_{arom}$), 129.9 (C_{arom}), 129.6 (CH$_{arom}$), 129.4 (CH$_{arom}$), 127.2 (CH$_{arom}$), 126.9 (CH$_{arom}$), 125.8 (CH$_{arom}$), 30.3 (apparent t, J = 13 Hz, CH$_{iPr}$), 27.9 (CH$_{3NCH3}$), 24.5 (apparent t, J = 19 Hz, CH$_{iPr}$), 20.5 (CH$_{3iPr}$), 20.3 (CH$_{3iPr}$), 19.4 (CH$_{3iPr}$), 18.0 (CH$_{3iPr}$), 7.2 (Si*Me*). ^{31}P{^{1}H} NMR (202.5 MHz, benzene-d_6): δ 63.7. ^{29}Si NMR (99.4 MHz, benzene-d_6): δ 36.0. IR (Thin Film, cm^{-1}): 2279 (m, Ir-H), 2095 (m, Ir-H).

[Cy-PSiP]Ir(H)NHNC$_5$H$_{10}$ (3-19). Method 1: A solution of LiNHNC$_5$H$_{10}$ (0.019 g, 0.18 mmol) in ca. 4 mL of THF was added dropwise via pipette to a solution of **2-1** (0.150 g, 0.18 mmol) in ca. 4 mL of THF at room temperature. A gradual color change from yellow to orange was observed over 1 hour at room temperature. The reaction mixture was evaporated to dryness, and the remaining residue was extracted with ca. 8 mL of benzene. The benzene extract was filtered through Celite and the filtrate was dried under vacuum. The remaining solid residue was triturated with pentane (3 × 5 mL) to afford **3-19** as an orange solid (0.152 g, 96%). **Method 2:** A solution of Me$_3$CCH$_2$Li (0.076 g, 0.098 mmol) in ca. 4 mL of cyclohexane was added to a solution of **2-1** (0.080 g, 0.098 mmol) in ca. 4 mL of cyclohexane. An immediate color change from yellow to orange was observed. Neat H$_2$NNC$_5$H$_{10}$ (11.6 μL, 0.011 g, 0.108 mmol) was added to the reaction mixture, and the solution was heated at 65 °C for 14 h. A gradual color change from orange to dark orange was observed. The reaction mixture was evaporated to dryness, and the remaining residue was extracted with ca. 4 mL of benzene. The benzene extract was filtered through Celite and the filtrate was dried under vacuum. The remaining solid residue was triturated with pentane (3 × 5 mL) to afford **3-19** as an orange solid (0.077 g, 91%). ^{1}H NMR (500 MHz, benzene-d_6): δ 8.17 (d, 2 H, J = 7 Hz, H_{arom}), 7.56 (t, 1 H, J = 7 Hz, H_{arom}), 7.47 (t, 1 H, J = 7 Hz, H_{arom}), 7.24 (m, 2 H, H_{arom}),

7.12 (m, 2 H, H_{arom}), 6.51 (m, 1 H, N*H*), 3.56 (m, 1 H, P*Cy*), 3.31 – 3.22 (overlapping resonances, 2 H, P*Cy*), 2.59 – 2.41 (overlapping resonances, 7 H, P*Cy* + NC_5H_{10}), 2.17 – 1.13 (overlapping resonances, 36 H, P*Cy* + NC_5H_{10}), 0.97 (s, 3 H, Si*Me*), 0.85 (m, 8 H, P*Cy*), -20.64 (t, 1 H, $^2J_{HP}$ = 16 Hz, Ir*H*). $^{13}C\{^1H\}$ NMR (125.8 MHz, benzene-d_6): δ 161.7 (C_{arom}), 146.1 (C_{arom}), 132.6 (apparent d, *J* = 16 Hz, CH_{arom}), 132.3 (apparent d, *J* = 15 Hz, CH_{arom}), 130.7 (CH_{arom}), 129.2 (CH_{arom}), 129.0 (CH_{arom}), 126.8 (CH_{arom}), 34.5 – 33.8 (overlapping resonances, CH_{Cy}), 32.9 (CH_{Cy}), 32.8 (CH_{Cy}), 31.0 (CH_{2Cy}), 30.7 (CH_{2Cy}), 30.4 (CH_{2Cy}), 28.9 (CH_{2Cy}), 28.1 – 26.9 (overlapping resonances CH_{2Cy} + $CH_{2NC5H10}$), 24.9 (CH_{2Cy}), 6.4 (Si*Me*). $^{31}P\{^1H\}$ NMR (202.5 MHz, benzene-d_6): δ 55.6 (AB quartet). ^{29}Si NMR (99.4 MHz, benzene-d_6): δ 15.1. ^{15}N NMR (50.7 MHz, benzene-d_6): δ -185.0. IR (Thin Film, cm^{-1}): 3157 (br, w, N-H), 2132 (m, Ir-H). Anal. Calcd for $C_{42}H_{67}IrN_2P_2Si$: C, 57.18; H, 7.65; N, 3.18. Found: C, 57.00; H, 7.52; N, 2.78.

[Cy-PSiP]Ir(H)NHN(CH$_2$CH$_2$)$_2$NMe (3-20) Method 1: A solution of LiNHN(CH$_2$CH$_2$)$_2$NMe (0.022 g, 0.18 mmol) in ca. 4 mL of THF was added dropwise via pipette to a solution of **2-1** (0.150 g, 0.18 mmol) in ca. 4 mL of THF at room temperature. A gradual color change from yellow to orange was observed over 1 hour at room temperature. The reaction mixture was evaporated to dryness, and the remaining residue was extracted with ca. 8 mL of benzene. The benzene extract was filtered through Celite and the filtrate was dried under vacuum. The remaining solid residue was triturated with pentane (3 × 5 mL) to afford **3-20** as an orange solid (0.149 g, 92%). **Method 2:** A solution of Me$_3$CCH$_2$Li (0.0023 g, 0.024 mmol) in ca. 1 mL of cyclohexane was added to a solution of **2-1** (0.020 g, 0.024 mmol) in ca. 1 mL of cyclohexane. An immediate color change from yellow to orange was observed. Neat H$_2$NN(CH$_2$CH$_2$)$_2$NMe (3.2 μL, 0.0031 g, 0.027 mmol) was added to the reaction mixture, and the solution was heated at 65 °C for 14 h. A gradual color change from orange to dark orange was observed. The reaction mixture was evaporated to dryness, and the remaining residue was extracted with ca. 4 mL of benzene. The benzene extract was filtered through Celite and the filtrate was dried under vacuum. The remaining solid

residue was triturated with pentane (3 × 5 mL) to afford **3-20** as an orange solid (0.017 g, 80%). ^{1}H NMR (500 MHz, benzene-d_6): δ 8.17 (d, 2 H, J = 7 Hz, H_{arom}), 7.55 (t, 1 H, J = 7 Hz, H_{arom}), 7.47 (t, 1H, J = 7 Hz, H_{arom}), 7.25 (m, 2 H, H_{arom}), 7.17 – 7.10 (overlapping resonances, 2 H, H_{arom}), 6.45 (d, 1 H, J = 9 Hz, N*H*), 3.56 (m, 1 H, P*Cy*), 3.42 (br s, 1 H, P*Cy*), 3.28 (m, 1 H, P*Cy*), 3.17 (br s, 1 H, P*Cy*), 2.71 – 2.22 (overlapping resonances, 14 H, P*Cy* + N(CH_2CH_2)$_2$NMe), 2.17 (s, 3 H, N(CH$_2$CH$_2$)$_2$N*Me*), 2.13 – 1.13 (overlapping resonances, 28 H, P*Cy* + C$H_{2N(CH2CH2)2NMe}$), 0.97 (s, 3 H, Si*Me*), 0.90 – 0.78 (overlapping resonances, 6 H, P*Cy*), -20.62 (t, 1 H, $^{2}J_{HP}$ = 16 Hz, Ir*H*). ^{13}C{^{1}H} NMR (125.8 MHz, benzene-d_6): δ 162.1 (C_{arom}), 144.8 (C_{arom}), 132.6 (apparent d, J = 16 Hz, CH_{arom}), 132.4 (apparent d, J = 13 Hz, CH_{arom}), 130.7 (apparent d, J = 11 Hz, CH_{arom}), 129.3 (CH_{arom}), 129.0 (CH_{arom}), 126.9 (CH_{arom}), 63.2 (C$H_{2N(CH2CH2)2NMe}$), 56.6 (C$H_{2N(CH2CH2)2NMe}$), 46.6 (C$H_{3N(CH2CH2)2NMe}$), 34.5 – 33.7 (overlapping resonances, CH_{Cy}), 33.0-32.8 (overlapping resonances, CH_{Cy}), 31.0 (CH_{2Cy}), 30.6 (CH_{2Cy}), 30.4 (CH_{2Cy}), 29.3 (CH_{2Cy}), 28.9 (CH_{2Cy}), 28.5 (CH_{2Cy}), 28.2 – 27.2 (overlapping resonances CH_{2Cy}), 26.9 (CH_{2Cy}), 6.4 (Si*Me*). ^{31}P{^{1}H} NMR (202.5 MHz, benzene-d_6): δ 55.8 (AB quartet). ^{29}Si NMR (99.4 MHz, benzene-d_6): δ 14.9. ^{15}N NMR (50.7 MHz, benzene-d_6): δ -190.2. IR (Thin Film, cm^{-1}): 3162 (br, w, N-H), 2124 (m, Ir-H). Anal. Calcd for $C_{42}H_{68}IrN3P_2Si$: C, 56.22; H, 7.64; N, 4.68. Found: C, 56.48; H, 7.65; N, 4.54.

[^{i}Pr-PSiP]Ir(H)NHNC$_5$H$_{10}$ (3-21). Method 1: A solution of LiNHNC$_5$H$_{10}$ (0.013 g, 0.122 mmol) in ca. 3 mL of THF was added dropwise via pipette to a solution of **3-2** (0.080 g, 0.122 mmol) in ca. 3 mL of THF at room temperature. A gradual color change from yellow to orange was observed over 1 hour at room temperature. The reaction mixture was evaporated to dryness, and the remaining residue was extracted with ca. 6 mL of benzene. The benzene extract was filtered through Celite and the filtrate was dried under vacuum. The remaining solid residue was triturated with pentane (3 × 5 mL) to afford **3-21** as an orange solid (0.064 g, 73%). **Method 2:** A solution of Me$_3$CCH$_2$Li (0.0023 g, 0.024 mmol) in ca. 2 mL of cyclohexane was added to a solution of **3-2** (0.020 g, 0.024 mmol) in ca. 2 mL of cyclohexane. An immediate color change from yellow to

orange was observed. Neat $H_2NNC_5H_{10}$ (2.9 μL, 0.0027 g, 0.027 mmol) was added to the reaction mixture, and the solution was heated at 65 °C for 14 h. A gradual color change from orange to dark orange was observed. The reaction mixture was evaporated to dryness, and the remaining residue was extracted with ca. 4 mL of benzene. The benzene extract was filtered through Celite and the filtrate was dried under vacuum. The remaining solid residue was triturated with pentane (3 × 5 mL) to afford **3-21** as an orange solid (0.017 g, 78%). ^{1}H NMR (500 MHz, benzene-d_6): δ 8.13 (d, 2 H, J = 7 Hz, H_{arom}), 7.45 (apparent t, 1 H, J = 7 Hz, H_{arom}), 7.35 (apparent t, 1H, J = 7 Hz, H_{arom}), 7.22 (m, 2 H, H_{arom}), 7.09 (m, 2 H, H_{arom}), 6.58 (m, 1 H, N*H*), 3.50 (m, 1 H, P^i*Pr*), 2.60 (m, 1 H, P^i*Pr*), 2.43 (m, 1 H, P^i*Pr*), 2.19 (m, 1 H, P^i*Pr*), 1.61 (br s, 5 H, NC_5H_{10}), 1.38 – 0.81 (overlapping resonances, 32 H, P^i*Pr* + NC_5H_{10} + Si*Me*; SiMe at 0.91 ppm), -20.33 (t, 1 H, $^2J_{HP}$ = 16 Hz, Ir*H*). ^{13}C{^{1}H} NMR (125.8 MHz, benzene-d_6): δ 161.6 (C_{arom}), 144.8 (C_{arom}), 135.5 (CH_{arom}), 132.6 – 132.3 (overlapping resonances, CH_{arom}), 130.6 (CH_{arom}), 129.4 (CH_{arom}), 129.1 (CH_{arom}), 126.8 (CH_{arom}), 27.0 ($CH_{2NC5H10}$), 24.9 (CH_{iPr}), 24.5 – 24.3 (overlapping resonances, CH_{iPr}), 23.3 – 23.1 (overlapping resonances, CH_{iPr}), 22.5 – 22.9 (overlapping resonances, CH_{iPr}), 21.1 – 20.8 (overlapping resonances, CH_{3iPr}), 19.2 (CH_{3iPr}), 18.5 (CH_{3iPr}), 18.2 (CH_{3iPr}), 17.1 (CH_{3iPr}), 6.3 (Si*Me*). ^{31}P{^{1}H} NMR (202.5 MHz, benzene-d_6): δ 62.6 (AB quartet). ^{29}Si NMR (99.4 MHz, benzene-d_6): δ 15.4. ^{15}N NMR (50.7 MHz, benzene-d_6): δ -182.7. IR (Thin Film, cm^{-1}): 3157 (br, w, N-H), 2122 (m, Ir-H).

[^{i}Pr-PSiP]Ir(H)NHN(CH$_2$CH$_2$)$_2$NMe (3-22) Method 1: A solution of LiNHN(CH$_2$CH$_2$)$_2$NMe (0.015 g, 0.122 mmol) in ca. 2 mL of THF was added dropwise via pipette to a solution of **3-2** (0.080 g, 0.122 mmol) in ca. 2 mL of THF at room temperature. An immediate color change from yellow to orange was observed at room temperature. The reaction mixture was evaporated to dryness, and the remaining residue was extracted with ca. 4 mL of benzene. The benzene extract was filtered through Celite and the filtrate was dried under vacuum. The remaining solid residue was triturated with pentane (3 × 5 mL) to afford **3-22** as an orange solid (0.081 g, 90%). **Method 2:** A

solution of Me_3CCH_2Li (0.011 g, 0.122 mmol) in ca. 4 mL of cyclohexane was added to a solution of **3-2** (0.080 g, 0.121 mmol) in ca. 4 mL of cyclohexane. An immediate color change from yellow to orange was observed. Neat $H_2NN(CH_2CH_2)_2NMe$ (14.6 μL, 0.014 g, 0.122 mmol) was added to the reaction mixture, and the solution was heated at 65 °C for 14 h. A gradual color change from orange to dark orange was observed. The reaction mixture was evaporated to dryness, and the remaining residue was extracted with ca. 8 mL of benzene. The benzene extract was filtered through Celite and the filtrate was dried under vacuum. The remaining solid residue was triturated with pentane (3 × 5 mL) to afford **3-22** as an orange solid (0.073 g, 82%). ^{1}H NMR (500 MHz, benzene-d_6): δ 8.12 (d, 2 H, J = 8 Hz, H_{arom}), 7.44 (m, 1 H, H_{arom}), 7.34 (m, 1H, H_{arom}), 7.25 – 7.04 (overlapping resonances, 4 H, H_{arom}), 6.50 (m, 1 H, N*H*), 3.51 (m, 1 H, P^i*Pr*), 3.35 (m, 1 H, P^i*Pr*), 3.15 (m, 1 H, P^i*Pr*), 3.03 (m, 1 H, P^i*Pr*), 2.64 – 2.58 (m, 4 H, N(CH_2CH_2)$_2$NMe), 2.42 – 2.38 (m, 4 H, N(CH_2CH_2)$_2$NMe), 2.17 (s, 3 H, N(CH$_2$CH$_2$)$_2$N*Me*), 1.34 – 0.83 (overlapping resonances, 27 H, P^i*Pr*$_2$ + Si*Me*), -20.40 (t, 1 H, $^2J_{HP}$ = 16 Hz, Ir*H*). ^{13}C{^{1}H} NMR (125.8 MHz, benzene-d_6): δ 161.2 (C_{arom}), 145.1 (C_{arom}), 132.7 (m, CH$_{arom}$), 130.8 (CH$_{arom}$), 129.6 (CH$_{arom}$), 127.0 (CH$_{arom}$), 46.7 (CH$_{3N(CH2CH2)2NMe}$), 25.0 – 23.8 (overlapping resonances, CH$_{iPr}$), 21.5 – 21.0 (overlapping resonances, CH$_{2N(CH2CH2)2NMe}$), 20.3 – 16.2 (overlapping resonances, CH$_{3iPr}$), 6.6 (Si*Me*). ^{31}P{^{1}H} NMR (202.5 MHz, benzene-d_6): δ 62.7 (AB quartet). ^{29}Si NMR (99.4 MHz, benzene-d_6): δ 15.2. ^{15}N NMR (50.7 MHz, benzene-d_6): δ -189.2. IR (Nujol, cm^{-1}): 3163 (br, w, N-H), 2124 (m, Ir-H).

[Cy-PSiP]Ir(H)NH(CO)Ph (3-23). A solution of Me_3SiCH_2Li (0.012 g, 0.122 mmol) in ca. 4 mL of cyclohexane was added to a solution of **2-1** (0.100 g, 0.122 mmol) in ca. 4 mL of cyclohexane. An immediate color change from yellow to orange was observed. The reaction mixture was analyzed by ^{31}P NMR spectroscopy to confirm the complete consumption of **2-1**. $H_2N(CO)Ph$ (0.016 g, 0.122 mmol) was added to the reaction mixture, and the solution was heated at 65 °C for 2 h. The reaction mixture was evaporated to dryness, and the remaining residue was extracted with ca. 4 mL of benzene.

The benzene extract was filtered through Celite and the filtrate was dried under vacuum. The remaining solid residue was triturated with pentane (3 × 5 mL) to afford **3-23** as an orange solid (0.109 g, 99%). ^{1}H NMR (500 MHz, benzene-d_6): δ 8.13 (d, 2 H, J = 7 Hz, H_{arom}), 7.80 (d, 2 H, J = 7 Hz, H_{arom}), 7.49 (m, 2 H, H_{arom}), 7.25 (m, 2 H, J = 7 Hz, H_{arom}), 7.15 – 7.13 (overlapping resonances, 2 H, H_{arom}), 7.09 – 7.06 (overlapping resonances, 3 H, H_{arom}), 5.73 (br m, 1 H, N*H*), 2.59 (m, 2 H, P*Cy*), 2.41 (m, 4 H, P*Cy*), 2.27 (m, 6 H, P*Cy*), 2.11 (m, 4 H, P*Cy*), 1.90 – 0.89 (overlapping resonances, 33 H, P*Cy*), 0.74 (s, 3 H, Si*Me*), -20.89 (t, 1 H, $^{2}J_{HP}$ = 16 Hz, Ir*H*). ^{13}C{^{1}H} NMR (125.8 MHz, benzene-d_6): δ 159.2 (apparent t, J = 14 Hz, C_{arom}), 144.5 (apparent t, J = 26 Hz, C_{arom}), 139.9 (C_{arom}), 139.4 (apparent t, J = 14 Hz, CH$_{arom}$), 130.3 (CH$_{arom}$), 130.0 (CH$_{arom}$), 129.3 (CH$_{arom}$), 127.5 (CH$_{arom}$), 126.6 (CH$_{arom}$), 37.2 (CH$_{Cy}$), 36.7 (CH$_{2Cy}$), 30.5 (CH$_{2Cy}$), 30.3 (CH$_{2Cy}$), 29.8 (CH$_{2Cy}$), 29.7 (CH$_{2Cy}$), 28,4 – 27.0 (overlapping resonances, CH$_{2Cy}$), 4.6 (Si*Me*). ^{31}P{^{1}H} NMR (202.5 MHz, benzene-d_6): δ 50.9. ^{29}Si NMR (99.4 MHz, benzene-d_6): δ 11.9. IR (Thin Film, cm^{-1}): 3400 (br, w, N-H), 2174 (m, Ir-H). X-Ray quality crystals of **3.20** were grown from slow evaporation from a concentrated benzene solution at room temperature.

[Cy-PSiP]Ir(H)NH(CO)C$_6$F$_5$ (3-24). A solution of Me$_3$SiCH$_2$Li (0.012 g, 0.122 mmol) in ca. 4 mL of cyclohexane was added to a solution of **2-1** (0.100 g, 0.122 mmol) in ca. 4 mL of cyclohexane. An immediate color change from yellow to orange was observed. The reaction mixture was analyzed by ^{31}P NMR spectroscopy to confirm the complete consumption of **2-1**. H$_2$N(CO)C$_6$F$_5$ (0.028 g, 0.134 mmol) was added to the reaction mixture, and the solution was heated at 65 °C for 2 h. The reaction mixture was evaporated to dryness, and the remaining residue was extracted with ca. 4 mL of benzene. The benzene extract was filtered through Celite and the filtrate was dried under vacuum. The remaining solid residue was triturated with pentane (3 × 5 mL) to afford **3-24** as an orange solid (0.110 g, 91%). ^{1}H NMR (500 MHz, benzene-d_6): δ 8.10 (d, 2 H, J = 7 Hz, H_{arom}), 7.50 (m, 2 H, H_{arom}), 7.24 (t, 2 H, J = 8 Hz, H_{arom}), 7.15 (m, 2 H, H_{arom}), 5.24 (br s, 1 H, N*H*), 2.73 (m, 2 H, P*Cy*), 2.51 – 2.39 (overlapping resonances, 4 H, P*Cy*), 2.21 (m, 2

H, P*Cy*), 2.13 (m, 2 H, P*Cy*), 2.03 (m, 2 H, P*Cy*), 1.92 (m, 2 H, P*Cy*), 1.78 – 1.56 (overlapping resonances, 14 H, P*Cy*), 1.45 – 1.20 (overlapping resonances, 10 H, P*Cy*), 0.95 – 0.85 (overlapping resonances, 6 H, P*Cy*), 0.72 (s, 3 H, Si*Me*), -21.13 (t, 1 H, $^{2}J_{HP}$ = 17 Hz, Ir*H*). $^{13}C\{^{1}H\}$ NMR (125.8 MHz, benzene-d_6): δ 162.4 (C_{arom}), 158.4 (apparent t, J = 21 Hz, C_{arom}), 143.3 (apparent t, J = 28 Hz, C_{arom}), 132.3 (apparent t, J = 9 Hz, CH_{arom}), 130.4 (CH_{arom}), 130.0 (CH_{arom}), 129.5 (CH_{arom}), 127.6 (CH_{arom}), 36.1 (apparent t, J = 15 Hz, CH_{Cy}), 34.7 (apparent t, J = 11 Hz, CH_{Cy}), 30.6 (CH_{2Cy}), 29.8 (CH_{2Cy}), 29.0 (CH_{2Cy}), 28.1 – 27.6 (overlapping resonances, CH_{2Cy}), 27.0, (CH_{2Cy}), 4.2 (Si*Me*). $^{31}P\{^{1}H\}$ NMR (202.5 MHz, benzene-d_6): δ 52.9. ^{29}Si NMR (99.4 MHz, benzene-d_6): δ 9.6. IR (Thin Film, cm^{-1}): 3383 (br, w, N-H), 2186 (m, Ir-H).

[^{i}Pr-PSiP]Ir(H)NH(CO)Ph (3-25). A solution of Me_3SiCH_2Li (0.003 g, 0.030 mmol) in ca. 0.4 mL of cyclohexane was added to a solution of **3-2** (0.020 g, 0.030 mmol) in ca. 0.4 mL of cyclohexane. An immediate color change from yellow to orange was observed. The reaction mixture was analyzed by ^{31}P NMR spectroscopy to confirm the complete consumption of **3-2**. $H_2N(CO)Ph$ (0.004 g, 0.030 mmol) was added to the reaction mixture, and the solution was heated at 65 °C for 14 h. The reaction mixture was evaporated to dryness, and the remaining residue was extracted with ca. 4 mL of benzene. The benzene extract was filtered through Celite and the filtrate was dried under vacuum. The remaining solid residue was triturated with pentane (3 ×3 mL) to afford **3-25** as an light orange solid (0.016 g, 70 %). ^{1}H NMR (500 MHz, benzene-d_6): δ 8.10 (d, 2 H, J =7 Hz, H_{arom}), 7.78 (d, 2 H, J = 7 Hz, H_{arom}), 7.36 (m, 2 H, H_{arom}), 7.22 (overlapping resonances, 3 H, H_{arom}), 7.15 – 7.09 (overlapping resonances, 4 H, H_{arom}), 5.73 (br m, 1 H, N*H*), 2.69 (m, 2 H, P^{i}*Pr*$_2$), 2.36 (m, 2 H, P^{i}*Pr*$_2$), 1.48 (m, 6 H, P^{i}*Pr*$_2$), 1.10 – 0.97 (overlapping resonances, 18 H, P^{i}*Pr*$_2$), 0.76 (s, 3 H, Si*Me*), -21.34 (t, 1 H, $^{2}J_{HP}$ = 16 Hz, Ir*H*). $^{13}C\{^{1}H\}$ NMR (125.8 MHz, benzene-d_6): δ 159.4 (apparent t, J = 16 Hz, C_{arom}), 144.5 (C_{arom}), 139.8 (C_{arom}), 132.6 (apparent t, J = 9 Hz, CH_{arom}), 130.4 (CH_{arom}), 130.3 (CH_{arom}), 127.6 (CH_{arom}), 126.8 (CH_{arom}), 27.3 (CH_{iPr}), 26.4 (CH_{iPr}), 21.0 (CH_{3iPr}), 20.1 (CH_{3iPr}), 19.1 (CH_{3iPr}), 18.1 (CH_{3iPr}), 4.4 (Si*Me*). $^{31}P\{^{1}H\}$ NMR (202.5

MHz, benzene-d_6): δ 57.9. ^{29}Si NMR (99.4 MHz, benzene-d_6): δ 11.2. IR (thin film, cm^{-1}): 3382 (br, w, N-H), 2182 (m, Ir-H).

[^{i}Pr-PSiP]Ir(H)NH(CO)C$_6$F$_5$ (3-26). A solution of Me_3SiCH_2Li (0.009 g, 0.122 mmol) in ca. 3 mL of cyclohexane was added to a solution of **3-2** (0.080 g, 0.122 mmol) in ca. 3 mL of cyclohexane. An immediate color change from yellow to orange was observed. The reaction mixture was analyzed by ^{31}P NMR spectroscopy to confirm the complete consumption of **3-2**. $H_2N(CO)C_6F_5$ (0.026 g, 0.122 mmol) was added to the reaction mixture, and the solution was heated at 65 °C for 14 h. The reaction mixture was evaporated to dryness, and the remaining residue was extracted with ca. 6 mL of benzene. The benzene extract was filtered through Celite and the filtrate was dried under vacuum. The remaining solid residue was triturated with pentane (3 × 5 mL) to afford **3-26** as an light yellow solid (0.098 g, 98 %). ^{1}H NMR (500 MHz, benzene-d_6): δ 8.06 (d, 2 H, J = 7 Hz, H_{arom}), 7.35 (m, 2 H, H_{arom}), 7.22 (t, 2 H, J = 7 Hz, H_{arom}), 7.11 (t, 2 H, J = 8 Hz, H_{arom}), 5.25 (br s, 1 H, N*H*), 2.73 (m, 2 H, P^i*Pr*$_2$), 2.63 (m, 2 H, P^i*Pr*$_2$), 1.54 (m, 6 H, P^i*Pr*$_2$), 1.15 – 0.95 (overlapping resonances, 18 H, P^i*Pr*$_2$), 0.67 (s, 3 H, Si*Me*), -21.28 (t, 1 H, $^2J_{HP}$ = 17 Hz, Ir*H*). ^{13}C{^{1}H} NMR (125.8 MHz, benzene-d_6): δ 162.5 (C_{arom}), 158.4 (apparent t, J = 21 Hz, C_{arom}), 143.1 (apparent t, J = 28 Hz, C_{arom}), 132.3 (apparent t, J = 9 Hz, CH$_{arom}$), 130.3 (CH$_{arom}$), 129.6 (CH$_{arom}$), 127.6 (CH$_{arom}$), 26.8 (apparent t, J = 15 Hz, CH$_{iPr}$), 25.6 (apparent t, J = 13 Hz, CH$_{iPr}$), 20.8 (CH$_{3iPr}$), 20.1 (CH$_{3iPr}$), 18.7 (CH$_{3iPr}$), 17.7 (CH$_{3iPr}$), 4.1s (Si*Me*). ^{31}P{^{1}H} NMR (202.5 MHz, benzene-d_6): δ 60.1. ^{29}Si NMR (99.4 MHz, benzene-d_6): δ 9.8. IR (Nujol, cm^{-1}): 3398 (br, w, N-H), 2175 (m, Ir-H). Anal. Calcd for $C_{32}H_{41}F_5IrNOP_2Si$: C, 46.14 H, 4.96; N, 1.68. Found: C, 46.74; H, 4.96; N, 1.68.

[Cy-PSiP]Rh(NH$_2$Ad) (3-28). A solution of Me_3SiCH_2Li (0.002 g, 0.021 mmol) in ca. 0.4 mL of benzene-d_6 was added to a solution of **2-2** (0.015 g, 0.021 mmol) in ca. 0.4 mL of benzene-d_6. An immediate color change from yellow to orange was observed. The reaction mixture was analyzed by ^{1}H and ^{31}P NMR spectroscopy to confirm the complete consumption of **2-2** and the formation of 1 equiv. of Me_4Si. Adamantyl amine

(0.016 g, 0.103 mmol) was added to the reaction mixture, and the solution was subsequently analyzed by use of NMR techniques, which confirmed the clean formation of putative **3-28**. The coordinated amine in **3-28** was readily displaced in vacuo, precluding the isolation of this compound. Moreover, the presence of excess amine in the in situ generated solution of **3-25** precluded the comprehensive assignment of ^{1}H and ^{13}C NMR resonances for this compound. ^{1}H NMR (500 MHz, benzene-d_6): δ8.30 (d, 2 H, J = 7 Hz, H_{arom}), 7.56 (d, 2 H, J = 8 Hz, H_{arom}), 7.34 (t, 2H, J = 7 Hz, H_{arom}), 7.24 (t, 2 H, J = 8 Hz, H_{arom}), 5.73 (br m, 2 H, NH_2), 2.44 (br m, 4 H, P*Cy*), 2.08 – 1.01 (overlapping resonances, 55 H, P*Cy* + NH_2*Ad*), 0.97 (s, 3 H, Si*Me*). ^{13}C{^{1}H} NMR (125.8 MHz, benzene-d_6): δ 161.2 (C_{arom}), 146.3 (C_{arom}), 132.0 (m, CH_{arom}), 129.2 (CH_{arom}), 128.2 (CH_{arom}), 126.5 (CH_{arom}), 40.1 (CH_{Cy}), 38.9 (CH_{Cy}), 31.9 – 26.1 (overlapping resonances, $CH_{2NC5H10}$ + CH_{2Cy}), 8.6 (Si*Me*). ^{31}P{^{1}H} NMR (202.5 MHz, benzene-d_6): δ 51.5 (d, J_{RhP} = 184 Hz). ^{29}Si NMR (99.4 MHz, benzene-d_6): δ 58.7.

[Cy-PSiP]Rh($NH_2{}^tBu$) (3-29). A solution of Me_3SiCH_2Li (0.002 g, 0.021 mmol) in ca. 0.4 mL of benzene-d_6 was added to a solution of **2-2** (0.015 g, 0.021 mmol) in ca. 0.4 mL of benzene-d_6. An immediate color change from yellow to orange was observed. The reaction mixture was analyzed by ^{1}H and ^{31}P NMR spectroscopy to confirm the complete consumption of **2-2** and the formation of 1 equiv. of Me_4Si. *Tert*-butyl amine (10.9 μL, 0.008 g, 0.103 mmol) was added to the reaction mixture, and the solution was subsequently analyzed by use of NMR techniques, which confirmed the clean formation of putative **3-29**. The coordinated amine in **3-29** was readily displaced in vacuo, precluding the isolation of this compound. Moreover, the presence of excess amine in the in situ generated solution of **3-26** precluded the comprehensive assignment of ^{1}H and ^{13}C NMR resonances for this compound. ^{1}H NMR (500 MHz, benzene-d_6): δ 8.27 (d, 2 H, J = 7 Hz, H_{arom}), 7.53 (d, 2 H, J = 7 Hz, H_{arom}), 7.33 (t, 2H, J = 8 Hz, H_{arom}), 7.23 (t, 2 H, J = 8 Hz, H_{arom}), 2.34 (br m, 4 H, P*Cy*), 2.08 – 1.00 (overlapping resonances, 40 H, P*Cy*), 0.94 (s, 3 H, Si*Me*). ^{13}C{^{1}H} NMR (125.8 MHz, benzene-d_6): δ 132.7 (m, CH_{arom}), 130.0 (CH_{arom}), 129.2 (CH_{arom}), 127.2 (CH_{arom}), 32.1 (CH_{2Cy}), 30.8 (CH_{2Cy}), 30.0 (CH_{2Cy}), 28.5

– 26.2 (overlapping resonances, CH_{2Cy}), 8.6 (Si*Me*), 0.4 (CH_{3tBu}). $^{31}P\{^{1}H\}$ NMR (202.5 MHz, benzene-d_6): δ 52.3 (d, J_{RhP} = 180 Hz). ^{29}Si NMR (99.4 MHz, benzene-d_6): δ 60.2.

[Cy-PSiP]Rh(NH_2Cy) (3-30). A solution of Me_3SiCH_2Li (0.002 g, 0.021 mmol) in ca. 0.4 mL of benzene-d_6 was added to a solution of **2-2** (0.015 g, 0.021 mmol) in ca. 0.4 mL of benzene-d_6. An immediate color change from yellow to orange was observed. The reaction mixture was analyzed by ^{1}H and ^{31}P NMR spectroscopy to confirm the complete consumption of **2-2** and the formation of 1 equiv. of Me_4Si. Cyclohexylamine (11.8 μL, 0.010 g, 0.103 mmol) was added to the reaction mixture, and the solution was subsequently analyzed by use of NMR techniques, which confirmed the clean formation of putative **3-30**. The coordinated amine in **3-30** was readily displaced in vacuo, precluding the isolation of this compound. Moreover, the presence of excess amine in the in situ generated solution of **3-30** precluded the comprehensive assignment of ^{1}H and ^{13}C NMR resonances for this compound. ^{1}H NMR (500 MHz, benzene-d_6): δ 8.27 (d, 2 H, J = 7 Hz, H_{arom}), 7.57 (d, 2 H, J = 7 Hz, H_{arom}), 7.35 (t, 2 H, J = 7 Hz, H_{arom}), 7.25 (t, 2 H, J = 7 Hz, H_{arom}), 2.48 – 0.85 (overlapping resonances, 47 H, P*Cy* + Si*Me*). $^{13}C\{^{1}H\}$ NMR (125.8 MHz, benzene-d_6): δ 132.3 (CH_{arom}), 129.8 (CH_{arom}), 129.2 (CH_{arom}), 126.6 (CH_{arom}), 30.4 (CH_{2Cy}), 29.7 (CH_{2Cy}), 28.8 – 26.3 (overlapping resonances, CH_{2Cy}), 6.9 (Si*Me*). $^{31}P\{^{1}H\}$ NMR (202.5 MHz, benzene-d_6): δ 54.0 (d, J_{RhP} = 184 Hz). ^{29}Si NMR (99.4 MHz, benzene-d_6): δ 61.3.

[Cy-PSiP]Rh(NH_2Pr) (3-31). Method 1: A solution of LiNH(Pr) (0.002g, 0.027 mmol) in ca. 0.4 mL of benzene-d_6 was added dropwise via pipette to a solution of **2.2** (0.020 g, 0.027 mmol) in ca. 0.4 mL of benzene-d_6 at room temperature. An immediate color change from yellow to orange was observed. The solution was subsequently analyzed by use of NMR techniques, which confirmed the clean formation of putative **3-31**. The coordinated amine in **3-31** was readily displaced in vacuo, precluding the isolation of this compound. **Method 2:** A solution of Me_3CCH_2Li (0.0016 g, 0.021 mmol) in ca. 0.4 mL of benzene-d_6 was added to a solution of **2-2** (0.015 g, 0.021 mmol) in ca. 0.4 mL of benzene-d_6. An immediate color change from yellow to

red was observed. The reaction mixture was analyzed by ^{1}H and ^{31}P NMR spectroscopy to confirm the complete consumption of **2-2** and the formation of 1 equiv. of CMe_4. Five equivalents of H_2NPr (8.5 μL, 0.0061 g, 0.10 mmol) were added to the reaction mixture, at which point ^{1}H and ^{31}P NMR analysis of the reaction mixture indicated the quantitative formation of **3-31**. The coordinated amine in **3-31** was readily displaced in vacuo, precluding the isolation of this compound. ^{1}H NMR (500 MHz, benzene-d_6): δ 8.32 (d, 2 H, J = 7 Hz, H_{arom}), 7.56 (d, 2 H, J = 8 Hz, H_{arom}), 7.35 (t, 2 H, J = 7 Hz, H_{arom}), 7.25 (t, 2 H, J = 8 Hz, H_{arom}), 2.66 (m, 2 H, P*Cy*), 2.31 (m, 4 H, P*Cy*), 2.13 (m, 2 H, P*Cy*), 1.97 (m, 2 H, P*Cy*), 1.88 (m, 2 H, P*Cy*), 1.74 – 1.15 (overlapping resonances, 36 H, P*Cy* + CH_{2Pr}), 0.91 (s, 3 H, Si*Me*), 0.80 (t, 3 H, J = 8 Hz, CH_{3Pr}). ^{13}C{^{1}H} NMR (125.8 MHz, benzene-d_6): δ 162.0 (C_{arom}), 146.7 (C_{arom}), 132.7 (m, CH_{arom}), 129.9 (CH_{arom}), 129.0 (CH_{arom}), 127.2 (CH_{arom}), 47.1 (CH_{2Pr}), 41.0 (CH_{Cy}), 39.0 (CH_{Cy}), 32.2 (CH_{2Cy}), 31.8 (CH_{2Cy}), 30.8 (CH_{2Cy}), 30.3 (CH_{2Cy}), 28.6 – 26.2 (overlapping resonances, CH_{2Cy} + CH_{2Pr}), 12.0 (CH_{3Pr}), 9.3 (Si*Me*). ^{31}P{^{1}H} NMR (202.5 MHz, benzene-d_6): δ 54.4 (d, J = 182 Hz). ^{29}Si NMR (99.4 MHz, benzene-d_6): δ 60.8.

[Cy-PSiP]Rh(NH_2Oct) (3-32). Method 1: A solution of LiNH(Oct) (0.0037g, 0.027 mmol) in ca. 0.4 mL of benzene-d_6 was added dropwise via pipette to a solution of **2-2** (0.020 g, 0.027 mmol) in ca. 0.4 mL of benzene-d_6 at room temperature. An immediate color change from yellow to orange was observed. The solution was subsequently analyzed by use of NMR techniques, which confirmed the clean formation of putative **3-32**. The coordinated amine in **3-32** was readily displaced in vacuo, precluding the isolation of this compound. **Method 2:** A solution of Me_3CCH_2Li (0.0016 g, 0.021 mmol) in ca. 0.4 mL of benzene-d_6 was added to a solution of **2-2** (0.015 g, 0.021 mmol) in ca. 0.4 mL of benzene-d_6. An immediate color change from yellow to red was observed. The reaction mixture was analyzed by ^{1}H and ^{31}P NMR spectroscopy to confirm the complete consumption of **2-2** and the formation of 1 equiv. of CMe_4. Five equivalents of H_2N^nOct (17.0 μL, 0.013 g, 0.10 mmol) were added to the reaction mixture, at which point ^{1}H and ^{31}P NMR analysis of the reaction mixture indicated the

quantitative formation of **3-32**. The coordinated amine in **3-32** was readily displaced in vacuo, precluding the isolation of this compound. ^{1}H NMR (500 MHz, benzene-d_6): δ 8.34 (d, 2 H, J = 7 Hz, H_{arom}), 7.59 (d, 2 H, J = 7 Hz, H_{arom}), 7.36 (t, 2 H, J = 8 Hz, H_{arom}), 7.27 (t, 2 H, J = 8 Hz, H_{arom}), 2.67 (m, 2 H, P*Cy*), 2.34 – 2.28 (overlapping resonances, 8 H, P*Cy*), 1.79 – 1.03 (overlapping resonances, 44 H, P*Cy* + CH_{2Oct}), 0.93 – 0.86 (overlapping resonances, 6 H, CH_{3Oct} + Si*Me*; SiMe at 0.93 ppm). ^{13}C{^{1}H} NMR (125.8 MHz, benzene-d_6): δ 162.2 (C_{arom}), 146.8 (C_{arom}), 132.8 (m, CH_{arom}), 129.9 (CH_{arom}), 129.0 (CH_{arom}), 127.2 (CH_{arom}), 40.8 (CH_{Cy}), 39.5 (CH_{Cy}), 34.9 (CH_{2Cy}), 32.6 – 27.1 (overlapping resonances, CH_{2Cy} + CH_{2Oct}), 25.8 (CH_{2Pr}), 23.4 (CH_{2Pr}), 23.2 (CH_{2Pr}), 14.6 (CH_{3Pr}), 9.4 (Si*Me*). ^{31}P{^{1}H} NMR (202.5 MHz, benzene-d_6): δ 56.7 (br s). ^{29}Si NMR (99.4 MHz, benzene-d_6): δ 61.2.

[Cy-PSiP]Rh(NH$_2$CH$_2$Ph) (3-33). A solution of Me_3SiCH_2Li (0.019 g, 0.21 mmol) in ca. 4 mL of C_6H_6 was added to a solution of **2-2** (0.150 g, 0.21 mmol) in ca. 4 mL of C_6H_6. An immediate color change from pale yellow to bright orange was observed. Neat $H_2N(CH_2Ph)$ (22.5 μL, 0.022 g, 0.21 mmol) was added to the reaction mixture, and the solution was stirred at room temperature for 20 minutes. The reaction mixture was evaporated to dryness, and the remaining residue was extracted with ca. 10 mL of benzene. The benzene extract was filtered through Celite and the filtrate was dried under vacuum. The remaining solid residue was triturated with pentane (3 × 5 mL) to afford **3-33** as an orange solid (0.156g, 93 %). ^{1}H NMR (500 MHz, benzene-d_6): δ 8.33 (d, 2 H, J = 7 Hz, H_{arom}), 7.55 – 7.50 (overlapping resonances, 4 H, H_{arom}), 7.35 (t, 2 H, J = 7 Hz, H_{arom}) 7.25 (t, 2 H, J = 7 Hz, H_{arom}), 7.19 (t, 2 H, J = 8 Hz, H_{arom}), 7.08 (t, 1 H, J = 8 Hz, H_{arom}), 3.89 (broad s, 2 H, NH_2) 2.24 – 1.15 (overlapping resonances, 36 H, P*Cy* + CH_2), 0.98 (s, 3 H, Si*Me*). ^{13}C{^{1}H} NMR (125.8 MHz, benzene-d_6): δ 161.6 (C_{arom}), 147.1 (C_{arom}), 142.4 (C_{arom}), 132.7 (CH_{arom}), 129.8 (CH_{arom}), 129.2 (CH_{arom}), 129.0 – 128.0 (overlapping resonances, CH_{arom}), 127.3 (CH_{arom}), 49.6 (CH_{2Cy}), 31.8 (CH_{2Cy}), 30.8 (CH_{2Cy}), 30.1 (CH_{2Cy}), 28.3 – 27.6 (overlapping resonances, CH_{2Cy}), 27.0 (CH_{2Cy}), 23.1

(CH_{2Cy}), 9.3 (Si*Me*). $^{31}P\{^{1}H\}$ NMR (202.5 MHz, benzene-d_6): δ 54.3 (d, J_{RhP} = 180 Hz). ^{29}Si NMR (99.4 MHz, benzene-d_6): δ 60.6.

[Cy-PSiP]Rh(H)NHNC$_5$H$_{10}$ (3-34). A solution of LiNHNC$_5$H$_{10}$ (0.022 g, 0.21 mmol) in ca. 5 mL of THF was added dropwise via pipette to a solution of **2-2** (0.150 g, 0.21 mmol) in ca. 5 mL of THF at room temperature. A gradual color change from yellow to dark orange was observed over 1 hour at room temperature. The reaction mixture was evaporated to dryness, and the remaining residue was extracted with ca. 10 mL of benzene. The benzene extract was filtered through Celite and the filtrate was dried under vacuum. The remaining solid residue was triturated with pentane (3 × 5 mL) to afford **3-34** as an orange solid (0.151 g, 90%). ^{1}H NMR (500 MHz, benzene-d_6): δ 8.09 (d, 2 H, J = 7 Hz, H_{arom}), 7.50 (m, 2 H, H_{arom}), 7.27 (apparent t, 2 H, J = 7 Hz, H_{arom}), 7.16 (m, 2 H, H_{arom}), 4.75 (m, 1 H, N*H*), 2.54 (m, 2 H, P*Cy*), 2.35 (m, 4 H, P*Cy*), 2.16 – 1.90 (overlapping resonances, 14 H, P*Cy* + NC$_5$*H$_{10}$*), 1.71 – 1.18 (overlapping resonances, 34 H, P*Cy* + NC$_5$*H$_{10}$*), 0.99 (s, 3 H, Si*Me*), -16.74 (apparent q, 1 H, $^{2}J_{HP}$ = 16 Hz, Rh*H*). $^{13}C\{^{1}H\}$ NMR (125.8 MHz, benzene-d_6): δ 159.6 (C_{arom}), 142.8 (C_{arom}), 132.5 (apparent t, J = 9 Hz, CH_{arom}), 130.8 (CH_{arom}), 129.2 (CH_{arom}), 127.0 (CH_{arom}), 34.1 (apparent t, J = 14 Hz, CH_{Cy}), 31.2 (CH_{Cy}), 30.7 (CH_{Cy}), 29.1 (CH_{Cy}), 28.1 – 26.8 (overlapping resonances CH_{2Cy} + $CH_{2NC5H10}$), 23.1 (CH_{2Cy}), 10.0 (Si*Me*). $^{31}P\{^{1}H\}$ NMR (202.5 MHz, benzene-d_6): δ 63.7 (br s). ^{29}Si NMR (99.4 MHz, benzene-d_6): δ 41.2. IR (thin film, cm^{-1}): 3256 (br, w, N-H), 2095 (m, Ir-H). Anal. Calcd for $C_{42}H_{67}RhN_2P_2Si$: C, 63.62; H, 8.52; N, 3.53. Found: C, 62.31; H, 8.41; N, 3.52.

[Cy-PSiP]Rh(H)NHN(CH$_2$CH$_2$)$_2$NMe (3-35). A solution of LiNHN(CH$_2$CH$_2$)$_2$NMe (0.025 g, 0.21 mmol) in ca. 5 mL of THF was added dropwise via pipette to a solution of **2-2** (0.150 g, 0.21 mmol) in ca. 5 mL of THF at room temperature. A gradual color change from yellow to orange was observed over 1 hour at room temperature. The reaction mixture was evaporated to dryness, and the remaining residue was extracted with ca. 10 mL of benzene. The benzene extract was filtered through Celite and the filtrate was dried under vacuum. The remaining solid residue was

triturated with pentane (3 × 5 mL) to afford **3-35** as an orange solid (0.117 g, 69%). ^{1}H NMR (500 MHz, benzene-d_6): δ 8.09 (d, 2 H, J = 8 Hz, H_{arom}), 7.49 (m, 2 H, H_{arom}), 7.27 (apparent t, 2 H, J = 7 Hz, H_{arom}), 7.15 (m, 2 H, H_{arom}), 4.69 (m, 1 H, N*H*), 3.26 (m, 3 H, P*Cy*), 2.85 – 2.33 (overlapping resonances, 16 H, P*Cy* + N(CH_2CH_2)$_2$NMe), 2.20 (s, 3 H, N(CH_2CH_2)$_2$N*Me*), 2.16 – 1.17 (overlapping resonances, 33 H, P*Cy*), 0.99 (s, 3 H, Si*Me*), -16.78 (apparent q, 1 H, $^{2}J_{HP}$ = 17 Hz, Rh*H*). ^{13}C{^{1}H} NMR (125.8 MHz, benzene-d_6): δ 159.6 (C_{arom}), 141.3 (C_{arom}), 132.4 (apparent d, J = 10 Hz, *C*H$_{arom}$), 130.8 (*C*H$_{arom}$), 129.3 (*C*H$_{arom}$), 129.3 (*C*H$_{arom}$), 129.3 (*C*H$_{arom}$), 127.1 (*C*H$_{arom}$), 64.2 (*C*H$_{2N(CH2CH2)2NMe}$), 57.0 (*C*H$_{2N(CH2CH2)2NMe}$), 46.7 (*C*H$_{3N(CH2CH2)2NMe}$), 35.3 (apparent t, J = 13 Hz, *C*H$_{Cy}$), 34.0 (apparent t, J = 15 Hz, *C*H$_{Cy}$), 31.1 (*C*H$_{2Cy}$), 30.7 (*C*H$_{2Cy}$), 30.2 (*C*H$_{2Cy}$), 29.3 (*C*H$_{2Cy}$), 28.1 – 26.7 (overlapping resonances, *C*H$_{2Cy}$), 23.1 (*C*H$_{2Cy}$), 10.1 (Si*Me*). ^{31}P{^{1}H} NMR (202.5 MHz, benzene-d_6): δ 63.7 (br s). ^{29}Si NMR (99.4 MHz, benzene-d_6): δ 41.1. IR (Thin Film, cm^{-1}): 3253 (br, w, N-H), 2096 (m, Ir-H).

[Cy-PSiP]Rh(NH$_2$NC$_5$H$_{10}$) (3-36). A solution of Me$_3$SiCH$_2$Li (0.002 g, 0.021 mmol) in ca. 0.4 mL of benzene-d_6 was added to a solution of **2-2** (0.015 g, 0.021 mmol) in ca. 0.4 mL of benzene-d_6. An immediate color change from yellow to orange was observed. The reaction mixture was analyzed by ^{1}H and ^{31}P NMR spectroscopy to confirm the complete consumption of **2-2** and the formation of 1 equiv. of Me$_4$Si. 1-Aminopiperidine (2.2 μL, 0.002 g, 0.021 mmol) was added to the reaction mixture, and the solution was subsequently analyzed by use of NMR techniques, which confirmed the clean formation of putative **3-36**. The coordinated amine in **3-36** was readily displaced in vacuo, precluding the isolation of this compound. Moreover, the presence of excess amine in the in situ generated solution of **3-36** precluded the comprehensive assignment of ^{1}H and ^{13}C NMR resonances for this compound. ^{1}H NMR (500 MHz, benzene-d_6): δ 8.32 (d, 2 H, J = 10 Hz, H_{arom}), 7.59 (d, 2 H, J = 7 Hz, H_{arom}), 7.36 (t, 2 H, J = 7 Hz, H_{arom}), 7.27 (t, 2 H, J = 7 Hz, H_{arom}), 3.56 (broad s, 2 H, NH_2), 2.63 – 0.99 (overlapping resonances, 54 H, PCy + NC$_5$*H$_{10}$*), 0.89 (s, 3 H, Si*Me*). ^{13}C{^{1}H} NMR (125.8 MHz, benzene-d_6): δ 161.2 (C_{arom}), 146.3 (C_{arom}), 132.0 (m, *C*H$_{arom}$), 129.2 (*C*H$_{arom}$), 128.2

(CH_{arom}), 126.5 (CH_{arom}), 40.1 (CH_{Cy}), 38.9 (CH_{Cy}), 31.9 – 26.1 (overlapping resonances, $CH_{2NC5H10}$ + CH_{2Cy}), 8.6 (Si*Me*). $^{31}P\{^{1}H\}$ NMR (202.5 MHz, benzene-d_6): δ 54.8 (d, J_{RhP} = 182 Hz). ^{29}Si NMR (99.4 MHz, benzene-d_6): δ 60.9.

[Cy-PSiP]Rh($NH_2N(CH_2CH_2)_2NMe$) (3-37). A solution of Me_3SiCH_2Li (0.002 g, 0.021 mmol) in ca. 0.4 mL of benzene-d_6 was added to a solution of **2-2** (0.015 g, 0.021 mmol) in ca. 0.4 mL of benzene-d_6. An immediate color change from yellow to orange was observed. The reaction mixture was analyzed by ^{1}H and ^{31}P NMR spectroscopy to confirm the complete consumption of **2-2** and the formation of 1 equiv. of Me_4Si. 4-methyl-1-aminopiperazine (12.4 μL, 0.012 g, 0.103 mmol) was added to the reaction mixture, and the solution was subsequently analyzed by use of NMR techniques, which confirmed the clean formation of putative **3-37**. The coordinated amine in **3-37** was readily displaced in vacuo, precluding the isolation of this compound. Moreover, the presence of excess amine in the in situ generated solution of **3-37** precluded the comprehensive assignment of ^{1}H and ^{13}C NMR resonances for this compound. ^{1}H NMR (500 MHz, benzene-d_6): δ 8.32 (d, 2 H, J = 7 Hz, H_{arom}), 7.58 (d, 2 H, J = 7 Hz, H_{arom}), 7.36 (m, 2 H, H_{arom}), 7.27 (m, 2 H, H_{arom}), 3.45 (br m, 2 H, NH_2), 2.28 – 1.15 (overlapping resonances, 55 H, N(CH_2CH_2)$_2$NMe + N(CH_2CH_2)$_2$N*Me* + P*Cy*), 0.89 (s, 3 H, Si*Me*). $^{13}C\{^{1}H\}$ NMR (125.8 MHz, benzene-d_6): δ 162.3 (C_{arom}), 141.1 (C_{arom}), 132.9 (m, CH_{arom}), 130.2 (CH_{arom}), 129.2 (CH_{arom}), 127.5 (CH_{arom}), 55.6 ($CH_{2N(CH2CH2)2NMe}$), 46.3 ($CH_{3N(CH2CH2)2NMe}$), 41.0 (CH_{Cy}), 39.5 (CH_{Cy}), 32.3 – 27.5 (overlapping resonances, CH_{Cy}), 9.48 (Si*Me*). $^{31}P\{^{1}H\}$ NMR (202.5 MHz, benzene-d_6): δ 54.8 (d, $^{2}J_{RhP}$ = 182 Hz). ^{29}Si NMR (99.4 MHz, benzene-d_6): δ 60.2.

[Cy-PSiP]Rh($NC_5H_4NMe_2$) (3-38). A solution of Me_3SiCH_2Li (0.002 g, 0.021 mmol) in ca. 1 mL of benzene was added to a solution of **2-2** (0.015 g, 0.021 mmol) in ca. 1 mL of benzene. An immediate color change from yellow to orange was observed. A solution of 4-dimethylaminopyridine (0.0028 g, 0.023 mmol) was added to the reaction mixture. A gradual color change from orange to lighter orange was observed over the course of 30 minutes. The reaction mixture was evaporated to dryness, and the remaining

residue was extracted with ca. 2 mL of benzene. The benzene extract was filtered through Celite and the filtrate was dried under vacuum. The remaining solid residue was triturated with pentane (3 × 2 mL) to afford **3-38** as a light orange solid (0.015 g, 95 %). ^{1}H NMR (500 MHz, benzene-d_6): δ 8.63 (br s, 2 H, H_{arom}), 8.45 (d, 2 H, J = 7 Hz, H_{arom}), 7.68 (d, 2 H, J = 8 Hz, H_{arom}), 7.41 (t, 2 H, J = 7 Hz, H_{arom}), 7.30 (t, 2 H, $_J$ = 7 Hz, H_{arom}), 6.10 (d, 2 H, J = 5 Hz, H_{arom}), 2.80 (br m, 2H, P*Cy*), 2.54 (m, 2 H, P*Cy*), 2.34 – 2.20 (overlapping resonances, 6 H, P*Cy*), 2.14 (br s, 10 H, P*Cy* + N*Me*$_2$), 2.01 (m, 3 H, P*Cy*), 1.88 – 1.13 (overlapping resonances, 25 H, P*Cy*), 0.97 (s, 3 H, Si*Me*), 0.86 (m, 4 H, P*Cy*). ^{13}C{^{1}H} NMR (125.8 MHz, benzene-d_6): δ 163.1 (apparent t, J = 28 Hz, C_{arom}), 147.2 (C_{arom}), 132.8 (apparent t, J = 13Hz, CH_{arom}), 130.0 (CH_{arom}), 128.8 (CH_{arom}), 127.1 (CH_{arom}), 107.2 (CH_{arom}), 39.1 (apparent t, J = 13 Hz, CH_{Cy}), 38.6 ($CH_{3pyridine}$), 38.2 (apparent t, J = 8 Hz, CH_{Cy}), 31.3 (CH_{2Cy}), 31.1 (CH_{2Cy}), 30.6 (CH_{2Cy}), 30.1 (CH_{2Cy}), 28.6 – 26.7 (overlapping resonances, CH_{2Cy}), 10.3 (Si*Me*). ^{31}P{^{1}H} NMR (202.5 MHz, benzene-d_6): δ 53.0 (d, J_{RhP} = 178 Hz). ^{29}Si NMR (99.4 MHz, benzene-d_6): δ 59.9. X-Ray quality crystals of **3-38** were grown from a concentrated Et_2O/THF solution at -30 °C.

[Cy-PSiP]Rh(H)NH(NCPh$_2$) (3-40). A solution of Me_3SiCH_2Li (0.019 g, 0.21 mmol) in ca. 8 mL of benzene was added to a solution of **2-2** (0.150 g, 0.21 mmol) in ca. 8 mL of benzene. An immediate color change from yellow to red was observed. A solution of benzophenone hydrazone (0.040 g, 0.21 mmol) was added to the reaction mixture, and the solution was heated at 65 °C for 14 h. A gradual color change from red to dark orange was observed. The reaction mixture was evaporated to dryness, and the remaining residue was extracted with ca. 15 mL of benzene. The benzene extract was filtered through Celite and the filtrate was dried under vacuum. The remaining solid residue was triturated with pentane (3 × 5 mL) to afford **3-40** as an orange solid (0.160 g, 86%). ^{1}H NMR (300K, 500 MHz, benzene-d_6): δ 8.35 (br s, 1 H, H_{arom}), 8.03 (d, 2 H, J = 7 Hz, H_{arom}), 7.95 (d, 2 H, J = 8 Hz, H_{arom}), 7.44 (m, 2 H, H_{arom}), 7.35 – 7.23 (overlapping resonances, 6 H, H_{arom}), 7.13 – 7.06 (overlapping resonances, 5 H, H_{arom}),

4.99 (br s, 1 H, N*H*), 2.80 (br m, 2 H, P*Cy*), 2.40 (m, 4 H, P*Cy*), 2.16 (m, 2 H, P*Cy*), 2.03 – 1.11 (overlapping resonances, 32 H, P*Cy*), 0.98 (s, 3 H, Si*Me*), 0.80 (m, 4 H, P*Cy*), -17.33 (apparent q, 1 H, J = 16 Hz, Rh-*H*). $^{13}C\{^{1}H\}$ NMR (125.8 MHz, benzene-d_6): δ 159.4 (apparent t, J = 23 Hz, C_{arom}), 142.8 (C_{arom}), 142.7 (C_{arom}), 140.0 (C_{arom}), 138.1 (C_{arom}), 132.4 (apparent t, J = 9 Hz, CH_{arom}), 131.9 (CH_{arom}), 131.2 (CH_{arom}), 129.9 (CH_{arom}), 129.6 (CH_{arom}), 127.6 (CH_{arom}), 127.4 (CH_{arom}), 125.6 (CH_{arom}), 124.9 (CH_{arom}), 34.7 (apparent t, J = 11 Hz, CH_{Cy}), 34.0 (apparent t, J = 10 Hz, CH_{Cy}), 31.0 (CH_{2Cy}), 30.8 (CH_{2Cy}), 28.0 (CH_{2Cy}), 27.8 – 27.5 (overlapping resonances, CH_{2Cy}), 26.9 (CH_{2Cy}), 9.8 (Si*Me*). $^{31}P\{^{1}H\}$ NMR (202.5 MHz, benzene-d_6): δ 63.1 (d, 2 P, J_{RhP} = 126 Hz, Cy-*P*Si*P*). ^{29}Si NMR (99.4 MHz, benzene-d_6): δ 41.9. IR (Thin Film, cm^{-1}): 3420 (br, w, N-H), 2045 (m, Ir-H).

[Cy-PSiP]Rh(NH_2-N=C(*p*-ClC_6H_5)$_2$) (3-41). A solution of Me_3SiCH_2Li (0.010 g, 0.11 mmol) in ca. 2 mL of benzene was added to a solution of **2-2** (0.080 g, 0.11 mmol) in ca. 2 mL of benzene. An immediate color change from yellow to red was observed. A solution of 4,4'-dichlorobenzophenone hydrazone (0.029 g, 0.11 mmol) was added to the reaction mixture, and the solution was stirred at room temperature for 30 min. A gradual color change from red to orange was observed. The reaction mixture was evaporated to dryness, and the remaining residue was extracted with ca. 8 mL of benzene. The benzene extract was filtered through Celite and the filtrate was dried under vacuum. The remaining solid residue was triturated with pentane (3 × 5 mL) to afford **3-41** as an orange solid (0.088 g, 83%). ^{1}H NMR (500 MHz, benzene-d_6): δ 8.28 (d, 1 H, J = 7 Hz, H_{arom}), 7.95 (d, 1 H, J = 7 Hz, H_{arom}), 7.88 (d, 2 H, J = 7 Hz, H_{arom}), 7.78 (d, 1 H, J = 7 Hz, H_{arom}), 7.66 (m, 1 H, H_{arom}), 7.46 (m, 2 H, H_{arom}), 7.29 (d, 2 H, J = 8 Hz, H_{arom}), 7.21 – 7.06 (overlapping resonances, 4 H, H_{arom}), 6.97 (d, 2 H, J = 7 Hz, H_{arom}), 3.14 (br m, 2 H, P*Cy*), 2.88 (m, 2 H, P*Cy*), 2.26 – 0.81 (overlapping resonances, 37 H, P*Cy* + Si*Me*, SiMe at 0.99 ppm), 0.83 (m, 4 H, P*Cy*), 0.56 (m, 2 H, P*Cy*). $^{13}C\{^{1}H\}$ NMR (125.8 MHz, benzene-d_6): δ 156.8 (apparent t, J = 20 Hz, C_{arom}), 142.1 (C_{arom}), 13 (C_{arom}), 138.1 (C_{arom}), 132.4 (apparent t, J = 9 Hz, CH_{arom}), 131.9 (CH_{arom}), 131.2 (CH_{arom}), 129.9

(CH$_{arom}$), 129.6 (CH$_{arom}$), 127.6 (CH$_{arom}$), 127.4 (CH$_{arom}$), 125.6 (CH$_{arom}$), 124.9 (CH$_{arom}$), 34.7 (apparent t, J = 11 Hz, CH$_{Cy}$), 34.0 (apparent t, J = 10 Hz, CH$_{Cy}$), 31.0 (CH$_{2Cy}$), 30.8 (CH$_{2Cy}$), 28.0 (CH$_{2Cy}$), 27.8 – 27.5 (overlapping resonances, CH$_{2Cy}$), 26.9 (CH$_{2Cy}$), 9.8 (Si*Me*). ^{31}P{^{1}H} NMR (202.5 MHz, benzene-d_6): δ 47.3 (d, 2 P, J_{RhP} = 113 Hz, Cy-*P*Si*P*). ^{29}Si NMR (99.4 MHz, benzene-d_6): δ 46.2.

3.4.3 Crystallographic Solution and Refinement Details

Crystallographic data for each of **3-2**, **3-8**, **3-11**, **3-22**, **3-24·C$_6$H$_6$**, **3-37**, and **3-38·Et$_2$O** were obtained at 193(±2) K on a Bruker D8/APEX II CCD diffractometer using a graphite-monochromated Mo Kα (λ = 0.71073 Å) radiation, employing a sample that was mounted in inert oil and transferred to a cold gas stream on the diffractometer. Programs for diffractometer operation, data collection, and data reduction (including SAINT) were supplied by Bruker. Gaussian integration (face-indexed) was employed as the absorption correction method in each case. The structure for **3-24·C$_6$H$_6$** was solved by the use of direct methods, while all remaining structures were solved by use of the Patterson search/structure expansion. All structures were refined by use of full-matrix least-squares procedures (on F^2) with R_1 based on $F_o^2 \geq 2\sigma(F_o^2)$ and wR_2 based on $F_o^2 \geq -3\sigma(F_o^2)$. Unless otherwise specified, anisotropic displacement parameters were employed throughout for the non-hydrogen atoms. During the solution and refinement process for **3-11** disorder involving the Ir-*NHAd* group was identified. The nitrogen atom of the disordered Ir-*NHAd* group was refined anisotropically over two positions, where N1A was refined with an occupancy factor of 0.55 and N1B was refined with an occupancy factor of 0.45. The Ir–N1A and Ir–N1B distances were constrained to be equal (within 0.05 Å) during refinement. The carbon atoms of the disordered Ir-*NHAd* group were refined over two positions, where C50A - C59A were refined with an occupancy factor of 0.55, while C50B - C59B were refined with an occupancy factor of 0.45. The following groups of chemically-equivalent atoms were refined with common isotropic displacement parameters: {C50A, C50B}, {C51A, C55A, C56A, C51B, C55B,

C56B}, {C52A, C54A, C57A, C52B, C54B, C57B}, {C53A, C58A, C59A, C53B, C58B, C59B}. The N1A–C50A and N1B–C50B distances were constrained to be equal (within 0.03 Å) during refinement. The C–C bond distances within the two conformers of the disordered 1-adamantyl group were constrained to be equal (within 0.03 Å) to a common refined value. During the structure solution process for **3-24·C_6H_6** an equivalent of benzene was located in the asymmetric unit and refined in a satisfactory manner. During the structure solution process for **3-38·Et_2O** an equivalent of diethyl ether was located in the asymmetric unit and refined in a satisfactory manner. The Ir-*H* in **3-8** was not located in the difference map. Instead, an initial Ir-*H* position similar to that found in related complexes such as **2-7** was selected, and in the subsequent refinement cycles the Ir-H distance was fixed (1.55 Å) and the other parameters (X-Ir-H angles, Ir-*H* thermal parameter) were allowed to vary. The Ir-*H* position in **3-8** following refinement in this manner was similar to that found in **2-7**. The Ir-*H* atoms in **3-2**, **3-11**, **3-22**, and **3-24·C_6H_6** were each located in the difference map and refined isotropically. The N-*H* atoms in **3-22**, **3-24·C_6H_6** and **3-37** were each located in the difference map and refined isotropically. Otherwise, all hydrogen atoms were added at calculated positions and refined by use of a riding model employing isotropic displacement parameters based on the isotropic displacement parameter of the attached atom. Additional crystallographic information is provided in Appendix A.

Chapter 4: Attempts Towards the Insertion of Unsaturated Substrates into [R-PSiP]Ir Amido Hydride Complexes

4.1 Introduction

Transition metal catalyzed amination chemistry of alkenes and alkynes represents a versatile methodology for forming new C-N bonds, ideally through the use of the most abundant source of nitrogen, ammonia. Classic methods to synthesize amines involve either substitution reactions of alkyl halides or reductive amination chemistry where carbonyl groups are converted to amines. Unfortunately, these methods are often unselective and have poor atom economy. Transition metal catalyzed methods for the formation of C-N bonds, therefore, have emerged as a promising methodology for the synthesis of amines. More specifically hydroamination, or the formation of a new C-N bond via addition of an N-H bond across an unsaturated substrate, has recently become a prolific research area.[74] Significant challenges remain associated with this reaction. Notably, the intermolecular hydroamination of unactivated alkenes with simple amines (alkyl, aryl, or ammonia) is rare.[75]

The development of hydroamination processes that operate via N-H bond oxidative addition to a metal center may provide a new pathway for accessing such intermolecular amination reactions. A proposed cycle for the hydroamination of unsaturated substrates via N-H bond activation is shown in Figure 4-1. In addition to challenging N-H bond oxidative addition, the cycle also features an intermolecular transfer of an amido group to an olefin through insertion chemistry. Currently, there are few examples of insertion of unactivated olefins into the M-N bond of isolated amido complexes,[38b,76] which stands in contrast to the breadth of chemistry focused on transfer of alkyl or aryl groups to olefins by insertion mechanisms.[77] A seminal example of this type of chemistry was pubished by Milstein and co-workers on the Ir^{I} catalyzed hydroamination of the activated alkene norbornene with aniline via a catalytic cycle related to that shown in Figure 4-1.[38b] However, this system was limited to the amination

of norbornene with aniline and required the stoichiometric addition of the Lewis acid $ZnCl_2$ to achieve relatively poor turnover numbers (TON) of 2-6.[38b]

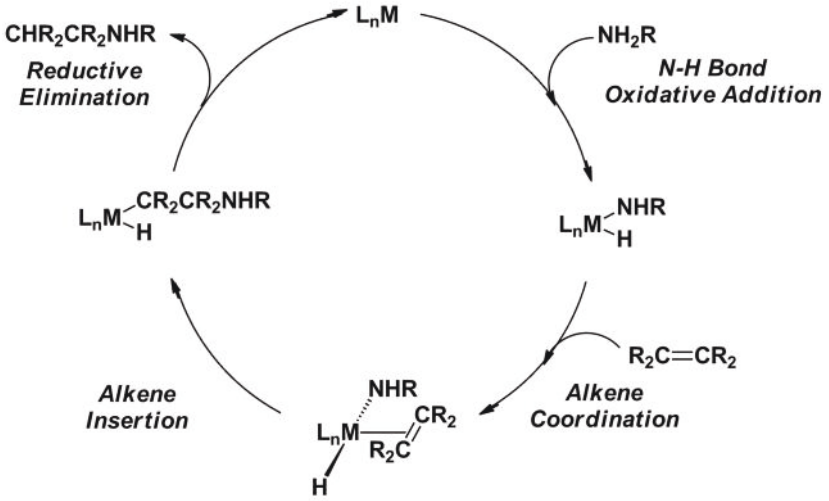

Figure 4-1. Proposed catalytic cycle for the functionalization of amines via N-H bond oxidative addition to L_nM

In more recent examples, the Hartwig group has reported a monomeric rhodium arylamido complex $(PEt_3)_3RhNHAr$ that reacts with excess (15-30 equiv) styrene, 1-hexene or 1-propene to generate products containing new C-N bonds, resulting from insertion of the olefin into the Rh-amide bond. (Scheme 4-2A).[76a] Moreover, ethylene was also observed to insert into the Pd-N bond of isolated Pd amido complexes, with evidence for an intermediate that features ethylene coordinated to the metal center of a Pd amido species (Figure 4-2B).[76b,c] Although the Rh and Pd amido complexes studied by Hartwig and co-workers were not generated by N-H bond oxidative addition, this work establishes precedent for the formation of intermediates that contain both an amido ligand and a coordinated alkene on the pathway to migratory insertion into a metal-amido linkage.

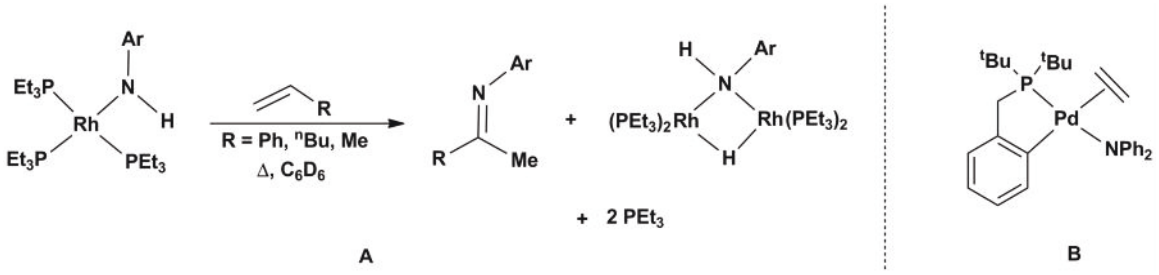

Figure 4 -2. Formation of (**A**) new C-N bonds by insertion of alkenes into a Rh-N bond and (**B**) an ethylene amido intermediate proposed by Hartwig and co-workers[102a,b]

Comparably, the iridium catalyzed intermolecular addition of N-H bonds of anilines, benzamides, and sulfonamides to bicyclic alkenes was recently reported to involve N-H bond oxidative addition steps followed by alkene migratory insertion to form the new C-N bond.[78] Therefore, the incorporation of N-H bond oxidative addition steps into the hydroamination process may provide new pathways for accessing intermolecular amination chemistry. Towards these ends, the work presented in this chapter will detail stoichiometric studies involving the insertion chemistry of complexes of the type [R-PSiP]Ir(H)NHR' (R = Cy, ^{i}Pr; R' = H, alkyl, aryl).

4.2 Results and Discussion

4.2.1 Reactivity of [R-PSiP]Ir(H)(NHR') Complexes with Simple Alkenes and Alkynes

To investigate the insertion chemistry of [R-PSiP]Ir(H)(NHR') (R = Cy, ^{i}Pr; R' = H, alkyl, aryl), the complexes [Cy-PSiP]Ir(H)(NHPh) (**2-6**), [Cy-PSiP]Ir(H)(NH^{t}Bu) (**3-9**), [Cy-PSiP]Ir(H)(NH_2) (**2-10**), and [^{i}Pr-PSiP]Ir(H)NH_2 (**3-7**) were selected as representative products of the N-H bond oxidative addition process described in previous chapters. Correspondingly, reactions of these complexes with unactivated alkenes and alkynes were attempted. Treatment of either **2-6** or **3-9** with 1 or 20 equiv of 1-hexene in benzene-d_6 solution did not result in any reactivity (by ^{1}H and ^{31}P NMR), even after heating of the reaction mixtures for up to 2 days at 70 °C. Similar treatment of a

benzene-d_6 solution of **2-10** or **3-7** with 1-hexene (10-20 equiv) and subsequent heating at 70 ^{o}C appeared to leave **2-10** and **3-7** intact (by ^{1}H and ^{31}P NMR), while also giving rise to new olefinic resonances between 4 and 6 ppm in the ^{1}H NMR spectrum of the reaction mixtures. The appearance of new olefinic resonances likely results from isomerization of the terminal double bond in 1-hexene to an internal position via insertion of the olefin into the Ir-H bond, followed by subsequent β-hydride elimination, which would regenerate **2-10** or **3-7** (Scheme 4-1). This result was somewhat surprising as some computational studies have suggested that it is more favorable for olefins to insert into the M-N bond of a late transition metal amido hydride complex, rather than insert into the M-H bond.[79]

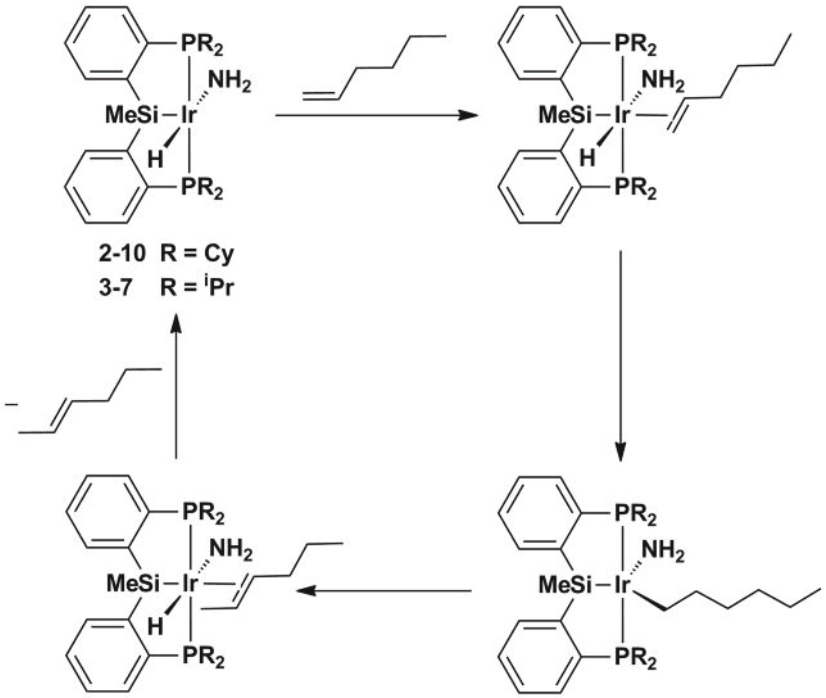

Scheme 4-1. Proposed isomerization of 1-hexene by [R-PSiP]Ir(H)(NH_2)

The insertion of the simplest alkene, ethylene, was also attempted. Reaction mixtures of the appropriate amido hydride complex in benzene-d_6 were degassed via three freeze-pump-thaw cycles and ethylene gas (ca. 1 atm) was added to the reaction

mixture. In all experiments, no initial reaction was observed and subsequent heating (up to 100 ^{o}C) led to no further reaction. Specifically, when **2-10** was treated with excess ethylene in this manner, no reaction was observed upon heating for 3 days at 65 ^{o}C, followed by heating for 4 days at 80 ^{o}C, and subsequent heating for 1 day at 100 ^{o}C. Conversely, since the ethylene coordination product [Cy-PSiP]Ir(C_2H_4) (**2-3**) could be isolated, the hydroamination of **2-3** with ammonia was also attempted. Unfortunately degassing a cyclohexane-d_{12} solution of **2-3** and introduction of 1 atm of anhydrous ammonia did not produce any new product and no reactivity was observed, even after heating for 3 days at 65 ^{o}C, followed by heating for 4 days at 80 ^{o}C. During the course of these experiments Leitner and coworkers published a theoretical study examining the potential of (PCP)Ir and (PSiP)Ir complexes to mediate intermolecular hydroamination of ethylene with ammonia.[80] This work assessed the potential of two types of catalytic cycles where (i) coordination of ethylene to an amido hydride complex followed by insertion into either the Ir-H or Ir-NH_2 bond and subsequent NH_3 coordination allowing for σ-bond metathesis or (ii) initial generation of an Ir-NH_3 adduct followed by N-H bond oxidative addition to form the amido hydride complex which coordinates ethylene, undergoes migratory insertion into Ir-H or Ir-NH_2, resulting in species that undergoes reductive elimination of ethylamine. In the (PSiP)Ir case, it was found that the energetic barriers for the catalytic turnover for the hydroamination of ethylene with ammonia would not be surmountable experimentally in either σ-bond metathesis ($\Delta G^{\ddagger}$ = 26.3 – 54.7 kcal/mol) or oxidative addition/reductive elimination pathways ($\Delta G^{\ddagger}$ = 26.3 – 40.1 kcal/mol). The same barriers in the (PCP)Ir system were also insurmountable experimentally ($\Delta G^{\ddagger}$ = 19.8 – 67.9 kcal/mol).[80]

When 20 equiv of phenylacetylene was added to a benzene-d_6 solution of the aryl amido hydride complex **2-6** or the alkyl amido hydride complex **3-9**, spectroscopic analysis of the reaction mixture revealed the quantitative formation of a new product (**4-1**), as indicated by the appearance of a new ^{31}P NMR resonance at 39.0 ppm. The ^{1}H NMR spectrum of complex **4-1** does not contain a hydride resonance. Comparably, when

the parent amido hydride complex **2-10** was treated with excess (five equiv) of phenylacetylene, an immediate reaction to form **4-1** in 70% yield by ^{31}P NMR spectroscopy. The tentative assignment of **4-1** as a alkyne adduct [Cy-PSiP]Ir(Ph-C≡C-H) (Scheme 4-2), from the elimination of an equivalent of NH_2R (R = H or ^{t}Bu) could not be definitively confirmed. Complex **4-1** was isolated in 72 % yield, and featured a ^{1}H NMR resonance at 5.65 ppm could be due to an acetylene C-*H* (correlating to a ^{13}C NMR resonance at 121.3 ppm in a ^{1}H-^{13}C HSQC experiment) or from an enyne coordinated organometallic product resulting from insertion of a second equivalent of phenylacetylene into an iridium alkynyl bond. Complex **4-1** could not be prepared by generation of [Cy-PSiP]Ir^I (from **2-1** and $TMSCH_2Li$ in cyclohexane solution) and subsequent treatment with phenylacetylene (Scheme 4-2). No immediate reaction was observed upon addition of phenylacetlyene to [Cy-PSiP]Ir^I and heating of the reaction mixture for 14 h at 70 ^{o}C led to an intractable mixture of products (^{31}P NMR). In relation, treatment of **3-7** with 10 equivalents of phenylactylene showed >90% conversion to a new product at 45.8 ppm (^{31}P NMR). As in the case of **4-1**, the identity of **4-2** was not straightforward and although **4-2** could be [^{i}Pr-PSiP]Ir(Ph-C≡C-H) (Scheme 4-2), an iridium enyne product could also be postulated. **4-2** was generated by independent synthesis through generation of [^{i}Pr-PSiP]Ir^I (from **3-2** and $TMSCH_2Li$ in cyclohexane solution) and subsequent treatment with excess phenylacetylene. Complex **4-2** was isolated in 88% yield as a bright orange solid and features a ^{1}H NMR (benzene-d_6) acetylene C-*H* resonance at 5.76 ppm (correlates to a ^{13}C NMR resonance at 121.4 ppm in a ^{1}H-^{13}C HSQC experiment). Further investigation is required to unambiguously assign the structure of **4-1** and **4-2**.

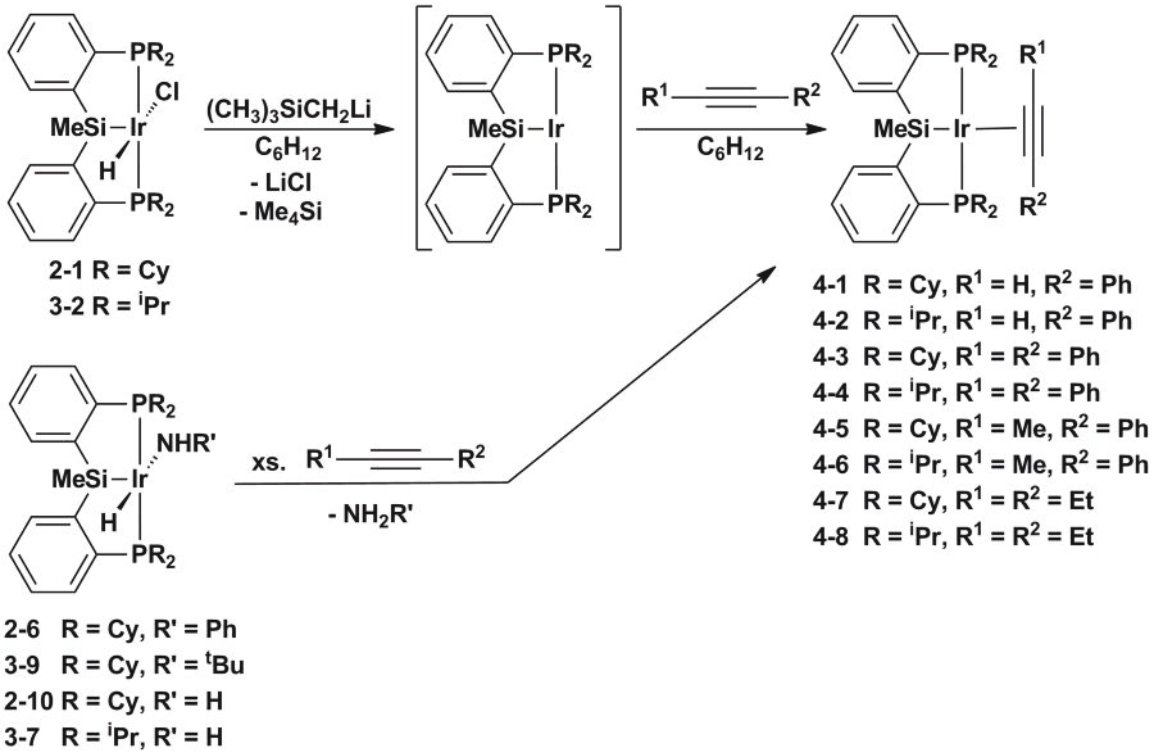

Scheme 4-2. Formation of iridium alkyne adducts [R-PSiP]Ir(R^1-C≡C-R^2) (**4-1** – **4-8)**

Treatment of complexes **2-6**, **3-9**, **2-10** and **3-7** with diphenylacetylene, which led to the formation of the iridium alkyne adducts [R-PSiP]Ir(Ph-C≡C-Ph) (**4-3**, R = Cy; **4-4**, R = ^{i}Pr; Scheme 4-2). Treatment of **2-6** with one equivalent of diphenylacetylene led to no initial reaction at room temperature. Monitoring the reaction by ^{31}P NMR spectroscopy showed that upon heating the reaction mixture for 3 days at 65 ^{o}C, a new product (**4-3**), giving rise to a resonance at 50.4 ppm, began to form. Continued heating at 80 ^{o}C (3 days) led to a 1:1 mixture of **2-6**:**4-3**. ^{1}H NMR analysis of this reaction mixture (benzene-d_6) indicated that **4-3** does not give rise to an Ir-*H* resonance. Similarly, treatment of **3-9** with one equivalent of diphenylacetylene and subsequent heating for 4 days at 65 ^{o}C led to the quantitative (^{31}P NMR) formation of **4-3**. Complex **2-10** did not react with one equivalent of diphenylacetylene upon addition. However, after heating for 4 days at 65 ^{o}C, a 30 % conversion to **4-3** was noted (^{31}P NMR). Continued heating of this reaction mixture at 100 ^{o}C for 2 days did not lead to further

clean conversion to **4-3**, resulting instead in the formation of an intractable mixture of products. Moreover the reaction of **3-7** with 10 equivalents of diphenylacetylene showed 50 % conversion by ^{31}P NMR (benene-d_6) to a new product at 57.0 ppm (**4-4**) with no new hydride appearing in the ^{1}H NMR. Prolonged reaction times (1 week) and elevated temperatures (65 ^{o}C) did not lead to further conversion to **4-4** and decomposition was observed. Both alkyne adducts **4-3** and **4-4** were prepared independently in 95 and 89 % isolated yields, by treating cyclohexane solutions of *in situ* generated [R-PSiP]Ir^{I} with one equivalent of diphenylacetylene (Scheme 4-2). The ^{13}C NMR spectra of **4-3** and **4-4** feature resonances at 143.9 and 143.2 ppm, respectively, for the alkynyl carbon atoms.

The reactivity of 1-phenyl-1-propyne (Ph-C≡C-Me) with complexes **2-6**, **3-9**, **2-10** and **3-7** was also investigated. No reaction was observed upon treatment of these amido hydride complexes with one equivalent of 1-phenyl-1-propyne at room temperature, and subsequent heating for 12 h at 70 ^{o}C led to complex reaction mixtures (by ^{31}P NMR) from which no pure product could be isolated. The synthesis of the alkyne coordination products [R-PSiP]Ir(Ph-C≡C-Me) (R = Cy, **4-5**; R = ^{i}Pr, **4-6**) was attempted in order to determine if **4-5** or **4-6** were generated in the course of these reactions. Treatment of a cyclohexane solution of *in situ* generated [R-PSiP]Ir^{I} with one equivalent of 1-phenyl-1-propyne led to the clean generation of **4-5** and **4-6** (Scheme 4-2), which were isolated as orange powders in 91 and 98% yield. Unlike **4-1** – **4-4,** which each feature one ^{31}P NMR resonance corresponding to the symmetry equivalent phosphino donors of the silyl pincer ligand, **4-5** and **4-6** each gave rise to two doublets centered at 55.8 and 48.6 ppm ($^{2}J_{PPcis}$ = 24 Hz), as well as 63.8 and 56.6 ($^{2}J_{PPcis}$ = 75 Hz) in the ^{31}P NMR spectrum of the isolated complex, consistent with nonequivalent phosphino groups. The ^{1}H NMR spectrum indicates that this complex adopts a C_1-symmetric structure where the Cy-PSiP ligand is bound in a facial manner as the ligand halves are inequivalent. Furthermore the resonance corresponding to the Me group of the coordinated Ph-C≡C-Me correlates to the Cy-PSiP ligand Si in a ^{1}H-^{29}Si HMBC experiment, which suggests the possibility of an interaction of the Me group with the Ir

metal center (Figure 4-3). Having rationally synthesized the 1-phenyl-1-propyne adduct, analysis of the reaction mixtures of the amido hydride complexes with 1-phenyl-1-propyne reveal the presence of either **4-5** or **4-6**. For **2-6**, **3-9**, and **2-10**, after 4 days at 70 ^{o}C about 45, 40, and 50% conversion to **4-5** was noted, whereas 40% conversion to **4-6** was observed for **3-7**.

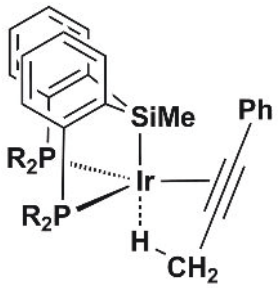

Figure 4-3. Proposed structure of [R-PSiP]Ir(Ph-C≡C-Me) (**4-5**, R = Cy; **4-6**, R = ^{i}Pr)

Lastly, the reactivity of aliphatic alkynes with complexes **2-6**, **3-9**, **2-10** and **3-7** was also investigated. Treatment of these amido hydride species with 1-hexyne resulted in complex reaction mixtures from which no clean products could be isolated. In contrast, treatment of **2-6** and **3-9** with one equivalent of 3-hexyne did not show any reaction, even upon heating (2 days at 70 ^{o}C). However, treatment of the parent amido hydride complex **2-10** with one equivalent of 3-hexyne and subsequent heating at 70 ^{o}C (12 h) gave rise to a new product (**4-7**, 40% conversion by ^{31}P NMR) that features a ^{31}P NMR resonance at 53.3 ppm. Complex **4-7** was also generated upon treatment of [Cy-PSiP]Ir^{I} with 3-hexyne, and is assigned as the corresponding alkyne adduct [Cy-PSiP]Ir(Et-C≡C-Et) (Scheme 4-2). Consistent with this formulation, the ^{1}H NMR spectrum of isolated **4-7** does not feature an Ir-*H* resonance, while the ^{13}C NMR spectrum features a resonance at 161.0 ppm corresponding to the alkyne carbons. Similarly reaction of **3-7** with 10 equivalents of 3-hexyne followed by heating at 70 ^{o}C for 3 days produced the alkyne adduct [^{i}Pr-PSiP]Ir(Et-C≡C-Et) (**4-8**) quantitatively by ^{31}P NMR. Complex **4-8** was alternatively prepared by treatment of in situ generated [^{i}Pr-PSiP]Ir^{I} with 10 equivalents of 3-hexyne and subsequent heating for 14 h at 70 ^{o}C. The ^{1}H NMR

spectrum of **4-8** does not reveal a hydride resonance and the ^{13}C NMR spectrum exhibits a resonance at 161.5 ppm for the alkyne carbons.

4.2.2 Reactivity of [R-PSiP]Ir(H)(NHR') Complexes with Activated Alkenes and Allenes

Due to the lack of alkene and alkyne insertion chemistry noted thus far for complexes **2-6**, **3-9**, **2-10** and **3-7**, the reactivity of activated alkene substrates was investigated with the hope of promoting C-N bond formation processes. In light of the report by Milstein and coworkers of an Ir^I complex that catalyzed the addition of aniline across the olefin of norbornene (nbe) via a pathway involving N-H bond oxidative addition steps,[46b] the reactivity of norbornene was investigated initially. Treatment of **2-6** or **3-9** with one or 20 equivalent of norbornene did not lead to any observed reactivity, even after prolonged heating (7 days at 70 °C) of the reaction mixture. Similar reactions were attempted with the parent amido hydride **2-10** and treatment of a benzene-d_6 solution of **2-10** with 20 equivalents of norbornene led to complete conversion to two new products (**4-9a** and **4-9b**, ^{31}P NMR) upon heating for 2 days at 70 °C. ^{31}P NMR spectroscopy indicated that these two complexes were present in a 3:2 ratio, as indicated by two resonances at 62.7 (**4-9a**) and 61.1 ppm (**4-9b**). No hydride resonance was observed in the ^1H NMR spectrum of the product mixture. Attempts to isolate either product from this reaction mixture were unsuccessful. To confirm the identity of **4-9a** and **4-9b**, a cyclohexane solution of in situ generated [Cy-PSiP]Ir^I was treated with one equivalent of norbornene to form the same 3:2 product ratio (^{31}P NMR) of **4-9a** and **4-9b**. Heating a solution (3 days at 75 ^oC) of **4-9a** and **4-9b** did not result in conversion to either product and attempts to separate the products were not successful. These results suggest that **4-9a** and **4-9b** likely correspond to isomeric versions of an Ir norbornene complex (Scheme 4-3). During the course of these investigations, Shimada and co-workers published the synthesis of [Cy-PSiP]$Ir(H)_4$, and reported that this complex

reacted with three equivalents of norbornene to yield the same mixture of **4-9a** and **4-9b**, which the authors also describe as a mixture of isomers.[15o] The authors were able to obtain a crystal structure of [Cy-PSiP]Ir(nbe), where back bonding from Ir to the coordinated norbornene was noted based on the elongated C-C bond distance of 1.433(4)Å (cf. 1.334(1) Å in free norbornene).[15o]

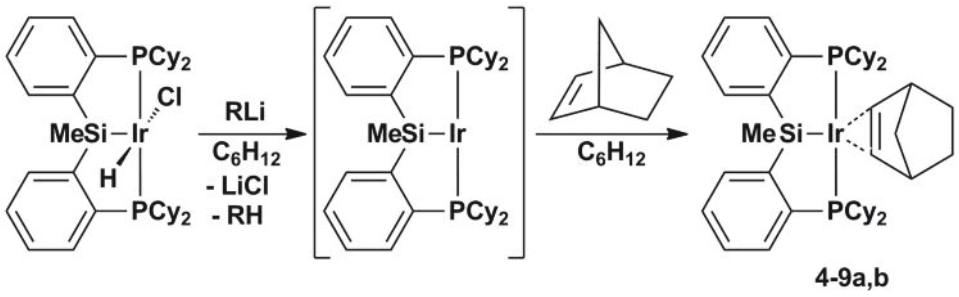

Scheme 4-3. Synthesis of [Cy-PSiP]Ir(nbe) isomers (**4-9a**,**b**)

Styrene, methyl acrylate, and dimethoxyacetylene dicarboxylate were also investigated as substrates in a similar series of reactions with **2-6**, **3-9**, **2-10** and **3-7**. In the case of styrene, an excess (10-20 equivalents) was added to benzene-d_6 solution of the appropriate amido hydride complex and the course of the reactions were monitored by ^{31}P and ^{1}H NMR spectroscopy. No reactivity was observed even after prolonged heating at elevated temperatures (up to 4 days at 65 °C and 2 days at 100 °C).

Treatment of both **2-6** and **3-9** with one equivalent of methyl acrylate showed no initial reactivity and heating of the reaction mixtures for 14 h at 70 °C produced multiple unidentified products. In contrast, treatment of a benzene-d_6 solution of **2-10** with one equivalent of methyl acrylate led to the immediate formation of a new product (**4-10**) featuring a ^{31}P NMR resonance at 43.0 ppm. Attempts to isolate this product led to decomposition, however in situ (benzene-d_6) characterization revealed that **4-10** features olefinic resonances at 7.23 (^{1}H-^{13}C HSQC), 5.38 (br d, 1 H, $^{3}J_{HHtrans}$ = 13 Hz,) and 4.62 (d, 1 H, $^{3}J_{HHcis}$ = 7 Hz), as well as a hydride resonance at -18.63 ppm (t, $^{2}J_{HP}$ = 18 Hz). A resonance at 165.8 ppm in the ^{13}C NMR was observed for the CO group. Based on this

data, **4-10** is proposed to be [CyPSiP]Ir(H)(OC(NH_2)(OMe)CH=CH_2) containing either an O,O or N,O κ^2-ligand (Scheme 4-4). This product would result from an insertion of the C=O group of methyl acrylate into the Ir-N bond.

The related reactions of **2-6**, **3-9**, **2-10** and **3-7** respectively, with one equivalent of dimethoxyacetylene dicarboxylate resulted in intractable mixtures (^{31}P NMR) from which no pure product could be isolated. This is not surprising given the reactive nature of this activated alkyne and the potential for decarbonylation chemistry.

The allene 3-methyl-1,2-butadiene was also reacted with benzene-d_6 solutions of the amido hydride complexes **2-6**, **3-9**, **2-10** and **3-7**. In all cases no initial reactivity was observed and both metal complex and free 3-methyl-1,2-butadiene were observed in the ^{1}H NMR. Unremarkably, heating the reaction mixture at 70 °C for 3 days did not show any change.

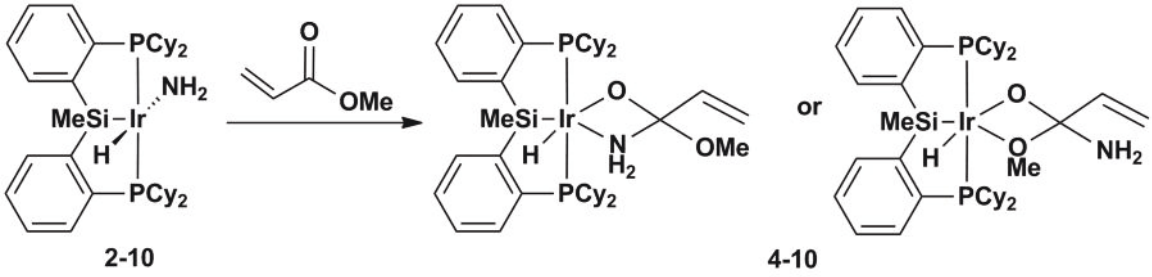

2-10 4-10

Scheme 4-4. Synthesis of [CyPSiP]Ir(H)(OC(NH_2)(OMe)CH=CH_2) (**4-10**)

4.2.3 Reactivity of [Cy-PSiP]Ir(H)(NHR') Complexes with Unsaturated Substrates that Possess Polar C-X (X = O or N) Multiple Bonds

A natural extension of the chemistry described so far includes a study of the reactivity of [Cy-PSiP]Ir amido hydride complexes with substrates containing C=O, C≡O, and C≡N bonds. The reactivity of other late transition metal amido complexes with these types of substrates have been reported in the literature to probe the basicity of the coordinated nitrogen.[81] Insertion into the N-H bond of (Cp*)(PMe_3)(Ph)Ir(NH_2) was observed with isocyanates, carbodiimides, whereas the reactivity of isocyanides lead to

loss of NH_3 and generation of an unusual η^4-tetramethyl fullvene complex.[81e] The reaction of $(DMPE)_2Ru(H)NH_2$ with phenylacetonitrile resulted in deprotonation of phenylacetonitrile and loss of NH_3.[81c] Furthermore, insertion of CO_2 and dimethoxyactylene dicarboxylate into the M-N or M-H bond of the Ni anilide complex $Ni(PMe_3)_2(NHPh)(Mes)$ has been reported.[81h] Perhaps the most extensive example of insertion chemistry with late transition metal amide complexes involved the reactivity of [PCP]Ru(CO)(PMe)(NHPh) with nitriles, carbodiimides, isocyanates and benzaldehyde.[81i] The resulting complexes were formed via coordination followed by insertion of the unsaturated substrate into the Ru-N bond to form κ^2-ligands.[81i] Based on the extent of reactivity possible, probing the chemistry of [R-PSiP]Ir amido hydride complexes with similar polar substrates is part of a complete study of insertion chemistry.

Benzene-d_6 solutions of **2-6**, **3-9**, and **2-10** were degassed via freeze-pump-thaw cycles and an excess of CO (~1 atm) was added to the reaction mixtures. In all cases, analysis of the reaction mixtures by ^{31}P and ^{1}H NMR spectroscopy indicated the formation of multiple hydride-containing products, but prolonged reaction times and temperatures did not lead to the formation of a single isolable species.

Addition of either one or five equivalents of benzaldehyde to a benzene-d_6 solution of **2-6** at room temperature resulted in the formation of two new products that exhibited ^{31}P NMR resonances at 53.6 and 47.9 ppm, respectively. Attempts to drive the reaction to one of these products by heating at 70 °C led to the formation of an intractable mixture of products. Alternatively, when five equivalents of benzaldehyde were added to a benzene-d_6 solution of **3-9**, ^{31}P NMR analysis of the reaction mixture indicated the formation of a single product (**4-11**) featuring a resonance at 53.6 ppm (^{31}P NMR). The ^{1}H NMR spectrum of **4-11** displayed an Ir-*H* resonance at -26.54 ppm (t, $^{2}J_{HP}$ = 16 Hz). Complex **4-11** was isolated in 78% yield and featured a ^{13}C NMR shift at 177.2 ppm as well as a C=O stretch at 1721 cm^{-1} by IR spectroscopy. This complex decomposes in benzene-d_6 solution to unidentified products. Based on this data, complex **4-11** is tentatively proposed to be the acyl hydride complex [Cy-PSiP]Ir(H)C(O)Ph (Scheme 4-

5). Attempts to obtain crystals to unambiguously identify **4-11** have thus far remained ineffective. These types of acyl complexes with open coordination sites on the metal center typically undergo decarbonylation or reductive elimination of the aldehyde.[82] However, there are examples of stable coordinatively unsaturated acyl hydride complexes that have been isolated[83] including a comparable $(Cp^*)(PMe)_3Ir(H)C(O)Ph$ which only underwent decarbonylation during thermolysis.[83e]

Complex **4-11** could result from elimination of $NH_2{}^tBu$ upon coordination of benzaldehyde, followed by Ir-mediated C-H bond cleavage of the aldehydic C-H to yield the observed product (Scheme 4-5). Similarly, the reaction of **2-10** with five equivalents of benzaldehyde also led to the rapid formation of **4-11** (^1H and ^{31}P NMR), likely via loss of NH_3.

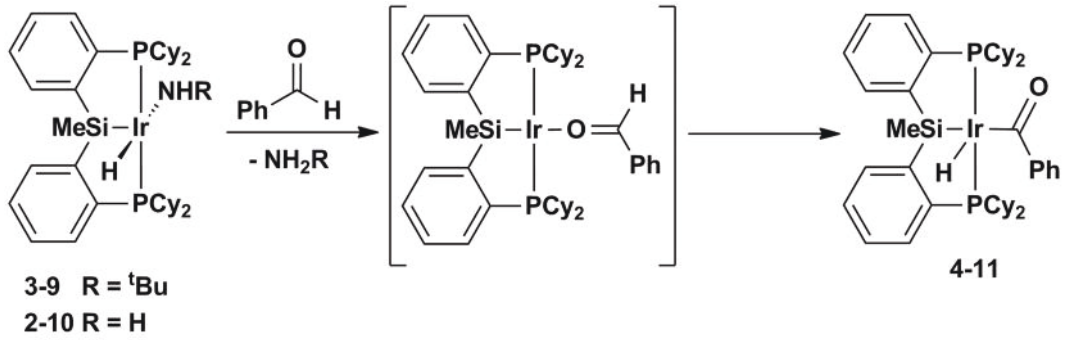

Scheme 4-5. Potential mechanism for formation of [Cy-PSiP]Ir(H)C(O)Ph (**4-11**)

The reaction of **2-6** with one equivalent of xylyl isocyanide at room temperature led to the first observation of clean insertion chemistry into the Ir-N linkage of [Cy-PSiP]Ir(H)(NHR) species. The insertion product [Cy-PSiP]Ir(H)(C(NHPh)(N(2,6-$Me_2C_6H_3$)) (**4-12**) was isolated as an orange solid in 98% yield (Scheme 4-6). The ^{31}P NMR spectrum of **4-12** exhibited a single resonance at 34.9 ppm, consistent with the formation of a C_s-symmetric complex. In addition, the ^1H NMR spectrum (benzene-d_6) of the product featured a hydride resonance at -19.29 (t, $^2J_{HP}$ = 17 Hz), and a singlet at 2.50 ppm that was assigned to the *ortho*-Me substituents of the xylyl fragment. An IR stretch of 1591 cm^{-1} was also found to correspond to the C=N group of the insertion

product. Unfortunately, reacting **3-9** with one or two equivalents of xylyl isocyanide generated multiple products that were not isolated.

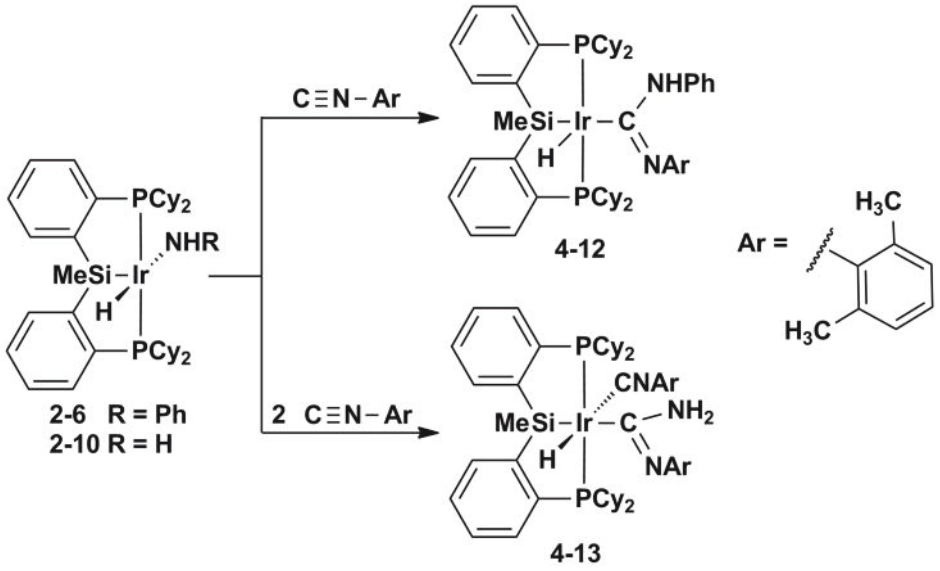

Scheme 4-6. Synthesis of the insertion products [Cy-PSiP]Ir(H)(C(NHPh)(N(2,6-$Me_2C_6H_3$)) (**4-12**) and [Cy-PSiP]Ir(H)(CN(2,6-$Me_2C_6H_3$))(C(NH_2)(N(2,6-$Me_2C_6H_3$)) (**4-13**)

When analogous reactivity was attempted with **2-10**, a different insertion product resulted. Treatment of **2-10** with one equivalent of xylyl isocyanide initially resulted in a 1:1 mixture of two products giving rise to ^{31}P NMR resonances at 41.5 and 40.7 ppm, respectively. Addition of a second equivalent of xylyl isocyanide led to complete conversion to the complex giving rise to the latter resonance (**4-13**), which was obtained as a orange solid in 84% isolated yield (Scheme 4-6). The solid state structure of **4-13** was determined by the use of single crystal X-ray crystallographic techniques (Figure 4-4, Table 4-1) and revealed a six-coordinate complex featuring one equivalent of xylyl isocyanide coordinated to the Ir metal center and a second inserted into the Ir-N bond of the parent amido complex to form a complex of the type [Cy-PSiP]Ir(H)(CN(2,6-$Me_2C_6H_3$))(C(NH_2)(N(2,6-$Me_2C_6H_3$)). The coordinated xylyl isocyanide ligand had a C-N bond distance of 1.167(5) Å, consistent with a C-N triple bond. The inserted xylyl isocyanide group had C-N bond distances of 1.285(5) Å and 1.387(5) Å, for the C=NAr

and C–NH_2 groups, respectively. The ^{13}C NMR spectrum of **4-13** (benzene-d_6) featured a single set of [Cy-PSiP] ligand backbone aromatic resonances, as well as resonances at 171.6 and 68.2 ppm, consistent with the *C*≡N fragment of the xylyl isocyanide ligand coordinated Ir and the N=*C*–NH_2 fragment of the inserted xylyl isocyanide, respectively. Furthermore, the IR spectrum of **4-13** featured bands at 2117 (*C*≡N) and 1590 (C=N). Notably, when two equivalents of xylyl isocyanide were added to **2-6**, coordination of a second equivalent to the Ir center was not observed. The difference in reactivity between **2-6** and **2-10** with xylyl isocyanide may be attributed to steric hindrance involved in coordination of the second equivalent of xylyl isocyanide when the insertion product contains a N-*Ph* rather than N-*H* substituent.

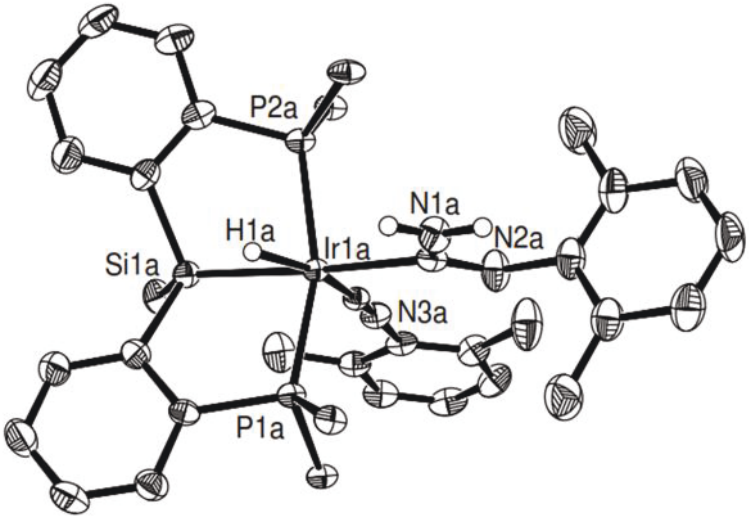

Figure 4-4. The crystallographically determined structure of **4-13**, shown with 50% displacement ellipsoids. With the exception of H1 and N-*H*, some C atoms, all H atoms as well as the Et_2O and solvate have been omitted for clarity.

Table 4-1. Selected interatomic distances (Å) and angles (º) for **4-13·OEt$_2$**

Bond Lengths (Å)			
Ir-P1	2.3414(18)	Ir-C2	2.177(6)
Ir-P2	2.2488(18)	Ir-I0	2.6982(6)
Ir-Si	2.2810(18)		
Bond Angles (°)			
P1-Ir-P2	97.53(6)	Si-Ir-I0	124.29(5)
Si-Ir-C2	89.22(18)		

4.3 Conclusions

The work detailed in this chapter was initiated to investigate the propensity for bis(phosphino)silyl Ir amido hydride complexes [R-PSiP]Ir(H)NHR' (R = Cy, ^{i}Pr; R' = H, alkyl, aryl) to insert unsaturated substrates into Ir-N or Ir-H bonds. This type of reactivity could provide insight into new or improved amination chemistry based on complexes derived from N-H oxidative addition.

Stoichiometric studies involving representative amido hydride complexes [Cy-PSiP]Ir(H)(NHPh) (**2-6**), [Cy-PSiP]Ir(H)(NH^{t}Bu) (**3-9**), [Cy-PSiP]Ir(H)(NH_2) (**2-10**), and [^{i}Pr-PSiP]Ir(H)(NH_2) (**3-7**) began with unactivated alkenes and alkynes. In most instances, insertion chemistry was not observed and instead elimination of the corresponding amine and formation of the Ir^{I} alkene/alkyne adduct resulted. Notably, the reactivity of the parent amido hydride complexes **2-10** and **3-7** with 1-hexene did promote the isomerization of 1-hexene to internal alkenes, which would be a direct consequence of insertion into the Ir-H bond followed by β-hydride elimination.

To circumvent the challenging nature of this type of insertion process more activated unsaturated substrates were targeted for further studies. The strained alkene norbornene did not insert into the Ir-H or Ir-N bonds and instead an isomeric mixture of norbornene coordinated Ir^{I} centers resulted. Moreover, reactions with 3-methyl-1,2-butadiene and dimethoxyacetylene dicarboxylate lead to no reactivity or complex reaction mixtures. However, treatment of **2-10** with methyl acrylate lead to the first

observation of insertion chemistry to form [Cy-PSiP]Ir(H)(NH_2)($CH_2CH(CO)OMe$) (**4-11**), representing a rare instance of C-N bond formation by a complex generated via N-H bond oxidative addition. Unfortunately, this complex undergoes decomposition over time in solution.

The reactivity of polar substrates containing multiple bonds was also probed. Although no products were isolated from reaction mixtures of the amido hydride complexes with CO, the reactivity of **3-9** and **2-10** with excess benzaldehyde resulted in formation of a new product tentatively assigned as [Cy-PSiP]Ir(H)C(O)Ph (**4-11**). The generation of this complex could result from initial amine loss, followed by C-H bond cleavage of the aldehyde. Further reactivity was also observed in the reaction of the strongly coordinating xylyl isocyanide [Cy-PSiP]Ir(H)(NHPh) (**2-6**) and [Cy-PSiP]Ir(H)NH_2 (**2-10**). In both reactions, one equivalent of xylyl isocyanide cleanly inserted into the Ir-N bond, and in the case of **2-6**, the insertion product [Cy-PSiP]Ir(H)(C(NHPh)(N(2,6-$Me_2C_6H_3$)) resulted. Comparatively, the parent amido hydride complex **2-10** coordinated a second equivalent of xylyl isocyanide to cleanly generate [Cy-PSiP]Ir(H)(CN(2,6-$Me_2C_6H_3$))(C(NH_2)(N(2,6-$Me_2C_6H_3$)) (**4-13**). These latter two reactions with xylyl isocyanide represent a rare example of C-N bond formation involving a metal amido fragment derived from N-H bond oxidative addition.

4.4 Experimental Section

4.4.1 General Considerations

All experiments were conducted under nitrogen in an MBraun glovebox or using standard Schlenk techniques. Dry, oxygen-free solvents were used unless otherwise indicated. All non-deuterated solvents were deoxygenated and dried by sparging with nitrogen and subsequent passage through a double-column solvent purification system purchased from MBraun Inc. Tetrahydrofuran and diethyl ether were purified over two activated alumina columns, while benzene, toluene, and pentane were purified over one activated alumina column and one column packed with activated Q-5. All purified

solvents were stored over 4 Å molecular sieves. Benzene-d_6 was degassed via three freeze-pump-thaw cycles and stored over 4 Å molecular sieves. The compounds [Cy-PSiP]Ir(H)Cl,[15b] Me_3SiCH_2Li,[65] and NpLi[67] were prepared according to literature procedures. Anhydrous ammonia and ethylene were purchased from Air Liquide Canada and used as received. All other reagents were purchased from Aldrich and used without further purification. Unless otherwise stated, ^1H, ^{13}C, ^{31}P NMR, ^{15}N, and ^{29}Si characterization data were collected at 300K on a Bruker AV-500 spectrometer operating at 500.1, 125.8, 202.5, 50.7 and 99.4 MHz (respectively) with chemical shifts reported in parts per million downfield of $SiMe_4$ (for ^1H, ^{13}C, and ^{29}Si), $MeNO_2$ (for ^{15}N), or 85% H_3PO_4 in D_2O (for ^{31}P). ^1H and ^{13}C NMR chemical shift assignments are based on data obtained from ^{13}C-DEPTQ, ^1H-^1H COSY, ^1H-^{13}C HSQC, and ^1H-^{13}C HMBC NMR experiments. ^{29}Si NMR assignments are based on ^1H-^{29}Si HMQC and ^1H-^{29}Si HMBC experiments. ^{15}N NMR assignments are based on ^1H-^{15}N HMQC experiments. In some cases, fewer than expected unique ^{13}C NMR resonances were observed, despite prolonged acquisition times. Elemental analyses were performed by Canadian Microanalytical Service Ltd. of Delta, British Columbia, Canada and by Columbia Analytical Services of Tucson, Arizona. Infrared spectra were recorded as Nujol mulls between NaCl plates using a Bruker TENSOR 27 FT-IR spectrometer at a resolution of 4 cm^{-1}. X-ray data collection, solution, and refinement were carried out by Drs. Robert MacDonald and Michael J. Ferguson at the University of Alberta X-ray Crystallography Laboratory, Edmonton, Alberta.

4.4.2 Synthetic Details and Characterization Data

[Cy-PSiP]Ir(Ph-C≡C-H) (4-1). Ten equivalents of phenylacetylene (94.1 µL, 0.088 g, 0. 86 mmol) was added to a solution of **2-6** (0.075 g, 0.086 mmol) in ca. 5 mL of benzene producing an immediate colour change to orange. The volatile components were subsequently removed under vacuum, the remaining residue was triturated with pentane (3 × 5 mL) to afford **4-1** as an orange powder (0.063 g, 83%). ^1H NMR (500

MHz, benzene-d_6): δ 7.98 (d, 2 H, J = 7 Hz, H_{arom}), 7.67 (d, 2 H, J = 7 Hz, H_{arom}), 7.50 (m, 2 H, H_{arom}), 7.38 (m, 2 H, H_{arom}), 7.18 – 7.08 (overlapping resonances, 5 H, H_{arom}), 5.65 (s, 1 H, C≡C-*H*), 3.06 (br t, 1 H, J = 12 Hz, P*Cy*), 2.96 (br m, 2 H, P*Cy*), 2.77 (br m, 1 H, P*Cy*), 2.61 (br m, 2 H, P*Cy*), 2.50 – 2.15 (overlapping resonances, 10 H, P*Cy*), 1.90 (m, 2 H, P*Cy*), 1.75 – 1.00 (overlapping resonances, 24 H, PCy), 0.89 (s, 3 H, Si*Me*), 0.712 (m, 2 H, P*Cy*). $^{13}C\{^1H\}$ NMR (125.8 MHz, benzene-d_6): δ 168.2 (*C*≡C), 156.7 (apparent t, J = 19 Hz, C_{arom}), 153.9 (C_{arom}), 141.1 (apparent t, J = 28 Hz, C_{arom}), 131.3 (apparent t, J = 10 Hz, CH_{arom}), 130.3 (CH_{arom}), 129.5 (CH_{arom}), 129.0 (CH_{arom}), 127.6 (CH_{arom}), 126.1 (CH_{arom}), 124.6 (CH_{arom}), 121.3 (C≡*C*), 38.1 (apparent t, J = 16 Hz, CH_{Cy}), 36.1 (apparent t, J = 15 Hz, *C*HCy), 33.0 (CH_{2Cy}), 30.1 (CH_{2Cy}), 29.0 (CH_{2Cy}), 28.4 – 27.9 (overlapping resonances, CH_{2Cy}), 27.3 (CH_{2Cy}), 27.1 (CH_{2Cy}), 26.7 (CH_{2Cy}) 7.4 (Si*Me*). $^{31}P\{^1H\}$ NMR (202.5 MHz, benzene-d_6): δ 39.0. ^{29}Si NMR (99.4 MHz, benzene-d6): δ 7.3. IR (thin film, cm^{-1}): 2092 (m, C≡C).

[^{i}Pr-PSiP]Ir(Ph-C≡C-H) (4-2). A solution of **3-2** (0.150 g, 0.228 mmol) in ca. 5 mL of cyclohexane was treated with a 5 mL cyclohexane solution of Me_3CCH_2Li (0.0215 g, 0.0228 mmol). Phenylacetylene (125.0 μL, 0.115 g, 1.14 mmol) was added to the reaction mixture, producing an immediate colour change to orange. The volatile components were subsequently removed under vacuum, the residue was extracted with ca. 5 mL of benzene, and the extract was filtered through Celite. The filtrate was dried in vacuo, and the remaining residue was triturated with pentane (3 × 5 mL) to afford **4-2** as an orange powder (0.147 g, 88%). ^1H NMR (500 MHz, benzene-d_6): δ 7.97 (d, 2 H, J = 7 Hz, H_{arom}), 7.55 (d, 2 H, J = 7 Hz, H_{arom}), 7.37 (m, 2 H, H_{arom}), 7.31 (t, 2 H, J = 7 Hz, H_{arom}), 7.19 – 7.06 (overlapping resonances, 5 H, H_{arom}), 5.76 (br m, 1 H, C≡C-*H*), 3.00 (m, 2 H, P^i*Pr*), 2.0 (m, 2 H, P^i*Pr*), 1.63 (m, 6 H, P^i*Pr*), 1.12 (m, 6 H, P^i*Pr*), 1.07 – 0.99 (overlapping resonances, 12 H, P^i*Pr*), 0.98 (s, 3 H, Si*Me*). $^{13}C\{^1H\}$ NMR (125.8 MHz, benzene-d_6): δ 165.7 (*C*≡C), 156.6 (d, J = 19 Hz, C_{arom}), 154.3 (C_{arom}), 141.5 (d, J = 27 Hz, C_{arom}), 131.2 (apparent t, J = 9 Hz, CH_{arom}), 130.5 (CH_{arom}), 129.3 (CH_{arom}), 129.0 (CH_{arom}), 127.5 (CH_{arom}), 126.2 (CH_{arom}), 124.0 (CH_{arom}), 28.0 (apparent t, J = 14 Hz,

*C*H$_{iPr}$), 27.2 (apparent t, *J* = 14 Hz, *C*H$_{iPr}$), 23.3 (*C*H$_{3iPr}$), 20.2 (*C*H$_{3iPr}$), 19.7 (*C*H$_{3iPr}$), 19.0 (*C*H$_{3iPr}$), 7.6 (Si*Me*). ^{31}P{^{1}H} NMR (202.5 MHz, benzene-d_6): δ 45.8. ^{29}Si NMR (99.4 MHz, benzene-d6): δ 7.7.

[Cy-PSiP]Ir(Ph-C≡C-Ph) (4-3). A solution of **2-1** (0.060 g, 0.073 mmol) in ca. 2 mL of cyclohexane was treated with a 2 mL cyclohexane solution of Me_3CCH_2Li (0.0057 g, 0.073 mmol). Diphenylacetylene (0.013 g, 0.073 mmol) was added to the reaction mixture, and the solution was heated at 65 °C for 14 h, yielding a dark orange solution. The volatile components were subsequently removed under vacuum, the residue was extracted with ca. 5 mL of benzene, and the extract was filtered through Celite. The filtrate was dried in vacuo, and the remaining residue was triturated with pentane (3 × 2 mL) to afford **4-3** as an orange powder (0.068 g, 95%). ^{1}H NMR (500 MHz, benzene-d_6): δ 7.83 (d, 2 H, *J* = 7 Hz, *H*$_{arom}$), 7.50 (m, 2 H, *H*$_{arom}$), 7.33 (d, 4 H, *J* = 7 Hz, *H*$_{arom}$), 7.19 (t, 2 H, *J* = 7 Hz, *H*$_{arom}$), 7.11 – 7.04 (overlapping resonances, 4 H, *H*$_{arom}$), 7.00 – 6.91 (overlapping resonances, 4 H, *H*$_{arom}$), 2.66 (m, 2 H, P*Cy*), 2.20 (m, 4 H, P*Cy*), 1.92 (m, 2 H, P*Cy*), 1.76 (m, 2 H, P*Cy*), 1.61 – 1.06 (overlapping resonances, 22 H, PCy), 0.93 – 0.77 (overlapping resonances, 13 H, P*Cy* + Si*Me*; SiMe at 0.87 ppm), 0.62 (m, 2 H, P*Cy*). ^{13}C{^{1}H} NMR (125.8 MHz, benzene-d_6): δ 158.0 (d, *J* = 50 Hz, *C*$_{arom}$), 146.9 (d, *J* = 44 Hz, *C*$_{arom}$), 143.9 (*C*≡*C*), 132.5 – 132.3 (overlapping resonances, *C*H$_{arom}$), 129.4 (*C*H$_{arom}$), 128.9 (*C*H$_{arom}$), 128.7 (*C*H$_{arom}$), 127.5 (*C*H$_{arom}$), 126.2 (*C*H$_{arom}$), 121.1 (*C*≡*C*), 39.6 (*C*H$_{Cy}$), 37.9 (*C*H$_{Cy}$), 31.6 (*C*H$_{2Cy}$), 29.8 (*C*H$_{2Cy}$), 29.6 (*C*H$_{2Cy}$), 28.6 (*C*H$_{2Cy}$), 28.2 (*C*H$_{2Cy}$), 27.6 – 27.1 (overlapping resonances, *C*H$_{2Cy}$), 26.3 (*C*H$_{2Cy}$), 2.9 (Si*Me*). ^{31}P{^{1}H} NMR (202.5 MHz, benzene-d_6): δ 50.4. ^{29}Si NMR (99.4 MHz, benzene-d6): δ 26.0.

[^{i}Pr-PSiP]Ir(Ph-C≡C-Ph) (4-4). A solution of **3-2** (0.060 g, 0.091 mmol) in ca. 2 mL of cyclohexane was treated with a 2 mL cyclohexane solution of Me_3SiCH_2Li (0.0086 g, 0.091 mmol). Diphenylacetylene (0.016 g, 0.091 mmol) was added to the reaction mixture, and the solution was heated at 65 °C for 14 h, yielding an orange solution. The volatile components were subsequently removed under vacuum, the

residue was extracted with ca. 5 mL of benzene, and the extract was filtered through Celite. The filtrate was dried in vacuo, and the remaining residue was triturated with pentane (3 × 2 mL) to afford **4-4** as an orange powder (0.060 g, 82%). ^{1}H NMR (500 MHz, benzene-d_6): δ 7.86 (d, 2 H, J = 7 Hz, H_{arom}), 7.51 (d, 2 H, J = 7 Hz, H_{arom}), 7.34 (d, 4 H, J = 7 Hz, H_{arom}), 7.19 – 6.92 (overlapping resonances, 10 H, H_{arom}), 2.66 (m, 2 H, P^{i}*Pr*), 2.39 (m, 2 H, P^{i}*Pr*), 1.25 (m, 6 H, P^{i}*Pr*), 1.03 (m, 6 H, P^{i}*Pr*), 0.93 – 0.84 (overlapping resonances, 9 H, P^{i}*Pr* + SiMe; SiMe at 0.87), 0.65 (m, 6 H, P^{i}*Pr*). ^{13}C{^{1}H} NMR (125.8 MHz, benzene-d_6): δ 165.6 (d, J = 47 Hz, C_{arom}), 157.9 (d, J = 49 Hz, C_{arom}), 146.1 (apparent d, J = 44 Hz, C_{arom}), 143.2 (*C*≡*C*), 132.5 – 132.3 (overlapping resonances, *C*H$_{arom}$), 129.6 (*C*H$_{arom}$), 128.8 (*C*H$_{arom}$), 128.5 (*C*H$_{arom}$), 127.4 (*C*H$_{arom}$), 126.4 (*C*H$_{arom}$), 29.0 (apparent t, J = 10 Hz, *C*H$_{iPr}$), 27.9 (*C*HCy), 20.6 (*C*H$_{3iPr}$), 19.9 (*C*H$_{3iPr}$), 19.7 (*C*H$_{3iPr}$), 19.2 (*C*H$_{3iPr}$), 2.0 (Si*Me*). ^{31}P{^{1}H} NMR (202.5 MHz, benzene-d_6): δ 57.0. ^{29}Si NMR (99.4 MHz, benzene-d6): δ 27.0.

[Cy-PSiP]Ir(Ph-C≡C-Me) (4-5). A solution of **2-1** (0.050 g, 0.061 mmol) in ca. 2 mL of cyclohexane was treated with a 2 mL cyclohexane solution of Me_3CCH_2Li (0.0048 g, 0.061 mmol). 1-pheynyl-1-propyne (7.6 μL, 0.0071 g, 0.061 mmol) was added to the reaction mixture, producing an immediate colour change to dark orange. The volatile components were subsequently removed under vacuum, the residue was extracted with ca. 5 mL of benzene, and the extract was filtered through Celite. The filtrate was dried in vacuo, and the remaining residue was triturated with pentane (3 × 2 mL) to afford **4-5** as an orange powder (0.051 g, 91%). ^{1}H NMR (500 MHz, benzene-d_6): δ 7.87 (d, 1 H, J = 7 Hz, H_{arom}), 7.74 (d, 1 H, J = 7 Hz H_{arom}), 7.64 (m, 1 H, H_{arom}), 7.47 (m, 1 H, H_{arom}), 7.26 – 7.22 (overlapping resonances, 3 H, H_{arom}), 7.13 – 7.06 (overlapping resonances, 5 H, H_{arom}), 6.98 (m, 1 H, H_{arom}), 2.92 (apparent d, 3 H, J_{HP} = 5 Hz, CH_3) 2.69 (m, 1 H, P*Cy*), 2.59 (m, 1 H, P*Cy*), 2.39 (m, 1H, P*Cy*), 2.16 (m, 3 H, P*Cy*), 2.02 (m, 2 H, P*Cy*), 1.82 – 0.91 (overlapping resonances, 34 H, P*Cy*), 0.80 – 0.75 (overlapping resonances, 4 H, P*Cy* + Si*Me*; SiMe at 0.80 ppm), 0.24 (m, 1H, P*Cy*). ^{13}C{^{1}H} NMR (125.8 MHz, benzene-d_6): δ 162.3 (*C*≡C), 158.2 (d, J = 50 Hz, C_{arom}),

147.4 (d, J = 30 Hz, C_{arom}), 146.2 (d, J = 34 Hz, C_{arom}), 145.0 (C_{arom}), 132.3 (apparent t, J = 23 Hz, CH_{arom}), 129.5 (CH_{arom}), 129.3 (CH_{arom}), 128.9 (CH_{arom}), 128.8 (CH_{arom}), 127.9 (CH_{arom}), 127.5 – 127.4 (overlapping resonances, CH_{arom}), 125.6 (CH_{arom}), 40.2 (apparent d, J = 18 Hz, CH_{Cy}), 39.5 (apparent d, J = 18 Hz, CH_{Cy}), 38.2 (apparent d, J = 29 Hz, CH_{Cy}), 37.6 (apparent d, J = 29 Hz, CH_{Cy}), 33.3 (CH_{2Cy}), 30.2 (CH_{2Cy}), 29.8 (CH_{2Cy}), 29.1 (CH_{2Cy}), 28.7 – 28.5 (overlapping resonances, CH_{2Cy}), 28.0 (CH_{2Cy}), 27.6 – 27.3 (overlapping resonance, CH_{2Cy}), 26.9 (CH_{2Cy}), 26.5 (CH_{2Cy}), 20.4 (CH_3), 3.2 (Si*Me*). $^{31}P\{^1H\}$ NMR (202.5 MHz, benzene-d_6): δ 55.8 (d, $^2J_{PPcis}$ = 24 Hz), 48.6 (d, $^2J_{PPcis}$ = 24 Hz). ^{29}Si NMR (99.4 MHz, benzene-d_6): δ 26.9.

[^{i}Pr-PSiP]Ir(Ph-C≡C-Me) (4-6). A solution of **2-1** (0.045 g, 0.068 mmol) in ca. 2 mL of cyclohexane was treated with a 2 mL cyclohexane solution of Me_3SiCH_2Li (0.0064 g, 0.068 mmol). 1-pheynyl-1-propyne (8.6 µL, 0.0079 g, 0.068 mmol) was added to the reaction mixture, producing an immediate colour change to dark orange. The volatile components were subsequently removed under vacuum, the residue was extracted with ca. 5 mL of benzene, and the extract was filtered through Celite. The filtrate was dried in vacuo, and the remaining residue was triturated with pentane (3 × 2 mL) to afford **4-6** as an orange powder (0.050 g, 98%). ^1H NMR (500 MHz, benzene-d_6): δ 7.88 (d, 1 H, J = 7 Hz, H_{arom}), 7.75 (d, 1 H, J = 7 Hz H_{arom}), 7.52 (m, 1 H, H_{arom}), 7.30 – 6.95 (overlapping resonances, 10 H, H_{arom}), 2.77 (apparent d, 3 H, J_{HP} = 5 Hz, CH_3) 2.69 (m, 2 H, P^i*Pr*), 2.37 (m, 1 H, P^i*Pr*), 2.20 (m, 1H, P^i*Pr*), 1.28 – 1.16 (overlapping resonances, 9 H, P^i*Pr*), 1.00 – 0.83 (overlapping resonances, 12 H, P^i*Pr*), 0.76 (s, 3 H, Si*Me*), 0.21 (dd, 3 H, $^3J_{HP}$ = 15 Hz, $^3J_{HH}$ = 7 Hz). $^{13}C\{^1H\}$ NMR (125.8 MHz, benzene-d_6): δ 162.5 (apparent d, J = 55 Hz, *C*≡*C*), 160.1 (apparent d, J = 45 Hz, *C*≡*C*), 158.0 (d, J = 53 Hz, C_{arom}), 146.9 (d, J = 34 Hz, C_{arom}), 145.7 (apparent d, J = 43 Hz, C_{arom}), 144.6 (C_{arom}), 132.3 (apparent t, J = 20 Hz, CH_{arom}), 129.7 (CH_{arom}), 129.4 (CH_{arom}), 129.0 (CH_{arom}), 128.0 (CH_{arom}), 127.6 – 127.4 (overlapping resonances, CH_{arom}), 125.7 (CH_{arom}), 30.1 (d, J = 20 Hz, CH_{iPr}), 28.5 – 28.0 (overlapping resonances, CH_{iPr}), 27.5 (d, J = 28 Hz, CH_{Cy}), 22.8 (CH_{3iPr}), 20.8 – 17.8 (overlapping resonances,

CH_{3iPr} + $CH_{3C\equiv C\text{-}Me}$), 3.3 (Si*Me*). $^{31}P\{^1H\}$ NMR (202.5 MHz, benzene-d_6): δ 63.8 (d, $^2J_{PPcis}$ = 75 Hz), 56.6 (d, $^2J_{PPcis}$ = 75 Hz). ^{29}Si NMR (99.4 MHz, benzene-d_6): δ 28.2.

[Cy-PSiP]Ir(Et-C≡C-Et) (4-7). A solution of **2-1** (0.045 g, 0.055 mmol) in ca. 2 mL of cyclohexane was treated with a 2 mL cyclohexane solution of Me_3SiCH_2Li (0.0052 g, 0.055 mmol). 3-hexyne (6.2 µL, 0.0045 g, 0.055 mmol) was added to the reaction mixture, and the solution was heated at 65 °C for 14 h, yielding a dark orange solution. The volatile components were subsequently removed under vacuum, the residue was extracted with ca. 5 mL of benzene, and the extract was filtered through Celite. The filtrate was dried in vacuo, and the remaining residue was triturated with pentane (3 × 2 mL) to afford **4-7** as an orange powder (0.043 g, 90%). ^1H NMR (500 MHz, benzene-d_6): δ 7.78 (d, 2 H, J = 7 Hz, H_{arom}), 7.55 (d, 2 H, J = 7 Hz, H_{arom}), 7.15 (m, 2 H, H_{arom}), 7.08 (t, 2 H, J = 7 Hz, H_{arom}), 3.53 (br m, 2 H, $CH_{2hexyne}$), 3.20 (m, 2 H, $CH_{2hexyne}$), 2.62 (m, 2 H, P*Cy*), 2.14 – 2.04 (overlapping resonances, 6 H, P*Cy*), 1.79 – 1.10 (overlapping resonances, 40 H, P*Cy* + $CH_{3hexyne}$; $CH_{3hexyne}$ at 1.24 ppm), 0.93 (m, 2 H, P*Cy*), 0.76 (s, 3 H, Si*Me*). $^{13}C\{^1H\}$ NMR (125.8 MHz, benzene-d_6): δ 161.0 (*C*≡*C*), 157.7 (d, J = 49 Hz, C_{arom}), 146.0 (d, J = 42 Hz, C_{arom}), 131.7 (CH_{arom}), 128.7 (CH_{arom}), 128.3 (CH_{arom}), 126.7 (CH_{arom}), 39.2 (CH_{Cy}), 37.2 (CH_{Cy}), 30.9 (CH_{2Cy}), 29.4 (CH_{2Cy}), 29.6 (CH_{2Cy}), 27.6 ($CH_{2hexyne}$), 27.4 – 26.3 (overlapping resonances, CH_{2Cy}), 14.4 ($CH_{3hexyne}$), 3.2 (Si*Me*). $^{31}P\{^1H\}$ NMR (202.5 MHz, benzene-d_6): δ 52.5. ^{29}Si NMR (99.4 MHz, benzene-d6): δ 26.8.

[^{i}Pr-PSiP]Ir(Et-C≡C-Et) (4-8). A solution of **3-2** (0.045 g, 0.068 mmol) in ca. 2 mL of cyclohexane was treated with a 2 mL cyclohexane solution of Me_3SiCH_2Li (0.0064 g, 0.068 mmol). 3-hexyne (7.8 µL, 0.0056 g, 0.068 mmol) was added to the reaction mixture, and the solution was heated at 65 °C for 14 h, yielding an orange solution. The volatile components were subsequently removed under vacuum, the residue was extracted with ca. 5 mL of benzene, and the extract was filtered through Celite. The filtrate was dried in vacuo, and the remaining residue was triturated with pentane (3 × 2 mL) to afford **4-8** as an orange powder (0.046 g, 98%). ^1H NMR (500

MHz, benzene-d_6): δ 7.79 (d, 2 H, J = 7 Hz, H_{arom}), 7.41 (m, 2 H, H_{arom}), 7.14 (m, 2 H, H_{arom}), 7.05 (t, 2H, J = 7 Hz, H_{arom}), 3.39 (m, 2 H, C$H_{2hexyne}$), 3.16 (m, 2 H, C$H_{2hexyne}$), 2.68 (m, 2 H, P^i*Pr*), 2.35 (m, 2 H, P^i*Pr*), 1.22 (t, 6 H, J = 7 Hz, C$H_{3hexyne}$), 1.12 (m, 12 H, P^i*Pr*), 1.00 (m, 6 H, P^i*Pr*), 0.78 (s, 3 H, Si*Me*), 0.74 (m, 6 H, P^i*Pr*). ^{13}C{^{1}H} NMR (125.8 MHz, benzene-d_6): δ 161.5 (*C*≡*C*), 158.5 (d, J = 53 Hz, C_{arom}), 150.9 (C_{arom}), 132.2 apparent t, J = 42 Hz, *C*H$_{arom}$), 129.5 (*C*H$_{arom}$), 128.8 (*C*H$_{arom}$), 127.2 (*C*H$_{arom}$), 29.1 (apparent t, J = 35 Hz, *C*H$_{iPr}$), 27.8 (*C*H$_{2hexyne}$), 20.8 (*C*H$_{3iPr}$), 20.3 (*C*H$_{3iPr}$), 19.6 (*C*H$_{3iPr}$), 18.9 (*C*H$_{3iPr}$), 14.7 (*C*H$_{3hexyne}$) 4.0 (Si*Me*). ^{31}P{^{1}H} NMR (202.5 MHz, benzene-d_6): δ 61.2. ^{29}Si NMR (99.4 MHz, benzene-d6): δ 29.2.

[Cy-PSiP]Ir(nbe) (4-9). A solution of **2-1** (0.089 g, 0.11 mmol) in ca. 4 mL of cyclohexane was treated with a 4 mL cyclohexane solution of Me_3CCH_2Li (0.010 g, 0.11 mmol). Norbornene (0.010 g, 0.11 mmol) was added to the reaction mixture, and the solution was left at room temperature for 14 h, yielding a dark orange solution. The volatile components were subsequently removed under vacuum, the residue was extracted with ca. 8 mL of benzene, and the extract was filtered through Celite. The filtrate was dried in vacuo, and the remaining residue was triturated with pentane (3 × 5 mL) to afford a 3:2 mixture (^{31}P NMR) of **4-9a** and **4-9b** as an orange powder (0.064 g, 68%). ^{1}H NMR (500 MHz, benzene-d_6): δ 8.24 (d, 2 H, J = 7 Hz, H_{arom} in **4-9a**), 7.61 – 7.58 (overlapping resonances, 4 H, H_{arom} in **4-9b**), 7.49 (d, 2 H, J = 7 Hz, H_{arom} in **4-9a**), 7.31 (t, 2 H, J = 7 Hz, H_{arom} in **4-9a**), 7.17 (t, 2 H, J = 7 Hz, H_{arom} in **4-9a**), 7.08 (m, 4 H, $_{arom}$ in **4-9b**), 3.62 (br s, 1 H, CH_{nbe} in **4-9a**), 3.36 (br m, 2 H, CH_{nbe} in **4-9a** + **4-9b**), 3.14 (br s, CH_{nbe}, in **4-9a** + **4-9b**), 2.91 (m, 3 H, PCy in **4-9a** + **4-9b**), 2.73 (m, 3 H, PCy in **4-9a** + **4-9b**), 2.20 – 1.10 (82 H, PCy + nbe in **4-9a** + **4-9b**), 0.76 (s, 3 H in **4-9a**, Si*Me*), 0.35 (s, 3 H in **4-9b**, Si*Me*), - 0.48 (d, 1H, J = 9 Hz, CH_{nbe} in **4-9b**). ^{13}C{^{1}H} NMR (125.8 MHz, benzene-d_6): δ 159.9 (apparent t, J = 29 Hz, C_{arom}), 155.0 (d, J = 51 Hz, C_{arom}), 145.8 (apparent t, J = 24 Hz, C_{arom}), 132.8 (apparent t, J = 11 Hz, *C*H$_{arom}$), 131.4 (d, J = 21 Hz, *C*H$_{arom}$), 129.9 (*C*H$_{arom}$), 129.2 (*C*H$_{arom}$), 129.0 (*C*H$_{arom}$), 128.7 (*C*H$_{arom}$), 127.7 (*C*H$_{arom}$), 127.1 (*C*H$_{arom}$), 55.3 (*C*H$_{nbe}$), 51.6 (*C*H$_{nbe}$), 47.4 (*C*H$_{nbe}$), 44.0 (d, J = 28

Hz, CH_{Cy}), 43.2 (CH_{2nbe}), 41.7 – 41.3 (overlapping resonances, CH_{Cy} + CH_{nbe}), 38.5 (CH_{Cy}), 37.1 (CH_{2Cy}), 36.8 (CH_{2Cy}), 36.0 (CH_{Cy}), 34.8 (CH_{2Cy}), 32.8 (CH_{2Cy}), 31.5 (CH_{2Cy}), 30.4 – 27.0 (overlapping resonances, CH_{2Cy} + CH_{2nbe}), 23.1 (CH_{2Cy}) 5.4 (Si*Me* in **4-9a**), - 2.4 (Si*Me* in **4-9b**). $^{31}P\{^1H\}$ NMR (202.5 MHz, benzene-d_6): δ 62.7 (s, **4-9a**), 61.0 (br s, **4-9b**). ^{29}Si NMR (99.4 MHz, benzene-d6): δ 62.7 (**4-9a**), 5.1 (**4-9b**).

[CyPSiP]Ir(H)(OC(NH$_2$)(OMe)CH=CH$_2$) (4-10). A solution of **2-10** (0.015 g, 0.019 mmol) in ca. 0.4 mL of benzene-d_6 was treated with a 0.4 mL benzene-d_6 solution of Me_3CCH_2Li (0.0015 g, 0.019 mmol). One equivalent of methyl acrylate was (1.7 μL, 0.0016 g, 0.019 mmol) was added to the reaction mixture, at which point ^1H and ^{31}P NMR analysis of the reaction mixture indicated the quantitative formation of **4-10**. Attempts to isolate **4-10** upon exposure to vacuum lead to multiple products and **4-10** was characterized in situ. ^1H NMR (500 MHz, benzene-d_6): δ 8.14 (d, 2 H, J = 7 Hz, H_{arom}), 7.56 (m, 2 H, H_{arom}), 7.25 (m, 3 H, H_{arom} + $HC{=}CH_2$), 7.18 – 7.08 (overlapping resonances, 4 H, H_{arom} + NH_2), 5.38 (br d, 1 H, $^3J_{HHtrans}$ = 13 Hz, HC=CH_2), 4.62 (d, 1 H, $^3J_{HHcis}$ = 7 Hz, HC=CH_2), 3.68 (s, 3 H, CO_2Me), 2.61 (br t, 2 H, J = 11 Hz, P*Cy*), 2.44 (br t, 2 H, J = 12 Hz, P*Cy*), 2.02 – 20.79 (overlapping resonances, 40 H, P*Cy*), 0.45 (s, 3 H, Si*Me*), -18.63 (t, 1 H, $^2J_{HP}$ = 18 Hz, Ir-*H*). $^{13}C\{^1H\}$ NMR (125.8 MHz, benzene-d_6): δ 165.8 (*C*-O), 160.6 ($CH_{C=C}$), 159.2 (apparent t, J = 21 Hz, C_{arom}), 145.0 (apparent t, J = 26 Hz, C_{arom}), 132.7 (t, J = 9 Hz, CH_{arom}), 129.9 (CH_{arom}), 129.3 (CH_{arom}), 127.7 (d, J = 23 Hz, CH_{arom}), 77.5 ($CH_{2C=C}$), 50.3 (CH_{3OMe}), 37.2 (apparent t, J = 10 Hz, CH_{Cy}), 36.1 (apparent t, J = 13 Hz, CH_{Cy}), 29.7 (CH_{2Cy}), 29.1 – 27.0 (overlapping resonances, CH_{2Cy}), 2.5 (Si*Me*). $^{31}P\{^1H\}$ NMR (202.5 MHz, benzene-d_6): δ 43.0. ^{29}Si NMR (99.4 MHz, benzene-d6): δ 12.8.

[Cy-PSiP]Ir(H)C(O)Ph (4-11). A solution of **3-9** (0.015 g, 0.018 mmol) in ca. 0.8 mL of benzene was treated with five equivalents of benzaldehyde (8.9 μL, 0.0093 g, 0.88 mmol) was added to the reaction mixture, producing an immediate colour change to yellow. The volatile components were subsequently removed under vacuum, the residue was triturated with pentane (3 × 2 mL) to afford **4-11** as an yellow film (0.015 g, 94%).

Rapid decomposition in benzene-d_6 solution prevented the comprehensive assignment of ^{1}H and ^{13}C NMR resonances for this complex. ^{1}H NMR (500 MHz, benzene-d_6): δ 8.45 (d, 2 H, J = 7 Hz, H_{arom}), 7.45 (m, 2 H, H_{arom}), 7.25 (t, 2 H, J = 7 Hz, H_{arom}), 7.26 – 7.01 (overlapping resonances, 7 H, H_{arom}), 2.56 – 0.84 (overlapping resonances, 47 H, P*Cy* + Si*Me*). ^{13}C{^{1}H} NMR (125.8 MHz, benzene-d_6): δ 177.2 (C=O), 159.2 (C_{arom}), 137.1 (C_{arom}), 130.6 (CH_{arom}), 129.5 (CH_{arom}), 128.7 (CH_{arom}), 35.6 (CH_{Cy}), 34.4 (CH_{Cy}), 30.8 – 2683 (overlapping resonances, CH_{2Cy}). IR (thin film, cm^{-1}): 2225 (m, Ir-H), 1721 (s, C=O).

[Cy-PSiP]Ir(H)(C(NHPh)(N(2,6-Me$_2$C$_6$H$_3$)) (4-12). A solution of 2,6-xylylisocyanide (0.012g, 0.091 mmol) in ca. 5 mL of C_6H_6 was added dropwise via pipette to a solution of **2-6** (0.080 g, 0.091 mmol) in ca. 5 mL of C_6H_6 at room temperature leading to a color change from red to orange. The reaction mixture was evaporated to dryness under vacuum. The remaining solid residue was triturated with pentane (3 × 5 mL) to afford **4-7** as an orange solid (0.091 g, 98%). ^{1}H NMR (250 MHz, benzene-d_6): δ 8.45 (d, 2 H, J = 7 Hz, H_{arom}), 8.12 (d, 2 H, J = 7 Hz, H_{arom}), 7.45 (m, 3 H, H_{arom}), 7.17 – 7.15 (overlapping resonances, 3 H, H_{arom}), 6.76 – 6.69 (overlapping resonances, 4 H, H_{arom}), 6.57 (d, 1 H, J = 7 Hz, H_{arom}), 6.43 (t, 1 H, J = 7 Hz, H_{arom}), 2.69 (m, 2 H, P*Cy*), 2.55 – 2.44 (overlapping resonances, 8 H, P*Cy* + NAr*Me*$_2$; a singlet at 2.50 ppm was assigned as NAr*Me* resonances on the basis of ^{1}H-^{13}C HMBC experiment), 2.25 (m, 2 H, P*Cy*), 2.11 – 2.05 (overlapping resonances, 5 H, P*Cy*), 1.73 – 1.39 (overlapping resonances, 20 H, P*Cy*), 1.25 – 1.04 (overlapping resonances, 16 H, P*Cy*), 0.76 (s, 3 H, Si*Me*), -19.29 (t, 1 H, $^2J_{HP}$ = 17 Hz, Ir*H*). ^{13}C{^{1}H} NMR (125.8 MHz, benzene-d_6): δ 161.3 (C_{arom}), 159.6 (apparent t, J = 21 Hz, C_{arom}), 153.8 (C_{arom}), 144.6 (apparent t, J = 28 Hz, C_{arom}), 135.7 (C_{arom}), 135.1 (C_{arom}), 133.5 (apparent t, J = 9 Hz, CH_{arom}), 129.9 – 129.7 (overlapping resonances, CH_{arom}), 129.2 (CH_{arom}), 128.8 (CH_{arom}), 127.8 (CH_{arom}), 108.2 (CH_{arom}), 38.1 (apparent t, J = 13 Hz, CH_{Cy}), 37.5 (apparent t, J = 14 Hz, CH_{Cy}), 29.9 (CH_{2Cy}), 29.6 (CH_{2Cy}), 28.8 (CH_{2Cy}), 28.3 (CH_{2Cy}), 28.1 (CH_{2Cy}), 27.9 (CH_{2Cy}), 27.6 – 27.5 (overlapping resonances, CH_{2Cy}), 27.1 (CH_{2Cy}), 20.0 (NAr*Me*), 19.7

(NAr*Me*), 4.1 (Si*Me*). $^{31}P\{^{1}H\}$ NMR (202.5 MHz, benzene-d_6): δ 34.9. ^{29}Si NMR (99.4 MHz, benzene-d_6): δ 39.9. IR (thin film, cm^{-1}): 3380 (br, w, N-H), 2097 (m, Ir-H), 1591 (s, N=C).

[Cy-PSiP]Ir(H)(CN(2,6-$Me_2C_6H_3$))(C(NH_2)(N(2,6-$Me_2C_6H_3$)) **(4-13).** A solution of 2,6-xylylisocyanide (0.013g, 0.10 mmol) in ca. 4 mL of C_6H_6 was added dropwise via pipette to a solution of [Cy-PSiP]Ir(H)NH_2 (0.040 g, 0.050 mmol) in ca. 4 mL of C_6H_6 at room temperature. No colour change was observed. The reaction mixture was evaporated to dryness under vacuum. The remaining solid residue was triturated with pentane (3 × 5 mL) to afford **4-8** as an orange solid (0.045 g, 84%). ^{1}H NMR (500 MHz, benzene-d_6): δ 8.27 (d, 2 H, J = 7 Hz, H_{arom}), 7.68 (m, 2 H, H_{arom}), 7.32 – 7.28 (overlapping resonances, 3 H, H_{arom}), 7.18 (m, 2 H, H_{arom}), 7.02 (m, 1 H, H_{arom}), 6.74 – 6.70 (overlapping resonances, 4 H, H_{arom} + NH_2), 6.58 (d, 2 H, J = 7 Hz, H_{arom}), 3.15 (m, 2 H, P*Cy*), 2.87 (m, 3 H, P*Cy*), 2.63 (s, 6 H, NArMe_2), 2.58 – 2.31 (overlapping resonances, 8 H, P*Cy*), 2.06 (s, 6 H, NArMe_2), 1.82 (m, 3 H, P*Cy*), 1.80 – 1.00 (overlapping resonances, 26 H, P*Cy*), 0.98 (s, 3 H, Si*Me*), 0.57 (m, 2 H, P*Cy*), -13.09 (t, 1 H, $^{2}J_{HP}$ = 19 Hz, Ir*H*). $^{13}C\{^{1}H\}$ NMR (125.8 MHz, benzene-d_6): δ 171.6 (N=*C*-N), 163.6 (C_{arom}), 161.1 (apparent t, J = 20 Hz, C_{arom}), 153.5 (C_{arom}), 147.4 (apparent t, J = 29 Hz, C_{arom}), 135.6 (C_{arom}), 133.4 (apparent t, J = 11 Hz, CH_{arom}), 130.1 (CH_{arom}), 129.6 (CH_{arom}), 128.7 (CH_{arom}), 128.0 (CH_{arom}), 127.7 (CH_{arom}), 120.6 (CH_{arom}), 68.2 (*C*≡NAr), 38.8 (apparent t, J = 14 Hz, CH_{Cy}), 38.2 (apparent t, J = 15 Hz, CH_{Cy}), 29.6 (CH_{2Cy}), 29.3 (CH_{2Cy}), 28.9 (CH_{2Cy}), 28.2 (CH_{2Cy}), 27.6 – 26.7 (overlapping resonances, CH_{2Cy}), 26.4 (CH_{2Cy}), 21.5 (NAr*Me*), 19.0 (NArMe), 9.3 (Si*Me*). $^{31}P\{^{1}H\}$ NMR (300K, 202.5 MHz, benzene-d_6): δ 40.7. ^{29}Si NMR (99.4 MHz, benzene-d_6): δ 33.7. IR (Nujol, cm^{-1}): 3452 (br, w, N-H), 3234 (br, w, N-H), 2280 (m, Ir-H), 2117 (s, C≡N), 1590 (s, C=N). X-Ray quality crystals of **4-13** were grown from a concentrated Et_2O/THF solution at -30 °C.

4.4.3 Crystallographic Solution and Refinement Details

Crystallographic data for **4-13·Et$_2$O** were obtained at 173(±2) K on a Bruker D8/APEX II CCD diffractometer using a graphite-monochromated Mo Kα (λ = 0.71073 Å) radiation, employing a sample that was mounted in inert oil and transferred to a cold gas stream on the diffractometer. Programs for diffractometer operation, data collection, and data reduction (including SAINT) were supplied by Bruker. Gaussian integration (face-indexed) was employed as the absorption correction method. The structure was solved by use of direct methods and was refined by use of full-matrix least-squares procedures (on F^2) with R_1 based on $F_o^2 \geq 2\sigma(F_o^2)$ and wR_2 based on $F_o^2 \geq -3\sigma(F_o^2)$. Unless otherwise specified, anisotropic displacement parameters were employed for the non-hydrogen atoms. During the structure solution process two crystallographically independent molecules of [Cy-PSiP]Ir(H)(CN(2,6-Me$_2$C$_6$H$_3$))(C(NH$_2$)(N(2,6-Me$_2$C$_6$H$_3$)) (A and B) along with two equivalents of diethyl ether were located in the asymmetric unit; for convenience, only molecule A is discussed in the text. One ether molecule refined satisfactorily, while a second was disordered. The corresponding oxygen and carbon atoms of the disordered ether molecule were modeled over two positions (O2S, O3S, C5S - C12S) and were refined with an occupancy of 0.50 and a common isotropic displacement parameter. The C–C and C–O distances within the disordered solvent diethyl ether molecules were restrained to be 1.530(5) and 1.430(5) Å, respectively. The Ir-*H* was located in the difference map and the Ir-H distance was fixed at 1.55 Å during refinement. Otherwise, all hydrogen atoms were added at calculated positions and refined by use of a riding model employing isotropic displacement parameters based on the isotropic displacement parameter of the attached atom. Additional crystallographic information is provided in Appendix A.

Chapter 5: The Synthesis and Reactivity of Cationic [R-PSiP]Ir^{III} Complexes

5.1 Introduction

As discussed previously in this document, Ir pincer complexes have proven highly effective in a variety of bond activation processes, most notably C-H bond oxidative addition chemistry, which has led to their use in catalytic alkane and alkyl group dehydrogenation reactions. The catalytically relevant species is typically a neutral, three coordinate Ir^{I} fragment that can readily undergo oxidative addition reactions to generate Ir^{III} products. In the search for new reactivity mediated by Ir pincer complexes, while variation of the ligand framework has received significant attention, much less emphasis has been placed on modifying the electrophilicity of the Ir center by generating cationic Ir^{III} pincer complexes.

Pioneering work by Bergman with the cationic Ir^{III} system $[Cp^*(PMe_3)Ir(R)]^+$ (R = H, Me) has shown the importance of cationic Ir^{III} complexes in bond activation chemistry, such as the activation of silane Si-H bonds, aldehyde C-H bonds, and mild C-H bond activation of methane and other hydrocarbons.[84] The choice of counter anion plays an important role in this reactivity, with the most "non-coordinating" anion leading to the most highly reactive Ir species.[84d] The mechanism of bond activation by such cationic Ir^{III} species has been the subject of some debate, with the two most likely pathways being either direct oxidative addition to generate an Ir^{V} intermediate, or σ-bond metathesis.[84c,g] The synthesis of cationic Ir^{III} pincer complexes has been initiated by the groups of both Tilley and Brookhart, respectively. Tilley and co-workers have reported the synthesis of cationic (PNP) supported Ir silylene species that have been shown to undergo alkene hydrosilation, alcoholysis and aminolysis.[85] Brookhart and co-workers have reported on the synthesis of cationic complexes of the type $[(POCOP)Ir(H)]^+$ that can facilitate the reduction of alkyl halides with Et_3SiH, hydrosilylation of carbonyl containing compounds and epoxides, the reduction of tertiary amides to amines, as well as the reduction of carbon dioxide to methane.[44-49]

In an effort to access increasingly reactive silyl pincer complexes that can mediate challenging bond cleavage processes, the synthesis and reactivity of cationic iridium^{III} pincer species supported by [Cy-PSiP] ligation was investigated. Complexes of the type [R-PSiP]Ir(R')(X) (R = Cy, ^{i}Pr; R' = H, CH_3; X = OTf, BF_4, and $B(C_6F_5)_4$) were targeted, and their synthesis will be discussed in this chapter. Furthermore, the interaction of these complexes with the C-H bonds of arenes and aldehydes, as well as, the Si-H bonds of silanes will be discussed.

5.2 Results and Discussion

5.2.1 Synthesis and Characterization of Cationic [R-PSiP]Ir^{III} Complexes

As an entry point into the chemistry of cationic iridium^{III} silyl pincer complexes, the synthesis of complexes of the type $\{[R\text{-}PSiP]Ir(R')\}^{+}[X]^{-}$ (**5-1**: R = Cy, R' = H, X = OTf; **5-2**: R = ^{i}Pr; R' = H, X = OTf; **5-3**: R = Cy, R' = H, X = BF_4; **5-4**: R = ^{i}Pr, R' = H, X = BF_4; **5-5**: R = Cy, R' = H, X = $B(C_6F_5)_4$; **5-6**: R = ^{i}Pr, R' = H, X = $B(C_6F_5)_4$)) was initially targeted. The extent of charge separation in complexes such as **5-1** - **5-6** will depend on the nature of the anion X and its ability to coordinate to the Ir center, such that for X = OTf, the formation of complexes that feature inner sphere OTf ligands is anticipated, whereas for X = $B(C_6F_5)_4$, the anion is expected to be outer sphere.[86] Tetrafluoroborate anions originally described as non-coordinating are significantly more likely to coordinate to the metal center than $B(C_6F_5)_4$.[86] The iridium hydride species **5-1** - **5-6** were prepared by reacting either **2-1** or **3-2**, respectively, with one equivalent of the appropriate silver or lithium salt of X^{-} in CH_2Cl_2 or C_6H_5F solution at room temperature (Scheme 5-1).

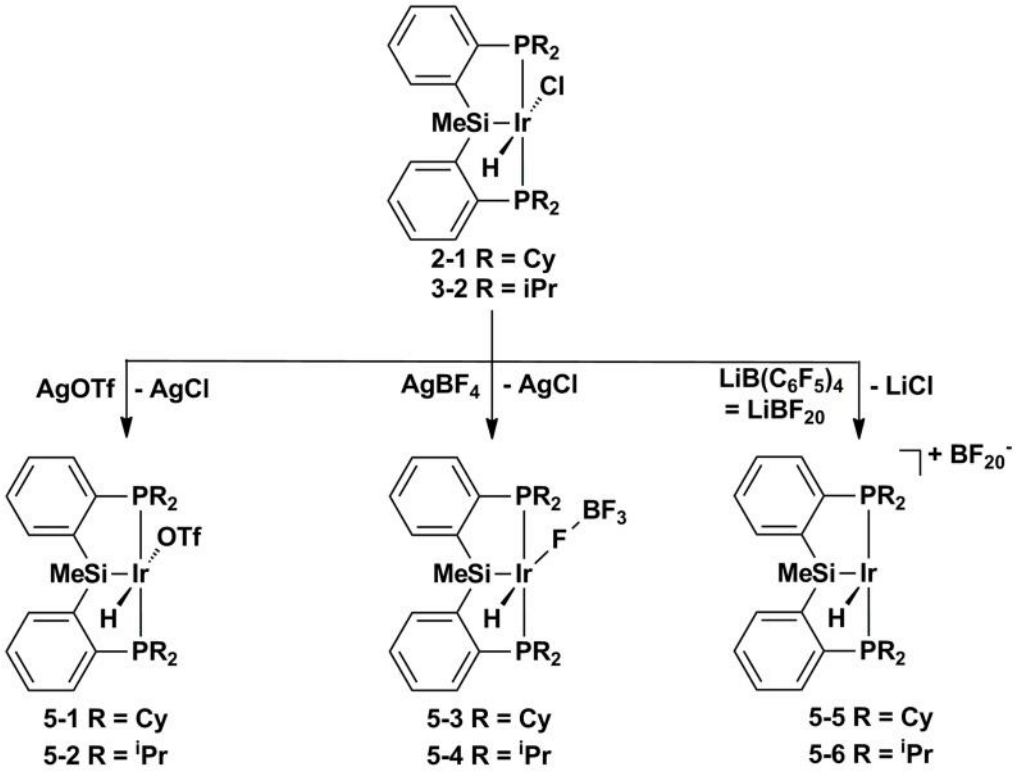

Scheme 5-1. Synthesis of Ir^{III} complexes [R-PSiP]Ir(H)(X) (R = Cy, ^{i}Pr; X = OTf, BF_4, $B(C_6F_5)_4$)

The formation of **5-1** - **5-6** was quantitative by in situ $^{31}P\{^{1}H\}$-NMR analysis of the reaction mixtures and the complexes were isolated as yellow or orange powders in 72 – 97% yields. Spectroscopic data for the isolated complexes (Table 5-1) support the formation of C_s-symmetric species, as indicated by the presence of a single $^{31}P\{^{1}H\}$ NMR resonance for each complex in conjunction with symmetry equivalent ligand aryl resonances. In addition, the ^{1}H NMR spectra of **5-1** - **5-6**, respectively, feature a characteristic downfield-shifted hydride resonance (Table 5-1), consistent with the formulations given in Scheme 5-1. The ^{11}B, ^{19}F, and ^{29}Si spectroscopic data (Table 5-1) are also in agreement with the structures proposed in Scheme 5-1. Complexes **5-3** and **5-4** exhibit broad singlets at -177.6 and -179.1 ppm in the ^{19}F NMR spectrum (benzene-d_6), indicating a dynamic process where coordination/decoordination of the fluorine atoms of

BF_4^- to the iridium centers is likely occurring. This η^1-BF_4 coordination is not unprecedented in the literature as examples of similar structures have been reported with metals across the periodic table[87] including Rh[87g,h] and Ir[87i,j]. Variable temperature NMR experiments were conducted in toluene-d_8 to attempt to freeze out separate ^{19}F resonances of the terminal and bridging fluorine atoms of the coordinated η^1-BF_4, however, separate resonances were not observed. In a room temperature toluene-d_8 solution, a single broad ^{19}F resonance at -170.7 ppm ($\Delta\nu_{1/2}$ = 647 Hz) observed. In contrast, a broad ^{19}F resonance at -177.6 ppm ($\Delta\nu_{1/2}$ = 108 Hz) was noted in room temperature benzene-d_6 solution. The cause of these solvent effects remains unclear. Upon decreasing the temperature of a toluene-d_8 solution of **5-3**, no decoalescence was detected. Despite the lack of decoalescence, a BF_4^- interaction with iridium is inferred from the broad nature of the ^{19}F resonance and was later confirmed in the solid state structure (*vide infra*). Moreover, the ^{19}F resonance has a temperature dependent chemical shift, which implies an equilibrium process, likely between coordinated and decoordinated BF_4 containing species. Similar spectral features were observed for $IrMe_2(PMe_2Ph)_3(FBF_3)$ and related rhodium species [PCP]Rh(Me)(FBF_3).[87h,i]

Table 5-1. Selected NMR spectroscopic data (ppm) for complexes **5-1** - **5-6**

Complex	$^{31}P\{^1H\}$ NMR	^1H NMR hydride[a]	$^{11}B\{^1H\}$ NMR	$^{19}F\{^1H\}$ NMR	^{29}Si NMR[b]
[Cy-PSiP]Ir(H)OTf (**5-1**)	61.2	-20.21 (t)	-	-76.1	7.3
[^{i}Pr-PSiP]Ir(H)OTf (**5-2**)	67.6	-29.49 (t)	-	-76.4	8.0
[Cy-PSiP]Ir(H)BF_4 (**5-3**)	62.2	-32.98 (t)	0.6	-177.6 (br s)	5.6
[^{i}Pr-PSiP]Ir(H)BF_4 (**5-4**)	69.1	-33.30 (t)	0.7	-179.1 (br s)	5.4
[Cy-PSiP]Ir(H)B(C_6F_5)$_4$ (**5-5**)	61.5	-25.07 (t)	-16.0	-132.6 (br s), -162.0 (t), -166.2 (br t)	8.9
[Cy-PSiP]Ir(H)B(C_6F_5)$_4$ (**5-6**)	72.1	-27.03 (t)	-16.0	-132.4 (d), -162.2 (t), -166.5 (br t)	11.8

[a] benzene-d_6; [b] resonances determined on the basis of ^1H-^{29}Si HMBC experiments

The solid state structures of **5-1**·$(C_6H_6)_{0.5}$ and **5-3**·C_6H_5F were determined using single crystal X-ray diffraction techniques (Figure 5-1, Table 5-2). The structures for

both complexes feature a five-coordinate Ir center due to inner sphere coordination of the OTf and BF_4 anions, respectively, in the solid state. In both cases the metal center exhibits distorted square-based pyramidal coordination geometry with Si occupying the apical position, similar to the geometries observed for the [Cy-PSiP]Ir^{III} structures discussed in previous chapters. In the case of **5-1**·$(C_6H_6)_{0.5}$ the Ir–O interatomic distance of 2.288(2) Å is longer than Bergman's Cp*(PMe_3)Ir(Me)(OTf) Ir–O distance of 2.216(10) Å.[84a] In the case of **5-3**·C_6H_5F the Ir-F1 distance of 2.288(3) Å is shorter than the Ir-F distance of 2.389(7) Å in $IrMe_2(PMe_2Ph)_3(FBF_3)$[87i] but comparable to that of $IrH(PPh_3)_2Cl(CO)(FBF_3)$ (2.272 Å).[87j] Complex **5-3** also features a relatively short Ir···F2 distance of 2.553(3) Å in the solid state which is within the sum of the van der Waals radii. Examples of an additional M–F interaction in other mononuclear BF_4 coordinated complexes are rare as only examples of Mo, Ag, and Zn complexes with a M-F interaction besides the terminal κ^1-bound BF_4, have been crystallographically characterized.[88] The short Ir···F2 distance may simply be due to coincidental orientation of the bound BF_4. Although the BF_4 anion appears to be coordinated to the Ir center of complex **5-3** in the solid state, in benzene or toluene solution at room temperature there is no ^{19}F NMR evidence for inequivalent F atoms (*vide supra*), indicating that the BF_4 anion may exchange fluorines intramolecularly or exhibit fluxionality between inner and outer sphere coordination modes in solution. As in the case of the solid state structure of [Cy-PSiP]IrHCl (**2-1**) and all other [Cy-PSiP]Ir^{III} structures discussed herein, both **5-1**·$(C_6H_6)_{0.5}$ and **5-3**·C_6H_5F feature relatively acute Si–M–H1 angles (78.3(10)º for **5-1**·$(C_6H_6)_{0.5}$ and 80.2(19)º for **5-3**·C_6H_5F). Notably these bis(phosphino)silyl Ir^{III} complexes adopt a structure that differs from that of the related cationic species $\{[POCOP]Ir(H)(acetone)\}^+[B(C_6F_5)_4]^-$, which exhibit square-based pyramidal geometry with the hydride ligand positioned in the apical site.[44b] This phenomenon likely reflects the strong trans-directing properties of the silyl group.[15f,50]

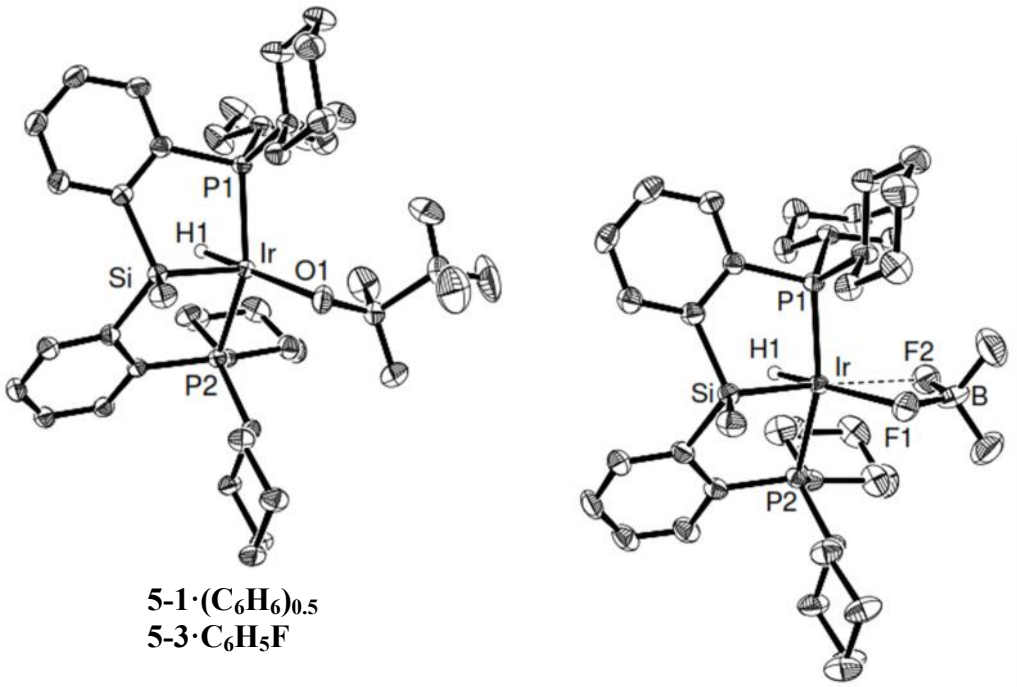

5-1·$(C_6H_6)_{0.5}$
5-3·C_6H_5F

Figure 5-1. The crystallographically determined structures of **5-1**·$(C_6H_6)_{0.5}$ and **5-3**·C_6H_5F shown with 50% displacement ellipsoids. With the exception of H1, all H atoms, as well as the C_6H_6 and C_6H_5F solvates, have been omitted for clarity.

Table 5-2. Selected interatomic distances (Å) and angles (º) for **5-1**·$(C_6H_6)_{0.5}$ and **5-3**·C_6H_5F.

Bond Lengths (Å)				
5-1·$(C_6H_6)_{0.5}$	Ir-P1	2.3198(7)	Ir-H1	1.47(3)
	Ir-P2	2.3041(7)	Ir-O1	2.288(2)
	Ir-Si	2.2618(7)		
5-3·C_6H_5F	Ir-P1	2.2968(9)	Ir-H1	1.494(10)
	Ir-P2	2.3102(11)	Ir-F1	2.288(3)
	Ir-Si	2.2600(11)	Ir-F2	2.553(3)
Bond Angles (º)				
5-1·$(C_6H_6)_{0.5}$	P1-Ir-P2	156.97(2)	Si-Ir-O1	105.28(5)
	Si-Ir-H1	78.3(10)		
5-3·C_6H_5F	P1-Ir-P2	163.34(5)	Si-Ir-F1	113.84(9)
	Si-Ir-H1	80.2(19)		

In an effort to assess the lability of the coordinated OTf and BF_4 ligands in **5-1** and **5-3**, the strongly donating neutral donor ligands PMe_3 and DMAP were introduced.

Treatment of a benzene solution of **5-1** with one equivalent of PMe_3 led to an immediate colour change from yellow to pale yellow. Analysis of the reaction mixture by ^{31}P NMR spectroscopy indicated the formation of a mixture of two major products in a 2:1 ratio. Attempts to drive the reaction mixture to one product by heating (14 h at 65 ºC) did not change the ratio of these products. However, if two equivalents of PMe_3 were added to **5-1**, quantitative formation of $\{[Cy\text{-}PSiP]Ir(H)(PMe_3)_2\}^+[OTf]^-$ (**5-7**) was observed (Scheme 5-2). Not surprisingly, the OTf ligand becomes non-coordinating upon the introduction of the strong L-donor PMe_3. Complex **5-7** was isolated as a pale yellow solid in 84% yield where the ^{31}P NMR of **5-2** exhibits a broad singlet at 26.6 ppm for ligand phosphine groups as well as two multiplets exhibiting second order splitting at -71.1 and -73.0 ppm for the coordinated PMe_3 groups. The ^1H NMR contains one set of ligand resonances for the symmetry equivalent halves of the ligand, as well as a doublet of multiplets centered at -14.91 ppm ($^2J_{HPtrans}$ = 94 Hz) for the Ir bound hydride.

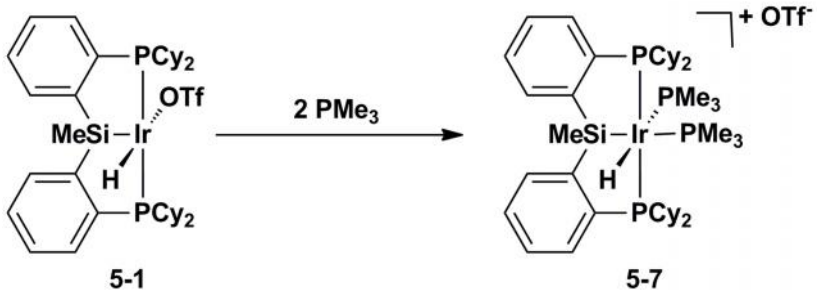

5-1 5-7

Scheme 5-2. Reactivity of [R-PSiP]Ir(H)(OTf) with PMe_3

In a related experiment, treatment of **5-1** with one equivalent of DMAP led to the quantitative (^{31}P NMR) formation of a new product (**5-8**) that featured a broad ^{31}P NMR resonance at 50.3 ppm and is tentatively assigned as the DMAP adduct [Cy-PSiP]Ir(H)(OTf)(DMAP) (Scheme 5-3). Complex **5-8** was isolated as a pale yellow solid in 96% yield. Spectroscopic data (benzene-d_6) are consistent with the formation of a C_s-symmetric species as indicated by the single set of ligand aryl resonances (^1H and ^{13}C NMR). The ^1H NMR spectrum of **5-8** features sharp aryl resonances corresponding to

the bound DMAP ligand, as well as a broad resonance at -21.7 ppm that corresponds to the Ir-H. The broad NMR features suggest a dynamic behavior that may be indicative of the reversible coordination of the OTf ligand to the Ir center. Variable temperature NMR studies (toluene-d_8) revealed decoalescence of the $^{31}P\{^1H\}$ NMR resonance at 0 °C and three phosphorus resonances were clearly observed at -30 °C at 50.3, 33.5 and 33.1 ppm. The peak at 50.3 is expected to correspond to $\{[Cy\text{-}PSiP]Ir(H)(DMAP)\}^+[OTf]^-$ (**5-8c**) where the OTf ligand is no longer coordinated to the metal center, whereas the two peaks at 33.5 and 33.1 ppm are likely due to [Cy-PSiP]Ir(H)(OTf)(DMAP) isomers with similar chemical shifts where the OTf ligand is inner sphere and either *trans* to the Ir-H (**5-8a**) or the ligand backbone Si-Me (**5-8b**) (Scheme 5-3, Figure 5-2).

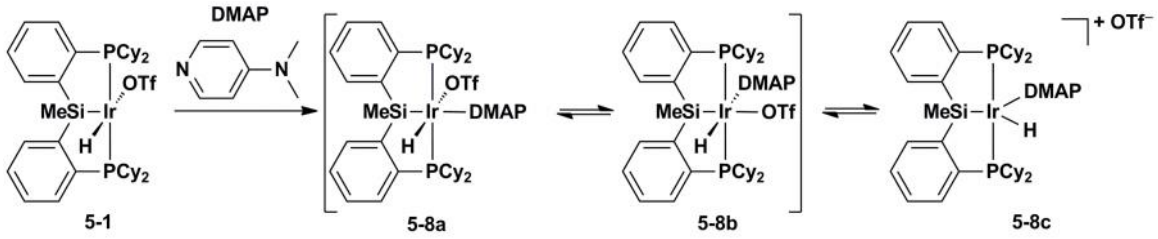

Scheme 5-3. Reactivity of [R-PSiP]Ir(H)(OTf) with DMAP

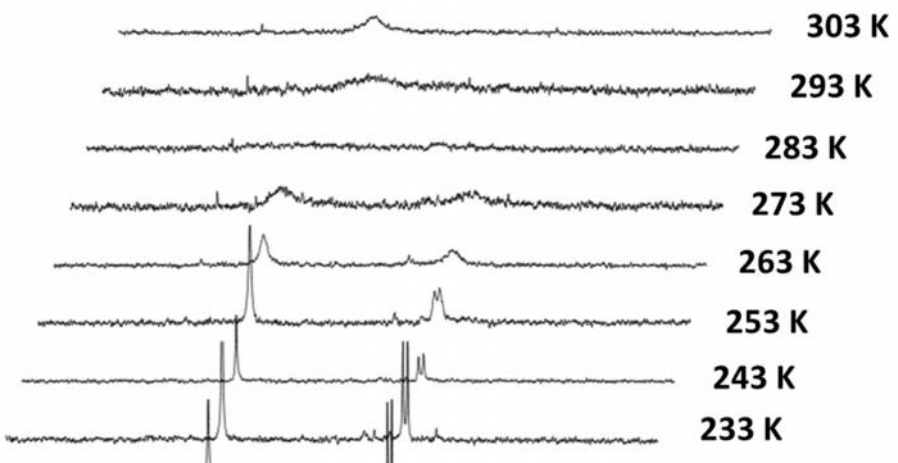

Figure 5-2. Partial $^{31}P\{^{1}H\}$ NMR spectrum (300 MHz, toluene-d_8) of [Cy-PSiP]Ir(H)(DMAP)(BF_4) as a function of temperature

Comparable reactivity was investigated with **5-3** to evaluate the lability of the coordinated BF_4 anion. In contrast to the **5-1**, **5-3** reacts cleanly with one equivalent of PMe_3 to quantitatively generate a new product **5-9** by $^{31}P\{^{1}H\}$ NMR where a doublet at 52.8 ($^{2}J_{PP}$ = 16 Hz) corresponds to the two ligand phosphine donors and a triplet at -22.3 ($^{2}J_{PP}$ = 16 Hz) is observed for the PMe_3 ligand. Complex **5-9** was isolated as a pale yellow powder in 91% yield and this C_s-symmetric product assigned as {[Cy-PSiP]Ir(H)(PMe_3)}$^{+}$[BF_4]$^{-}$ (**5-9**, Scheme 5-4) based on solution NMR data including a $^{19}F\{^{1}H\}$ shift of -152.1, corresponding to free (non-coordinated) BF_4^{-}. Furthermore, addition of DMAP to a fluorobenzene solution of **5-3** yielded a broad $^{31}P\{^{1}H\}$ NMR (benzene-d_6) resonance at 55.0 ppm. This product was isolated as a pale yellow solid in 93% yield and is tentatively assigned as {[Cy-PSiP]Ir(H)(DMAP)}$^{+}$[BF_4]$^{-}$ (**5-10**), based on $^{31}P\{^{1}H\}$, ^{1}H, and ^{13}C NMR (benzene-d_6) (Scheme 5-4). The broad $^{31}P\{^{1}H\}$ NMR resonance indicates dynamic behaviour, anticipated to be analogous to the reactivity of **5-1** with DMAP where structures of both coordinated and uncoordinated OTf anion were revealed at low temperatures (*vide supra*). Interestingly, a sharp $^{19}F\{^{1}H\}$ NMR resonance at -151.4 ppm (benzene-d_6) for **5-10** is observed at room temperature, implicating non-coordinated BF_4.

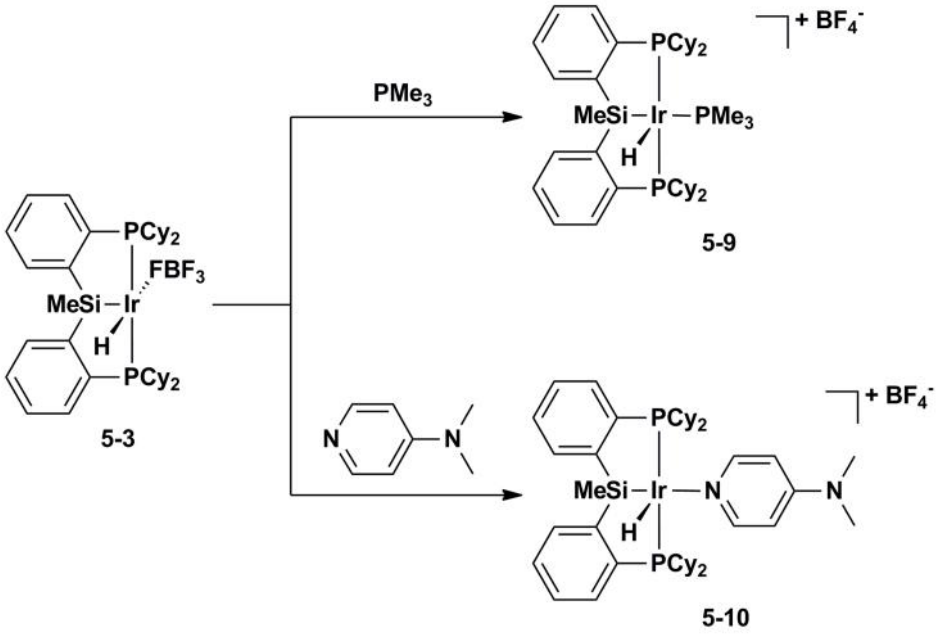

Scheme 5-4. Reactivity of [Cy-PSiP]Ir(H)BF_4 with L-donors (PMe_3 and DMAP)

The synthesis of cationic bis(phosphino)silyl iridium methyl complexes was also pursued, due to their direct relation to the Cp*(PMe_3)Ir(Me)$^+$ cation that has demonstrated remarkable bond activation reactivity.[84] In order to access [Cy-PSiP]Ir(Me)$^+$ species, the corresponding [Cy-PSiP]Ir(Me)(I) (**5-11**) complex were first targeted as it represents a convenient precursor for anion exchange via salt metathesis reactions similar to those used for the synthesis of [R-PSiP]Ir(H)$^+$ species (*vide supra*). Treatment of an in situ generated [Cy-PSiP]Ir^I with MeI led to intractable reaction mixtures. Alternatively, treatment of [Cy-PSiP]Ir(C_2H_4) with MeI in THF yielded the desired [Cy-PSiP]Ir(Me)(I) complex as a dark orange solid in 52% isolated yield (Scheme 5-5). Complex **5-11** exhibits C_s-symmetry in solution based on a single broad

$^{31}P\{^{1}H\}$ NMR resonances at 35.7 ppm. As the solid state structure of **5-11** reveals a facial binding mode of the ligand (vide infra), the broad $^{31}P\{^{1}H\}$ NMR spectrum likely indicates a fluxional process where both *fac*-PSiP and *mer*-PSiP ligand orientations are exchanging. Furthermore, the ^{1}H NMR (benzene-d_6) spectra of **5-11** features a resonance corresponding to an Ir-*Me* ligand at 2.06 ppm.

Scheme 5-5. Synthesis of [Cy-PSiP]Ir(Me)(I) (**5-11**)

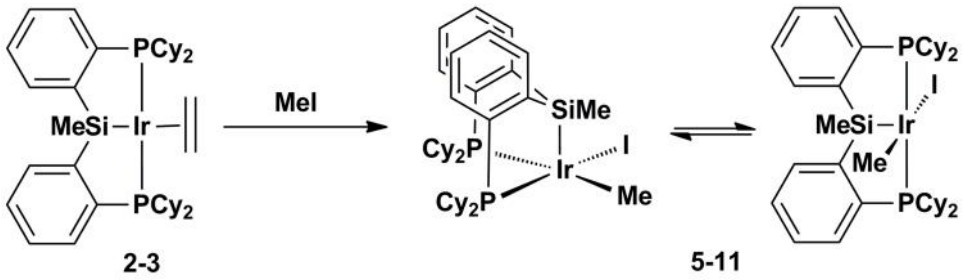

2-3 **5-11**

The solid state structure of **5-11** was obtained using single crystal X-ray diffraction techniques (Figure 5-3, Table 5-3). The five-coordinate complex adopts a distorted square based pyramidal structure with the [Cy-PSiP] ligand bound in a facial manner, such that the phosphino donors are *cis*-disposed, with one phosphine arm bound *trans* to a Me group while the other is coordinated *trans* to the iodide ligand (Figure 5-3). The silyl donor is bound in the apical position *trans* to an empty coordination site. Interestingly, although there have been previous examples of *fac*-[Cy-PSiP] metal complexes reported,[15f] this is the first example of a crystallographically characterized [Cy-PSiP]Ir species where the tridentate ligand is not bound to Ir in a meridonal fashion.[89] It is noteworthy that all previous examples of crystallographically characterized *mer*-[Cy-PSiP]Ir complexes also feature hydrido ligands (e.g. *mer*-[Cy-PSiP]Ir(H)(Cl), **2-1**), and highly acute Si-Ir-H angles (66.2 – 79.3^{o}), which are potentially indicative of a Si-H interaction in the solid state.[90] It is possible that such an Si-H interaction facilitates the *mer*-[Cy-PSiP] coordination observed for these Ir complexes. In the absence of a hydride ligand, **5-11** adopts the observed *fac*-[Cy-PSiP] structure.

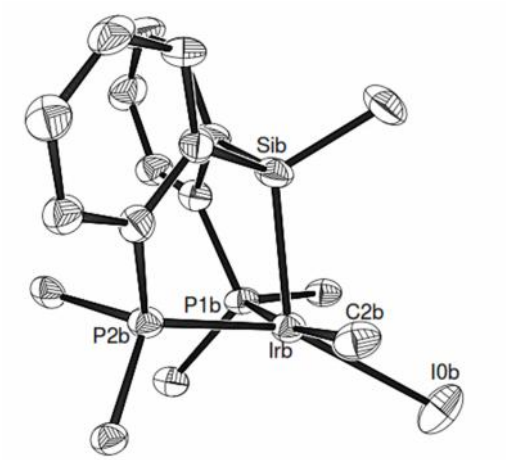

Figure 5-3. The crystallographically determined structure of **5-11** shown with 50% displacement ellipsoids. Only one of the two crystallographically-independent molecules of **5-11** is shown. All H atoms and some C atoms have been omitted for clarity.

Table 5-3. Selected interatomic distances (Å) and angles (º) for **5-11**

Bond Lengths (Å)			
Ir-P1	2.3414(18)	Ir-C2	2.177(6)
Ir-P2	2.2488(18)	Ir-I0	2.6982(6)
Ir-Si	2.2810(18)		
Bond Angles (º)			
P1-Ir-P2	97.53(6)	Si-Ir-I0	124.29(5)
Si-Ir-C2	89.22(18)		

Note: Distances and angles of only one of the two crystallographically-independent molecules of **5-11** are given

Attempts to access [Cy-PSiP]Ir(Me)$^+$ species via treatment of **5-11** with the silver or lithium salt of X^- (X = OTf, BF_4, or $B(C_6F_5)_4$) were hindered due to challenges associated with clean synthesis of precursor **5-11**. As a result, only [Cy-PSiP]Ir(Me)(OTf) (**5-12**) was synthesized by treatment of **5-11** with AgOTf and isolated as an orange solid in 81% yield (Scheme 5-5). The ^{31}P NMR spectrum of **5-12** features two doublets centered at 52.5 and -24.5 ppm ($^2J_{PP}$ = 300 Hz), respectively, indicative of a C_1-symmetric species. In addition, the ^{1}H and ^{13}C NMR spectra (benzene-d_6) of **5-12**

indicate two sets of ligand aryl resonances, which is also consistent with a C_1-symmetric complex that features *fac*-[Cy-PSiP] coordination. Furthermore, the ^{1}H NMR spectrum of **5-12** also features two Me resonances at 1.13 and -0.12 ppm for the ligand Si-*Me* and Ir-*Me*, respectively. A correlation between the ligand Si and both Me groups (^{1}H-^{29}Si HMBC) indicates the Ir-Me is trans to Si (Scheme 5-6). Unfortunately, further reactivity was not pursued due to the difficulties in reliable synthesis of **5-11**.

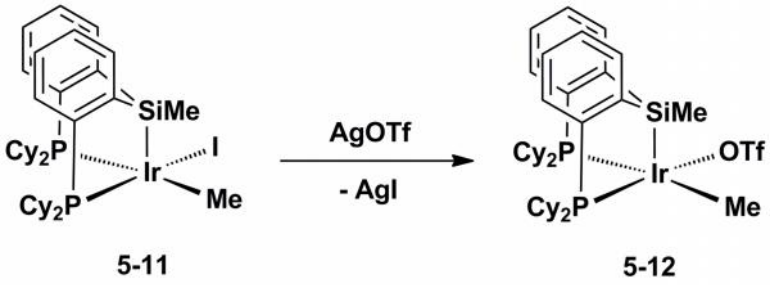

5-11 5-12

Scheme 5-6. Synthesis of [Cy-PSiP]Ir(Me)(OTf) (**5-12**)

5.2.2 Reactivity of [Cy-PSiP]Ir(H)(X) (X = OTf, BF_4, $B(C_6F_5)_4$) Complexes

The reactivity of complexes **5-1**, **5-3** and **5-5** with simple hydrocarbons was initially probed by dissolving the complexes in benzene, THF, or cyclohexane. Prolonged heating (up to 5 days at 100 ºC) did not result in any reactivity and limited decomposition. Subsequently cleavage of the *sp*-hybridized terminal CH bond of phenylacetylene was investigated by treatment of fluorobenzene solutions of **5-1**, **5-3** and **5-5** with 1 equiv of phenylacetylene. These reactions resulted in the formation of intractable reaction mixtures that contained multiple products, as evidenced by ^{31}P NMR spectroscopy. Subsequent heating of these reaction mixtures for 14 h at 70 ºC did not lead to clean product formation (^{31}P NMR).

The reactivity of complexes **5-1**, **5-3** and **5-5** with aldehyde C-H bonds was also investigated. Treatment of fluorobenzene solutions of either **5-1** or **5-5** with

benzaldehyde (either 1 or 5 equiv) or acetaldehyde (20 equiv) did not result in any reactivity at room temperature or upon heating at temperatures up to 70 ºC. Conversely, treatment of fluorobenzene solutions of **5-3** with 5 equiv of benzaldehyde led to the immediate quantitative formation of a new product (**5-13**) featuring a ^{31}P NMR resonance at 57.8 ppm. Exposure of this reaction mixture to vacuum (ca. 0.01 mm Hg), led to the isolation of a 1:1 mixture of [Cy-PSiP]Ir(H)C(O)Ph (**4-11**) and **5-3** (^{31}P and ^{1}H NMR). These results suggest that the reaction of **5-3** with benzaldehyde initially forms an intermediate (**5-13**), which is likely a benzaldehyde adduct of the type {[Cy-PSiP]Ir(H)(O=CPhH)$_2$}(BF$_4$) (Scheme 5-7).[91] Subsequent exposure of **5-13** to vacuum can lead to loss of the coordinated benzaldehyde to reform **5-3**. Upon loss of only one equivalent of coordinated benzaldeyde from **5-13**, C-H activation of the remaining aldehyde ligand may occur and subsequent loss of HBF$_4$ would provide the observed acyl complex [Cy-PSiP]Ir(H)C(O)(Ph) (**4-11**) (Scheme 5-6)

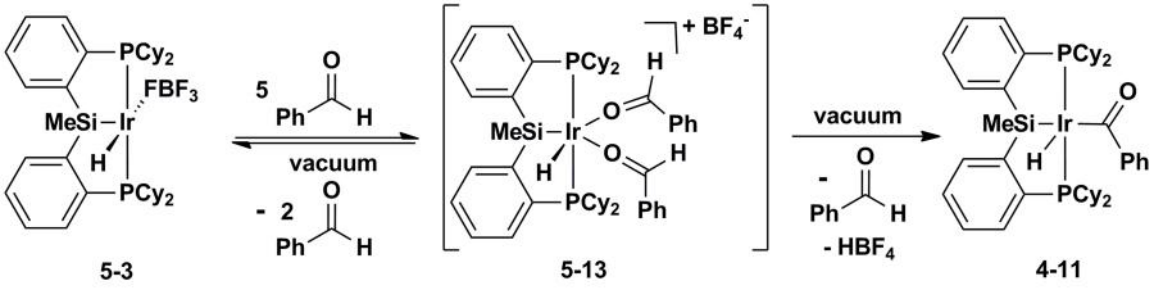

Scheme 5-7. Reactivity of [Cy-PSiP]Ir(H)(BF$_4$) (**5-3**) with benzaldehyde

The reactivity of complexes **5-1**, **5-3**, and **5-5** with the Si-H bonds of hydrosilanes was also explored. Treatment of a fluorobenzene solution of **5-1** with one equivalent of Et$_3$SiH resulted in ca. 50% conversion (^{31}P NMR) to a new species (**5-14**) that featured a ^{31}P NMR resonance at 42.7 ppm. Subsequent addition of a second equivalent of Et$_3$SiH resulted in quantitative (^{31}P NMR) formation of **5-14**. Complex **5-14** was isolated as a pale yellow solid (62 % yield) where the ^{1}H NMR spectrum (benzene-d_6) of **5-14** features

two broad hydride signals at -10.23 (2 H) and -12.48 (1 H) ppm. On the basis of these data **5-14** was tentatively assigned as the trihydride complex [Cy-PSiP]Ir$(H)_3(SiEt_3)$. The ^{29}Si resonance (^{1}H-^{29}Si HMQC) at 3.1 ppm corresponding to the $SiEt_3$ ligand shows no correlation with the Ir hydride ligands. Although no coupling is observed, Si-H interactions cannot be ruled out (see below for discussion). Variable temperature NMR studies (toluene-d_8) reveal decoalescence of the upfield Ir bound hydride signals to three peaks at -9.87, -10.33, and -12.55 ppm at 273 K. Measurement of the T_1 relaxation times at different temperatures using the null method[92] revealed estimated T_{1min} of 188 ms (243 K), 216 ms (253 K) and 209 ms (253 K) at 300 MHz. Moreover, the IR spectrum of **5-14** shows broad bands at 1997, and 1965 cm^{-1} for the Ir bound hydrides, none of which indicate Si-H interactions as these are typically observed as broad, intense bands between 1650 and 1800 cm^{-1}.[93] This collection of data indicates the presence of classical iridium bound hydride ligands.[94]

The formation of **5-14** can be envisioned to occur via the initial reaction of one equivalent of Et_3SiH with **5-1** to form either an Ir^{III} σ-Si-H complex or an Ir^{V} silyl hydride (Scheme 5-8). Subsequent loss of Et_3SiOTf, followed by oxidative addition of a second equivalent of Et_3SiH yields **5-14**. Consistent with this formulation, a ^{1}H-^{29}Si HMBC experiment revealed two Si resonances for **5-14** at 3.1 ppm (for the Ir-bound $SiEt_3$ ligand) and 37.4 ppm (for the SiMe of the ligand backbone), as well as a resonance at 44.0 ppm that corresponds to free Et_3SiOTf.[95]

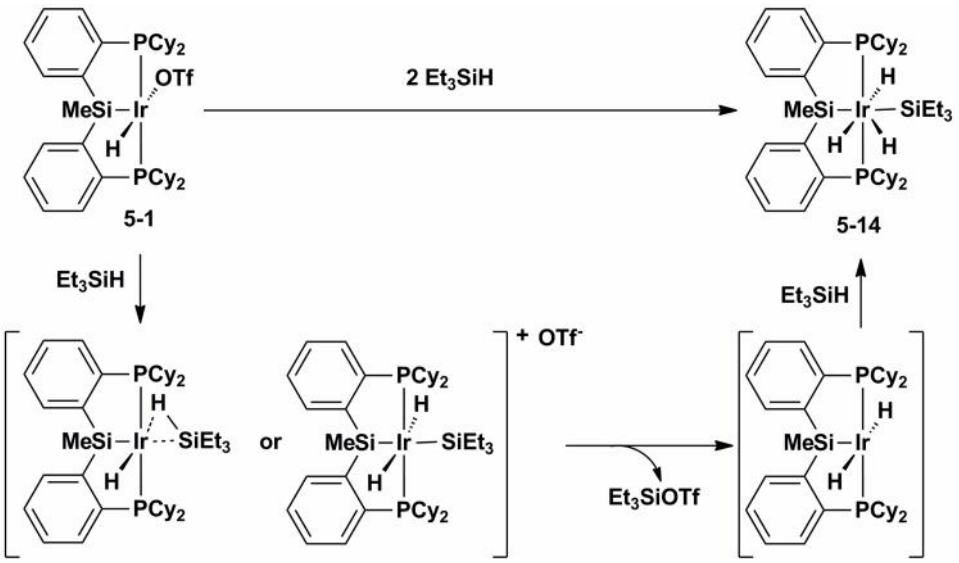

Scheme 5-8. Potential mechanism for formation of [Cy-PSiP]Ir(H)$_2$(H)(SiEt$_3$) (**5-14**)

A single crystal suitable for X-ray diffraction was obtained from a concentrated benzene solution of **5-14** at room temperature. The resulting structure (Figure 5-4, Table 5-4) revealed a complex where an equivalent of H_2 was lost from **5-14** to generate the silyl hydride complex **5-15**·$(C_6H_6)_{0.5}$. The five coordinate complex exhibits a distorted square-based pyramidal geometry at Ir, with the $SiEt_3$ ligand occupying the apical coordination site. The structure features an acute Si2-Ir-H1 angle between the $SiEt_3$ and hydride ligands (67.5(19)º). Unlike related crystallographically characterized complexes of the type [Cy-PSiP]Ir(H)(X), which feature acute Si-Ir-H angles involving the hydride ligand and the pincer silyl donor, **5-15** does not contain a potentially π-donating X ligand in the Ir coordination sphere. Such a π-donor has previously been implicated in the preference for "Y-shaped" coordination geometry in d^6 ML_5 complexes.[96] This suggests that the acute Si2-Ir-H1 angle observed in the solid state structure of **5-15** may derive from an alternative source, such as a weak Si-H interaction in the solid state. The Ir-Si1 distance of 2.3850(10) Å is shorter than the Ir-Si2 distance of 2.4966(11) Å, likely due to the steric profile of the bulky $SiEt_3$ group.

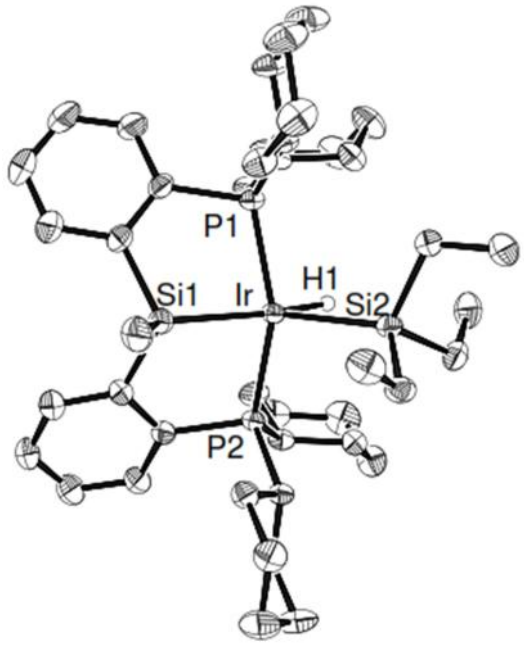

Figure 5-4. The crystallographically determined structure of **5-15**·$(C_6H_6)_{0.5}$ shown with 50% displacement ellipsoids. With the exception of H1, all H atoms, as well as the C_6H_6 solvate, have been omitted for clarity.

Table 5-4. Selected interatomic distances (Å) and angles (º) for **5-15**·$(C_6H_6)_{0.5}$.

Bond Lengths (Å)			
Ir-P1	2.3114(9)	Ir-H1	1.51(5)
Ir-P2	2.3127(9)	Ir-Si2	2.4966(1)
Ir-Si1	2.3850(10)		
Bond Angles (º)			
P1-Ir-P2	152.80(3)	Si2-Ir-H1	67.5(19)
Si1-Ir-H1	159.5(19)	Si1-Ir-Si2	132.95(4)

Treatment of a fluorobenzene solution of **5-3** with one equivalent of Et_3SiH resulted in 50% conversion (^{31}P NMR) to a new [Cy-PSiP]Ir species (**5-16**) that features a ^{31}P NMR resonance at 52.3 ppm. Addition of a second equivalent of Et_3SiH to this reaction mixture led to quantitative conversion to **5-16**, which was isolated in 94% yield. The ^{1}H and ^{13}C NMR spectra of **5-16** (benzene-d_6) are consistent with a C_s-symmetric

species, as indicated by the observation of only one set of ligand aromatic resonances. The ^{1}H NMR spectrum of **5-16** also contained three broad Ir-*H* resonances at -6.59, -9.20, and -14.4 ppm, each integrating to one H. The hydride resonances at -6.59 and -9.20 sharpen in the $^{1}H\{^{11}B\}$ NMR to broad triplets with $^{2}J_{HP}$ = 34 Hz and $^{2}J_{HP}$ = 26 Hz, indicating that these H atoms are closely associated with a boron atom. The IR spectrum of **5-16** reveals a sharp peak at 2138 cm^{-1} for the terminal Ir-H as well as a broad band at 1844 cm^{-1}, in the range for a bridging B-H stretch in an η^2 complex.[97] In the $^{19}F\{^{1}H\}$ NMR a peak at -54.9 ppm was observed for **5-16**. Also, the ^{11}B NMR has a single broad resonance at 30.5 ppm, which sharpens upon ^{1}H decoupling.

The solid state structure of **5-16**·C_6H_6 was determined by use of single crystal X-ray diffraction techniques, and revealed the formation of the hydroborate complex [Cy-PSiP]Ir(H)(η^2:η^2-H_2BF_2) (Figure 5-5, Table 5-5), which is consistent with the solution NMR data available for this complex. The six coordinate complex exhibits a pseudo octahedral geometry where the ligand phosphine donors occupy the axial positions and the silicon, hydride and bridging B-H groups occupy the equatorial plane. The structure features an acute Si-Ir-H1 angle (77.3(14)º), comparable to related [Cy-PSiP]Ir^{III} crystallographically characterized complexes described herein. Although, no literature examples were found containing hydroborates of the type $BH_2F_2^-$, related tetrahydroborate η^2-BH_4 transition metal complexes have been reported in the literature for pincer complexes, including [PNX]Ru(H)(BH_4) (X = P, N),[97d] [^{tBu}PCP]Ni(BH_4),[97b] [^{R}POCOP]Ni(BH_4) (R = ^{t}Bu, ^{i}Pr, ^{c}Pe)[97c] and [^{tBu}POCOP]Ir(H)$_2$(BH_3)[97a] where the complex is described more as an Ir σ-BH_3 complex with a second activated B-H bond. The bridging B-H bond distances in **5-16** (B-H1ba = 1.44(3) Å, B-H1bb = 1.25(3) Å) are comparable to that of [^{tBu}POCOP]Ir(H)$_2$(BH_3), which has a σ-B–H bond distance of 1.45(5) Å. Furthermore the Ir···B bond distance of 2.158(3) Å for **5-16** is shorter than the η^1-BH_3 of [^{tBu}POCOP]Ir(H)$_2$(BH_3) and is slightly shorter than that of related Ni and Ru pincer complexes containing η^2-borate ligands (2.180 - 2.214 Å)[97c,d].

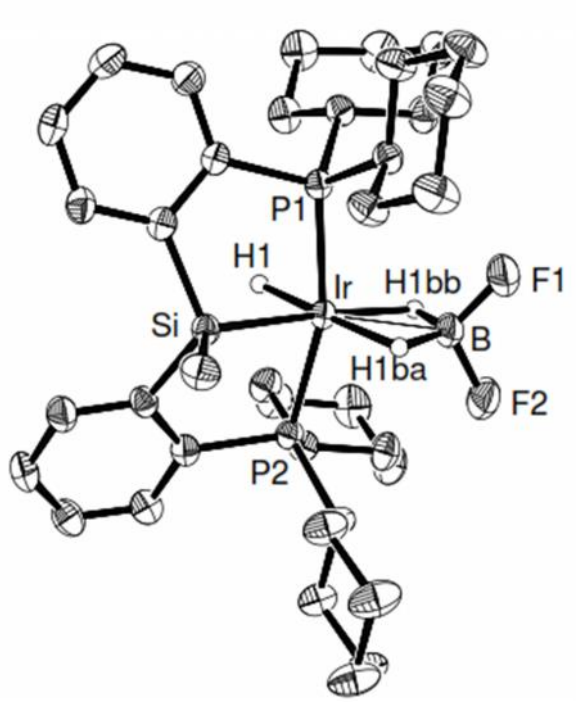

Figure 5-5. The crystallographically determined structure of **5-16** shown with 50% displacement ellipsoids. With the exception of H1, H1ba, and H1bb, all H atoms, as well as the C_6H_6 solvate, have been omitted for clarity.

Table 5-5. Selected interatomic distances (Å) and angles (º) for **5-16.**

Bond Lengths (Å)			
Ir-P1	2.3003(7)	Ir···B	2.158(3)
Ir-P2	2.3079(7)	B-H1ba	1.44(3)
Ir-Si	2.3477(7)	B-H1bb	1.25(3)
Ir-H1	1.55(4)	B-F1	1.351(4)
Ir-H1ba	1.77(3)	B-F2	1.350(4)
Ir-H1bb	1.91(3)		
Bond Angles (º)			
P1-Ir-P2	163.42(3)	Si-Ir-H1ba	102.0(10)
Si-Ir-H1	77.3(14)	Si-Ir-H1bb	176.7(9)

The formation of **5-16** from **5-3** and 2 equiv Et_3SiH could result from an H/F exchange process where two of the F atoms of the η^1-BF_4 unit in **5-3** are progressively transferred to Si in Et_3SiH (Scheme 5-9). Although the exact mechanism of this process

remains ambiguous, theoretical calculations on various isomers of [^{tBu}PCP]Ni(BF_xH_{4-x}) (x = 1-3) have shown that η^1- and η^2-borohydride Ni complexes are predicted on the pathway interconverting [^{tBu}PCP]Ni(BH_3F) to [^{tBu}PCP]Ni(BF_4).[97b] In situ ^{19}F NMR spectroscopy of reaction mixtures in which **5-16** is generated feature a resonance at -54.9 ppm for **5-16** as well as a resonance at -175.1 ppm for free Et_3SiF, consistent with the evolution of fluorosilane during the formation of **5-16**.[98] Unfortunately the reaction of Et_3SiH (1 or 5 equivalents) with **5-5** did not yield any new isolable product.

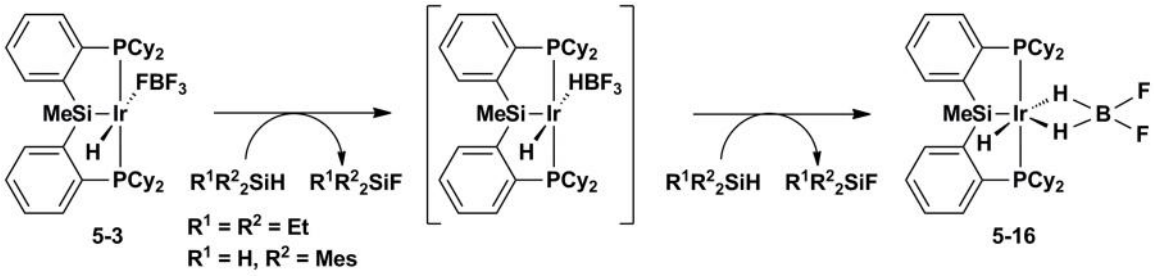

Scheme 5-9. Proposed mechanism for formation of [Cy-PSiP]Ir(H)(η^2: η^2-H_2BF_2) (**5-16**)

The reactivity of secondary silanes with [Cy-PSiP]Ir(H)(X) (X = OTf, BF_4, $B(C_6F_5)_4$) was also explored. In this regard, addition of one or two equivalents of Mes_2SiH_2 to **5-1** did not result in any observed reaction, even upon heating of the reaction mixtures to 80 ºC. Treatment of a fluorobenzene solution of **5-3** with two equivalents of Mes_2SiH_2 led to the quantitative (^{31}P NMR) formation of **5-16**. The ^{19}F NMR spectrum of the reaction mixture features a resonance at -54.9 ppm for **5-16**, as well as a resonance at -167.2 ppm for free Mes_2SiHF. The ^{29}Si NMR spectroscopy (^{29}Si-^{1}H HMBC) of the reaction mixture also revealed a resonance at -10.1 ppm, due to liberation of Mes_2SiHF. The mechanism to generate **5-16** and Mes_2SiHF likely follows similar steps to those depicted in Scheme 5-9.

Complex **5-5** also reacted with one equivalent of Mes_2SiH_2 to afford quantitative (^{31}P NMR) formation of a new [Cy-PSiP]Ir species (**5-17**) that featured a ^{31}P NMR

resonance at 46.9 ppm. Complex **5-17** was isolated as an orange solid in 92% yield and is tentatively assigned on the basis of ^{1}H and ^{29}Si NMR spectroscopy as the dimesitylsilane complex [Cy-PSiP]Ir(H)(η^2:η^2-H_2SiMes_2) that features bis(σ-Si–H) coordination (Scheme 5-10). The ^{1}H NMR spectrum of **5-17** (benzene-d_6) features three upfield-shifted resonances at -15.00 (br s), -5.06 (br s) and -0.67 (br s) ppm that correspond to the terminal Ir-*H* and the two σ-Si-*H* ligands, respectively. The latter two resonances correlate to a ^{29}Si resonance at 62.7 ppm in a ^{1}H-^{29}Si HMQC experiment, with one bond Si-H coupling constants of 140 and 101 Hz, respectively, which fall in the range commonly associated with η^2-silane complexes (typical $^{1}J_{SiH}$ values in free silanes fall near 200 Hz, while $^{1}J_{SiH}$ values in metal silyl species range between ca. 140 - 220 Hz)[93] Furthermore, in keeping with η^2-Si-H coordination to a metal center, the IR spectrum of **5-17** exhibits IR bands at 2155 cm^{-1} for the terminal Ir-H, as well as bands at 1643 and 1605 cm^{-1}, a region characteristic of η^2-Si-H metal species.[93]

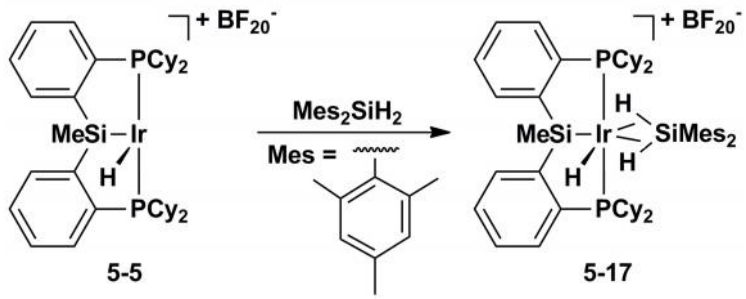

Scheme 5-10. Synthesis of [Cy-PSiP]Ir(H)(η^2:η^2-H_2SiMes_2) (**5-17**)

Alternatively, the reaction of **5-1** with one equivalent of Ph_2SiH_2 led to quantitative (^{31}P NMR) formation of a new complex (**5-18**) featuring a ^{31}P NMR resonance at 42.0 ppm. Complex **5-18** was isolated in 92% yield and has been assigned as [Cy-PSiP]Ir(H)$_3$(SiPh$_2$OTf) on the basis of ^{1}H and ^{29}Si NMR data. The ^{1}H NMR spectrum of isolated **5-18** (benzene-d_6) features two Ir-*H* resonances at -8.83 (2 H) and -12.13 (1 H) ppm. The ^{29}Si NMR spectrum of **5-18** exhibits two resonances at 28.0 and

57.7 ppm, corresponding to the ligand *Si*Me group and the coordinated *Si*Ph_2OTf ligand, respectively. ^{29}Si-^{1}H correlation experiments did not show any Si-H coupling, however Si-H interactions cannot be ruled out (*vide infra*). IR bands were observed at 2037, and 1968 cm^{-1}, in the range of terminal iridium hydrides. Low temperature NMR studies (toluene-d_8) showed the presence of three upfield resonances at – 11.55, - 11.91, and – 14.19 at 283 K that exhibited estimated (null method) T_1 relaxation times of 215 ms (253 K), 247 ms (263 K) and 241 ms (253 K) at 300 MHz. This data indicates the presence of classical iridium bound hydride ligands.[92,94] Attempted crystallization of **5-18** from a concentrated fluorobenzene solution afforded single crystals that upon X-ray diffraction analysis proved to be [Cy-PSiP]Ir(H)(SiPh$_2$OTf) (**5-19**·(**C_6H_5F)$_{1.25}$**, Figure 5-6, Table 5-6), the product of H_2 loss from **5-19**·(**C_6H_5F)$_{1.25}$**. The five coordinate complex exhibits a distorted square-based pyramidal geometry at Ir, with the SiPh$_2$OTf ligand occupying the apical coordination site, comparable to the structure of **5-15**·$(C_6H_6)_{0.5}$ also bearing a silyl ligand. The structure features an acute Si2-Ir-H1 angle between the SiPh$_2$OTf and hydride ligand (71.6(16)º). The Ir-Si1 distance of 2.4074(10) is comparable in length to the Ir-Si2 distance of 2.3853(11) Å.

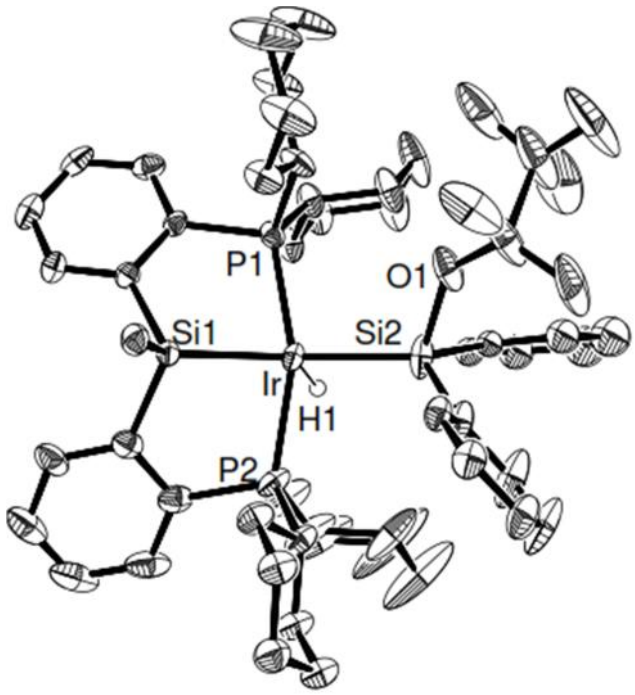

Figure 5-6. The crystallographically determined structure of **5-19**·$(C_6H_5F)_{1.25}$ shown with 50% displacement ellipsoids. With the exception of H1, all H atoms, as well as the C_6H_5F solvate, have been omitted for clarity.

Table 5-6. Selected interatomic distances (Å) and angles (º) for **5-19**·$(C_6H_5F)_{1.25}$.

Bond Lengths (Å)			
Ir-P1	2.3330(10)	Ir-Si1	2.4074(10)
Ir-P2	2.3316(11)	Ir-Si2	2.3853(11)
Ir-H1	1.498(10)	Si2-O1	1.807(3)
Bond Angles (º)			
P1-Ir-P2	159.37(4)	Si2-Ir-H1	71.6(16)
Si1-Ir-H1	139.3(16)		

Possible routes for the generation of **5-18** would proceed via the initial formation of an Ir silyl species either through Si-H oxidative addition to generate an Ir^V intermediate, similar to those proposed by Bergman and Tilley in the silane Si-H bond cleavage mediated by Cp*(PMe_3)Ir(Me)(OTf),[84g] or alternatively via σ-bond metathesis to generate an Ir^{III} silyl triflate complex and H_2, which may coordinate to the metal center

(Scheme 5-11). Dissociation of the OTf ligand would provide an open coordination site at the metal, allowing for an α-hydride migration from Si to Ir to generate a cationic Ir silylene hydride species.[84] Cationic metal silylene species are known to be highly electrophilic at Si and often exhibit reactivity analogous to silylium cations. Thus, such a cationic Ir silylene species would readily coordinate OTf to generate **5-18** (Scheme 5-11).[84]

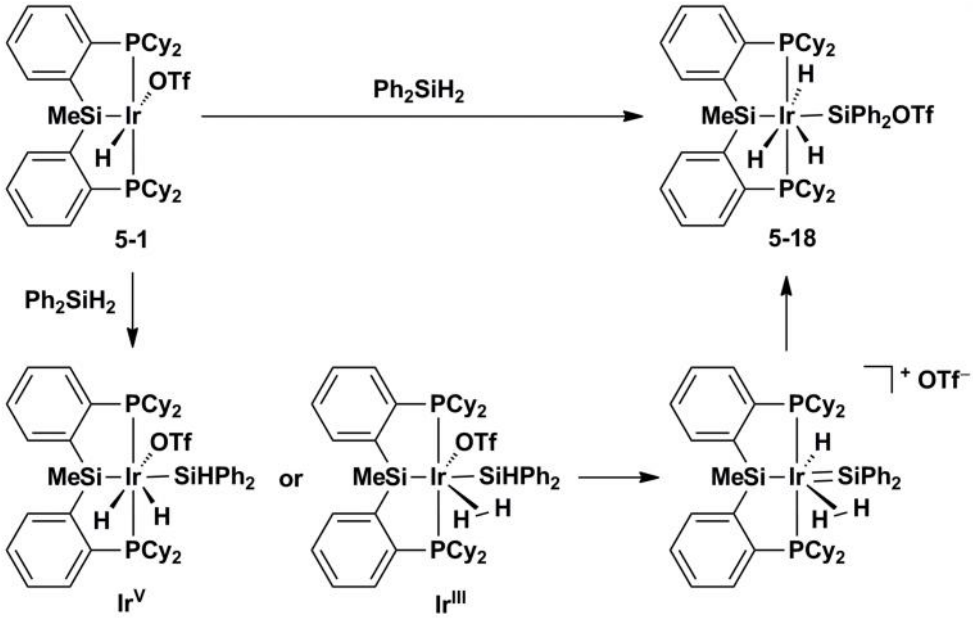

Scheme 5-11. Possible mechanisms for formation of [Cy-PSiP]Ir(H_2)(H)($SiPh_2OTf$) (**5-18**)

The reaction of **5-3** with one equivalent of Ph_2SiH_2 led to the quantitative (^{31}P NMR) formation of a new product (**5-20**) that featured a ^{31}P NMR resonance at 43.9 ppm. Complex **5-20** was isolated as an orange solid in 79% yield, and is assigned on the basis of ^{1}H, ^{19}F and ^{29}Si NMR spectroscopy as an analogue of **5-18** featuring a π-donor stabilized Ir silylene IrSi(BF_4)Ph_2 ligand derived from an electrophilic diphenylsilylene intermediate, likely formed from an initial Si-H activation followed by α-H migration (Scheme 5-12). Base stabilized silylenes are fairly well known in the literature and are often precursors to base-free metal silylene species.[85] As in the case of **5-18**, the ^{1}H NMR spectrum (benzene-d_6) of **5-20** features two upfield shifted resonances at -9.27 (2

H) and -11.86 (1 H) ppm, consistent with three Ir-*H* ligands also observed in the IR spectrum as bands at 2004, and 1957 cm^{-1}. Variable temperature ^{1}H NMR (toluene-d_8) showed that at 323 K the hydride signals coalesce into one broad resonance at -9.82 ppm. At 273 K the hydride resonances decoalesce into three peaks integrating to 1 H each at -9.02, -9.58 and -11.90 ppm with estimated (null method)[92] T_1(min) values of 202 ms (253 K), 214 ms (263 K) and 214 ms (263 K), respectively, supporting the trihydride nature of **5-20**. The ^{11}B NMR features a single resonance at 0.51 ppm, while the $^{19}F\{^{1}H\}$ NMR shows resonances at -130.4 ppm and -141.7 for the BF_4 unit coordinated to Si through one F atom. Two ^{29}Si NMR resonances were observed for **5-20** (^{29}Si-^{1}H HMBC) at 32.1 ($^{1}J_{SiF}$ = 237 Hz) and 35.2 ppm, corresponding to the Ir-*Si*Ph_2BF_4 and Ir-*Si*Me, groups respectively. Interestingly, unlike the reactivity observed for **5-3** with Et_3SiH and Mes_2SiH_2, no evidence for the formation of **5-16** was observed. However, when two equivalents of Ph_2SiH_2 were initially added to **5-3**, ^{31}P NMR spectroscopy reveals the generation of both **5-20** and **5-16** (2:1 ratio). Unfortunately, the reaction of **5-5** with either one or two equivalents of Ph_2SiH_2 generated multiple products (^{31}P NMR), none of which could be identified or isolated.

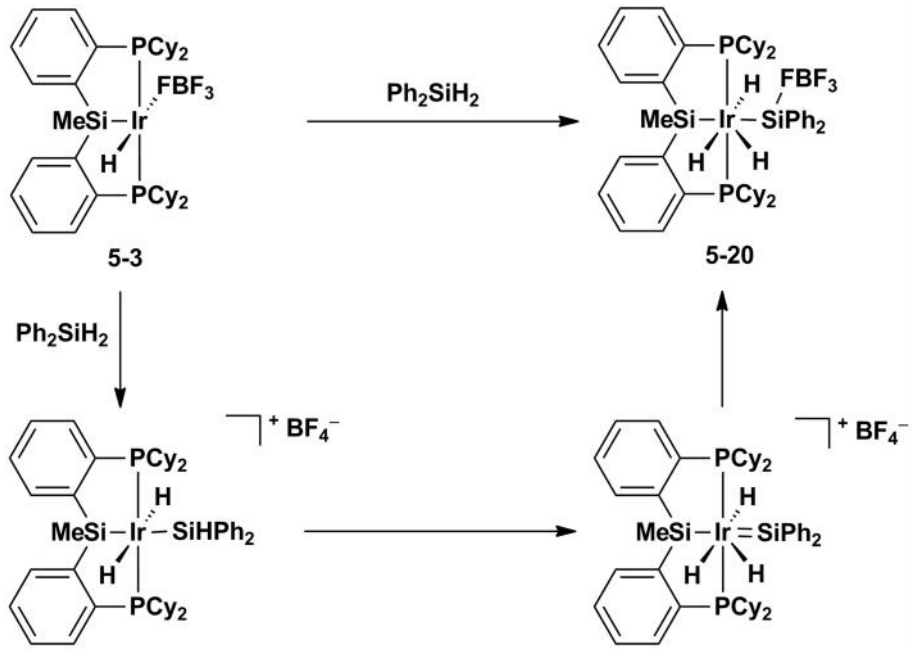

Scheme 5-12. Possible mechanism for formation of [Cy-PSiP]Ir(H)$_3$(SiPh$_2$BF$_4$) (**5-20**)

The reactivity of the primary silane PhSiH$_3$ was also investigated during the course of these studies. A fluorobenzene solution of **5-1** reacted cleanly with one equiv of PhSiH$_3$ to quantitatively (^{31}P NMR) generate a new product (**5-21**) featuring an AB quartet centered at 43.6 ppm by ^{31}P NMR spectroscopy, consistent with a [Cy-PSiP]Ir species that contains inequivalent phosphorus donors. Complex **5-21** was isolated as an orange solid in 96% yield. Spectroscopic data for **5-21** (benzene-d_6) are consistent with a formulation of the type [Cy-PSP]Ir(H)$_3$(SiHPhOTf) (Scheme 5-13). Thus, the ^{1}H NMR spectrum of **5-21** features three upfield-shifted resonances are observed at -9.21, -9.48, and -11.80 ppm, corresponding to the Ir-*H* ligands, respectively. In addition, the ^{1}H NMR spectrum of **5-21** contains an Si-*H* resonance at 7.7 ppm for the Ir-Si*H*PhOTF ligand that correlates to a ^{29}Si resonance at 32.5 ppm ($^1J_{SiH}$ = 190 Hz) in a ^{29}Si-^{1}H HMQC experiment. The Ir-*Si*Me group in the ligand backbone gives rise to a ^{29}Si NMR resonance at 31.5 ppm (^{29}Si-^{1}H HMBC). Moreover, the IR spectrum of **5-21** confirms the presence of terminal Ir-bound hydride atoms and an Si-H with peaks at 2113, 2033,

and 1975 cm^{-1}. All other [Cy-PSiP]Ir$(H)_3$X complexes described so far exhibit two IR bands for the Ir-H groups and no Si-H band. The formation of this complex likely occurs via a similar mechanism to that proposed for formation of **5-18** and **5-20** (Schemes 5-11 and 5-12) α-hydride migration from Si to Ir to form a silylene intermediate that could coordinate OTf to generate the observed product. Moreover, reactivity of **5-3** and **5-6** with the primary silane $PhSiH_3$ led to complex reaction mixtures with no isolable products.

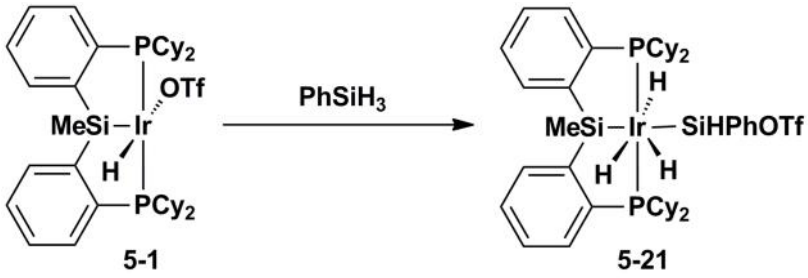

Scheme 5-13. Synthesis of [Cy-PSiP]Ir$(H)_3(SiHPh_2OTf)$ (**5-21**)

With respect to the reactivity of silanes with [Cy-PSiP]Ir^{III} complexes described herein, the unequivocal assignment of structure is challenging due to the presence of both silyl and hydride ligands which can exhibit non-classical interligand interactions. There have been many literature examples and reviews highlighting the difficulty in unambiguously assigning the extent of Si-H activation as either a classical silyl hydride or a non-classical η^2-silane, due to the potential for secondary interaction between Si and H atoms within the metal sphere.[93,99,100] Although no long range Si-H coupling constants were observed in ^{29}Si-^{1}H HMBC experiments for the [Cy-PSiP]Ir^{III} silyl polyhydride complexes, this does not preclude a σ-interaction as $^{1}J_{SiH}$ and $^{2}J_{SiH}$ values could have opposite signs and lead to a lower observed J_{SiH}.[100]

5.3 Conclusions

In summary, the work discussed in this chapter highlights the continuing study of new bis(phosphino)silyl Ir pincer complexes, with focus placed on the synthesis of (PSiP)Ir^{III} species, including their ability to activate E-H bonds. Specifically, the work in this chapter places emphasis on modifying the electrophilicity of the Ir center by targeting Ir^{III} complexes of the type [R-PSiP]Ir(R')(X) (R = Cy, ^{i}Pr; R' = H, CH_3; X = OTf, BF_4, and $B(C_6F_5)_4$). Solid state structures showed that both OTf and BF_4 coordinated directly to the metal center. Through the addition of coordinating ligands, the lability of the anions were assessed showing that both OTf and BF_4 anions can be displaced in solution.

The reactivity of [Cy-PSiP]Ir(H)(X) (X = OTf, BF_4, and $B(C_6F_5)_4$) with simple hydrocarbons, terminal alkynes and aldehydes was probed. However the most extensive reactivity of these Ir^{III} species was observed with hydrosilanes, yielding products of Si-H activation where the coordinating anion (X) often behaves in a non-innocent fashion and is involved in formation of the final products. Specifically, the reaction of [Cy-PSiP]Ir(H)(OTf) (**5-1**) or [Cy-PSiP]Ir(H)(BF_4) (**5-3**) with two equivalents of Et_3SiH led to the formation of [Cy-PSiP]Ir(H)$_3$SiEt_3 (**5-14**) and the hydroborate complex [Cy-PSiP]Ir(H)(η^2:η^2-H_2BF_2) (**5-16**), respectively. Formation of **5-16** resulting from loss of two equivalents of Et_3SiF highlights the non-innocent nature of the anions. In the case of {[Cy-PSiP]Ir(H)}$^+$[$B(C_6F_5)_4$]$^-$ (**5-5**) reaction with Mes_2SiH_2 generated the dimesitylsilane complex [Cy-PSiP]Ir(H)(η^2:η^2-H_2SiMes_2) (**5-17**) that features bis(σ-Si–H) coordination.

Finally, The reaction of Ph_2SiH_2 or $PhSiH_3$ with [Cy-PSiP]Ir(H)(OTf) (**5-1**) yielded [Cy-PSiP]Ir(H)$_3$(SiOTfR^1R^2) (R^1 = R^2 =Ph or R^1 = H and R^2 = Ph), proposed to form via initial Si-H cleavage, followed by OTf ligand dissociation and an α-hydride migration from Si to Ir to generate an intermediate cationic Ir silylene hydride species that subsequently coordinated the OTf anion. In comparable reactivity, [Cy-

PSiP]Ir(H)(BF_4) (**5-3**) reacted with Ph_2SiH_2 to produce the analogue [Cy-PSiP]Ir(H)$_3$(Si(BF_4)Ph_2) (**5-20**), where the BF_4^- anion is coordinated to the Si center.

5.4 Experimental Section

5.4.1 General Considerations

All experiments were conducted under nitrogen in an MBraun glovebox or using standard Schlenk techniques. Dry, oxygen-free solvents were used unless otherwise indicated. All non-deuterated solvents were deoxygenated and dried by sparging with nitrogen and subsequent passage through a double-column solvent purification system purchased from MBraun Inc. Tetrahydrofuran and diethyl ether were purified over two activated alumina columns, while benzene, toluene, and pentane were purified over one activated alumina column and one column packed with activated Q-5. All purified solvents were stored over 4 Å molecular sieves. Benzene-d_6 and bromobenzene-d_5 were degassed via three freeze-pump-thaw cycles and stored over 4 Å molecular sieves. All other reagents, were purchased from Aldrich and used without further purification. Unless otherwise stated, ^{1}H, ^{13}C, ^{31}P NMR, and ^{29}Si characterization data were collected at 300K on a Bruker AV-500 spectrometer operating at 500.1, 125.8, 202.5, 50.7 and 99.4 MHz (respectively) with chemical shifts reported in parts per million downfield of $SiMe_4$ (for ^{1}H, ^{13}C, and ^{29}Si) or 85% H_3PO_4 in D_2O (for ^{31}P). All ^{11}B and ^{19}F characterization data were collected at 300K on a Bruker AV-300 spectrometer operating at 96.3 and 282.3 MHz with chemical shifts reported in parts per million downfield of BF_3•OEt_2 and relative to a standard sample of 0.5% $CF_3C_6H_5$ in chloroform-*d* at -63.7 ppm, respectively. ^{1}H and ^{13}C NMR chemical shift assignments are based on data obtained from ^{13}C-DEPTQ, ^{1}H-^{1}H COSY, ^{1}H-^{13}C HSQC, and ^{1}H-^{13}C HMBC NMR experiments. ^{29}Si NMR assignments are based on ^{1}H-^{29}Si HMQC and ^{1}H-^{29}Si HMBC experiments. In some cases, fewer than expected unique ^{13}C NMR resonances were observed, despite prolonged acquisition times. Relaxation rate (T_1) experiments were

measured using the T_1 null method. This technique involves finding the value of the recovery delay in the standard inversion recovery experiment that yields a null signal (τ_{null}) and calculating T_1 according to $T_1 = 1.443(\tau_{null})$.[92] Elemental analyses were performed by Canadian Microanalytical Service Ltd. of Delta, British Columbia, Canada and by Columbia Analytical Services of Tucson, Arizona. Infrared spectra were recorded as thin films between NaCl plates using a Bruker TENSOR 27 FT-IR spectrometer at a resolution of 4 cm^{-1}. X-ray data collection, solution, and refinement were carried out by Drs. Robert MacDonald and Michael J. Ferguson at the University of Alberta X-ray Crystallography Laboratory, Edmonton, Alberta.

5.4.2 Synthetic Details and Characterization Data

[Cy-PSiP]Ir(H)OTf (5-1). A solution of AgOTf (0.031g, 0.122 mmol) in ca. 5 mL of CH_2Cl_2 was added dropwise via pipette to a solution of **2-1** (0.100 g, 0.122 mmol) in ca. 5 mL of CH_2Cl_2 or C_6H_5F at room temperature. An immediate precipitate was observed with no observable color change from yellow. The reaction mixture was filtered through Celite and dried under vacuum. The remaining solid was triturated with pentane (3 × 5 mL) to afford **5-1** as a pale yellow solid (0.107 g, 94%). ^{1}H NMR (500 MHz, benzene-d_6): δ 7.92 (d, 2 H, J = 7 Hz, H_{arom}), 7.32 (m, 2 H, H_{arom}), 7.18 (t, 2 H, J = 7 Hz, H_{arom}), 7.08 (t, 2 H, J = 8 Hz, H_{arom}), 2.94 (m, 2 H, P*Cy*), 2.79 (m, 2 H, P*Cy*), 2.49 (m, 2 H, P*Cy*), 2.29 (m, 2 H, P*Cy*), 2.28 (m, 2 H, P*Cy*), 2.03 (m, 2 H, P*Cy*), 1.69 (m, 2 H, P*Cy*), 1.61 – 1.17 (overlapping resonances, 24 H, P*Cy*), 0.79 – 0.71 (overlapping resonances, 7 H, P*Cy* + Si*Me*; Si*Me* at 0.77), -20.21 (t, 1 H, $^2J_{HP}$ = 15 Hz, Ir*H*). ^{13}C{^{1}H} NMR (125.8 MHz, benzene-d_6): δ 156.3 (C_{arom}), 141.1 (C_{arom}), 132.3 (apparent t, J = 9 Hz, CH$_{arom}$), 131.4 (CH$_{arom}$), 130.1 (CH$_{arom}$), 128.3 (CH$_{arom}$), 35.5 (apparent t, J = 16 Hz, CH$_{Cy}$), 35.2 (apparent t, J = 12 Hz, CH$_{Cy}$), 31.0 (CH$_{2Cy}$), 30.1 (CH$_{2Cy}$), 29.9 (CH$_{2Cy}$), 28.6 (CH$_{2Cy}$), 28.0 – 27.4 (overlapping resonances, CH$_{2Cy}$), 26.9 (CH$_{2Cy}$), 2.5 (Si*Me*). ^{31}P{^{1}H} NMR (202.5 MHz, benzene-d_6): δ 61.2. ^{29}Si NMR (99.4 MHz, benzene-d_6): δ 7.3. ^{19}F

NMR (282.4 MHz, benzene-d_6): δ -76.1. IR (film, cm^{-1}): 2283 (m, Ir-*H*). X-Ray quality crystals of **5-1** were grown from vapour diffusion of pentane into a concentrated benzene solution at room temperature.

[^{i}Pr-PSiP]Ir(H)OTf (**5-2**). A solution of AgOTf (0.039 g, 0.152 mmol) in ca. 5 mL of C_6H_5F was added dropwise via pipette to a solution of **3-2** (0.100 g, 0.152 mmol) in ca. 5 mL of C_6H_5F at room temperature. An immediate precipitate was observed with no observable color change from yellow. The reaction mixture was filtered through Celite and dried under vacuum. The remaining solid was triturated with pentane (3 × 5 mL) to afford **5-2** as a pale yellow solid (0.112 g, 96%). ^{1}H NMR (500 MHz, benzene-d_6): δ 7.86 (d, 2 H, J = 7 Hz, H_{arom}), 7.15 – 7.11 (overlapping resonances, 4 H, H_{arom}), 7.01 (t, 2 H, J = 7 Hz, H_{arom}), 3.05 (m, 2 H, P^i*Pr*), 2.72 (m, 2 H, P^i*Pr*), 1.44 (m, 6 H, P^i*Pr*), 1.10 (m, 6 H, P^i*Pr*), 0.94 (m, 6 H, P^i*Pr*), 0.78 (m, 6 H, P^i*Pr*), 0.69 (s, 3 H, Si*Me*), -29.49 (t, 1 H, $^2J_{HP}$ = 15 Hz, Ir*H*). ^{13}C{^{1}H} NMR (125.8 MHz, benzene-d_6): δ 156.0 (apparent t, J = 20 Hz, C_{arom}), 140.5 (apparent t, J = 26 Hz, C_{arom}), 132.0 (apparent t, J = 9 Hz, CH_{arom}), 131.0 (CH_{arom}), 130.0 (CH_{arom}), 128.0 (CH_{arom}), 26.2 (apparent t, J = 16 Hz, CH_{iPr}), 25.7 (apparent t, J = 12 Hz, CH_{iPr}), 20.6 (CH_{3iPr}), 19.8 (CH_{3iPr}), 18.7 (CH_{3iPr}), 17.7 (CH_{3iPr}), 2.9 (Si*Me*). ^{31}P{^{1}H} NMR (202.5 MHz, benzene-d_6): δ 67.6. ^{29}Si NMR (99.4 MHz, benzene-d_6): δ 8.0. ^{19}F NMR (282.4 MHz, benzene-d_6): δ -76.4. IR (film, cm^{-1}): 2280 (m, Ir-*H*).

[Cy-PSiP]Ir(H)(FBF_3) (5-3). A solution of $AgBF_4$ (0.06g, 0.183 mmol) in ca. 5 mL of CH_2Cl_2 was added dropwise via pipette to a solution of **2-1** (0.150 g, 0.183 mmol) in ca. 5 mL of CH_2Cl_2 at room temperature. An immediate precipitate was observed with no observable color change from yellow. The reaction mixture was filtered through Celite and dried under vacuum. The remaining solid was triturated with pentane (3 × 5 mL) to afford **5-3** as a pale yellow/orange solid (0.155 g, 72%). ^{1}H NMR (500 MHz, benzene-d_6): δ 7.91 (d, 2 H, J = 8 Hz, H_{arom}), 7.30 (m, 2 H, H_{arom}), 7.18 (t, 2 H, J = 7 Hz, H_{arom}), 7.08 (t, 2 H, J = 8 Hz, H_{arom}), 2.89 (m, 2 H, P*Cy*), 2.68 (m, 2 H, P*Cy*), 2.41 (m, 2

H, P*Cy*), 2.30 (m, 2 H, P*Cy*), 2.28 (m, 2 H, P*Cy*), 2.03 (m, 2 H, P*Cy*), 1.83 – 1.76 (overlapping resonances, 4 H, P*Cy*), 1.64 – 1.46 (overlapping resonances, 14 H, P*Cy*), 1.39 – 1.00 (overlapping resonances, 14 H, P*Cy*), 0.74 (s, 3 H, Si*Me*), -32.98 (t, 1 H, $^{2}J_{HP}$ = 15 Hz, Ir*H*). $^{13}C\{^{1}H\}$ NMR (125.8 MHz, benzene-d_6): δ 156.0 (apparent t, J = 20 Hz, C_{arom}), 140.9 (apparent t, J = 26 Hz, C_{arom}), 132.2 (apparent t, J = 13 Hz, CH$_{arom}$), 131.3 (CH$_{arom}$), 130.0 (CH$_{arom}$), 128.1 (CH$_{arom}$), 36.3 (apparent t, J = 11 Hz, CH$_{Cy}$), 35.8 (apparent t, J = 15 Hz, CH$_{Cy}$), 34.8 (CH$_{2Cy}$), 30.6 (CH$_{2Cy}$), 29.9 (CH$_{2Cy}$), 29.5 (CH$_{2Cy}$), 28.6 (CH$_{2Cy}$), 27.7 – 27.4 (overlapping resonances, CH$_{2Cy}$), 26.6 (CH$_{2Cy}$), 2.9 (Si*Me*). $^{31}P\{^{1}H\}$ NMR (202.5 MHz, benzene-d_6): δ 62.2. ^{29}Si NMR (99.4 MHz, benzene-d_6): δ 5.6. ^{11}B NMR (96.3 MHz, benzene-d_6): δ 0.6. ^{19}F NMR (282.4 MHz, benzene-d_6): δ -177.6. IR (film, cm^{-1}): 1960 (m, Ir-*H*). Anal. Calcd for $C_{37}H_{56}BF_4IrP_2Si$: C, 51.09; H, 6.49. Found: C, 50.79; H, 6.26. X-Ray quality crystals of **5-3** were grown from vapour diffusion of pentane into a concentrated fluorobenzene solution at room temperature.

[^{i}Pr-PSiP]Ir(H)(FBF$_3$) (5-4). A solution of $AgBF_4$ (0.034 g, 0.173 mmol) in ca. 5 mL of C_6H_5F was added dropwise via pipette to a solution of **3-2** (0.114 g, 0.173 mmol) in ca. 5 mL of C_6H_5F at room temperature. An immediate precipitate was observed with no observable color change from yellow. The reaction mixture was filtered through Celite and dried under vacuum. The remaining solid was triturated with pentane (3 × 5 mL) to afford **5-4** as a pale yellow/orange solid (0.111 g, 92%). ^{1}H NMR (500 MHz, benzene-d_6): δ 7.86 (d, 2 H, J = 7 Hz, H_{arom}), 7.15 – 7.03 (overlapping resonances, 4 H, H_{arom}), 7.03 (t, 2 H, J = 7 Hz, H_{arom}), 2.95 (m, 2 H, P^{i}*Pr*), 2.65 (m, 2 H, P^{i}*Pr*), 1.43 (m, 6 H, P^{i}*Pr*), 1.13 (m, 6 H, P^{i}*Pr*), 0.94 (m, 6 H, P^{i}*Pr*), 0.74 (m, 6 H, P^{i}*Pr*), 0.65 (s, 3 H, Si*Me*), - 33.30 (t, 1 H, $^{2}J_{HP}$ = 15 Hz, Ir*H*). $^{13}C\{^{1}H\}$ NMR (125.8 MHz, benzene-d_6): δ 156.0 (apparent t, J = 20 Hz, C_{arom}), 140.5 (apparent t, J = 26 Hz, C_{arom}), 132.1 (apparent t, J = 9 Hz, CH$_{arom}$), 131.1 (CH$_{arom}$), 130.0 (CH$_{arom}$), 127.3 (CH$_{arom}$), 26.7 (apparent t, J = 11 Hz, CH$_{iPr}$), 26.4 (apparent t, J = 15 Hz, CH$_{iPr}$), 20.4 (CH$_{3iPr}$), 19.7 (CH$_{3iPr}$), 18.4 (CH$_{3iPr}$), 18.0 (CH$_{3iPr}$), 2.7 (Si*Me*). $^{31}P\{^{1}H\}$ NMR (202.5 MHz, benzene-d_6): δ 69.1. ^{29}Si

NMR (99.4 MHz, benzene-d_6): δ 5.4. ^{11}B NMR (96.3 MHz, benzene-d_6): δ 0.7. ^{19}F NMR (282.4 MHz, benzene-d_6): δ - 179.1 (br s). IR (film, cm^{-1}): 2199 (m, Ir-*H*).

[Cy-PSiP]Ir(H){B(C$_6$F$_5$)$_4$} (5-5). A solution of LiB(C$_6$F$_5$)$_4$·2Et$_2$O (0.106g, 0.122 mmol) in ca. 5 mL of CH_2Cl_2 was added dropwise via pipette to a solution of **2-1** (0.100 g, 0.122 mmol) in ca. 5 mL of CH_2Cl_2 at room temperature. An immediate color change from yellow to orange was observed. The reaction mixture was filtered through Celite and dried under vacuum. The remaining solid was triturated with pentane (3 × 5 mL) to afford **5-5** as an orange solid (0.173 g, 97%). ^{1}H NMR (500 MHz, benzene-d_6): δ 7.91 (d, 2 H, J = 7 Hz, H_{arom}), 7.30 (m, 2 H, H_{arom}), 7.21 (t, 2 H, J = 7 Hz, H_{arom}), 7.12 (t, 2 H, J = 8 Hz, H_{arom}), 2.72 (m, 2 H, P*Cy*), 2.59 (m, 2 H, P*Cy*), 2.19 (m, 2 H, P*Cy*), 2.10 (m, 2 H, P*Cy*), 1.82 – 0.72 (overlapping resonances, 36 H, P*Cy*), 0.65 (s, 3 H, Si*Me*), -25.1 (br s, 1 H, Ir*H*). ^{13}C{^{1}H} NMR (125.8 MHz, benzene-d_6): δ 150.4 (C_{arom}), 148.4 (C_{arom}), 140.3 (C_{arom}), 138.3 (C_{arom}), 136.3 (C_{arom}), 132.3 (CH_{arom}), 131.2 (CH_{arom}), 130.5 (CH_{arom}), 130.2 (CH_{arom}), 35.3 (CH_{Cy}), 34.9 (CH_{Cy}), 31.0 (CH_{2Cy}), 30.6 (CH_{2Cy}), 29.7 (CH_{2Cy}), 28.0 – 26.5 (overlapping resonances, CH_{2Cy}), 4.6 (Si*Me*). ^{31}P{^{1}H} NMR (202.5 MHz, benzene-d_6): δ 61.5. ^{29}Si NMR (99.4 MHz, benzene-d_6): δ 8.9. ^{11}B NMR (96.3 MHz, benzene-d_6): δ -16.0. ^{19}F NMR (282.4 MHz, benzene-d_6): δ -132.6 (br s, B(C$_6$*F*$_5$)$_4$), -162.0 (J = 22 Hz, B(C$_6$*F*$_5$)$_4$), -166.2 (br t, J = 18 Hz, B(C$_6$*F*$_5$)$_4$). IR (film, cm^{-1}): 2246 (m, Ir-*H*). Anal. Calcd for $C_{61}H_{56}BF_{20}IrP_2Si$: C, 50.11; H, 3.86. Found: C, 49.85; H, 4.01.

[^{i}Pr-PSiP]Ir(H){B(C$_6$F$_5$)$_4$} (5-6). A solution of LiB(C$_6$F$_5$)$_4$·2Et$_2$O (0.040g, 0.023 mmol) in ca. 2 mL of C_6H_5F was added dropwise via pipette to a solution of **3-2** (0.030 g, 0.023 mmol) in ca. 2 mL of C_6H_5F at room temperature. An immediate color change from yellow to orange was observed. The reaction mixture was filtered through Celite and dried under vacuum. The remaining solid was triturated with pentane (3 × 5 mL) to afford **5-6** as an orange solid (0.025 g, 84%). ^{1}H NMR (500 MHz, benzene-d_6): δ 7.83 (d, 2 H, J = 7 Hz, H_{arom}), 7.20 – 7.12 (overlapping resonances, 6 H, H_{arom}), 2.71 (m, 2 H,

P*Cy*), 2.57 (m, 2 H, P*Cy*), 1.13 (m, 6 H, P^{i}*Pr*), 1.01 (m, 6 H, P^{i}*Pr*), 0.92 (m, 6 H, P^{i}*Pr*), 0.73 (m, 6 H, P^{i}*Pr*), 0.58 (s, 3 H, Si*Me*), -27.03 (br t, 1 H, J = 16 Hz, Ir*H*). ^{13}C{^{1}H} NMR (125.8 MHz, benzene-d_6): δ 150.4 (C_{arom}), 148.5 (C_{arom}), 140.3 (C_{arom}), 138.4 (C_{arom}), 136.5 (C_{arom}), 132.3 (CH_{arom}), 132.1 (apparent t, J = 16 Hz, CH_{arom}), 130.8 (CH_{arom}), 129.2 (CH_{arom}), 128.7 (CH_{arom}), 27.1 (br m, CH_{iPr}), 20.2 (CH_{3iPr}), 18.1 (CH_{3iPr}), 15.0 (CH_{3iPr}), 14.6 (CH_{3iPr}), 4.1 (Si*Me*). ^{31}P{^{1}H} NMR (202.5 MHz, benzene-d_6): δ 72.1. ^{29}Si NMR (99.4 MHz, benzene-d_6): δ 11.8. ^{11}B NMR (96.3 MHz, benzene-d_6): δ -16.0. ^{19}F NMR (282.4 MHz, benzene-d_6): δ -132.5 (d, J = 8.5 Hz, $B(C_6F_5)_4$), -162.2 (t, J = 20 Hz, $B(C_6F_5)_4$), -166.5 (br t, J = 17 Hz, $B(C_6F_5)_4$). IR (film, cm^{-1}): 2268 (m, Ir-*H*).

{[Cy-PSiP]Ir(H)(PMe$_3$)$_2$}$^{+}$[OTf]$^{-}$ (5-7). Two equiv of PMe_3 (9.8 μL, 0.0073 g, 0.097 mmol) were syringed into a solution of [Cy-PSiP]Ir(H)OTf (0.045 g, 0.048 mmol) in ca. 4 mL of benzene at room temperature. An immediate color change from yellow to pale yellow was observed. The reaction mixture was dried under vacuum. The remaining solid was triturated with pentane (3 × 3 mL) to afford **5-7** as a pale yellow solid (0.0414 g, 80%). ^{1}H NMR (500 MHz, benzene-d_6): δ 7.59 (d, 1 H, J = 7 Hz, H_{arom}), 7.54 (m, H_{arom}), 7.15 – 7.10 (overlapping resonances, 4 H, H_{arom}), 2.30 (m, 2 H, P*Cy*), 2.11 – 1.87 (overlapping resonances, 18 H, P*Cy* + P*Me*$_3$; P*Me*$_3$ at 1.96), 1.71 – 1.04 (overlapping resonances, 42 H, P*Cy* + P*Me*$_3$; P*Me*$_3$ at 1.42), 0.45 (s, 3 H, Si*Me*), -14.91 (m, Ir*H*). ^{13}C{^{1}H} NMR (125.8 MHz, benzene-d$_6$): δ 155.1 (C_{arom}), 144.1 (C_{arom}), 132.2 (apparent t, J = 9 Hz, CH_{arom}), 131.5 (CH_{arom}), 129.9 (CH_{arom}), 128.4 (CH_{arom}), 42.7 (apparent t, J = 14 Hz, CH_{Cy}), 40.3 (apparent t, J = 8 Hz, CH_{Cy}), 30.0 –26.5 (overlapping resonances, CH_{2Cy}), 25.1 (apparent d, J = 28 Hz, P*Me*$_3$), 24.1 (apparent d, J = 30 Hz, P*Me*$_3$), 9.0 (Si*Me*). ^{31}P{^{1}H} NMR (202.5 MHz, benzene-d_6): δ 26.6 (br s, Cy-*P*Si*P*), -71.1 (m, *P*Me$_3$), -73.0 (m, *P*Me$_3$). ^{29}Si NMR (99.4 MHz, benzene-d$_6$): δ 36.8. ^{19}F NMR (282.4 MHz, benzene-d$_6$): δ -77.3. IR (film, cm^{-1}): 2166 (m, Ir-H). Anal. Calcd for $C_{44}H_{74}F_3IrO_3P_4SSi$: C, 48.74; H, 6.88. Found: C, 48.88; H, 6.62.

[Cy-PSiP]Ir(H)(OTf)(DMAP) (5-8). A solution of 4-dimethylaminopyridine (0.004 g, 0.032 mmol) in ca. 2 mL of benzene was added dropwise via pipette to a solution of **5-1** (0.030 g, 0.032 mmol) in ca. 2 mL of benzene at room temperature. An immediate color change from yellow to pale yellow was observed. The reaction mixture was dried under vacuum. The remaining solid was triturated with pentane (3 × 3 mL) to afford **5-8** as a pale yellow solid (0.032 g, 96%). The NMR spectra of **5-8** at 300K exhibit line broadening. Where possible, variable temperature characterization data are provided. ^{1}H NMR (300K, 500 MHz, benzene-d_6): δ 8.72 (d, 2 H, J = 7 Hz, H_{arom}), 8.09 (d, 2 H, J = 7 Hz, H_{arom}), 7.47 (m, 2 H, H_{arom}), 7.26 (t, 2 H, J = 7 Hz, H_{arom}), 7.15 (m, 2 H, H_{arom}), 6.48 (d, 2 H, J = 5 Hz, H_{arom}), 2.31 – 2.22 (overlapping resonances, 10 H, P*Cy* + Me_{DMAP}), 2.09 (br s, 2 H, P*Cy*), 1.95 (br m, 4 H, P*Cy*), 1.80 (m, 2 H, P*Cy*), 1.70 – 0.87 (overlapping resonances, 28 H, P*Cy*), 0.75 (s, 3 H, Si*Me*), -21.69 (br s, 1 H, Ir*H*). ^{13}C{^{1}H} NMR (125.8 MHz, benzene-d_6): δ 154.6 (C_{arom}), 153.6 (CH_{arom}), 143.0 (C_{arom}), 132.4 (CH_{arom}), 130.6 (CH_{arom}), 129.8 (CH_{arom}), 129.1 (CH_{arom}), 38.9 (Me_{DMAP}), 36.7 (CH_{Cy}), 36.2 (CH_{Cy}), 29.7 (CH_{2Cy}), 29.1 (CH_{2Cy}), 28.4 (CH_{2Cy}), 27.9 – 26.7 (overlapping resonances, CH_{2Cy}), 26.1 (CH_{2Cy}), 4.7 (Si*Me*). ^{31}P{^{1}H} NMR (300K, 202.5 MHz, benzene-d_6): δ 50.3 (br s). ^{31}P{^{1}H} NMR (243K, 202.5 MHz, benzene-d_6): δ 50.3 (s, **5-8c**), 33.5 (s, **5-8a**), 33.1 (s, **5-8b**). ^{29}Si NMR (99.4 MHz, benzene-d_6): δ 5.6. ^{19}F NMR (282.4 MHz, benzene-d_6): δ -77.3. IR (film, cm^{-1}): 2184 (m, Ir-*H*).

{[Cy-PSiP]Ir(H)(PMe_3)}$^{+}$[BF_4]$^{-}$ (5-9). One equiv of PMe_3 (3.3 μL, 0.0044 g, 0.057 mmol) was syringed into a solution of **5-1** (0.050 g, 0.057 mmol) in ca. 4 mL of benzene at room temperature. An immediate color change from yellow to pale yellow was observed. The reaction mixture was dried under vacuum. The remaining solid was triturated with pentane (3 × 3 mL) to afford **5-9** as a pale yellow solid (0.047 g, 87%). ^{1}H NMR (500 MHz, benzene-d_6): δ 7.82 (d, 1 H, J = 7 Hz, H_{arom}), 7.31 (m, H_{arom}), 7.13 – 7.04 (overlapping resonances, 4 H, H_{arom}), 3.05 (m, 2 H, P*Cy*), 2.33 – 1.64 (overlapping resonances, 29 H, P*Cy* + PMe_3; PMe_3 at 1.79), 1.44 – 1.02 (overlapping resonances, 18 H,

P*Cy*), 0.60 (m, P*Cy*), 0.55 (s, 3 H, Si*Me*), 0.33 (m, P*Cy*), -10.62 (dt, 1 H, $^2J_{HPtrans}$ = 105 Hz, $^2J_{HPcis}$ = 19 Hz, Ir*H*). $^{13}C\{^1H\}$ NMR (125.8 MHz, benzene-d_6): δ 154.4 (C_{arom}), 142.8 (C_{arom}), 131.9 (apparent t, J = 9 Hz, CH_{arom}), 130.1 (CH_{arom}), 129.4 (CH_{arom}), 127.7 (CH_{arom}), 36.7 – 35.7 (overlapping resonances, CH_{Cy}), 30.8 (CH_{2Cy}), 29.7 (CH_{2Cy}), 28.1 – 26.2 (overlapping resonances, CH_{2Cy}), 20.6 (apparent d, J = 29 Hz, PMe_3), 4.0 (Si*Me*). $^{31}P\{^1H\}$ NMR (202.5 MHz, benzene-d_6): δ 52.8 (d, 2 P, $^2J_{PP}$ = 16 Hz, *P*Si*P*), - 22.3 (t, 1 P, $^2J_{PP}$ = 16 Hz, *P*Me$_3$). ^{29}Si NMR (99.4 MHz, benzene-d_6): δ 4.5. ^{11}B NMR (96.3 MHz, benzene-d_6): δ 0.2. (^{19}F NMR (282.4 MHz, benzene-d_6): δ -152.1. IR (film, cm^{-1}): 2104 (m, Ir-H).

{[Cy-PSiP]Ir(H)(DMAP)}$^+$[BF$_4$]$^-$ (5-10). A solution of 4-dimethylaminopyridine (0.006 g, 0.052 mmol) in ca. 3 mL of benzene was added dropwise via pipette to a solution of **5-3** (0.045 g, 0.052 mmol) in ca. 3 mL of benzene at room temperature. An immediate color change from yellow to pale yellow was observed. The reaction mixture was dried under vacuum. The remaining solid was triturated with pentane (3 × 3 mL) to afford **5-10** as a pale yellow solid (0.032 g, 96%). ^{1}H NMR (500 MHz, benzene-d_6): δ 8.43 (d, 2 H, J = 7 Hz, H_{arom}), 8.02 (d, 2 H, J = 7 Hz, H_{arom}), 7.40 (m, 2 H, H_{arom}), 7.25 (t, 2 H, J = 7 Hz, H_{arom}), 7.16 (m, 2 H, H_{arom}), 6.67 (d, 2 H, J = 5 Hz, H_{arom}), 2.62 (m, 2 H, P*Cy*), 2.46 (br s, 6 H, Me_{DMAP}), 2.41 (br s, 3 H, Me_{DMAP}), 2.22 – 2.15 (overlapping resonances, 8 H, P*Cy*), 1.67 – 0.80 (overlapping resonances, 40 H, P*Cy*), 0.75 (s, 3 H, Si*Me*), 0.62 (m, 2 H, P*Cy*), -21.35 (br s, 1 H, Ir*H*). $^{13}C\{^1H\}$ NMR (125.8 MHz, benzene-d_6): δ 156.5 (CH_{arom}), 154.7 (C_{arom}), 142.4 (C_{arom}), 132.2 (apparent t, J = 9 Hz, CH_{arom}), 130.8 (CH_{arom}), 130.0 (CH_{arom}), 128.4 (CH_{arom}), 39.1 (Me_{DMAP}), 37.1 (CH_{Cy}), 30.0 (CH_{2Cy}), 29.4 (CH_{2Cy}), 28.5 (CH_{2Cy}), 27.6 – 26.7 (overlapping resonances, CH_{2Cy}), 4.4 (Si*Me*). $^{31}P\{^1H\}$ NMR (303K, 202.5 MHz, benzene-d_6): δ 55.0 (br s). ^{29}Si NMR (99.4 MHz, benzene-d_6): δ 8.0. ^{11}B NMR (96.3 MHz, benzene-d_6): δ 0.4. ^{19}F NMR (282.4 MHz, benzene-d_6): δ -151.4. IR (film, cm^{-1}): 2184 (m, Ir-*H*).

[Cy-PSiP]Ir(Me)I (5-11). MeI (7.7 μL, 0.18 g, 0.123 mmol) was syringed into a solution of **2-3** (0.100 g, 0.123 mmol) in ca. 8 mL of THF at room temperature. A gradual colour change to red-brown was observed while stirring for 4 days at room temperature. The reaction mixture was dried under vacuum. The remaining solid was triturated with pentane (3 × 5 mL) to afford **5-10** as a dark orange-brown solid (0.059 g, 52%). ^{1}H NMR (500 MHz, benzene-d_6): δ 7.91 (d, 2 H, J = 7 Hz, H_{arom}), 7.40 (m, 2 H, H_{arom}), 7.22 (t, 2 H, J = 7 Hz, H_{arom}), 7.11 (t, 2 H, J = 7 Hz, H_{arom}), 3.37 (m, 2 H, P*Cy*), 2.88 (m, 2 H, P*Cy*), 2.40 (m, 2 H, P*Cy*), 2.11 (m, 2 H, P*Cy*), 2.07 (t, 3 H, $^{3}J_{HP}$ = 3 Hz, Ir-*Me*), 1.90 – 1.06 (overlapping resonances, 36 H, P*Cy*), 0.55 (s, 3 H, Si*Me*). ^{13}C{^{1}H} NMR (125.8 MHz, benzene-d_6): δ 163.1 (C_{arom}), 155.9 (C_{arom}), 133.2 (apparent t, J = 9 Hz, CH_{arom}), 131.7 (CH_{arom}), 130.2 (CH_{arom}), 41.2 (apparent t, J = 13 Hz, CH_{Cy}), 36.8 (apparent t, J = 13 Hz, CH_{Cy}), 31.4 (CH_{2Cy}), 30.6 (CH_{2Cy}), 30.4 (CH_{2Cy}), 9.3 (CH_{2Cy}), 28.3 – 26.8 (overlapping resonances, CH_{2Cy}), 4.0 (Si*Me*). ^{31}P{^{1}H} NMR (202.5 MHz, benzene-d_6): δ 35.7 (br s). ^{29}Si NMR (99.4 MHz, benzene-d_6): δ 24.6.

[Cy-PSiP]Ir(Me)OTf (5-12). A solution of AgOTf (0.014 g, 0.054 mmol) in ca. 3 mL of C_6H_5F was added dropwise via pipette to a solution of **5-11** (0.050 g, 0.054 mmol) in ca. 3 mL of C_6H_5F at room temperature. An immediate precipitate was observed with no observable color change from yellow. The reaction mixture was filtered through Celite and dried under vacuum. The remaining solid was triturated with pentane (3 × 5 mL) to afford **5-12** as a pale yellow solid (0.039 g, 76%). ^{1}H NMR (500 MHz, benzene-d_6): δ 7.37 (m, 2 H, H_{arom}), 7.13 – 7.09 (overlapping resonances, 2 H, H_{arom}), 6.64 – 6.61 (overlapping resonances, 2 H, H_{arom}), 6.50 – 6.46 (overlapping resonances, 2 H, H_{arom}), 6.20 (dd, J = 7 Hz, J = 4 Hz, H_{arom}), 3.12 (m, 1 H, P*Cy*), 2.70 – 2.59 (overlapping resonances, 4 H, P*Cy*), 2.39 – 1.96 (overlapping resonances, 9 H, P*Cy*), 1.80 – 1.18 (overlapping resonances, 22 H, P*Cy*), 1.14 (s, 3 H, Si*Me*), 1.10 – 0.91 (overlapping resonances, 8 H, P*Cy*), -0.12 (s, 3 H, Ir-*Me*). ^{13}C{^{1}H} NMR (125.8 MHz, benzene-d_6): δ 150.9 (C_{arom}), 145.8 (C_{arom}), 138.4 (C_{arom}), 137.4 (apparent d, J = 9 Hz,

CH_{arom}), 136.2 (C_{arom}), 133.3 (CH_{arom}), 133.1 (CH_{arom}), 132.0 (CH_{arom}), 130.8 (CH_{arom}), 129.9 (CH_{arom}), 129.1 (CH_{arom}), 128.6 (CH_{arom}), 127.4 (CH_{arom}), 123.3 (apparent d, J = 8 Hz, CH_{arom}), 43.9 – 43.5 (overlapping resonances, CH_{Cy}), 41.5 (CH_{Cy}), 37.7 (CH_{2Cy}), 37.5 (CH_{2Cy}), 36.1 – 34.9 (overlapping resonances, CH_{2Cy}), 4.4 (Si*Me*), 3.6 (Ir-*Me*). $^{31}P\{^1H\}$ NMR (202.5 MHz, benzene-d_6): δ 52.5 (d, $^2J_{PP}$ = 300 Hz), -24.5 (d, $^2J_{PP}$ = 300 Hz). ^{29}Si NMR (99.4 MHz, benzene-d_6): δ 14.5. ^{19}F NMR (282.4 MHz, benzene-d_6): δ -77.0.

[Cy-PSiP]Ir(H)(O=PhH)$_2$}$^+$[BF$_4$]$^-$ (5-13). 5 equiv of benzaldehyde (8.9 μL, 0.091 g, 0.086 mmol) were added to a 0.2 mL C_6D5_5Br solution of **5-3** (0.015 g, 0.017 mmol) at room temperature. An immediate color change from yellow to pale yellow was observed. The reaction mixture was transferred to an NMR tube and analyzed by use of NMR techniques, which confirmed the quantitative consumption of **5-3** and the clean formation of putative **5-13**. Attempts to isolate **5-13** by removing the volatile components in vacuo resulted in a 1:1 mixture of **4-6** and reformed **5-3**, as indicated by ^1H and ^{31}P NMR spectroscopy of the residue. Moreover, the presence of excess benzaldehyde in the in situ generated solution of **5-13** precluded the comprehensive assignment of ^1H and ^{13}C NMR resonances for this complex. ^1H NMR (500 MHz, bromobenzene-d_5): δ 8.26 (d, 2 H, J = 7 Hz, H_{arom}), 7.72 (br m, 2 H, H_{arom}), 7.49 (m, 2 H, H_{arom}), 7.38 (m, 2 H, H_{arom}), 3.07 – 0.89 (overlapping resonances, 44 H, P*Cy*), 0.87 (s, 3 H, Si*Me*). $^{13}C\{^1H\}$ NMR (125.8 MHz, cyclohexane-d_{12}): δ 191.3 (HC=O), 155.1 (C_{arom}), 140.6 (C_{arom}), 133.2 (CH_{arom}), 129.5 (CH_{arom}), 127.6 (CH_{arom}), 127.3 (CH_{arom}), 35.0 (apparent t, J = 11 Hz, CH_{Cy}), 34.2 (apparent t, J = 15 Hz, CH_{Cy}), 28.6 (CH_{2Cy}), 27.8 (CH_{2Cy}), 27.7 (CH_{2Cy}), 26.8 (CH_{2Cy}), 26.2 – 25.7 (overlapping resonances, CH_{2Cy}), 25.1 (CH_{2Cy}), 1.6 (Si*Me*). $^{31}P\{^1H\}$ NMR (bromobenzene-d_5): δ 57.8 (br s). ^{29}Si NMR (99.4 MHz, bromobenzene-d_5): δ 5.8. ^{11}B NMR (96.3 MHz, bromobenzene-d_5): δ -2.6. ^{19}F NMR (282.4 MHz, bromobenzene-d_5): δ -159.7 (br s). IR (C_6D_5Br, cm^{-1}): 2261 (m, Ir-*H*), 1704 (s, C=O).

[Cy-PSiP]Ir(H)$_3$SiEt$_3$ (5-14). Two equivs of Et_3SiH (20.6 μL, 0.015 g, 0.128 mmol) were syringed into a solution of **5-1** (0.060 g, 0.064 mmol) in ca. 4 mL of C_6H_5F at room temperature. An immediate color change from yellow to pale yellow was observed. The reaction mixture was dried under vacuum. The remaining solid was triturated with pentane (3 × 3 mL) to afford **5-14** as a pale yellow solid (0.046 g, 62%). ^{1}H NMR (500 MHz, benzene-d_6): δ 8.18 (d, 2 H, J = 7 Hz, H_{arom}), 7.34 (d, 2 H, J = 7 Hz, H_{arom}), 7.22 (t, 2 H, J = 7 Hz, H_{arom}), 7.06 (t, 2 H, J = 7 Hz, H_{arom}), 2.28 (m, 2 H, P*Cy*), 2.18 (m, 2 H, P*Cy*), 2.00 (m, 2 H, P*Cy*), 1.88 (m, 6 H, P*Cy*), 1.74 (m, 4 H, P*Cy*), 1.62 (m, 12 H, P*Cy*), 1.40 – 1.08 (overlapping resonances, 34 H, P*Cy* + Si*Et$_3$* + Si*Me*), -10.23 (br m, 2 H, Ir*H*), -12.48 (br m, 1 H, Ir*H*). ^{13}C{^{1}H} NMR (125.8 MHz, benzene-d_6): δ 159.0 (apparent t, J = 20 Hz, C_{arom}), 145.9 (C_{arom}), 133.1 (apparent t, J = 8 Hz, CH_{arom}), 129.5 (CH_{arom}), 129.3 (CH_{arom}), 127.1 (CH_{arom}), 36.7 (apparent t, J = 11 Hz, CH_{Cy}), 34.1 (CH_{Cy}), 30.8 (CH_{2Cy}), 30.2 (CH_{2Cy}), 29.3 (CH_{2Cy}), 28.5 (CH_{2Cy}), 27.9 – 26.9 (overlapping resonances, CH_{2Cy}), 13.3 (CH_{2SiEt3}), 9.5 (CH_{3SiEt3}), 8.2 (Si*Me*), 6.0 ($CH_{3SiEt3OTf}$), 5.2 ($CH_{2SiEt3OTf}$). ^{31}P{^{1}H} NMR (202.5 MHz, benzene-d_6): δ 42.7. ^{29}Si NMR (99.4 MHz, benzene-d_6): δ 44.0 ($SiEt_3OTf$), 37.4 (Si*Me*), 3.1 ($SiEt_3$). IR (film, cm^{-1}): 1997 (br m, Ir-*H*), 1965 (br m, Ir-*H*). Anal. Calcd for $C_{43}H_{764}IrP_2Si_2$: C, 57.10; H, 7.74. Found: C, 57.36; H, 8.17. X-Ray quality crystals of **[Cy-PSiP]Ir(H)SiEt$_3$ (5-15·(C$_6$H$_6$)$_{0.5}$)** were grown from vapour diffusion of pentane into a concentrated C_6H_6 solution at room temperature.

[Cy-PSiP]Ir(H)(η^2:η^2-BH$_2$F$_2$) (5-16). Method 1: Two equivs of Et_3SiH (22.0 μL, 0.016 g, 0.138 mmol) were syringed into a solution of **5-3** (0.060 g, 0.069 mmol) in ca. 4 mL of C_6H_5F at room temperature. An immediate color change from yellow to pale yellow was observed. The reaction mixture was dried under vacuum. The remaining solid was triturated with pentane (3 × 3 mL) to afford **5-16** as a pale yellow solid (0.056 g, 94%). **Method 2:** A solution of Mes_2SiH_2 (0.025 g, 0.092 mmol) in ca. 3 mL of C_6H_5F was added dropwise via pipette to a solution of **5-3** (0.040 g, 0.046 mmol) in ca. 3

mL of C_6H_5F at room temperature. An immediate colour change from yellow to pale yellow was observed. The reaction mixture was dried under vacuum. The remaining solid was triturated with pentane (3 × 5 mL) to afford **5-16** as a pale yellow solid (0.036 g, 94%). ^{1}H NMR (500 MHz, benzene-d_6): δ 8.12 (d, 2 H, J = 7 Hz, H_{arom}), 7.40 (m, 2 H, H_{arom}), 7.23 (t, 2 H, J = 8 Hz, H_{arom}), 7.09 (t, 2 H, J = 8 Hz, H_{arom}), 2.52 – 2.45 (overlapping resonances, 4 H, P*Cy*), 2.25 (m, 2 H, P*Cy*), 2.00 (m, 6 H, P*Cy*), 1.84 (m, 8 H, P*Cy*), 1.63 – 1.10 (overlapping resonances, 18 H, P*Cy*), 1.06 (s, 3 H, Si*Me*), 0.69 (m, 6 H, P*Cy*), -6.59 (br m, 1 H, Ir*H*), -9.20 (br m, 1 H, Ir*H*), -14.42 (br m, 1 H, Ir*H*). ^{13}C{^{1}H} NMR (125.8 MHz, benzene-d_6): δ 159.3 (apparent t, J = 21 Hz, C_{arom}), 143.2 (apparent t, J = 28 Hz, C_{arom}), 133.3 (apparent t, J = 10 Hz, CH$_{arom}$), 130.4 (CH$_{arom}$), 130.1 (CH$_{arom}$), 127.5 (CH$_{arom}$), 36.3 (apparent t, J = 15 Hz, CH$_{Cy}$), 32.9 (apparent t, J = 18 Hz, CH$_{Cy}$), 30.5 (CH$_{2Cy}$), 30.1 (CH$_{2Cy}$), 28.0 – 26.9 (overlapping resonances, CH$_{2Cy}$), 8.2 (Si*Me*). ^{31}P{^{1}H} NMR (202.5 MHz, benzene-d$_6$): δ 52.3. ^{29}Si NMR (99.4 MHz, benzene-d$_6$): δ 31.7. ^{19}F NMR (22.4 MHz, benzene-d$_6$): δ -54.9. IR (film, cm^{-1}): 2138 (m, Ir-*H*), 1840 (br m, η^2-B-*H*). Anal. Calcd for $C_{37}H_{58}BF_2IrP_2Si$: C, 53.29; H, 7.01. Found: C, 52.92; H, 7.01. X-Ray quality crystals of **5-16** were grown from vapour diffusion of pentane into a concentrated fluorobenzene solution at room temperature.

{[Cy-PSiP]Ir(H)(η^2:η^2-SiH$_2$Mes$_2$)}$^+${B(C$_6$F$_5$)$_4^-$} (5-17). A solution of Mes_2SiH_2 (0.015 g, 0.055 mmol) in ca. 2 mL of C_6H_5F was added dropwise via pipette to a solution of **5-5** (0.080 g, 0.055 mmol) in ca. 2 mL of C_6H_5F at room temperature. An immediate color change from orange to yellow was observed. The reaction mixture was dried under vacuum and the remaining solid was triturated with pentane (3 × 3 mL) to afford **5-17** as a pale yellow solid (0.087 g, 92%). ^{1}H NMR (500 MHz, benzene-d_6): δ 8.10 (m, 2 H, H_{arom}), 7.55 (m, 2 H, H_{arom}), 7.45 (t, 2 H, J = 8 Hz, H_{arom}), 7.08 (s, 2 H, H_{arom}), 7.03 (s, 2 H, H_{arom}), 6.87 (m, 2 H, H_{arom}), 2.80 (s, 6 H, CH_{3Mes}), 2.67 (s, 6 H, CH_{3Mes}), 2.38 – 1.10 (overlapping resonances, 4 H, P*Cy* + CH_{3Mes}), 2.25 (m, 2 H, P*Cy*), 2.00 (m, 6 H, P*Cy*), 1.84 (m, 8 H, P*Cy*), 1.63 – 1.10 (overlapping resonances, 18 H, P*Cy*), 1.06 (s, 3 H, Si*Me*),

0.69 (m, 6 H, P*Cy*), -6.59 (br m, 1 H, Ir*H*), -14.42 (br m, 1 H, Ir*H*). $^{13}C\{^{1}H\}$ NMR (125.8 MHz, bromobenzene-d_5): δ 152.7 (C_{arom}), 148.7 (C_{arom}), 146.8 (C_{arom}), 143.6 (C_{arom}), 133.3 (apparent t, J = 10 Hz, CH_{arom}), 130.4 (CH_{arom}), 130.1 (CH_{arom}), 127.5 (CH_{arom}), 36.3 (apparent t, J = 15 Hz, CH_{Cy}), 32.9 (apparent t, J = 18 Hz, CH_{Cy}), 30.5 (CH_{2Cy}), 30.1 (CH_{2Cy}), 28.0 – 26.9 (overlapping resonances, CH_{2Cy}), 8.2 (Si*Me*). $^{31}P\{^{1}H\}$ NMR (202.5 MHz, benzene-d_6): δ 46.9. ^{29}Si NMR (99.4 MHz, benzene-d_6): δ 62.8 (SiH_2Mes_2), 33.7 (*Si*Me). ^{11}B NMR (96.3 MHz, benzene-d_6): δ -15.9. ^{19}F NMR (22.4 MHz, benzene-d_6): δ -131.9 (d, J = 8 Hz, $B(C_6F_5)_4$), -162.5 (t, J = 20 Hz, $B(C_6F_5)_4$), -166.3 (br t, J = 20 Hz, $B(C_6F_5)_4$). IR (film, cm^{-1}): 2155 (m, Ir-*H*), 1643 (m, η^2-Si-*H*), 1605 (m, η^2-Si-*H*).

[Cy-PSiP]Ir(H)$_3$SiOTf(Ph)$_2$ (5-18). One equiv of Ph_2SiH_2 (15.9 μL, 0.016 g, 0.086 mmol) was syringed into a solution of **5-3** (0.080 g, 0.086 mmol) in ca. 5 mL of C_6H_5F at room temperature. An immediate color change from yellow to pale yellow was observed. The reaction mixture was dried under vacuum. The remaining solid was triturated with pentane (3 × 3 mL) to afford **5-18** as a pale yellow solid (0.088 g, 92%). ^{1}H NMR (500 MHz, benzene-d_6): δ 8.38 (d, 4 H, J = 7 Hz, H_{arom}), 8.10 (d, 2 H, J = 7 Hz, H_{arom}), 7.31 (t, 4 H, J = 8 Hz, H_{arom}), 7.24 – 7.17 (overlapping resonances, 6 H, H_{arom}), 7.02 (t, 2 H, J = 7 Hz, H_{arom}), 2.20 (m, 2 H, P*Cy*), 2.11 (m, 2 H, P*Cy*), 1.88 – 1.82 (overlapping resonances, 6 H, P*Cy*), 1.73 (m, 2 H, P*Cy*), 1.66 (m, 2 H, P*Cy*), 1.58 (m, 4 H, P*Cy*), 1.46 (m, 4 H, P*Cy*), 1.38 – 1.17 (overlapping resonances, 13 H, P*Cy* + Si*Me*), 1.03 – 0.89 (overlapping resonances, 8 H, P*Cy*), 0.57 (m, 2 H, P*Cy*), 0.30 (m, 2 H, P*Cy*), -8.83 (br m, 2 H, Ir*H*), -12.1 (br m, 1 H, Ir*H*). $^{13}C\{^{1}H\}$ NMR (125.8 MHz, benzene-d_6): δ 157.4 (apparent t, J = 19 Hz, C_{arom}), 144.9 (apparent t, J = 28 Hz, C_{arom}), 143.3 (C_{arom}), 137.2 (CH_{arom}), 132.9 (apparent t, J = 9 Hz, CH_{arom}), 129.9 (CH_{arom}), 129.7 (CH_{arom}), 127.9 (CH_{arom}), 127.8 (CH_{arom}), 35.2 (apparent t, J = 14 Hz, CH_{Cy}), 33.8 (apparent t, J = 18 Hz, CH_{Cy}), 29.8 (CH_{2Cy}), 29.2 (CH_{2Cy}), 27.4 – 26.2 (overlapping resonances, CH_{2Cy}), 8.6 (Si*Me*). $^{31}P\{^{1}H\}$ NMR (202.5 MHz, benzene-d_6): δ 42.0. ^{29}Si NMR (99.4 MHz,

benzene-d_6): δ 58.0 ($SiPh_2OTf$), 28.5 (Si*Me*). ^{19}F NMR (282.4 MHz, benzene-d_6): δ -76.3. IR (film, cm^{-1}): 2037 (m, Ir-*H*), 1968 (m, Ir-*H*). X-Ray quality crystals of **[Cy-PSiP]Ir(H)SiOTf(Ph)$_2$ (5-19·(C$_6$H$_5$F)$_{1.25}$)** were grown from vapour diffusion of pentane into a concentrated C_6H_5F solution at room temperature.

[Cy-PSiP]Ir(H)$_3$(Si(FBF$_3$)Ph$_2$) (5-20). One equiv Ph_2SiH_2 (12.8 μL, 0.013 g, 0.069 mmol) were syringed into a solution of **5-3** (0.060 g, 0.069 mmol) in ca. 5 mL of C_6H_5F at room temperature. An immediate color change from yellow to pale yellow was observed. The reaction mixture was dried under vacuum. The remaining solid was triturated with pentane (3 × 3 mL) to afford **5-20** as a pale yellow solid (0.054 g, 74%). ^1H NMR (500 MHz, benzene-d_6): δ 8.17 (d, 2 H, J = 7 Hz, H_{arom}), 8.06 (d, 2 H, J = 7 Hz, H_{arom}), 7.32 (m, 2 H, H_{arom}), 7.33 – 7.21 (overlapping resonances, 6 H, H_{arom}), 7.12 (t, 2 H, J = 7 Hz, H_{arom}), 7.06 (t, 2 H, H_{arom}), 2.28 – 2.19 (overlapping resonances, 4 H, P*Cy*), 1.99 (m, 2 H, P*Cy*), 1.84 – 0.93 (overlapping resonances, 37 H, P*Cy* + Si*Me*; Si*Me* at 1.35), 0.64 (m, 2 H, P*Cy*), 0.39 (m, 2 H, P*Cy*), -9.27 (br m, 2 H, Ir*H*), -11.8 (br m, 1 H, Ir*H*). $^{13}C\{^1H\}$ NMR (125.8 MHz, benzene-d_6): δ 158.8 (apparent t, J = 19 Hz, C_{arom}), 149.2 (apparent d, J = 21 Hz, C_{arom}), 145.4 (apparent t, J = 28 Hz, C_{arom}), 135.4 (CH_{arom}), 133.0 (apparent d, J = 9 Hz, CH_{arom}), 129.7 (CH_{arom}), 130.0 (CH_{arom}), 128.8 (CH_{arom}), 128.3 (CH_{arom}), 127.3 (CH_{arom}), 127.5 (CH_{arom}), 35.4 (apparent t, J = 15 Hz, CH_{Cy}), 33.7 (apparent t, J = 20 Hz, CH_{Cy}), 30.0 (CH_{2Cy}), 29.3 (CH_{2Cy}), 27.6 (CH_{2Cy}), 27.5 (CH_{2Cy}), 26.9 – 26.6 (overlapping resonances, CH_{2Cy}), 9.5 (Si*Me*). $^{31}P\{^1H\}$ NMR (202.5 MHz, benzene-d_6): δ 43.8. ^{29}Si NMR (99.4 MHz, benzene-d_6): δ 32.1 ($^1J_{SiF}$ = 237 Hz, *Si*(FBF$_3$)Ph$_2$), 35.2 (*Si*Me). ^{11}B NMR (96.3 MHz, benzene-d_6): δ 0.5. ^{19}F NMR (282.4 MHz, benzene-d_6): δ -130.4, -141.7. IR (film, cm^{-1}): 2004 (m, Ir-*H*), 1957 (m, Ir-*H*).

[Cy-PSiP]Ir(H)$_3$SiHPhOTf (5-21). One equiv of $PhSiH_3$ (10.6 μL, 0.0093 g, 0.086 mmol) were syringed into a solution of **5-1** (0.080 g, 0.086 mmol) in ca. 5 mL of C_6H_5F at room temperature. An immediate color change from yellow to pale yellow was observed. The reaction mixture was dried under vacuum. The remaining solid was

triturated with pentane (3 × 3 mL) to afford **5-21** as a pale yellow solid (0.088 g, 98%). ^{1}H NMR (500 MHz, benzene-d_6): δ 8.08 – 8.03 (overlapping resonances, 4 H, H_{arom}), 7.76 (m, 1 H, Si*H*(OTF)(Ph)), 7.30 (m, 1 H, H_{arom}), 7.27 – 7.23 (overlapping resonances, 3 H, H_{arom}), 7.19 (m, 2 H, H_{arom}), 7.09 (t, 1 H, J = 8 Hz, H_{arom}), 7.06 (m, 2 H, H_{arom}), 2.26 – 1.80 (overlapping resonances, 14 H, P*Cy*), 1.67 – 0.80 (overlapping resonances, 29 H, P*Cy* + Si*Me*), 0.62 (m, 2 H, P*Cy*), 0.46 (m, 1 H, P*Cy*), 0.34 (m, 1H, P*Cy*), -9.21 (br s, 1 H, Ir*H*), -9.48 (br s, 1 H, Ir*H*), -11.80 (br m, 1 H, Ir*H*). ^{13}C{^{1}H} NMR (125.8 MHz, benzene-d_6): δ 158.5 (C_{arom}), 158.2 (C_{arom}), 144.4 (C_{arom}), 143.3 (C_{arom}), 134.3 (CH_{arom}), 133.1 (apparent d, J = 8 Hz, CH_{arom}), 132.9 (apparent d, J = 9 Hz, CH_{arom}), 130.0 (CH_{arom}), 129.8 (CH_{arom}), 128.1 (CH_{arom}), 127.8 (CH_{arom}), 35.5 (apparent t, J = 6 Hz, CH_{Cy}), 35.3 (apparent t, J = 6 Hz, CH_{Cy}), 29.8 (CH_{2Cy}), 29.6 (CH_{2Cy}), 29.4 (CH_{2Cy}), 29.1 (CH_{2Cy}), 28.1 (CH_{2Cy}), 27.6 (CH_{2Cy}), 27.4 – 26.7 (overlapping resonances, CH_{2Cy}), 9.4 (Si*Me*). ^{31}P{^{1}H} NMR (202.5 MHz, benzene-d_6): δ 43.6 (AB Quartet). ^{29}Si NMR (99.4 MHz, benzene-d_6): δ 32.5 (d, $^{1}J_{SiH}$ = 190 Hz, *Si*HPhOTf), 31.5 (*Si*Me). ^{19}F NMR (282.4 MHz, benzene-d_6): δ -77.0. IR (film, cm^{-1}): 2113 (m, Ir-*H*), 2033 (m, Ir-*H*), 1976 (m, Si-*H*). Anal. Calcd for $C_{44}H_{64}F_3IrO_3P_2SSi_2$: C, 50.80; H, 6.20. Found: C, 50.54; H, 5.93.

5.4.3 Crystallographic Solution and Refinement Details

Crystallographic data for each of **5-1·$(C_6H_6)_{0.5}$**, **5-3·C_6H_5F**, **5-11·$(Et_2O)_{0.5}$**, **5-15·$(C_6H_6)_{0.5}$**, **5-16·C_6H_6**, **5-19·$(C_6H_5F)_{1.25}$** were obtained at 173(±2) K on a Bruker D8/APEX II CCD diffractometer using graphite-monochromated Mo Kα (λ = 0.71073 Å) radiation, employing a sample that was mounted in inert oil and transferred to a cold gas stream on the diffractometer. Programs for diffractometer operation, data collection, and data reduction (including SAINT) were supplied by Bruker. Gaussian integration (face-indexed) was employed as the absorption correction method in each case. All structures were solved by use of the Patterson search/structure expansion and were refined by use of full-matrix least-squares procedures (on F^2) with R_1 based on F_o^2

$\geq 2\sigma(F_o^2)$ and wR_2 based on $F_o^2 \geq -3\sigma(F_o^2)$. Unless otherwise noted, anisotropic displacement parameters were employed throughout for non-hydrogen atoms. During the structure solution process for **5-1·$(C_6H_6)_{0.5}$**, half an equivalent of C_6H_6 was located in the asymmetric unit and refined in a satisfactory manner. During the structure solution process for **5-3·C_6H_5F**, one equivalent of fluorobenzene was located in the asymmetric unit. The fluorine atom in the disordered fluorobenzene molecule was refined anisotropically over two positions (F1S and F2S) with an occupancy factor of 0.5. Restraints were applied to distances within the disordered fluorobenzene molecule: d(F1S–C1S) = d(F2S–C3S) = 1.33(1) Å; d(F1S···C2S) = d(F1S···C6S) = d(F2S···C2S) = d(F2S···C4S) = 2.36(1) Å. During the structure solution process for **5-11·$(Et_2O)_{0.5}$**, two crystallographically independent molecules of [Cy-PSiP]Ir(Me)(I) (A and B) along with an equivalent of diethyl ether were located in the asymmetric unit; for convenience, only molecule A is discussed in the text. The non-hydrogen atoms of the disordered diethyl ether solvate were refined with a common isotropic displacement parameter over two positions, where O1S and C1S - C4S were refined with an occupancy factor of 0.65, while O2S and C5S - C8S were refined with an occupancy factor of 0.35. Distances within the disordered diethyl ether molecule were restrained during refinement: d(O1S–C1S) = d(O1S–C3S) = d(O2S–C5S) = d(O2S–C7S) = 1.46(1) Å; d(C1S–C2S) = d(C3S–C4S) = d(C5S–C6S) = d(C7S–C8S) = 1.52(1) Å; d(O1S···C2S) = d(O1S···C4S) = d(O2S···C6S) = d(O2S···C8S) = 2.40(1) Å. During the structure solution process for **5-15·$(C_6H_6)_{0.5}$**, half an equivalent of benzene was located in the asymmetric unit. The benzene solvate was disordered across the crystallographic inversion center (1/2, 1/2, 1/2). Carbon atoms of the disordered solvent molecule (C1S - C6S) were refined with a common isotropic displacement parameter and an occupancy factor of 0.5. Bond distances within the disordered benzene molecule were restrained to be 1.39(2) Å during refinement. The six carbon atoms were constrained to be (nearly) coplanar during refinement, i.e. by defining them as the vertices of a polyhedron that could occupy a

volume of no more than 0.01 Å3 (*SHELXL-97* FLAT instruction). During the structure solution process for **5-16·C_6H_6**, one equivalent of benzene was located in the asymmetric unit. Carbon atoms of the disordered benzene solvate were refined with a common isotropic displacement parameter over two positions, where C11S – C16S were refined with an occupancy factor of 0.75 and C21S - C26S were refined with an occupancy factor of 0.25. During the structure solution process for **5-19·$(C_6H_5F)_{1.25}$**, 1.25 equivalents of fluorobenzene were located in the asymmetric unit. Disorder involving one P-*Cy* group, one Si-*Ph* group, and the fluorobenzene solvate was identified during refinement. Carbon atoms for the disordered cyclohexyl group (C51A - C56A and C51B - C56B) and for the disordered phenyl ring (C81A - C86A and C81B - C86B) were refined anisotropically over two positions with an occupancy factor of 0.5. The fluorine atom for one equivalent of fluorobenzene was refined isotropically over two positions (F1S and F2S) with an occupancy factor of 0.5. For the remaining 0.25 equivalents of fluorobenzene, the carbon atoms (C7S, C8S, and C9S) were refined isotropically with an occupancy factor of 0.5, while the fluorine atom F3S was refined isotropically with an occupancy factor of 0.25. The Ir-*H* in **5-1·$(C_6H_6)_{0.5}$**, **5-15·$(C_6H_6)_{0.5}$** and **5-16·C_6H_6** were located in the difference map and refined isotropically in a satisfactory manner. For **5-16·C_6H_6** the bridiging Ir-*H*-B hydrides (H1BA and H1BB) were also located in the difference map and refined with a common isotropic displacement parameter. For **5-3·C_6H_5F** and **5-19·$(C_6H_5F)_{1.25}$** the Ir-*H* (H1 for both structures) was located in the difference map and refined isotropically with the Ir-*H* distance restrained to an idealized value of 1.50(1) Å during refinement. Furthermore, for **5-19·$(C_6H_5F)_{1.25}$** the P1···H1 and P2···H1 distances were constrained to be equal (within 0.03 Å) during refinement. Otherwise, all hydrogen atoms were added at calculated positions and refined by use of a riding model employing isotropic displacement parameters based on the isotropic displacement parameter of the attached atom. Additional crystallographic information is provided in Appendix A.

Chapter 6: Conclusions

6.1 Summary and Conclusions

The synthesis of new Rh and Ir pincer complexes supported by bis(phosphino)silyl ligation, as well as their reactivity with C-H, N-H and Si-H bonds, have been detailed in this document. Building on previous studies showing that a [Cy-PSiP]Ir^{I} reactive intermediate was capable of mediating room temperature sp^2-C-H bond activation, the ability of this reactive intermediate to cleave N-H bonds in anilines and ammonia was detailed in Chapter 2. Such N-H bond cleavage reactivity occurred under relatively mild conditions to afford isolable, monomeric amido hydride complexes of the type [Cy-PSiP]Ir(H)(NHR) (R = H, aryl), several of which were crystallographically characterized. Unlike similar (PCP)Ir pincer species, these amido hydride complexes were shown to be resistant to N-H bond reductive elimination chemistry, even in the presence of arenes and alkenes. This divergent reactivity showcases the ability of the silyl pincer framework to support complexes with unique reactivity. Similar N-H bond cleavage chemistry was attempted by the [Cy-PSiP]Rh^{I} reactive intermediate, however upon introduction of aniline or ammonia, formation of Rh^{I} amine adducts of the type [Cy-PSiP]Rh(NH_2R) was observed.

Preliminary investigations into the nature of the [Cy-PSiP]Ir-mediated N-H bond cleavage were carried out using ^2H labeling experiments. It was found that upon treatment of *in situ* generated [Cy-PSiP]Ir^{I} with ammonia-d_3 and subsequent heating, the N-H activation product [Cy-PSiP]Ir(D)(ND_2) was observed, where deuterium had been incorporated exclusively into the hydride and amide positions. The lack of deuterium incorporation into the ligand PCy_2 groups is consistent with oxidative addition by a 14 e^- [Cy-PSiP]Ir^{I} intermediate (or a reactive equivalent) in the N-H bond cleavage step. A preliminary mechanism was therefore proposed to involve NH_3 coordination to [Cy-PSiP]Ir^{I} to form an initial amine adduct. Although the Ir amine adduct was not observed, indirect evidence for its formation comes from the characterization of related [Cy-PSiP]Rh(NH_3) complex (**2-12**). Subsequent N-H bond oxidative addition could then

yield the parent amido hydride complex [Cy-PSiP]Ir(H)(NH_2) (**2-10**). This example of ammonia N-H bond activation presented is exceedingly rare, and may provide inroads to new atom-economical chemical transformations that incorporate N-H bond oxidative addition steps in the functionalization of this abundant feedstock.

Due to the scarcity of complexes capable of mediating N-H bond oxidative addition, the work described in Chapter 3 expanded on the initial results presented in Chapter 2 and probed the reactivity of Rh and Ir silyl pincer complexes with a variety of N-H containing substrates, including alkyl amines, hydrazine derivatives, and benzamides. At the outset of these investigations, a diisopropylphosphino silyl ligand precursor [^{i}Pr-PSiP]H (**3-1**) was synthesized, as resulting [^{i}Pr-PSiP]M (M = Rh, Ir) complexes were envisioned to be less susceptible to potential cyclometalation processes that could occur in the [Cy-PSiP]M system. The N-H bond activation reactivity of such [^{i}Pr-PSiP]Ir complexes was investigated in parallel to that of the analogous [Cy-PSiP]Ir species.

Alkyl amines were initially targeted for N-H bond activation studies as they are notoriously difficult substrates to activate, as alkyl substitution at N renders the amine more nucleophilic and therefore the amine is more likely to simply coordinate to a metal center rather than undergo oxidative addition. Remarkably, highly reactive [R-PSiP]Ir^{I} (R = Cy, ^{i}Pr) species generated in situ were shown to mediate the oxidative addition of highly Lewis basic amines, such as adamantylamine, *tert*-butylamine, and in the case of [Cy-PSiP]Ir^{I}, cyclohexylamine. Extension of this reactivity to the N-H bond activation of benzylamine yielded the first example of room temperature N-H bond activation mediated by [^{i}Pr-PSiP]Ir^{I} to synthesize [^{i}Pr-PSiP]Ir(H)($NHCH_2Ph$) (**3-16**). The [Cy-PSiP]Ir(H)($NHCH_2Ph$) (**3-15**) analogue was also synthesized by N-H bond activation of benzylamine, but required heating in order to achieve this transformation. This observed difference in reactivity highlights the impact that phosphine substituents have on the resulting chemistry at Ir, and may reflect decreased steric bulk in the coordination sphere of [^{i}Pr-PSiP]Ir in relation to analogous [Cy-PSiP]Ir species. The reactivity of primary

and secondary amines that contained β-hydrogens was complicated by the occurrence of β-hydride elimination and other side reactions.

The reactivity of [Cy-PSiP]Rh^{I} with alkyl amines yielded amine adducts of the type [Cy-PSiP]Rh(NH_2R), in direct relation to the reactivity previously observed with ammonia and anilines. These adducts proved stable only in the presence of excess amine and were not isolable. Remarkably, the benzyl amine adduct [Cy-PSiP]Rh(NH_2CH_2Ph) (**3-33**) was the first instance where the amine adduct was isolable.

The N-H bonds of hydrazine derivatives were also targeted for bond activation studies, due to the potential for these substrates to be utilized as ammonia surrogates in reactions where reactivity with ammonia is challenging.[101] Specifically, [R-PSiP]Ir^{I} was shown to mediate the N-H bond activation of 1-aminopiperidine and 4-methyl-1-aminopiperazine, with no secondary reactions (e.g. α-H migration to Ir) occurring. Although N-H bond cleavage was not observed in the reactions of [Cy-PSiP]Rh^{I} with 1-aminopiperidine and 4-methyl-1-aminopiperazine, the first example of [Cy-PSiP]Rh^{I} mediated N-H bond activation was observed with the hydrazine derivative benzophenone hydrazone to yield [Cy-PSiP]Rh(H)NH-N=CPh_2 (**3-41**). This represents a rare example of N-H bond activation mediated by Rh and could provide insight into new methods for Rh catalyzed functionalization of N-H bonds.

The N-H bond activation of benzamides by [R-PSiP]Ir^{I} was also described in Chapter 3. Both the parent benzamide and pentafluorobenzamide were shown to undergo N-H bond activation with both [Cy-PSiP]Ir^{I} and [^{i}Pr-PSiP]Ir^{I} reactive species, where bond cleavage occurred after heating for two hours (compared to heating for 12-18 h typically required for other N-H containing substrates). The facile N-H bond activation may be promoted by coordination of the carbonyl oxygen to the Ir center.

The remarkable ability of bis(phosphino)silyl ligated Ir complexes to mediate the N-H bond activation of a wide variety of N-H containing substrates is unprecedented. This N-H bond oxidative addition chemistry could potentially be harnessed for the development of new pathways for the formation of C-N bonds. For example, a

hydroamination processes that operates via transition metal catalyzed N-H bond oxidative addition to a metal center followed by insertion of an unsaturated substrate into the M-N or M-H bond may provide new types of selectivity in such amination chemistry. Along these lines, Chapter 4 details the reactivity of a variety of unsaturated substrates with [R-PSiP]Ir amido hydride complexes derived from N-H oxidative addition, where [Cy-PSiP]Ir(H)(NHPh), [Cy-PSiP]Ir(H)(NH^{t}Bu), [Cy-PSiP]Ir(H)(NH_2), and [^{i}Pr-PSiP]Ir(H)(NH_2) were chosen as representative complexes for the investigation.

Initial attempts at insertion chemistry looked at the reaction of the representative amido hydride complexes with unactivated alkenes and alkynes. Although no insertion chemistry was observed with ethylene or 1-hexene, the parent amido hydride complexes [R-PSiP]Ir(H)(NH_2) (**2-10**, R = Cy; **3-7**, R = ^{i}Pr) promoted the isomerization of 1-hexene to internal alkenes. Isomerization would result from insertion of the terminal alkene into the Ir-H bond, followed by β-hydride elimination to move the double bond to an internal position. These results were unexpected as previously reported calculations had predicted that alkene insertion into M-N bonds is more favourable than into M-H bonds.[79]

Treatment of the representative amido hydride complexes with unactivated alkynes (phenyl acetylene, diphenyl acetylene, 1-phenyl-1-propyne, and 3-hexyne) led to elimination of the corresponding amine and the formation of Ir^I alkyne complexes of the type [R-PSiP]Ir(R'-C≡C-R") (R = Cy, ^{i}Pr; R', R" = aryl, alkyl).

These results highlighted the challenging nature of such insertion processes involving unsaturated substrates and Ir amido species. Interestingly, after the initiation of these investigations, a computational study was published that predicted that pathways for the catalytic hydroamination of ethylene with ammonia via the insertion of ethylene into either [Cy-PSiP]Ir(H)(NH_2) or (PCP)Ir(H)(NH_2) (PCP = [κ^3-(^{t}Bu$_2$*P*C$_2$H$_4$)$_2$*C*H]$^-$) complexes are too high in energy for turnover to occur.[80] As a result, more activated unsaturated substrates were targeted for further studies. In this context, the reactivity of the strained alkene norbornene was investigated and it was found that this substrate also did not undergo insertion, leading instead to amine loss followed by alkene coordination

to the Ir^{I} center. In addition, no reactivity was observed with the allene 3-methyl-1,2-butadiene, and complex reaction mixtures resulted from the reaction of the amido hydride complexes with dimethoxyacetylene dicarboxylate. The first observation of insertion chemistry, however, resulted upon treatment of [Cy-PSiP]Ir(H)NH_2 (**2-10**) with one equivalent of methyl acrylate. The carbonyl group inserts into the Ir-N bond generating [Cy-PSiP]Ir(H)(OC(NH_2)(OMe)CH=CH_2) (**4-10**). Although this complex underwent decomposition over time in solution, it's observation provides insight into potential C-N bond forming processes involving products of N-H bond oxidative addition.

Finally, the reactivity of the amido hydride complexes with molecules containing polar bonds was also examined. The addition of an atmosphere of CO to the representative complexes led to the formation of multiple products that were not isolable. Alternatively, when excess benzaldehyde was reacted with [R-PSiP]Ir(H)(NHR') (R = Cy, ^{i}Pr; R' = Ph, ^{t}Bu, H), the formation of [Cy-PSiP]Ir(H)C(O)Ph (**4-11**) was observed, likely resulting from amine elimination, followed by aldehyde C-H bond cleavage. The strongly coordinating xylyl isocyanide also showed reactivity with [Cy-PSiP]Ir(H)(NHPh) and [Cy-PSiP]Ir(H)NH_2. One equivalent of xylyl isocyanide cleanly inserted into the Ir-N bond of the aryl amido hydride [Cy-PSiP]Ir(H)(NHPh) to generate [Cy-PSiP]Ir(H)(C(NHPh)(N(2,6-$Me_2C_6H_3$)). Comparatively, two equivalents of xylyl isocyanide were necessary for the complete conversion of [Cy-PSiP]Ir(H)(NH_2) to the insertion product [Cy-PSiP]Ir(H)(CN(2,6-$Me_2C_6H_3$))(C(NH_2)(N(2,6-$Me_2C_6H_3$)), which also features an equivalent of the isocyanide coordinated to the Ir center. These latter two reactions with xylyl isocyanide represent a rare example of C-N bond formation involving a metal amido fragment derived from N-H bond oxidative addition.

Having probed aspects of C-H and N-H bond activation chemistry facilitated by [R-PSiP]Ir^{I} species, the focus of Chapter 5 was to examine how altering the electrophilicity of the Ir center by targeting cationic [Cy-PSiP]Ir^{III} complexes would affect E-H bond cleavage chemistry. As an entry point into this chemistry, the synthesis of complexes of the type {[R-PSiP]Ir(H)}$^{+}$[X]$^{-}$ (R = Cy, ^{i}Pr; X = OTf, BF_4, $B(C_6F_5)_4$)

was pursued. Both the OTf and BF_4 derivatives featured inner-sphere coordination of the anion in the solid state. Related methyl derivatives of the type $\{[R\text{-}PSiP]Ir(Me)\}^+[X]^-$ were also pursued but their isolation proved to be synthetically challenging.

The hydride complexes $\{[Cy\text{-}PSiP]Ir(H)\}^+[X]^-$ showed extensive reactivity with primary, secondary, and tertiary hydrosilanes. The products typically resulted from Si-H activation and interactions with the X^- anion. More specifically, the reaction of [Cy-PSiP]Ir(H)(OTf) (**5-1**) with two equivalents of Et_3SiH led to the formation of [Cy-PSiP]Ir$(H)_3SiEt_3$ (**5-14**) with the concomitant loss of Et_3SiOTf. Comparatively, the reaction of [Cy-PSiP]Ir$(H)(BF_4)$ (**5-3**) with two equivalents of either Et_3SiH or Mes_2SiH_2 produced the hydroborate complex [Cy-PSiP]Ir$(H)(\eta^2\text{:}\eta^2\text{-}H_2BF_2)$ (**5-16**) resulting from loss of two equivalents of Et_3SiF or Mes_2SiHF, respectively. In the case of $\{[Cy\text{-}PSiP]Ir(H)\}^+[B(C_6F_5)_4]^-$ (**5-5**) reaction with Mes_2SiH_2 generated the dimesitylsilane complex [Cy-PSiP]Ir$(H)(\eta^2\text{:}\eta^2\text{-}H_2SiMes_2)$ (**5-17**) that features bis(σ-Si–H) coordination.

The reaction of Ph_2SiH_2 or $PhSiH_3$ with $\{[Cy\text{-}PSiP]Ir(H)\}^+[B(C_6F_5)_4]^-$ (**5-5**) did not yield any new, isolable products. However, similar reactions with [Cy-PSiP]Ir(H)(OTf) (**5-1**) yielded [Cy-PSiP]Ir$(H)_3(SiOTfR^1R^2)$ ($R^1 = R^2$ =Ph or R^1 = H and R^2 = Ph). These complexes likely resulted from initial Si-H cleavage, OTf ligand dissociation and an α-hydride migration from Si to Ir to generate an intermediate cationic Ir silylene hydride species that subsequently coordinated the OTf anion. Alternatively, the reaction of [Cy-PSiP]Ir$(H)(BF_4)$ (**5-3**) with Ph_2SiH_2 yielded a comparable analogue [Cy-PSiP]Ir$(H)_3(Si(BF_4)Ph_2)$ (**5-20**), where the $BF4^-$ anion is coordinated to the Si center. These studies profile the rich reaction chemistry of [Cy-PSiP]Ir^{III} species with Si-H bonds and highlight the significant influence of the counter anion on the reactivity of cationic metal complexes.

6.2 Future Work

Building on the success of the 14-electron [R-PSiP]Ir^{I} (R = Cy, ^{i}Pr) fragment in the activation of both C-H and N-H bonds, future efforts will also be directed towards exploring the possibility of other types of E-H (E = main group element; e.g. B, Si, P, O) bond activation reactions mediated by [R-PSiP]M^{I} (M = Rh, Ir). Towards these ends, preliminary studies of complexes of the type [R-PSiP]M(H)(PR_2) and [R-PSiP]M(H)(OR) (M = Rh, Ir; R = alkyl, aryl, or H) were undertaken. Preliminary results suggest that the Rh and Ir phosphido products obtained from the reaction of [Cy-PSiP]M(H)Cl with LiPHMes exhibit divergent reactivity. The Ir product appears isolable as [Cy-PSiP]Ir(H)(PHMes) (Scheme 6-1, Figure 6-1), whereas the Rh analogue appears to undergo P-H reductive elimination to form [Cy-PSiP]Rh(PH_2Mes) (Scheme 6-1). Reductive elimination is also observed upon attempted synthesis of [Cy-PSiP]Ir(H)($P^{i}Pr_2$), as the final product from the reaction of [Cy-PSiP]Ir(H)Cl with Li$P^{i}Pr_2$ appears to be the Ir^{I} species [Cy-PSiP]Ir($PH^{i}Pr_2$) (Figure 6-1).

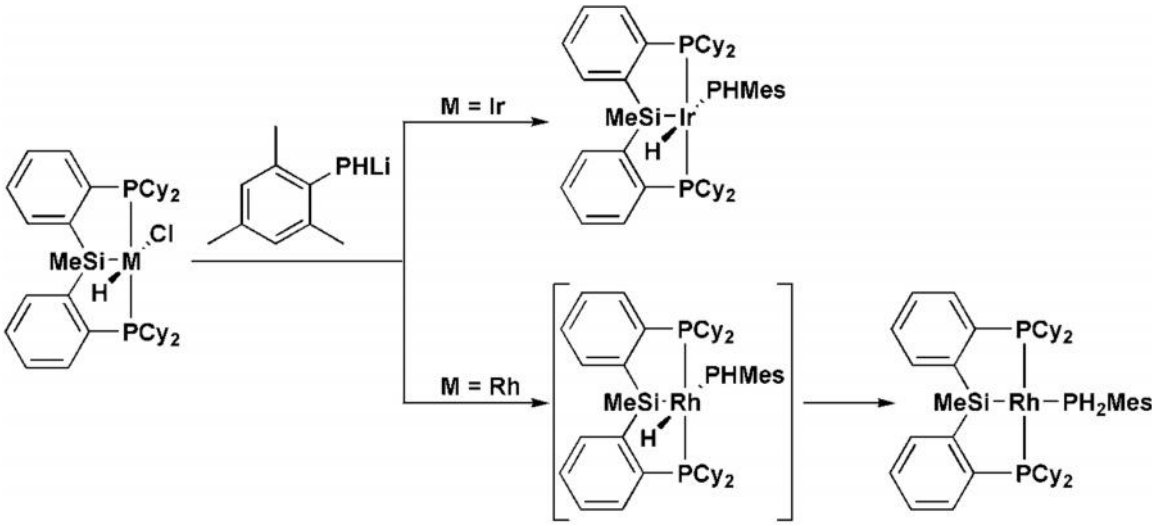

Scheme 6-1. Generation of [Cy-PSiP]Rh(PH_2Mes) and [Cy-PSiP]Ir(H)(PHMes)

Preliminary results also indicate that complexes of the type [Cy-PSiP]Ir(H)(O^{t}Bu) can be synthesized by the reaction of [Cy-PSiP]Ir(H)Cl with KO^{t}Bu. Future work is aimed at the isolation and complete characterization of such alkoxo and phosphido complexes and the exploration of their reactivity, as well as at pursuing O-H and P-H bond oxidative addition routes for their synthesis, respectively.

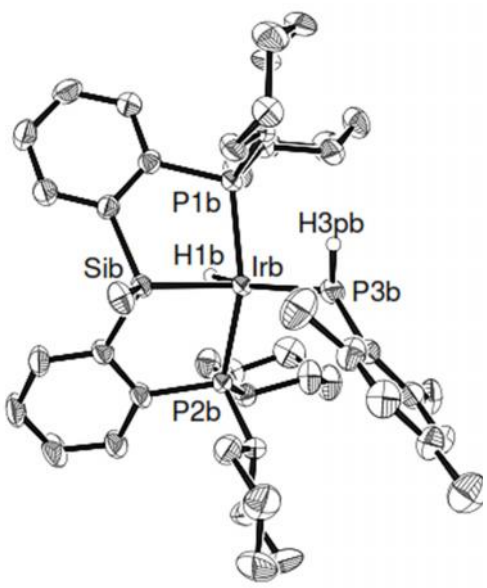

[Cy-PSiP]Ir(H)PHMes

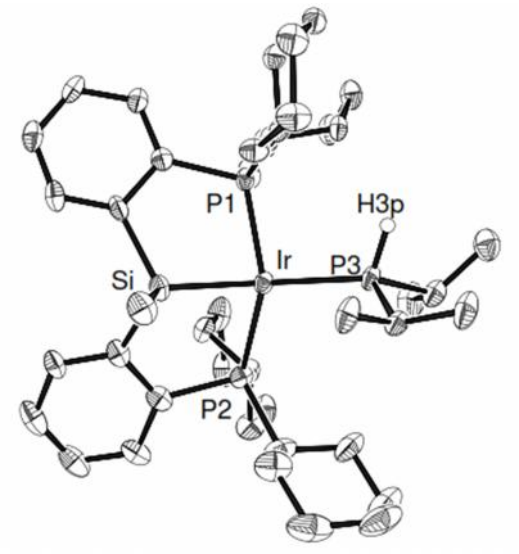

[Cy-PSiP]Ir(PH^{i}Pr$_2$)

Figure 6-1. The crystallographically determined structures of [Cy-PSiP]Ir(H)PHMes and [Cy-PSiP]Ir(PH^{i}Pr$_2$)

In the course of examining the reactivity of [Cy-PSiP]Ir(H)(OTf) with hydrosilanes, products of the type [Cy-PSiP]Ir(H)$_3$(SiOTfR^{1}R^2) (R^1 = R^2 = Ph; R^1 = H, R^2 = Ph) were isolated. Interestingly, these complexes can be viewed as base stabilized silylene complexes where the OTf$^-$ anion coordinates to an electrophilic Si center. Transition metal silylene complexes featuring a double bond between silicon and a metal center are of interest as they are often proposed as intermediates in a number of catalytic cycles involving organosilicon compounds.[68] Thus there has been significant effort dedicated to the synthesis of silylene complexes in order to probe the structures and reactivity properties of these often difficult to isolate species. As such, abstraction of the

Lewis basic OTf group from [Cy-PSiP]Ir(H)$_3$(SiOTfR^{1}R^2) could act as an entry point for synthesizing cationic [Cy-PSiP]Ir=SiR^{1}R^2 species. Indeed, preliminary research reveals that treatment of a C_6H_5F solution of [Cy-PSiP]Ir(H)$_3$(SiOTfPh$_2$) with LiB(C_6F_5)$_4$·2Et$_2$O led to quantitative (^{31}P NMR) formation of a new product featuring a ^{31}P NMR resonance at 43.6 ppm. However, the presence of Et$_2$O in the reaction mixture is undesirable, as it is likely to coordinate to the silylene fragment. As such, alternative sources of B(C_6F_5)$_4^-$, such as AgB(C_6F_5)$_4$ could be utilized to attempt the synthesis and isolation of cationic [Cy-PSiP]Ir=SiR^{1}R^2 species (Scheme 6-2).

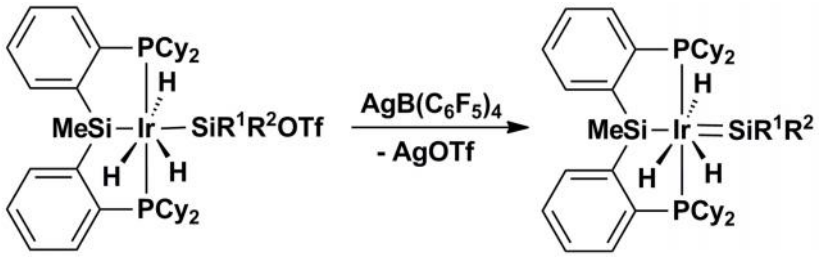

Scheme 6-2. Proposed synthesis of [Cy-PSiP]Ir=SiR^{1}R^2 species

Finally, as the [R-PSiP] ligand system used throughout these investigations has a modular design, it may be beneficial to investigate the effects of varying the ligand backbone and/or the nature of the substituents on phosphorus in order to see how reactivity is affected by changes in the steric and/or electronic properties of the pincer ligand. Potential new ligand architectures to pursue as well as possible synthetic routes to such ligands are depicted in Scheme 6-3. As previous results from PCP-pincer systems have clearly demonstrated (*vide supra*), changes in ligand backbone and in the donor substituents can lead to pronounced changes in the reactivity of the resulting complexes.

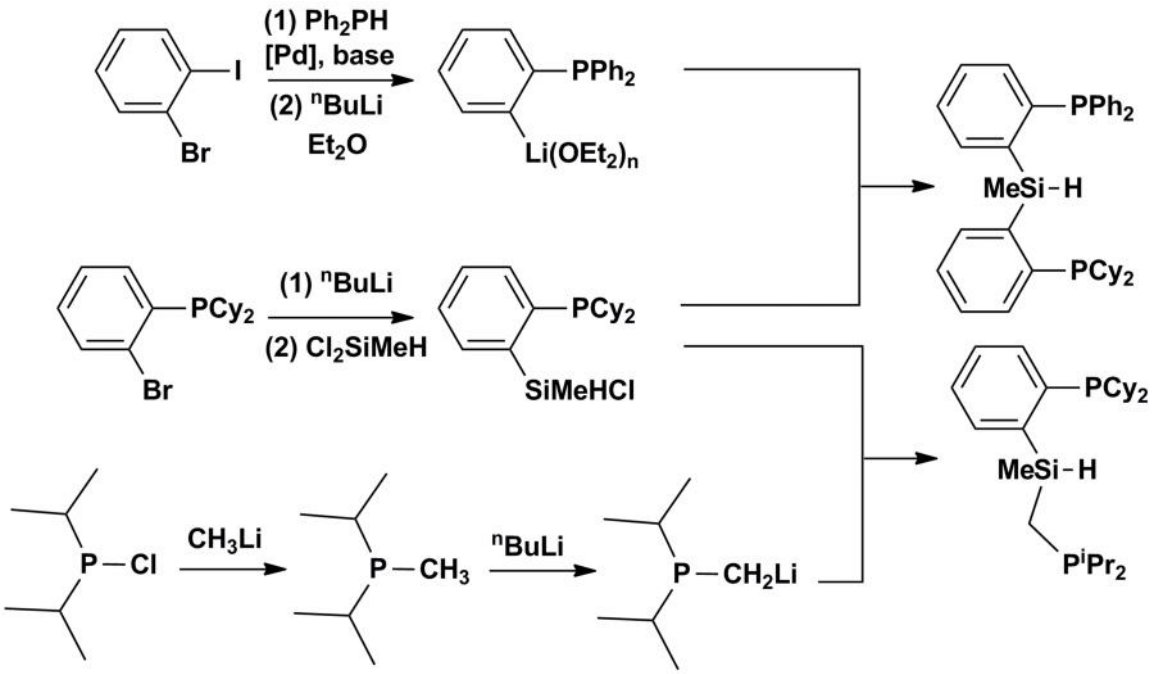

Scheme 6-3. Synthetic routes to new silyl pincer ligands

Appendix A: Crystallographic Experimental Details

Table A1. Crystallographic Experimental Details for [{κ^3–Me<u>Si</u>(C_6H_4<u>P</u>Cy_2)$_2$} Rh(PMe_3)] (**2-5**).

A. Crystal Data	
formula	$C_{40}H_{64}P_3RhSi$
formula weight	768.82
crystal dimensions (mm)	0.45 × 0.25 × 0.19
crystal system	monoclinic
space group	$P2_1/c$ (No. 14)
unit cell parameters	
a (Å)	11.9620 (6)
b (Å)	18.5340 (9)
c (Å)	18.7300 (10)
β (deg)	103.2047 (6)
V (Å^3)	4042.7 (4)
Z	4
ρ_{calcd} (g cm^{-3})	1.263
μ (mm^{-1})	0.597
B. Data Collection and Refinement Conditions	
diffractometer	Bruker D8/APEX II CCD
radiation (λ [Å])	graphite-monochromated Mo Kα (0.71073)
temperature (°C)	–100
scan type	ω scans (0.3°) (20 s exposures)
data collection 2θ limit (deg)	55.04
total data collected	35047 (-15 ≤ h ≤ 15, -23 ≤ k ≤ 24, -24 ≤ l ≤ 24)
independent reflections	9291 (R_{int} = 0.0248)
number of observed reflections (*NO*)	8142 [$F_o^2 \geq 2\sigma(F_o^2)$]
structure solution method	Patterson/structure expansion (*DIRDIF–2008*)
refinement method	full-matrix least-squares on F^2 (*SHELXL–97*)
absorption correction method	Gaussian integration (face-indexed)
range of transmission factors	0.8966–0.7738
data/restraints/parameters	9291 [$F_o^2 \geq -3\sigma(F_o^2)$] / 0 / 406
goodness-of-fit (S)	1.038 [$F_o^2 \geq -3\sigma(F_o^2)$]
final R indices[f]	
R_1 [$F_o^2 \geq 2\sigma(F_o^2)$]	0.0264
wR_2 [$F_o^2 \geq -3\sigma(F_o^2)$]	0.0693
largest difference peak and hole	1.131 and –0.483 e Å^{-3}

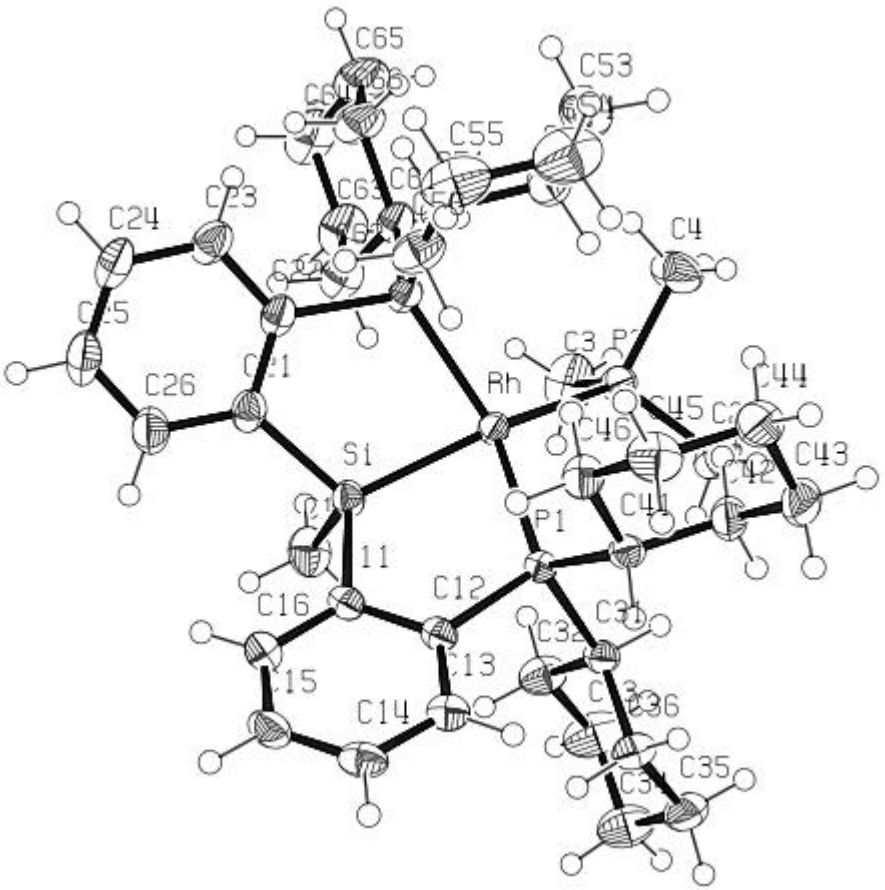

Figure A1. ORTEP diagram of [Cy-PSiP]Rh(PMe_3) (**2-5**)

***Table* A2.** Crystallographic Experimental Details for [{κ^3–Me<u>Si</u>(C_6H_4<u>P</u>Cy_2)$_2$}IrH (NHPh)]·Et_2O (**2-6·OEt$_2$**)

A. Crystal Data	
formula	$C_{47}H_{72}IrNOP_2Si$
formula weight	949.29
crystal dimensions (mm)	0.38 × 0.26 × 0.14
crystal system	orthorhombic
space group	*Pbca* (No. 61)
unit cell parameters	
a (Å)	18.8460 (6)
b (Å)	17.5996 (5)
c (Å)	27.5460 (8)
V (Å^3)	9136.5 (5)
Z	8
ρ_{calcd} (g cm^{-3})	1.380
μ (mm^{-1})	3.053
B. Data Collection and Refinement Conditions	
diffractometer	Bruker D8/APEX II CCD
radiation (λ [Å])	graphite-monochromated Mo Kα (0.71073)
temperature (°C)	–100
scan type	ω scans (0.3°) (20 s exposures)
data collection 2θ limit (deg)	55.06
total data collected	76763 (-24 ≤ *h* ≤ 24, -22 ≤ *k* ≤ 22, -35 ≤ *l* ≤ 35)
independent reflections	10506 (R_{int} = 0.0353)
number of observed reflections (*NO*)	8132 [$F_o^2 \geq 2\sigma(F_o^2)$]
structure solution method	Patterson/structure expansion (*DIRDIF–2008*)
refinement method	full-matrix least-squares on F^2 (*SHELXL–97*)
absorption correction method	Gaussian integration (face-indexed)
range of transmission factors	0.6816–0.3916
data/restraints/parameters	10506 [$F_o^2 \geq -3\sigma(F_o^2)$] / 8[a] / 575
goodness-of-fit (*S*)[f]	1.088 [$F_o^2 \geq -3\sigma(F_o^2)$]
final *R* indices[g]	
R_1 [$F_o^2 \geq 2\sigma(F_o^2)$]	0.0236
wR_2 [$F_o^2 \geq -3\sigma(F_o^2)$]	0.0618
largest difference peak and hole	1.048 and –0.430 e Å^{-3}

[a] The N–C2A and N–C2B distances (within the disordered HNPh group) were constrained to be equal (within 0.01 Å) during refinement. Distances involving

analogous pairs of atoms within the solvent diethyl ether molecule were constrained to be equal (within 0.03 Å) during refinement: d(O1S–C1S) = d(O2S–C5S); d(O1S–C3S) = d(O2S–C7S); d(C1S–C2S) = d(C5S–C6S); d(C3S–C4S) = d(C7S–C8S); d(O1S···C2S) = d(O2S···C6S); d(O1S···C4S) = d(O2S···C8S); d(C1S···C3S) = d(C5S···C7S).

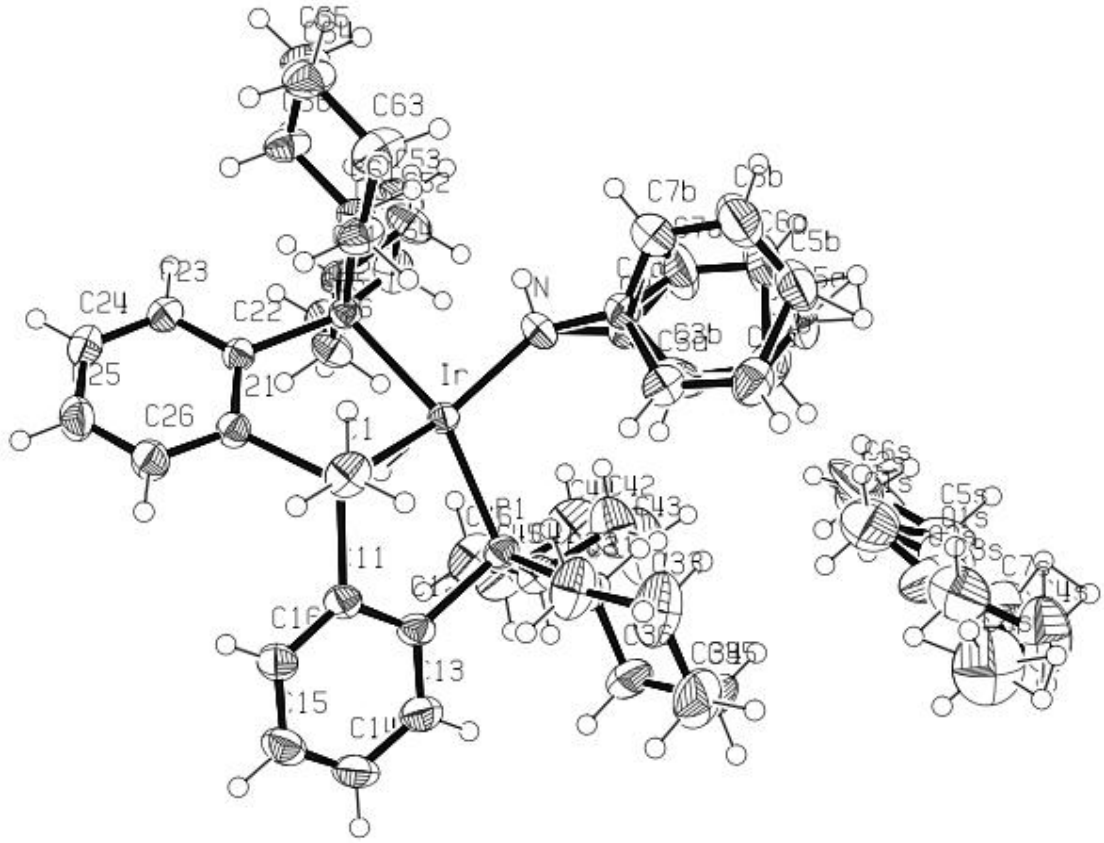

Figure A2. ORTEP diagram of [Cy-PSiP]Ir(H)NHPh·OEt_2 (**2-6·OEt_2**)

Table A3. Crystallographic Experimental Details for [{κ^3–Me<u>Si</u>(C_6H_4<u>P</u>Cy_2)$_2$}IrH(NHC_6H_3-2,6-Me_2)] (**2-7**)

A. Crystal Data	
formula	$C_{45}H_{66}IrNP_2Si$
formula weight	903.22
crystal dimensions (mm)	0.26 × 0.18 × 0.12
crystal system	monoclinic
space group	$P2_1/n$ (an alternate setting of $P2_1/c$ [No. 14])
unit cell parameters	
a (Å)	12.0501 (6)
b (Å)	19.8548 (10)
c (Å)	17.7790 (9)
β (deg)	91.6341 (7)
V (Å^3)	4251.9 (4)
Z	4
ρ_{calcd} (g cm^{-3})	1.411
μ (mm^{-1})	3.275
B. Data Collection and Refinement Conditions	
diffractometer	Bruker D8/APEX II CCD
radiation (λ [Å])	graphite-monochromated Mo Kα (0.71073)
temperature (°C)	–100
scan type	ω scans (0.3°) (25 s exposures)
data collection 2θ limit (deg)	54.86
total data collected	36901 (-15 ≤ h ≤ 15, -25 ≤ k ≤ 25, -22 ≤ l ≤ 23)
independent reflections	9694 (R_{int} = 0.0380)
number of observed reflections (*NO*)	8035 [$F_o^2 \geq 2\sigma(F_o^2)$]
structure solution method	Patterson/structure expansion (*DIRDIF–2008*)
refinement method	full-matrix least-squares on F^2 (*SHELXL–97*)
absorption correction method	Gaussian integration (face-indexed)
range of transmission factors	0.6947–0.4820
data/restraints/parameters	9694 [$F_o^2 \geq -3\sigma(F_o^2)$] / 0 / 454
goodness-of-fit (S)	1.043 [$F_o^2 \geq -3\sigma(F_o^2)$]
final R indices[f]	
R_1 [$F_o^2 \geq 2\sigma(F_o^2)$]	0.0262
wR_2 [$F_o^2 \geq -3\sigma(F_o^2)$]	0.0610
largest difference peak and hole	1.210 and –0.533 e Å^{-3}

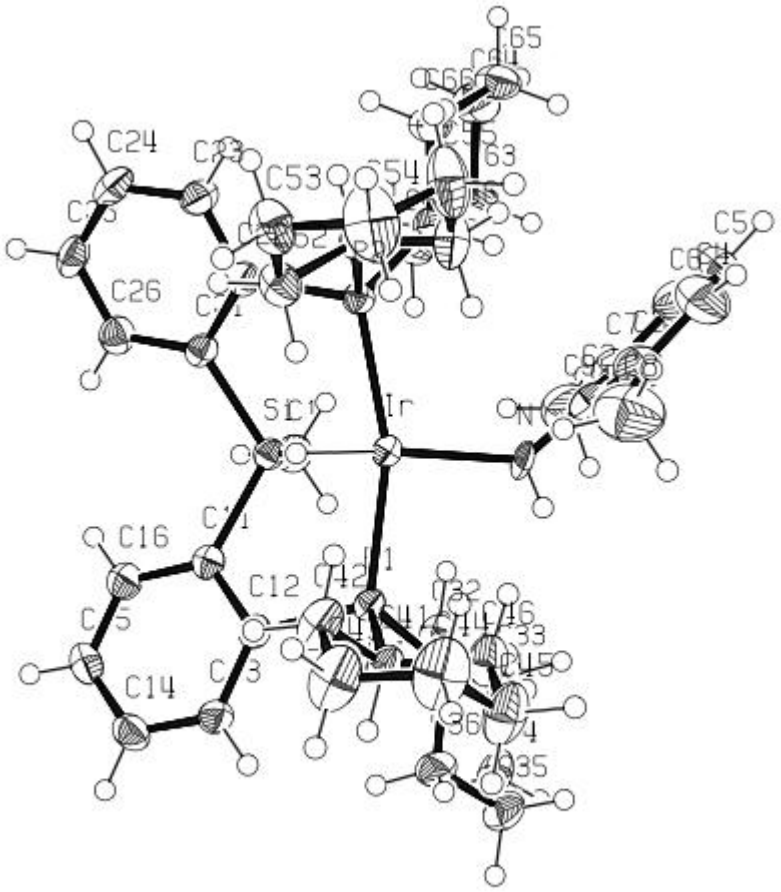

Figure A3. ORTEP diagram of [Cy-PSiP]Ir(H)NH(2,6-$Me_2C_6H_3$) (**2-7**)

Table A4. Crystallographic Experimental Details for [{κ^3–MeSi(C$_6$H$_4$PCy$_2$)$_2$}RhH (NHPh)] (**2-8**)

A. Crystal Data	
formula	$C_{43}H_{62}NP_2RhSi$
formula weight	785.88
crystal dimensions (mm)	0.24 × 0.23 × 0.06
crystal system	monoclinic
space group	$P2_1/c$ (No. 14)
unit cell parameters	
a (Å)	11.7712 (19)
b (Å)	17.415 (3)
c (Å)	20.937 (3)
β (deg)	105.739 (2)
V (Å^3)	4131.1 (11)
Z	4
ρ_{calcd} (g cm^{-3})	1.264
μ (mm^{-1})	0.549
B. Data Collection and Refinement Conditions	
diffractometer	Bruker D8/APEX II CCD
radiation (λ [Å])	graphite-monochromated Mo Kα (0.71073)
temperature (°C)	–100
scan type	ω scans (0.3°) (25 s exposures)
data collection 2θ limit (deg)	50.76
total data collected	25644 (-13 ≤ h ≤ 14, -21 ≤ k ≤ 21, -25 ≤ l ≤ 25)
independent reflections	7558 (R_{int} = 0.0974)
number of observed reflections (*NO*)	4460 [$F_o^2 \geq 2\sigma(F_o^2)$]
structure solution method	Patterson/structure expansion (*DIRDIF–2008*)
refinement method	full-matrix least-squares on F^2 (*SHELXL–97*)
absorption correction method	Gaussian integration (face-indexed)
range of transmission factors	0.9657–0.8776
data/restraints/parameters	7558 [$F_o^2 \geq -3\sigma(F_o^2)$] / 0 / 434
goodness-of-fit (S)	1.009 [$F_o^2 \geq -3\sigma(F_o^2)$]
final R indices[f]	
R_1 [$F_o^2 \geq 2\sigma(F_o^2)$]	0.0519
wR_2 [$F_o^2 \geq -3\sigma(F_o^2)$]	0.1241
largest difference peak and hole	0.869 and –0.600 e Å^{-3}

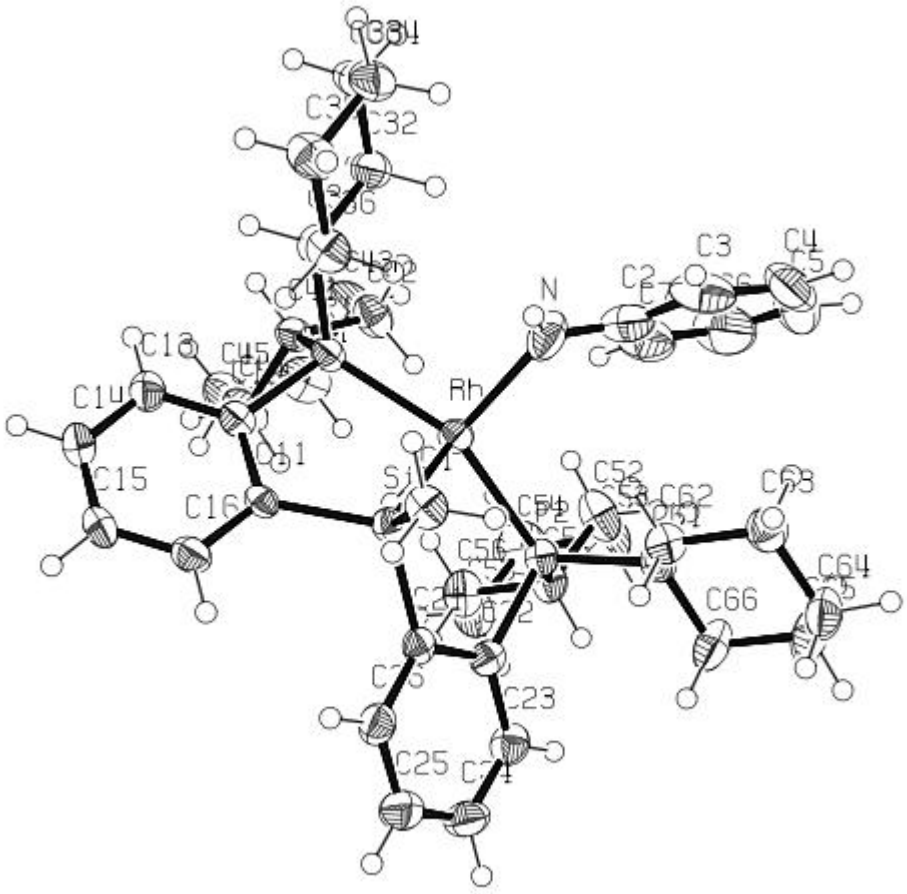

Figure A4. ORTEP diagram of [Cy-PSiP]Rh(H)NHPh (**2-8**)

Table A5. Crystallographic Experimental Details for [{κ^3–Me<u>Si</u>(C_6H_4<u>P</u>Cy_2)$_2$}IrH(NH_2)] (**2-10**)

A. Crystal Data	
formula	$C_{37}H_{58}IrNP_2Si$
formula weight	799.07
crystal dimensions (mm)	0.33 × 0.33 × 0.14
crystal system	triclinic
space group	$P\bar{1}$ (No. 2)
unit cell parameters	
a (Å)	12.6766 (9)
b (Å)	14.0704 (11)
c (Å)	21.2108 (16)
α (deg)	79.8717 (10)
β (deg)	89.5751 (10)
γ (deg)	76.8335 (10)
V (Å^3)	3624.3 (5)
Z	4
ρ_{calcd} (g cm^{-3})	1.464
μ (mm^{-1})	3.831
B. Data Collection and Refinement Conditions	
diffractometer	Bruker D8/APEX II CCD
radiation (λ [Å])	graphite-monochromated Mo Kα (0.71073)
temperature (°C)	–100
scan type	ω scans (0.3°) (30 s exposures)
data collection 2θ limit (deg)	55.34
total data collected	86270 (-16 ≤ h ≤ 16, -17 ≤ k ≤ 18, -27 ≤ l ≤ 27)
independent reflections	16571 (R_{int} = 0.0532)
number of observed reflections (*NO*)	13255 [$F_o^2 \geq 2\sigma(F_o^2)$]
structure solution method	direct methods (*SHELXS–97*[c])
refinement method	full-matrix least-squares on F^2 (*SHELXL–97*)
absorption correction method	multi-scan (*TWINABS*)
range of transmission factors	0.6161–0.3681
data/restraints/parameters	16571 / 0 / 784
goodness-of-fit (S) [all data]	1.036
final R indices[e]	
R_1 [$F_o^2 \geq 2\sigma(F_o^2)$]	0.0300
wR_2 [all data]	0.0719
largest difference peak and hole	1.551 and –1.017 e Å^{-3}

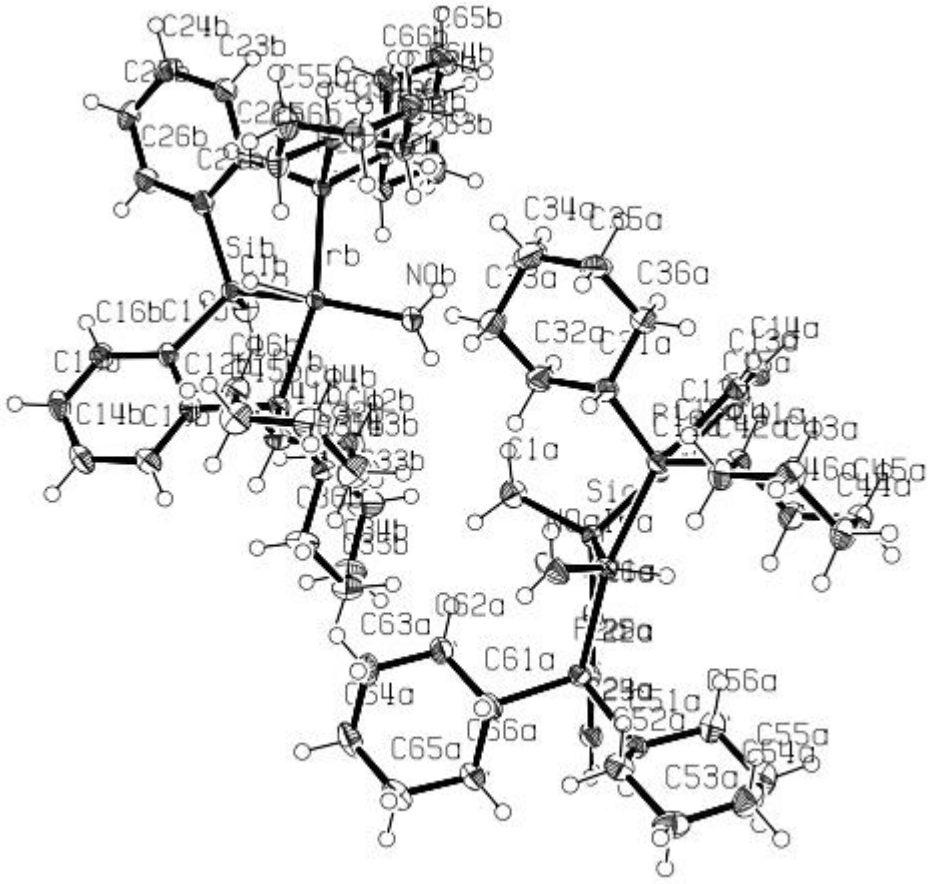

Figure A5. ORTEP diagram of [Cy-PSiP]Ir(H)NH_2 (**2-10**)

Table A6. Crystallographic Experimental Details for [{κ^3–MeSi(C$_6$H$_4$P^{i}Pr$_2$)$_2$}IrHCl] (**3-2**)

A. Crystal Data	
formula	$C_{25}H_{40}ClIrP_2Si$
formula weight	658.25
crystal dimensions (mm)	0.22 × 0.21 × 0.06
crystal system	monoclinic
space group	*C*2/*c* (No. 15)
unit cell parameters	
a (Å)	32.2169 (15)
b (Å)	11.5194 (5)
c (Å)	15.4081 (7)
β (deg)	99.6903 (6)
V (Å^3)	5636.7 (4)
Z	8
ρ_{calcd} (g cm^{-3})	1.551
μ (mm^{-1})	4.999
B. Data Collection and Refinement Conditions	
diffractometer	Bruker D8/APEX II CCD
radiation (λ [Å])	graphite-monochromated Mo Kα (0.71073)
temperature (°C)	–100
scan type	ω scans (0.3°) (20 s exposures)
data collection 2θ limit (deg)	55.06
total data collected	24449 (-41 ≤ *h* ≤ 41, -14 ≤ *k* ≤ 14, -19 ≤ *l* ≤ 19)
independent reflections	6460 (R_{int} = 0.0386)
number of observed reflections (*NO*)	5219 [$F_o^2 \geq 2\sigma(F_o^2)$]
structure solution method	Patterson/structure expansion (*DIRDIF–2008*)
refinement method	full-matrix least-squares on F^2 (*SHELXL–97*)
absorption correction method	Gaussian integration (face-indexed)
range of transmission factors	0.7603–0.4073
data/restraints/parameters	6460 / 0 / 275
goodness-of-fit (*S*) [all data]	1.026
final *R* indices[f]	
R_1 [$F_o^2 \geq 2\sigma(F_o^2)$]	0.0235
wR_2 [all data]	0.0512
largest difference peak and hole	0.633 and –0.647 e Å^{-3}

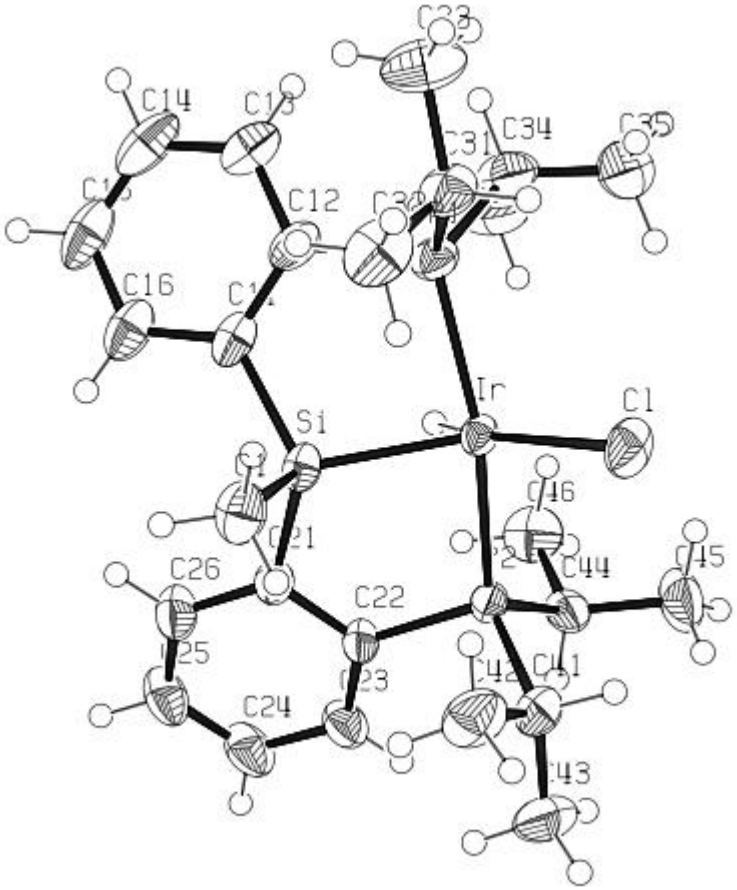

Figure A6. ORTEP diagram of [^{i}Pr-PSiP]Ir(H)Cl (**3-2**)

Table A7. Crystallographic Experimental Details for [{κ^3–MeSi(C_6H_4PCy_2)2IrH{HN (1-adamantyl)}] (**3-8**)

A. Crystal Data	
formula	$C_{47}H_{72}IrNP_2Si$
formula weight	933.29
crystal dimensions (mm)	0.34 × 0.33 × 0.13
crystal system	monoclinic
space group	$P2_1/c$ (No. 14)
unit cell parameters	
a (Å)	12.2243 (5)
b (Å)	17.5649 (7)
c (Å)	21.0860 (8)
β (deg)	101.4818 (4)
V (Å^3)	4437.0 (3)
Z	4
ρ_{calcd} (g cm^{-3})	1.397
μ (mm^{-1})	3.140
B. Data Collection and Refinement Conditions	
diffractometer	Bruker D8/APEX II CCD
radiation (λ [Å])	graphite-monochromated Mo Kα (0.71073)
temperature (°C)	–100
scan type	ω scans (0.3°) (15 s exposures)
data collection 2θ limit (deg)	54.96
total data collected	38895 (-15 ≤ h ≤ 15, -22 ≤ k ≤ 22, -27 ≤ l ≤ 27)
independent reflections	10156 (R_{int} = 0.0231)
number of observed reflections (*NO*)	8658 [$F_o^2 \geq 2\sigma(F_o^2)$]
structure solution method	Patterson/structure expansion (*DIRDIF–2008*)
refinement method	full-matrix least-squares on F^2 (*SHELXL–97*)
absorption correction method	Gaussian integration (face-indexed)
range of transmission factors	0.6856–0.4193
data/restraints/parameters	10156 / 0 / 470
goodness-of-fit (*S*)[e] [all data]	1.091
final R indices[f]	
R_1 [$F_o^2 \geq 2\sigma(F_o^2)$]	0.0252
wR_2 [all data]	0.0598
largest difference peak and hole	1.377 and –1.096 e Å^{-3}

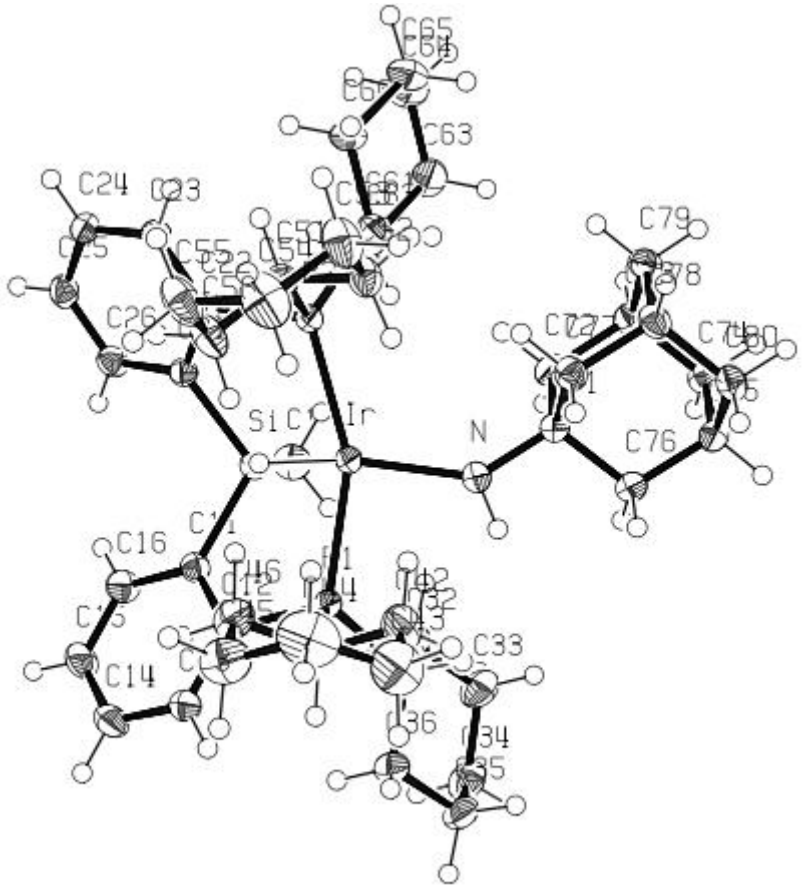

Figure A7. ORTEP diagram of [Cy-PSiP]Ir(H)NHAd (**3-8**)

Table A8. Crystallographic Experimental Details for [{κ^3–Me<u>Si</u>(C_6H_4<u>P</u>^{i}Pr$_2$)$_2$}IrH {HN(1-adamantyl)}] (**3-11**)

A. Crystal Data	
formula	$C_{35}H_{56}IrNP_2Si$
formula weight	773.04
crystal dimensions (mm)	0.29 × 0.24 × 0.16
crystal system	monoclinic
space group	$P2_1/c$ (No. 14)
unit cell parameters	
a (Å)	11.0624 (3)
b (Å)	10.5841 (3)
c (Å)	29.9001 (9)
β (deg)	90.3705 (4)
V (Å^3)	3500.80 (17)
Z	4
ρ_{calcd} (g cm^{-3})	1.467
μ (mm^{-1})	3.963
B. Data Collection and Refinement Conditions	
diffractometer	Bruker PLATFORM/APEX II CCD
radiation (λ [Å])	graphite-monochromated Mo Kα (0.71073)
temperature (°C)	–100
scan type	ω scans (0.3°) (15 s exposures)
data collection 2θ limit (deg)	54.70
total data collected	29918 (-14 ≤ h ≤ 14, -13 ≤ k ≤ 13, -38 ≤ l ≤ 38)
independent reflections	7892 (R_{int} = 0.0251)
number of observed reflections (*NO*)	6355 [$F_o^2 \geq 2\sigma(F_o^2)$]
structure solution method	Patterson/structure expansion (*DIRDIF–2008*)
refinement method	full-matrix least-squares on F^2 (*SHELXL–97*)
absorption correction method	Gaussian integration (face-indexed)
range of transmission factors	0.5626–0.3907
data/restraints/parameters	7892 / 26[a] / 350
goodness-of-fit (*S*)[f] [all data]	1.084
final R indices[g]	
R_1 [$F_o^2 \geq 2\sigma(F_o^2)$]	0.0453
wR_2 [all data]	0.1107
largest difference peak and hole	2.229 and –5.006 e Å^{-3}

[a] The Ir–N1A and Ir–N1B distances were constrained to be equal (within 0.05 Å) during refinement. (b) The N1A–C50A and N1B–C50B distances were constrained to be equal

(within 0.03 Å) during refinement. (c) The C–C bond distances within the two conformers of the disordered 1-adamantyl group were constrained to be equal (within 0.03 Å) to a common refined value.

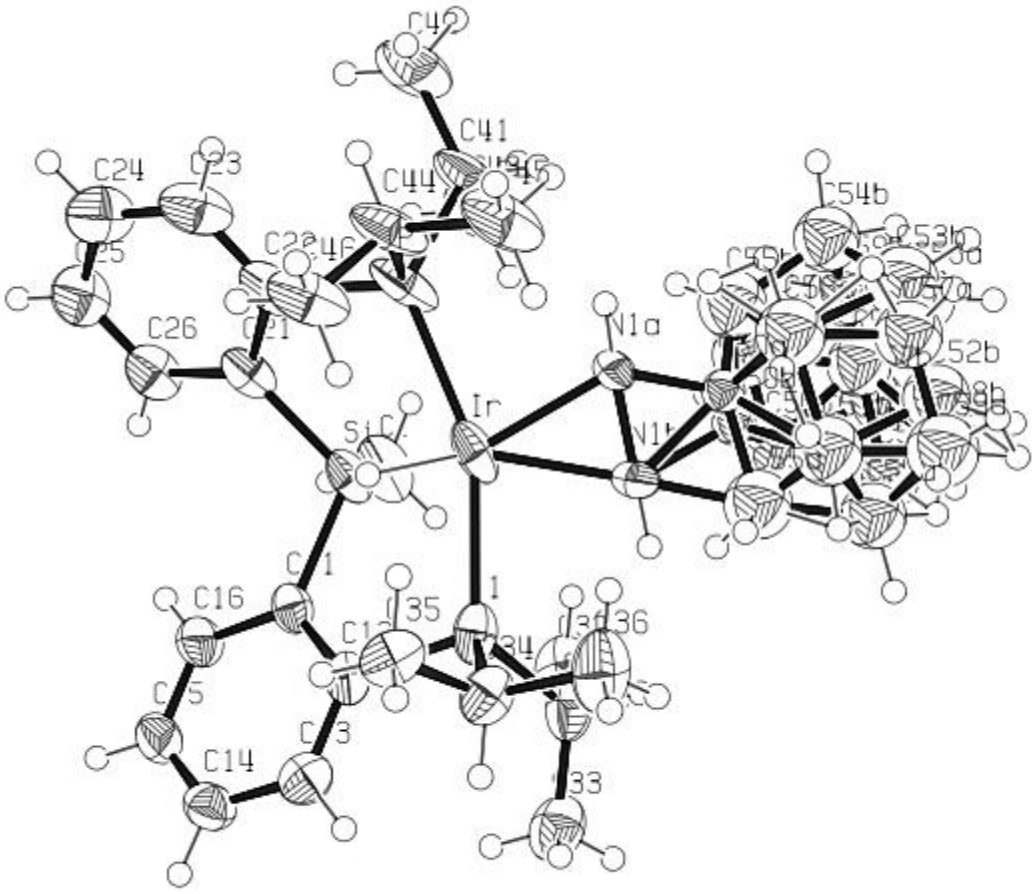

Figure A8. ORTEP diagram of [^{i}Pr-PSiP]Ir(H)NHAd (**3-11**)

Table A9. Crystallographic Experimental Details for [{κ^3–MeSi($C_6H_4P^iPr_2$)$_2$}IrH{(4-methylpiperazin-1-yl)amide}] (**3-22**)

A. Crystal Data	
formula	$C_{30}H_{52}IrN_3P_2Si$
formula weight	736.98
crystal dimensions (mm)	0.23 × 0.17 × 0.15
crystal system	monoclinic
space group	$P2_1/c$ (No. 14)
unit cell parameters	
a (Å)	12.1108 (4)
b (Å)	14.1354 (5)
c (Å)	19.5155 (7)
β (deg)	91.5654 (4)
V (Å^3)	3339.6 (2)
Z	4
ρ_{calcd} (g cm^{-3})	1.466
μ (mm^{-1})	4.152
B. Data Collection and Refinement Conditions	
diffractometer	Bruker D8/APEX II CCD
radiation (λ [Å])	graphite-monochromated Mo Kα (0.71073)
temperature (°C)	–100
scan type	ω scans (0.3°) (20 s exposures)
data collection 2θ limit (deg)	55.08
total data collected	29269 (-15 ≤ h ≤ 15, -18 ≤ k ≤ 18, -25 ≤ l ≤ 25)
independent reflections	7688 (R_{int} = 0.0374)
number of observed reflections (*NO*)	6519 [$F_o^2 \geq 2\sigma(F_o^2)$]
structure solution method	Patterson/structure expansion (*DIRDIF–2008*)
refinement method	full-matrix least-squares on F^2 (*SHELXL–97*)
absorption correction method	Gaussian integration (face-indexed)
range of transmission factors	0.5673–0.4472
data/restraints/parameters	7688 / 0 / 342
goodness-of-fit (S) [all data]	1.020
final R indices	
R_1 [$F_o^2 \geq 2\sigma(F_o^2)$]	0.0226
wR_2 [all data]	0.0510
largest difference peak and hole	0.816 and –0.780 e Å^{-3}

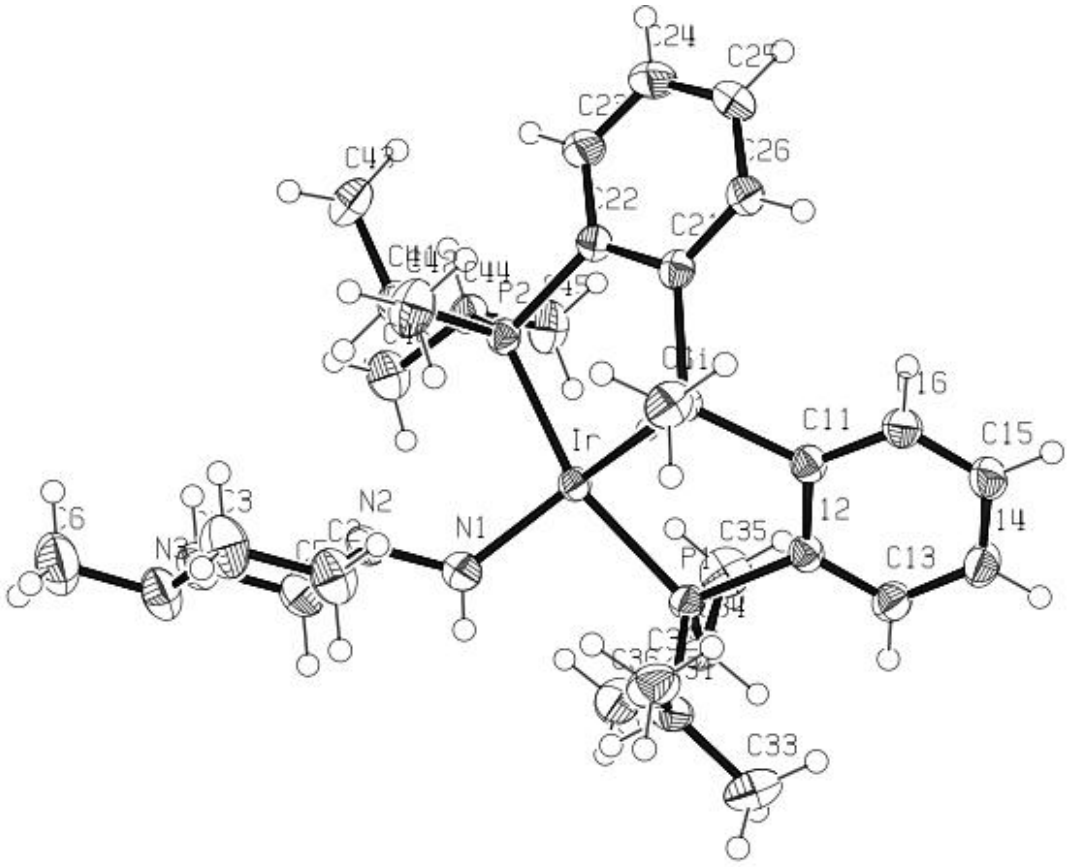

Figure A9. ORTEP diagram of [^{i}Pr-PSiP]Ir(H)NHN(CH_2CH_2)$_2$NMe (**3-22**)

Table A10. Crystallographic Experimental Details for [{MeSi(PCy_2)$_2$}IrH($NHCOC_6F_5$)]•C_6H_6 (**3-24•C_6H_6**)

A. Crystal Data	
formula	$C_{50}H_{63}F_5IrNOP_2Si$
formula weight	1071.24
crystal dimensions (mm)	0.49 × 0.45 × 0.10
crystal system	triclinic
space group	$P\bar{1}$ (No. 2)
unit cell parameters	
a (Å)	10.6476 (4)
b (Å)	14.1039 (5)
c (Å)	16.3130 (6)
α (deg)	77.7977 (4)
β (deg)	83.6358 (4)
γ (deg)	89.2749 (4)
V (Å^3)	2379.52 (15)
Z	2
ρ_{calcd} (g cm^{-3})	1.495
μ (mm^{-1})	2.955
B. Data Collection and Refinement Conditions	
diffractometer	Bruker D8/APEX II CCD
radiation (λ [Å])	graphite-monochromated Mo Kα (0.71073)
temperature (°C)	–100
scan type	ω scans (0.3°) (20 s exposures)
data collection 2θ limit (deg)	54.98
total data collected	20915 (-13 ≤ h ≤ 13, -18 ≤ k ≤ 18, -21 ≤ l ≤ 21)
independent reflections	10754 (R_{int} = 0.0148)
number of observed reflections (*NO*)	10183 [$F_o^2 \geq 2\sigma(F_o^2)$]
structure solution method	direct methods (*SHELXS–97*[c])
refinement method	full-matrix least-squares on F^2 (*SHELXL–97*)
absorption correction method	Gaussian integration (face-indexed)
range of transmission factors	0.7566–0.3271
data/restraints/parameters	10754 / 0 / 559
goodness-of-fit (S) [all data]	1.068
final R indices[e]	
R_1 [$F_o^2 \geq 2\sigma(F_o^2)$]	0.0173
wR_2 [all data]	0.0458
largest difference peak and hole	0.830 and –0.308 e Å^{-3}

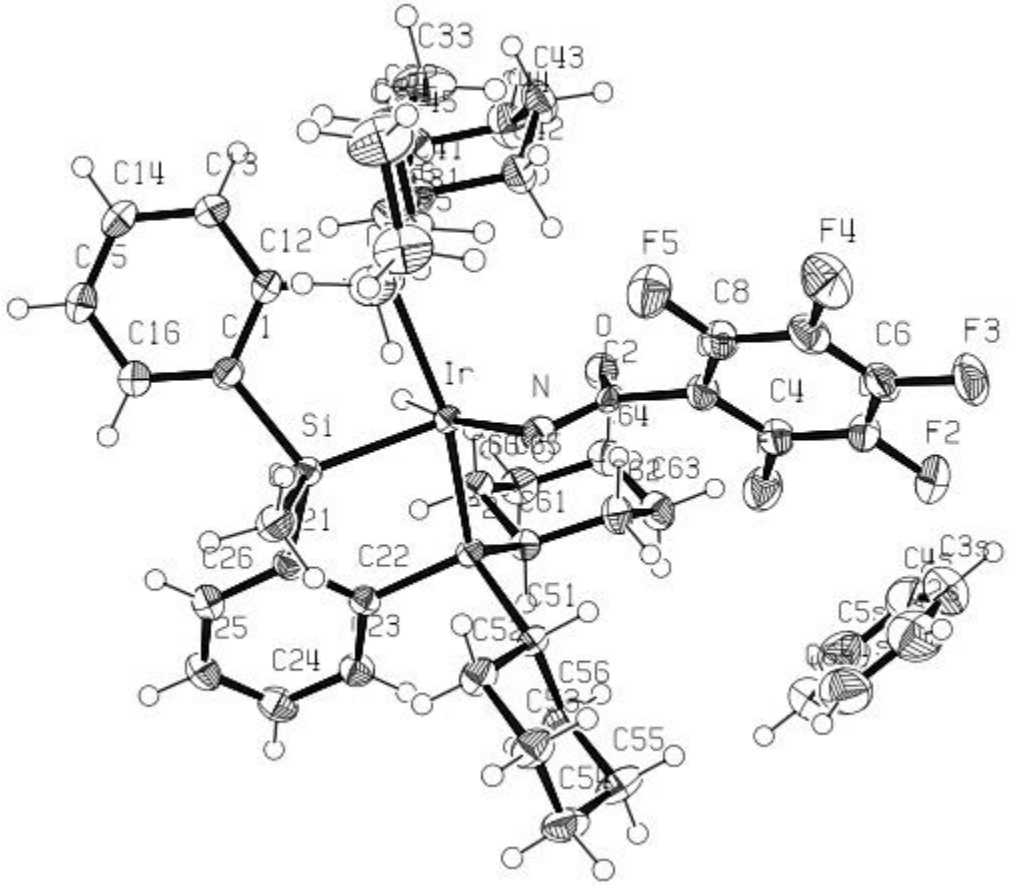

Figure A10. ORTEP diagram of [Cy-PSiP]Ir(H)NH(CO)$C_6F_5 \cdot C_6H_6$ (**3-24·C_6H_6**)

Table A11. Crystallographic Experimental Details for [{κ^3–Me<u>Si</u>(C_6H_4<u>P</u>Cy_2)$_2$}Rh(4-methylpiperazin-1-amine)] (**3-37**)

A. Crystal Data	
formula	$C_{42}H_{68}N_3P_2RhSi$
formula weight	807.93
crystal dimensions (mm)	0.24 × 0.18 × 0.13
crystal system	monoclinic
space group	$P2_1/c$ (No. 14)
unit cell parameters	
a (Å)	9.7964 (4)
b (Å)	23.7656 (10)
c (Å)	18.0199 (8)
β (deg)	98.7288 (6)
V (Å^3)	4146.8 (3)
Z	4
ρ_{calcd} (g cm^{-3})	1.294
μ (mm^{-1})	0.550
B. Data Collection and Refinement Conditions	
diffractometer	Bruker D8/APEX II CCD
radiation (λ [Å])	graphite-monochromated Mo Kα (0.71073)
temperature (°C)	–100
scan type	ω scans (0.3°) (30 s exposures)
data collection 2θ limit (deg)	52.88
total data collected	33197 (-12 ≤ h ≤ 12, -29 ≤ k ≤ 29, -22 ≤ l ≤ 22)
independent reflections	8520 (R_{int} = 0.0609)
number of observed reflections (*NO*)	6427 [$F_o^2 \geq 2\sigma(F_o^2)$]
structure solution method	Patterson/structure expansion (*DIRDIF–2008*)
refinement method	full-matrix least-squares on F^2 (*SHELXL–97*)
absorption correction method	Gaussian integration (face-indexed)
range of transmission factors	0.9329–0.8793
data/restraints/parameters	8520 / 0 / 451
goodness-of-fit (*S*) [all data]	1.008
final R indices[f]	
R_1 [$F_o^2 \geq 2\sigma(F_o^2)$]	0.0396
wR_2 [all data]	0.0926
largest difference peak and hole	1.397 and –0.688 e Å^{-3}

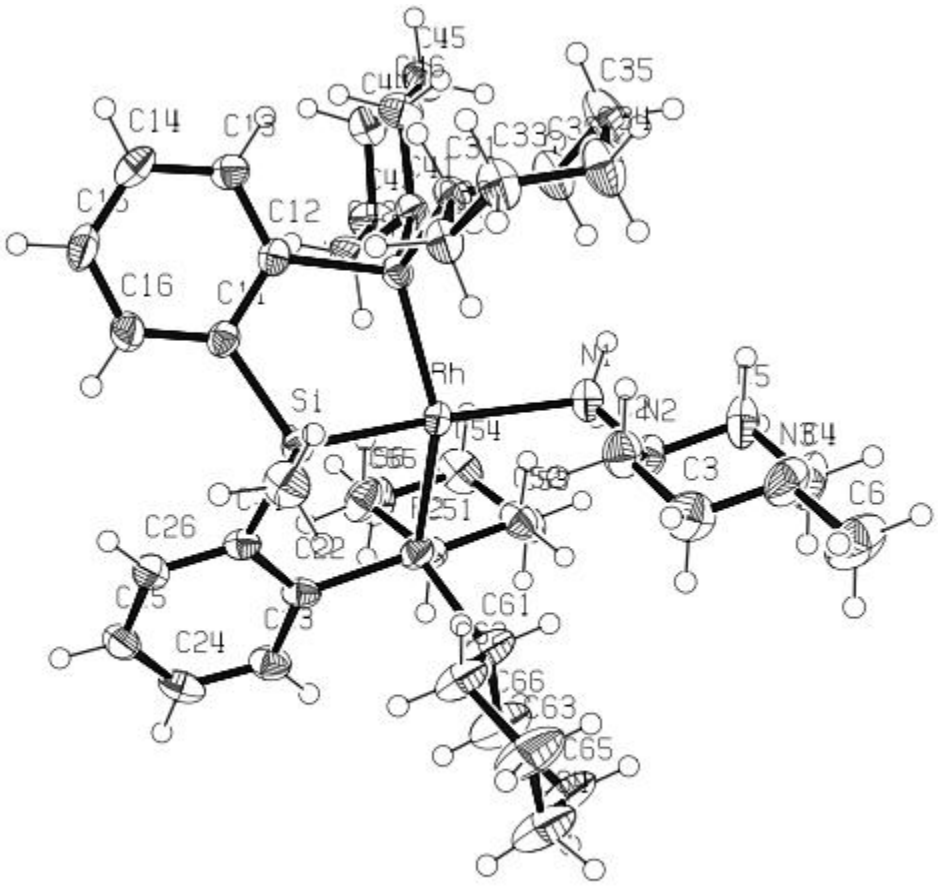

Figure A11. ORTEP diagram of [Cy-PSiP]Rh($NH_2N(CH_2CH_2)_2NMe$) (**3-37**)

Table A12. Crystallographic Experimental Details for [{κ^3–MeSi(C_6H_4PCy_2)$_2$}Rh(4-dimethylaminopyridine)]•Et_2O (**3-38·Et_2O**)

A. Crystal Data	
formula	$C_{48}H_{75}N_2OP_2RhSi$
formula weight	889.04
crystal dimensions (mm)	0.53 × 0.36 × 0.32
crystal system	monoclinic
space group	$P2_1/c$ (No. 14)
unit cell parameters	
a (Å)	10.7149 (4)
b (Å)	21.9879 (8)
c (Å)	20.2091 (8)
β (deg)	100.6717 (5)
V (Å^3)	4678.9 (3)
Z	4
ρ_{calcd} (g cm^{-3})	1.262
μ (mm^{-1})	0.495
B. Data Collection and Refinement Conditions	
diffractometer	Bruker D8/APEX II CCD
radiation (λ [Å])	graphite-monochromated Mo Kα (0.71073)
temperature (°C)	–100
scan type	ω scans (0.3°) (15 s exposures)
data collection 2θ limit (deg)	55.12
total data collected	41021 (-13 ≤ h ≤ 13, -28 ≤ k ≤ 28, -26 ≤ l ≤ 26)
independent reflections	10768 (R_{int} = 0.0261)
number of observed reflections (*NO*)	9482 [$F_o^2 \geq 2\sigma(F_o^2)$]
structure solution method	Patterson/structure expansion (*DIRDIF–2008*)
refinement method	full-matrix least-squares on F^2 (*SHELXL–97*)
absorption correction method	Gaussian integration (face-indexed)
range of transmission factors	0.8569–0.7801
data/restraints/parameters	10768 / 0 / 499
goodness-of-fit (S) [all data]	1.026
final R indices[f]	
R_1 [$F_o^2 \geq 2\sigma(F_o^2)$]	0.0269
wR_2 [all data]	0.0711
largest difference peak and hole	1.008 and –0.306 e Å^{-3}

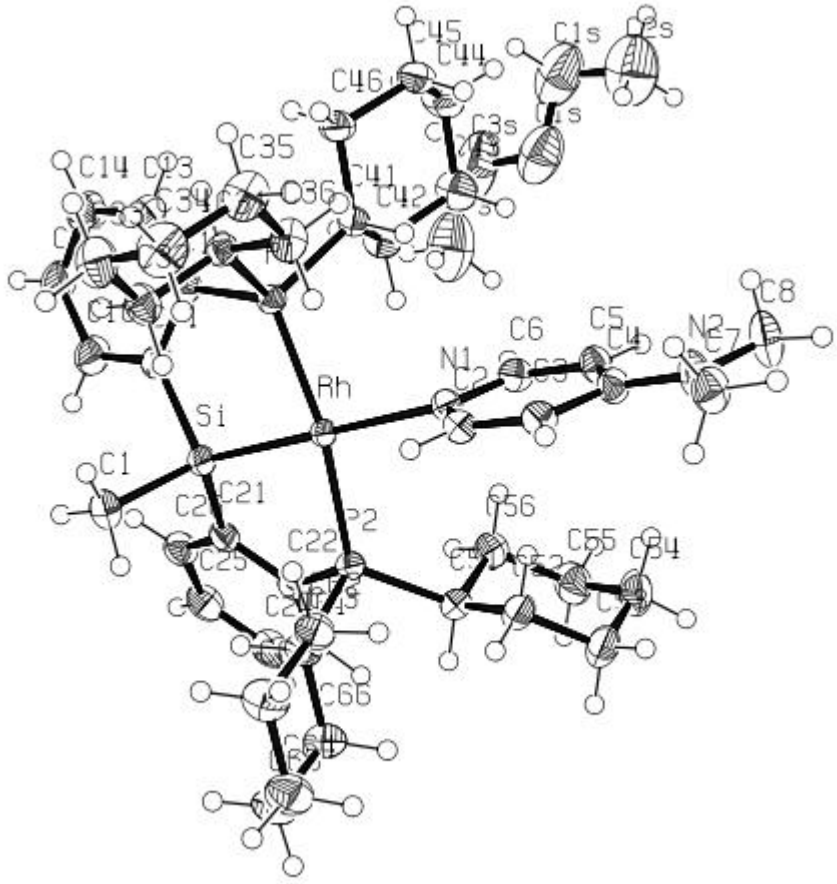

Figure A12. ORTEP diagram of [Cy-PSiP]Rh($NC_5H_4NMe_2$)·Et_2O (**3-38·Et_2O**)

Table A13. Crystallographic Experimental Details for [{MeSi($C_6H_4PCy_2$)$_2$}IrH {C(NH_2)$NC_6H_3Me_2$}{$CNC_6H_3Me_2$}]•$C_4H_{10}O$ (**4-13·Et_2O**)

A. Crystal Data	
formula	$C_{59}H_{86}IrN_3OP_2Si$
formula weight	1135.54
crystal dimensions (mm)	0.44 × 0.28 × 0.08
crystal system	monoclinic
space group	$P2_1/c$ (No. 14)
unit cell parameters[a]	
a (Å)	18.7880 (13)
b (Å)	23.8079 (17)
c (Å)	25.5213 (18)
β (deg)	96.0760 (10)
V (Å^3)	11351.6 (14)
Z	8
ρ_{calcd} (g cm^{-3})	1.329
μ (mm^{-1})	2.470
B. Data Collection and Refinement Conditions	
diffractometer	Bruker D8/APEX II CCD[b]
radiation (λ [Å])	graphite-monochromated Mo Kα (0.71073)
temperature (°C)	–100
scan type	ω scans (0.3°) (15 s exposures)
data collection 2θ limit (deg)	53.08
total data collected	90942 (-23 ≤ h ≤ 23, -29 ≤ k ≤ 29, -31 ≤ l ≤ 31)
independent reflections	23464 (R_{int} = 0.0413)
number of observed reflections (*NO*)	19527 [$F_o^2 \geq 2\sigma(F_o^2)$]
structure solution method	direct methods (*SHELXS–97*[c])
refinement method	full-matrix least-squares on F^2 (*SHELXL–97*[c])
absorption correction method	Gaussian integration (face-indexed)
range of transmission factors	0.8345–0.4068
data/restraints/parameters	23464 [$F_o^2 \geq -3\sigma(F_o^2)$] / 12[d] / 1203
goodness-of-fit (S)[e]	1.109 [$F_o^2 \geq -3\sigma(F_o^2)$]
final R indices[f]	
R_1 [$F_o^2 \geq 2\sigma(F_o^2)$]	0.0326
wR_2 [$F_o^2 \geq -3\sigma(F_o^2)$]	0.0875
largest difference peak and hole	2.867 and –1.218 e Å^{-3}

[a] The C–C and C–O distances within the disordered solvent diethylether molecules were restrained to be 1.530(5) and 1.430(5) Å, respectively.

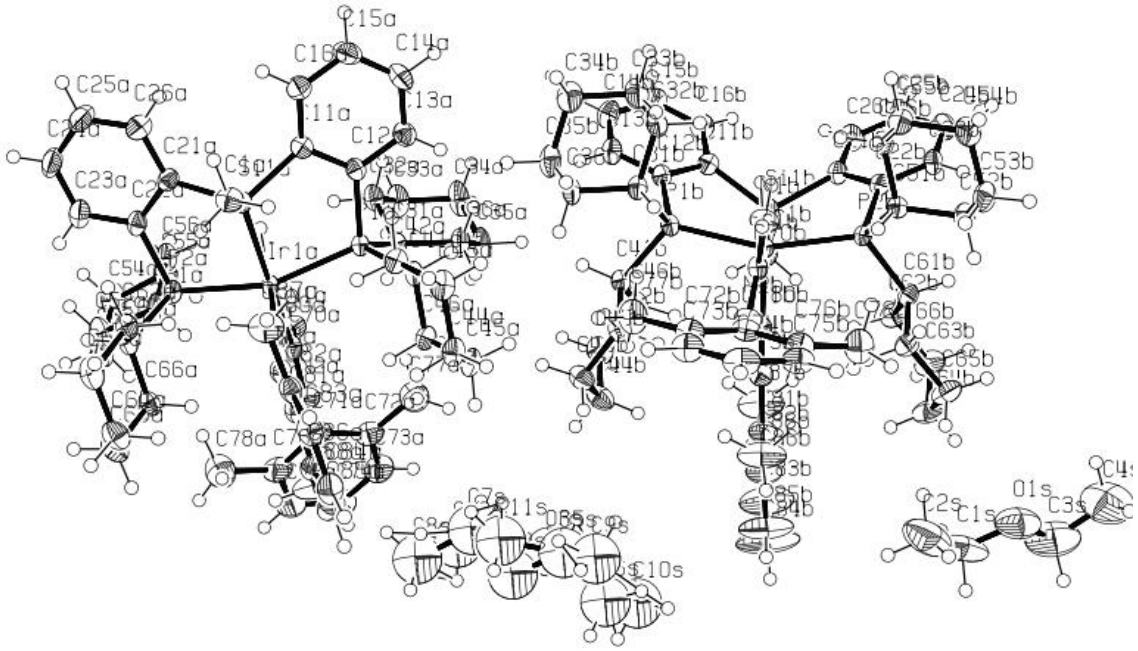

Figure A.13 ORTEP diagram of [Cy-PSiP]Ir(H)(CN(2,6-$Me_2C_6H_3$))(C(NH_2)(N(2,6-$Me_2C_6H_3$)) ·Et_2O (**4-13·Et_2O**)

Table A14. Crystallographic Experimental Details for [{κ^3–Me<u>Si</u>(C_6H_4<u>P</u>Cy_2)$_2$}IrH(OSO_2CF_3)]•0.5C_6H_6 (**5-1·(C_6H_6)$_{0.5}$**)

A. Crystal Data	
formula	$C_{41}H_{59}F_3IrO_3P_2SSi$
formula weight	971.17
crystal dimensions (mm)	0.22 × 0.13 × 0.07
crystal system	monoclinic
space group	$P2_1/n$ (an alternate setting of $P2_1/c$ [No. 14])
unit cell parameters[a]	
a (Å)	11.6753 (6)
b (Å)	17.4028 (9)
c (Å)	20.1125 (10)
β (deg)	92.6090 (6)
V (Å^3)	4082.3 (4)
Z	4
ρ_{calcd} (g cm^{-3})	1.580
μ (mm^{-1})	3.481
B. Data Collection and Refinement Conditions	
diffractometer	Bruker D8/APEX II CCD[b]
radiation (λ [Å])	graphite-monochromated Mo Kα (0.71073)
temperature (°C)	–100
scan type	ω scans (0.3°) (20 s exposures)
data collection 2θ limit (deg)	55.04
total data collected	35632 (-15 ≤ h ≤ 15, -22 ≤ k ≤ 22, -26 ≤ l ≤ 26)
independent reflections	9370 (R_{int} = 0.0392)
number of observed reflections (*NO*)	8011 [$F_o^2 \geq 2\sigma(F_o^2)$]
structure solution method	Patterson/structure expansion (*DIRDIF–2008*[c])
refinement method	full-matrix least-squares on F^2 (*SHELXL–97*[d])
absorption correction method	Gaussian integration (face-indexed)
range of transmission factors	0.7927–0.5175
data/restraints/parameters	9370 / 0 / 473
goodness-of-fit (*S*)[e] [all data]	1.021
final R indices[f]	
R_1 [$F_o^2 \geq 2\sigma(F_o^2)$]	0.0233
wR_2 [all data]	0.0536
largest difference peak and hole	0.717 and –1.238 e Å^{-3}

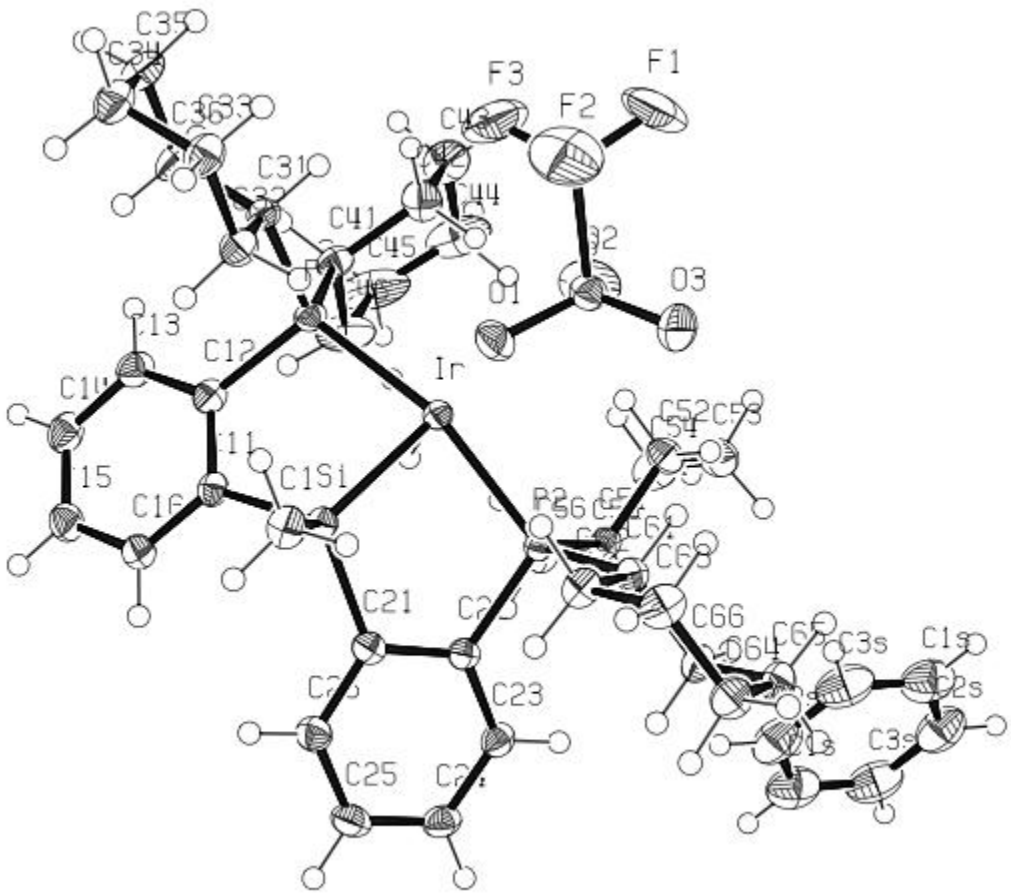

Figure A.14 ORTEP diagram of [Cy-PSiP]Ir(H)(OTf)·$(C_6H_6)_{0.5}$ (**5-1·$(C_6H_6)_{0.5}$**)

Table A15. Crystallographic Experimental Details for [{κ^3–Me<u>Si</u>(C_6H_4<u>P</u>Cy_2)$_2$}IrH(BF_4)]•PhF (**5-3·C_6H_5F**)

A. Crystal Data	
formula	$C_{43}H_{61}BF_5IrP_2Si$
formula weight	965.96
crystal dimensions (mm)	0.29 × 0.23 × 0.12
crystal system	orthorhombic
space group	$Pca2_1$ (No. 29)
unit cell parameters	
a (Å)	17.8330 (8)
b (Å)	13.4805 (6)
c (Å)	17.9199 (8)
V (Å^3)	4307.9 (3)
Z	4
ρ_{calcd} (g cm^{-3})	1.489
μ (mm^{-1})	3.252
B. Data Collection and Refinement Conditions	
diffractometer	Bruker D8/APEX II CCD
radiation (λ [Å])	graphite-monochromated Mo Kα (0.71073)
temperature (°C)	–100
scan type	ω scans (0.3°) (20 s exposures)
data collection 2θ limit (deg)	55.04
total data collected	33905 (-23 ≤ *h* ≤ 23, -17 ≤ *k* ≤ 17, -22 ≤ *l* ≤ 23)
independent reflections	9844 (R_{int} = 0.0383)
number of observed reflections (*NO*)	8675 [$F_o^2 \geq 2\sigma(F_o^2)$]
structure solution method	Patterson/structure expansion (*DIRDIF–2008*)
refinement method	full-matrix least-squares on F^2 (*SHELXL–97*)
absorption correction method	Gaussian integration (face-indexed)
range of transmission factors	0.7041–0.4481
data/restraints/parameters	9844 / 7[a] / 492
Flack absolute structure parameter[f]	–0.001(5)
goodness-of-fit (*S*)[g] [all data]	1.069
final *R* indices[h]	
R_1 [$F_o^2 \geq 2\sigma(F_o^2)$]	0.0240
wR_2 [all data]	0.0683
largest difference peak and hole	0.682 and –0.402 e Å^{-3}

[a] The Ir–H1 distance was restrained to a target value of 1.50(1) Å. Restraints were

applied to distances within the disordered solvent fluorobenzene molecule: d(F1S–C1S) = d(F2S–C3S) = 1.33(1) Å; d(F1S···C2S) = d(F1S···C6S) = d(F2S···C2S) = d(F2S···C4S) = 2.36(1) Å.

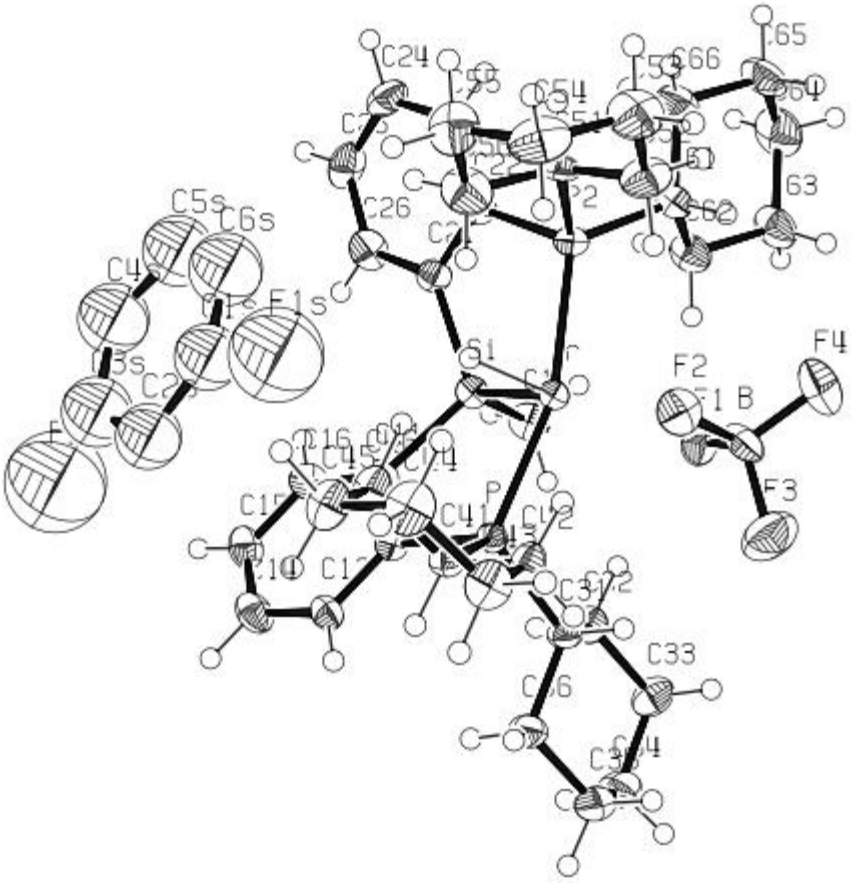

Figure A.15 ORTEP diagram of [Cy-PSiP]Ir(H)(FBF_3)·C_6H_5F (**5-3·C_6H_5F**)

Table A16. Crystallographic Experimental Details for [{κ^3–MeSi(C$_6$H$_4$PCy$_2$)$_2$}IrI(Me)]•$^1/_2$Et$_2$O (**5-11·(Et$_2$O)$_{0.5}$**)

A. Crystal Data	
formula	$C_{40}H_{63}IIrO_{0.5}P_2Si$
formula weight	961.03
crystal dimensions (mm)	0.16 × 0.11 × 0.08
crystal system	triclinic
space group	$P\bar{1}$ (No. 2)
unit cell parameters	
a (Å)	10.5671 (5)
b (Å)	19.6008 (9)
c (Å)	19.8145 (10)
α (deg)	91.2033 (6)
β (deg)	101.4191 (6)
γ (deg)	95.7738 (6)
V (Å^3)	3998.9 (3)
Z	4
ρ_{calcd} (g cm^{-3})	1.596
μ (mm^{-1})	4.249
B. Data Collection and Refinement Conditions	
diffractometer	Bruker D8/APEX II CCD
radiation (λ [Å])	graphite-monochromated Mo Kα (0.71073)
temperature (°C)	–100
scan type	ω scans (0.3°) (20 s exposures)
data collection 2θ limit (deg)	52.70
total data collected	31839 (-13 ≤ h ≤ 13, -24 ≤ k ≤ 24, -24 ≤ l ≤ 24)
independent reflections	16262 (R_{int} = 0.0574)
number of observed reflections (*NO*)	11303 [$F_o^2 \geq 2\sigma(F_o^2)$]
structure solution method	Patterson/structure expansion (*DIRDIF–2008*)
refinement method	full-matrix least-squares on F^2 (*SHELXL–97*)
absorption correction method	Gaussian integration (face-indexed)
range of transmission factors	0.7411–0.5497
data/restraints/parameters	16262 / 14[a] / 808
goodness-of-fit (S)[f] [all data]	0.998
final R indices[g]	
R_1 [$F_o^2 \geq 2\sigma(F_o^2)$]	0.0494
wR_2 [all data]	0.0873
largest difference peak and hole	1.042 and –1.469 e Å^{-3}

[a] Distances within the disordered solvent diethyl ether molecule were restrained during refinement: d(O1S–C1S) = d(O1S–C3S) = d(O2S–C5S) = d(O2S–C7S) = 1.46(1) Å; d(C1S–C2S) = d(C3S–C4S) = d(C5S–C6S) = d(C7S–C8S) = 1.52(1) Å; d(O1S···C2S) = d(O1S···C4S) = d(O2S···C6S) = d(O2S···C8S) = 2.40(1) Å.

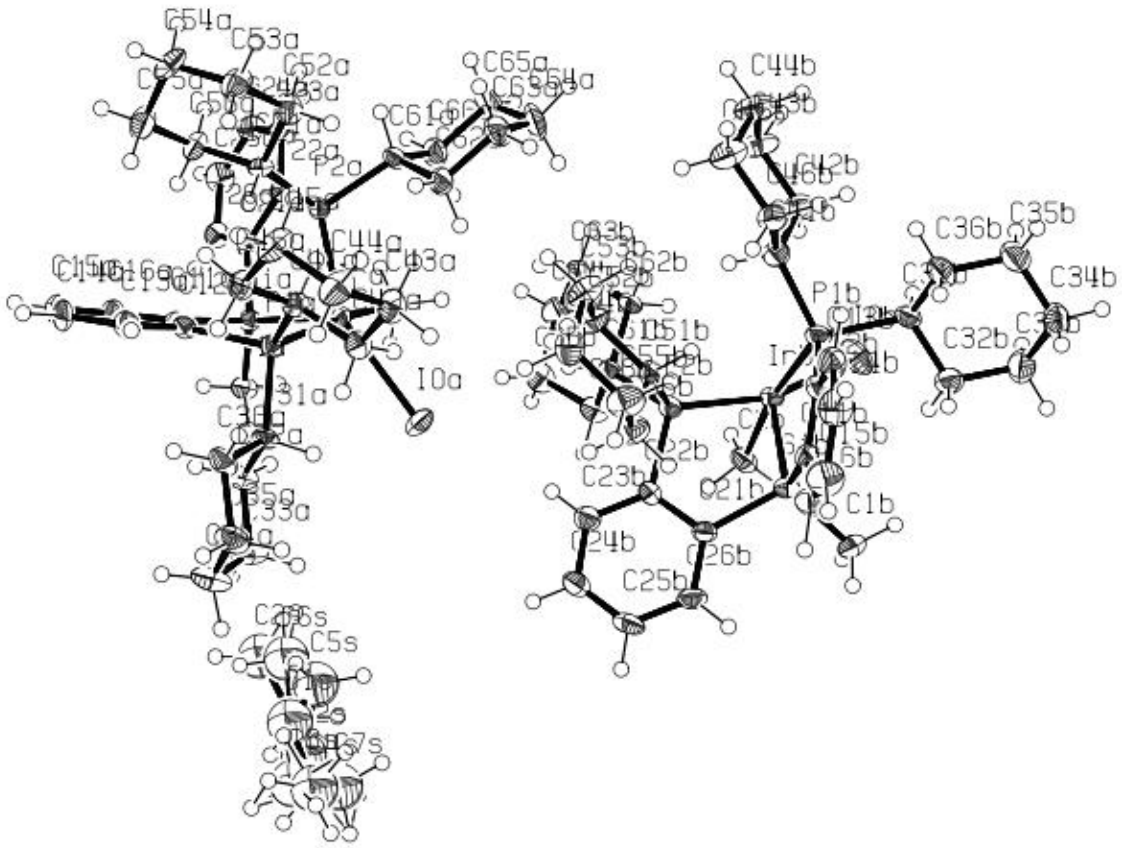

Figure A.16 ORTEP diagram of [Cy-PSiP]Ir(Me)I·$(Et_2O)_{0.5}$ (**5-11·$(Et_2O)_{0.5}$**)

Table A17. Crystallographic Experimental Details for [{κ^3–Me<u>Si</u>(C_6H_4<u>P</u>Cy_2)$_2$} IrH($SiEt_3$)]•0.5C_6H_6 (**5-15·(C_6H_6)$_{0.5}$**)

A. Crystal Data	
formula	$C_{46}H_{74}IrP_2Si_2$
formula weight	937.37
crystal dimensions (mm)	0.58 × 0.38 × 0.27
crystal system	triclinic
space group	$P\bar{1}$ (No. 2)
unit cell parameters	
a (Å)	11.1098 (6)
b (Å)	14.2527 (8)
c (Å)	16.0056 (9)
α (deg)	77.3352 (6)
β (deg)	78.6419 (7)
γ (deg)	67.7812 (6)
V (Å^3)	2270.8 (2)
Z	2
ρ_{calcd} (g cm^{-3})	1.371
μ (mm^{-1})	3.093
B. Data Collection and Refinement Conditions	
diffractometer	Bruker D8/APEX II CCD
radiation (λ [Å])	graphite-monochromated Mo Kα (0.71073)
temperature (°C)	–100
scan type	ω scans (0.3°) (15 s exposures)
data collection 2θ limit (deg)	55.12
total data collected	20137 (-14 ≤ h ≤ 14, -18 ≤ k ≤ 18, -20 ≤ l ≤ 20)
independent reflections	10340 (R_{int} = 0.0164)
number of observed reflections (*NO*)	9743 [$F_o^2 \geq 2\sigma(F_o^2)$]
structure solution method	Patterson/structure expansion (*DIRDIF–2008*)
refinement method	full-matrix least-squares on F^2 (*SHELXL–97*)
absorption correction method	Gaussian integration (face-indexed)
range of transmission factors	0.4867–0.2671
data/restraints/parameters	10340 / 9[a] / 457
goodness-of-fit (*S*) [all data]	1.091
final *R* indices	
R_1 [$F_o^2 \geq 2\sigma(F_o^2)$]	0.0317
wR_2 [all data]	0.0777
largest difference peak and hole	5.664 and –2.443 e Å^{-3}

[a] The solvent benzene molecule was disordered across the crystallographic inversion center ($^1/_2$, $^1/_2$, $^1/_2$). Bond distances within this molecule were restrained to be 1.39(2) Å during refinement. The six carbon atoms were constrained to be (nearly) coplanar during refinement, i.e. by defining them as the vertices of a polyhedron that could occupy a volume of no more than 0.01 Å^3 (*SHELXL-97* FLAT instruction).

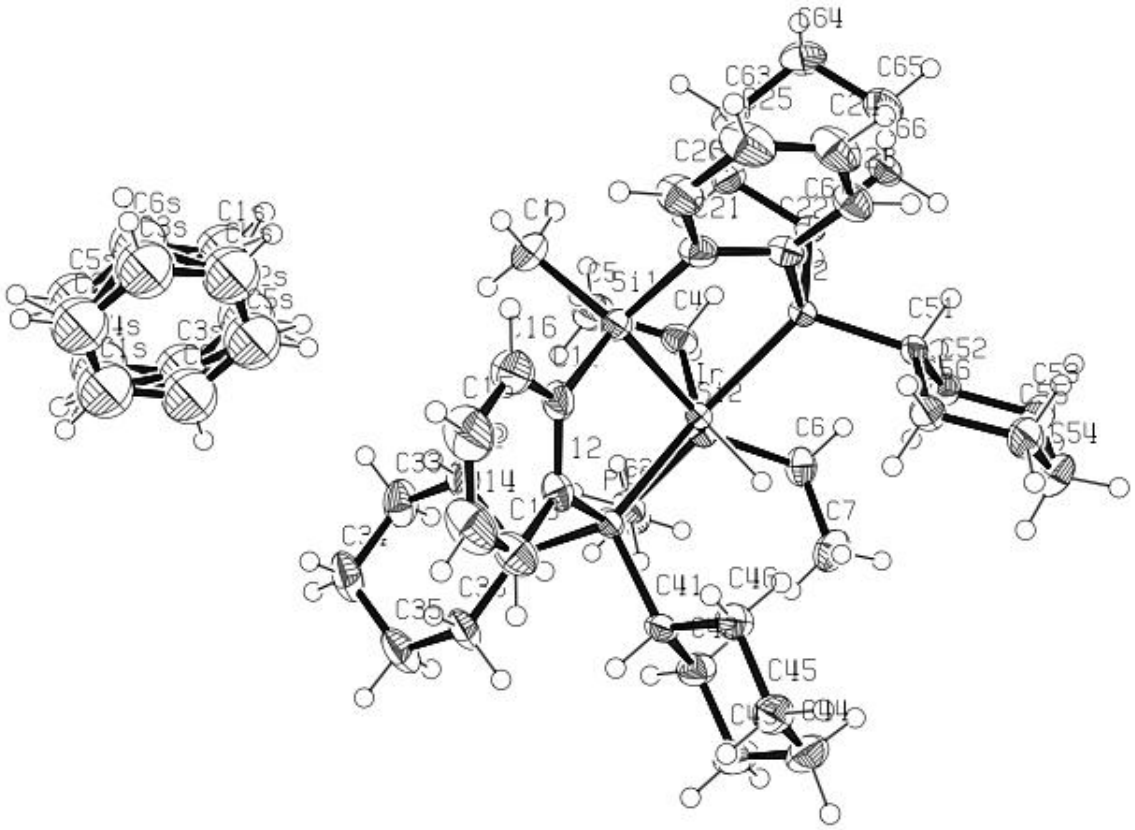

Figure A.17 ORTEP diagram of [Cy-PSiP]Ir(H)SiEt$_3$·(C$_6$H$_6$)$_{0.5}$ **(5-15·(C$_6$H$_6$)$_{0.5}$)**

Table A18. Crystallographic Experimental Details for [{κ^3–Me<u>Si</u>(C_6H_4<u>P</u>Cy_2)$_2$}IrH(H_2BF_2)]•C_6H_6 (**5-16·C_6H_6**)

A. Crystal Data	
formula	$C_{43}H_{64}BF_2IrP_2Si$
formula weight	911.98
crystal dimensions (mm)	0.33 × 0.31 × 0.21
crystal system	triclinic
space group	$P\bar{1}$ (No. 2)
unit cell parameters	
a (Å)	10.2859 (4)
b (Å)	12.4678 (5)
c (Å)	19.1353 (8)
α (deg)	103.1939 (4)
β (deg)	96.5031 (4)
γ (deg)	114.1028 (4)
V (Å^3)	2121.21 (15)
Z	2
ρ_{calcd} (g cm^{-3})	1.428
μ (mm^{-1})	3.288
B. Data Collection and Refinement Conditions	
diffractometer	Bruker D8/APEX II CCD
radiation (λ [Å])	graphite-monochromated Mo Kα (0.71073)
temperature (°C)	–100
scan type	ω scans (0.3°) (15 s exposures)
data collection 2θ limit (deg)	55.12
total data collected	18888 (-13 ≤ h ≤ 13, -16 ≤ k ≤ 16, -24 ≤ l ≤ 24)
independent reflections	9675 (R_{int} = 0.0173)
number of observed reflections (*NO*)	8963 [$F_o^2 \geq 2\sigma(F_o^2)$]
structure solution method	Patterson/structure expansion (*DIRDIF–2008*)
refinement method	full-matrix least-squares on F^2 (*SHELXL–97*)
absorption correction method	Gaussian integration (face-indexed)
range of transmission factors	0.5451–0.4064
data/restraints/parameters	9675 / 0 / 423
goodness-of-fit (S) [all data]	1.055
final R indices[f]	
R_1 [$F_o^2 \geq 2\sigma(F_o^2)$]	0.0249
wR_2 [all data]	0.0639
largest difference peak and hole	1.313 and –0.609 e Å^{-3}

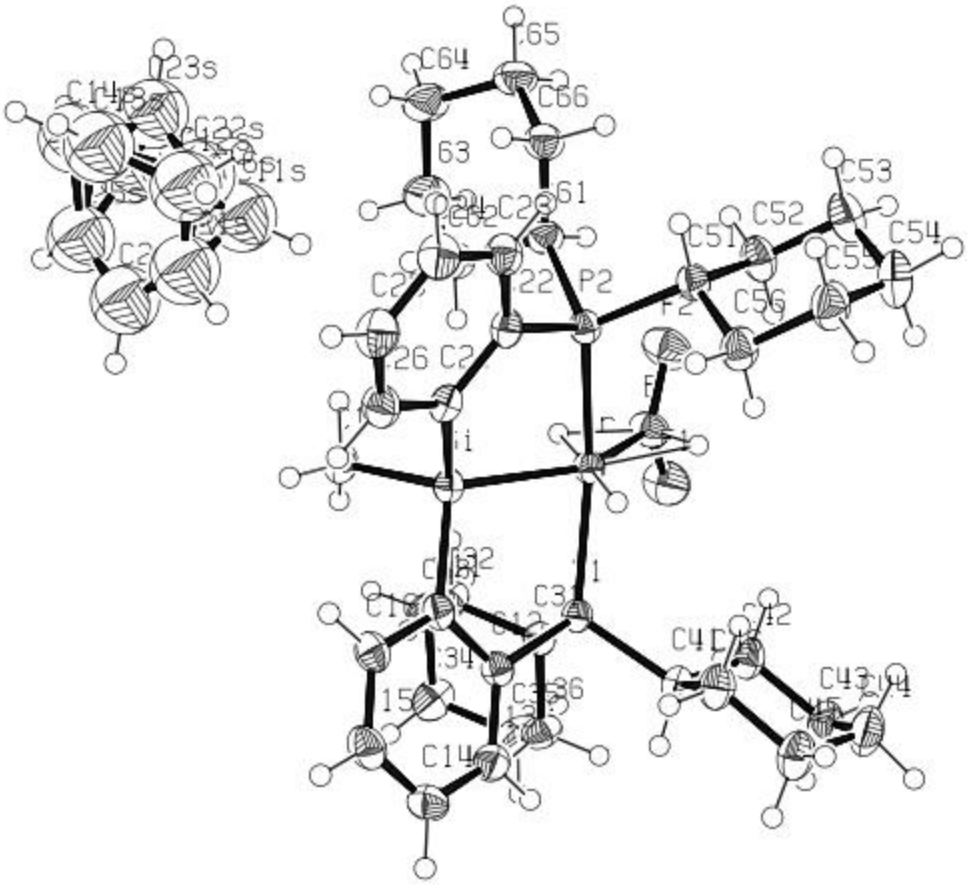

Figure A.18 ORTEP diagram of [Cy-PSiP]Ir(H)(η^2:η^2-H_2BF_2)·C_6H_6 (**5-16·C_6H_6**)

Table A19. Crystallographic Experimental Details for [{κ^3–Me<u>Si</u>(C_6H_4<u>P</u>Cy_2)$_2$}IrH{Si(OTf)Ph_2}]•1.25PhF **(5-19·(C_6H_5F)$_{1.25}$)**

A. Crystal Data	
formula	$C_{57.5}H_{72.25}F_{4.25}IrO_3P_2SSi_2$
formula weight	1234.53
crystal dimensions (mm)	0.32 × 0.16 x 0.16
crystal system	monoclinic
space group	$P2_1/n$ (an alternate setting of $P2_1/c$ [No. 14])
unit cell parameters[a]	
a (Å)	12.8714 (6)
b (Å)	16.4929 (8)
c (Å)	26.1916 (13)
β (deg)	93.9390 (7)
V (Å^3)	5547.0 (5)
Z	4
ρ_{calcd} (g cm^{-3})	1.478
μ (mm^{-1})	2.603
B. Data Collection and Refinement Conditions	
diffractometer	Bruker D8/APEX II CCD[b]
radiation (λ [Å])	graphite-monochromated Mo Kα (0.71073)
temperature (°C)	–100
scan type	ω scans (0.3°) (20 s exposures)
data collection 2θ limit (deg)	53.14
total data collected	39888 (-16 ≤ h ≤ 16, -20 ≤ k ≤ 20, -32 ≤ l ≤ 32)
independent reflections	11514 (R_{int} = 0.0490)
number of observed reflections (*NO*)	9151 [$F_o^2 \geq 2\sigma(F_o^2)$]
structure solution method	Patterson/structure expansion (*DIRDIF–2008*[c])
refinement method	full-matrix least-squares on F^2 (*SHELXL–97*[d])
absorption correction method	Gaussian integration (face-indexed)
range of transmission factors	0.6778–0.4869
data/restraints/parameters	11514 / 2[e] / 749
goodness-of-fit (*S*)[f] [all data]	1.020
final R indices[g]	
R_1 [$F_o^2 \geq 2\sigma(F_o^2)$]	0.0336
wR_2 [all data]	0.0850
largest difference peak and hole	1.316 and –0.945 e Å^{-3}

[a] The Ir–H1 distance was constrained to be 1.50(1) Å during refinement. (b) The P1···H1

and P2···H1 distances were constrained to be equal (within 0.03 Å) during refinement.

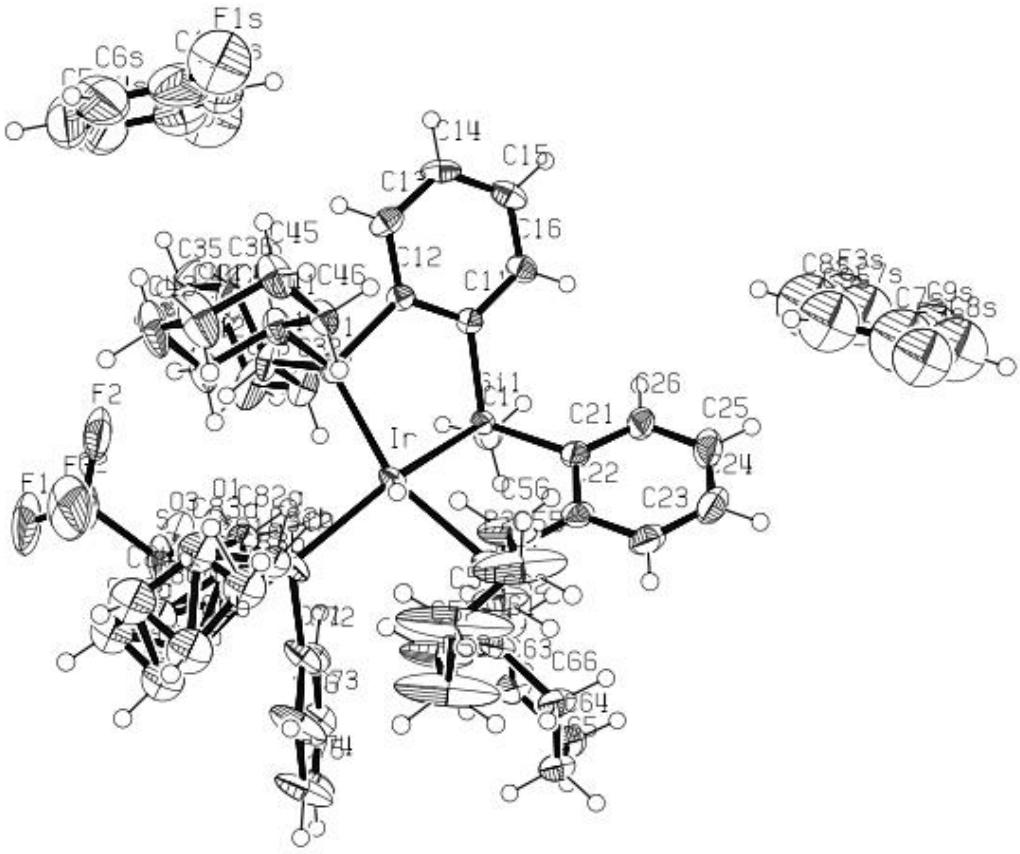

Figure A.19 ORTEP diagram of [Cy-PSiP]Ir(H)($SiPh_2OTf$)·$(C_6H_5F)_{1.25}$ **(5-19·$(C_6H_5F)_{1.25}$)**

References

(1) J. F. Hartwig, *Organotransition Metal Chemistry: From Bonding to Catalysis*, University Science Books, Sausalito, **2010**.

(2) (a) Knowles, W. S. *Angew. Chem. Int. Ed.* **2002**, *45*, 1998. (b) Noyori, R. *Angew. Chem. Int. Ed.* **2002**, *45*, 2008. (c) Sharpless, K. B. *Angew. Chem. Int. Ed.* **2002**, *45*, 2024.

(3) (a) Chauvin, Y. *Angew. Chem. Int. Ed.* **2006**, *45*, 3740. (b) Schrock, R. R. *Angew. Chem. Int. Ed.* **2006**, *45*, 3748. (c) Grubbs, R. H. *Angew. Chem. Int. Ed.* **2006**, *45*, 3760.

(4) Wu, X. F.; Anbarasan, P.; Neumann, H.; Beller, M. *Angew. Chem. Int. Ed.* **2010**, *48*, 9047.

(5) (a) Morales-Morales, D. and Jensen, C. M. *The Chemistry of Pincer Compound*s, Elsevier B. V.: Oxford, 2007. (b) Elschenbroich, C. *Organometallics, Third Completely Revised and Extended Edition*; Wiley: Weinheim, 2006; chapter 18. (c) Albrecht, M.; van Koten, G. *Angew. Chem. Int. Ed.* **2001**, *40*, 3750. (d) van der Boom, M. E.; Milstein, D. *Chem. Rev.* **2003**, *103*, 1759. (d) Lindner, M. M.; Albrecht, M. *Dalton Trans.* **2011**, *40*, 8733.

(6) Slagt, M. Q.; van Zwieten D. A. P.; Moerkerk, A. J. C. M.; Klein Gebbink, R. J. M.; van Koten, G. *Coord. Chem. Rev.* **2004**, *248*, 2275.

(7) Fischer, J.; Schürmann, M.; Mehring, M.; Zachwieja, U.; Jurkschat, K. *Organometallics* **2006**, *25*, 2886.

(8) (a) Espinet, P.; Garcia-Orodea, E.; Miguel, J. A. *Chem. Mater.* **2004**, *16*, 551. (b) Zim, D.; Gruber, A. S.; Ebeling, G.; Dupont, J.; Monteiro, A. L. *Org. Lett.* **2000**, *2*, 2881.

(9) (a) Yao, Q.; Sheets, M. *J. Org. Chem.* **2006**, *71*, 5384. (b) Olsson, V. J.; Sevelius, S.; Selander, N.; Szabó, K. J. *J. Am. Chem. Soc.* **2006,** *128*, 4588.

(10) Pugh, D.; Danopoulos, A. A. *Coord. Chem. Rev.* **2007**, *251*, 4588.

(11) (a) Brück, A.; Gallego, D.; Wang, W.; Irran, E.; Driess, M.; Hartwig, J. F. *Angew. Chem. Int. Ed.* **2012**, *51*, 11478. (b) Wang, W.; Inoue, S.; Irran, E.; Driess, M. *Angew. Chem. Int. Ed.* **2012**, *51*, 3691. (c) Lee, C. -I.; Zhou, J.; Ozerov, O. V. *J. Am. Chem. Soc.* **2013**, *135*, 3560.

(12) For bis(phosphino)phosphido PPP pincer examples, see: (a) Mankad, N. P.; Rivard, E.; Harkins, S. B.; Peters, J. C. *J. Am. Chem. Soc.* **2005**, *127*, 16032. (b) Mazzeo, M.; Lamberti, M.; Massa, A.; Scettri, A.; Pellecchia, C.; Peters, J. C.

Organometallics, **2008**, *27*, 5741. (c) Mazzeo, M.; Strianese, M.; Kuhl, O.; Peters, J. C. *Dalton Trans.* **2011**, *40*, 9026. (d) Bauer, R. C.; Gloaguen, Y.; Lutz, M.; Reek, J. N. H.; de Bruin, B.; van der Vlugt, J. I. *Dalton Trans.*, **2011**, *40*, 8822. (e) Pan, B.; Bezpalko, M. W.; Foxman, B. M.; Thomas, C. M. *Organometallics*, **2011**, *30*, 5560. (f) D'Auria, I.; Lamberti, M.; Mazzeo, M.; Milione, S.; Roviello, G.; Pellecchia, C. *Chem. Eur. J.* **2012**, *18*, 2349. (g) Gloaguen, Y.; Jacobs, W.; de Bruin, B.; Lutz, M.; van der Vlugt, J. I. *Inorg. Chem.* **2013**, *52*, 1682.

(13) For bis(phosphino)boryl PBP pincer examples, see: (a) Segawa, Y.; Yamashita, M.; Nozaki, K. *J. Am. Chem. Soc.* **2009**, *131*, 9201. (b) Segawa, Y.; Yamashita, M.; Nozaki, K. *Organometallics*, **2009**, *28*, 6234. (c) Hasegawa, M.; Segawa, Y.; Yamashita, M.; Nozaki, K. *Angew. Chem. Int. Ed.* **2012**, *51*, 6956. (d) Ogawa, H.; Yamashita, M. *Dalton Trans.* **2013**, *42*, 625.

(14) For bis(phosphino)germyl PGeP or bis(phosphino)stannyl PSnP pincer examples, see: (a) Hajime, K.; Ishii, S.; Nakazawa, H. *Dalton Trans.* **2012**, *41*, 11386. (b) Takaya, J.; Nakamura, S.; Iwasawa, N. *Chem. Lett.* **2012**, *41*, 967.

(15) For bis(phosphino)silyl PSiP pincer examples, see: (a) MacInnis, M. C.; MacLean, D. F.; Lundgren, R. J.; McDonald, R.; Turculet, L. *Organometallics* **2007**, *26*, 6522. (b) MacLean, D. F.; McDonald, R.; Ferguson, M. J.; Caddell, A. J.; Turculet, L. *Chem. Commun.* **2008**, 5146. (c) Mitton, S. J.; McDonald, R.; Turculet, L. *Organometallics* **2009**, *28*, 5122. (d) Mitton, S. J.; McDonald, R.; Turculet, L. *Angew. Chem. Int. Ed.* **2009**, *48*, 8568. (e) Morgan, E.; MacLean, D. F.; McDonald, R.; Turculet, L. *J. Am. Chem. Soc.* **2009**, *131*, 14234. (f) MacInnis, M. C.; McDonald, R.; Ferguson, M. J.; Tobisch, S.; Turculet, L. *J. Am. Chem. Soc*. **2011,** *133*, 13622. (g) Mitton, S. J.; Turculet, L. *Chem. Eur. J.* **2012***, 18*, 258. (h) Korshin, E. E.; Leitus, G.; Shimon, L. J. W.; Konstantinovski, L.; Milstein, D. *Inorg. Chem.* **2008**, *47*, 7177. (i) J. Takaya, N. Iwasawa, *J. Am. Chem. Soc.* **2008**, *130*, 15254. (j) Takaya, J.; Iwasawa, N. *Organometallics*, **2009**, *28*, 6636. (k) Takaya, J.; Iwasawa, N. *Dalton Trans.* **2011**, *40*, 8814. (l) Takaya, J.; Kirai, N.; Iwasawa, N. *J. Am. Chem. Soc.* **2011**, *133*, 12980. (m) Takaya, J.; Sasano, K.; Iwasawa, N. *Org. Lett.* **2011**, *13*, 1698. (n) Kirai, N.; Takaya, J.; Iwasawa, N. *J. Am. Chem. Soc.* **2013**, *135*, 2493. (o) Fang, H.; Choe, Y.-K.; Li, Y.; Shimada, S. *Chem. Asian J.* **2011**, *6*, 2512. (p) Joost, M.; Mallet-Ladeira, S.; Miqueu, K.; Amgoune, A.; Bourissou, D. *Organometallics*, **2013**, *32*, 898.

(16) (a) Liang, L. C. *Coord. Chem. Rev.* **2006**, *250*, 1152. (b) Ozerov, O. V.; Guo, C.; Papkov, V. A.; Foxman, B. M. *J. Am. Chem. Soc.* **2004**, *126*, 4792. (c) Mindiola, D. J. *Acc. Chem. Res.* **2006**, *39*, 813. (d) Csok, Z.; Vechorkin, O.; Harkins, S. B.; Scopelliti, R.; Hu, X. *J. Am. Chem. Soc.* **2008**, *130*, 8156. (e) Wei, W.; Qin, Y.; Loo, M.; Xia, P.; Wong, M. S. *Organometallics* **2008**, *27*, 2268. (f) Fryzuk, M. D. *Can. J. Chem.* **1992**, *70*, 2839. (g) Watson, L. A.; Ozerov, O. V.; Pink, M; Caulton, K. G. *J. Am. Chem. Soc.* **2003**, *125*, 8426.

(17) Leis, W.; Mayer, H. A.; Kaska, W. C. *Coord. Chem. Rev.* **2008**, *252*, 1787.

(18) (a) Moulton, C. J.; Shaw, B. L. *J. Chem. Soc. Dalton* **1976**, 1020. (b) Empsall, H. D.; Hyde, E. M.; Markham, R.; McDonald, W. S.; Norton, M. C.; Shaw, B. L.; Weeks, B. *J. Chem. Soc. Chem. Comm.* **1977**, 589. (c) Crocker, C.; Errington, R. J.; McDonald, W. S.; Odell, K. J.; Shaw, B. L. *J. Chem. Soc. Chem. Comm.* **1979**, 498. (d) Crocker, C.; Errington, R. J.; Markham, R.; Moulton, C. J.; Odell, K. J.; Shaw, B. L. *J. Am. Chem. Soc.* **1980**, *102*, 4373.

(19) Arndtsen, B. A.; Bergman, R. G.; Mobley, T. A.; Peterson, T. H. *Acc. Chem. Res.* **1995**, *28*, 154.

(20) Labinger, J. A.; Bercaw, J. E. *Nature* **2002**, *417*, 507.

(21) (a) Janowicz, A. H.; Bergman, R.G. *J. Am. Chem. Soc.* **1982**, *104*, 352. (b) Hoyano, J. K.; Graham, W. A. G. *J. Am. Chem. Soc.* **1982**, *104*, 3723.

(22) For select examples of transition metal mediated transfer dehydrogenation see: (a) Baudry, D.; Ephritikhine, M.; Felkin, H.; Holmes-Smith, R. *J. Chem. Soc., Chem. Commun*. **1983**, 788. (b) Burk, M. W.; Crabtree, R. H.; McGrath, D. V. *J. Chem. Soc., Chem. Commun.* **1985**, 1829. (c) Belli, J.; Jensen, C. M. *Organometallics*, **1996**, *15*, 1532

(23) (a) Maguire, J. A.; Goldman, A. S. *J. Am. Chem. Soc.* **1991**, *113*, 6706. (b) Maguire, J. A.; Petrillo, A.; Goldman, A. S. *J. Am. Chem. Soc.* **1992**, *114,* 9492.

(24) (a) Gupta, M.; Hagen, C.; Flesher, R. J.; Kaska, W. C.; Jensen, C. M. *Chem. Commun.* **1996**, 2083. (b) Gupta, M.; Hagen, C.; Kaska, W. C.; Cramer, R. E.; Jensen, C. M. *J. Am. Chem. Soc.* **1997**, *119*, 840.

(25) Crabtree, R. H.; Parnell, C. P.; Uriarte, R. J. *Organometallics* **1987**, *6*, 696.

(26) Jensen, C. M. *Chem. Commun*. **1999**, 2443.

(27) Lee, D. W.; Kaska, W. C.; Jensen, C. M. *Organometallics* **1998**, *17*, 1.

(28) Kanzelberger, M.; Singh, B.; Czerw, M.; Krogh-Jespersen, K.; Goldman, A. S. *J. Am. Chem. Soc.* **2000**, *122*, 11017.

(29) Liu, F.; Pak, E. B.; Singh, B.; Jensen, C. M.; Goldman, A. S. *J. Am. Chem. Soc.* **1999**, *121*, 4086.

(30) Biswas, S.; Huang, Z.; Choliy, Y.; Wang. D. Y.; Brookhart, M.; Krogh-Jespersen, K.; Goldman, A. S. *J. Am. Chem. Soc.* **2012**, *134*, 13276.

(31) Xu, W.-W.; Rosini, G. P.; Gupta, M.; Jensen, C. M.; Kaska, W. C.; Krogh-Jespersen, K.; Goldman, A. *Chem. Commun.* **1997**, 2273.

(32) Liu, F.; Goldman, A. S. *Chem. Commun.* **1999**, 655.

(33) Punji, B.; Emge, T. J.; Goldman, A. S. *Organometallics*, **2010**, *29*, 2702.

(34) (a) Krogh-Jespersen, K.; Czerw, M.; Kanzelberger, M.; Goldman, A. S. *J. Chem. Inf. Comput. Sci*. **2001**, *41*, 56. (b) Krogh-Jespersen, K.; Czerw, M.; Zhu, K.; Singh, B.; Kanzelberger, M.; Darji, N.; Achord, P. D.; Renkema, K. B.; Goldman, A. S. *J. Am. Chem. Soc.* **2002**, *124*, 10797 (c) Renkema, K. B.; Kissin, Y. V.; Goldman, A. S. *J. Am. Chem. Soc.* **2003**, *125*, 7770.

(35) (a) Göttker-Schnetmann, I.; White, P.; Brookhart, M. *J. Am. Chem. Soc.* **2004**, *126*, 1804. (b) Göttker-Schnetmann, I.; Brookhart, M. *J. Am. Chem. Soc.* **2004**, *126*, 9330.

(36) Choi, J.; Roy MacArthur, A. H.; Brookhart, M.; Goldman, A. S. *Chem. Rev.* **2011**, *111*, 1761.

(37) Kuklin, S. A.; Sheloumov, A. M.; Dolgushin, F. M.; Ezernitskaya, M. G.; Peregudov, A. S.; Petrovskii, P. V.; Koridze, A. A. *Organometallics*, **2006**, *25*, 5466.

(38) (a) Zhao, J.; Goldman, A. S.; Hartwig, J. F. *Science* **2005**, *307,* 1080. (b) Casalnuovo, A. L.; Clabrese, J. C.; Milstein, D. *Inorg. Chem.* **1987**, *26*, 973. (c) Hillhouse, G. L.; Bercaw, J. E. *J. Am. Chem. Soc.* **1984**, *106*, 5472. (d) Koelliker, V. R.; Milstein, D. *Angew. Chem., Int. Ed. Engl.* **1991**, *30,* 707.

(39) Kanzelberger, M.; Zhang, X.; Ernge, T. J.; Goldman, A. S.; Zhao, J.; Incarvito, C.; Hartwig, J. F. *J. Am. Chem. Soc.* **2003**, *125*, 13644.

(40) Huang, Z.; Zhou, J.; Hartwig, J. F. *J. Am. Chem. Soc.*, **2010**, *132*, 11458.

(41) Sykes, A. C.; White, P.; Brookhart, M. *Organometallics*, **2006**, *25*, 1664.

(42) Gunanathan, C.; Milstein, D. *Acc. Chem Res.* **2011**, *44*, 588.

(43) (a) Khaskin, E.; Iron, M. A.; Shimon, L. J. W.; Zhang, J.; Milstein, D., *J. Am. Chem. Soc.* **2010**, *132*, 8542. (b) Feller, M.; Diskin-Posner, Y.; Shimon, L. J. W.; Ben-Ari, E.; Milstein, D., *Organometallics,* **2012**, *31*, 4083.

(44) (a) Yang, J.; Brookhart, M. *Adv. Synth. Catal.*, **2009**, *351*, 175. (b) Yang, J.; Brookhart, M. *J. Am. Chem. Soc.* **2007**, *129*, 12656.

(45) Yang, J.; White, P. S.; Schauer, C. K.; Brookhart, M. *Angew. Chem. Int. Ed.*, **2008,** *47,* 4141.

(46) Yang, J.; White, P. S.; Brookhart, M. *J. Am. Chem. Soc.*, **2008**, *130*, 17509.

(47) Park, S.; Brookhart, M. *Organometallics*, **2010**, *29,* 6057. (b) Park, S.; Brookhart, M. *Chem. Commun*. **2011**, *47*, 3643.

(48) Park. S.; Bézier, D.; Brookhart, M. *J. Am. Chem. Soc.*, **2012**, *134*, 11404.

(49) Park, S.; Brookhart, M. *J. Am. Chem. Soc.* **2012**, *134*, 640.

(50) For a comparison of the *trans*-labilizing properties of silyl, alkyl, and hydride ligated Ir complexes see: Aizenberg, M.; Milstein, D. *J. Am. Chem. Soc*. **1995**, *117*, 6456.

(51) (a) Auburn, M. J.; Stobart, S. R. *Inorg. Chem.* **1985**, *24*, 318. (b) Joslin, F. L; Stobart, S. R. *J. Chem. Soc., Chem. Commun.* **1989**, 504. (c) Auburn, M. J.; Holmes-Smith, R. D.; Stobart, S. R.; Bakshi, P. K.; Cameron, T. S. *Organometallics* **1996**, *15*, 3032. (d) Gossage, R. A.; McLennan, G. D.; Stobart, S. R. *Inorg. Chem.* **1996**, *35*, 1729. (e) Brost, R. D.; Bruce, G. C.; Joslin, F. L.; Stobart, S. R. *Organometallics* **1997**, *16*, 5669. (f) Bushnell, G. W.; Casado, M. A.; Stobart, S. R. *Organometallics* **2001**, *20*, 601.

(52) (a) Stradiotto, M.; Fujdala, K. L.; Tilley, T. D. *Chem. Commun.* **2001**, 1200. (b) Sangtrirutnugul, P.; Stradiotto, M.; Tilley, T. D. *Organometallics* **2006**, *25*, 1607. (c) Sangtrirutnugul, P.; Tilley, T. D. *Organometallics* **2007**, *26*, 5557. (d) Sangtrirutnugul, P.; Tilley, T. D. *Organometallics* **2008**, *27*, 2223.

(53) (a) Tilley, T. D. In *The Silicon-Heteroatom Bond*; Patai, S., Rappoport, Z., Eds; Wiley: New York, 1991. (b) Corey, J. Y.; Braddock-Wilking, J. *Chem. Rev.* **1999**, *99*, 175.

(54) Göttker-Schnetmann, I.; White, P.S.; Brookhart, M. *Organometallics* **2004**, *23*, 1766.

(55) *CRC Handbook of Chemistry and Physics*, 63rd ed.; West, R. C., Ed.; CRC Press: Boca Raton, FL, 1982; Appendix F, p 186.

(56) (a) Gatard, S.; Celenligil-Cetin, R.; Guo, C.; Foxman, B. M.; Ozerov, O. V. *J. Am. Chem. Soc.* **2006***, 128*, 2808. (b) Verat, A. Y.; Pink, M.; Fan, H.; Tomaszewski, J.; Caulton, K. G. *Organometallics* **2008**, *27*, 166. (c) Fan, L; Parkin, S; Ozerov, O. V. *J. Am. Chem. Soc.* **2005**, *127*, 16772.

(57) (a) Dorta, R.; Goikhman, R.; Milstein, D. *Organometallics* **2003**, *22*, 2806. (b) Chaplin, A. B.; Poblador-Bahamonde, A. I.; Sparkes, H. A.; Howard, J. A. K.;

Macgregor, S. A.; Weller, A. S. *Chem. Commun.* **2009**, 244. (c) Douglas, T. M.; Chaplin, A. B.; Weller, A. S. *Organometallics* **2008**, *27*, 2918. (d) Urtel, H.; Meier, C; Eisenträger, F.; Rominger, F.; Joschek, J. P.; Hofmann, P. *Angew. Chem. Int. Ed.* **2001**, *40*, 781. (e) Dorta, R.; Stevens, E. D.; Nolan, S. P. *J. Am. Chem. Soc.* **2004**, *126*, 5054. (f) Pike, S. D.; Thompson, A. L.; Algarra, A. G.; Apperley, D. C.; Macgregor, S. A.; Weller, A. S. *Science*, **2012**, *337*, 1648.

(58) The Rh-*H* in **2-8** and the Ir-*H* in **2-7** were each located in the difference map and refined the M-*H* distance fixed at 1.55 Å. In the final refinement cycles, this distance restraint was removed; the previously determined hydride thermal parameter was retained and the hydride position was refined. For **2-6·OEt$_2$** the Ir-*H* was not located in the difference map. Instead, an initial Ir-*H* position similar to that found in **2-7** was selected, and the Ir-H distance was fixed (1.55 Å) while the other parameters (X-Ir-H angles, Ir-*H* thermal parameter) were allowed to vary. The Ir-*H* position in **2-6·OEt$_2$** following refinement in this manner was similar to that found in **2-7**.

(59) (a) Albinati, A.; Bakhmutov, V. I.; Caulton, K. G.; Clot, E.; Eckert, J.; Eisenstein, O.; Gusev, D. G.; Grushin, V. V.; Hauger, B. E.; Klooster, W. T.; Koetzle, T. F.; McMullan, R. K.; O'Loughlin, T. J.; Pelissier, M.; Ricci, J. S.; Sigalas, M. P.; Vymenits, A. B. *J. Am. Chem. Soc.* **1993**, *115*, 7300. (b) Riehl, J.-F.; Jean, Y.; Eisenstein, O.; Pelissier, M. *Organometallics*, **1992**, *11*, 729. (c) Thorn, D. L.; Hoffmann, R. *New J. Chem.* **1979**, *3*, 39.

(60) Lachaize, S.; Sabo-Etienne, S. *Eur. J. Inorg. Chem.* **2006**, 2115.

(61) Two examples of σ-Si-H coordination to a late metal center involving [R-P*Si*(μ-H)P]*M* ligation have been previously reported; see reference 15c and 15j

(62) (a) Pouy, M. J.; Stanley, L. M.; Hartwig, J. F. *J. Am. Chem. Soc.* **2009**, *131*, 11312. (b) Vo, G. D.; Hartwig, J. F. *J. Am. Chem. Soc.* **2009**, *131*, 11049. (c) Lavallo, V.; Frey, G. D.; Donnadieu, B.; Soleilhavoup, M.; Bertrand, G. *Angew. Chem. Int. Ed.* **2008**, *47*, 5224. (d) Surry, D. S.; Buchwald, S. L. *J. Am. Chem. Soc.* **2007**, *129*, 10354. (e) Seayad, A.; Ahmed, M.; Klein, H.; Jackstell, R.; Gross, T.; Beller, M. *Science* **2002**, *297*, 1676. (f) Roundhill, D. M. *Chem. Rev.* **1992**, *71*, 23. (g) Lundgren, R. J.; Peters, B. D.; Alsabeh, P. G.; Stradiotto, M. *Angew. Chem. Int. Ed.* **2010**, *49*, 4071. (h) Lundgren, R. J.; Sappong-Kumankumah, A.; Stradiotto, M. *Chem. Eur. J.* **2010**, *16*, 1983.

(63) (a) Fulton, J. R.; Holland, A. W.; Fox, D. J.; Bergman, R. G. *Acc. Chem. Res.* **2002**, *35*, 44, and references contained therein. (b) Kaplan, A. W.; Ritter, J. C. M.; Bergman, R. B. *J. Am. Chem. Soc.* **1998**, *120*, 6828.

(64) Zhou, J.; Hartwig, J. F. *Angew. Chem. Int. Ed.* **2008**, *47*, 5783.

(65) Tessier-Youngs, C.; Beachley, O. T. *Inorg. Synth.* **1986**, *25*, 95.

(66) Schlosser, M.; Hartmann, J. *Angew. Chem., Int. Ed. Engl.* **1973**, *12*, 508.

(67) Fellmann, J. D.; Schrock, R. R. *J. Am. Chem. Soc.* **1978**, *100*, 3359.

(68) Murata, M.; Buchwald, S. L. *Tetrahedron* **2004**, *60*, 7397.

(69) (a) Korshin, E.E.; Leitus, G.; Shimon, L. J. W.; Konstantinovski, L.; Milstein, D. *Inorg. Chem.* **2008**, *47*, 7177; (b) Tamm, M.; Drebel, B.; Baum, K.; Lugger, T.; Pape, T. *J. Organomet. Chem.* **2003**, *677*, 1.

(70) Sircoglou, M M.; Saffon, N.; Coppel, Y.; Boudhadir, G.; Maron, L.; Bourissou, D. *Angew. Chem. Int. Ed.* **2009**, *48*, 3454.

(71) During the course of this work, the synthesis of [κ^3-(2-^{i}Pr$_2$PC$_6$H$_4$)$_2$SiMe]H (^{i}Pr-PSiP)H) was reported (see reference 15o) to involve the same steps as [Cy-PSiP]H.[15b] However, attempts to follow the same synthetic protocol were not successful and the procedure was modified.

(72) (a) Brookhart, M.; Green, M. L. H. *J. Organomet. Chem.* **1983**, *250*, 395. (b) Brookhart, M.; Green, M. L. H.; Parkin, G. *Proc. Natl. Acad. Sci. U.S.A*. **2007**, *104*, 6908.

(73) Cooper, A. C.; Huffman, J. C.; Caulton, K. G. *Inorg. Chim. Acta*, **1998**, *270*, 261.

(74) (a) Hesp, K. D.; Stradiotto, M. *Chem. Cat. Chem.*, **2010**, *2*, 1192. (b) Müller, T. E.; Hultzsch, K. C.; Yus, M.; Foubelo, F.; Tada, M. *Chem. Rev*. **2008**, *108*, 3795 (c) Hartwig, J. F. *Nature*, **2008**, *455*, 314 (d) Severin, R.; Doye, S. *Chem. Soc. Rev.* **2007**, *36*, 1407 (e) Alonso, F.; Beletskaya, I. P.; Yus, M. *Chem. Rev.* **2004**, *104*, 3079 (f) Pohlki, F.; Doye, S. *Chem. Soc. Rev.* **2003**, *32*, 104 (g) Müller, R. E.; Beller, M. *Chem. Rev.* **1998**, *98*, 675.

(75) For examples, see: (a) Rodriguez-Zubiri, M.; Baudequin, C.; Bethegnies, A.; Brunet, J. J. *Chem. Plus. Chem.* **2012**, *77*, 445. (b) Reznichenko, A. L.; Nguyen, H. N.; Hultzsch, K. C. *Angew. Chem. Int. Ed.* **2010**, *49*, 8984. (c) Dub, P. A.; Rodriguez-Zubiri, M.; Daran, J. -C.; Brunet, J. -J.; Poli, R. *Organometallics*, **2009**, *28*, 4764. (d) Yi, C. S.; Yun, S. Y. *Org. Lett.* **2005**, *7*, 2181. (e) Khedkar, V.; Tillack, A.; Benisch, C.; Melder, J. -P.; Meller, M. *J. Mol. Catal. A*. **2005**, *241*, 175. (f) Brunet, J. -J.; Chu, N. C.; Diallo, O. *Organometallics*, **2005**, *24*, 3104. (g) Ryu, J. -S.; Li, G. Y.; Marks, T. J. *J. Am. Chem. Soc.* **2003**, *125*, 12584. (h) Li, Y.; Marks, T. J. *Organometallics,* **1996**, *15*, 3770.

(76) (a) Zhao, P.; Krug, P.; Hartwig, J. F. *J. Am. Chem. Soc.* **2005**, *127*, 12066. (b) Hanley, P. S.; Marković; Hartwig, J. F. *J. Am. Chem. Soc.* **2010**, *132*, 6302. (c) Hanley, P. S.; Hartwig, J. F. *J. Am. Chem. Soc.* **2011**, *133*, 15661. (d) Sevov, C. S.; Zhou, J.; Hartwig, J. F. *J. Am. Chem. Soc.* **2012**, *134*, 11960.

(77) For examples of reviews see: (a) Bryliakov, K. P.; Talsi, E. P.; Coord. Chem. Rev. **2012**, *256*, 2994. (b) Lamberti, M.; Mazzeo, M.; Pappalardo, D.; Pellecchia, C. *Coord. Chem. Rev.* **2002**, *35*, 905. (c) Hou, Z.; Luo, Y.; Li, X. *J. Organomet. Chem*. **2006**, *691*, 3114. (d) Drent, E.; Budzelaar, P. H. M. *Chem. Rev*. **1996**, *96*, 663. (e) Resconi, L.; Cavallo, L.; Fait, A.; Piemontesi, F. *Chem. Rev*. **2000**, *100*, 1253. (f) Angermund, K.; Fink, G.; Jensen, V. R.; Kleinschmidt, R. *Chem. Rev*. **2000**, *100*, 1457. (g) Corradini, P.; Guerra, G.; Cavallo, L. *Acc. Chem. Res*. **2004**, *37*, 231. (h) Erker, G. *Acc. Chem. Res*. **2001**, *34*, 309. (i) Coates, G. W.; Hustad, P. D.; Reinartz, S. *Angew. Chem.,Int. Ed*. **2002**, *41*, 2236. (j) Chen, E. Y. X.; Marks, T. J. *Chem. Rev*. **2000**. (k) Widenhoefer, R. A. *Acc. Chem. Res*. **2002**, *35*, 905.

(78) (a) Zhou, J.; Hartwig, J. F. *J. Am. Chem. Soc.* **2008**, *130*, 12220. (b) Sevov. C. S.; Zhou, J.; Hartwig, J. F. *J. Am. Chem. Soc.* **2012**, *134*, 11960.

(79) Müller, R. E.; Hultzsch, K. C.; Yus, M.; Foubelo, F.; Tada, M. *Chem. Rev.* **2008**, *108*, 3795.

(80) Uhe, A.; Hölscher, M.; Leitner, W. *Chem. Eur. J.* **2013**, *19*, 1020.

(81) (a) Glueck, D. S.; Newman Winslow, L. J.; Bergman, R. G. *Organometallics*, **1991**, *10*, 1462. (b) Fulton, J. R.; Bouwkamp, M. W.; Bergman, R. G. *J. Am. Chem. Soc.* **2000**, *122*, 8799. (c) Fulton, J. R.; Sklenak, S.; Bouwkamp, M. W.; Bergman, R. G. *J. Am. Chem. Soc.* **2002**, *124*, 4722. (d) Holland, A. W.; Bergman, R. G. *J. Am. Chem. Soc.* **2002**, *124*, 14684. (e) Rais, D.; Bergman, R. G. *Chem. Eur. J.* **2004**, *10*, 3970. (f) Jayaprakash, K. N.; Gunnoe, T. B.; Boyle, P. D. *Inorg. Chem.* **2001**, *40*, 6481. (g) Conner, D.; Jayaprakash, K. N.; Cundari, T. R.; Gunnoe, T. B. *Organometallics*, **2004**, *23*, 2724. (h) VanderLende, D. D.; Abboud, K. A.; Boncella, J. M. *Inorg. Chem.* **1995**, *34*, 5319. (i) Gunnoe, T. B. *Eur. J. Inorg. Chem.* **2007**, 1185.

(82) Garralda, M. A. *Dalton Trans.* **2009**, 3635 and references therein.

(83) (a) Milstein, D.; Calabrese, J. C. *J. Am. Chem. Soc.* **1982**, *104*, 3773 (b) Bianchini, A. Meli, M. Peruzzini, J. A. Ram´ırez, A. Vacca, F. Vizza and F. Zanobini, *Organometallics*, **1989**, *8*, 337. (c) Goikhman, R.; Milstein, D. *Angew. Chem. Int. Ed.* **2001**, *40*, 1119. (d) V. Circu, M. A. Fernandes and L. Carlton, *Inorg. Chem.* **2002**, *41*, 3859. (e) Peterson, T. H.; Golden, J. T.; Bergman, R. G. *Organometallics*, **1999**, *18*, 2005.

(84) (a) Burger, P.; Bergman, R. G. *J. Am. Chem. Soc.* **1993**, *115*, 10462. (b) Luecke. H. F.; Arndtsen, B. A.; Burger, P.; Bergman, R. G. *J. Am. Chem. Soc.* **1996**, *118*, 2517. (c) Alaimo, P. J.; Arndtsen, B. A.; Bergman, R. G. *J. Am. Chem. Soc.* **1997**, *119*, 5269. (d) Arndtsen, B. A.; Bergman, R. G. *Science*, **1995**, *270*, 1970. (e) Alaimo, P. J.; Bergman, R. G. *Organometallics*, **1999**, *18*, 2707. (f) Strout, D.

L.; Zarić, S.; Niu, S. Q.; Hall, M. B. *J. Am. Chem. Soc.*, **1996,** *118,* 6068. (g) Klei, S. R.; Tilley, T. D.; Bergman, R. G. *J. Am. Chem. Soc.*, **2000**, *122*, 1816.

(85) (a) Waterman, R.; Hayes, P. G.; Tilley, T. D. *Acc. Chem. Res.* **2007**, *40*, 712, and references contained therein. (b) Calimano, E.; Tilley, T. D. *J. Am. Chem. Soc.* **2008**, *130*, 9226. (c) Calimano, E.; Tilley, T. D. *J. Am. Chem. Soc.* **2009**, *131*, 11161. (d) Calimano, E.; Tilley, T. D. *Organometallics*, **2010**, *29*, 1680. (e) Fasula, M. E.; Tilley, T. D. *Organometallics*, **2012**, *31*, 5049.

(86) (a) Díaz-Torres, R.; Alvarex, S. *Dalton Trans.* **2011**, *40*, 10742. (b) Krossing, I.; Raabe, I. *Angew. Chem. Int. Ed.* **2004**, *43*, 2066. (c) Strauss, S. H. *Chem. Rev.* **1993**, 927. (d) Beck, W.; Sünkel, K. *Chem. Rev.* **1988**, *88*, 1405.

(87) (a) Cheng, T.-Y.; Szalda, D. J.; Franz, J. A.; Bullock, R. M. *Inorg. Chim. Acta*, **2010**, *363*, 581. (b) Cipot, J.; Wechsler, D.; McDonald, R.; Ferguson, M. J.; Stradiotto, M. *Organometallics*, **2005**, *24*, 1737. (c) Yang, C. S.; Horng, H. C.; Liao, F. L.; Cheng. C. P. *J. Chem. Soc. Chem. Commun.* **1994**, 1637. (d) Carballo, R.; Castiñeiras, A.; García-Fontá, S.; Losada-González, P.; Abram, U.; Vázquez-Lópex, E. *Polyhedron*, **2001**, *20*, 2371. (e) Vela, J.; Smith, J.; Yu, Y.; Ketterer, N. A.; Flaschenriem, C. J.; Lachiocotte, R. J.; Holland, P. L. *J. Am. Chem. Soc.* **2005**, *127*, 7857. (f) Ogasawara, M.; Huang, D.; Streib, W. E.; Huffman, J. C.; Gallego-Planas, N.; Maseras, F.; Eisenstein, O.; Caulton, K. G. *J. Am. Chem. Soc.* **1997**, *119*, 8642. (g) Rybtchinski, B.; Oevers, S.; Montag, M.; Vigalok, A.; Rozenberg. H.; Martin, J. M. L.; Milstein, D. *J. Am. Chem. Soc.* **2001**, *123*, 9064. (h) Gandelman, M.; Konstantinovski, L.; Rozenberg, H.; Milstein, D. *Chem. Eur. J.* **2003**, *9*, 2595. (i) Lundquist, E. G.; Folting, K.; Huffman, J. D.; Caulton, K. G. *Organometallics*, **1990**, *9*, 2254. (j) Olgmöller, B.; Bauer, H.; Löbermann, H.; Nagel, U.; Beck, W. *Chem. Ber.* **1982**, *115*, 2271. (k) Tomlinson, A. A. G.; Bonamico, M.; Dessy, G.; Fares, V.; Scaramuzza, L. *J. Chem. Soc. Dalton*, **1972**, 1671. (l) Rheingold, A. L.; Wu, G.; Heck, R. F. *Inorg. Chim. Acta*, **1987**, *131*, 147.

(88) (a) Cimadevilla, F.; Garćia, M. E.; Garćia-Vivó, D.; Ruiz, M. A.; Rueda, M. T.; Halut, S. *J. Organomet. Chem.* **2012**, *699*, 67. (b) Fenton, H.; Tidmarsh, I. S.; Ward, M. D. *Dalton Trans.* **2010**, *39*, 3805. (c) Poorters, L.; Armspach, D.; Matt, D.; Toupe, L.; Jones, P. *Angew. Chem. Int. Ed.* **2007**, *46*, 2663. (d) Varonka, M. S.; Warren, T. H. *Inorg. Chem.* **2009**, *48*, 5605.

(89) Complexes **3-15** and **3-16** [R-PSiP]Ir(H)($NHCH_2Ph$) (**3-15**, R = Cy; **3-16**, R = ^{i}Pr), were determined to adopt a related *fac*-[Cy-PSiP] structure on the basis of ^{1}H and ^{31}P NMR spectroscopy, but these compounds have not been crystallographically characterized.

(90) No evidence was found for such an interaction in solution. See ref 15f.

(91) See related Ir acetone complexes (a) Shapely, J. R.; Schrock, R. R.; Osborn, J. A. *J. Am. Chem. Soc.* **1969**, *91*, 2816. (b) Crabtree, R. H.; Mellea, M. F.; Mihelcic, J. M.; Quirk, J. M. *J. Am. Chem. Soc.* **1982**, *104*, 107. (c) Crabtree, R. H.; Demou, P. C.; Eden, D.; Mihelcic, J. M.; Parnell, C. A.; Quirk, J. M.; Morris, G. E. *J. Am. Chem. Soc.* **1982**, *104*, 6994. (d) Crabtree, R. H.; Mellea, M. F.; Mihelcic, J. M. *Inorg. Chim. Acta*, **1989**, *28*, 56.

(92) T. D. W. Claridge, *High-Resolution NMR Techniques in Organic Chemistry*, Pergamon, New York, **1999**.

(93) (a) Corey, J. Y.; Braddock-Wilking, J. *Chem. Rev.* **1999**, *99*, 175. (b) Corey, J. Y. *Chem. Rev.* **2011**, *111*, 863.

(94) (a) Hamilton, D. G.; Crabtree, R. H. *J. Am. Chem. Soc.* **1988**, *110*, 4126. (b) Crabtree, R. H. *Acc. Chem. Res.* **1990**, *23*, 95.

(95) Olah, G. A.; Laall, K.; Farooq, O. *Organometallics*, **1984**, *3*, 1337.

(96) Riehl, J. -F.; Jean, Y.; Eisenstein, O.; Pélissier, M. *Organometallics*, **1992**, *11*, 729.

(97) (a) Hebden, T. J.; Denney, M. C.; Pons, V.; Piccoli, P. M. B.; Koetzle, T. F.; Schultz, A. J.; Kaminsky, W.; Goldberg, K. I.; Heinekey, D. M. *J. Am. Chem. Soc.* **2008**, *130*, 10812. (b) Rossin, A.; Peruzzini, M.; Zanobini, F. *Dalton Trans.* **2011**, *40*, 4447. (c) Chakraborty, S.; Zhang, J.; Patel, Y. J.; Krause, J. A.; Guan, H. *Inorg. Chem.* **2013**, *52*, 37. (d) Zhang, J.; Balaraman, E.; Leitus, G.; Milstein, D. *Organometallics*, **2011**, *30*, 5716. (e) Marks, T. J.; Kolb, J. R. *Chem. Rev.* **1977**, *71*, 263.

(98) Luehmann, N.; Panisch, R.; Müeller, T. *Appl. Organomet. Chem.* **2010**, *24*, 533.

(99) (a) Kubas, G. J. *Metal Dihydrogen and σ-Bond Complexes*; Kluwer Academic: New York, 2001. (b) Lin, Z. *Chem. Soc. Rev*. **2002**, *31*, 239. (c) Nikonov, G. *Adv. Organomet. Chem.* **2005**, *53*, 217. (d) Lachaize, S.; Sabo-Etienne, S. *Eur. J. Inorg. Chem*. **2006**, 2115.

(100) It has been suggested that, in the absence of independent corroborating evidence, J_{SiH} values < 70 Hz may not be a definitive measure of the extent of Si-H interaction: (a) Dubberley, S. R.; Ignatov, S. K.; Rees, N. H.; Razuvaev, A. G.; Mountford, P.; Nikonov, G. I. *J. Am. Chem. Soc*. **2003**, *125*, 642. (b) Ignatov, S. K.; Rees, N. H.; Tyrrell, B. R.; Dubberley, S. R.; Razuvaev, A. G.; Mountford, P.; Nikonov, G. I. *Chem. Eur. J.* **2004**, *10*, 4991.

(101) Johns, A. M.; Liu, Z.; Hartwig, J. F. *Angew. Chem. Int. Ed.* **2007**, *46*, 7259.